NOAA Technical Memorandum NMFS-AFSC-373
doi:10.7289/V5/TM-AFSC-373

Model-based Essential Fish Habitat Definitions for Gulf of Alaska Groundfish Species

S. Rooney, C. N. Rooper, E. Laman, K. Turner, D. Cooper, and M. Zimmermann

U.S. DEPARTMENT OF COMMERCE
National Oceanic and Atmospheric Administration
National Marine Fisheries Service
Alaska Fisheries Science Center

March 2018

NOAA Technical Memorandum NMFS

The National Marine Fisheries Service's Alaska Fisheries Science Center uses the NOAA Technical Memorandum series to issue informal scientific and technical publications when complete formal review and editorial processing are not appropriate or feasible. Documents within this series reflect sound professional work and may be referenced in the formal scientific and technical literature.

The NMFS-AFSC Technical Memorandum series of the Alaska Fisheries Science Center continues the NMFS-F/NWC series established in 1970 by the Northwest Fisheries Center. The NMFS-NWFSC series is currently used by the Northwest Fisheries Science Center.

This document should be cited as follows:

> Rooney, S., C. N. Rooper, E. Laman, K. Turner, D. Cooper, and M. Zimmermann. 2018. Model-based essential fish habitat definitions for Gulf of Alaska groundfish species. U.S. Dep. Commer., NOAA Tech. Memo. NMFS-AFSC-373, 370 p.
>
> Document available: http://www.afsc.noaa.gov/Publications/AFSC-TM/NOAA-TM-AFSC-373.pdf

Reference in this document to trade names does not imply endorsement by the National Marine Fisheries Service, NOAA.

NOAA Technical Memorandum NMFS-AFSC-373
doi:10.7289/V5/TM-AFSC-373

Model-based Essential Fish Habitat Definitions for Gulf of Alaska Groundfish Species

S. Rooney, C. N. Rooper, E. Laman, K. Turner, D. Cooper, and M. Zimmermann

Resource Assessment and Conservation Engineering Division
Alaska Fisheries Science Center
National Marine Fisheries Service
National Oceanic and Atmospheric Administration
7600 Sand Point Way N.E.
Seattle, WA 98115

www.afsc.noaa.gov

U.S. DEPARTMENT OF COMMERCE
Wilbur L. Ross Jr., Secretary
National Oceanic and Atmospheric Administration
RDML Timothy Gallaudet (ret.), Acting Under Secretary and Administrator
National Marine Fisheries Service
Chris Oliver, Assistant Administrator for Fisheries

March 2018

This document is available to the public through:

National Technical Information Service
U.S. Department of Commerce
5285 Port Royal Road
Springfield, VA 22161

www.ntis.gov

ABSTRACT

Defining essential habitats for fishes and invertebrates is an important step in managing groundfish species in Alaska waters. Species distribution models have been widely used to describe the potential habitat of species found in marine and terrestrial systems. The models themselves can take a number of forms, from relatively simple frameworks such as generalized linear or additive models to complex modeling frameworks such as Maximum Entropy Modeling (MaxEnt). We used several modeling methods and data from scientific surveys and commercial fisheries to define essential habitats for 36 species from the Gulf of Alaska. Adult, juvenile, larval and egg stages were seasonally modeled where data were available. Bottom depth was the dominant variable determining the distribution of most adult and juvenile life history stages. Sea surface temperature was the most important predictor of ichthyoplankton distribution. The model results were used to develop maps that depicted the boundaries delineating essential fish habitat for each species and life stage. These maps will be used for marine spatial planning and assessing impacts of anthropogenic activities in Alaska's marine environment.

CONTENTS

ABSTRACT iii
INTRODUCTION 1
MATERIALS AND METHODS 3
Study Area 3
Survey Data 4
Species Distribution Data -- Recruitment Processes Data 7
Species Distribution Data -- Groundfish Bottom Trawl Surveys 10
Species Distribution Data -- Commercial Catch (Observer) Data 15
Habitat Covariates 17
Habitat Covariates for Early Life History Stage Models 17
Habitat Covariates for Bottom Trawl Survey Models 19
Habitat Covariates for Commercial Catch Models 23
Modeling Methods -- Recruitment Processes Data 28
Modeling Methods -- Bottom Trawl Survey Data 28
Modeling Methods -- Commercial Catch (Observer) Data 30
Model Validation 31
Essential Fish Habitat Maps 32
RESULTS 34
Flatfishes 34
Arrowtooth Flounder (*Atheresthes stomias*) 34
Rex Sole (*Glyptocephalus zachirus*) 47
Flathead Sole (*Hippoglossoides elassodon*) 58
Northern Rock Sole (*Lepidopsetta polyxystra*) 69
Southern Rock Sole (*Lepidopsetta bilineata*) 81
Yellowfin Sole (*Limanda aspera*) 87
Alaska Plaice (*Pleuronectes quadrituberculatus*) 96
Dover Sole *(Microstomus pacificus)* 105
Roundfishes 116
Sablefish (*Anoplopoma fimbria*) 116
Walleye Pollock (*Gadus chalcogrammus*) 128
Pacific Cod (*Gadus macrocephalus*) 140

Yellow Irish Lord (*Hemilepidotus jordani*) 151
Bigmouth Sculpin (*Hemitripterus bolini*) 162
Great Sculpin (*Myoxocephalus polyacanthocephalus*) 173
Atka Mackerel (*Pleurogrammus monopterygius*) 181
Rockfishes (*Sebastes* spp.) 190
Pacific Ocean Perch (*Sebastes alutus*) 191
Rougheye Rockfish (*Sebastes aleutianus*) 202
Redbanded Rockfish (*Sebastes babcocki*) 211
Northern Rockfish (*Sebastes polyspinis*) 219
Shortraker Rockfish (*Sebastes borealis*) 228
Silvergray Rockfish (*Sebastes brevispinis*) 236
Dark Rockfish (*Sebastes ciliatus*) 244
Quillback Rockfish (*Sebastes maliger*) 250
Black Rockfish (*Sebastes melanops*) 257
Blackspotted Rockfish (*Sebastes melanostictus*) 263
Redstriped Rockfish (*Sebastes proriger*) 268
Yelloweye Rockfish (*Sebastes ruberrimus*) 276
Dusky Rockfish (*Sebastes variabilis)* 284
Harlequin Rockfish (*Sebastes variegatus*) 292
Pygmy Rockfish (*Sebastes wilsoni*) 300
Sharpchin Rockfish (*Sebastes zacentrus*) 304
Shortspine Thornyhead (*Sebastolobus alascanus*) 312
Longspine Thornyhead (*Sebastolobus altivelis*) 323
Skates 328
Alaska Skate (*Bathyraja parmifera*) 328
Aleutian Skate (*Bathyraja aleutica*) 337
Bering Skate (*Bathyraja interrupta*) 346
Invertebrates 351
Octopus Unidentified 351
ACKNOWLEDGMENTS 359
CITATIONS 361

INTRODUCTION

The 1996 reauthorization of the Magnuson-Stevens Fishery Conservation and Management Act (MSFCMA) mandates that the National Marine Fisheries Service (NMFS) identify habitats essential for managed species and conserve habitats from adverse effects of fishing and other anthropogenic activities. Essential Fish Habitat (EFH) is defined under the act as 'those waters and substrates necessary to fish for spawning, breeding, feeding or growth to maturity.' As part of this mandate, EFH descriptions for all species listed under a Fisheries Management Plan (FMP) in Alaska waters are needed. In addition, these descriptions are routinely revisited under a 5-year cycle that reviews and updates EFH information (including species descriptions) with new data and research.

Essential fish habitat descriptions consist of maps of EFH and text descriptions. In Alaska, most EFH descriptions for groundfish have been limited to qualitative statements on the distribution of adult life stages. These are useful, but could be relatively easily refined both in terms of spatial extent and life history stage using species distribution models (SDMs) and data available from a variety of NOAA sources. Distribution models have been widely used in conservation biology and terrestrial systems to define the potential habitat for organisms of interest (e.g., Delong and Collie 2004, Lozier et al. 2009, Elith et al. 2011, Sagarese et al. 2014). Recently SDMs have been developed for various groundfishes in the eastern Bering Sea (McConnaughey and Syrjala 2009, Laman et al. 2017), and for coral and sponge species in the Gulf of Alaska and Aleutian Islands (Rooper et al. 2014, Sigler et al. 2015, Rooper et al. 2016).

Species distribution models themselves can take a number of forms, from relatively simple frameworks such as generalized linear or additive models to more complex methods including computer learning methods (boosted regression trees, maximum entropy models, and random forest models) or multi-stage models. The models can be used to predict potential habitat, abundance, or

probability of presence, but they all have some features in common: 1) the underlying data consist of some type of independent variables (predictors) and a dependent response variable (presence, presence/absence or abundance), 2) raster maps of independent variables are used to predict a response map, and 3) confidence bounds around the predictions and partitioning of the data can be used to produce test statistics useful for evaluating the model. The outputs of SDMs are raster maps that can show the predicted abundance of a species at each of the raster cells. This type of product is useful for EFH descriptions, as it lends itself to producing maps of areas of high abundance or hotspots of distribution and the models themselves can be used to generate the required text descriptions.

The goal of this study was to predict spatial distributions from habitat covariates (i.e., vessel position, bottom depth, maximum tidal current speed, presence /absence of corals or sponges) using SDMs and to use the resulting maps to re-describe EFH for all federally managed species of groundfishes and invertebrates in the Gulf of Alaska (GOA). The SDMs predicted either abundance (for bottom trawl survey data) or probability of suitable habitat based on presence observations (for early life history data, commercial catch data, and some bottom trawl survey data for rarer species). The SDMs used were generalized additive models (GAM or hurdle-GAM) for abundance data and maximum entropy models (MaxEnt) or presence-absence (PA) for presence-only data. Complementary accompanying NOAA Technical Memoranda were generated for Aleutian Islands (Turner et al. 2017) and eastern Bering Sea (Laman et al. 2017) fishes and invertebrates. We used several sources of both measured and model derived data to parameterize the early life history and adult fish distribution models. After model parametrization, we extended our analysis to make predictions for areas of the GOA where conditions were known, but fishes and invertebrates were not directly sampled. We generated models describing components of EFH for each species' life stage where data existed for egg, larval, juvenile, and adult life history stages. In addition, we produced

distribution maps that showed the location of EFH for all major groundfish species. It is anticipated that this research establishes a foundation for future updates to EFH through integration of new data and studies.

MATERIALS AND METHODS

Study Area

The GOA continental shelf and upper continental slope represent a diverse mosaic of benthic habitats stretching from Dixon Entrance (131° W) in the southeastern GOA to Unimak Pass (165° W) in the eastern Aleutian Islands. The GOA continental shelf here ranges in width from 20 km to greater than 200 km and the continental slope is steep and features gullies and submarine canyons extending into the continental shelf (Fig. 1). The Alaska Coastal Stream and Alaska Coastal Current flow westward (counter-clockwise) around the GOA from Dixon Entrance to the end of the Aleutian Islands. These currents result in downwelling of surface water at the Alaska coast. Seasonal freshwater discharge results in a highly stratified system in the summer, with nutrient limitation in the photic zone of the water column. The seafloor of the GOA is diverse, with extensive rocky substrate that has been uplifted due to tectonic activity and the retreat of glaciation. Much of the continental shelf is dominated by soft unconsolidated sediments.

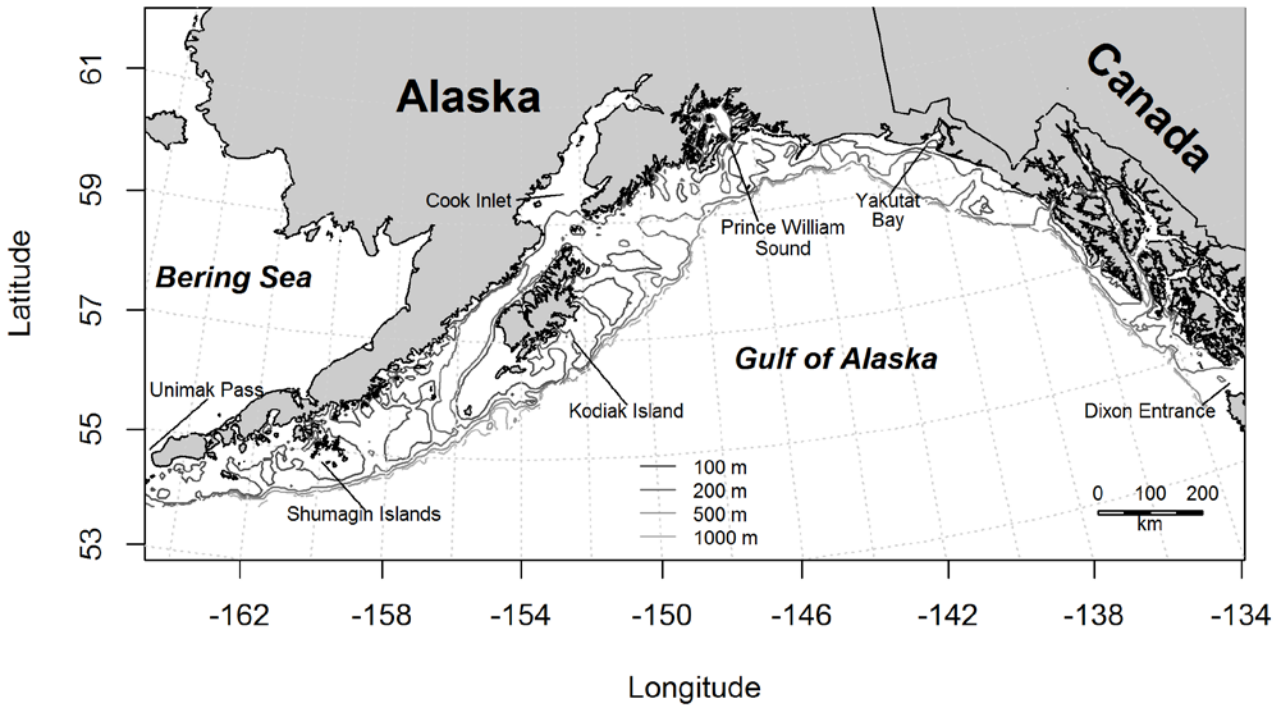

Figure 1. -- Gulf of Alaska from Dixon Entrance to Unimak Pass where this modeling study was carried out.

Survey Data

Data detailing the distribution and abundance of fishes and invertebrates in the GOA came from three different sources. The distribution data for the early life history stages (ELHS) of fishes (eggs, larvae, and pelagic juveniles) were collected by the Ecosystems and Fisheries-Oceanography Coordinated Investigations (EcoFOCI) ichthyoplankton surveys and provided from their ECODAAT database (https://access.afsc.noaa.gov/ichthyo/). EcoFOCI is a joint research program between the Alaska Fisheries Science Center (AFSC) and Pacific Marine Environmental Laboratory (PMEL). Species-specific ichthyoplankton data were separated into oceanographic seasons based on presence of ELHS in the water column. Distributions of settled juvenile and adult stages were modeled using the AFSC's Resource Assessment and Conservation Engineering Division Groundfish Assessment Program's (RACE-GAP) summer bottom trawl survey database (RACEBASE: http://www.akfin.org/). The fall, winter, and spring distributions of what we assumed were primarily

adult animals were modeled using commercial catches from the Alaska Regional Office's (AKRO) fishery observer program VMS-Observer Enabled Catch-in-Areas database (VOE-CIA; S. Lewis, NMFS, Alaska Regional Office. Anchorage, Alaska). These data were divided into fall (October-November), winter (December-February), spring (March-May), and summer (June-September) seasons. All fishes and invertebrates examined were separated into generic, specific, or broader taxonomic groupings and then parsed into ontogenetic stages where prevalence and *a priori* sampling considerations were used to determine which species distribution modeling approach was applied to each data source, taxon, life stage, and season (Table 1).

Table 1. -- Life history stages of fishes and invertebrates collected on Ecosystems and Fisheries Oceanography Cooperative Investigations ichthyoplankton surveys (EcoFOCI) and NMFS Alaska Fisheries Science Center Resource Assessment and Conservation Engineering-Groundfish Assessment Program summer bottom trawl surveys (RACE-GAP) of the Gulf of Alaska indicating the species distribution modeling technique used to describe their distributions.

Species	Eggs	Larvae	Pelagic juveniles	Settled juveniles	Adults
Arrowtooth flounder (*Atheresthes stomias*)	*Atheresthes* spp.				
Rex sole (*Glyptocephalus zachirus*)					
Dover sole (*Microstomus pacificus*)					
Flathead sole (*Hippoglossoides elassodon*)					
Yellowfin sole (*Limanda aspera*)					
Southern rock sole (*Lepidopsetta bilineata*)					
Northern rock sole (*Lepidopsetta polyxystra*)					
Alaska plaice (*Pleuronectes quadrituberculatus*)					
Walleye pollock (*Gadus chalcogrammus*)					
Pacific cod (*Gadus macrocephalus*)					
Sablefish (*Anoplopoma fimbria*)					
Atka mackerel (*Pleurogrammus monopterygius*)					
Yellow Irish lord (*Hemilepidotus jordani*)					
Great sculpin (*Myoxocephalus polyacanthocephalus*)					
Bigmouth sculpin (*Hemitripterus bolini*)					
Pacific ocean perch (*Sebastes alutus*)		*Sebastes* spp.			
Northern rockfish (*Sebastes polyspinis*)					
Shortraker rockfish (*Sebastes borealis*)					
Rougheye rockfish (*Sebastes aleutianus*)					
Blackspotted rockfish (*Sebastes melanostictus*)					
Dusky rockfish (*Sebastes variabilis*)					
Yelloweye rockfish (*Sebastes ruberrimus*)					
Redbanded rockfish (*Sebastes babcocki*)					
Silvergray rockfish (*Sebastes brevispinis*)					
Dark rockfish (*Sebastes ciliatus*)					
Quillback rockfish (*Sebastes maliger*)					
Black rockfish (*Sebastes melanops*)					
Redstripe rockfish (*Sebastes proriger*)					
Harlequin rockfish (*Sebastes variegatus*)					
Pygmy rockfish (*Sebastes wilsoni*)					
Sharpchin rockfish (*Sebastes zacentrus*)					
Shortspine thornyhead (*Sebastolobus alascanus*)					
Longspine thornyhead (*Sebastolobus altivelis*)					
Alaska skate (*Bathyraja parmifera*)					
Bering skate (*Bathyraja interrupta*)					
Aleutian skate (*Bathyraja aleutica*)					
Octopus unidentified					

	Insufficient data to model
	Presence or presence-absence models
	Density (CPUE) models

Species Distribution Data -- Recruitment Processes Data

Observations of ELHS of fishes (eggs, larvae, and pelagic juveniles) from the EcoFOCI program's Data Access and Analysis Tool (ECODAAT) database (Fig. 2) were used in species distribution modeling. For our analysis, we included catches in the GOA from 1991 to 2013. These data were collected in pursuit of a variety of survey objectives, often opportunistically, and on several different types of surveys (Matarese et al. 2003). Sampling design, gear type, mesh size, and seasonality varied over the history of these surveys as well. Collection methods included bongo nets, Multiple Opening/Closing Net and Environmental Sensing System (MOCNESS) tows, as well as Methot and Tucker trawls (Matarese et al. 2003). Over the years, samples were collected in all 12 months, although not all month-year combinations occurred in the database. These ichthyoplankton collections were also not uniformly spatially distributed and most samples came from the central GOA which reflects this program's historic focus on pollock recruitment mechanisms during this time period. Inter-annual differences in survey design and coverage as well as species-season-life stage prevalence combined with our intent to generate a single ELHS EFH map for each species' life stages based on average conditions predicated combining all years of recruitment processes data for our analyses. The distribution of sampling effort should be considered when drawing conclusions from maps produced from these data. For example, most of the historical ichthyoplankton samples were collected on a grid near Kodiak Island; therefore, predictions of suitable habitat in southeastern Alaska may be unsupported by data.

Temporal periodicity and prevalence of each taxon's ELHS was determined from the recruitment processes data (Table 2). Oceanographic seasonality for taxa and life stages present was defined as the months when they were present in the water column. Prevalence was used to determine whether there were sufficient data to model distribution. There had to be 50 or more presence observations for a taxon-life stage combination to qualify for species distribution modeling

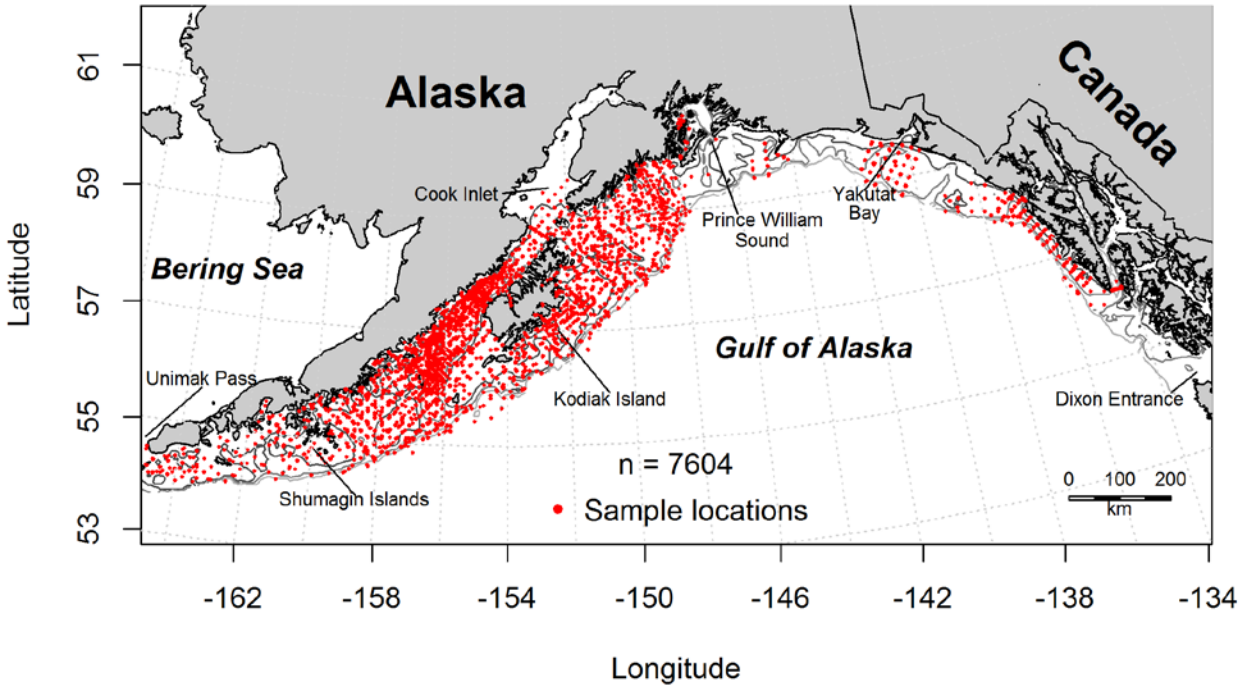

Figure 2. -- Locations of EcoFOCI ichthyoplankton data collections in the Gulf of Alaska from 1991to 2013. These data were used in the modeling of early life history stages of fish and invertebrate essential fish habitat.

Table 2 -- Oceanographic seasons for early life history stages of taxa collected during Ecosystems and Fisheries-Oceanography Cooperative Investigations ichthyoplankton surveys (EcoFOCI) of the Gulf of Alaska (1991-2013) were defined by months present in the water column; prevalence (number of presence observations) is indicated in parentheses.

Species	Eggs	Larvae	Pelagic juveniles
Alaska plaice (*Pleuronectes quadrituberculatus*)	Mar - Sept (490)	Apr - Sept (270)	--
Atheresthes spp.	Jan - Mar (42)	Jan - Sept (1386)	Apr - Sept (8)
Atka mackerel (*Pleurogrammus monopterygius*)	--	Feb - Apr (13)	--
Bigmouth sculpin (*Hemitripterus bolini*)	--	Apr - May (8)	Jun (1)
Dover sole (*Microstomus pacificus*)	Jan - Sept (1851)	Apr - Sept (257)	--
Northern rock sole (*Lepidopsetta polyxystra*)	--	Feb - Oct (1742)	Jun (1)
Pacific cod (*Gadus macrocephalus*)	Apr - Jul (9)	Apr - Jul (2348)	Jun - Sept (73)
Rex sole (*Glyptocephalus zachirus*)	Apr - Oct (1789)	Apr - Sept (354)	--
Rockfish (*Sebastes* spp.)	--	Apr - Oct (2996)	Apr - Sept (19)
Sablefish (*Anoplopoma fimbria*)	Feb - Jun (11)	Apr - Jul (351)	May - Jun (2)
Southern rock sole (*Lepidopsetta bilineata*)	--	Apr - Oct (1426)	--
Thornyhead rockfish (*Sebastolobus* spp.)	Apr - Jul (48)	May - Aug (30)	--
Walleye pollock (*Gadus chalcogramma*)	Feb - Oct (3133)	Feb - Sept (4834)	May - Sept (122)
Yellow Irish lord (*Hemilepidotus jordani*)	Jan - Sept (30)	Apr - Jun (15)	Feb - Apr (13)
Yellowfin sole (*Limanda aspera*)	May - Sept (107)	Apr - Sept (44)	--

Species Distribution Data -- Groundfish Bottom Trawl Surveys

The NMFS AFSC RACE-GAP has conducted bottom-trawl surveys in the GOA since 1984 (von Szalay and Raring 2016), either triennially (1993-99) or biennially (2001-13), under a rigorous and repeatable statistical sampling design. The GOA survey has been conducted on a regular 5 km × 5 km grid that covers the continental shelf and upper continental slope to 1,000 m depth. The survey uses a stratified random sampling protocol and includes a random mix of both previously sampled and unsampled grid cells using a modified Neyman optimum allocation sampling strategy (Cochran 1977). Strata have been based on a combination of depth intervals, geographic regions, and habitat types. We included trawl survey data from 1993 to 2013 (Fig. 3) in our analyses, but the window of informative survey results varied by species due to the evolution of species identification and taxonomy. RACE-GAP bottom trawl data were combined across the GOA region (Dixon Entrance to Unimak Pass) for all survey years inclusive since 1993. This approach was driven by our desire to generate a single EFH map based on average conditions and representative of a wide range of conditions. When parameterizing the SDMs from the groundfish bottom trawl data, we used habitat covariates collected in association with the catch (e.g., depth and temperature) so that the best fitting models were trained on local conditions and incorporated inter-annual variability in these predictors.

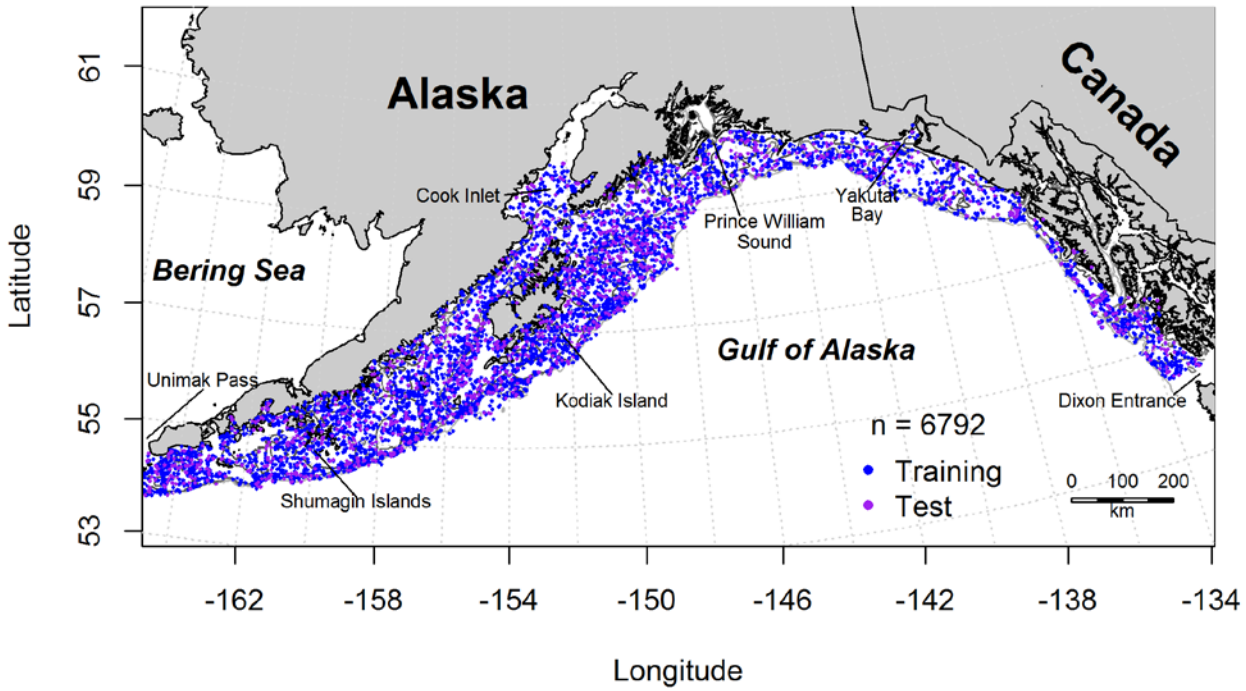

Figure 3. -- RACE-GAP bottom trawl survey locations in the Gulf of Alaska from 1993 to 2013 used in modeling essential fish habitat for fishes and invertebrates. Training data were used to parameterize the models, while testing data were used to test model performance (see Model Validation section for details).

The GOA bottom trawl survey has been conducted under nationally accepted standard protocols (Stauffer 2004) and utilizes a poly Nor'Eastern high-opening bottom trawl with a 27.2 m headrope and 24.2 m footrope configured with roller gear comprised of 20 cm rubber bobbins separated by 10 cm rubber disks with "flying wing" sections outboard. Trawl hauls were conducted at a target speed of 5.6 km h^{-1} (3 knots) with a targeted bottom contact duration of 15 (since 1996) or 30 minutes (prior to 1996) in "on bottom" configuration. Bottom contact, distance fished, and net dimensions were recorded throughout each trawl.

Groundfish bottom trawl data records were screened for inclusion in the SDMs. To qualify in the initial cut, trawl performance was satisfactory and the geographic position, distance fished, average bottom depth, and water temperature were recorded. Trawl hauls were satisfactory if the net opening was within a predetermined "normal" range, the footrope maintained contact with the seafloor, and the net suffered little or no damage during towing. A total of 7,314 bottom trawl survey hauls conducted between 1993 and 2013 met the criteria for initial inclusion in our analyses.

Bottom trawl survey catch abundance was standardized as catch-per-unit-effort (CPUE in units of no. ha^{-1}) using the area swept method (Alverson and Pereyra 1969) and computational approach of Wakabayashi et al. (1985). For catch processing at sea, all fishes and invertebrates caught in the trawl during a survey trawl haul were sorted either by species or into broader taxonomic groups and their total weight (kg) and number in the catch were determined and recorded. Effort in the form of area swept was calculated from measured net width averaged over the trawl haul duration and multiplied by the distance fished derived from positioning data collected with a vessel-mounted GPS receiver. For some species, both juvenile and adult sizes were captured in trawl catches. For our analyses, an approximate length at maturity taken from extant literature (Table 3) was used to apportion the catches into settled juvenile and adult stages using proportionality from the random

length subsample taken from the catch. For some species, only a subset of the available years was used for modeling due to changing confidence in our ability to distinguish taxa over the time series. For example, rougheye and blackspotted rockfish and were not confidently distinguished from each other on the GOA surveys until around 2006 (Orr and Hawkins 2008); so only data since and including 2006 surveys were used to parameterize models for these two species.

Table 3. -- Taxa from RACE-GAP summer bottom trawl surveys that were used for species distribution modeling: the years included in the modeling efforts, the prevalence of settled juveniles and adults (frequency of occurrence) in the bottom trawl hauls, and the length at first maturity (presented here as the maximum juvenile length) with sources indicated; "All" years modeled = 1993-2013.

Species	Years modeled	% Prevalence of settled juveniles	% Prevalence of adults	Maximum juvenile length (cm)	Length@Maturity Source
Alaska plaice (*Pleuronectes quadrituberculatus*)	All	0.5	5.1	28	Tenbrink and Wilderbuer 2015
Alaska skate (*Bathyraja parmifera*)	1990-	1.2	1.0	92	Matta 2006
Aleutian skate (*Bathyraja aleutica*)	1990-	6.6	1.8	132	Ebert et al. 2007
Arrowtooth flounder (*Atheresthes stomias*)	1993-	75.6	85.9	35	Zimmermann 1997
Atka mackerel (*Pleurogrammus monopterygius*)	All	0.4	9.8	27	Cooper et al. 2010
Bering skate (*Bathyraja interrupta*)	1990-	5.0	4.6	69	Ebert et al. 2007
Bigmouth sculpin (*Hemitripterus bolini*)	All	1.4	2.8	51	Tenbrink and Hutchinson 2009
Black rockfish (*Sebastes melanops*)	All	0.2	0.6	40	Rooper 2008
Blackspotted rockfish (*Sebastes melanostictus*)	2007-	4.7	2.5	43	Rooper 2008
Dark rockfish (*Sebastes ciliatus*)	1996-	0.9	0.5	42	Rooper 2008
Dover sole (*Microstomus pacificus*)	All	34.7	38.9	38	Abookire and Macewicz 2003
Dusky rockfish (*Sebastes variabilis*)	1996-	1.5	12.0	29	Chilton 2010
Flathead sole (*Hippoglossoides elassodon*)	All	38.1	49.2	29	Stark 2004
Great sculpin (*Myoxocephalus polyacanthocephalus*)	All	3.8	3.9	51	Tenbrink and Hutchinson 2009
Harlequin rockfish (*Sebastes variegatus*)	All	3.1	5.0	23	Rooper 2008
Longspine thornyhead (*Sebastolobus altivelis*)	All	--	1.1		
Northern rock sole (*Lepidopsetta polyxystra*)	2001-	21.9	26.2	30	Stark 2012a
Northern rockfish (*Sebastes polyspinis*)	All	3.2	15.1	26	Chilton 2007
Octopus unidentified	All	--	4.4		
Pacific cod (*Gadus macrocephalus*)	All	29.7	56.7	42	Stark 2007
Pacific ocean perch (*Sebastes alutus*)	All	24.2	33.0	25	Rooper 2008
Walleye Pollock (*Gadus chalcogrammus*)	All	49.5	51.4	37	Dorn et al. 2016
Pygmy rockfish (*Sebastes wilsoni*)	All	--	0.8		
Quillback rockfish (*Sebastes maliger*)	All	0.2	0.7	29	Rooper 2008
Redbanded rockfish (*Sebastes babcocki*)	All	8.6	3.2	42	Rooper 2008
Redstripe rockfish (*Sebastes proriger*)	All	1.0	2.3	28	Rooper 2008
Rex sole (*Glyptocephalus zachirus*)	All	28.1	59.5	24	Abookire 2006
Rougheye rockfish (*Sebastes aleutianus*)	2007-	7.4	3.3	43	Rooper 2008
Sablefish (*Anoplopoma fimbria*)	All	6.8	35.9	40	D. Hanselman, ABL (pers comm)
Sharpchin rockfish (*Sebastes zacentrus*)	All	5.8	4.8	25	Rooper 2008
Shortraker rockfish (*Sebastes borealis*)	All	2.6	8.1	44	Rooper 2008
Shortspine thornyhead (*Sebastolobus alascanus*)	All	19.4	23.6	21	Rooper 2008
Silvergray rockfish (*Sebastes brevispinis*)	All	1.7	5.5	40	Rooper 2008
Southern rock sole (*Lepidopsetta bilineata*)	2001-	23.2	34.2	30	Stark 2012b
Yellow Irish lord (*Hemilepidotus jordani*)	All	2.5	12.5	22	Tenbrink and Buckley 2013
Yelloweye rockfish (*Sebastes ruberrimus*)	All	0.8	2.0	45	Rooper 2008
Yellowfin sole (*Limanda aspera*)	All	3.4	5.8	25	Nichol 1997

Species distribution modeling approach used:

Standard GAM model
Hurdle GAM model
Maximum entropy model

Species Distribution Data -- Commercial Catch (Observer) Data

Distribution data collected by fishery observers aboard commercial fishing vessels (2001-2015) and reported from the VOE-CIA database were used to parameterize SDMs for species caught in commercial catches during the fall, winter, and spring seasons (Table 4). Summer VOE-CIA data were not included in our analyses because summer distributions were modeled from RACE-GAP groundfish bottom trawl survey data. The VOE-CIA data were provided by John V. Olson and Steve Lewis (AKRO). Species presence from observed catches, regardless of the type of fishing gear, was combined across years for our analyses. These presence-only data were used to parameterize MaxEnt models if the number of presence observations for a species exceeded 50. The fishes and invertebrates recorded by fishery observers were assumed to be adult life history stages since the commercial fisheries typically target mature animals. Because commercial fisheries by definition focus effort on their target species, the distribution of observer presence observations is mainly dependent upon the fishing activity. In other words, instead of being a regular survey conducted over a regular grid, these catch presence observations are typically clustered around areas of high catches for a target species (e.g., walleye pollock). As such, the resulting SDMs should be viewed with some caution compared to the models informed by fishery-independent data.

Table 4. -- Numbers of presence records (catch of at least 1 individual in an observed haul) by species and season in the VMS-Observer Enabled Catch-in-Areas commercial database (VOE-CIA) for the Gulf of Alaska.

Species	Fall	Winter	Spring
Alaska plaice (*Pleuronectes quadrituberculatus*)	2	15	37
Alaska skate (*Bathyraja parmifera*)	289	178	149
Aleutian skate (*Bathyraja aleutica*)	574	363	993
Arrowtooth flounder (*Atheresthes stomias*)	1623	1315	5678
Atka mackerel (*Pleurogrammus monopterygius*)	275	104	283
Bigmouth sculpin (*Hemitripterus bolini*)	36	74	68
Black rockfish (*Sebastes melanops*)	12	21	34
Blackspotted, rougheye rockfish (*Sebastes aleutianus, S. melanostictus*)	182	98	2006
Dark rockfish (*Sebastes ciliatus*)	49	24	33
Dover sole (*Microstomus pacificus*)	400	103	1337
Dusky rockfish (*Sebastes variabilis*)	369	223	462
Flathead sole (*Hippoglossoides elassodon*)	889	849	2403
Great sculpin (*Myoxocephalus polyacanthocephalus*)	3	38	25
Harlequin rockfish (*Sebastes variegatus*)	47	8	65
Kamchatka flounder (*Atheresthes evermanni*)	38	5	124
Longspine thornyhead (*Sebastolobus altivelis*)	--	--	62
Northern rock sole (*Lepidopsetta polyxystra*)	296	417	733
Northern rockfish (*Sebastes polyspinis*)	383	261	610
Octopus unidentified	107	292	137
Pacific cod (*Gadus macrocephalus*)	1643	2277	2708
Pacific ocean perch (*Sebastes alutus*)	245	153	965
Pygmy rockfish (*Sebastes wilsoni*)	--	--	2
Quillback rockfish (*Sebastes maliger*)	6	2	5
Redbanded rockfish (*Sebastes babcocki*)	41	20	313
Redstripe rockfish (*Sebastes proriger*)	28	3	14
Rex sole (*Glyptocephalus zachirus*)	490	481	2083
Sablefish (*Anoplopoma fimbria*)	645	127	4833
Sharpchin rockfish (*Sebastes zacentrus*)	10	1	54
Shortraker rockfish (*Sebastes borealis*)	215	65	2173
Shortspine thornyhead (*Sebastolobus alascanus*)	249	62	4169
Silvergray rockfish (*Sebastes brevispinis*)	7	14	15
Southern rock sole (*Lepidopsetta bilineata*)	290	703	790
Walleye Pollock (*Gadus chalcogramma*)	1084	1039	2137
Yellow Irish lord (*Hemilepidotus jordani*)	73	170	126
Yelloweye rockfish (*Sebastes ruberrimus*)	321	59	201
Yellowfin sole (*Limanda aspera*)	1	59	24

Habitat Covariates

The independent covariates used to parameterize and then select the best fitting SDMs were chosen from a suite of habitat covariates typically collected on the bottom trawl survey plus some derived and modeled variables (Table 5, Fig. 3, Fig. 4). Observed, derived, or modeled point values were interpolated to regular spatial grids (rasters) on scales ranging from 100 m × 100 m to 1 km × 1 km using inverse distance weighting (Watson and Philip 1985) or ordinary kriging (Venables and Ripley 2002) with an exponential semi-variogram model. The potential for an independent habitat covariate to influence the distribution of the life stages of the fishes and invertebrates in the region was considered when identifying which predictors to include in the initial model formulations. For example, many fish ELHS are released to and complete much of their development in the water column. Therefore, surface water temperature, surface current speed, and surface current direction were among the covariates chosen to parameterize the ELHS models. We tested collinearity amongst the habitat covariates as a precursor to including them in the SDMs (Table 6). The largest correlations were between latitude and longitude ($r = 0.60$). The remaining pairwise correlations among variables were < 0.5. Variance inflation factors were calculated using the method of Zaur et al. (2009) for each of the covariates considered as model inputs and they ranged from 1.2 to 1.6. These values were all acceptable (below 5.0) and the habitat covariates were included in the models of habitat suitability, presence or absence, and fish or invertebrate abundance in the GOA.

Habitat Covariates for Early Life History Stage Models

We used seven habitat descriptors to parameterize ELHS MaxEnt SDMs (Table 5). The independent predictors used to train and test the SDMs included site-specific environmental variables collected during oceanographic surveys as well as derived and modeled covariates, but spatial predictions generated by the best fitting models utilized derived or modeled raster

surfaces as input. Derived habitat covariate surfaces like local slope which is inferred from depth changes consist of geo-referenced raster maps). These rasters generally consist of a matrix of cells organized into a grid where each cell contains a value representing information (e.g., local slope or surface current speed). Interpolated raster surfaces were based on extrapolation from point measures or modeled values such as satellite ocean color or maximum tidal current speed. The habitat covariates selected to parameterize the SDMs were chosen both for their availability and for their potential influence on the distribution of fishes and invertebrates based on previous studies.

The covariates describing surface currents and temperature were derived from the regional ocean modeling system (ROMS) run for the period 1969-2005 (Danielson et al. 2011). Surface current direction variability was considered an indication of potential eddy vorticity and was incorporated into these models. The initial data values were derived monthly on a 10 km × 10 km grid and were then interpolated via inverse distance weighting to a 1 km × 1 km grid for our SDMs (Fig. 5). The ROMS modeled data used were temporally synched to the months when the ELHS were present in the water column. For example, *Atheresthes* spp. larvae were collected on EcoFOCI ichthyoplankton surveys in the GOA from February until September, so the ROMS data from these months were input to the SDM.

The covariates describing bottom depth and slope were obtained from a gridded bathymetry raster for the GOA region that was derived from bathymetric point data (n > 1.75 million soundings) of National Ocean Service (NOS) smooth sheets and other data (Zimmermann and Benson 2013, Zimmermann and Prescott 2014, Zimmermann and Prescott 2015). These point data were linearly interpolated from a triangular irregular network (TIN) layer to a 100 m × 100 m raster grid and empty spaces were filled using data from AKRO. This interpolation was conducted using the Spatial

Analyst package in ArcMAP software[1]. Local slope was derived from this bathymetry raster and calculated for each raster grid cell as the maximum change in elevation over the distance between the cell and its eight neighbors using the slope tool from the Spatial Analyst package in ArcMAP. Local slope was also computed from the 100 m × 100 m bathymetry raster using the *raster* package[2] in R (R Core Development Team 2013).

To represent average ocean productivity ($g \cdot C \cdot m^{-2} \cdot day^{-1}$) at each of the ichthyoplankton survey sites, we employed satellite-based moderate-resolution imaging spectroradiometer (MODIS) ocean color data for the five spring-summer months (May-September) that encapsulated the spring-summer phytoplankton blooms in the GOA from 2003 to 2011 (Behrenfeld and Falkowski 2007). These data were downloaded from the Oregon State University's (OSU) Ocean Productivity website[3], were averaged by grid cell and month, and then averaged again by cell and year (to account for differences in the number of samples within each cell). The averages were then interpolated to a 1 km × 1 km raster grid using inverse distance weighting using the *raster* package in R.

Habitat Covariates for Bottom Trawl Survey Models

For bottom trawl survey data a different suite of habitat variables was used for modeling (Table 5). Vessel position, bottom depth, and bottom temperature were collected at each bottom trawling site. A start and end position for the vessel during the on-bottom portion of the trawl were collected using the vessel-mounted GPS receiver. Vessel position was corrected for the position of the bottom trawl itself by triangulating how far the net was behind the vessel (based on the seafloor depth and the wire out) and subtracting this distance from the vessel position in the direction of the

[1] ArcMap Desktop. Environmental Systems Research Institute. 2009. Redlands, CA.
[2] R v3.0.1; Hijams, R.J., J. van Etten, M. Mattiuzzi, M. Sumner, J.A. Greenberg, O.P., Lamigueiro, A. Bevan, E.B. Racine, and A. Shortridge. 2015. Geographic data analysis and modeling: package 'raster' version 2.3–24. 232 p.
[3] http://www.science.oregonstate.edu/ocean.productivity/

bottom trawl haul. We assumed that the bottom trawl was directly behind the vessel during the tow and that all bottom trawl hauls were conducted in a straight line from the beginning point to the end point. The mid-point of the start and end positions of the trawl haul was used as the location variable in the modeling. The longitude and latitude data for each tow (and all other geographical data including the raster layers described below) were projected into Alaska Albers Equal Area Conic projection (center latitude = 50°N and center longitude = 154°W) and degrees of latitude and longitude were transformed into 100 m × 100 m square grids of eastings and northings for modeling. The location variable was used to capture any significant spatial trends in bottom trawl survey catches across the GOA.

Bottom depth and temperature were routinely collected for each trawl haul on the GOA bottom trawl surveys from 1993 to 2013, but different instruments were used to measure these values through the years. Starting in 1993, Brancker XL200 digital bathythermographic data loggers (Richard Brancker Research, Ltd., Kanata, Ontario, Canada) recorded continuous temperature and depth recording at the trawl net, and the survey began reporting on-bottom depth and temperature averaged over the trawl haul duration. Starting in 2003, the Brancker data logger was replaced by the SeaBird SBE-39 microbathythermograph (Sea-Bird Electronics, Inc., Bellevue, WA). The SBE-39 is attached to the headrope of the net and the averaged gear depth is added to the averaged measured net height to come up with average bottom depth during the trawl haul.

Depth and temperature measured at the trawl net were used as independent habitat covariates to parameterize the SDMs while rasters of these and other features (e.g., bathymetry, current speed, and local slope) were used primarily for prediction but occasionally for parameterization. For example, the estimated slope derived from the bathymetry raster at each bottom trawl haul location was used as a habitat variable in the SDM, but the slope raster derived from bathymetry was used for prediction. Mean bottom temperatures from each trawl haul were also interpolated to the

100 m × 100 m grid of the GOA region using ordinary kriging (Venables and Ripley 2002) with an exponential semi-variogram model. The result was a single temperature raster layer that reflects the average bottom temperature conditions on the bottom trawl surveys from 1993 to 2013. This raster layer of average temperature was used for prediction.

Average ocean productivity ($g \cdot C \cdot m^{-2} \cdot day^{-1}$) at each of the bottom trawl survey sites was extracted from the ocean color raster to parameterize the SDMs. Similar to its inclusion in the ELHS models above, we used MODIS ocean color data for five spring-summer months (May-September) that encompassed the spring and summer phytoplankton blooms over eight years (2003-2011) in the GOA region (Behrenfeld and Falkowski 2007). The ocean color data downloaded from OSU's Ocean Productivity website were averaged by cell and month and then averaged again by cell and year (to account for differences in the number of samples within each cell). The averages were then interpolated to a 1 km × 1 km raster grid using inverse distance weighting and the *raster* package[4] in R (R Core Development Team 2013; Fig. 4). The complete raster of ocean productivity was the input to the best fitting SDMs when producing spatial predictions.

Two measures of water movement and its potential interaction with the seafloor were included as habitat covariates for modeling and prediction from the bottom trawl survey data. One variable was the maximum tidal current speed at the site of each bottom trawl haul. Tidal speeds were estimated for 368 consecutive days (1st January, 2009 to 3rd January, 2010) using a tidal inversion program parameterized for the GOA on a 1 km × 1 km grid (Egbert and Erofeeva 2002). Their tidal prediction model was used to produce a series of one lunar year tidal currents for spring and neap cycles at each bottom trawl survey location. The maximum predicted tidal current speed for the series at the bottom trawl survey haul site was extracted and used to parameterize the

[4] R v3.0.1; Hijams, R.J., J. van Etten, M. Mattiuzzi, M. Sumner, J.A. Greenberg, O.P., Lamigueiro, A. Bevan, E.B. Racine, and A. Shortridge. 2015. Geographic data analysis and modeling: package 'raster' version 2.3–24. 232 pages.

distribution models. Maximum tidal current speed at each bottom trawl survey site was also interpolated over the GOA region using ordinary kriging and an exponential semi-variogram (Venables and Ripley 2002) to interpolate a raster of maximum tidal current speed values on a 1 km × 1 km grid that was used for predictions. The second water movement variable was the predicted bottom water layer current speed from ROMS model runs from 1969 to 2005 (Danielson et al. 2011). This long-term current speed and direction were available as points on a 10 km × 10 km grid. The ROMS model was based on a three-dimensional grid with 60 depth tiers for each grid cell. For example, a point at 60 m water depth would have 60 depth bins at 1 m intervals, while a point at 120 m depth would have 60 depth bins at 2 m depth intervals, etc.). The bottom current speed and direction for the deepest depth bin at each point (closest to the seafloor) was used in our analyses. These regularly spaced data were interpolated to a 100 m × 100 m raster grid covering the GOA using inverse distance weighting (Fig. 4). Point values of bottom current speed were extracted from this raster layer at each of the bottom trawl survey haul locations and the mean current speed value computed for the path of each bottom trawl survey tow. The interpolated bottom current speed raster was also input to the best fitting SDMs for spatial predictions.

The biogenic habitat covariates included in bottom trawl survey SDMs were the concurrent catches of structure forming invertebrates (corals, sponges, and pennatulaceans). The binomial (presence or absence) factor for each of these categories of invertebrates was incorporated as a habitat covariate in the models. Complete raster surfaces from distribution models for each of these structure-forming invertebrates (Rooper et al. 2014, Sigler et al. 2015, Rooper et al. 2016) were used as input to the best fitting SDMs for spatial predictions.

Habitat Covariates for Commercial Catch Models

The same process and variables used to model and predict fish and invertebrate distributions with the NMFS bottom trawl survey data were used for the commercial catch data (CIA data), with the exception of the haul position and structure forming invertebrate layers (coral, sponge, and pennatulacean; Table 5).

Table 5. -- Habitat covariates used to model the distributions of fishes and invertebrates in the Gulf of Alaska.

Variable	Unit	Definition	Interpolation method	Source	Model
Geographic position	eastings, northings	Latitude and longitude of bottom trawl hauls in Alaska Albers projection corrected for the position of the trawl net relative to the vessel.	--	DGPS collected at bottom trawl hauls	1,3
Bottom depth	m	Bathymetry of the seafloor based on digitized and position corrected NOS charts.	Linear interpolation	Mean depth of bottom trawl hauls (modeling), Zimmermann, M, unpublished data (prediction)	1,3
Slope	percent	Maximum difference between a bottom depth measurement and its adjoining cells.	--	Zimmermann, M, unpublished data	1,3
Bottom temperature	°C	Mean summer bottom temperature for the region measured during bottom trawl surveys from 1996-2013.	Ordinary kriging	Temperature data collected at bottom trawl hauls	3
Surface temperature	°C	Ocean current speed predicted from the ROMS model during the years 1970-2004 and averaged on a 10 km x 10 km grid.	Inverse distance weighting	Danielson et al. 2011	1
Ocean color	$Carbon*m^{-2}*day^{-1}$	Net primary production in surface waters in May to September averaged by 1080 x 2160 grid cells then averaged across years (2002-2011).	Inverse distance weighting	Behrenfeld and Falkowski 1997	3
Bottom current speed	$m*sec^{-1}$	Seafloor ocean current speed predicted from the ROMS model during the years 1970-2004 and averaged on a 10 km x 10 km grid.	Inverse distance weighting	Danielson et al. 2011	3
Maximum tidal current	$cm*sec^{-1}$	Maximum of the predicted tidal current at each bottom trawl location over a 1-year cycle.	Ordinary kriging	Egbert and Erofeeva 2000	3
Surface current speed	$m*sec^{-1}$	Surface ocean current speed predicted from the ROMS model during the years 1970-2004 and averaged on a 10 km x 10 km grid.	Inverse distance weighting	Danielson et al. 2011	1
Surface current direction	angle	Mean surface ocean current direction predicted from the ROMS model during the years 1970-2004 and averaged on a 10 km x 10 km grid.	Inverse distance weighting	Danielson et al. 2011	1
Surface current direction variability	--	Variability in surface ocean current direction predicted from the ROMS model during the years 1970-2004 and averaged on a 10 km x 10 km grid.	Inverse distance weighting	Danielson et al. 2011	1
Coral presence or absence	--	Coral presence or absence in bottom trawl catch and raster of predicted presence or absence of Coral.	--	Catch data from bottom trawl hauls (modeling), Rooper et al. 2016 (prediction)	2
Sponge presence or absence	--	Sponge presence or absence in bottom trawl catch and raster of predicted presence or absence of Sponge.	--	Catch data from bottom trawl hauls (modeling), Rooper et al. 2016 (prediction)	2
Pennatulacean presence or absence	--	Pennatulacean presence or absence in bottom trawl catch and raster of predicted presence or absence of Pennatulacean	--	Catch data from bottom trawl hauls (modeling), Rooper et al. 2016 (prediction)	2

[1] Used to model early life history stages (egg, larval, and pelagic juvenile stages) only

[2] Used to model bottom trawl survey data only

[3] Used to model bottom trawl survey and commercial catch data only

Table 6. -- Variance inflation factors amongst habitat covariates from the Gulf of Alaska. NMFS Alaska Fisheries Science Center Resource Assessment and Conservation Engineering-Groundfish Assessment Program summer bottom trawl surveys (RACE-GAP), VMS-Observer Enabled Catch-in-Areas commercial catch observations (VOE-CIA), and Ecosystems and Fisheries-Oceanography Cooperative Investigations ichthyoplankton surveys (EcoFOCI).

Variable	Variance Inflation Factor (RACE-GAP trawl survey data)	Variance Inflation Factor (VOE-CIA data)	Variance Inflation Factor (EcoFOCI data)
Bottom depth	1.79	2.42	1.19
Slope	1.55	1.99	1.19
Bottom temperature	1.69	2.15	
Ocean color	1.24	1.60	1.10
Bottom current speed	1.28	1.53	
Tidal current speed	1.32	1.67	1.27
Coral	1.18		
Sponge	1.21		
Pennatulaceans (sea whips)	1.23		
Surface temperature			1.71
Surface current speed			2.49
Surface current variability			2.37

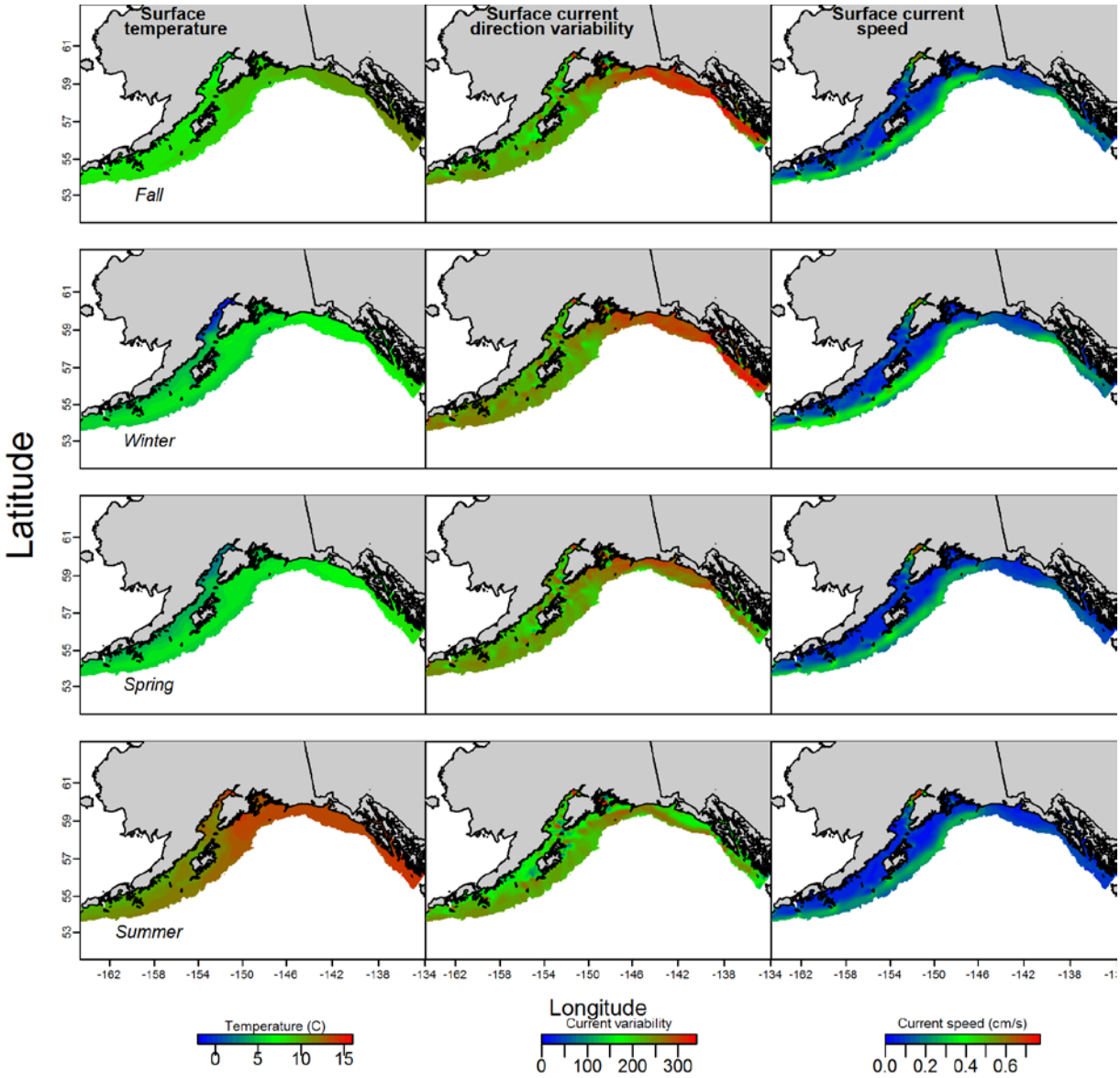

Figure 4. -- Habitat covariate rasters used in species distribution models for the settled juvenile and adult stages of fishes and invertebrates collected from RACE-GAP summer bottom trawl surveys in the Gulf of Alaska (Depth = bottom depth, Slope = kriged local slope, Bottom temperature = bottom temperature, Ocean color = ocean productivity, Bottom current speed = bottom current speed, Maximum tidal current = tidal maxima, Coral, Sponge, and Sea Whips are presence-absence).

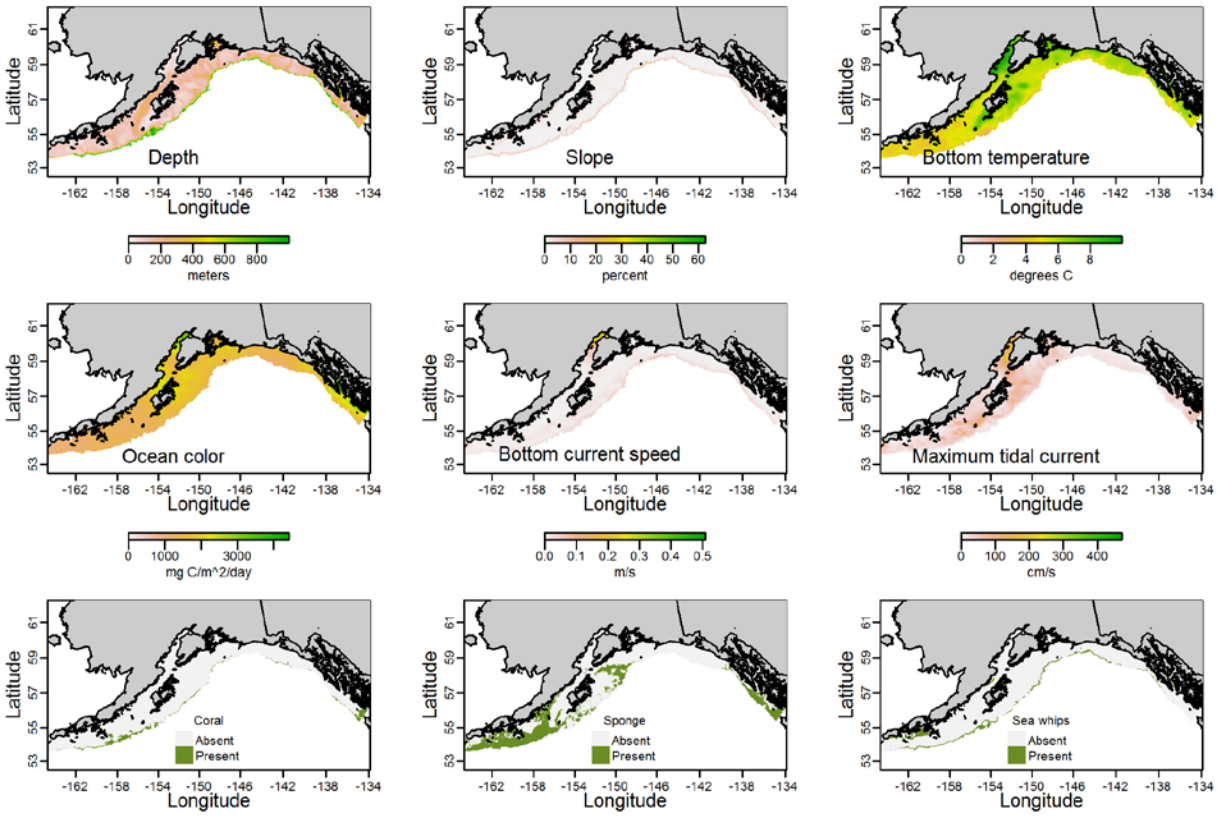

Figure 5. -- Habitat covariate rasters of surface temperature, surface current direction variability, and surface current speed from ROMS model runs (1969-2005; Danielson et al. 2011) for the Gulf of Alaska used in species distribution models for the early life history stages (ELHS) of species collected from EcoFOCI ichthyoplankton surveys.

Modeling Methods -- Recruitment Processes Data

Maximum entropy modeling (MaxEnt; Phillips et al. 2006, Elith et al. 2011) was used to predict species distribution for ELHS of fishes collected on EcoFOCI ichthyoplankton surveys of the EBS. MaxEnt modeling was implemented in R software using the *dismo* package[5]. A minimum prevalence of 50 presence observations was required to use the MaxEnt model. These models use only presence observations to predict the probability of suitable habitat from raster grids of habitat covariates and point observations of presence (i.e., given the bottom depth, temperature, slope, and current speed at a grid cell where the species and life-stage of interest was present - what is the probability that these were suitable conditions for that species?). Note that since predictions are made from a raster grid that geographic location is implicit in the results from MaxEnt models.

Modeling Methods -- Bottom Trawl Survey Data

Three types of distribution modeling were used to predict species distribution from RACE-GAP summer bottom trawl survey data. The choice of model was based on the prevalence of each species in the overall survey. For species that occurred in greater than 30% of bottom trawl hauls, such as arrowtooth flounder (Table 3), the best fitting standard generalized additive model (CPUE GAM; Hastie and Tibshirani 1990) describing the 4th-root transformed CPUE was identified through backward stepwise term selection and the resulting model was used to make spatial predictions of

[5] R, v3.0.1; Hijams, R.J., S. Phillips, J. Leathwick, and J. Elith. 2014. Species distribution modeling: package 'dismo' version 1.0–5. 65 p.

species distribution. Generalized additive models were applied to the trawl data using the *mgcv* package[6] in R, so that the full model was as follows:

$$y = s(geographic\ position) + s(slope) + s(maximum\ tidal\ current) + s(ocean\ current) + s(bottom\ current\ speed) + s(bottom\ temperature) + s(bottom\ depth) + \text{sponge presence/absence} + \text{coral presence/absence} + \text{pennatulacean presence/absence} + \varepsilon \quad ,$$

where y was the dependent variable, either presence/absence or log(CPUE), and s indicated a thin plate regression spline, and ε was an error term either binomial (for presence absence) or gaussian (CPUE). For each habitat covariate, the basis degrees of freedom used in the smoothing function were limited to ≤ 4 for univariate variables and ≤ 10 for the bivariate term (geographic location). To identify the best fitting GAM, insignificant terms (based on *p*-values) were sequentially removed until the generalized cross validation score (GCV) was minimized (Wood 2006). For each species, the formulation with the lowest AIC score was deemed the best fitting model and used for further prediction and validation. For species where frequency of occurrence was between 10% and 30%, a hurdle model (hGAM) was used (Cragg 1971, Potts and Elith 2006) to predict species distribution. Hurdle models predict the spatial distribution of abundance in three stages: 1) probability of presence is predicted from presence-absence data (PA) using the best fitting GAM and binomial distribution for each species; 2) a threshold presence probability is determined that defines presence or absence of the species; and 3) a hurdle GAM is constructed that predicts a species' abundance by modeling the fourth-root transformed CPUE data from the bottom trawl survey at locations where the probability of presence was predicted to meet or exceed the threshold established in step 2 above. As was done

[6] R, v3.0.1; Wood, S. 2014. Mixed GAM computation vehicle with GCV/AIC/REML smoothness estimation: package 'mgcv' version 1.8–4. 243 p.

for the standard GAM's above, the basis degrees of freedom used in the smoothing function were constrained and insignificant terms were sequentially removed to minimize the AIC and determine the best fitting model. For species with less than 10% frequency of occurrence, but greater than 50 presence observations, the MaxEnt model was used to describe the probability of suitable habitat.

For all SDMs, separate training (80%) and testing (20%) data were randomly selected. The training and testing data were selected before modeling began and remained the same during analyses of each data class. The larger (80%) segment of data was used to select and train the best fitting model while the remaining 20% was used to test and validate the model fit.

Modeling Methods -- Commercial Catch (Observer) Data

MaxEnt modeling was used to estimate species distribution from commercial fishery catch observer data from the VOE-CIA database. As above, MaxEnt was implemented in R software (R Core Development Team, 2013) using the *dismo* package. MaxEnt models use only presence observations and are based on raster grids of habitat covariates and point observations of presence so that geographic location is implicit in the MaxEnt results. As with the other models, separate training (80%) and testing (20%) data were randomly selected for MaxEnt modeling and the testing data were used to assess model performance. Commercial fishing activity occurred throughout the GOA, however, an important caveat to the SDMs developed using the VOE-CIA database is that for most species, the distribution of catches represent the distribution of fishing activity. So, instead of being a standardized survey conducted over a defined grid, these observations were typically clustered in areas of high densities for a target species. As such, they should be viewed with some caution compared to the bottom trawl survey distribution maps.

Model Validation

To test the performance of the best fitting models, the predictions were compared to the observations. For presence and presence-absence models, the area under the receiver operating characteristic curve (AUC) was computed to judge model performance. The AUC calculates the probability that a randomly chosen presence observation would have a higher probability of presence than a randomly chosen absence observation using rank data. We used the scale of Hosmer and Lemeshow (2005), where AUC value greater than 0.5 is estimated to be better than chance, a value greater than 0.7 is considered acceptable, and values greater than 0.8 and 0.9 are excellent and outstanding; we considered AUC values less than 0.5 to indicate models with questionable predictive ability. Confidence intervals for the AUC (95%) were calculated according to the methodology of DeLong et al. (1988).

The models were parameterized on a randomly chosen 80% partition of the original data and tested on the remaining 20% of the data that was left out for model validation. The performance of abundance models (i.e., GAMs and hGAMs) was measured by computing the R2 between the model predictions and the observations for the training data. The training model was also used to calculate predictions of CPUE for the test data set. These predictions of the test data based on the training model were compared to observations from the test data set by computing the R2 between test data observations and predictions of the test data from the training model. Because of space limitations, figures displaying the model validation results were not shown here.

Essential Fish Habitat Maps

Maps of essential habitat based on model predictions were developed for each species' life history stage and season modeled. These maps were produced as population quantiles from predictions of the distribution of suitable habitat (in cases where MaxEnt was used) or predictions of the distribution of abundance (for species where CPUE was modeled using either a GAM or hGAM). For each map of model predictions, 300,000 points were randomly sampled from the raster surface. These values were then ordered by cumulative distribution; zero abundance values and probabilities of suitable habitat < 0.05 were removed. Four population quantiles were selected from these cumulative distributions (5%, 25%, 50%, and 75%). These quantiles were then used as break points to translate the model predictions (maps of suitable habitat or abundance) into maps of the distribution quantiles. For example, if the 5% quantile of species A was 0.024 individuals $\cdot$ ha^{-1}, then this meant that 95% of the population occurred at values higher than 0.024. Similarly, a 75% quantile of species A at 2.1 individuals ha^{-1} meant that values above 2.1 represented the top 25% of the population of predictions, or the predicted highest abundance areas. The four population quantiles for each species, life history stage, and season were mapped to show the distribution of the areas containing 95%, 75%, 50%, and 25% of the population of predictions. It is important to note that these values were chosen somewhat arbitrarily, with the exception of the 95% level which is the current definition of EFH in Alaska for management purposes, and other values could be equally appropriate. For a more detailed discussion of how predictions of species distribution relate to the definition of EFH in Alaska resource management see Laman et al. (in press).

The above habitat descriptions include both text and maps. For the purposes of these descriptions, the GOA has been divided into three geographic regions based on the regulatory areas described within the latest FMP for GOA groundfishes (https://www.npfmc.org/wp-

content/PDFdocuments/fmp/GOA/GOAfmp.pdf). They are as follows: the Eastern Gulf (132°40'W to 147°W), Central Gulf (147°W to 159°W), and Western Gulf (159°W to 170°W).

RESULTS

Flatfishes

Arrowtooth Flounder (*Atheresthes stomias*)

Early life history stages of *Atheresthes* spp. -- Arrowtooth flounder eggs, larvae, and pelagic juveniles cannot be distinguished from the other species in the genus, Kamchatka flounder (*Atheresthes evermanni*), so *Atheresthes* spp. ELHS were combined and presented here. There were 42 ECODAAT records of *Atheresthes* spp. egg presence along the western and central GOA shelf break (Fig. 6), not enough to run the model.

There were 1,386 catches of *Atheresthes* spp. larvae in the EcoFOCI data. These observations were distributed throughout the central and western GOA, and in the eastern GOA between Yakutat and Cross Sound (Fig. 7). The AUC of the MaxEnt model was 0.70 for both the training and testing data. The model correctly classified 74% of the predictions from the training data and 70% of the predictions from the test data. The most important variables determining suitable habitat of larval *Atheresthes* spp. were bottom depth and surface current variability (relative importance: 0.44 and 0.18, respectively). The model predicted probable suitable habitat of *Atheresthes* spp. larvae throughout the western GOA, with higher suitability areas concentrated in Shelikof and Shumagin Gullies.

There were eight occurrences of pelagic juvenile *Atheresthes* spp. in the ECODAAT database. Most occurred on the inner and middle shelf in the western GOA (Fig. 8). However, there were insufficient observations to develop a model.

Juvenile and adult arrowtooth flounder distribution in the bottom trawl survey -- The catch of arrowtooth flounder in summer bottom trawl surveys indicates this species is broadly distributed in the GOA (Fig. 9). The best fitting GAM explained 31% of the variability in CPUE of settled juvenile arrowtooth flounder from the bottom trawl survey training data and 30% of the variability in the test data. Geographic location, bottom depth, and maximum tidal current were the most important habitat covariates in the model. Settled juvenile arrowtooth flounder were distributed throughout the GOA, with the highest abundances predicted to occur in the central GOA, around Shelikof Strait, and in the western GOA, around the Shumagin Islands (Fig. 9).

The best-fitting GAM indicated that bottom depth and ocean color were the most important factors predicting the abundance of adult arrowtooth flounder. The model explained 32% of the variability of the training data and 32% of the variability of the test data. Adult arrowtooth flounder were found in the highest abundance in the western GOA, particularly around Shelikof Strait (Fig. 10).

Arrowtooth flounder distribution in commercial fisheries -- The distribution of arrowtooth flounder based on presence in commercial fisheries catches in the GOA varied throughout the year. In the fall, bottom depth and ocean color were the most important model variables determining the probability of suitable habitat of arrowtooth flounder (relative importance: 0.40 and 0.18, respectively). The AUC of the fall MaxEnt model was 0.86 for the training data and 0.72 for the test data. The model correctly classified 78% of the predictions from the training data and 72% of the predictions from the test data. The model predicted probable suitable habitat of arrowtooth flounder in deeper areas of the western GOA, particularly off Unimak Island (Fig. 11).

In the winter, distribution of probable suitable habitat for arrowtooth flounder was generally consistent with that predicted based on fall commercial fisheries catches. Bottom depth and ocean color were the most important model variables determining the probability of suitable habitat of arrowtooth flounder (relative importance: 0.33 and 0.30, respectively). The AUC of the winter MaxEnt model was 0.83 for the training data and 0.74 for the test data. The model correctly classified 76% of the predictions from the training data and 74% of the predictions from the test data. The model predicted suitable habitat of arrowtooth flounder throughout the central GOA, particularly on Albatross and Portlock banks, as well as in western GOA, off Unimak Island (Fig. 12).

In the spring, catches of adult arrowtooth flounder tended to be higher than either during the fall or the winter. Bottom depth and bottom current speed were the most important model variables determining the probability of suitable habitat of arrowtooth flounder (relative importance: 0.59 and 0.15, respectively). The AUC of the MaxEnt spring model was 0.87 for the training data and 0.78 for the test data. The model correctly classified 78% the predictions of both the training and test data. Predicted spring arrowtooth flounder habitat was largely concentrated near the shelf break across the GOA (Fig. 13).

Arrowtooth flounder essential fish habitat maps and conclusions -- In general, habitat for ELHS of *Atheresthes* spp. and for settled juvenile and adult arrowtooth flounder was distributed throughout the GOA (Fig. 14). Core habitat for larval *Atheresthes* spp. (the top 25% of probable suitable habitat predicted from the MaxEnt model) was primarily located in the central and western GOA. Settled juvenile and adult arrowtooth flounder core habitat was found from Yakutat, through the Shelikof Strait, and out into the Shumagin Gully and Islands. High probability of suitable arrowtooth flounder

habitat predicted from their presence in commercial catches was centered on the continental shelf below Kodiak in fall and winter, but also overlapped with core habitat predicted in the Shumagins and Shelikof Strait from summer RACE-GAP bottom trawl surveys.

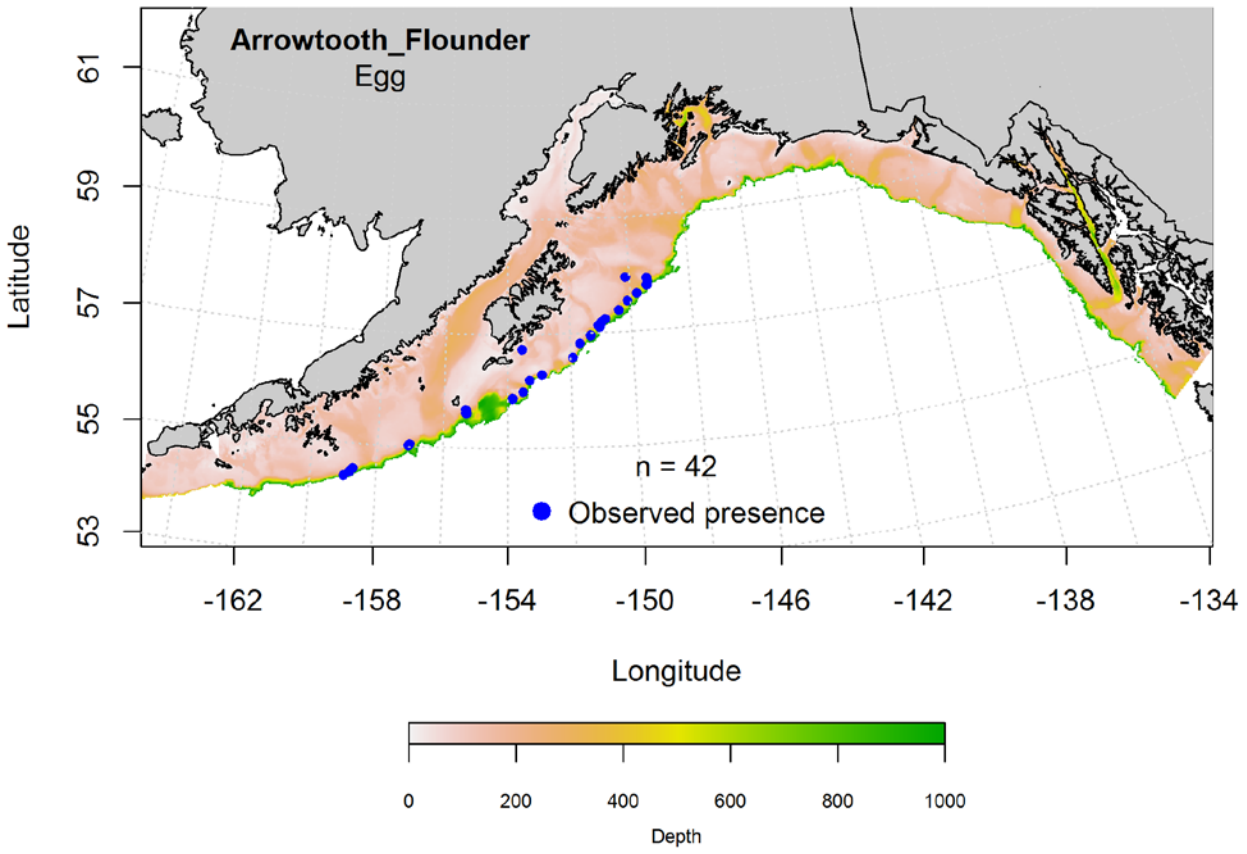

Figure 6. -- Distribution of *Atheresthes* spp. egg observations from EcoFOCI ichthyoplankton surveys in the Gulf of Alaska (January-March 1991-2013).

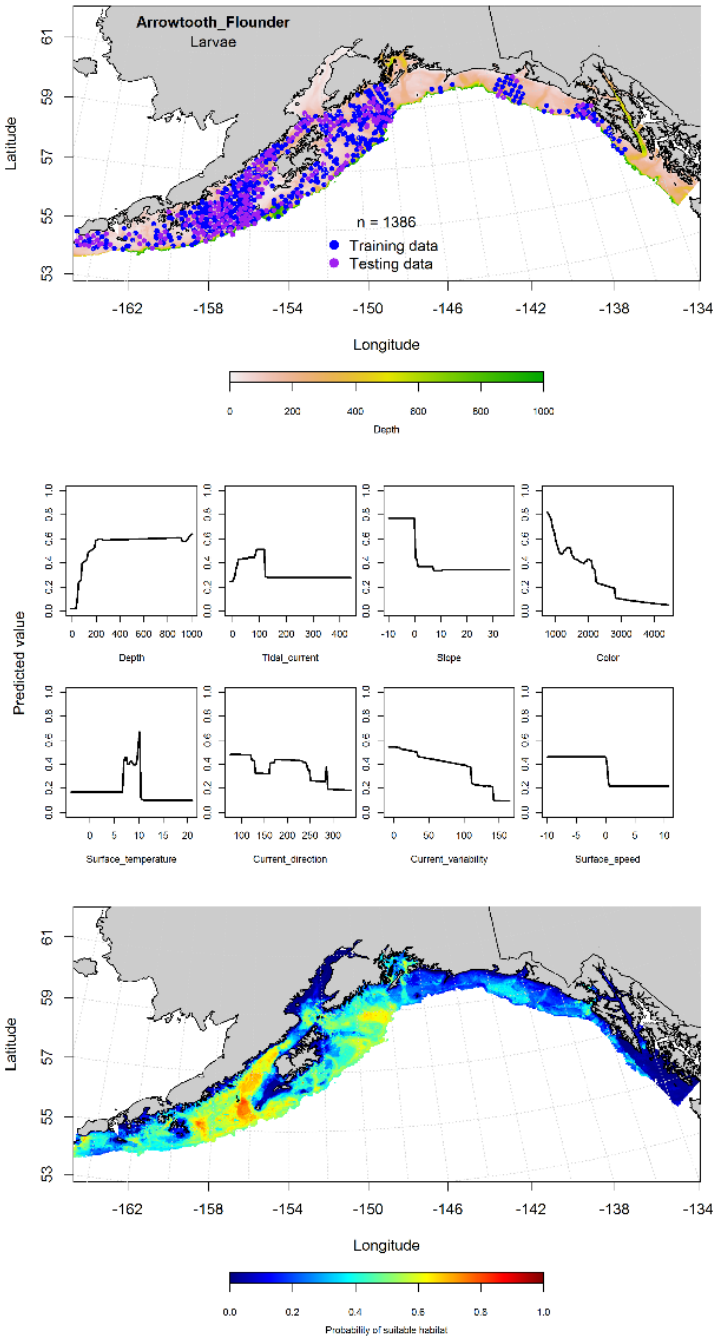

Figure 7. -- Presence of pelagic *Atheresthes* spp. larvae from EcoFOCI ichthyoplankton surveys (January-September 1991-2013) in the Gulf of Alaska (top panel) with training (blue dots) and testing (purple dots) data indicated, maximum entropy (MaxEnt) model effects (center panel), and the MaxEnt-predicted probability of suitable larval *Atheresthes* spp. habitat (bottom panel).

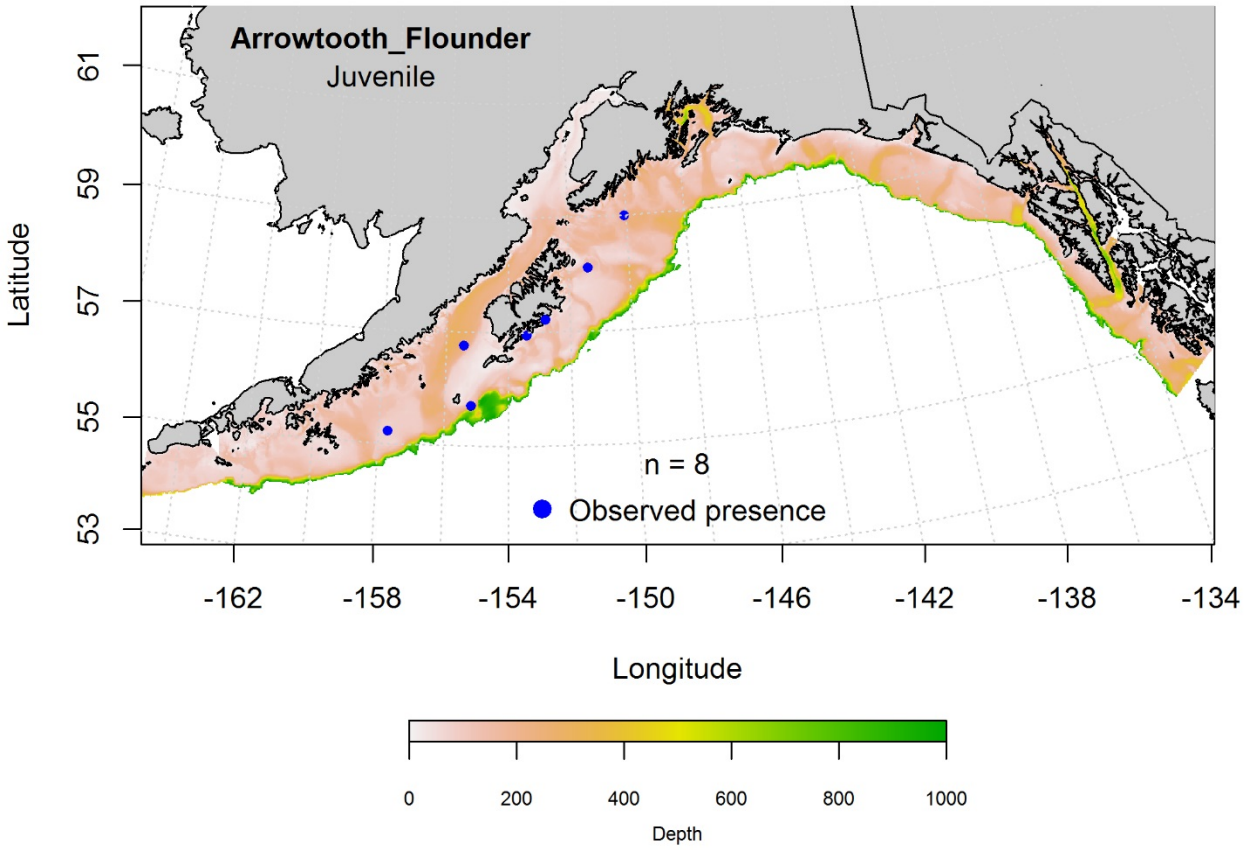

Figure 8. -- Distribution of pelagic *Atheresthes* spp. juvenile observations from EcoFOCI ichthyoplankton surveys in the Gulf of Alaska (April-September 1991-2012).

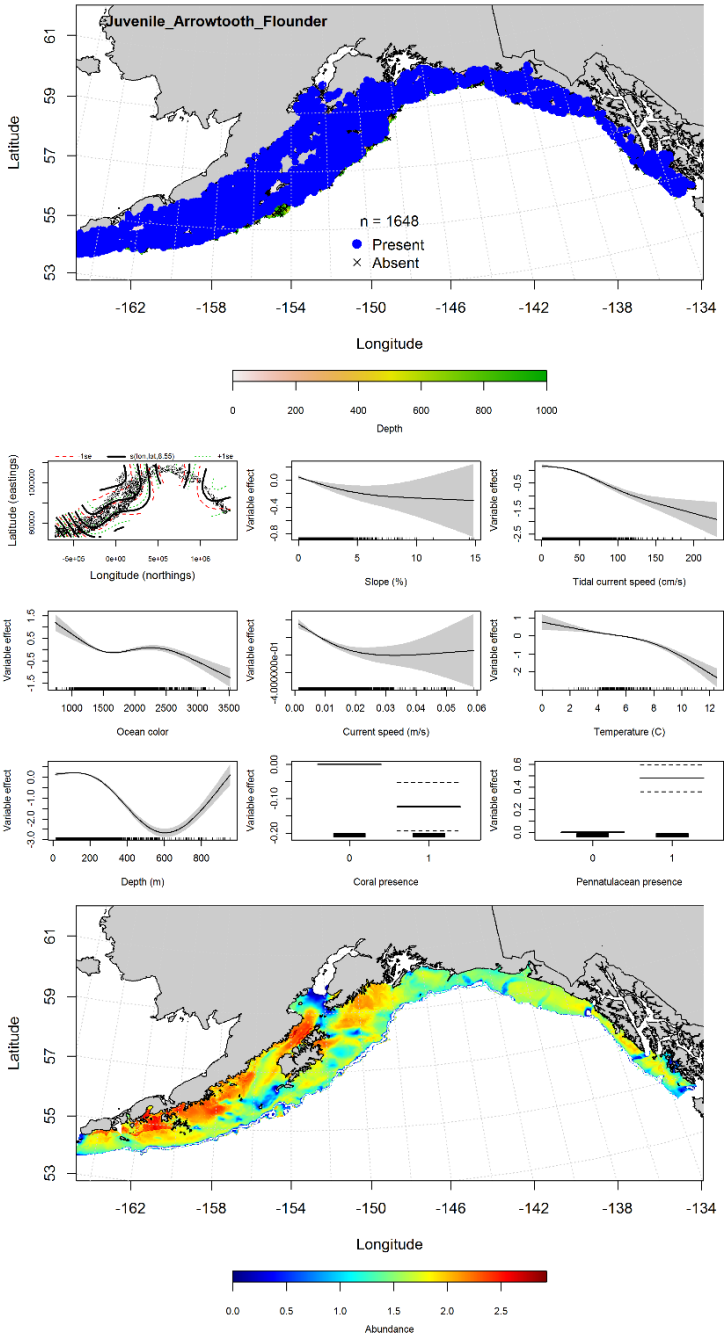

Figure 9. -- Catches of settled juvenile arrowtooth flounder from RACE-GAP summer bottom trawl surveys (1993-2013) in the Gulf of Alaska (top panel), significant relationships between CPUE and environmental variables in the best fitting generalized additive model (GAM; middle panels), and the GAM-predicted abundance of settled juvenile arrowtooth flounder (bottom panel).

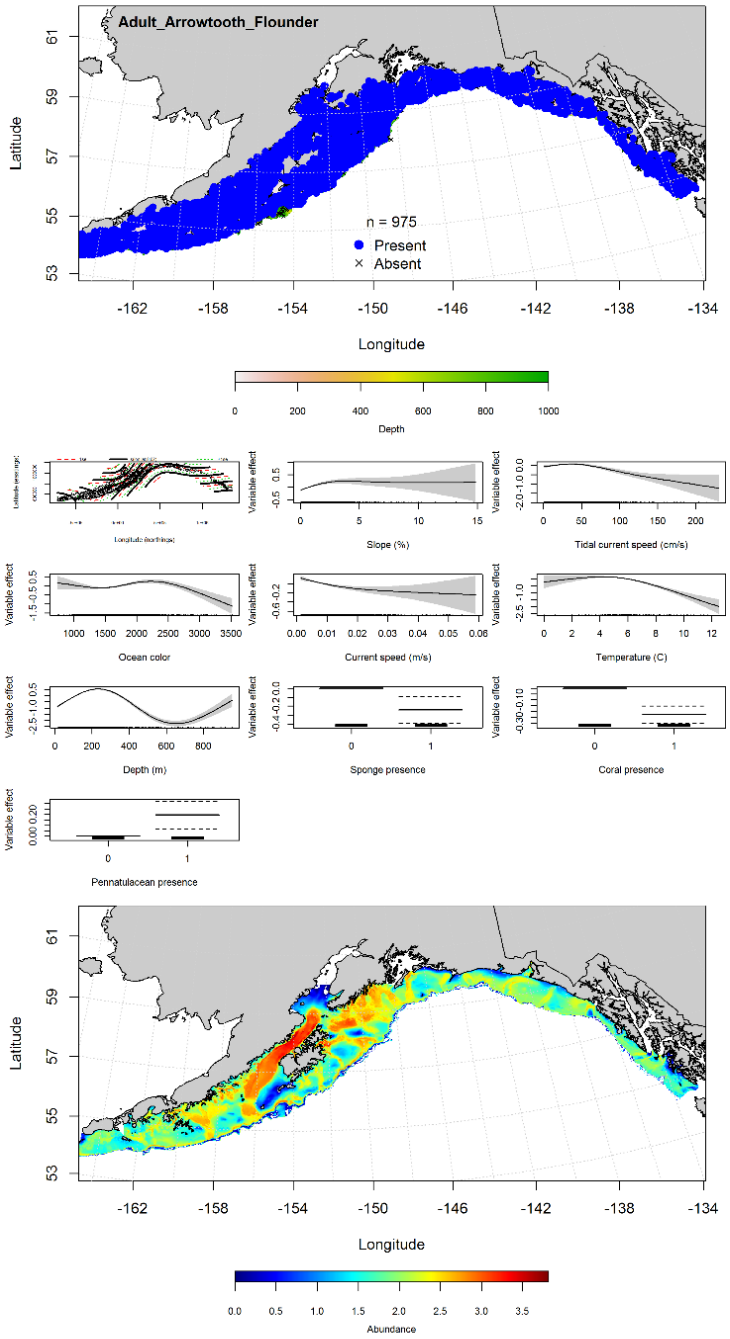

Figure 10. -- Catches of adult arrowtooth flounder from RACE-GAP summer bottom trawl surveys (1993-2013) in the Gulf of Alaska (top panel), significant relationships between CPUE and environmental variables in the best fitting generalized additive model (GAM; middle panels), and the GAM-predicted abundance of adult arrowtooth flounder (bottom panel).

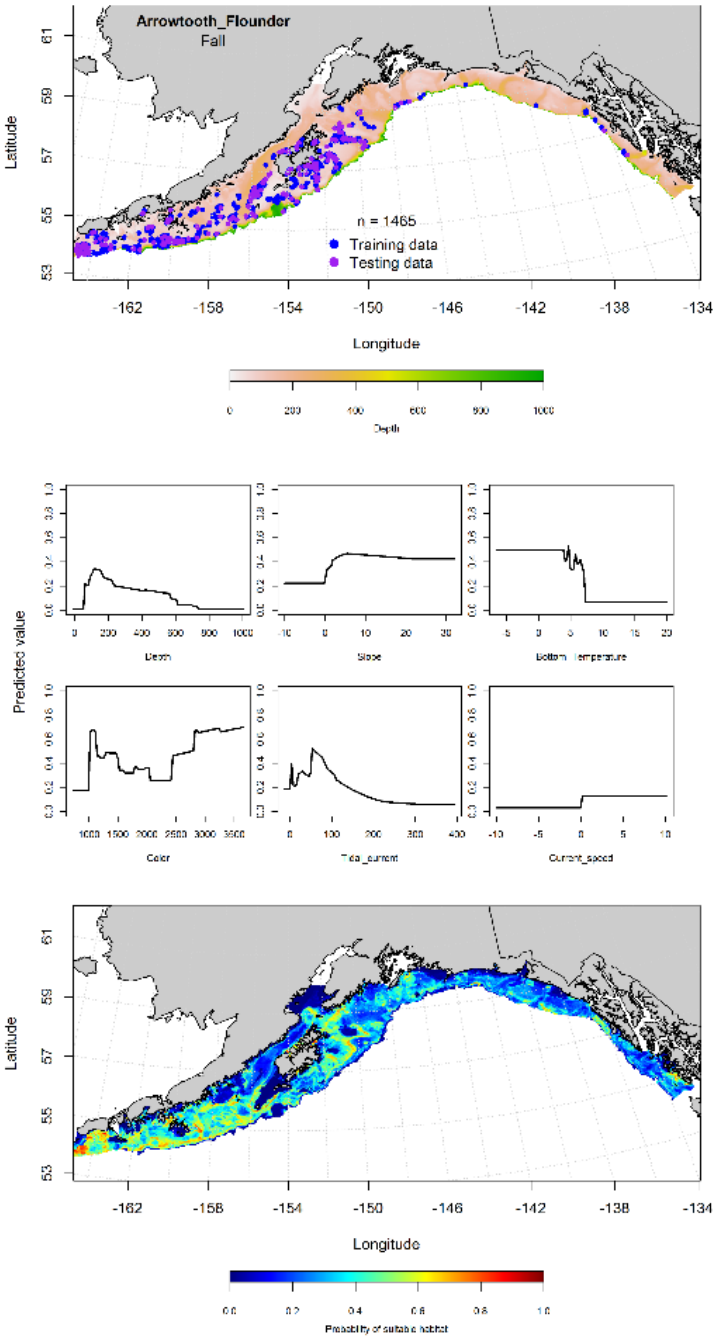

Figure 11. -- Locations of arrowtooth flounder from fall (September-November 2001-2015) commercial fisheries catches in the Gulf of Alaska (top panel), with training (blue dots) and testing (purple dots) data indicated, maximum entropy (MaxEnt) model effects (center panel), and the predicted probability of suitable adult arrowtooth flounder habitat (bottom panel).

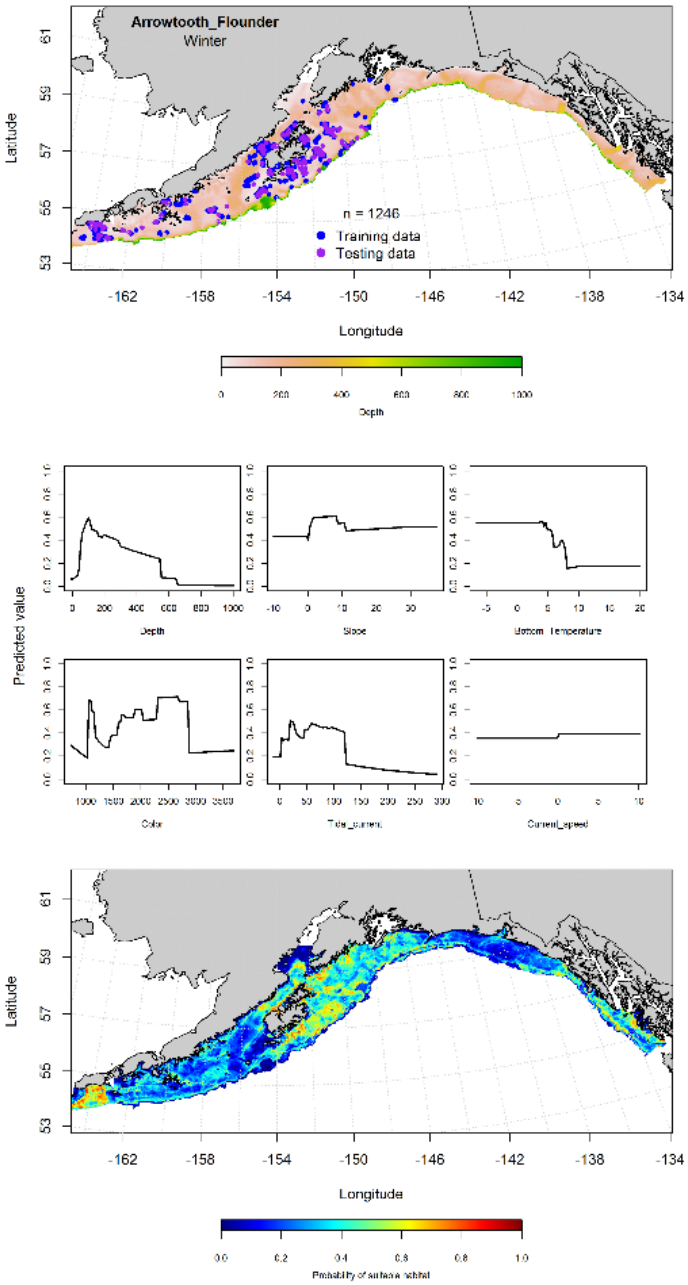

Figure 12. -- Locations of arrowtooth flounder from winter (December-February 2001-2015) commercial fisheries catches in the Gulf of Alaska (top panel), with training (blue dots) and testing (purple dots) data indicated, maximum entropy (MaxEnt) model effects (center panel), and the predicted probability of suitable adult arrowtooth flounder habitat (bottom panel).

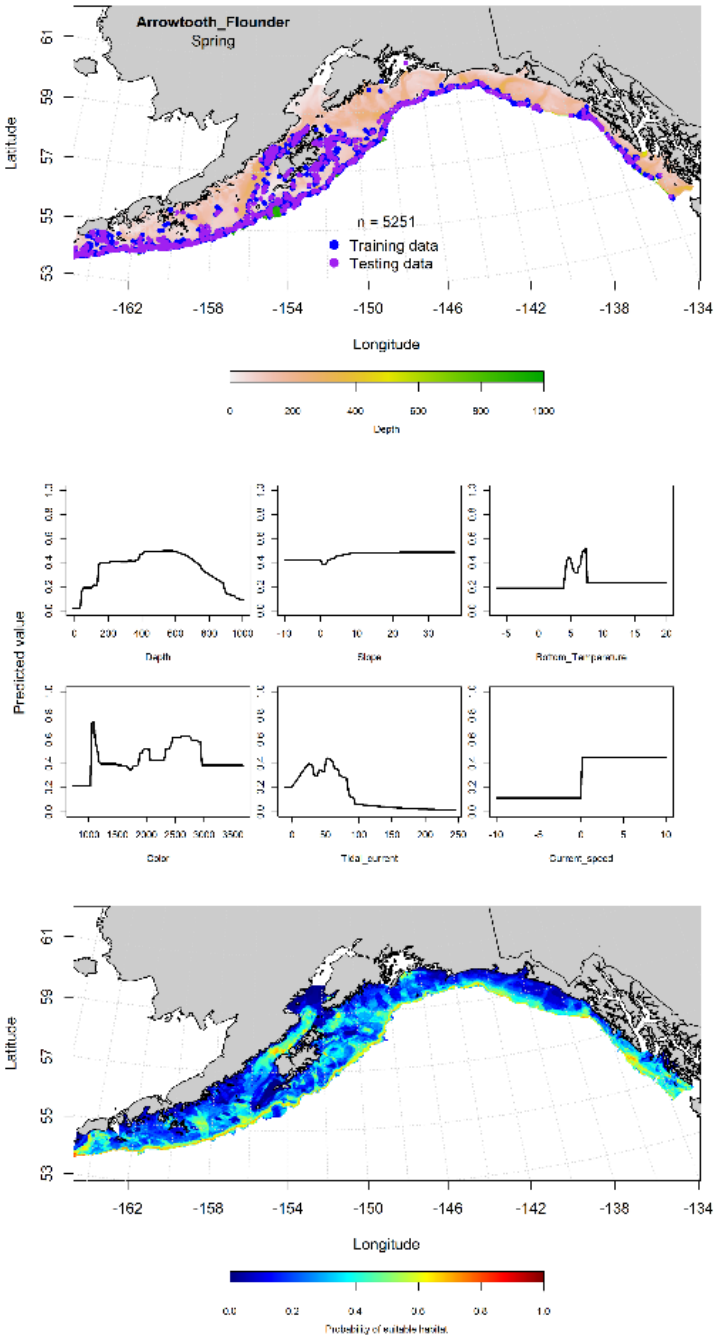

Figure 13. -- Locations of arrowtooth flounder from spring (March-May 2001-2015) commercial fisheries catches in the Gulf of Alaska (top panel), with training (blue dots) and testing (purple dots) data indicated, maximum entropy (MaxEnt) model effects (center panel), and the predicted probability of suitable adult arrowtooth flounder habitat (bottom panel).

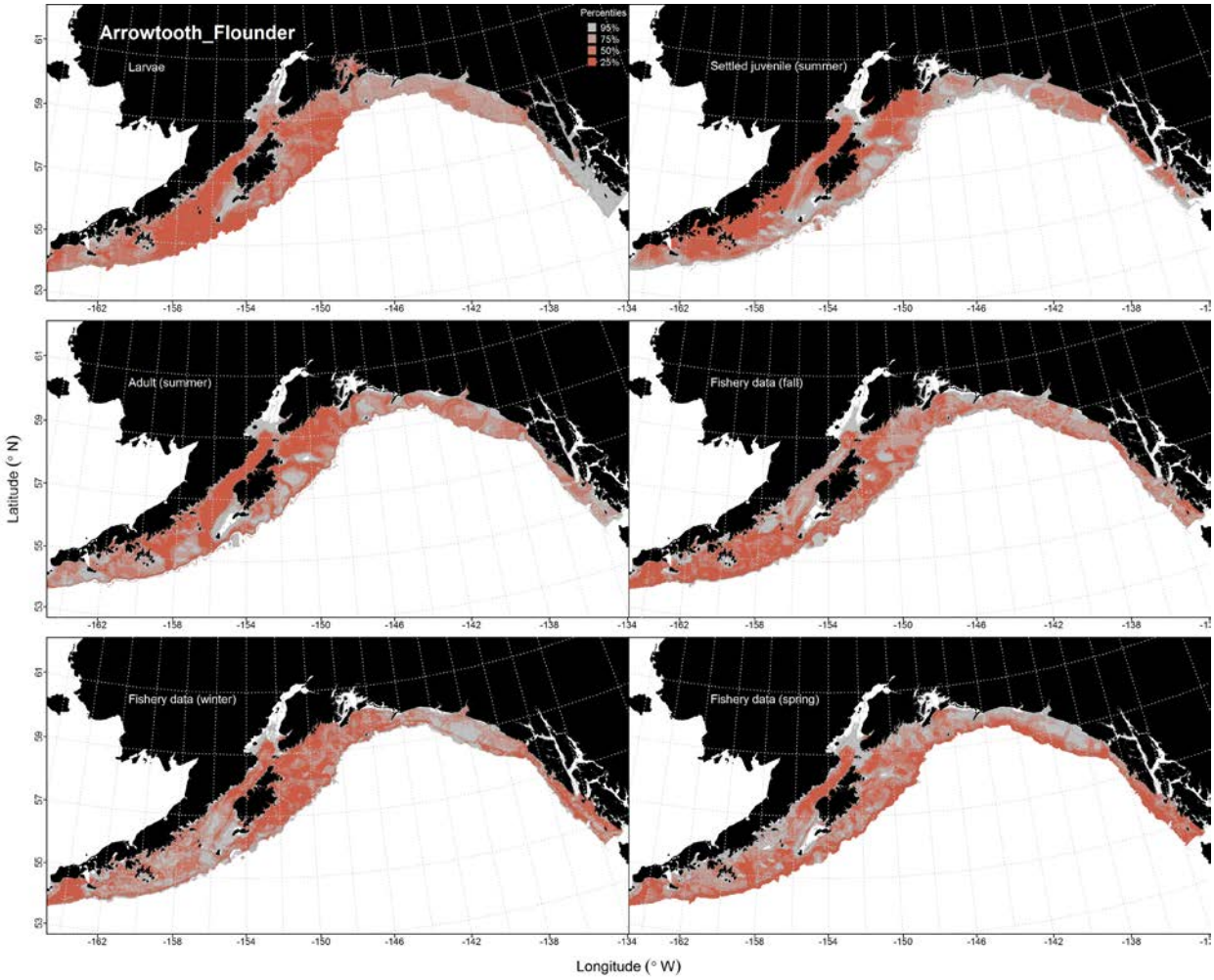

Figure 14. -- Predicted habitat quantiles for arrowtooth flounder life history stages based on species distribution modeling. Pelagic larval maps from EcoFOCI ichthyoplankton surveys are a combination of both species of *Atheresthes* spp. (*A. stomias and A. evermanni*). Settled juvenile and adult stages are based on RACE-GAP summer bottom trawl survey data (1993-2013), while the remaining seasonal maps (winter, spring, fall) are from VOE-CIA commercial fishery observer data (2001-2015).

Rex Sole (*Glyptocephalus zachirus*)

Early life history stages of rex sole -- There were 1,789 instances of rex sole eggs observed in the EcoFOCI collections from the GOA (Fig. 15). A MaxEnt model indicated that bottom depth and surface temperature were the most important model variables explaining the probability of suitable rex sole egg habitat (relative importance: 0.39 and 0.14, respectively). The AUC was 0.83 for the training and it was 0.74 for the testing data; with the model correctly classifying 74% of the training and 75% of the test data. The highest predicted probability of suitable habitat for rex sole eggs was in the central and western GOA, particularly around Shelikof Gully and the Shumagin Islands (Fig. 15).

There were 354 instances of rex sole pelagic larvae in the EcoFOCI collections, these were largely from the central and western GOA (Fig. 16). Surface temperature and bottom depth were the most important variables determining suitable habitat of larval rex sole (relative importance: 0.31 and 0.31, respectively). The AUC was 0.85 for the training data and 0.73 for the testing data. The model correctly classified 91% of the predictions from the training and 86% of the predictions from the test data. The model predicted suitable habitat for pelagic larval rex sole in the central and western GOA, particularly around Chirikof Island (Fig. 16).

There were no observations of pelagic juvenile rex sole in the EcoFOCI collections.

Juvenile and adult rex sole distribution in the bottom trawl survey -- An hGAM was used to predict the distribution of settled juvenile rex sole abundance. The PA GAM resulted in an AUC of 0.77 for the training data and 0.79 for the test data. The PA GAM indicated that geographic location, bottom temperature, ocean color, and bottom depth were the most important variables controlling settled juvenile rex sole distribution. The model predicted the probability of settled juvenile presence was distributed throughout the central and eastern GOA (Fig. 17). The important variables in the

CPUE GAM were geographic location, bottom temperature, and maximum tidal current. Overall, the hurdle model explained 15% of the variability in training data and 11% in test data. The areas of highest abundance were along the inner shelf in the eastern GOA, from the Kenai Peninsula to Yakutat (Fig. 17).

A GAM predicting the abundance of adult rex sole explained 33% of the variability in CPUE in the bottom trawl survey training data, and 46% of the variability in the test data. Bottom depth, maximum tidal current, and slope were the most important factors controlling catch of adult rex sole. Adult rex sole were distributed throughout the GOA, but most abundant in deeper areas, including in Shelikof Gully, Amatuli Trough, and off Prince of Wales Island (Fig. 18).

Rex sole distribution in commercial fisheries -- Presence of rex sole in commercial fisheries catches from the GOA were largely consistent throughout all seasons. In the fall, maximum tidal current, bottom depth, and ocean color were the most important variables determining probable suitable habitat for rex sole (relative importance: 0.29, 0.28, and 0.17, respectively). The AUC for the fall MaxEnt model was 0.92 for the training data and 0.81 for the test data. The best-fitting model correctly classified 83% of training data and 81% of test data. The model predicted suitable habitat was most abundant in the central GOA, particularly in off Kodiak Island, and in the western GOA off Unimak Island (Fig. 19).

In the winter, bottom depth, ocean color, and maximum tidal current were the most important variables determining probable suitable habitat for adult rex sole (relative importance: 0.31, 0.30, and 0.18, respectively). The AUC of the winter MaxEnt model was 0.92 for the training data and 0.80 for the test data. Eighty-five percent of the training data and 80% of the test data were correctly

classified. The model predicted suitable habitat of rex sole in the central GOA, with the highest probabilities concentrated around Albatross and Portlock banks (Fig. 20).

In the spring, bottom depth, bottom current speed, and ocean color were the most important variables determining probable suitable habitat of rex sole (relative importance: 0.44, 0.22, and 0.19, respectively). The AUC of the spring MaxEnt model was 0.91 for the training data and 0.81 for the test data. The model correctly classified 84% of the predictions from the training data and 81% of the predictions form the test data. The areas of predicted highest probability of suitable habitat in the central GOA, were around the Shumagin and Shelikof gullies; while in the western GOA, they were off Unimak Island (Fig. 21).

Rex sole essential fish habitat maps and conclusions -- Habitat for rex sole eggs and pelagic larvae was distributed extensively throughout the central and western GOA (Fig. 22). In contrast, habitat for settled juvenile rex sole was more limited, and largely concentrated in the eastern GOA (Fig. 22). Adult rex sole habitat was predicted to be extensively distributed throughout the GOA, with the higher suitability areas concentrated at deeper depths (Fig. 22). Predicted fall, winter, and spring distributions of suitable habitat predicted from commercial catch observations were similar across seasons, but slightly more concentrated near the outer shelf during the spring (Fig. 22).

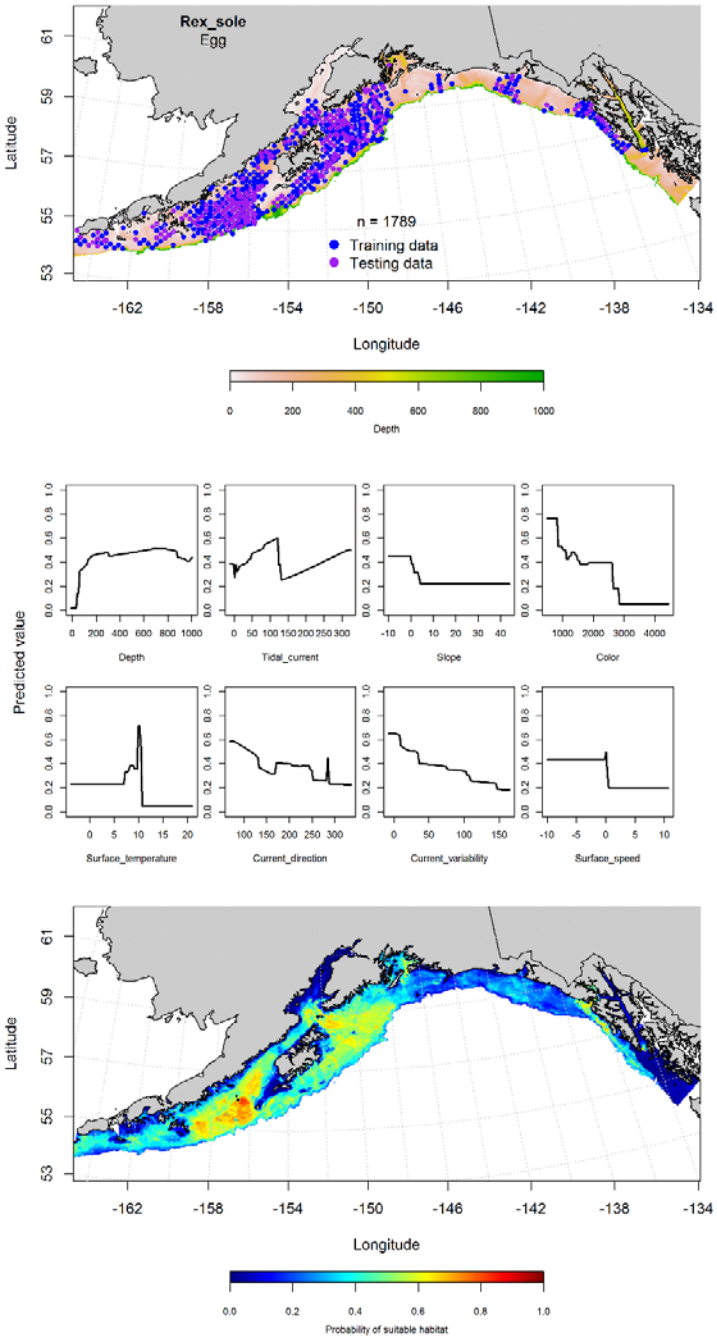

Figure 15. -- Distribution of rex sole eggs from EcoFOCI ichthyoplankton surveys (January-March 1991-2013) (top panel) with training (blue dots) and testing (purple dots) data indicated, maximum entropy (MaxEnt) model effects (center panel), and predicted probability of suitable rex sole egg habitat (bottom panel).

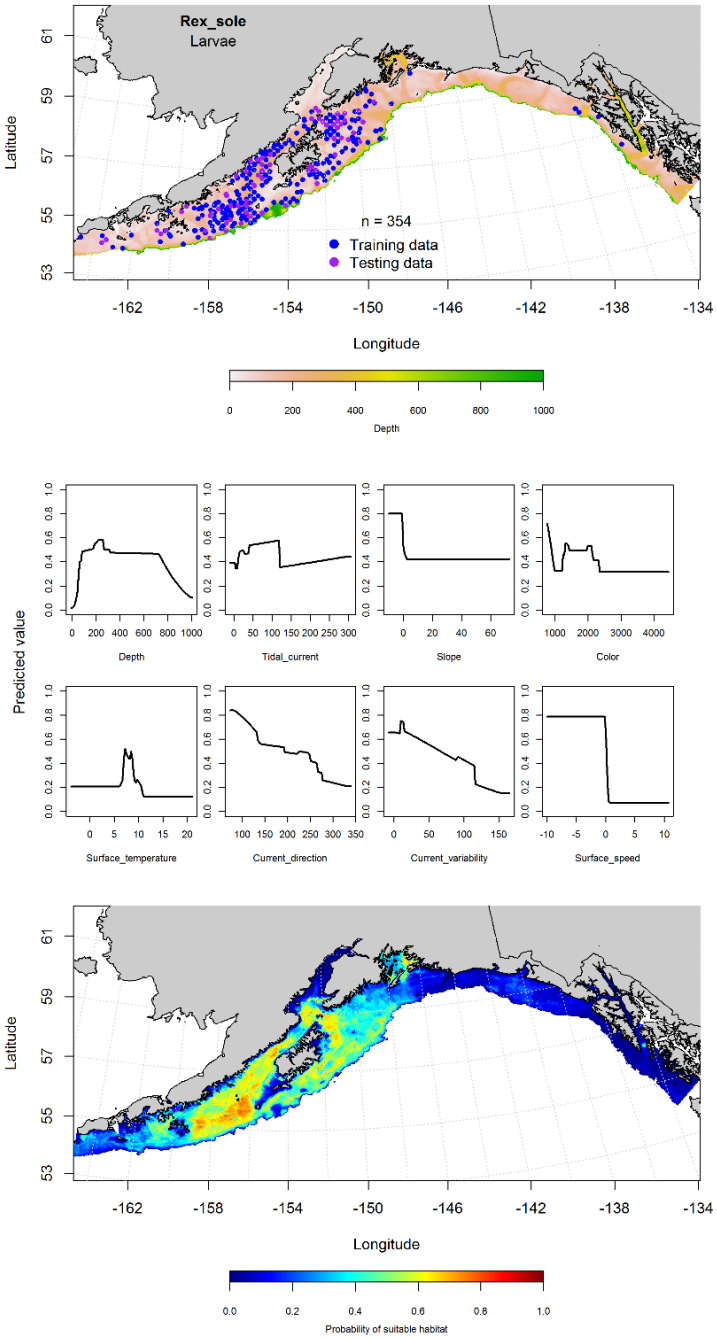

Figure 16. -- Presence of pelagic rex sole larvae from EcoFOCI ichthyoplankton surveys (January to September 1991-2013) in the Gulf of Alaska (top panel) with training (blue dots) and testing (purple dots) data indicated, maximum entropy (MaxEnt) model effects (center panel), and the predicted probability of suitable pelagic rex sole larval habitat (bottom panel).

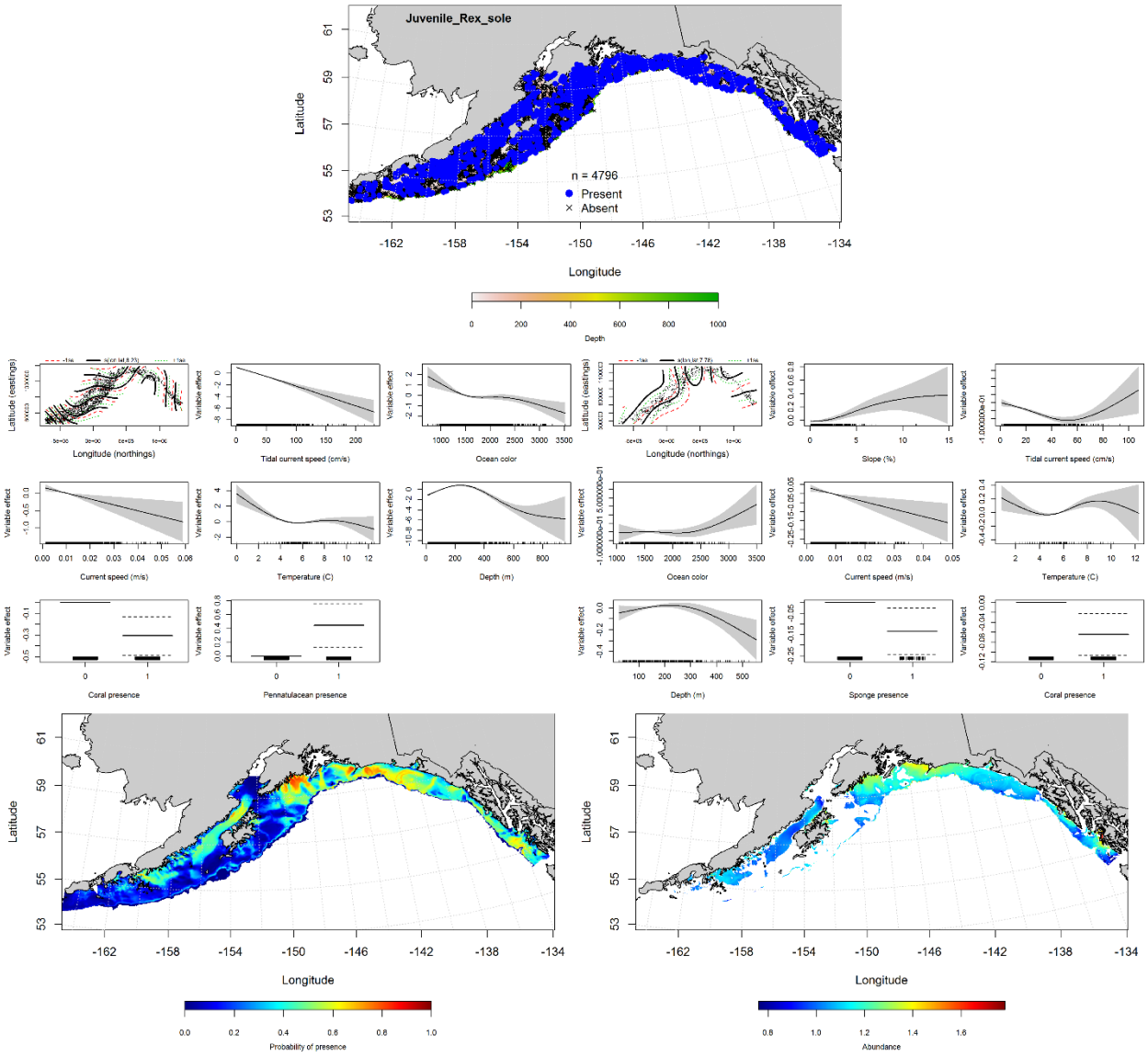

Figure 17. -- Distribution of settled juvenile rex sole in 1993-2013 RACE-GAP summer bottom trawl surveys conducted in the Gulf of Alaska (upper panel). Effects of retained habitat covariates in the best fitting generalized additive models (PA GAM) of presence-absence models (left center panel) and abundance (CPUE GAM; right center panel). Predicted spatial distribution of the probability of presence (bottom left panel) and abundance of settled juvenile rex sole based on the models (bottom right panel).

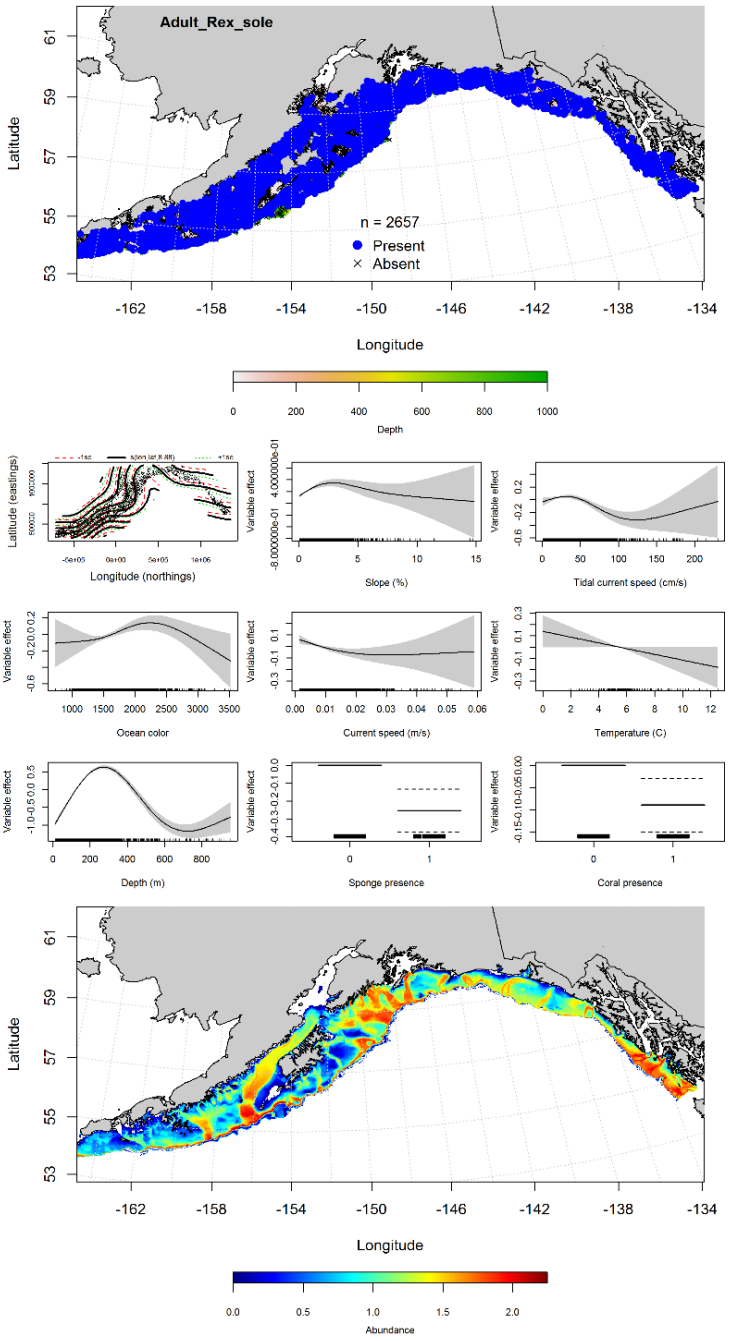

Figure 18. -- Catches of adult rex sole from RACE-GAP summer bottom trawl surveys (1993-2013) in the Gulf of Alaska (top panel), significant relationships between CPUE and environmental variables in the best fitting generalized additive model (GAM) for adult rex sole (middle panels), and the GAM-predicted abundance of adult rex sole (bottom panel).

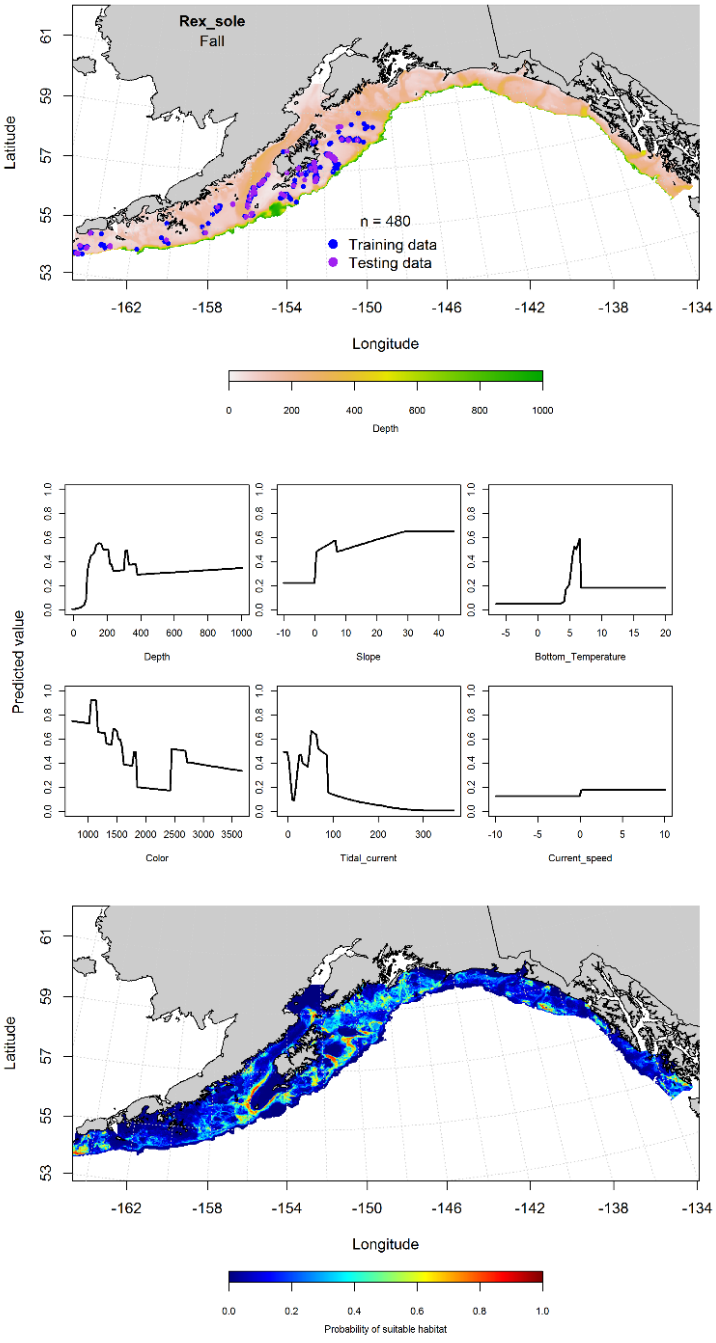

Figure 19. -- Locations of fall (September-November 2001-2015) commercial fisheries catches of rex sole (top panel), MaxEnt model effects (middle panels), and predicted probability of suitable habitat for rex sole based on the model (bottom panel).

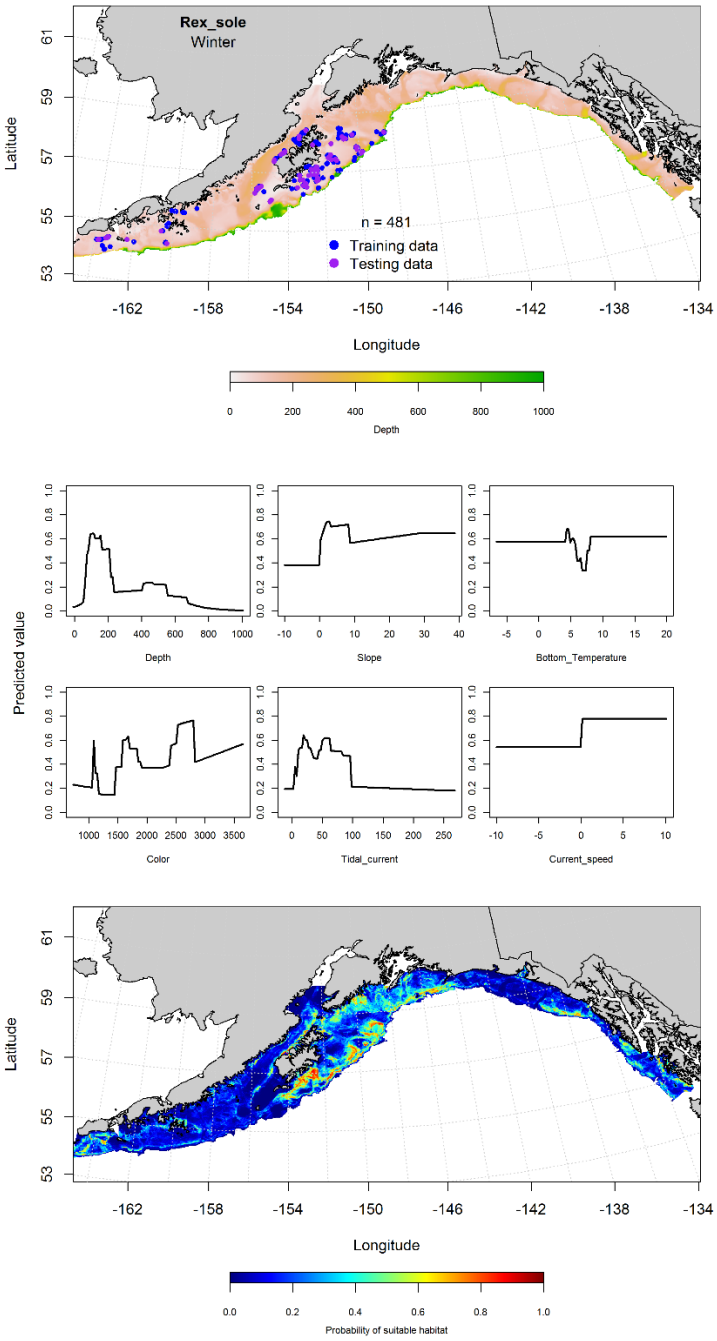

Figure 20. -- Locations of rex sole from fall (September-November 2001-2015) commercial fisheries catches in the Gulf of Alaska (top panel), MaxEnt model effects (middle panels), and predicted probability of suitable habitat for rex sole based on the model (bottom panel).

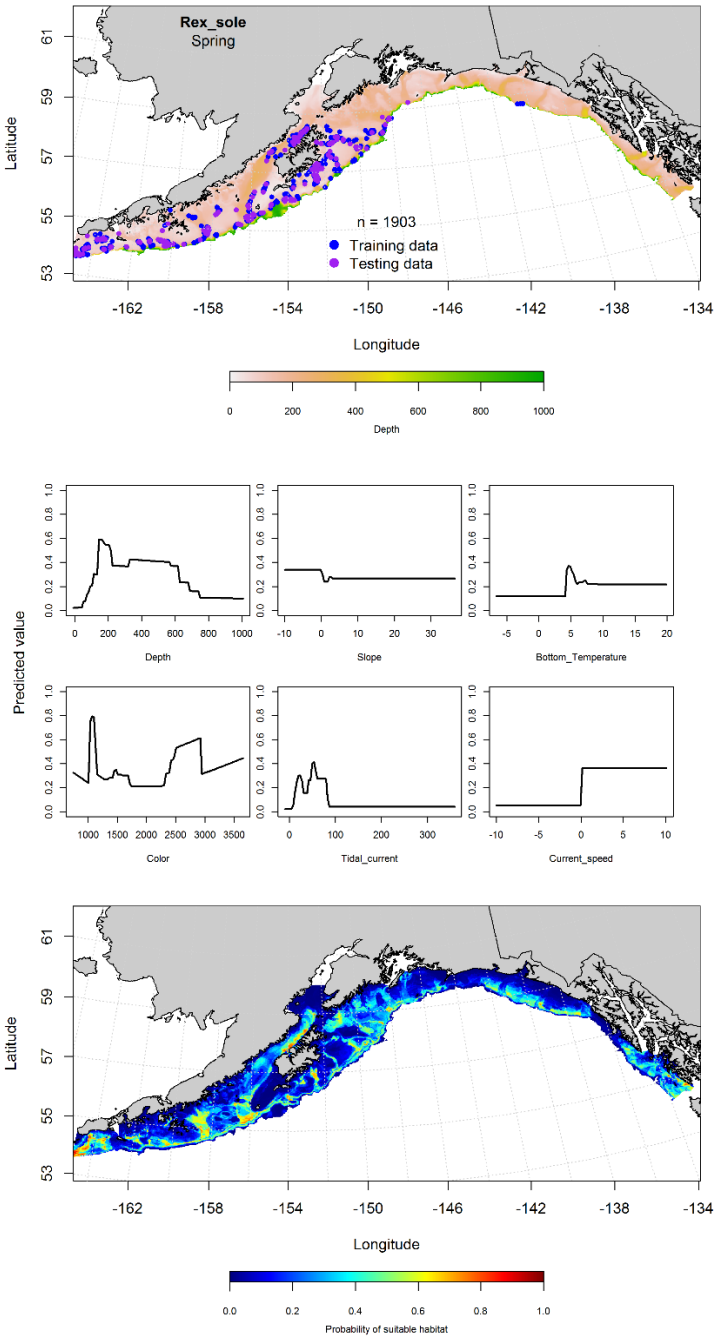

Figure 21. -- Locations of spring (March-May 2001-2015) commercial fisheries catches of rex sole (top panel), MaxEnt model effects (middle panels), and predicted probability of suitable habitat for rex sole based on the model (bottom panel).

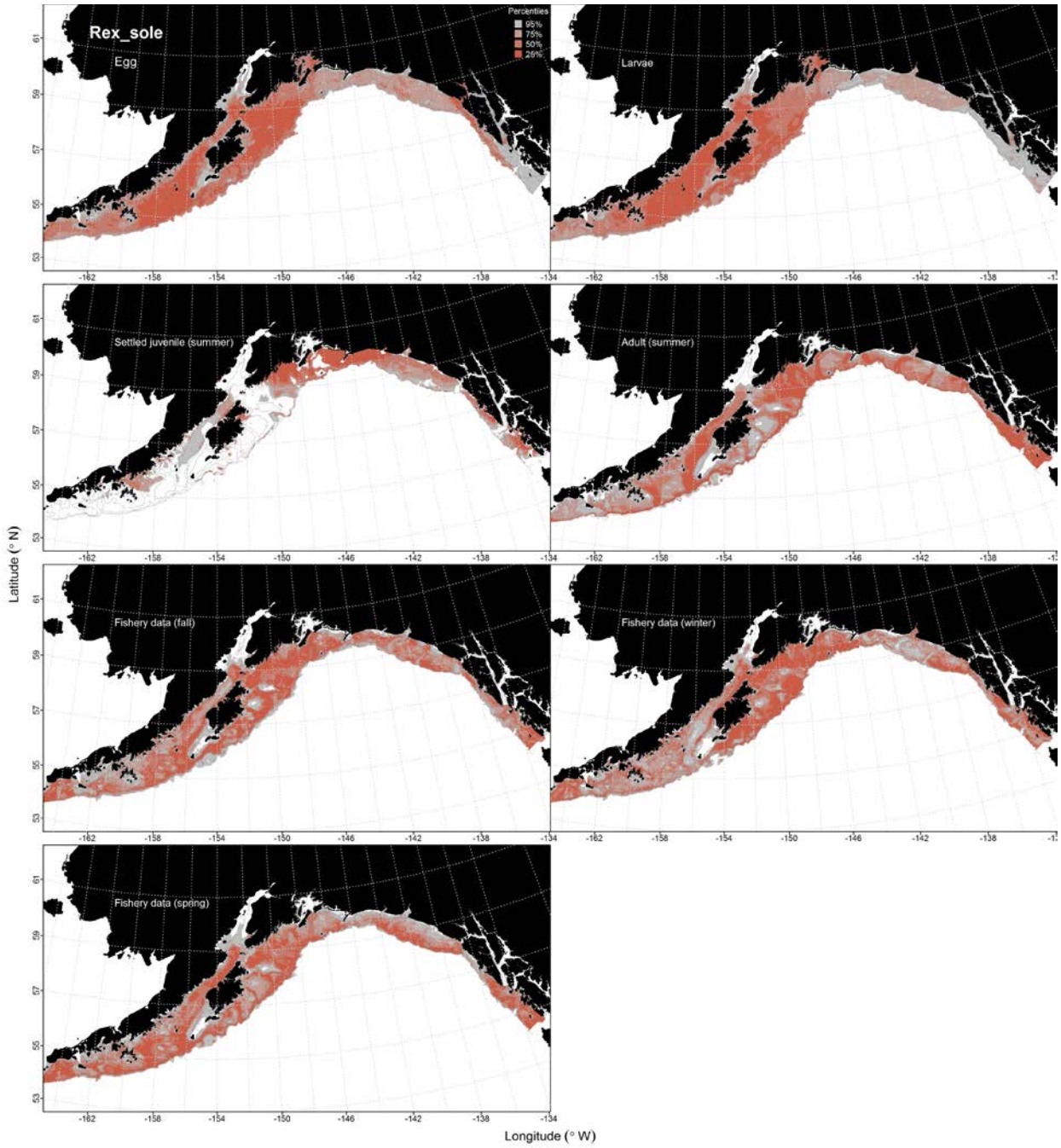

Figure 22. -- Habitat predicted for rex sole eggs from EcoFOCI ichthyoplankton surveys (1991-2012), settled juveniles and adults from RACE-GAP summertime bottom trawl surveys (1993-2013), and predicted from presence in commercial fishery catches (2001-2015) from fall, winter, and spring in the Gulf of Alaska.

Flathead Sole (*Hippoglossoides elassodon*)

Early life history stages of flathead sole -- There were 4,121 instances of flathead sole eggs observed in the EcoFOCI collections. A majority of these were from the central and western GOA (Fig. 23). Surface temperature, bottom depth, and surface current speed were the most important variables determining suitable habitat of flathead sole eggs (relative importance: 0.34, 0.31, and 0.16, respectively). The AUC for the MaxEnt model was 0.89 for the training data and 0.81 for the test data. The model correctly classified 81% of the predictions from both the training and test data. The model predicted suitable habitat for flathead sole eggs was concentrated in Shelikof Gully and along the Alaska Peninsula (Fig. 23).

There were 3,295 observations of flathead sole larvae in the EcoFOCI collections, with a majority of these occurring in the central and western GOA (Fig. 24). A MaxEnt model was used to predict the probability of suitable habitat for larval flathead sole. The AUC of the model was 0.89 for the training data and 0.79 for the testing data. The model correctly classified 80% of the predictions from the training data and 79% of the predictions from the test data. Surface temperature, bottom depth, and surface current speed were the most important variables explaining the probability of suitable larval flathead sole habitat (relative importance: 0.43, 0.26, and 0.13, respectively). The model predicted the highest probability of suitable habitat for larval flathead sole in the western GOA, particularly around Shelikof Gully (Fig. 24).

There were no observations of pelagic juvenile flathead sole in the EcoFOCI collections.

Juvenile and adult flathead sole distribution in the bottom trawl survey -- The catch of settled juvenile flathead sole in summer bottom trawl surveys of the GOA indicates this species is broadly distributed (Fig. 25). GAM predictions of the abundance of settled juvenile flathead sole explained

37% of the variability in CPUE for both the training and test data. Geographic location, ocean color, bottom depth, and maximum tidal current were the most important variables predicting catch of juvenile flathead sole. The model predicted settled juvenile flathead sole were most abundant in Shelikof Strait and along the Alaska Peninsula (Fig. 25).

As with the juveniles, the best fitting GAM indicated that geographic location, ocean color, and bottom depth were the most important factors determining the abundance of adult flathead sole. The model explained 43% of the variability of the training data and 44% of the variability of the test data. Adult flathead sole were distributed similarly to the settled juveniles, in Shelikof Strait and along the Alaska Peninsula (Fig. 26).

Flathead sole distribution in commercial fisheries -- Distribution of adult flathead sole in GOA commercial fisheries catches was generally consistent throughout all seasons. In the fall, bottom depth, ocean color, maximum tidal currents were the most important model variables determining probable suitable habitat of flathead sole (relative importance: 0.36, 0.27, and 0.17). The AUC for the fall MaxEnt model was 0.92 for the training and 0.76 for the test data. The model correctly classified 85% of the predictions from the training and 76% of the predictions from the test data. The model predicted suitable habitat of flathead sole habitat was patchy in distribution, with higher suitability habitats concentrated off Unimak and Kodiak Islands (Fig. 27).

Like the fall, bottom depth, ocean color, maximum tidal currents in the winter were the most important variables determining the distribution of flathead sole suitable habitat (relative importance: 0.33, 0.31, and 0.17). The AUC of the winter MaxEnt model was 0.87 for the training data and 0.78 for the test data. The model correctly classified 80% of the predictions from the training data and

78% of the predictions from the test data. The model predicted suitable habitat in deeper areas of the central and western GOA, particularly near Unimak and Kodiak Islands (Fig. 28).

In the spring, bottom depth and ocean color and were the most important variables determining the distribution of flathead sole suitable habitat (relative importance: 0.39 and 0.24). The AUC of the spring MaxEnt model was 0.80 for the training data and 0.81 for the test data. The model correctly classified 80% of the predictions from the training and 81% of the predictions from the test data. As with the other seasons, the model predicted probable suitable habitat for flathead sole at deeper depths in the central and western GOA (Fig. 29).

Flathead sole essential fish habitat maps and conclusions-- Predicted habitat for flathead sole eggs and pelagic larvae was broadly distributed across the GOA (Fig. 30). Settled juvenile and adult flathead had more narrowly distributed habitat than either of the ELHS. The model predicted probable suitable habitat of settled juvenile and adult flathead sole throughout the central and western GOA, though the highest probability of suitable habitat was predicted in Shelikof Strait and along the Alaska Peninsula (Fig. 30). The fall, winter, and spring distribution of flathead sole habitat was generally the same throughout the seasons in the GOA (Fig. 30). Interestingly, an area of high abundance predicted by bottom trawl survey GAM along Shelikof Strait and the Alaska Peninsula, was not observed in the commercial fisheries catch models. This may, in part, be due to differences in the fishing effort and timing of the commercial fisheries and the trawl surveys.

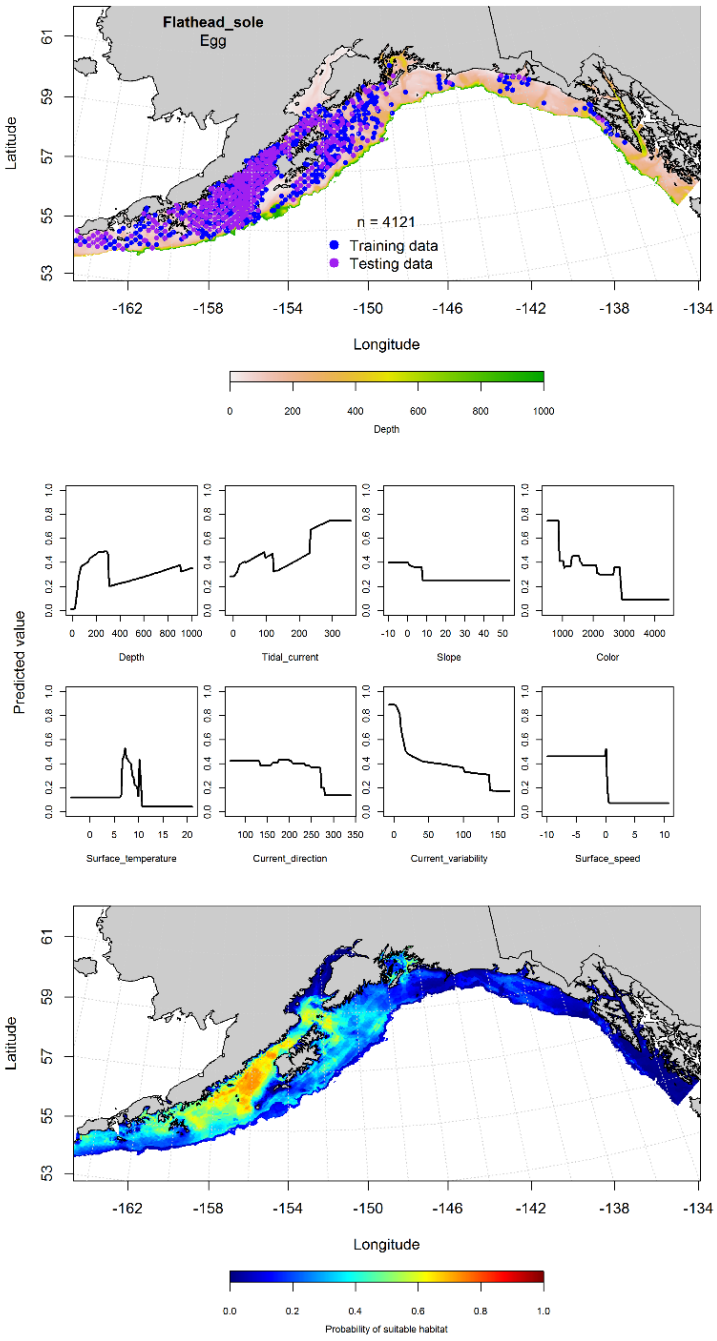

Figure 23. -- Distribution of flathead sole eggs from EcoFOCI ichthyoplankton surveys (January-March 1991-2013) (top panel) with training (blue dots) and testing (purple dots) data indicated, maximum entropy (MaxEnt) model effects (center panel), and predicted probability of suitable flathead sole egg habitat (bottom panel).

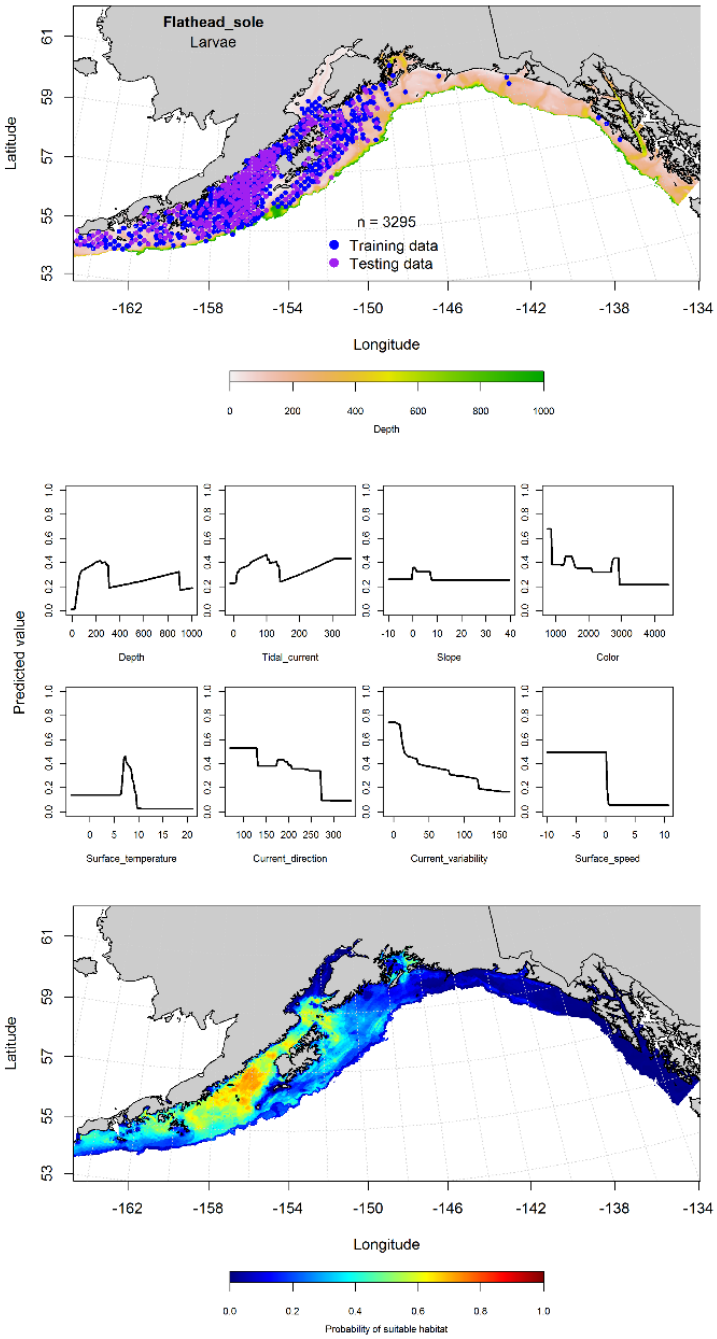

Figure 24. -- Distribution of pelagic flathead sole larvae observations from EcoFOCI ichthyoplankton surveys (April-September 1991-2012) in the Gulf of Alaska (top panel) with training (blue dots) and testing (purple dots) data indicated, maximum entropy (MaxEnt) model effects (center panel), and the predicted probability of suitable pelagic flathead sole larval habitat (bottom panel).

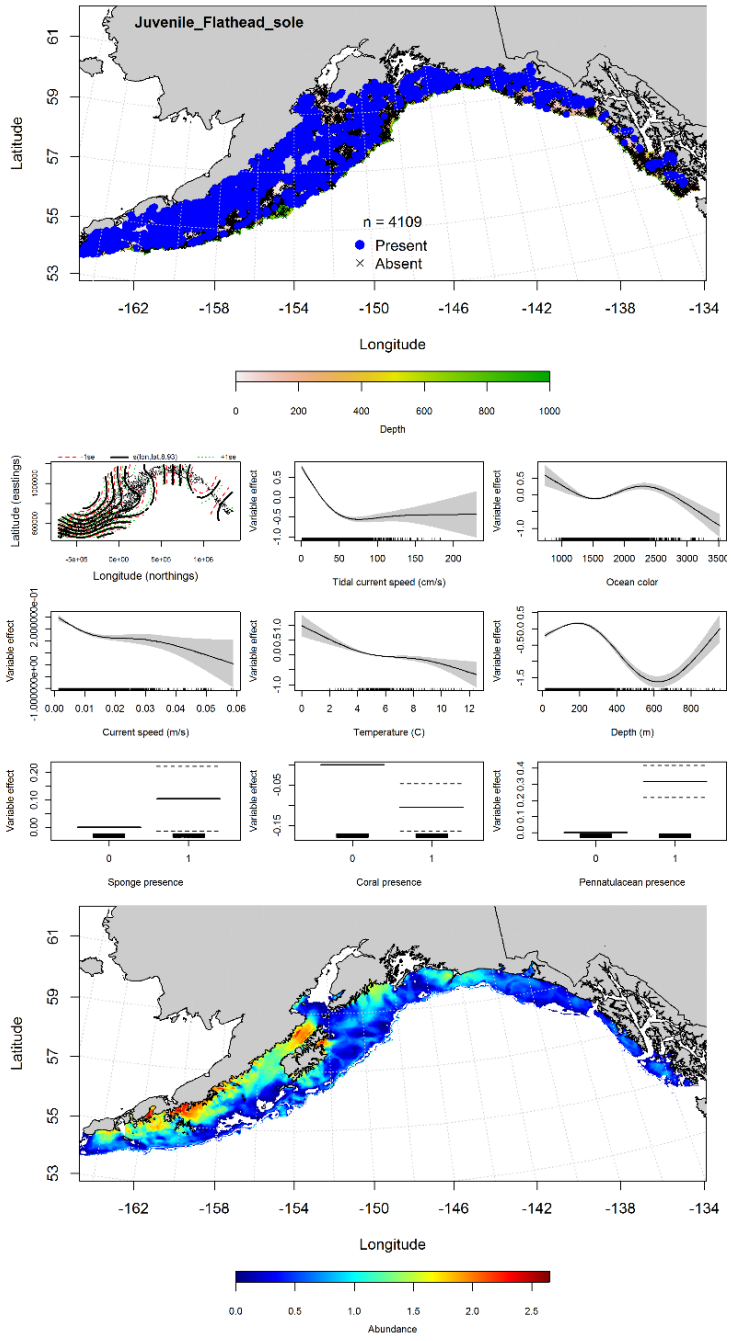

Figure 25. -- Catches of settled juvenile flathead sole from RACE-GAP summer bottom trawl surveys (1993-2013) in the Gulf of Alaska (top panel), significant relationships between CPUE and environmental variables in the best fitting generalized additive model (GAM; middle panels), and the GAM-predicted abundance of settled juvenile flathead sole (bottom panel).

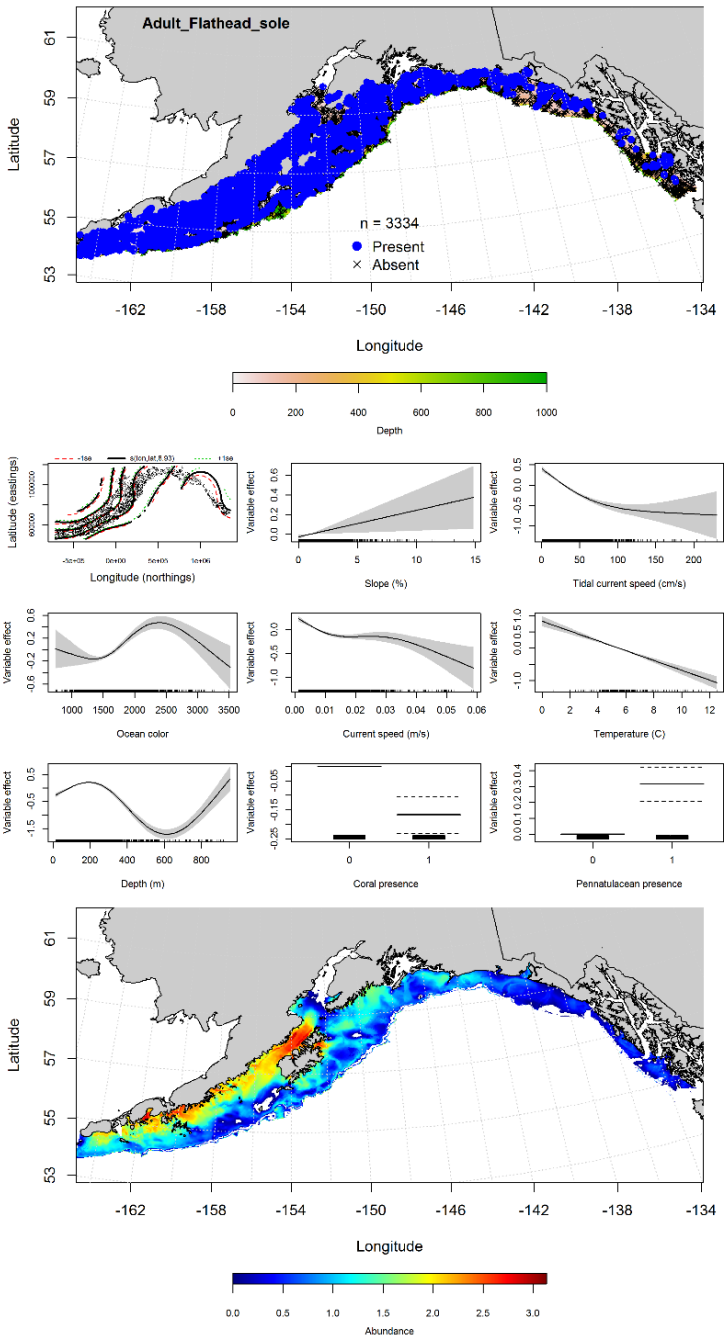

Figure 26. -- Catches of adult flathead sole from RACE-GAP summer bottom trawl surveys (1993-2013) in the Gulf of Alaska (top panel), significant relationships between CPUE and environmental variables in the best fitting generalized additive model (GAM; middle panels), and the GAM-predicted abundance of adult flathead sole (bottom panel).

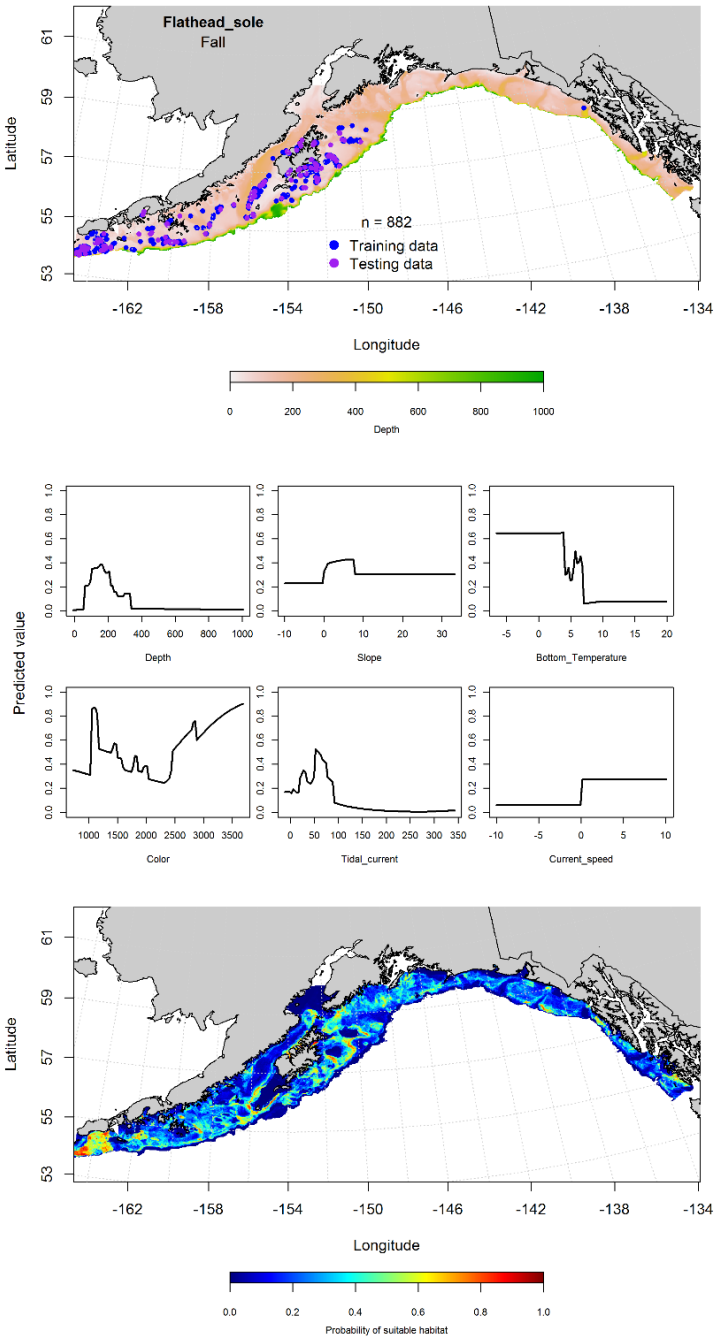

Figure 27. -- Locations of flathead sole from fall (September-November 2001-2015) commercial fisheries catches in the Gulf of Alaska (top panel), MaxEnt model effects (middle panels), and predicted probability of suitable habitat for flathead sole based on the model (bottom panel).

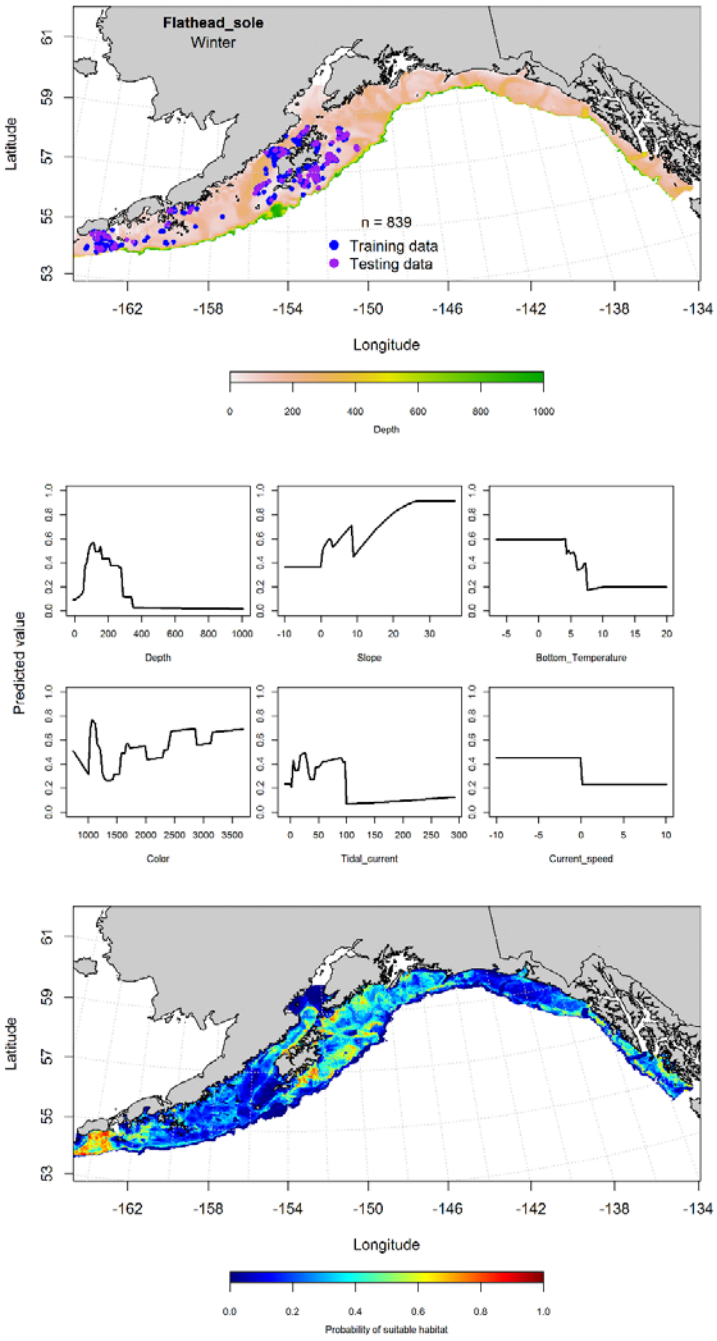

Figure 28. -- Locations of flathead sole from winter (December-February 2001-2015) commercial fisheries catches in the Gulf of Alaska (top panel), with training (blue dots) and testing (purple dots) data indicated, maximum entropy (MaxEnt) model effects (center panel), and the predicted probability of suitable adult flathead sole habitat (bottom panel).

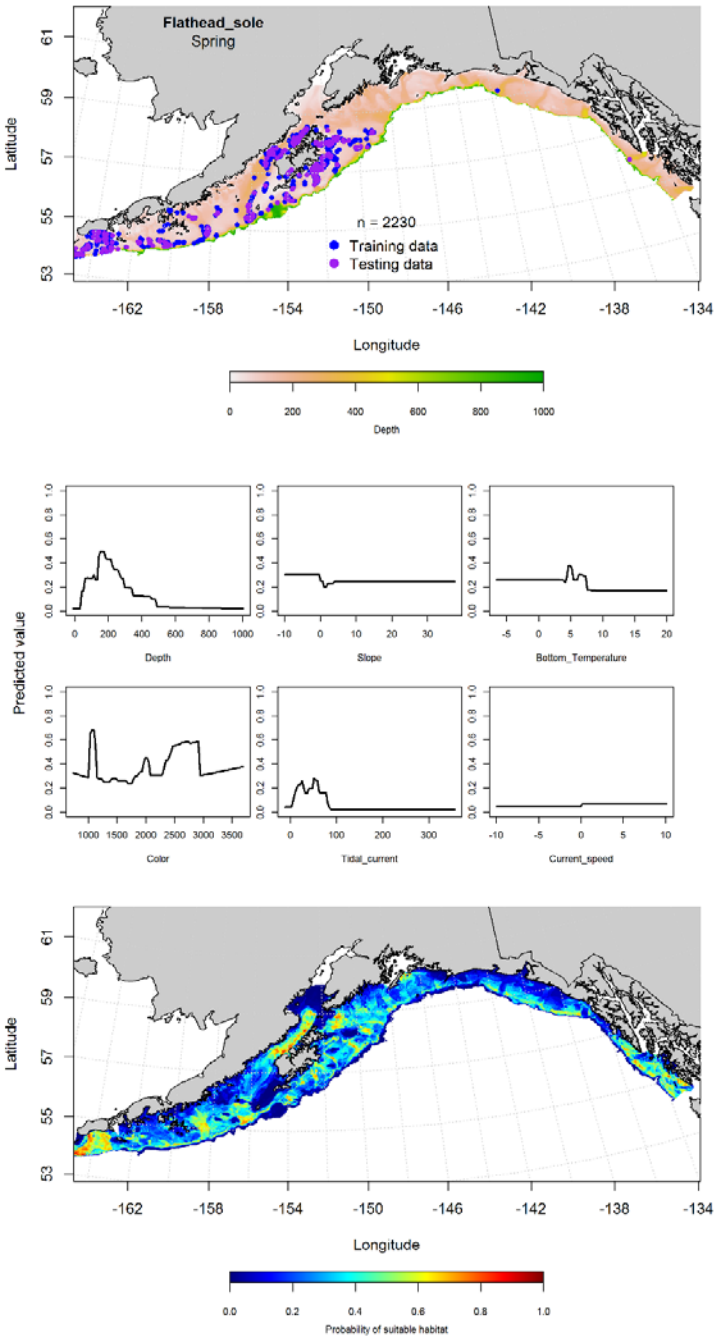

Figure 29. -- Locations of flathead sole from spring (March-May 2001-2015) commercial fisheries catches in the Gulf of Alaska (top panel), with training (blue dots) and testing (purple dots) data indicated, maximum entropy (MaxEnt) model effects (center panel), and the predicted probability of suitable adult flathead sole habitat (bottom panel).

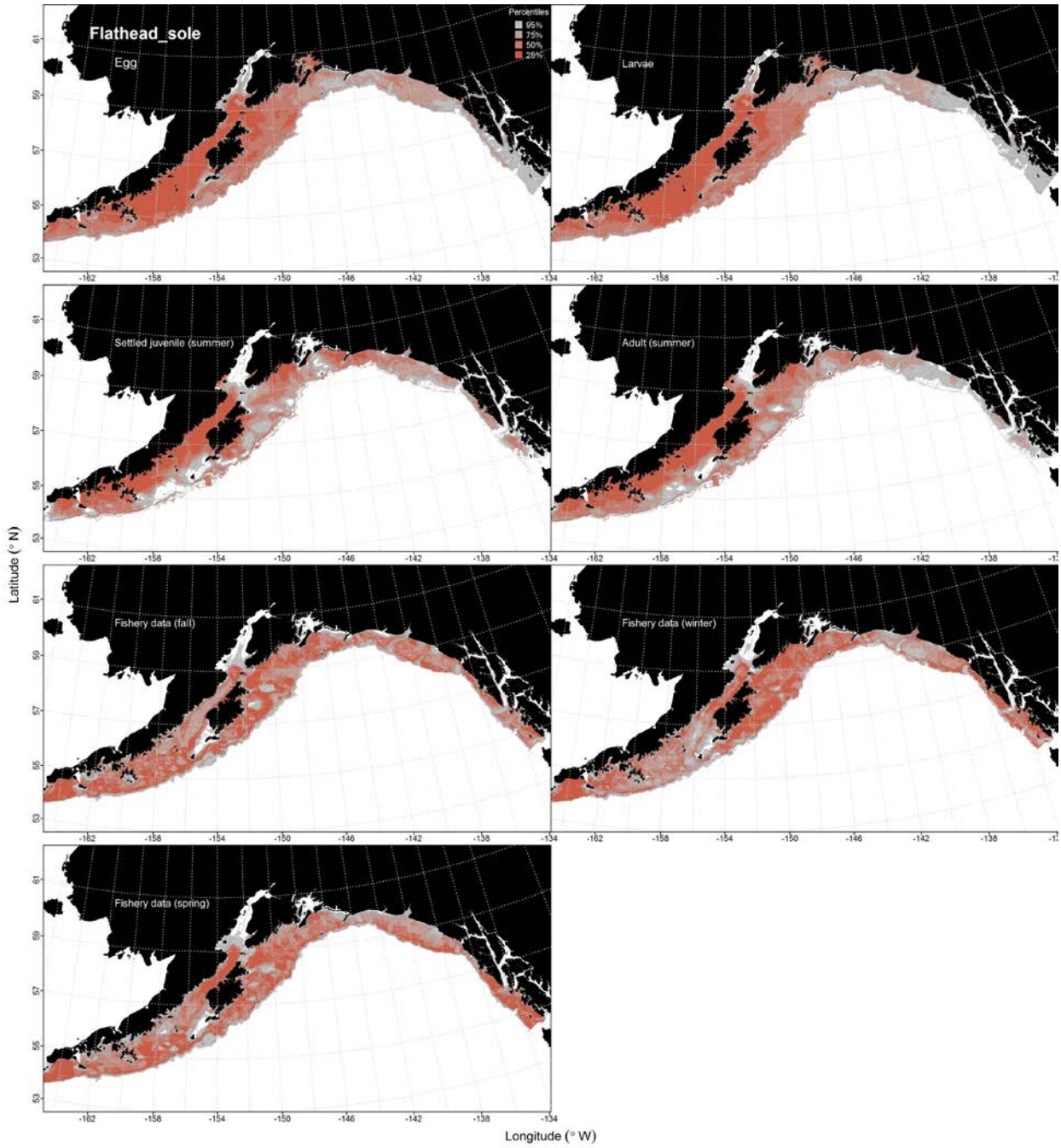

Figure 30. -- Habitat predicted for flathead sole eggs and pelagic larvae from EcoFOCI ichthyoplankton surveys (1991-2012), settled juveniles and adults from RACE-GAP summertime bottom trawl surveys (1993-2013), and predicted from presence in commercial fishery catches (2001-2015) from fall, winter, and spring in the Gulf of Alaska.

Northern Rock Sole (*Lepidopsetta polyxystra*)

Early life history stages of northern rock sole -- There were no observations of northern rock sole (NRS) eggs in the in the EcoFOCI collections.

There were 1,742 instances of larval NRS observed in the EcoFOCI collections, most of which were from the central and western GOA (Fig. 31). The most important variables in the MaxEnt model were surface temperature and bottom depth (relative importance: 0.52 and 0.26, respectively). The AUC for the training data was 0.89 and 0.77 for the testing data. The model correctly classified 80% of the predictions from the training and 77% of the predictions from the test data. The model predicted probable suitable habitat for larval NRS throughout the central and western GOA (Fig. 31).

There was a single instance of pelagic juvenile NRS in the EcoFOCI collections (Fig. 32), which was insufficient to populate a MaxEnt model.

Juvenile and adult northern rock sole distribution in the bottom trawl survey-- The catch of NRS in summer bottom trawl surveys indicates they are broadly distributed throughout the central and western GOA (Fig. 33). The first step of the hGAM used presence-absence data to predict the probability of settled juvenile NRS across the GOA had an AUC of 0.96 for the training data and 0.94 for the test data. Geographic location, ocean color, and bottom current speed were the most important variables in the model (Fig. 33). The PA GAM correctly classified 90% of the training data and 88% of the test data. The model predicted the highest probability of presence in the central GOA, around Kodiak; and in the western GOA, around the Shumagin and Unimak islands (Fig. 33). Geographic location and slope were the most important variables in the CPUE GAM. The model

explained 32% of the variance in the training data and 24% in the test data. The model predicted high CPUE in the western GOA, around the Alaska Peninsula and Unimak Island (Fig. 33).

An hGAM was used to predict the distribution of adult NRS abundance. The AUC for the PA GAM was 0.95 for the training data and 0.94 for the test data. Geographic location and bottom temperature were the most important variables explaining the abundance of adult NRS. The model correctly classified 92% of the predictions from the training and 91% of the predictions from the test data. Adult NRS were predicted to occur in the central GOA, around Kodiak; and in the western GOA, along the Alaska Peninsula (Fig. 34). The CPUE GAM found that bottom depth and maximum tidal current were the most important were the most important determinants of CPUE. Overall, the CPUE GAM explained 30% of the variability in the training data and 24% in the test data. The model predicted the highest CPUE in nearshore waters off Unimak Island and the Alaska Peninsula (Fig. 34).

Rock sole distribution in commercial fisheries

Northern and southern rock sole are not well distinguished in the commercial fisheries VOE-CIA database (D. Stevenson, AFSC, personal communication). Thus, these two species were considered as a generic group, *Lepidopsetta* spp., for seasonal modeling using MaxEnt methods. The distribution of rock sole in commercial fisheries catches was consistent throughout all seasons, with most occurring in the central and western GOA. In the fall, bottom depth and ocean color were the most important model variables (relative importance was 0.37 and 0.26, respectively). The AUC of the fall MaxEnt model was 0.94 for the training data and 0.81 for the testing data. The model correctly classified 87% of the predictions from the training data and 81% of the predictions from the

testing observations. The model predicted suitable habitat of rock sole was concentrated near Kodiak and Unimak Islands (Fig. 35).

In the winter, bottom depth, maximum tidal current, and ocean color and were the most important model variables (relative importance was 0.46, 0.23 and 0.14, respectively). Most catches were in the central GOA (Fig. 36). The AUC of the fall MaxEnt model was 0.93 for the training data and 0.83 for the testing data. The model correctly classified 86% of the predictions from the training data and 83% of the predictions from the test data. Suitable habitat was predicted in the central GOA, on Portlock and Albatross banks, as well as in the western GOA, on Davidson Bank (Fig. 36).

In the spring, ocean color, bottom depth, and maximum tidal current were the most important model variables (relative importance was 0.38, 0.27 and 0.15, respectively). Most of the catches were in the central and western GOA (Fig. 37). The AUC of the spring MaxEnt model was 0.91 for the training data and 0.83 for the testing data. The model correctly classified 83% of the predictions from both the training and testing data. The model predicted suitable habitat in the central GOA, on Albatross Banks, and in the western GOA, along Davidson Bank (Fig. 37).

Northern rock sole essential fish habitat maps and conclusions-- The MaxEnt-predicted probabilities of suitable habitat for larval northern rock sole and commercially harvested *Lepidopsetta* spp. indicate that their potential habitat extends throughout the GOA study area from southeast Alaska to the western Gulf (Fig. 38). Predictions of settled juvenile and adult habitat were constrained to areas in Kamishak Bay, to the west, south, and southeast of Kodiak Island, and to portions of the western GOA from the Shumagin Islands westward. The predicted distribution of larval northern rock sole habitat may reflect the pelagic nature of this life stage. In the bottom trawl survey data, the eastern limit of northern rock sole distribution is found in the central GOA east of

Kodiak Island. However, habitat distribution predicted from presence in commercial catches extends beyond there to the southeastern limit of the survey area. This may be due, in part, to combining northern and southern rock sole in the commercial fishery data used to populate the SDMs.

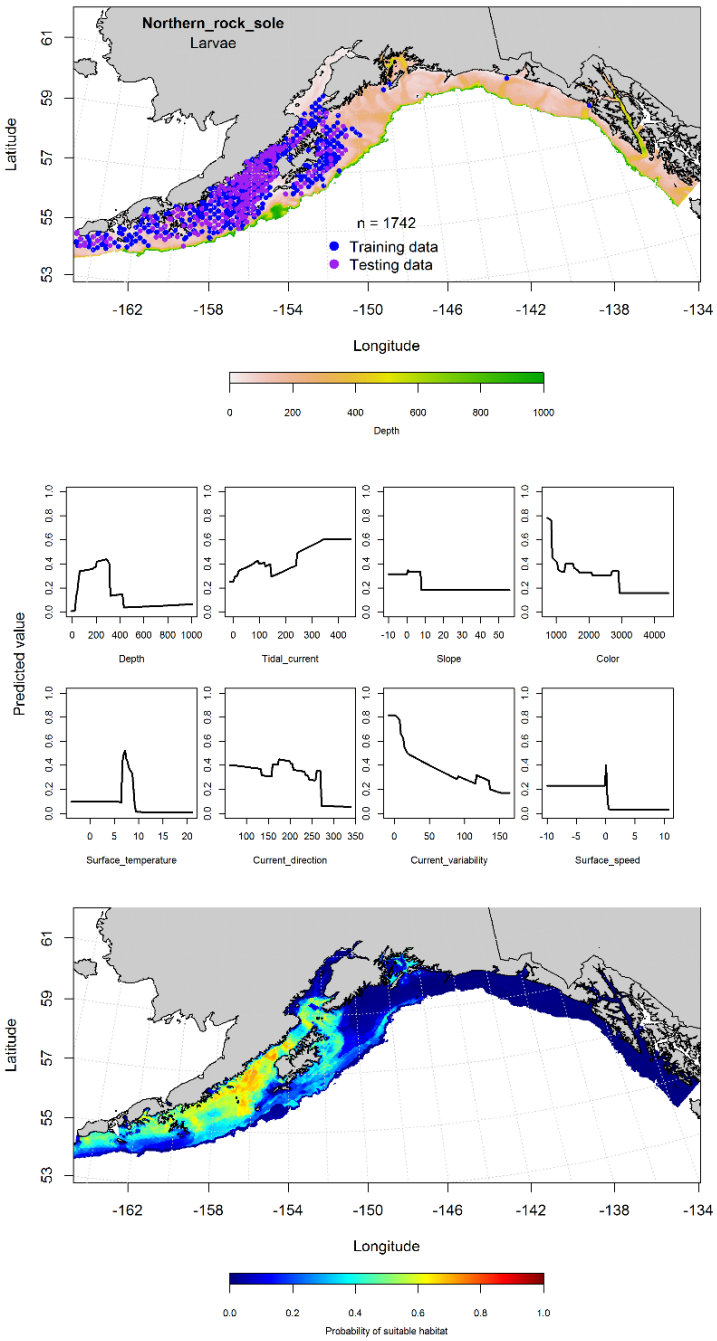

Figure 31. -- Distribution of pelagic northern rock sole larvae observations from EcoFOCI ichthyoplankton surveys (April-September 1991-2012) in the Gulf of Alaska (top panel) with training (blue dots) and testing (purple dots) data indicated, maximum entropy (MaxEnt) model effects (center panel), and the predicted probability of suitable pelagic northern rock sole larval habitat (bottom panel).

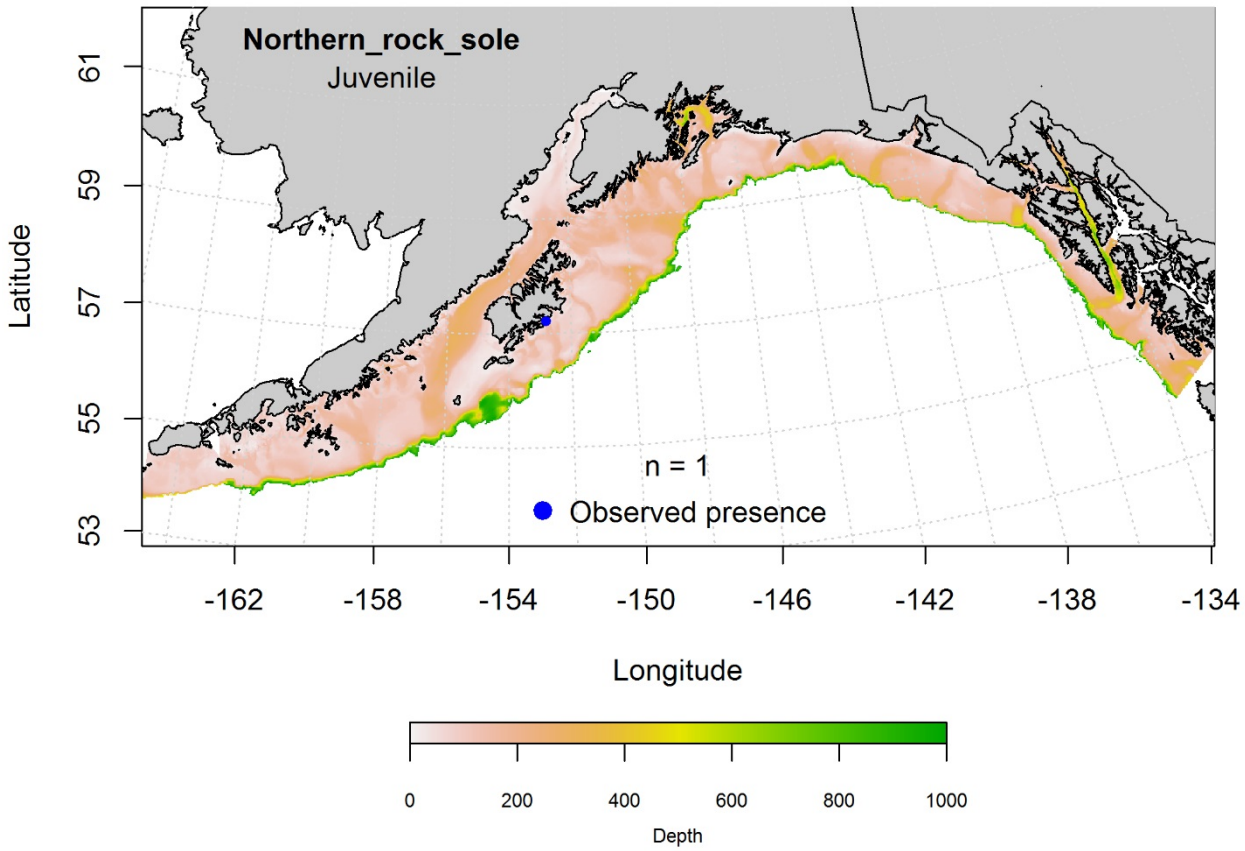

Figure 32. -- Distribution of pelagic juvenile northern rock sole observations from EcoFOCI ichthyoplankton surveys (April-September 1991-2012) in the Gulf of Alaska.

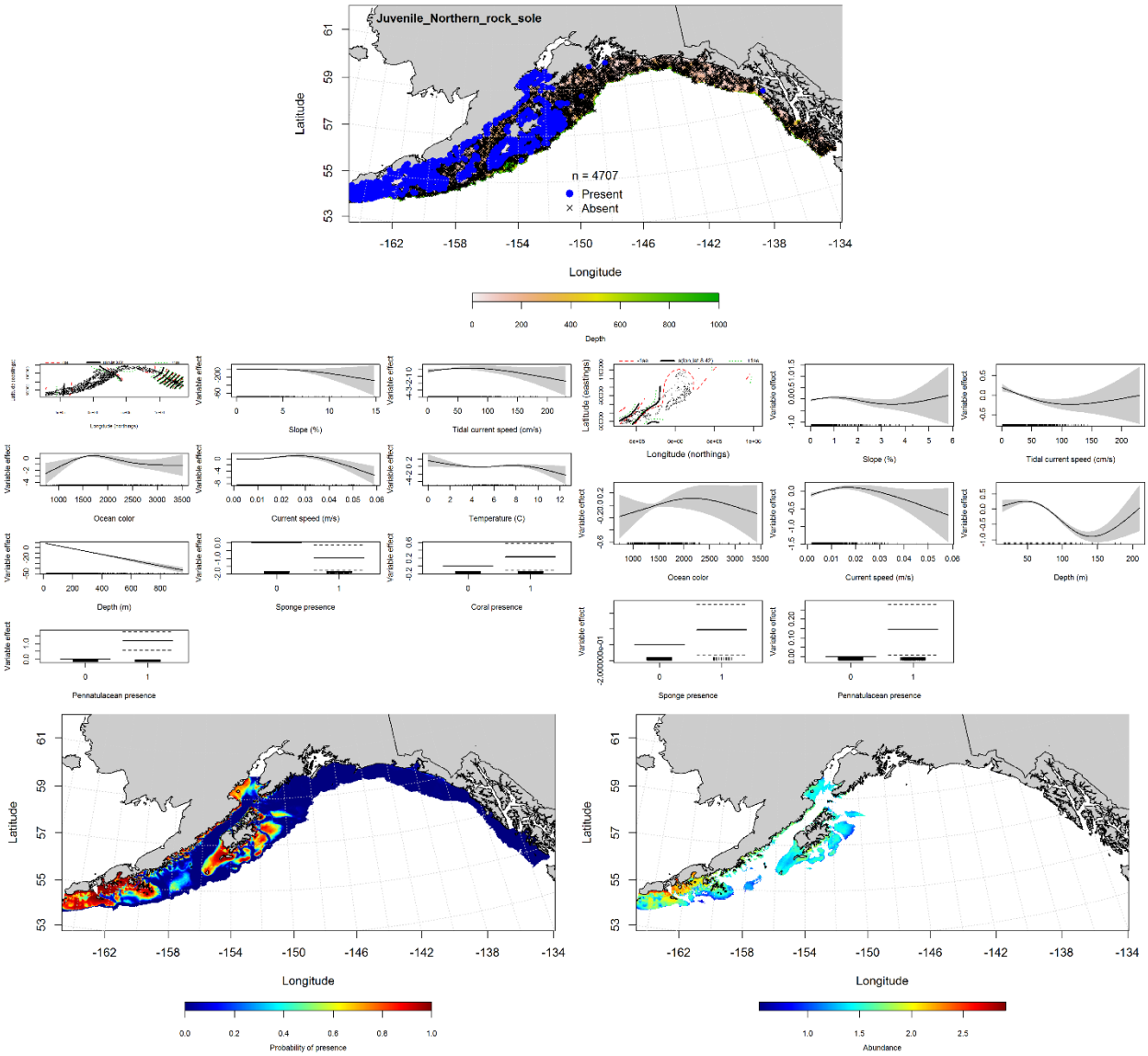

Figure 33. -- Distribution of settled juvenile northern rock sole in 1993-2013 RACE-GAP summer bottom trawl surveys conducted in the Gulf of Alaska (upper panel). Effects of retained habitat covariates in the best fitting generalized additive presence-absence models (PA GAM); left center panel) and abundance (CPUE GAM; right center panel). Predicted spatial distribution of the probability of presence (bottom left panel) and abundance of settled juvenile northern rock sole based on the models (bottom right panel).

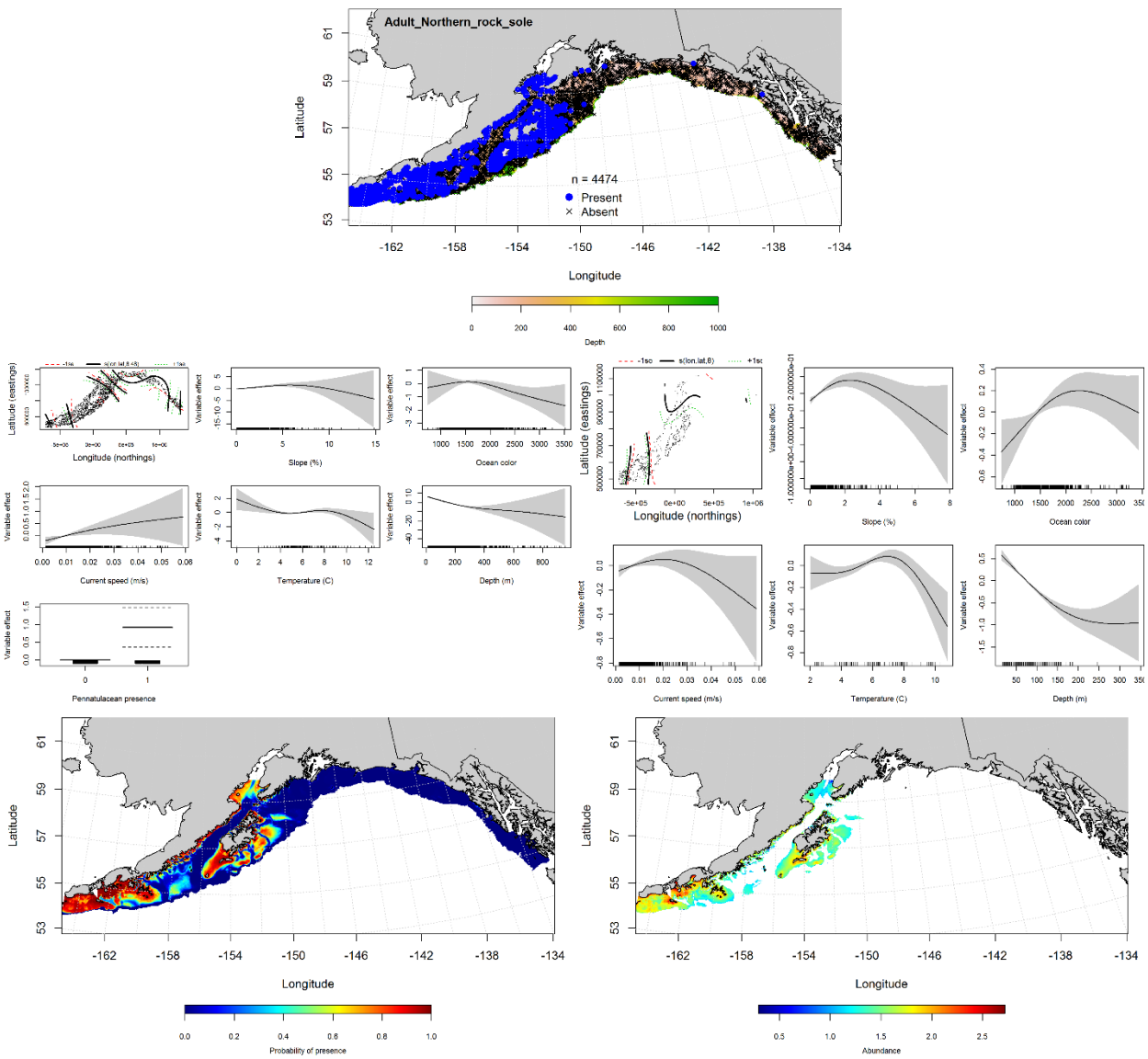

Figure 34. -- Distribution of adult northern rock sole in 1993-2013 RACE-GAP summer bottom trawl surveys conducted in the Gulf of Alaska (upper panel). Effects of retained habitat covariates in the best fitting generalized additive presence-absence models (PA GAM; left center panel) and abundance (CPUE GAM; right center panel). Predicted spatial distribution of the probability of presence (bottom left panel) and abundance of adult northern rock sole based on the models (bottom right panel).

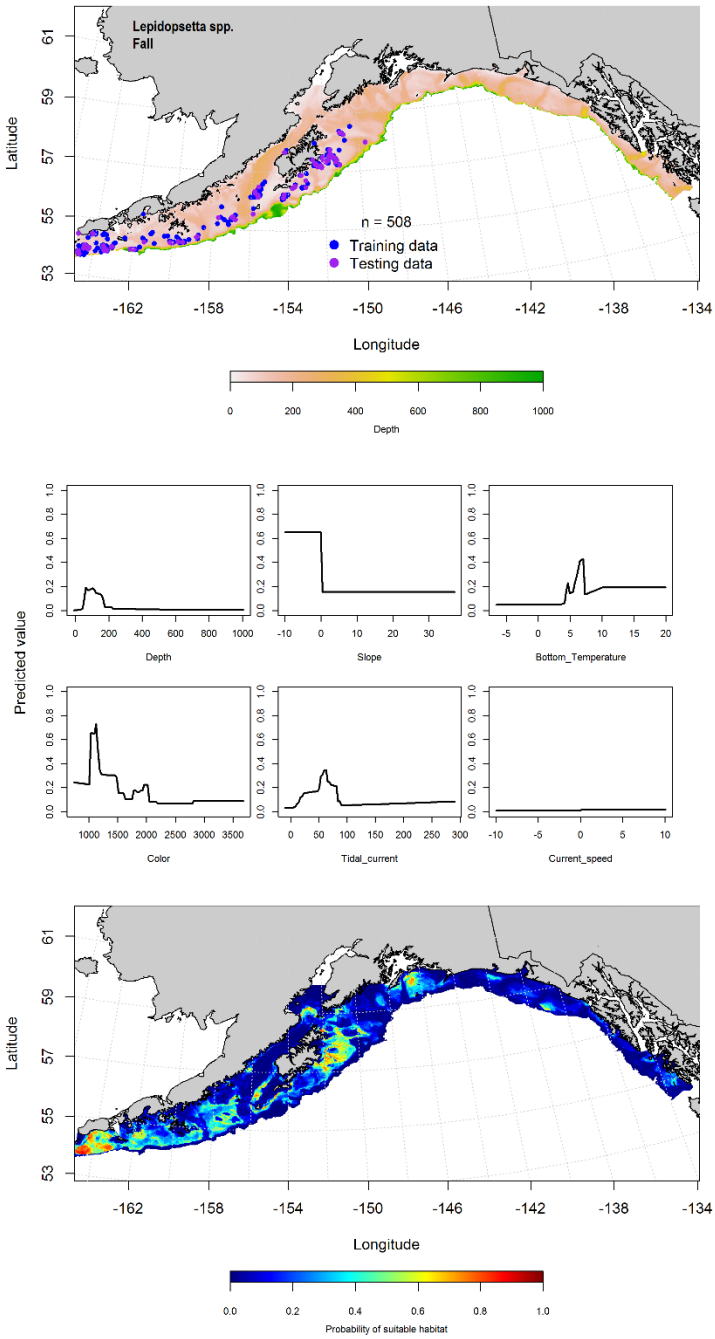

Figure 35. -- Locations of rock sole (*Lepidopsetta* spp.) from fall (September-November 2001-2015) commercial fisheries catches in the Gulf of Alaska (top panel), MaxEnt model effects (middle panels), and predicted probability of suitable habitat for rock sole based on the model (bottom panel).

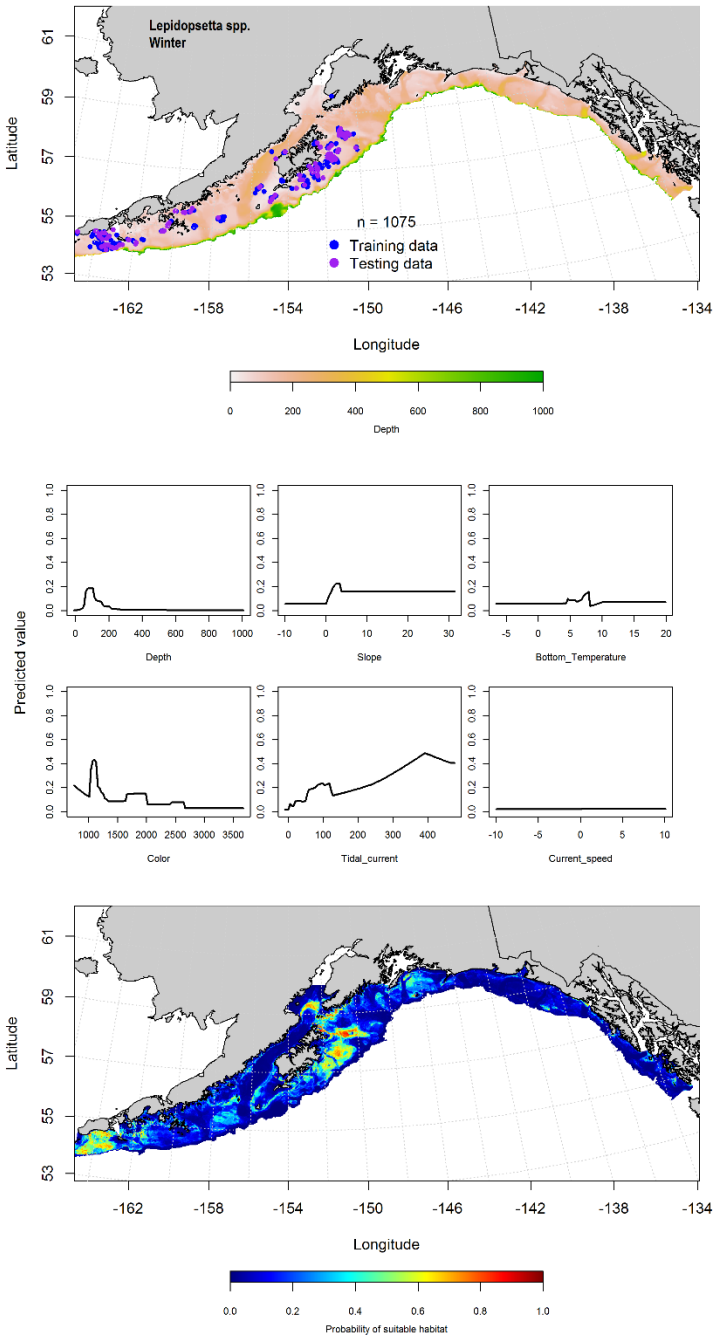

Figure 36. -- Locations of rock sole (*Lepidopsetta* spp.) from winter (December-February 2001-2015) commercial fisheries catches in the Gulf of Alaska (top panel), with training (blue dots) and testing (purple dots) data indicated, maximum entropy (MaxEnt) model effects (center panel), and the predicted probability of suitable rock sole habitat (bottom panel).

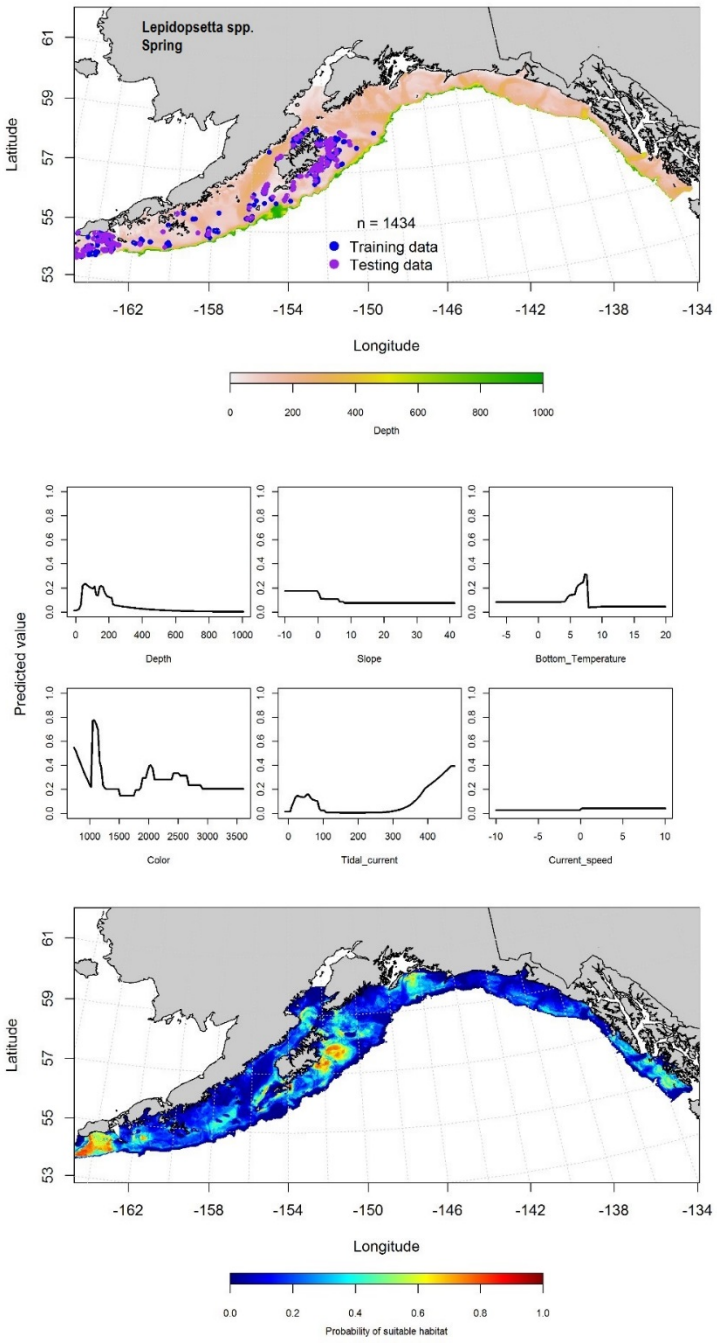

Figure 37. -- Locations of rock sole *(Lepidopsetta* spp.) from spring (March-May 2001-2015) commercial fisheries catches in the Gulf of Alaska (top panel), with training (blue dots) and testing (purple dots) data indicated, maximum entropy (MaxEnt) model effects (center panel), and the predicted probability of suitable rock sole habitat (bottom panel).

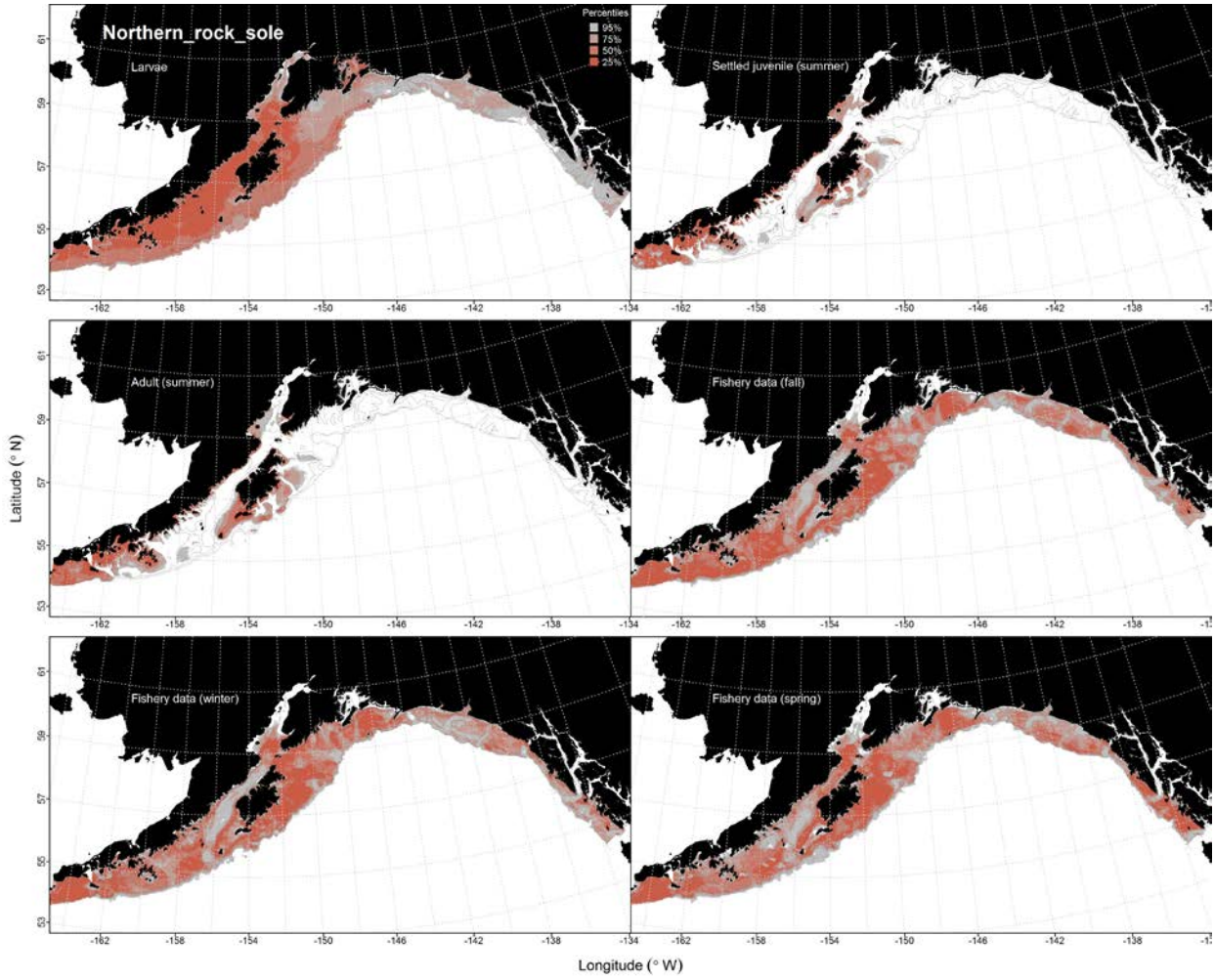

Figure 38. -- Habitat predicted for northern rock sole pelagic larvae from EcoFOCI ichthyoplankton surveys (1991-2012), settled juveniles and adults from RACE-GAP summertime bottom trawl surveys (1993-2013), and predicted from presence in commercial fishery catches (2001-2015) from fall, winter, and spring in the Gulf of Alaska.

Southern Rock Sole (*Lepidopsetta bilineata*)

Early life history stages of southern rock sole -- There were no observations of southern rock sole eggs in the in the EcoFOCI collections.

There were 1,426 instances of larval southern rock sole (SRS) observed in the EcoFOCI collections, most of which were from the central and western GOA (Fig. 39). The most important variables in the MaxEnt model were surface temperature and bottom depth (relative importance: 0.52 and 0.26, respectively). The AUC was 0.89 for the training data and 0.77 for the testing data. The model correctly classified with 80% percent of the predictions from the training data and 77% of the predictions from the test data. Predicted suitable habitat for larval SRS was concentrated in central and western GOA (Fig. 39).

There were no observations of pelagic juvenile SRS in the EcoFOCI collections.

Juvenile and adult southern rock sole distribution in the bottom trawl survey -- Distribution of settled juvenile SRS was modeled using an hGAM. The PA GAM indicated that geographic position, bottom current speed, and bottom temperature were the most important variables included in the model. The AUC of model was 0.92 for both the training and testing data. The model correctly classified 86% of the predictions from the training data and 85% of the predictions form the test data. The areas of predicted highest presence were concentrated in the central and western GOA, as well as in nearshore waters off southeast Alaska (Fig. 40). The CPUE GAM found geographic location, bottom depth, and maximum tidal current speed were the most important determinants of CPUE. Overall, the hGAM explained 23% of the variability of the training data set and 15% of the test data set. The model predicted the highest CPUE in the central GOA were around Kodiak while, in western GOA, they were near the Shumagin Islands (Fig. 40).

A GAM predicting the abundance of adult SRS explained 53% of the variability in the CPUE for the training data, and 48% of the variability for the test data. Geographic location, bottom depth, ocean color, and bottom temperature were the most important variables explaining the catch of adult SRS. The model predicted distributions of adult SRS were similar to those of settled juvenile SRS, and the highest catches were predicted to be concentrated around Kodiak and near the Shumagin Islands (Fig. 41).

Southern rock sole distribution in commercial fisheries -- Since observations of northern and southern rock sole are not well distinguished in the commercial fisheries observer database, the combined results for these species are reported above with northern rock sole.

Southern rock sole essential fish habitat maps and conclusions -- Predicted habitat for pelagic larval southern rock sole encompassed all of the GOA with core habitat centered on Kodiak Island and westward into the Shumagins (Fig. 42). Predicted summertime habitat for settled juvenile SRS was concentrated in the central and western GOA around Kodiak Island and along the Alaska Peninsula (Fig. 42). Predicted summertime habitat of adult SRS was more widely distributed than that of the settled juveniles, though there were common areas of high abundance (Fig. 42).

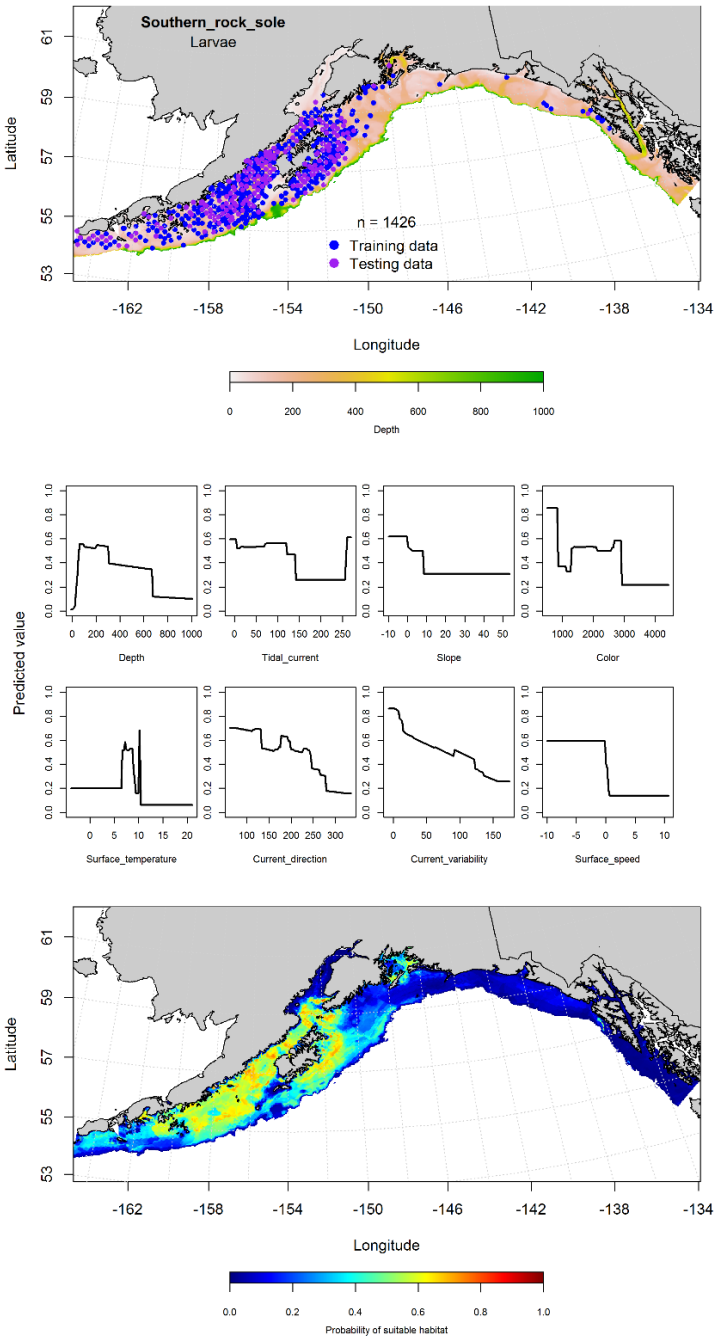

Figure 39. -- Distribution of pelagic southern rock sole larvae observations from EcoFOCI ichthyoplankton surveys (April-September 1991-2012) in the Gulf of Alaska (top panel) with training (blue dots) and testing (purple dots) data indicated, maximum entropy (MaxEnt) model relationships between probability of pelagic juvenile presence and habitat covariates (center panel), and the predicted probability of suitable pelagic southern rock sole larval habitat (bottom panel).

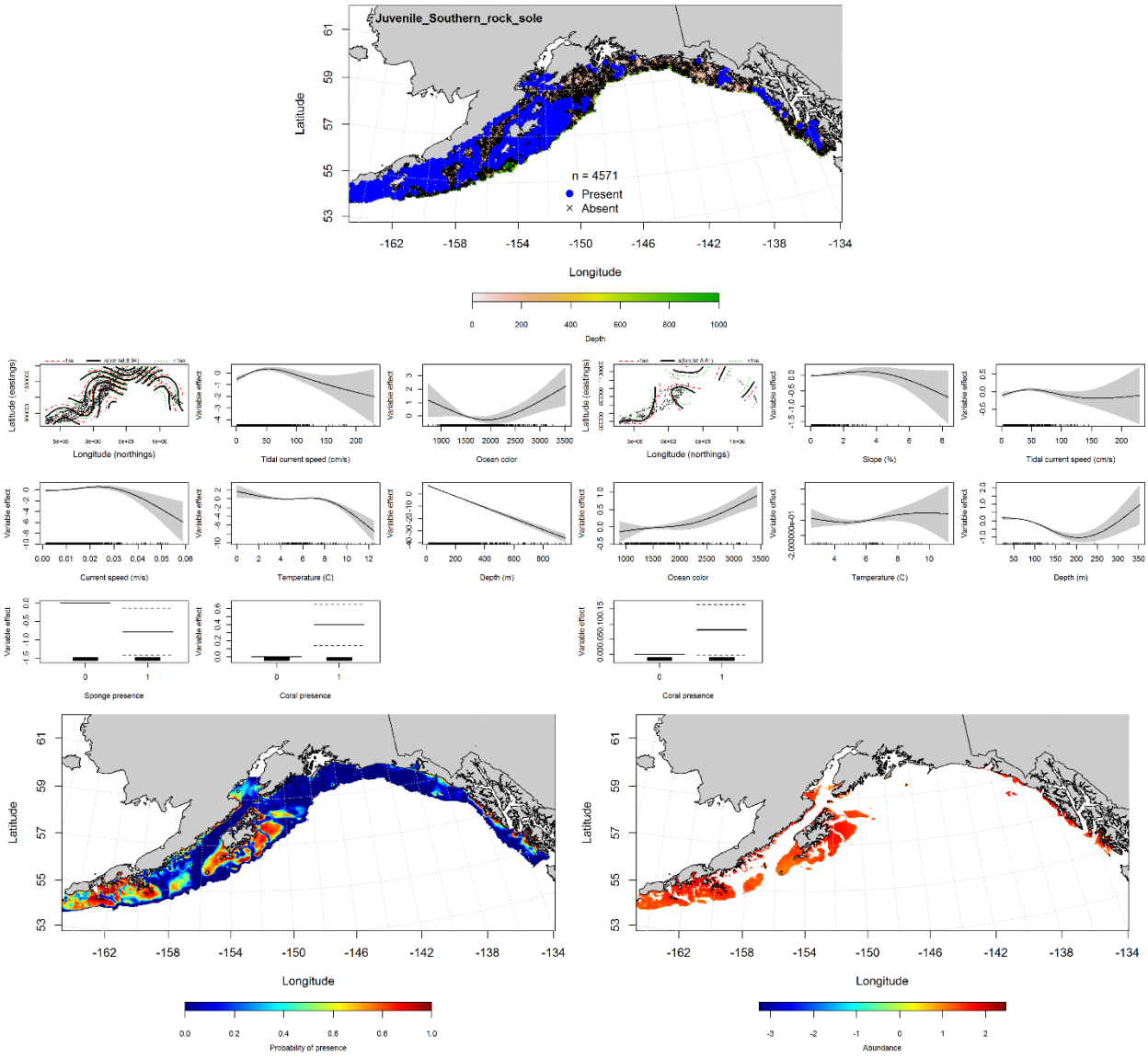

Figure 40. -- Distribution of settled juvenile southern rock sole in 1993-2013 RACE-GAP summer bottom trawl surveys conducted in the Gulf of Alaska (upper panel). Effects of retained habitat covariates in the best fitting generalized additive presence-absence models (PA GAM; left center panel) and abundance (CPUE GAM; right center panel). Predicted spatial distribution of the probability of presence (bottom left panel) and abundance of settled juvenile southern rock sole based on the models (bottom right panel).

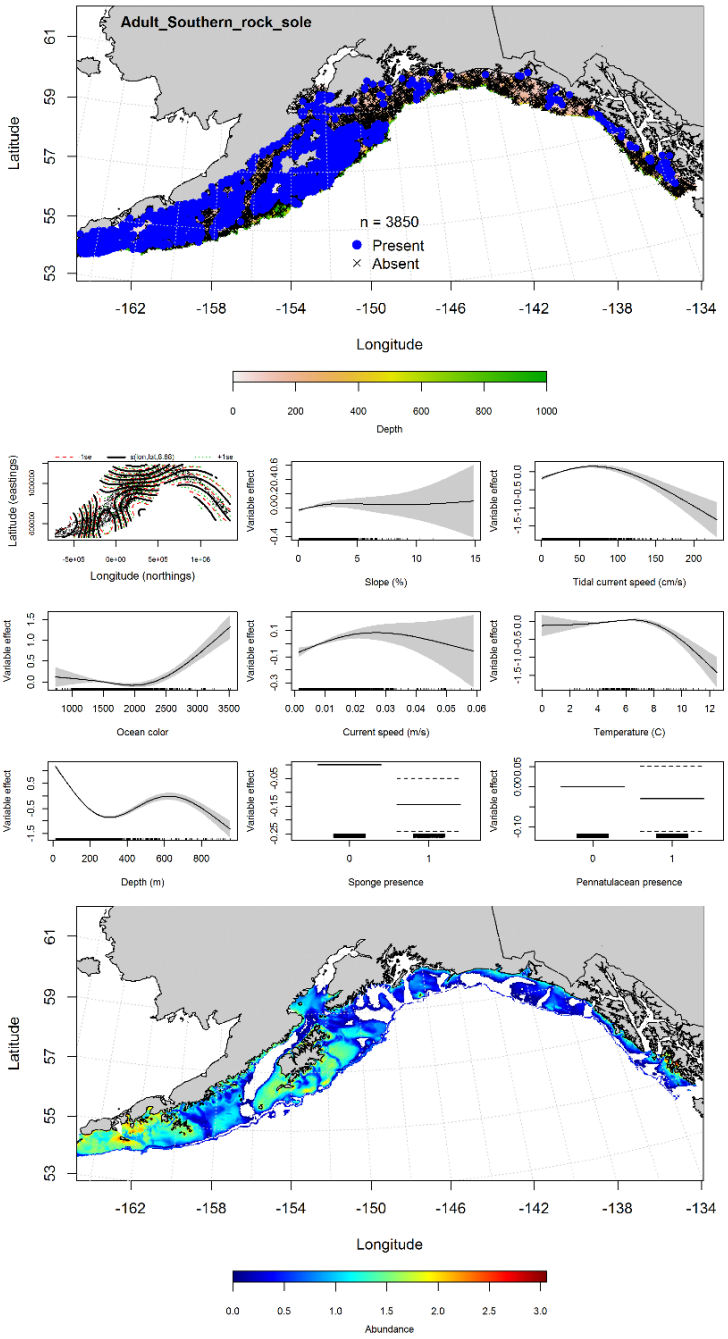

Figure 41. -- Presence of adult southern rock sole from RACE-GAP summer bottom trawl surveys (1993-2013) in the Gulf of Alaska (top panel) with training (blue dots) and testing (purple dots) data indicated, generalized additive model (GAM) effects (center panel), and the GAM-predicted abundance of adult southern rock sole (bottom panel).

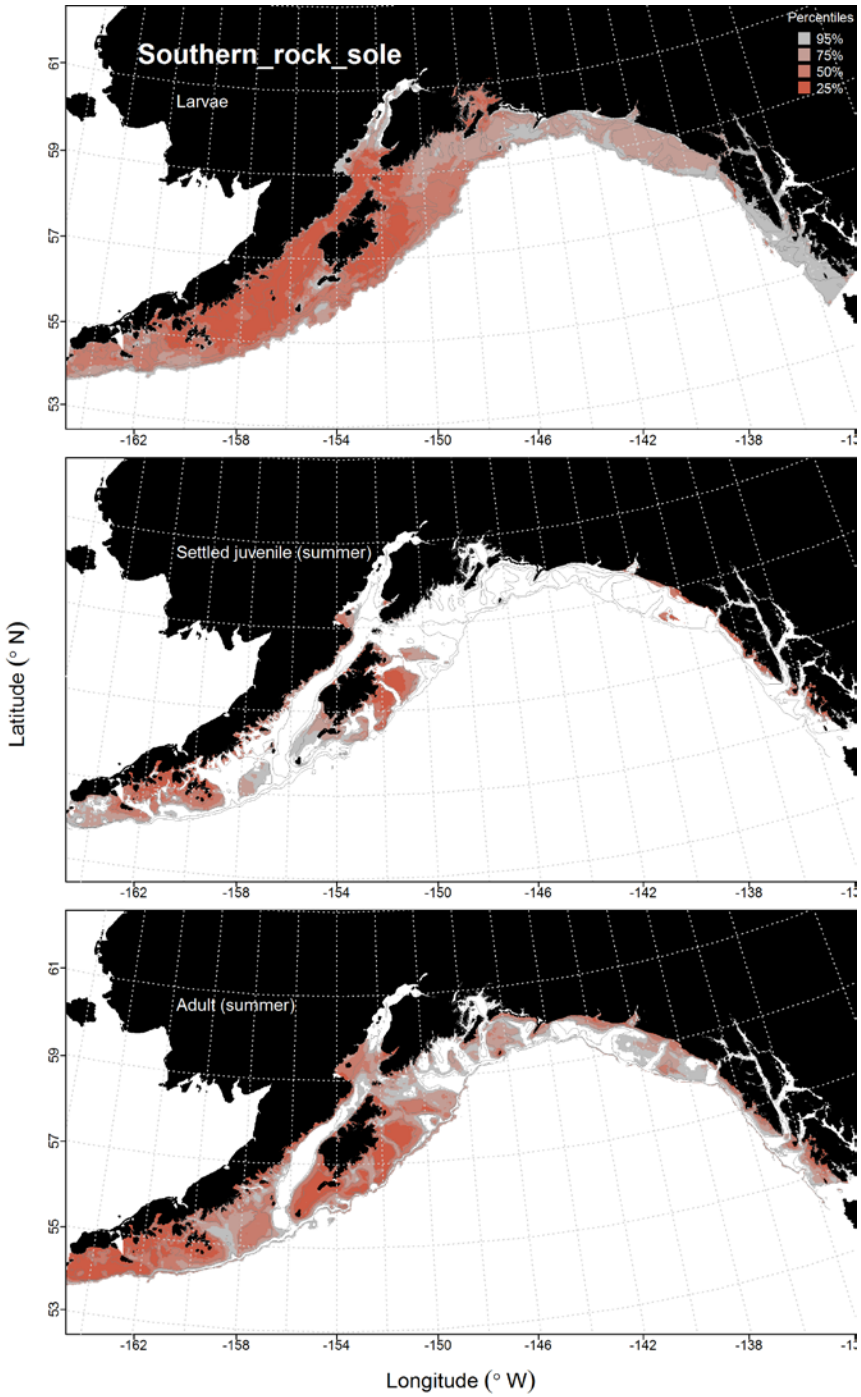

Figure 42. -- Habitat predicted for southern rock sole pelagic larvae from EcoFOCI ichthyoplankton surveys (1991-2012), settled juveniles and adults from RACE-GAP summertime bottom trawl surveys (1993-2013) in the Gulf of Alaska.

Yellowfin Sole (*Limanda aspera*)

Early life history stages of yellowfin sole -- There were 107 instances of yellowfin sole eggs observed in the EcoFOCI collections (Fig. 43); most from the central and western GOA. Surface temperature, ocean color, and bottom depth were the important variables predicting probability of suitable yellowfin sole egg habitat (relative importance: 0.23, 0.21, and 0.18, respectively). The AUC for the MaxEnt model was 0.96 for the training data and 0.90 for the test data. The model correctly classified 89% percent of the predictions from the training data and 90% of the predictions from the test data. The predicted suitable habitat for yellowfin sole eggs was in nearshore waters around Kodiak and the Alaska Peninsula (Fig. 43).

There were no observations of either larval or pelagic juvenile yellowfin sole in the EcoFOCI collections.

Juvenile and adult yellowfin sole distribution in the bottom trawl survey -- Distributions of settled juvenile and adult yellowfin sole were modeled using a MaxEnt model. The model predicted suitable habitat of settled juvenile yellowfin sole in nearshore waters across the GOA, with higher suitability areas concentrated around Kamishak Bay and the Alaska Peninsula (Fig. 44). The model AUC was 0.95 for the training data (89% correctly classified) and 0.90 for the test data (90% correctly classified). Bottom depth and maximum tidal current were the most important variables explaining the distribution of suitable settled juvenile yellowfin sole habitat (relative importance: 0.70 and 0.15, respectively).

Bottom depth, maximum tidal current, and bottom temperature were the most important factors in the MaxEnt model determining the probability of suitable habitat for adult yellowfin sole (relative importance: 0.58, 0.26, and 0.10, respectively). The model AUC was 0.94 for the training

data and 0.86 for the test data. The model correctly classified 87% of the predictions from the training data and 86% the predictions form the test data. The model predicted suitable habitat for adult yellowfin sole was similar to that of the settled juveniles and centered around Kamishak Bay and the Alaska Peninsula (Fig. 45).

Yellowfin sole distribution in commercial fisheries -- The distribution of adult yellowfin sole in commercial fisheries catches were limited, but spatially consistent throughout all seasons. There was one observation of yellowfin sole during the fall (Fig. 46).

In the winter, there were 49 observations of yellowfin sole, most of which occurred in nearshore waters around Kodiak and Unimak Islands (Fig. 47). These occurrences were insufficient to run a MaxEnt model.

In the spring, there were 23 observations of yellowfin sole, with most occurring around Kodiak and Unimak Islands (Fig. 48). These data were not modeled.

Yellowfin sole essential fish habitat maps and conclusions-- Yellowfin sole egg, settled juvenile, and adult habitat were predicted to be widely distributed throughout the GOA (Fig. 49). Core habitat for these three yellowfin sole life stages overlapped extensively and was found primarily across the shallower portions of inner and middle shelf around Kodiak Island and across the GOA (Fig. 49).

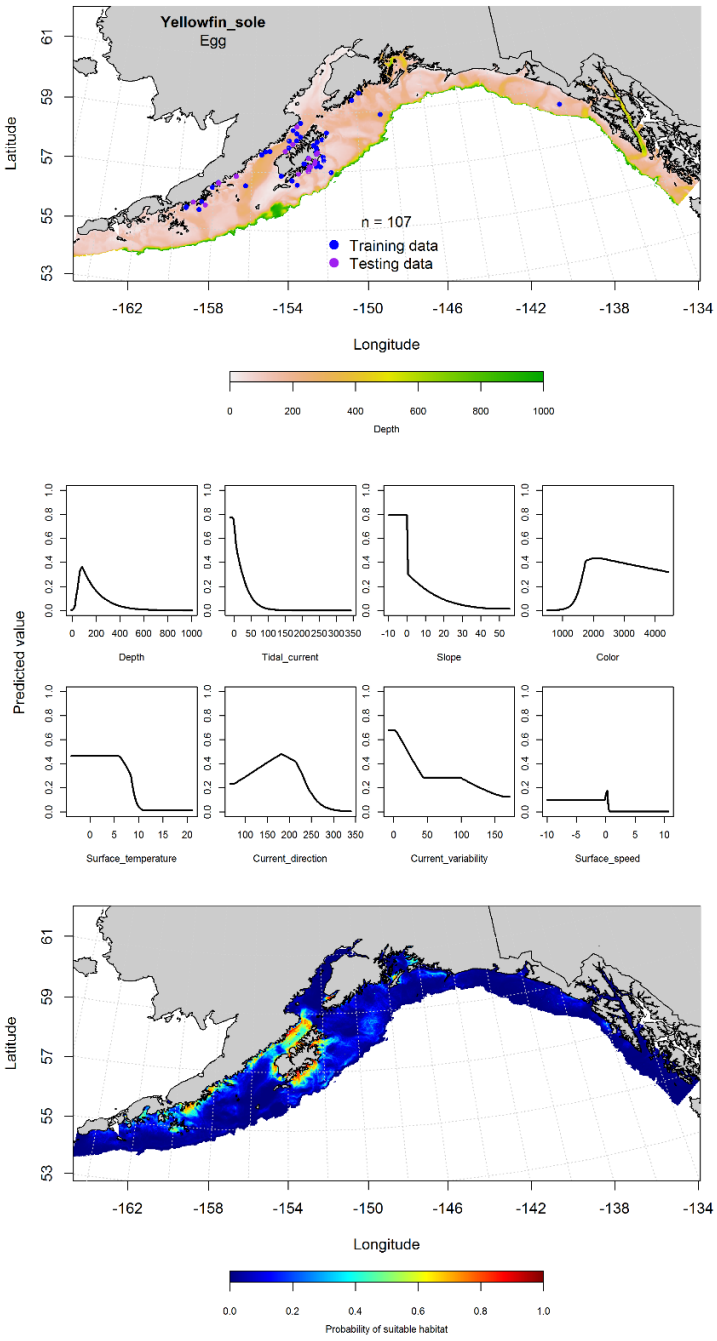

Figure 43. -- Distribution of yellowfin sole eggs from EcoFOCI ichthyoplankton surveys (January-March 1991-2013; top panel) with training (blue dots) and testing (purple dots) data, maximum entropy (MaxEnt) model effects (center panel), and predicted probability of suitable yellowfin sole egg habitat (bottom panel).

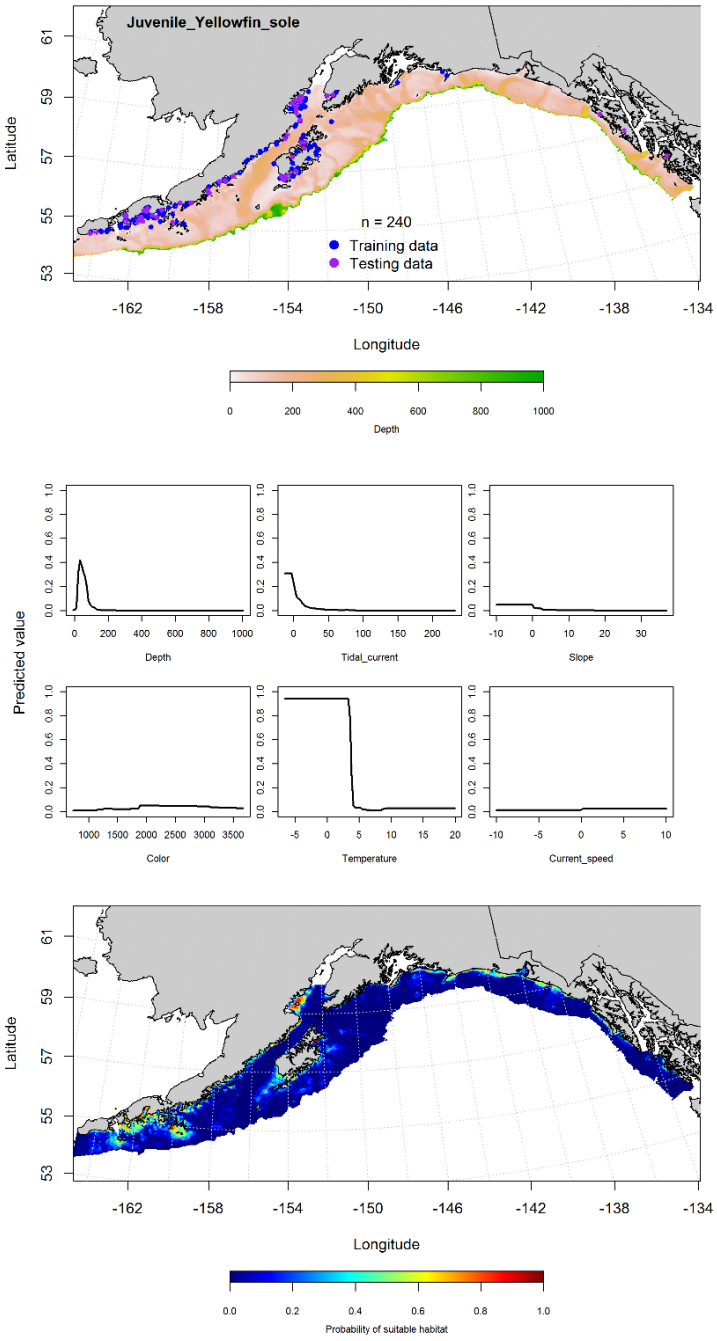

Figure 44. -- Presence of settled juvenile yellowfin sole from RACE-GAP summer bottom trawl surveys (1993-2013) in the Gulf of Alaska (top panel) with training (blue dots) and testing (purple dots) data indicated, maximum entropy (MaxEnt) model effects (center panel), and the MaxEnt-predicted probability of suitable juvenile yellowfin sole habitat (bottom panel).

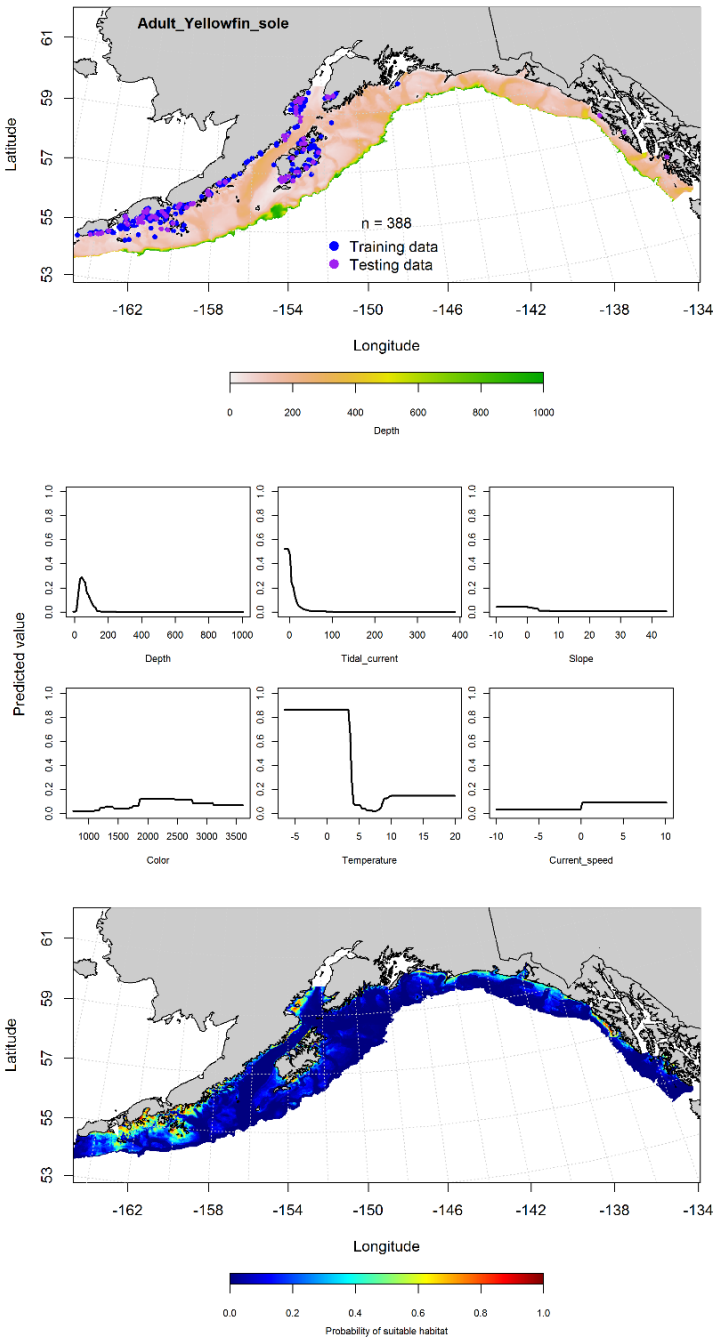

Figure 45. -- Presence of adult yellowfin sole from RACE-GAP summer bottom trawl surveys (1993-2013) in the Gulf of Alaska (top panel) with training (blue dots) and testing (purple dots) data indicated, maximum entropy (MaxEnt) model effects (center panel), and the MaxEnt-predicted probability of suitable adult yellowfin sole habitat (bottom panel).

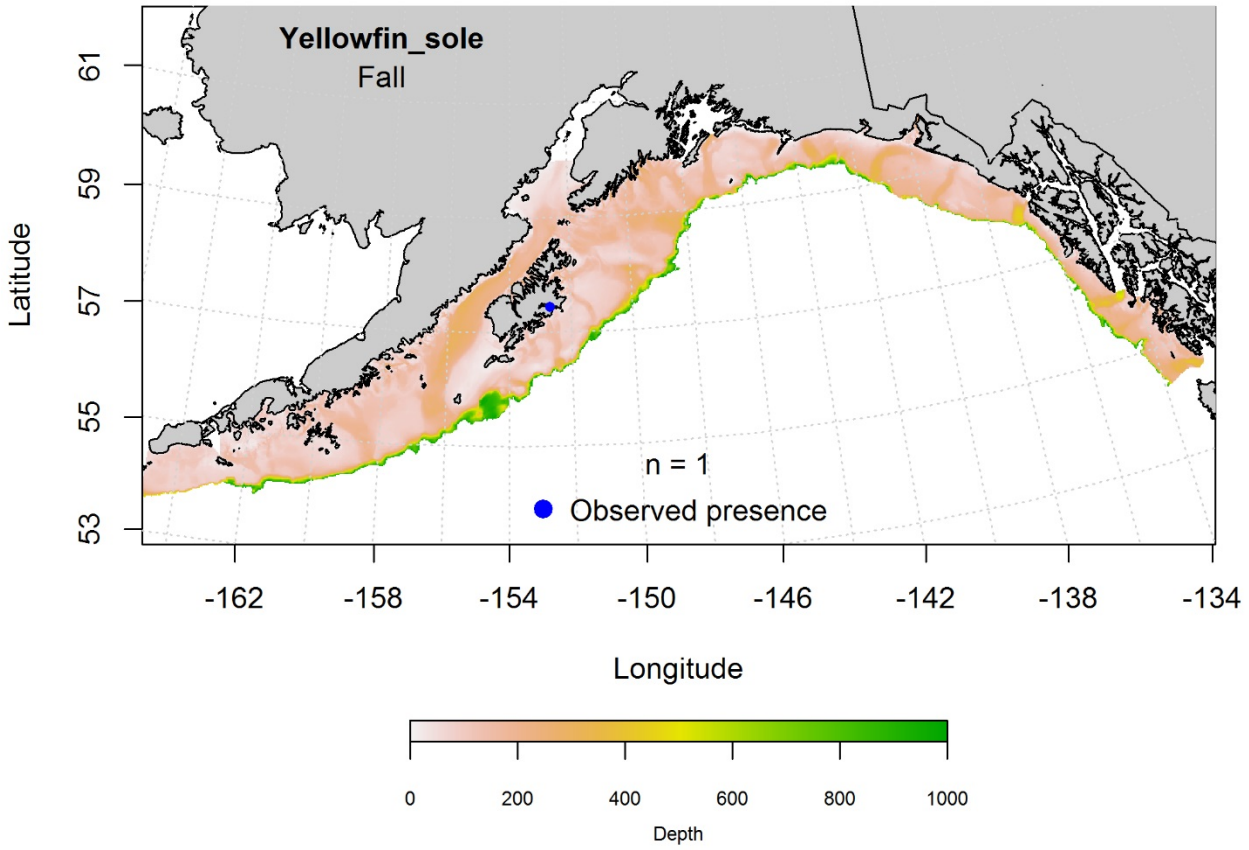

Figure 46. -- Locations of yellowfin sole from fall (September-November 2001-2015) commercial fisheries catches in the Gulf of Alaska.

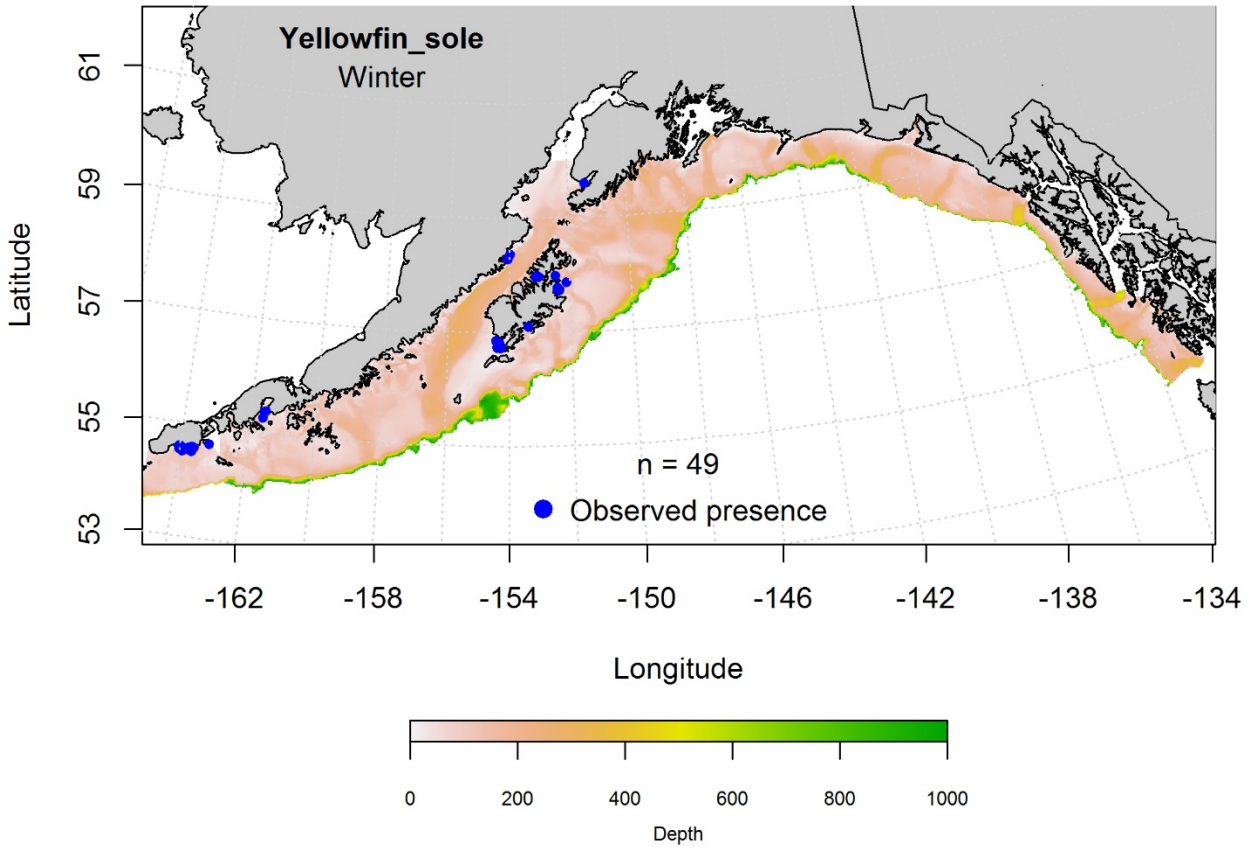

Figure 47. -- Locations of yellowfin sole from winter (December-February 2001-2015) commercial fisheries catches in the Gulf of Alaska.

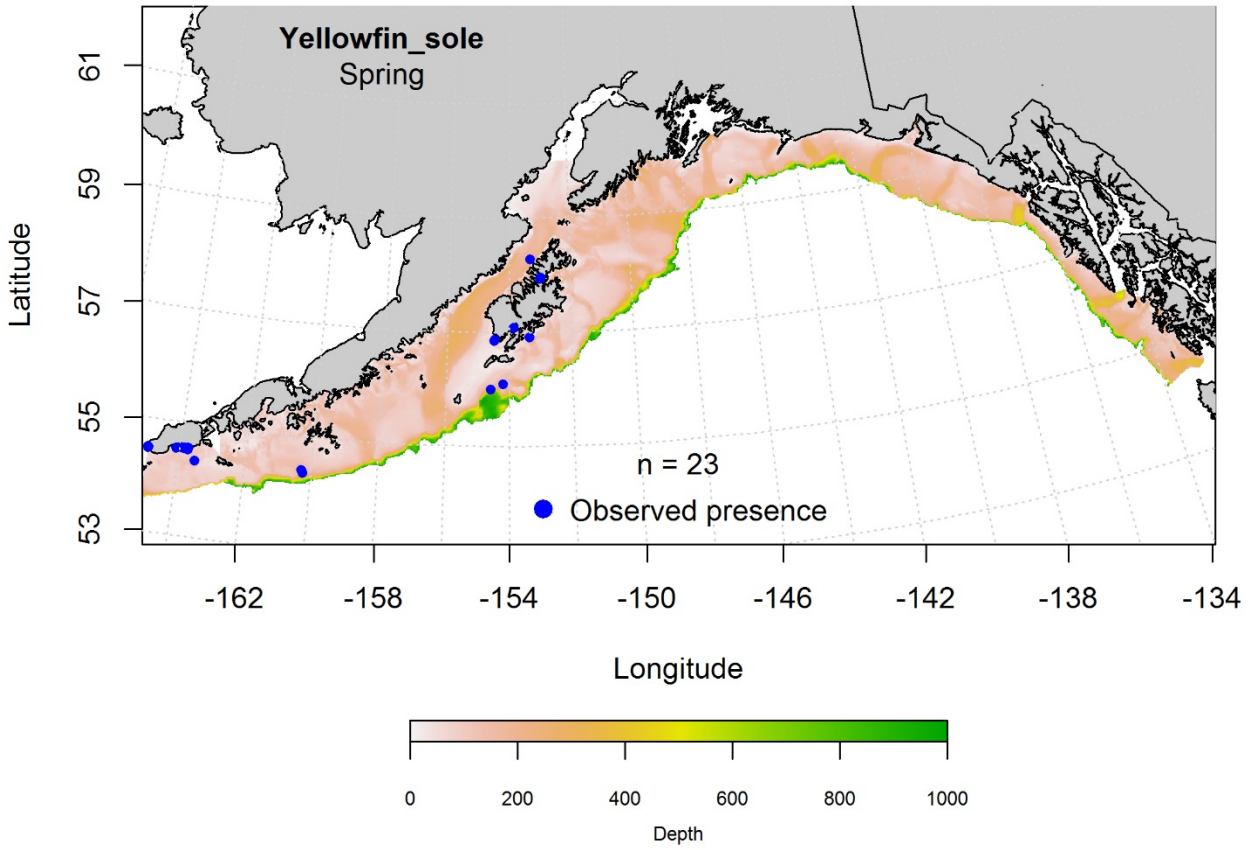

Figure 48. -- Locations of yellowfin sole from spring (March-May 2001-2015) commercial fisheries catches in the Gulf of Alaska.

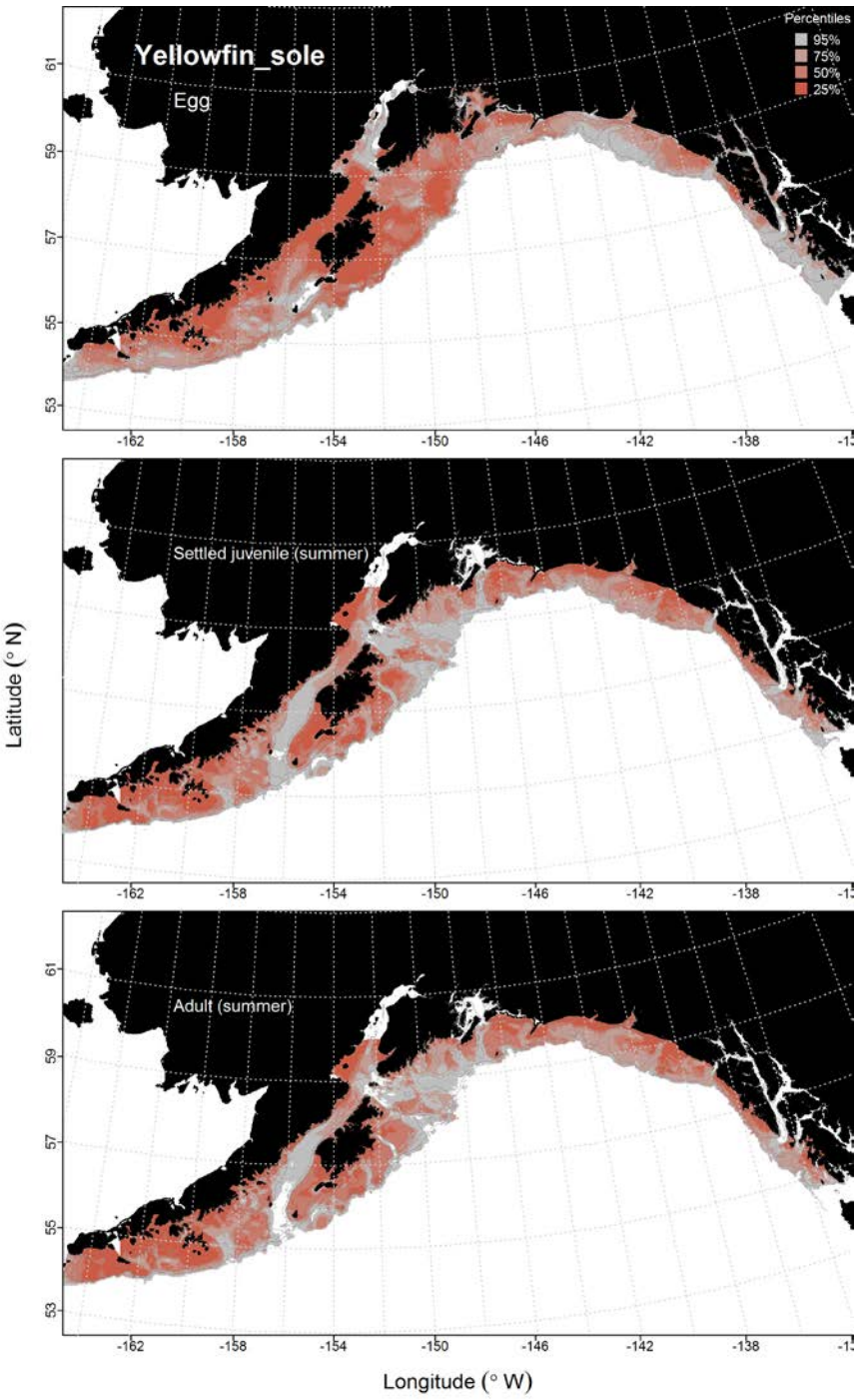

Figure 49. -- Habitat predicted for yellowfin sole eggs from EcoFOCI ichthyoplankton surveys (1991-2012), settled juveniles and adults from RACE-GAP summertime bottom trawl surveys (1993-2013) in the Gulf of Alaska.

Alaska Plaice (*Pleuronectes quadrituberculatus*)

Early life history stages of Alaska plaice -- There were 490 instances of Alaska plaice eggs observed in the EcoFOCI collections (Fig. 50), most from the central and western GOA. The MaxEnt model indicated that surface temperature, bottom depth, and bottom current speed (relative importance: 0.46, 0.32, and 0.11, respectively) were the most important variables determining the probability of suitable Alaska plaice egg habitat. The AUC for the model was 0.95 for the training data and 0.87 for the test data. Eighty-nine percent of the training data and 87% of the test data were correctly classified. The areas of predicted highest probability of suitable habitat were concentrated in Shelikof Strait and Shelikof Gully (Fig. 50).

There were 270 instances of pelagic Alaska plaice larvae in the ECODAAT database, with most of these observations from the central and western GOA (Fig. 51). Surface temperature, bottom depth, and surface current speed were the most important variables explaining the probability of suitable larval Alaska plaice habitat (relative importance: 0.46, 0.32, and 0.11, respectively). The AUC of the MaxEnt model was 0.91 for the training data and 0.81 for the test data set. The model predicted suitability of larval Alaska plaice habitat was highest along the Alaska Peninsula (Fig. 51).

There were no observations of pelagic juvenile Alaska plaice in the EcoFOCI collections.

Juvenile and adult Alaska plaice distribution in the bottom trawl survey -- There were no observations of settled juvenile Alaska plaice during the summer bottom trawl surveys.

A MaxEnt model was used to predict the probability of suitable habitat for adult Alaska plaice. The AUC of the model was 0.91 for the training data and 0.86 for the test data. The model correctly classified 84% of the predictions from the training data and 86% of the predictions from the

test data. The most important variables in the model were bottom depth and maximum tidal current (relative importance: 0.57 and 0.26, respectively). The highest probability of suitable habitat for adult Alaska plaice occurred in shallower areas of eastern GOA, including off Baranof and Chichagof islands; as well as in the western GOA, around the Shumagin Islands (Fig. 52).

Alaska plaice distribution in commercial fisheries -- Commercial fisheries catches of Alaska plaice in the GOA were limited, but spatially consistent throughout all seasons. In the fall, there were two observations of Alaska plaice (Fig. 53). In the winter, there were 15 observations of Alaska plaice, mostly from around Kodiak and the Shumagin islands (Fig. 54). In the spring, there were 37 observations of Alaska plaice, with most occurring around Kodiak (Fig. 55). There were, however, an insufficient number of observations to model any commercial catch data.

Alaska plaice essential fish habitat maps and conclusions-- In general, Alaska plaice egg and pelagic larval habitat were broadly distributed throughout the central and western GOA (Fig. 56), whereas adult Alaska plaice habitat was concentrated in shallower portions of inner and middleshelf throughout the GOA (Fig. 56).

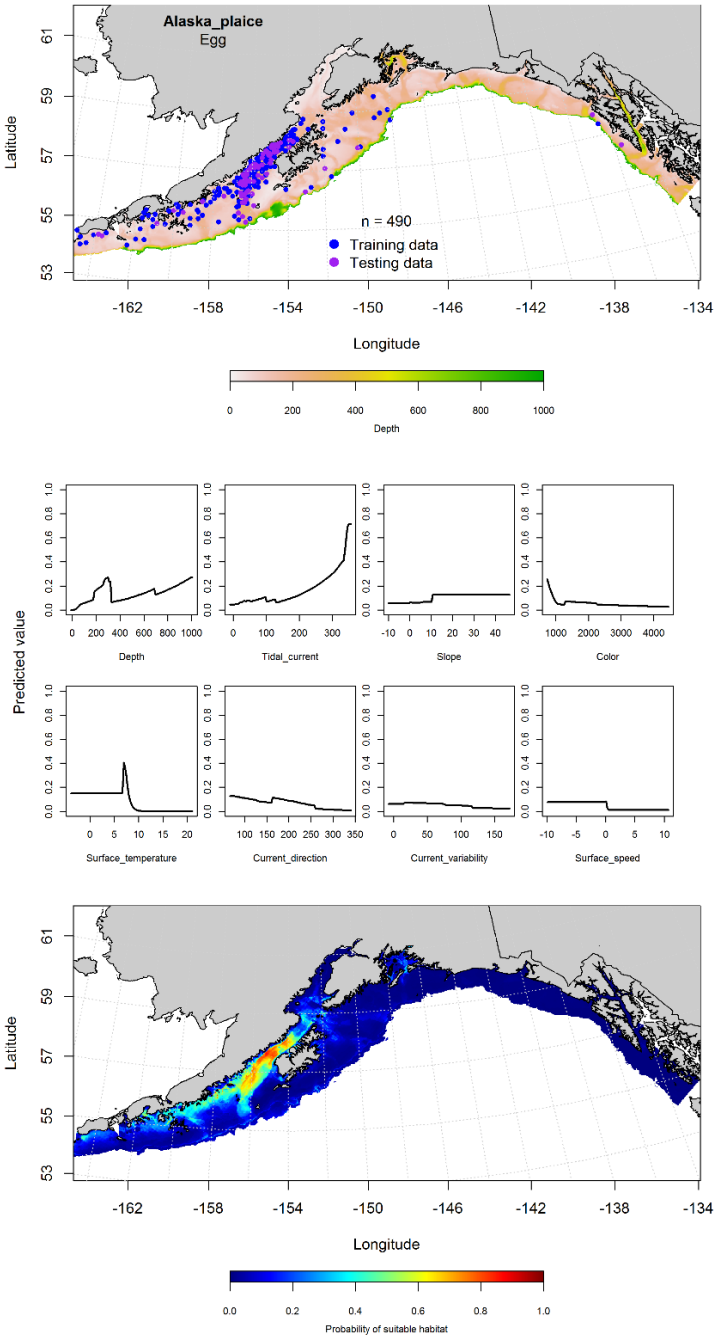

Figure 50. -- Distribution of Alaska plaice eggs from EcoFOCI ichthyoplankton surveys (January-March 1991-2013) (top panel) with training (blue dots) and testing (purple dots) data indicated, maximum entropy (MaxEnt) model effects (center panel), and predicted probability of suitable Alaska plaice egg habitat (bottom panel).

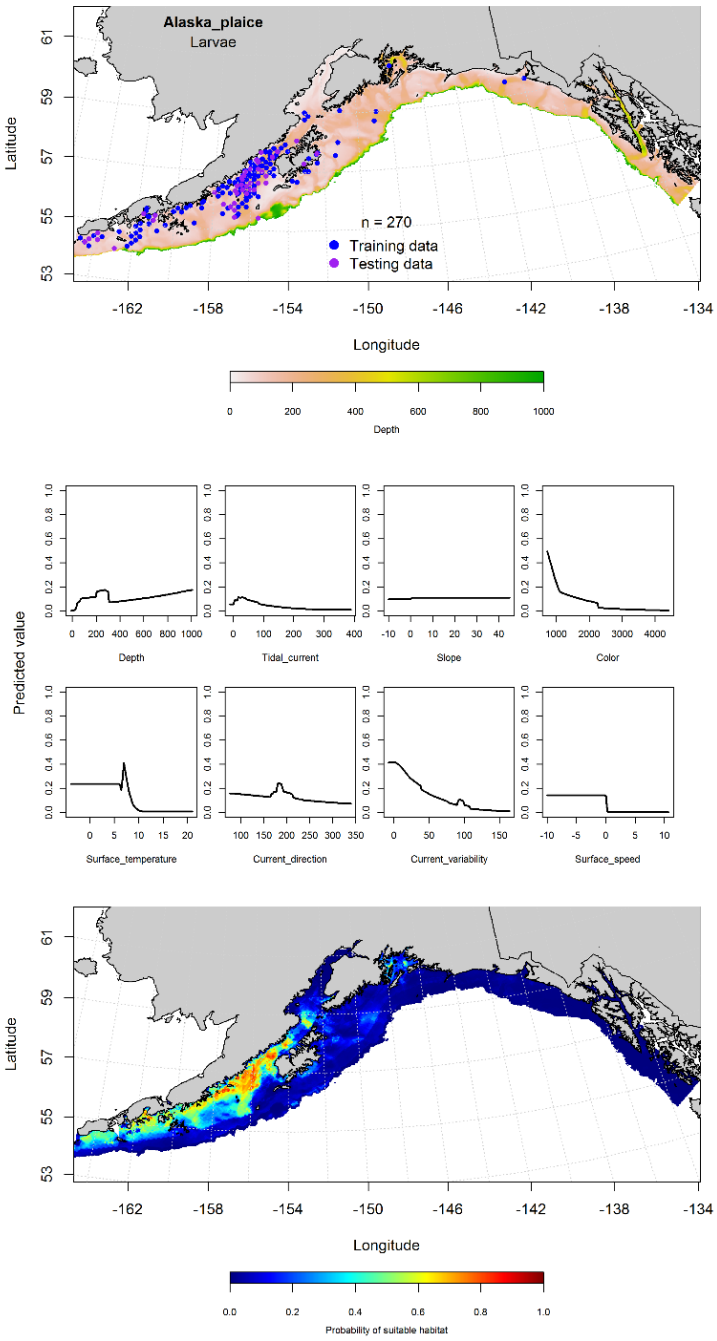

Figure 51. -- Presence of pelagic Alaska plaice larvae from EcoFOCI ichthyoplankton surveys (April-September 1991-2012) in the Gulf of Alaska (top panel) with training (blue dots) and testing (purple dots) data indicated, maximum entropy (MaxEnt) model effects (center panel), and the MaxEnt-predicted probability of suitable juvenile Alaska plaice habitat (bottom panel).

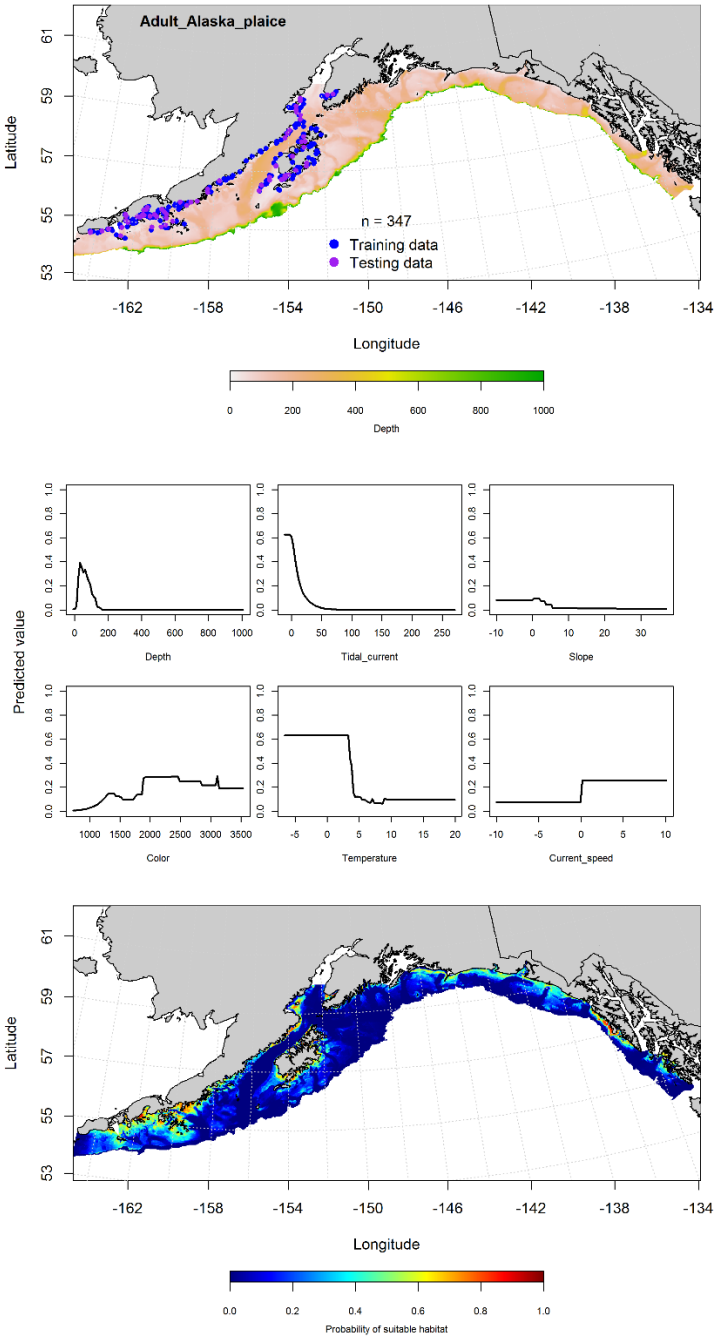

Figure 52. -- Presence of adult Alaska plaice from RACE-GAP summer bottom trawl surveys (1993-2013) in the Gulf of Alaska (top panel) with training (blue dots) and testing (purple dots) data indicated, maximum entropy (MaxEnt) model effects (center panel), and the MaxEnt-predicted probability of suitable adult Alaska plaice habitat (bottom panel).

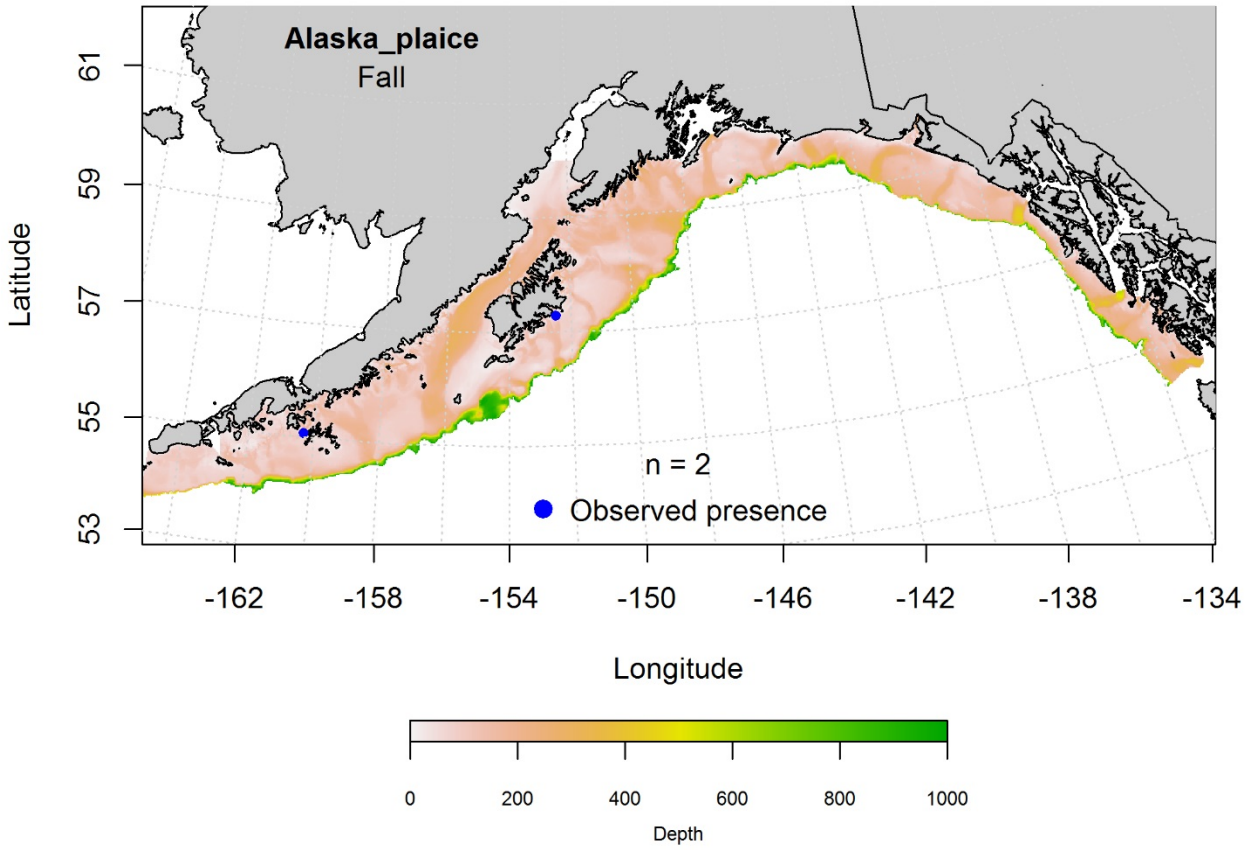

Figure 53. -- Locations of Alaska plaice from fall (September-November 2001-2015) commercial fisheries catches in the Gulf of Alaska.

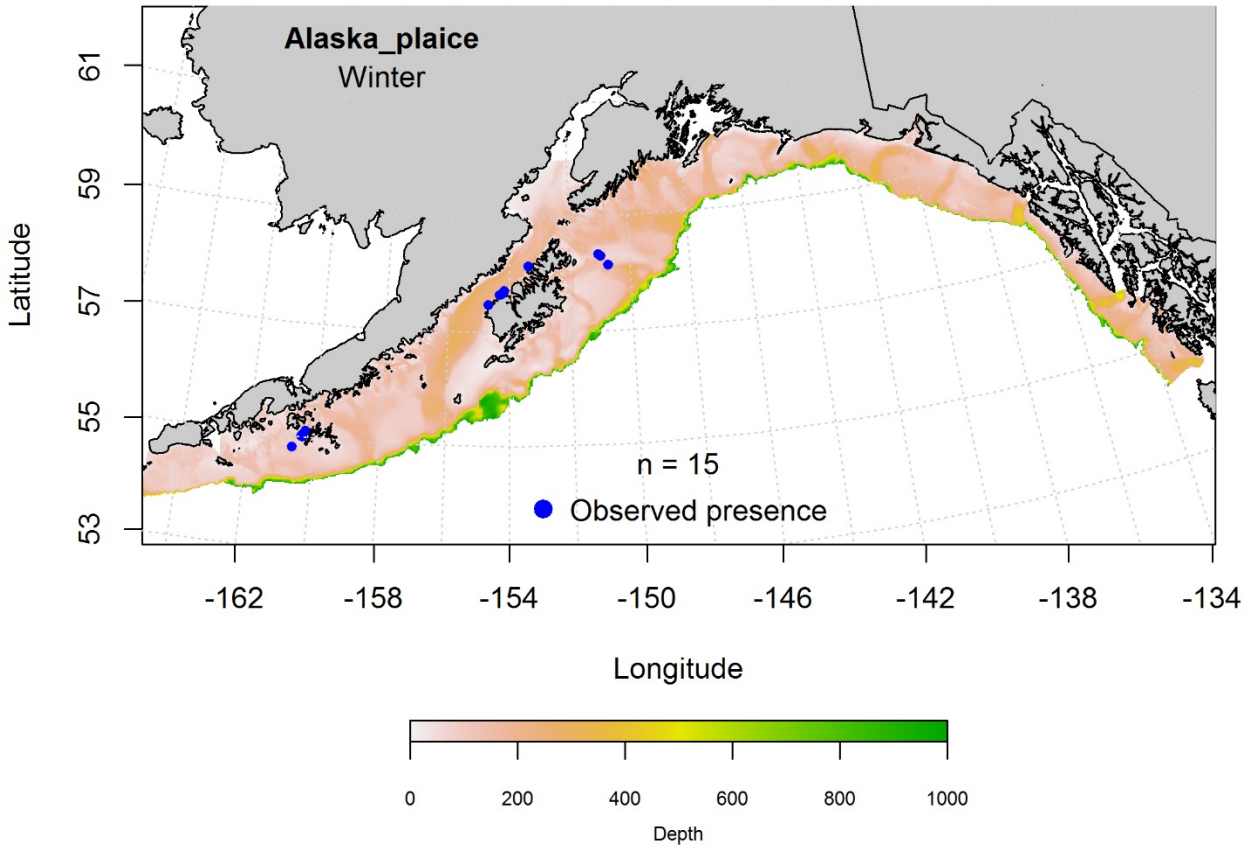

Figure 54. -- Locations of Alaska plaice from winter (December-February 2001-2015) commercial fisheries catches in the Gulf of Alaska.

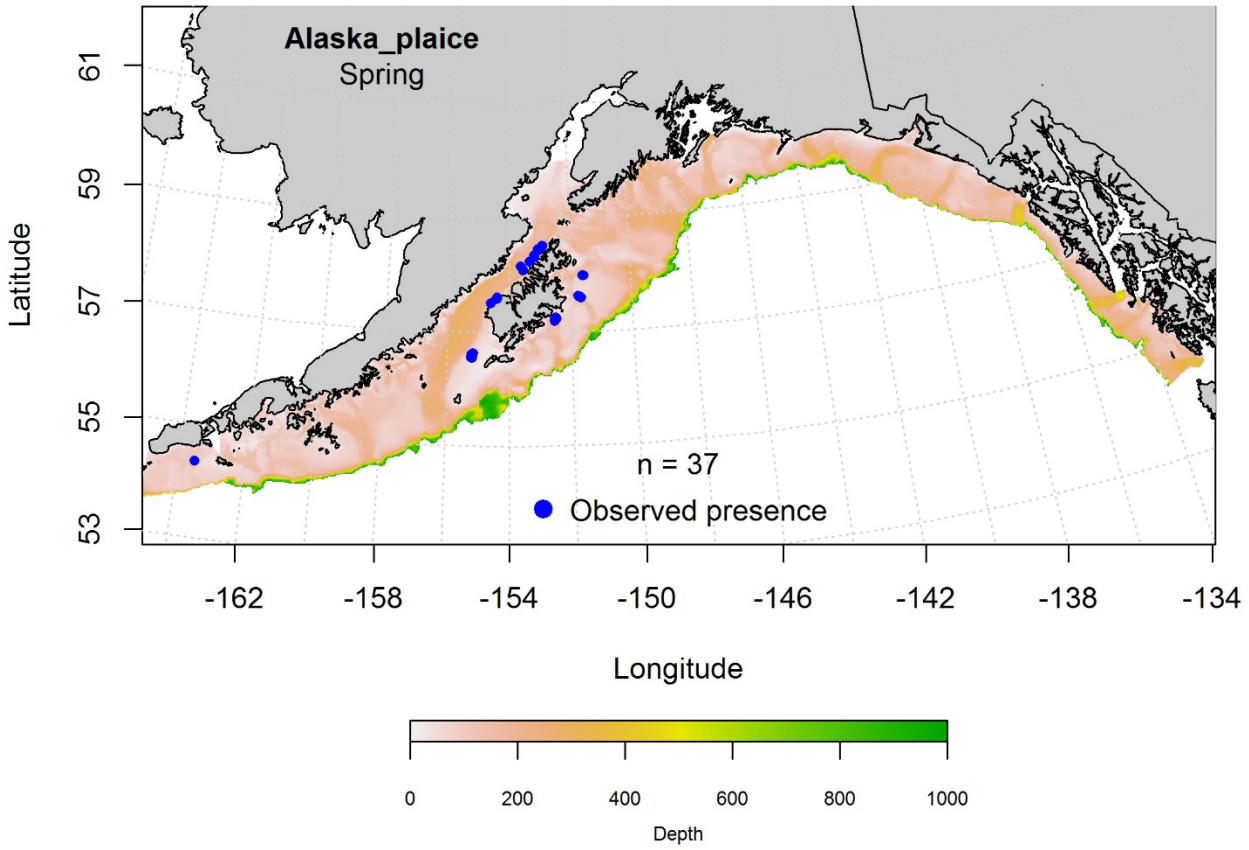

Figure 55. -- Locations of Alaska plaice from spring (March-May 2001-2015) commercial fisheries catches in the Gulf of Alaska.

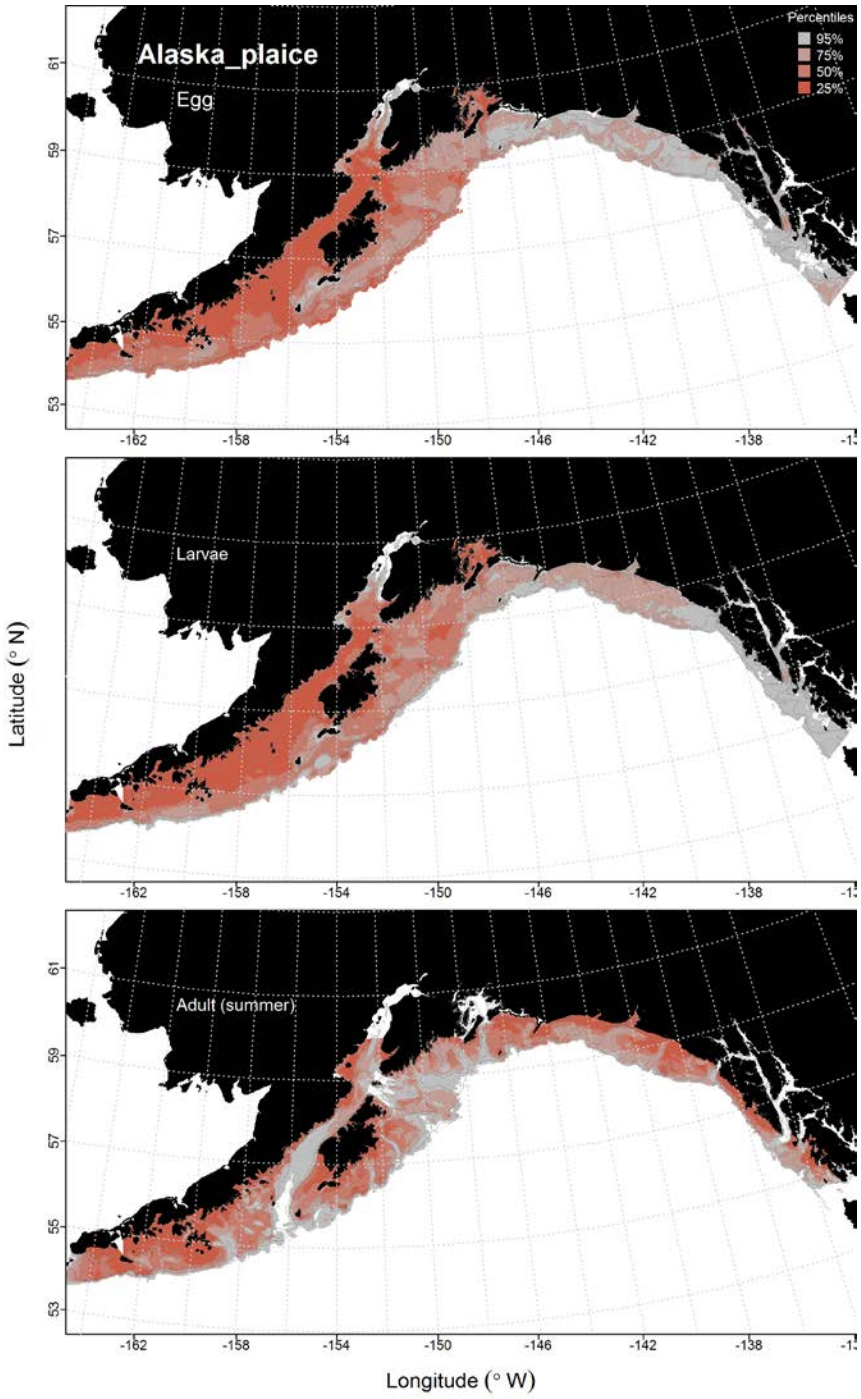

Figure 56. -- Habitat predicted for Alaska plaice eggs and pelagic larvae from EcoFOCI ichthyoplankton surveys (1991-2012), settled juveniles and adults from RACE-GAP summertime bottom trawl surveys (1993-2013) in the Gulf of Alaska.

Dover Sole *(Microstomus pacificus)*

Early life history stages of Dover sole -- There were 1,851 instances of Dover sole eggs observed in the EcoFOCI collections (Fig. 57). A MaxEnt model was used to predict suitable habitat of Dover sole eggs. The AUC of the model was 0.80 for the training data and (72% correctly classified) and 0.70 for the test data (70% correctly classified). Bottom depth, surface temperature, and surface current directions were the most important variables (relative importance: 0.45, 0.22, and 0.80, respectively). The model predicted probable suitable habitat of Dover sole eggs throughout the central and western GOA.

There were 257 catches of Dover sole larvae, all of which were from central or western GOA (Fig. 58). Surface temperature, bottom depth, and ocean color were the most important variables in the MaxEnt model (relative importance: 0.39, 0.24, and 0.12, respectively). The model AUCs were 0.86 (training data) and 0.76 (test data). Suitable larval Dover sole habitat was predicted in central and western GOA, with the highest probabilities around Shelikof Strait and Shelikof Gully (Fig. 58).

There were no observations of pelagic juvenile Dover sole in EcoFOCI collections.

Juvenile and adult Dover sole distribution in the bottom trawl survey -- The catch of Dover sole in summer bottom trawl surveys indicate this species is broadly distributed in the GOA. Generalized additive models predicting the abundance of settled juvenile Dover sole explained 30% of the variability in CPUE of training data and 29% of the variability in the test data. Geographic location, slope, ocean color, and bottom depth were the most important model variables. The highest abundance of settled juvenile Dover sole was predicted at around 400 m depth in the eastern and central GOA (Fig. 59).

The best fitting GAM indicated that geographic location, bottom depth, bottom temperature, and ocean color were the most important variables predicting the catch of adult Dover sole. The model explained 45% of the variability in CPUE for the training data, and 46% of the variability in the test data. Adult Dover sole abundance was higher in deeper waters and near the shelf break throughout the GOA (Fig. 60).

Dover sole distribution in commercial fisheries -- Distribution of adult Dover sole from commercial fisheries catches in the GOA was generally consistent throughout all seasons. In the fall, bottom depth and ocean color were the most important variables determining the distribution of suitable adult Dover sole habitat (relative importance: 0.30, 0.27, and 0.23, respectively). The AUC of the fall MaxEnt model was 0.89 for the training data and 0.78 for the test data. The model correctly classified 81% of the predictions from the training and 78% of the predictions from the test data. The model predicted suitable habitat of adult Dover sole throughout the central and western GOA, with highest suitability areas concentrated along the outer shelf (Fig. 61).

In the winter, ocean color, bottom current speed, and bottom depth were the most important variables determining suitable habitat for Dover sole (relative importance: 0.33, 0.28, and 0.16, respectively). The AUC of the MaxEnt model was 0.93 for the training data and 0.78 for the test data. The model correctly classified 85% of the predictions from the training and 78% of the predictions from the test data. The model predicted the distribution of suitable habitat for Dover sole throughout the GOA, with the highest suitability areas concentrated on the outer shelf in central and eastern GOA (Fig. 62).

In the spring, bottom depth, bottom temperature, and bottom current speed were the most important model variables determining suitable habitat for Dover sole (relative importance: 0.70,

0.10, and 0.08, respectively). The AUC of the spring MaxEnt model was 0.91 for the training data and 0.83 for the test data. The model correctly classified 84% of the predictions from the training data and 83% of the predictions from the test data. The model predicted probable suitable habitat for Dover sole throughout the GOA, with the highest suitability areas again concentrated along the outer shelf (Fig. 63).

Dover sole essential fish habitat maps and conclusions-- Predicted habitat for Dover sole eggs and larvae was widely distributed throughout the GOA, with higher probability areas concentrated in the central and western GOA (Fig. 64). Habitat of settled juvenile and adult Dover sole was also widely distributed, with adult habitat tending to be more concentrated in gullies and deeper areas along the middle and outer shelf (Fig. 64). The habitat predicted from commercial catches was also widely distributed throughout the GOA, particularly at deeper depths (Fig. 64). There does not appear to be much seasonal variability to the habitat distribution predicted for Dover sole from their presence in commercial catches.

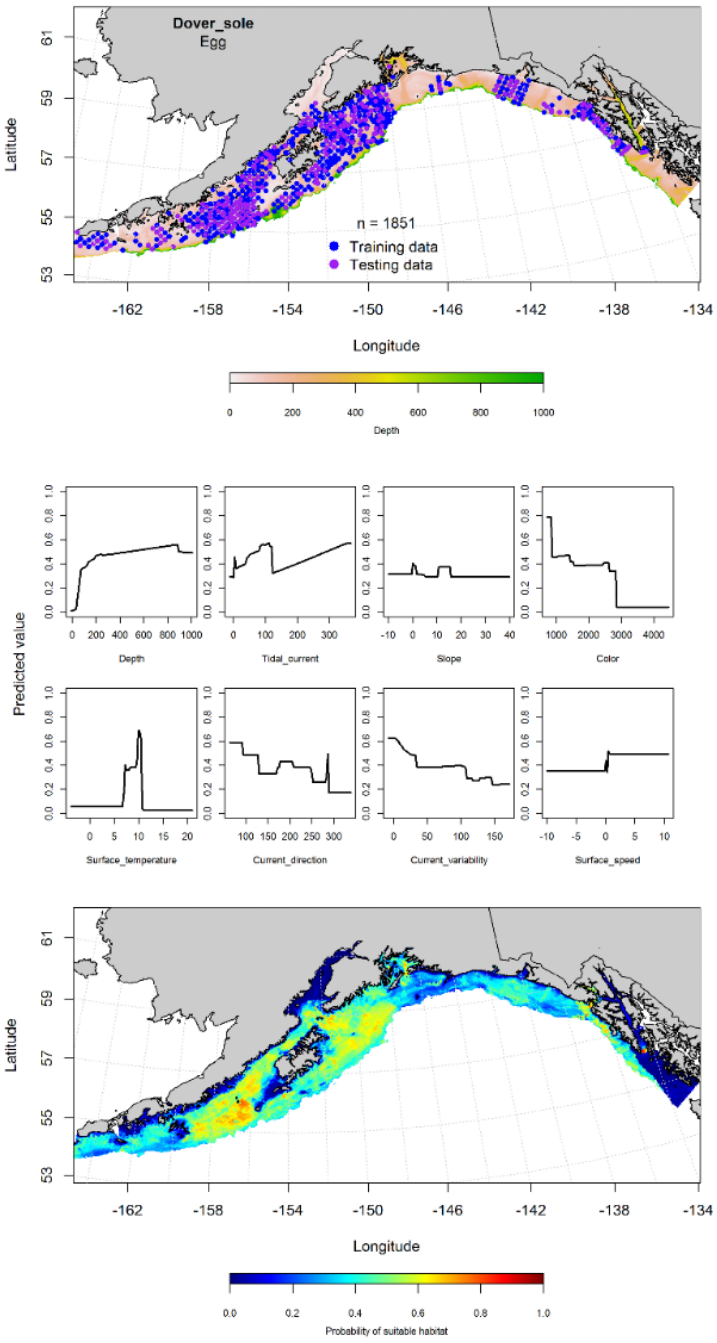

Figure 57. -- Distribution of Dover sole eggs from EcoFOCI ichthyoplankton surveys (January-March 1991-2013) (top panel) with training (blue dots) and testing (purple dots) data indicated, maximum entropy (MaxEnt) model effects (center panel), and predicted probability of suitable Dover sole egg habitat (bottom panel).

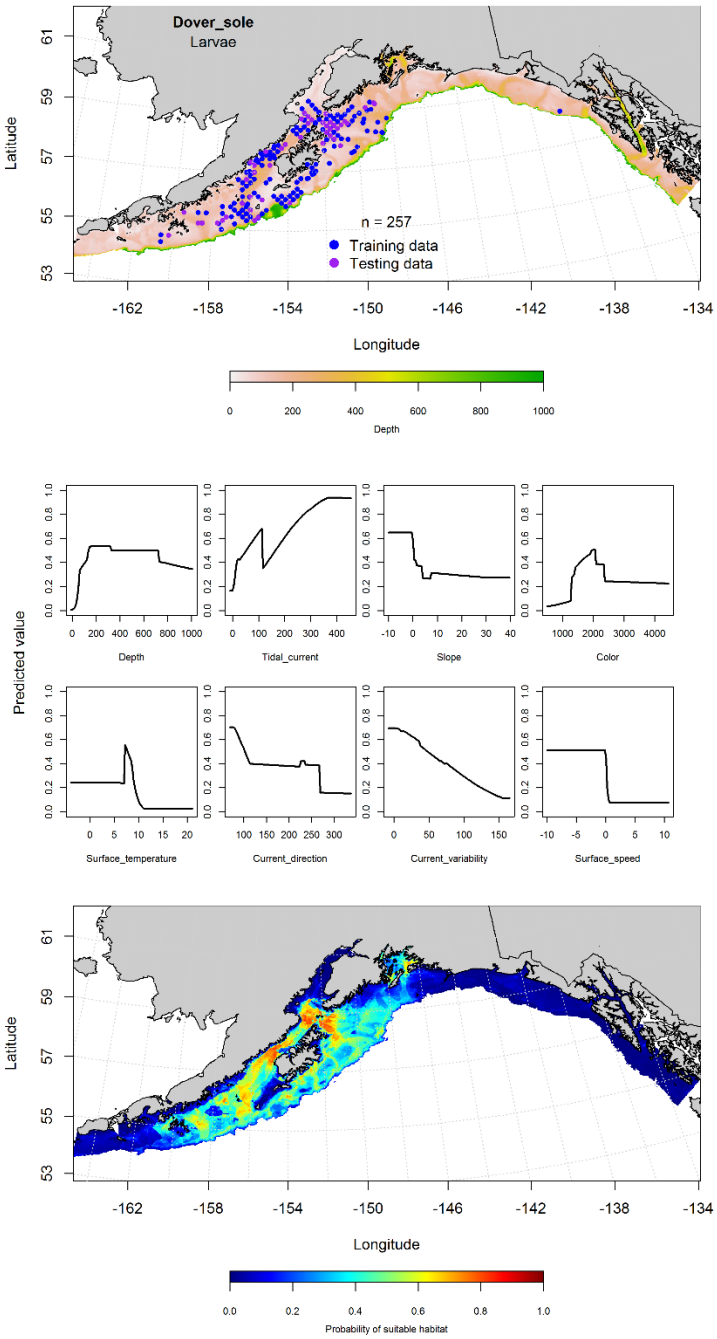

Figure 58. -- Distribution of pelagic Dover sole larvae observations from EcoFOCI ichthyoplankton surveys (April-September 1991-2012) in the Gulf of Alaska (top panel) with training (blue dots) and testing (purple dots) data indicated, maximum entropy (MaxEnt) model effects (center panel), and the predicted probability of suitable pelagic Dover sole larval habitat (bottom panel).

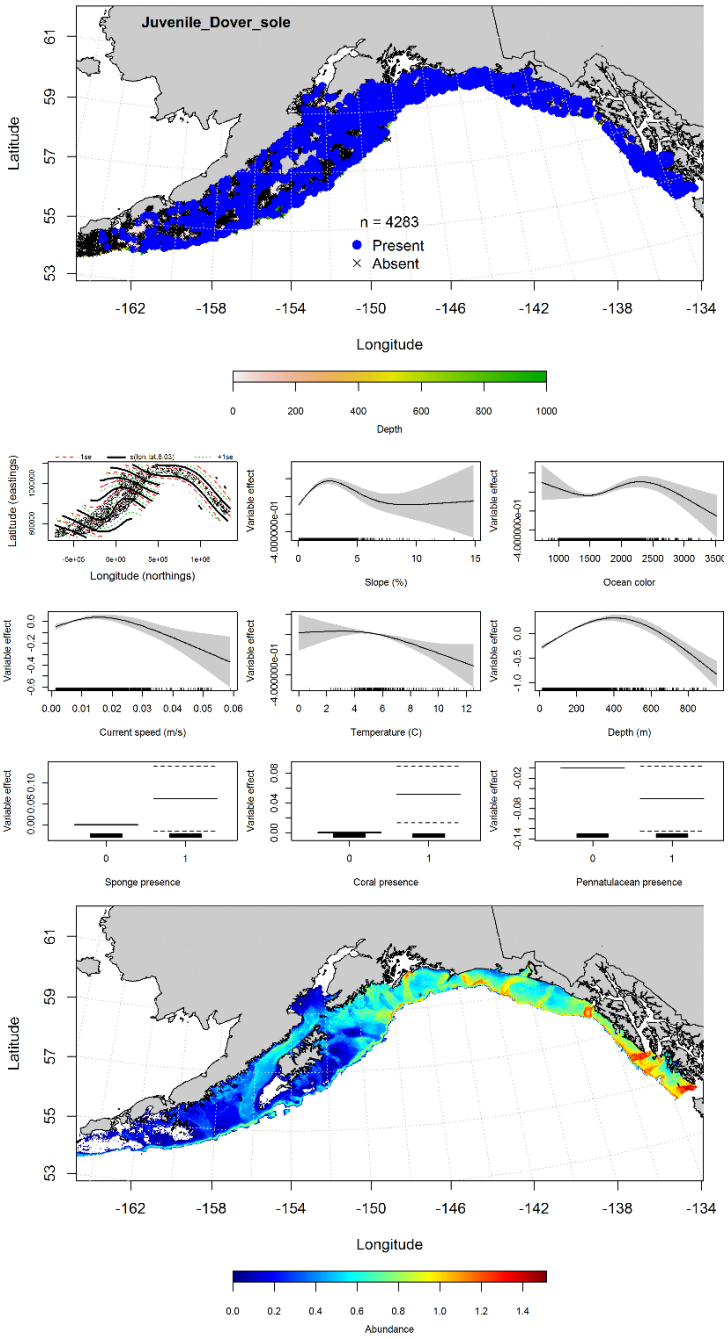

Figure 59. -- Presence of settled juvenile Dover sole from RACE-GAP summer bottom trawl surveys (1993-2013) in the Gulf of Alaska (top panel) with training (blue dots) and testing (purple dots) data indicated, generalized additive model (GAM) effects (center panel), and the GAM-predicted abundance of settled juvenile Dover sole (bottom panel).

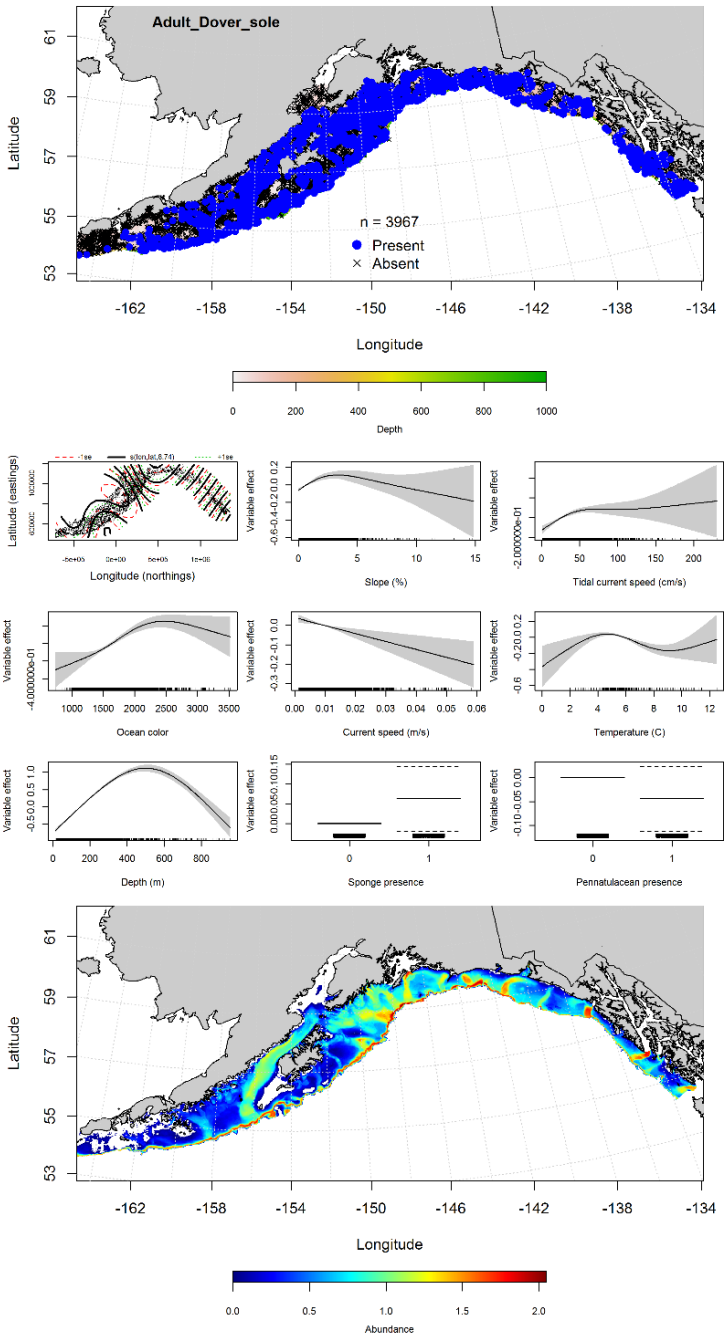

Figure 60. -- Presence of adult Dover sole from RACE-GAP summer bottom trawl surveys (1993-2013) in the Gulf of Alaska (top panel) with training (blue dots) and testing (purple dots) data indicated, generalized additive model (GAM) effects (center panel), and the GAM-predicted abundance of adult Dover sole (bottom panel).

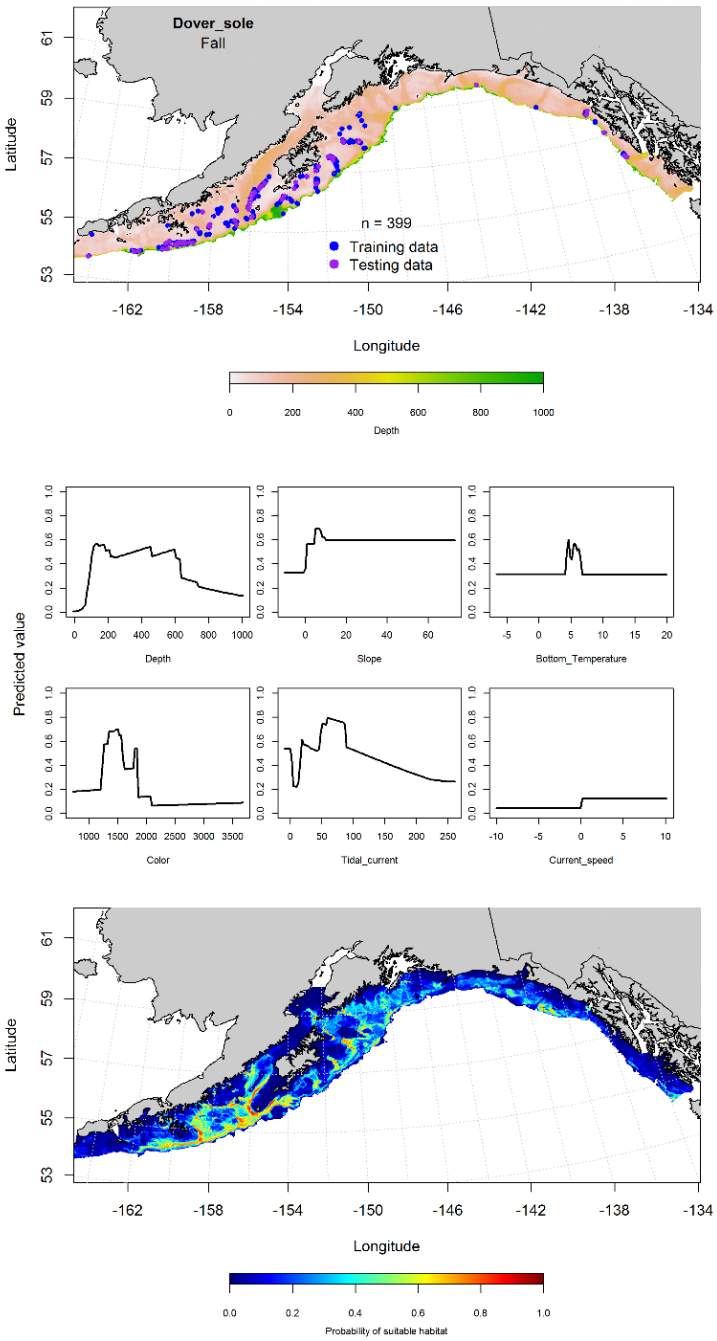

Figure 61. -- Locations of Dover sole from fall (September-November 2001-2015) commercial fisheries catches in the Gulf of Alaska (top panel), maximum entropy (MaxEnt) model effects (middle panels), and predicted probability of suitable habitat for Dover sole based on the model (bottom panel).

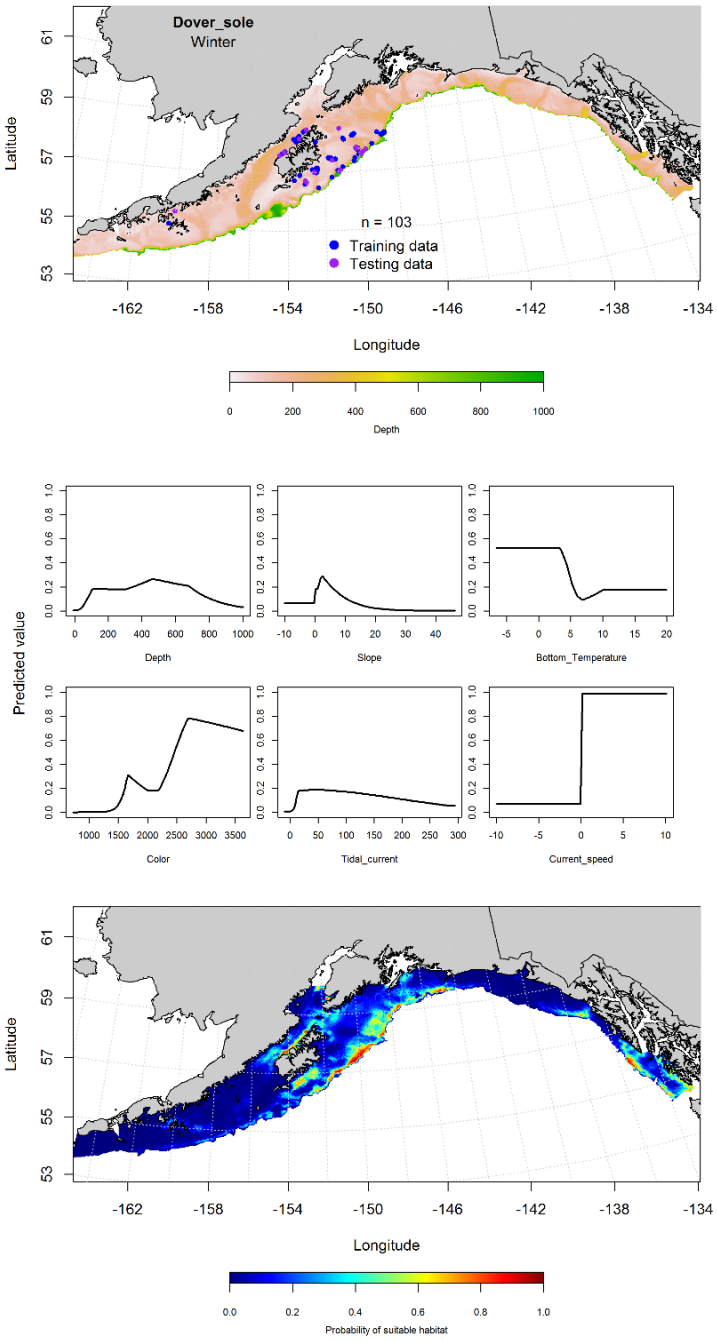

Figure 62. -- Locations of Dover sole from winter (December-February 2001-2015) commercial fisheries catches in the Gulf of Alaska (top panel), with training (blue dots) and testing (purple dots) data indicated, maximum entropy (MaxEnt) model effects (center panel), and the predicted probability of suitable adult Dover sole habitat (bottom panel).

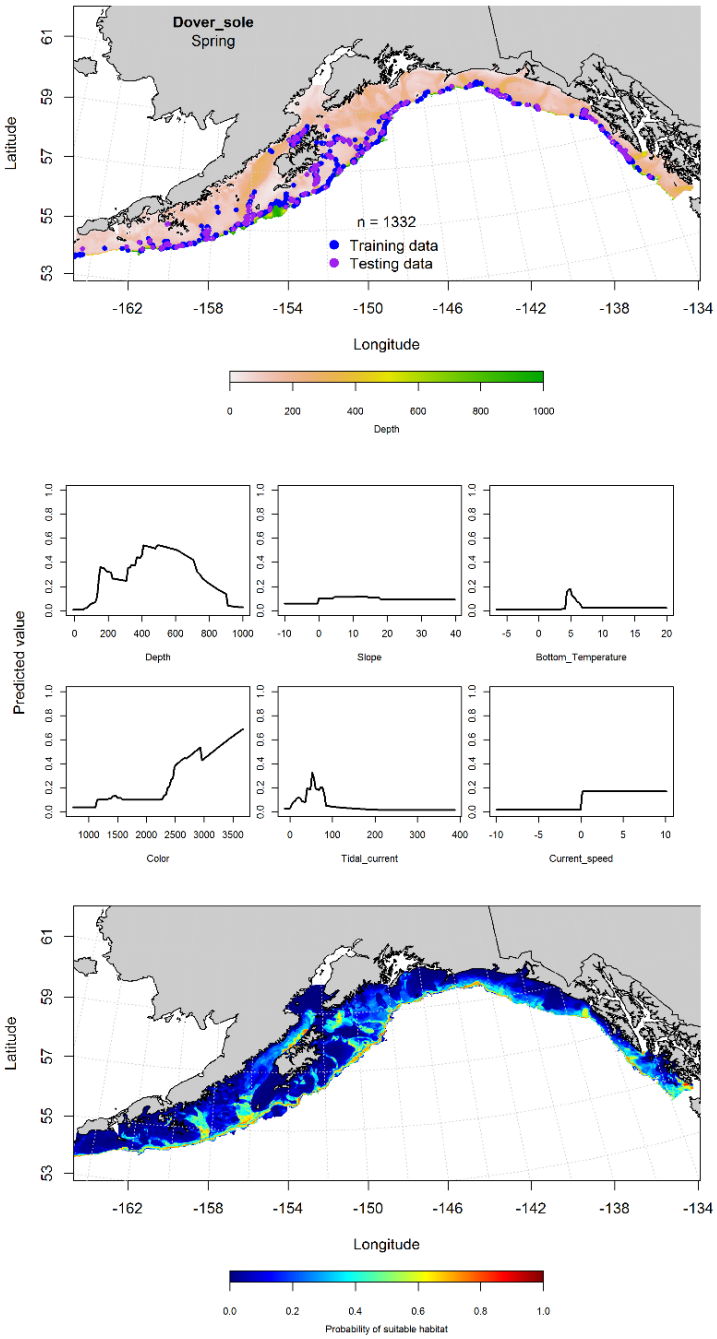

Figure 63. -- Locations of Dover sole from spring (March-May 2001-2015) commercial fisheries catches in the Gulf of Alaska (top panel), with training (blue dots) and testing (purple dots) data indicated, maximum entropy (MaxEnt) model effects (center panel), and the predicted probability of suitable adult Dover sole habitat (bottom panel).

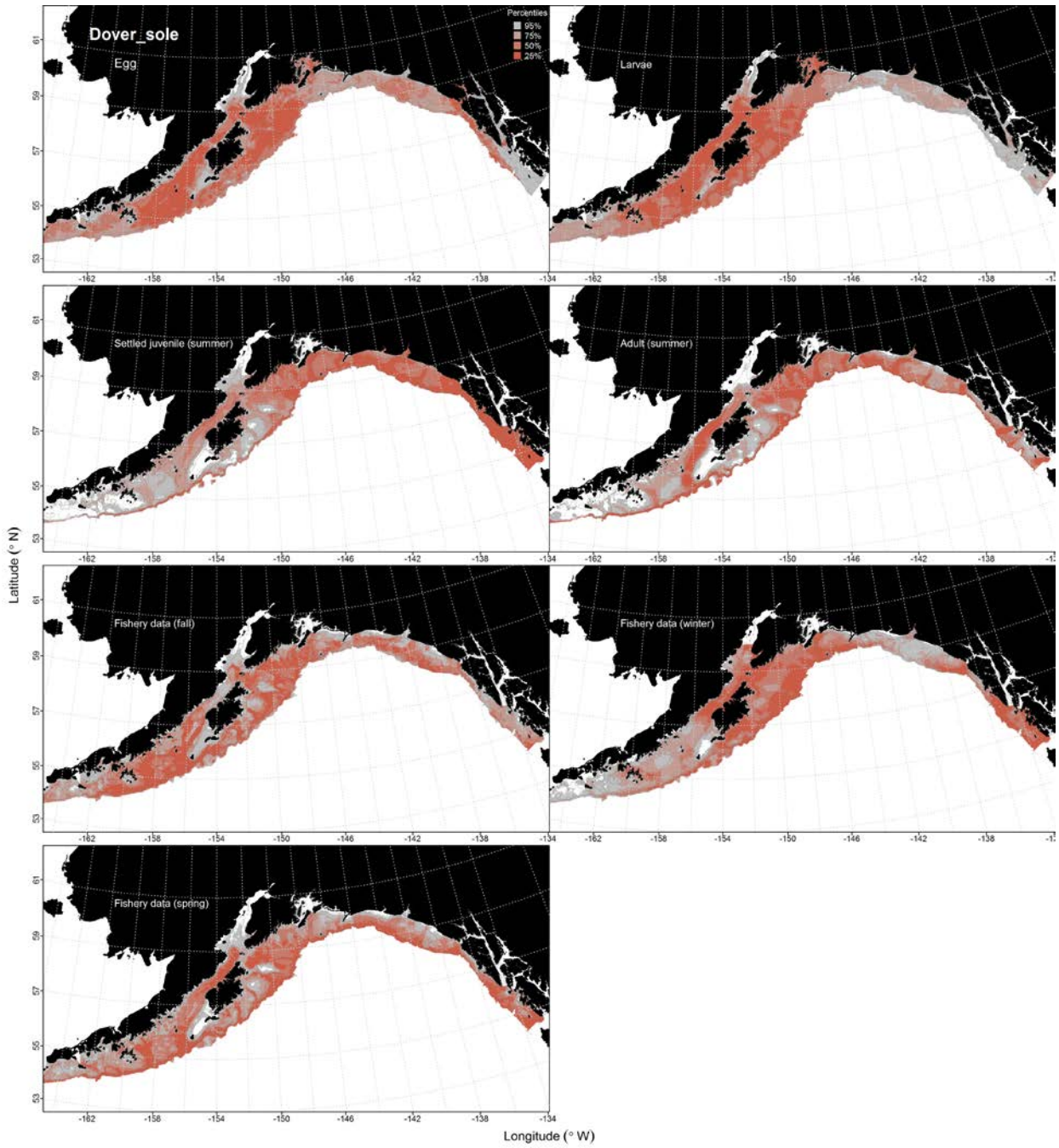

Figure 64. -- Habitat predicted for Dover sole eggs and pelagic larvae from EcoFOCI ichthyoplankton surveys (1991-2012), settled juveniles and adults from RACE-GAP summertime bottom trawl surveys (1993-2013), and predicted from presence in commercial fishery catches (2001-2015) from fall, winter, and spring in the Gulf of Alaska.

Roundfishes

Sablefish (*Anoplopoma fimbria*)

Early life history stages of sablefish -- There were 11 instances of sablefish eggs observed in the EcoFOCI collections, most of which occurred in the central GOA (Fig. 65). These were, however, not enough to run a model for this life stage.

The 351 instances of larval sablefish recorded in the ECODAAT database were widely distributed throughout the GOA (Fig. 66). Bottom depth, surface temperature, and ocean color were the most important model variables predicting suitable larval sablefish habitat (relative importance: 0.38, 0.33, and 0.12, respectively). The AUC was 0.99 for the training data and 0.90 for the test data. The model correctly classified 75% of the predictions from the training data and 72% of the predictions from the test data. The areas with the highest probability of suitable habitat were concentrated in the central GOA, around the Semidi Islands, as well as in the eastern GOA, around Chichagof Island (Fig. 66).

There were not enough instances (n = 2) of pelagic juvenile sablefish observed in the EcoFOCI collections to run the model for this life stage (Fig. 67).

Juvenile and adult sablefish distribution in the bottom trawl survey -- The first step of an hGAM predicting presence of settled juvenile sablefish had an AUC of 0.85 for the training data and 0.83 for the testing data. The most important variables determining presence or absence were geographic location and slope. Settled juveniles were predicted to be distributed throughout the GOA, though the highest probability of presence was in nearshore waters of the eastern GOA (Fig. 68). The CPUE-

GAM indicated that slope and geographic location were the most important variables explaining abundance of settled juvenile sablefish abundance where their presence was predicted. Overall the CPUE model step of the hGAM explained just 9% of the variability of the training data set and 4% of the test data. The areas of predicted highest abundance were nearshore waters in the eastern GOA, particularly between Dixon entrance and Yakutat (Fig. 68).

A GAM predicting the abundance of adult sablefish explained 53% of the variability in the CPUE of the training data and 55% of the variability in the test data. Geographic location, slope, bottom temperature, and ocean color were the most important variables explaining the distribution of adult sablefish. Adult sablefish were distributed at deeper depths and near the shelf break across the GOA (Fig. 69).

Sablefish distribution in commercial fisheries -- The distribution of sablefish in commercial fisheries catches varied by season with their occurrence being much more prevalent in spring. In the fall, bottom depth, slope, and bottom temperature were the most important model variables for predicting suitable habitat (relative importance: 0.38, 0.16, and 0.14, respectively). The AUC of the fall MaxEnt model was 0.90 for the training data and 0.80 for the test data. The model correctly predicted 82% of the training data set and 80% of the test data set. The model predicted that the probability of suitable habitat for sablefish was highest near the shelf break in the central and western GOA (Fig. 70).

In the winter, ocean color, bottom current speed, and bottom depth were the most important variables determining the probability of suitable habitat for sablefish (relative importance: 0.29, 0.23, and 0.16, respectively). The AUC of the winter MaxEnt model was 0.94 for the training data and 0.78 for the test data. The model correctly predicted 90% of the training data set and 78% of the test

data set. The model predicted that suitable sablefish habitat was concentrated near the shelf break in the central GOA (Fig. 71).

In the spring, when sablefish occurrences were concentrated along the shelf break across the GOA study area, bottom depth, bottom current speed, and slope were the most important model variables determining probable suitable habitat for sablefish (relative importance: 0.80, 0.07, and 0.07, respectively). The AUC of the spring MaxEnt model was 0.96 for the training data and 0.90 for the test data. The model correctly classified 91% of the predictions from the training data and 90% of the predictions from the test data. The model predicted that probable suitable habitat for sablefish was concentrated near the shelf break throughout the GOA (Fig. 72).

Sablefish essential fish habitat maps and conclusions-- Predicted habitat for larval sablefish was distributed throughout the GOA (Fig. 73). Settled juvenile sablefish habitat was more narrowly distributed along the inner shelf in the eastern GOA (Fig. 73). In contrast, the predicted habitat for adult sablefish was more broadly distributed throughout the GOA, particularly in gullies and deeper areas along the middle and outer shelf (Fig. 73). The fall, winter, and spring distributions of potential habitat predicted from commercial catches were similar across seasons, but slightly more concentrated at deeper depths during the spring (Fig. 73).

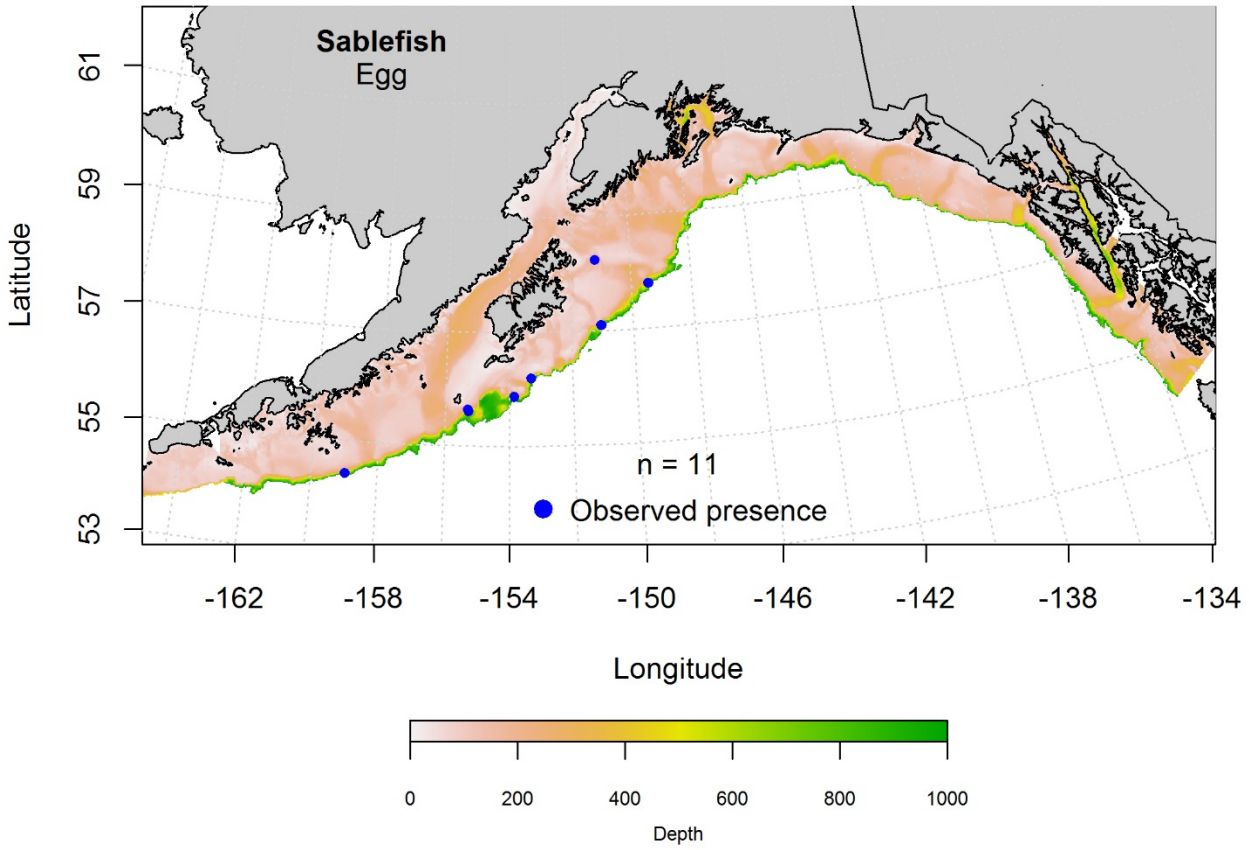

Figure 65. -- Distribution of sablefish eggs from EcoFOCI ichthyoplankton surveys (January-March 1991-2013).

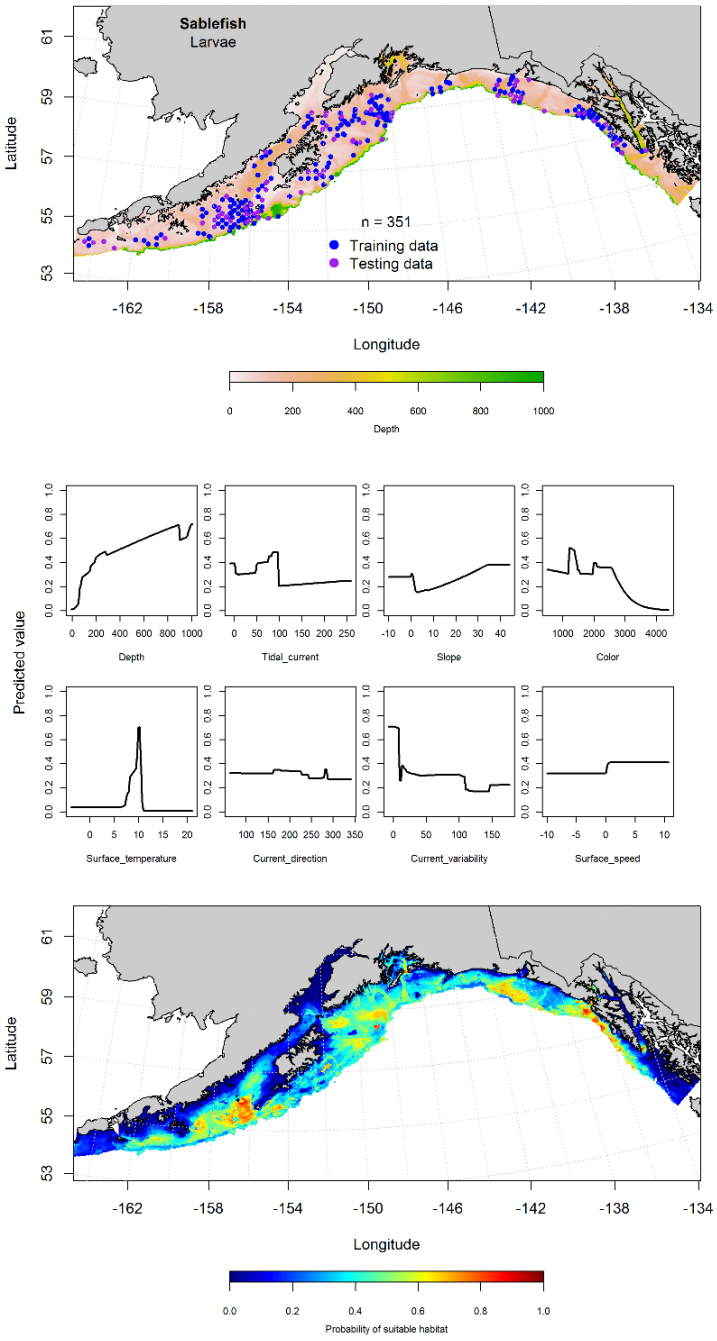

Figure 66. -- Distribution of pelagic sablefish larvae observations from EcoFOCI ichthyoplankton surveys (April-September 1991-2012) in the Gulf of Alaska (top panel) with training (blue dots) and testing (purple dots) data indicated, maximum entropy (MaxEnt) effects (center panel), and the predicted probability of suitable pelagic sablefish larval habitat (bottom panel)

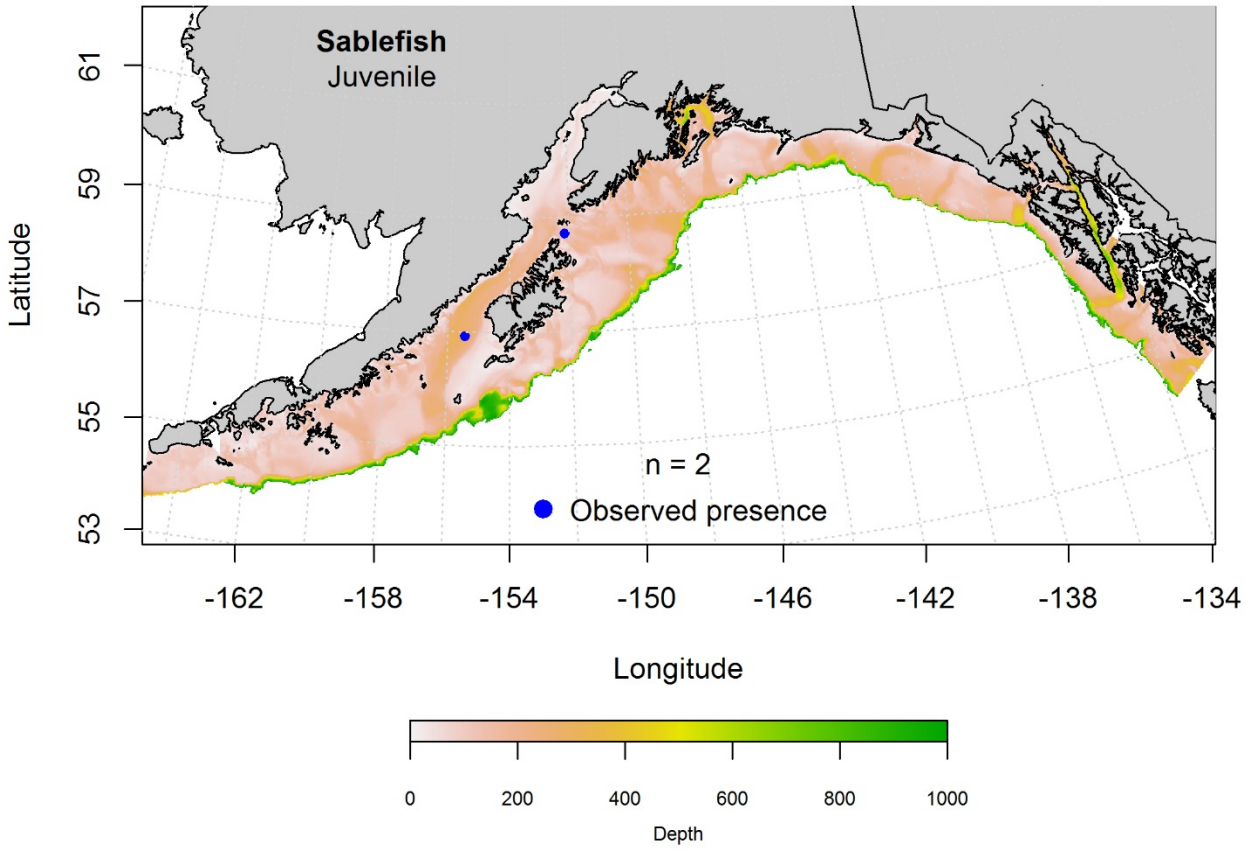

Figure 67. -- Distribution of pelagic juvenile sablefish observations from EcoFOCI ichthyoplankton surveys (April-September 1991-2012) in the Gulf of Alaska.

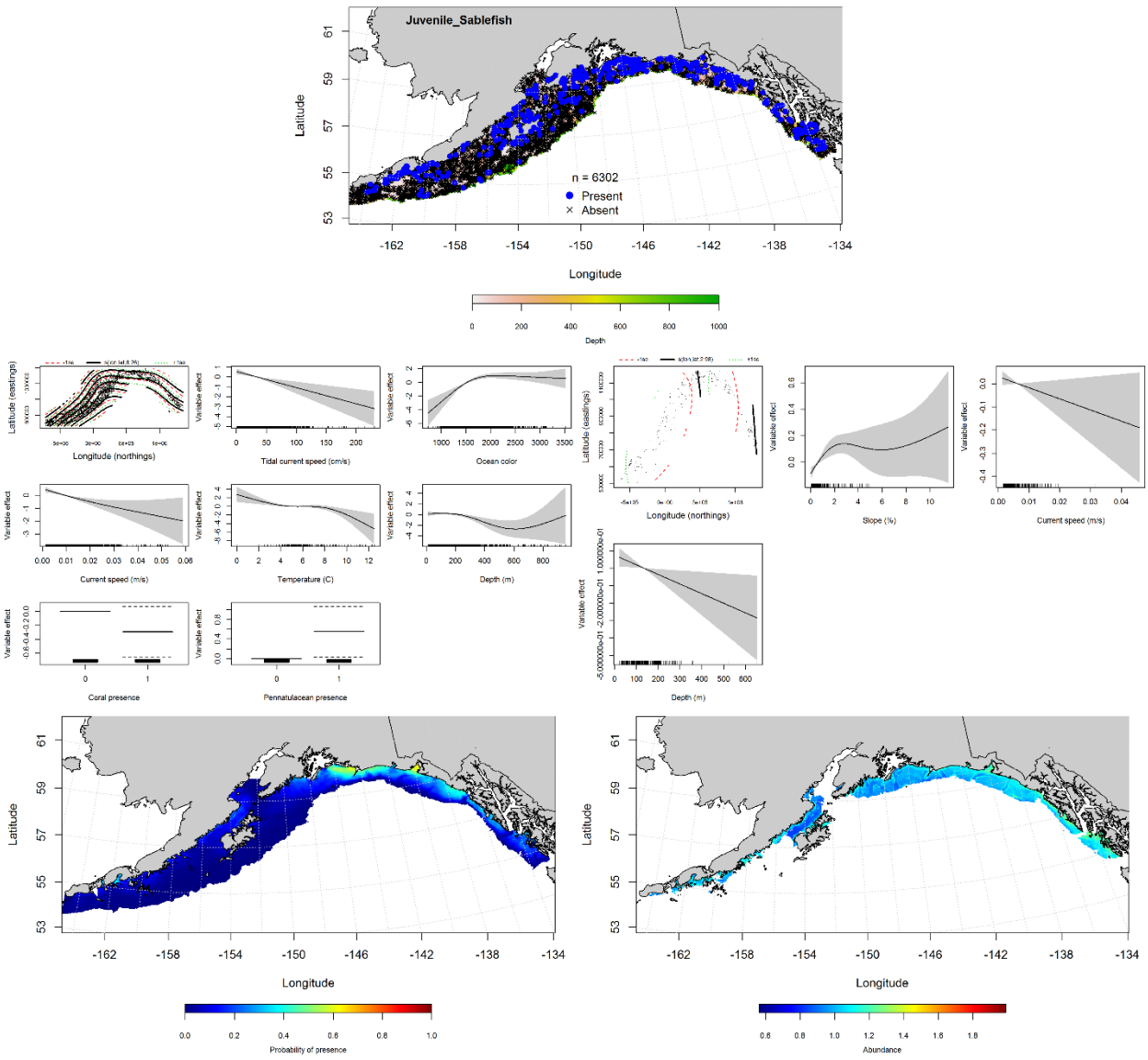

Figure 68. -- Distribution of settled juvenile sablefish in 1993-2013 RACE-GAP summer bottom trawl surveys conducted in the Gulf of Alaska (upper panel). Effects of retained habitat covariates in the best fitting generalized additive presence-absence models (PA GAM; left center panel) and abundance (CPUE GAM; right center panel). Predicted spatial distribution of the probability of presence (bottom left panel) and abundance of settled juvenile sablefish based on the models (bottom right panel).

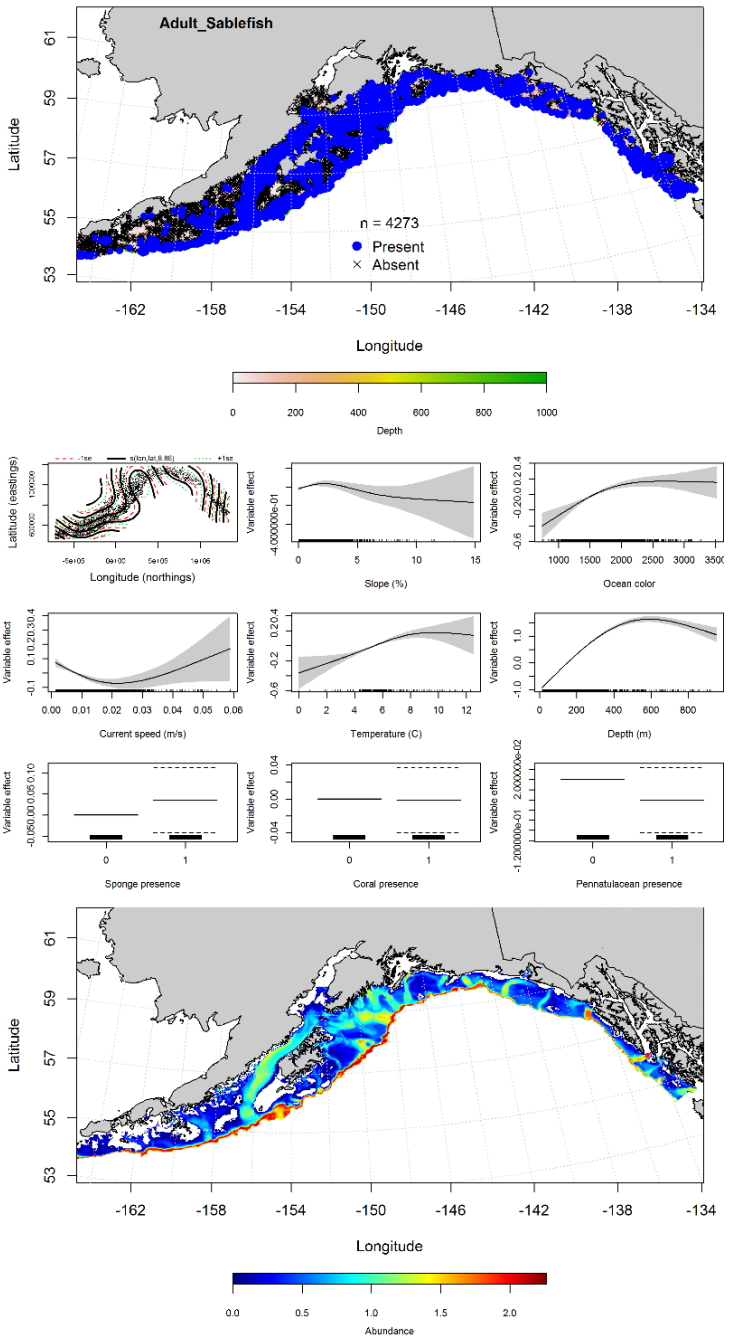

Figure 69. -- Distribution of adult sablefish in 1993-2013 RACE-GAP summer bottom trawl surveys conducted in the Gulf of Alaska (upper panel), effects of retained habitat covariates in the best fitting generalized additive models (GAM) of abundance (CPUE; center panel), and predicted spatial distribution of the abundance of adult sablefish (bottom panel).

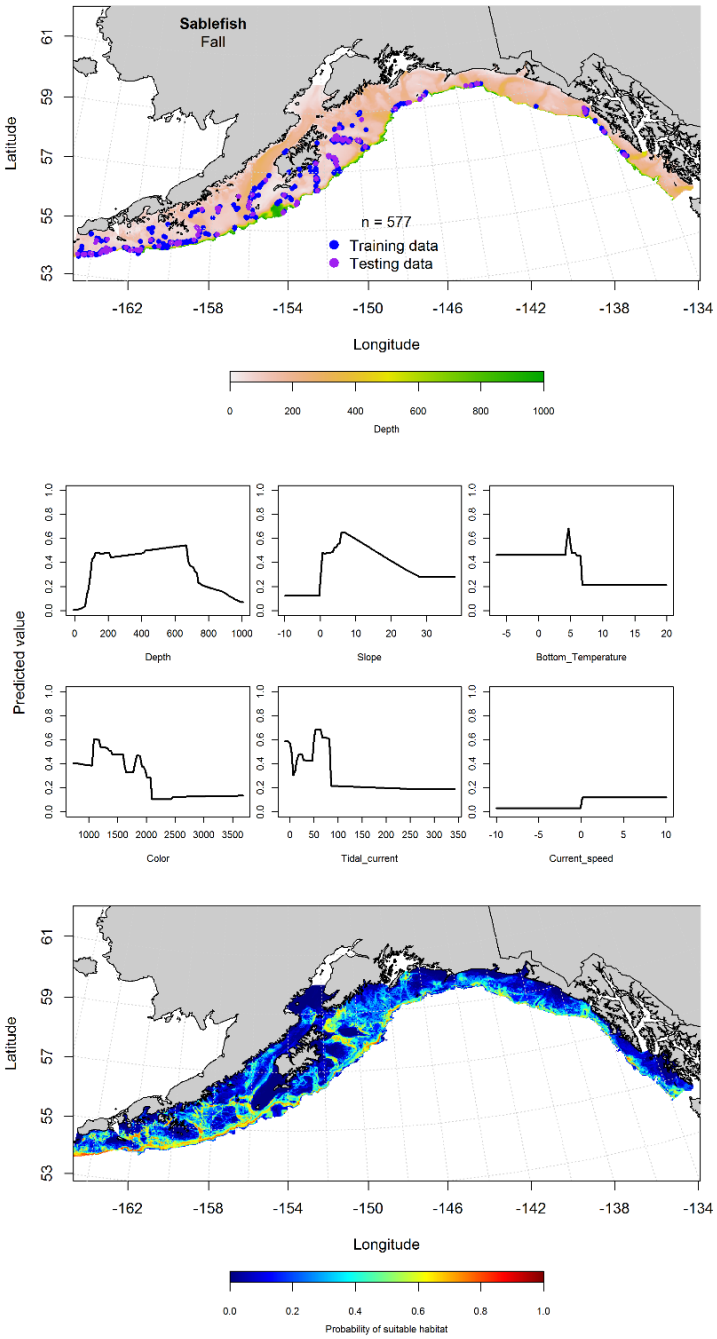

Figure 70. -- Locations of sablefish from fall (September-November 2001-2015) commercial fisheries catches in the Gulf of Alaska (top panel), MaxEnt model effects (middle panels), and predicted probability of suitable habitat for sablefish based on the model (bottom panel).

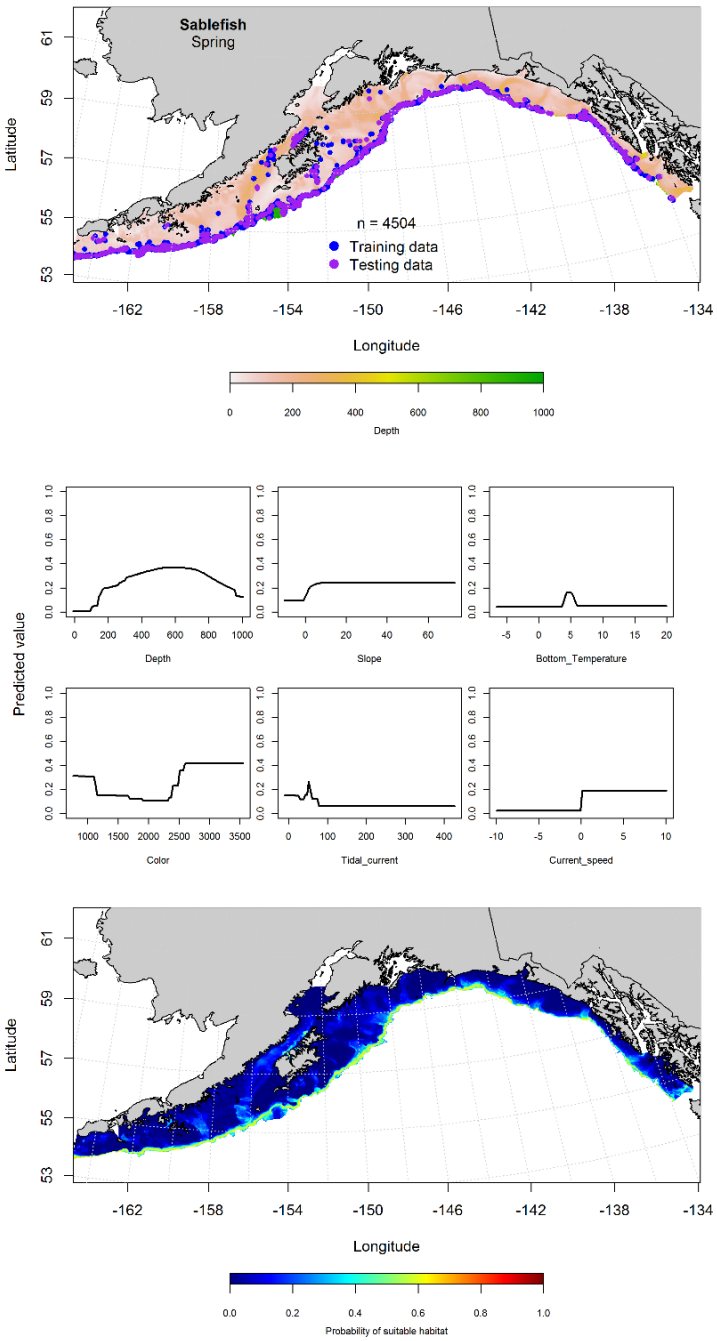

Figure 71. -- Locations of sablefish from winter (December-February 2001-2015) commercial fisheries catches in the Gulf of Alaska (top panel), with training (blue dots) and testing (purple dots) data indicated, maximum entropy (MaxEnt) model effects (center panel), and the predicted probability of suitable adult sablefish habitat (bottom panel).

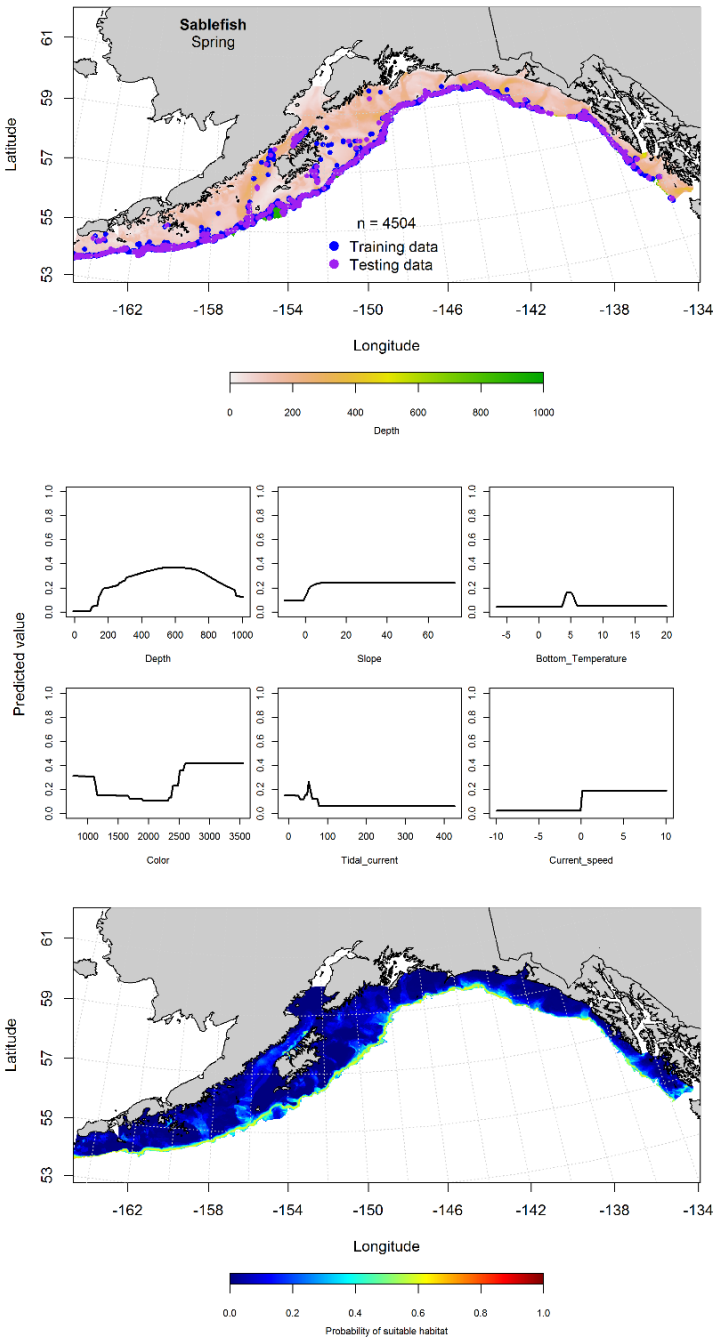

Figure 72. -- Locations of sablefish from spring (March-May 2001-2015) commercial fisheries catches in the Gulf of Alaska (top panel), with training (blue dots) and testing (purple dots) data indicated, maximum entropy (MaxEnt) model effects (center panel), and the predicted probability of suitable adult sablefish habitat (bottom panel).

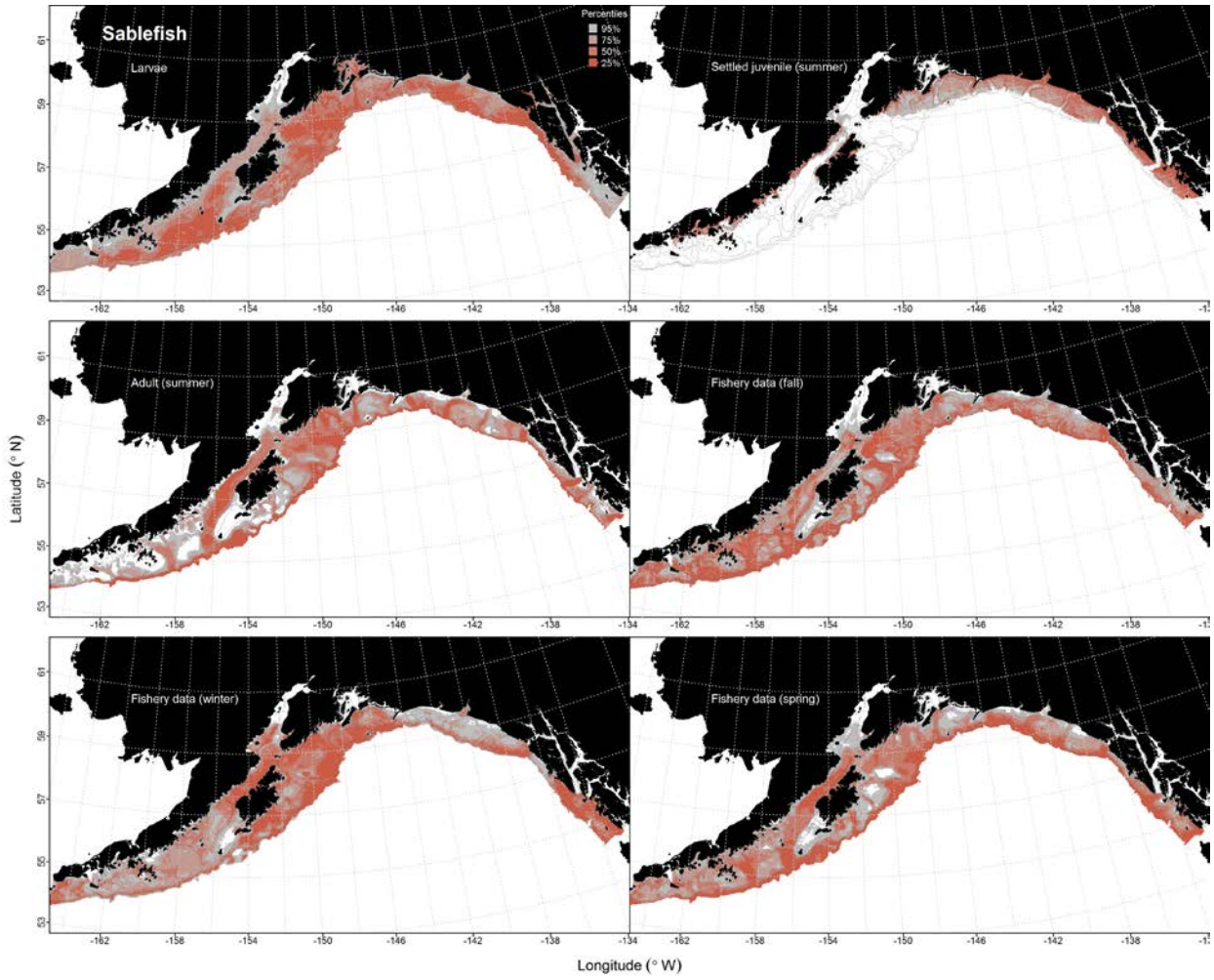

Figure 73. -- Habitat predicted for pelagic sablefish larvae from EcoFOCI ichthyoplankton surveys (1991-2012), settled juveniles and adults from RACE-GAP summertime bottom trawl surveys (1993-2013), and predicted from presence in commercial fishery catches (2001-2015) from fall, winter, and spring in the Gulf of Alaska.

Walleye Pollock (*Gadus chalcogrammus*)

Early life history stages of walleye pollock -- There were 3,133 instances of walleye pollock eggs observed in the EcoFOCI collections, most of which were from the central or western GOA (Fig. 74). Surface temperature, bottom depth, and surface current speed were the important variables for predicting probability of suitable habitat from the MaxEnt model (relative importance: 0.36, 0.35, and 0.14, respectively). The AUC was 0.89 for the training data and 0.81 for the test data. The model correctly classified 80% of the predictions from the training data and 79% of the predictions from the test data. The highest probability of suitable walleye pollock egg habitat was in Shelikof Strait and Shelikof Gully (Fig. 74).

There were 4,834 observations of larval walleye pollock in the EcoFOCI collections, primarily from the central and western GOA (Fig. 75). The most important variables in the MaxEnt model were surface temperature, bottom depth, and surface current speed (relative importance: 0.36, 0.29, and 0.10, respectively). The AUC was 0.89 for the training data and 0.80 for the testing data, and the model correctly classified 80% of the predictions from both the training and test data. Suitable habitat for larval pollock was distributed throughout the central GOA, with the highest probability habitat occurring in Shelikof Strait and Shelikof Gully (Fig. 75).

There were 122 observations of pelagic juvenile walleye pollock in the EcoFOCI collections, a majority of which occurred west of Chirikof Island (Fig. 76). The most important variables in the MaxEnt model were ocean color, surface temperature, and bottom depth (relative importance: 0.45, 0.28, and 0.16, respectively). The AUC was 0.94 for the training data and 0.88 for the test data. The model correctly classified 88% of the predictions from both the training and test data. The model predicted suitable habitat for pelagic juvenile walleye pollock in the central GOA, particularly around the Semidi Islands (Fig. 76).

Juvenile and adult walleye pollock distribution in the bottom trawl survey -- Settled juvenile walleye pollock distribution in the GOA was modeled using a standard GAM. Geographic location, bottom depth, ocean color and maximum tidal current were the important predictors of settled juvenile walleye pollock abundance. The model explained 17% of the variability of the training data, and 18% of the variability in the test data. Higher abundance of juvenile walleye pollock was predicted across the inner shelf of the GOA with the highest abundance predicted in Shelikof Strait (Fig. 77).

A GAM predicting the abundance of adult walleye pollock across the GOA explained 33% of the variability in CPUE for the training data, and 35% of the variability for test data. Geographic location, bottom depth, and bottom temperature were the most important model predictors. Adult walleye pollock were distributed throughout the GOA, with the highest abundances predicted to occur in Shelikof Strait (Fig. 78).

Walleye pollock distribution in commercial fisheries -- Distribution of adult walleye pollock in commercial fisheries catches from the GOA was generally consistent throughout all seasons. In the fall, bottom depth, ocean color, and bottom temperature were the most important model variables determining suitable habitat of walleye pollock (relative importance: 0.44, 0.19, and 0.11, respectively). The AUC of the fall MaxEnt model was 0.92 for the training and 0.79 for the test data, and 85% of the catches in training and 79% of the test data were correctly classified. The model predicted suitable walleye pollock habitat throughout the GOA with the highest probability habitats off Unimak Island and near the shelf break in the western GOA (Fig. 79).

In the winter, bottom depth, bottom current speed, and maximum tidal current were the most important variables determining suitable habitat for walleye pollock (relative importance: 0.40, 0.36,

and 0.12, respectively). The AUC of the winter MaxEnt model was 0.99 for the training data and 0.96 for the test data, with 94% of the catches in training data, with 96% in the test data predicted correctly. The model predicted that suitable habitat of walleye pollock was most probable in the central GOA, along Shelikof Strait, and in the western GOA off Unimak Island (Fig. 80).

In the spring, bottom depth, slope, and bottom current speed were the most important variables determining suitable habitat for walleye pollock (relative importance: 0.39, 0.25, and 0.12, respectively). The AUC of the spring MaxEnt model was 0.97 for the training and 0.93 for the test data, with 93% of the catches in both the training and test data correctly classified. The model predicted suitable habitat of walleye pollock across the GOA; including off Southeast Alaska, along Shelikof Strait, and off Unimak Island (Fig. 81).

Walleye pollock essential fish habitat maps and conclusions-- Predicted habitat for walleye pollock eggs and larvae was concentrated in the central and western GOA (Fig. 82). Pelagic juvenile walleye pollock habitat was also concentrated in the western GOA (Fig. 82). Summertime habitat of settled juvenile walleye pollock was distributed along the inner and middle shelf throughout the GOA. Adult walleye pollock were also broadly distributed throughout the GOA, but areas of higher predicted abundance were more prevalent along the outer shelf (Fig. 82). The fall, winter, and spring distribution of walleye pollock habitat from commercial catches was essentially the same throughout the seasons and spread throughout the GOA (Fig. 82).

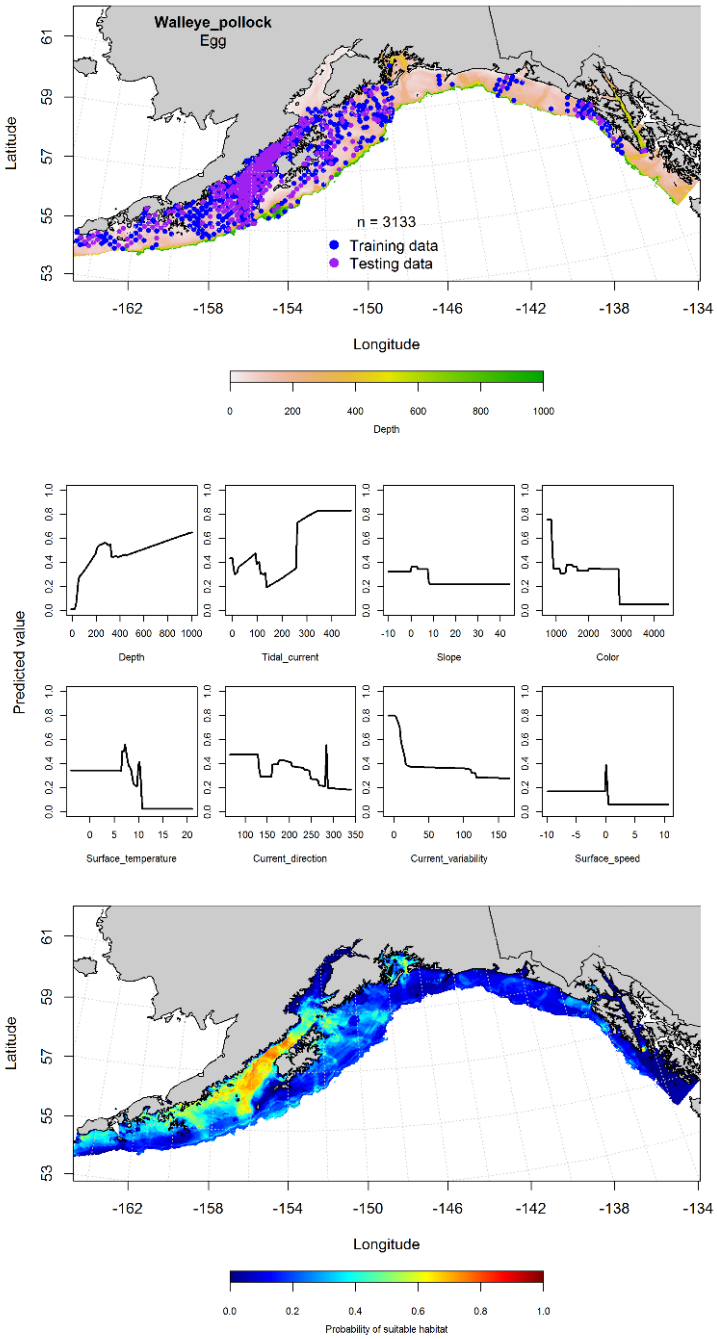

Figure 74. -- Distribution of walleye pollock eggs from EcoFOCI ichthyoplankton surveys (January-March 1991-2013) (top panel) with training (blue dots) and testing (purple dots) data indicated, maximum entropy (MaxEnt) model effects (center panel), and predicted probability of suitable walleye pollock egg habitat (bottom panel).

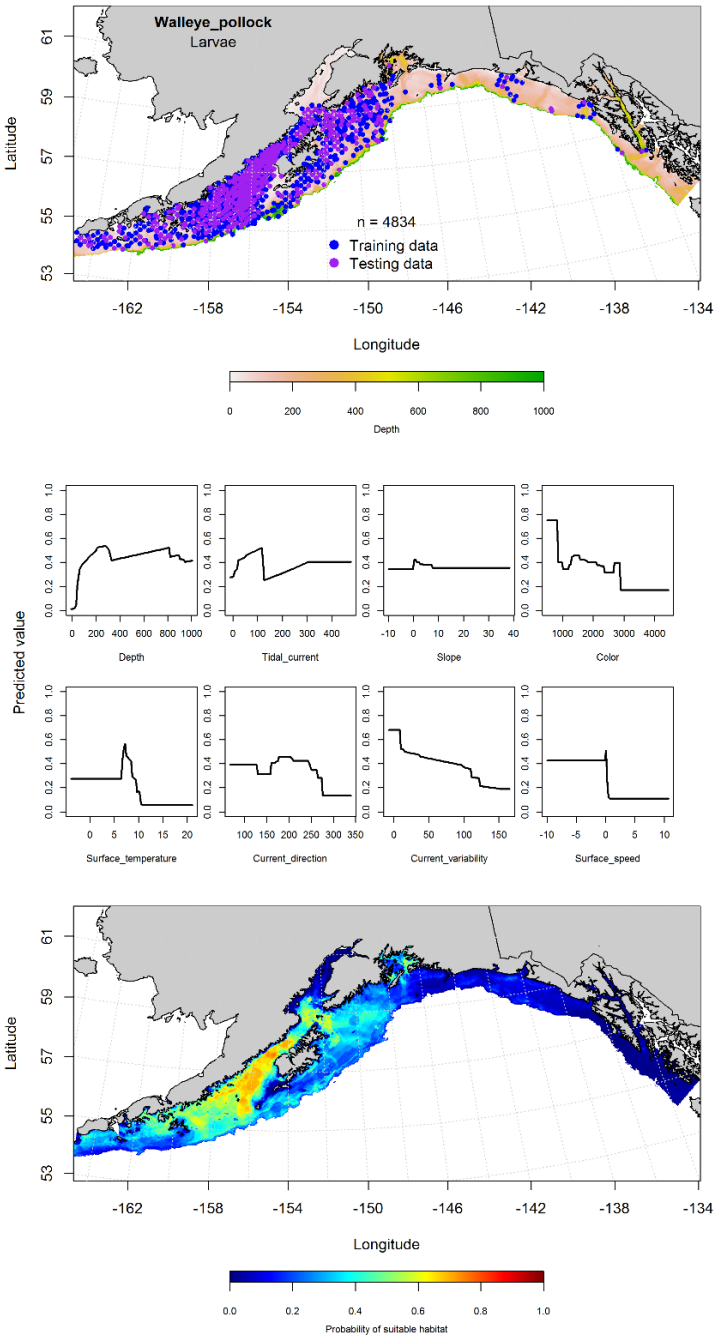

Figure 75. -- Distribution of pelagic walleye pollock larvae observations from EcoFOCI ichthyoplankton surveys (April-September 1991-2012) in the Gulf of Alaska (top panel) with training (blue dots) and testing (purple dots) data indicated, maximum entropy (MaxEnt) model effects (center panel), and the predicted probability of suitable pelagic walleye pollock larval habitat (bottom panel).

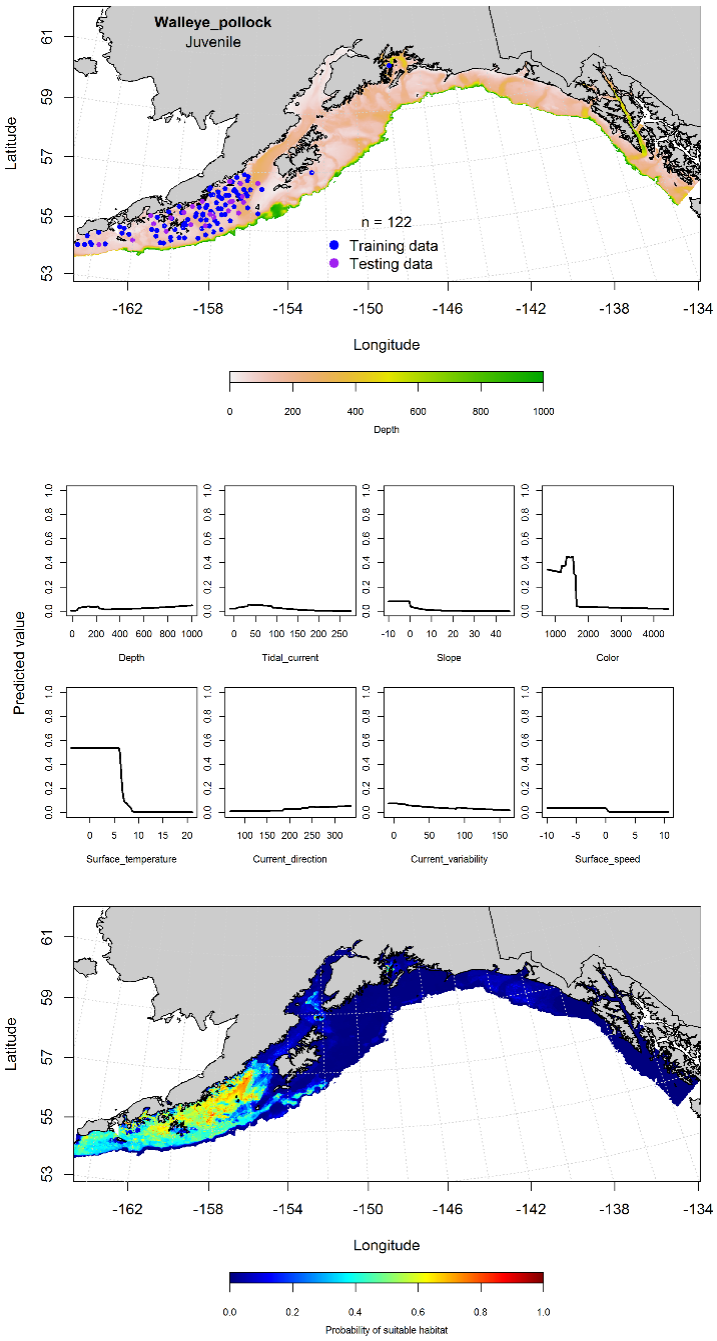

Figure 76. -- Distribution of pelagic juvenile walleye pollock observations from EcoFOCI ichthyoplankton surveys (April-September 1991-2012) in the Gulf of Alaska (top panel) with training (blue dots) and testing (purple dots) data indicated, maximum entropy (MaxEnt) model effects (center panel), and the predicted probability of suitable pelagic juvenile walleye pollock habitat (bottom panel).

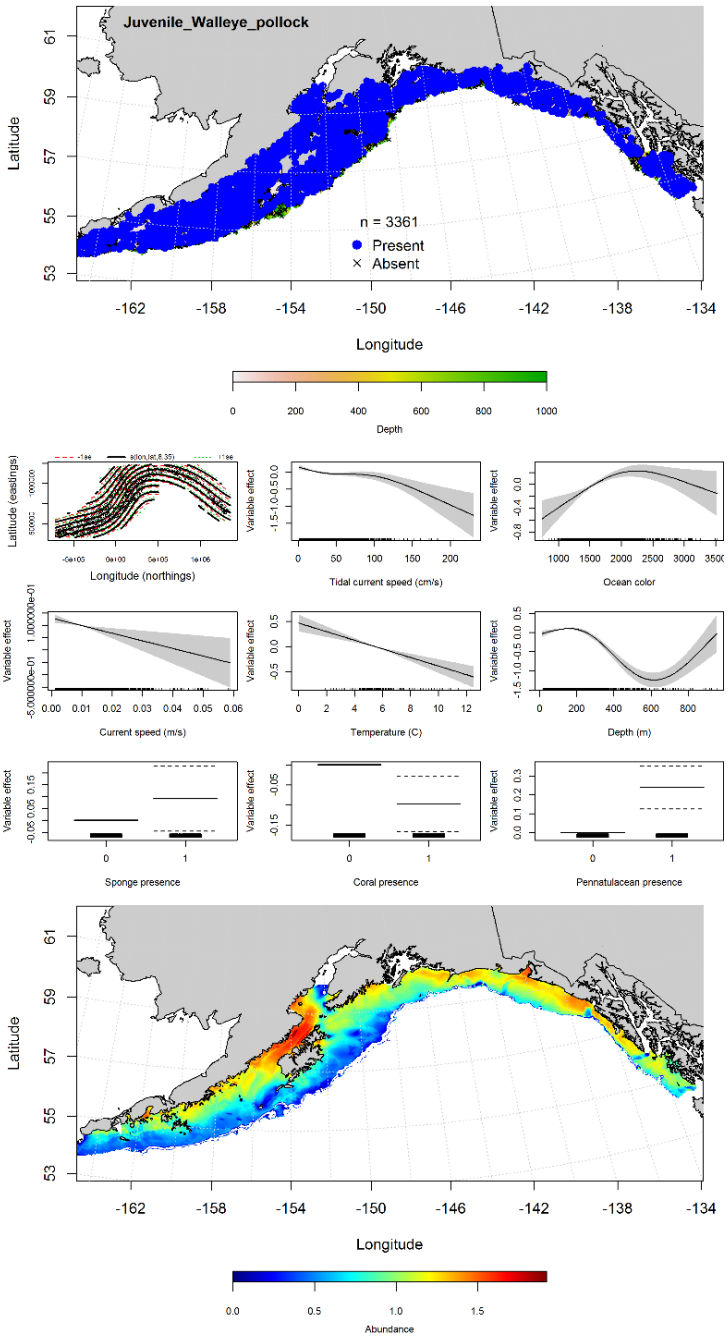

Figure 77. -- Catches of settled juvenile walleye pollock from RACE-GAP summer bottom trawl surveys (1993-2013) in the Gulf of Alaska (top panel), significant relationships between CPUE and environmental variables in the best fitting generalized additive model (GAM; middle panels), and the GAM-predicted abundance of settled juvenile walleye pollock (bottom panel).

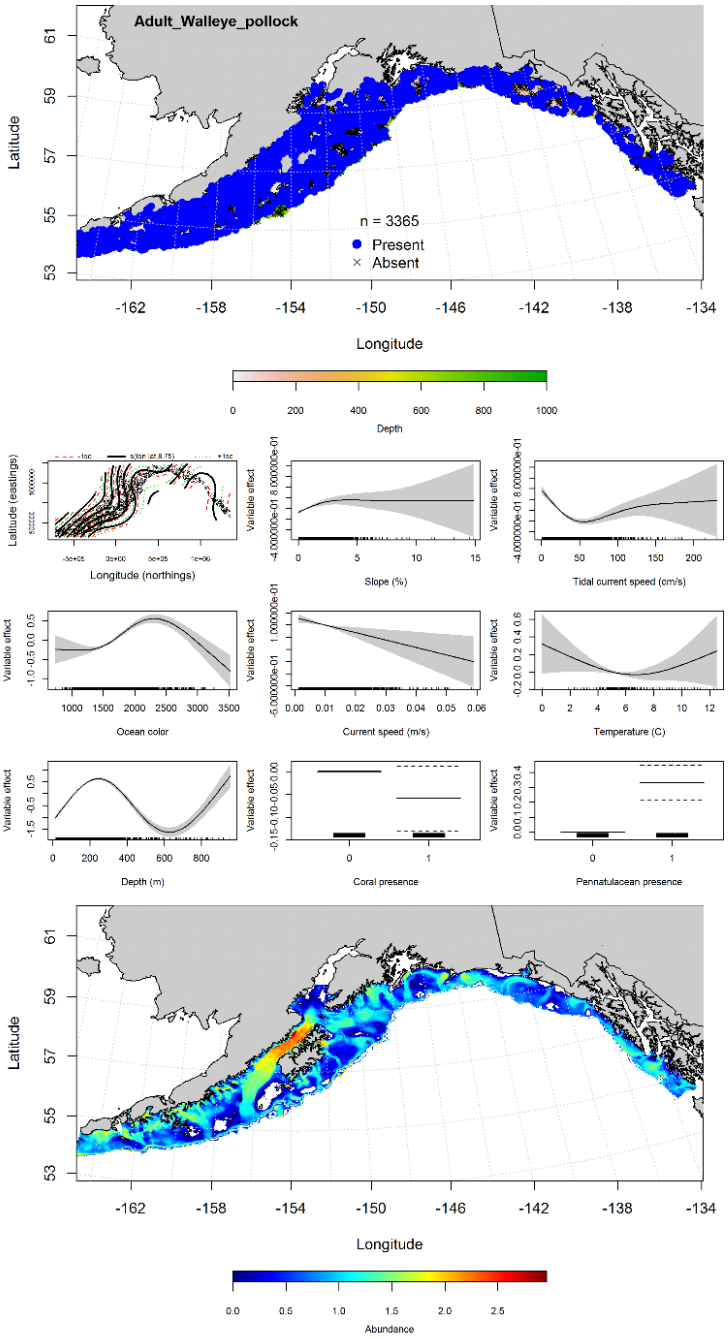

Figure 78. -- Catches of adult walleye pollock from RACE-GAP summer bottom trawl surveys (1993-2013) in the Gulf of Alaska (top panel), significant relationships between CPUE and environmental variables in the best fitting generalized additive model (GAM; middle panels), and the GAM-predicted abundance of adult walleye pollock (bottom panel).

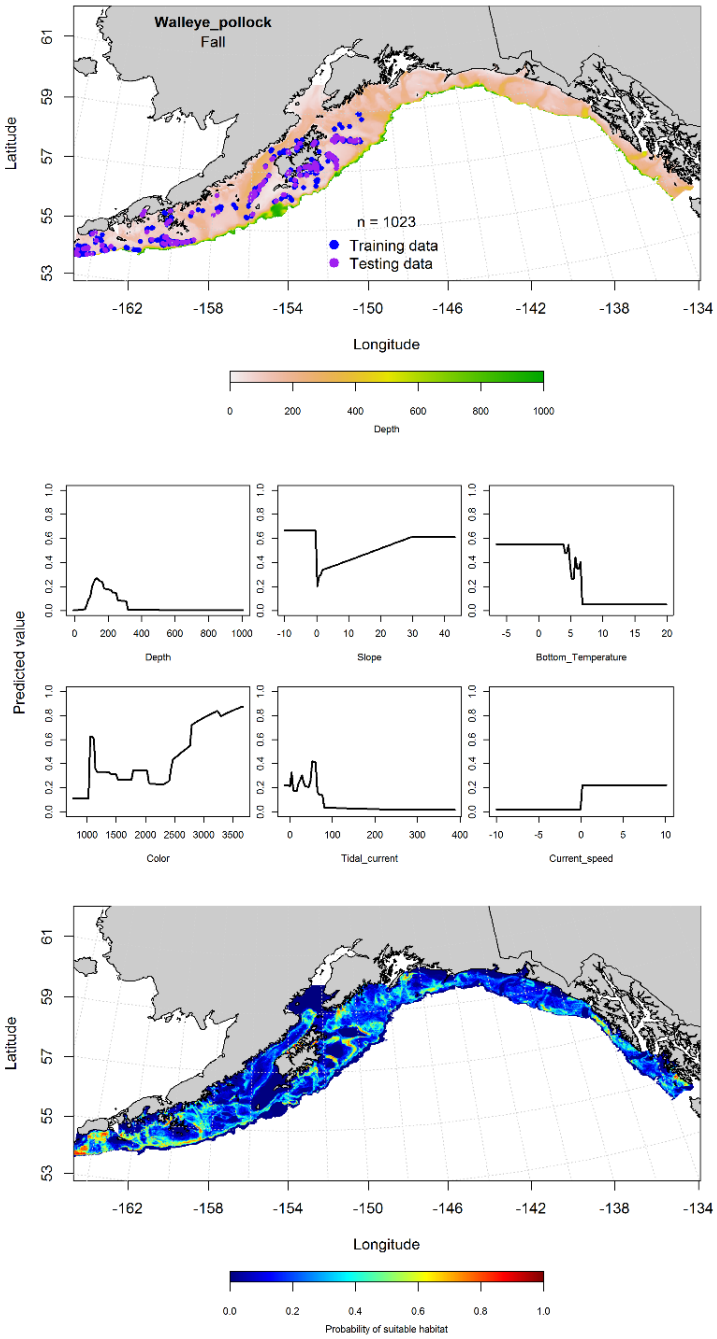

Figure 79. -- Locations of walleye pollock from fall (September-November 2001-2015) commercial fisheries catches in the Gulf of Alaska (top panel), MaxEnt model effects (middle panels), and predicted probability of suitable habitat for walleye pollock based on the model (bottom panel).

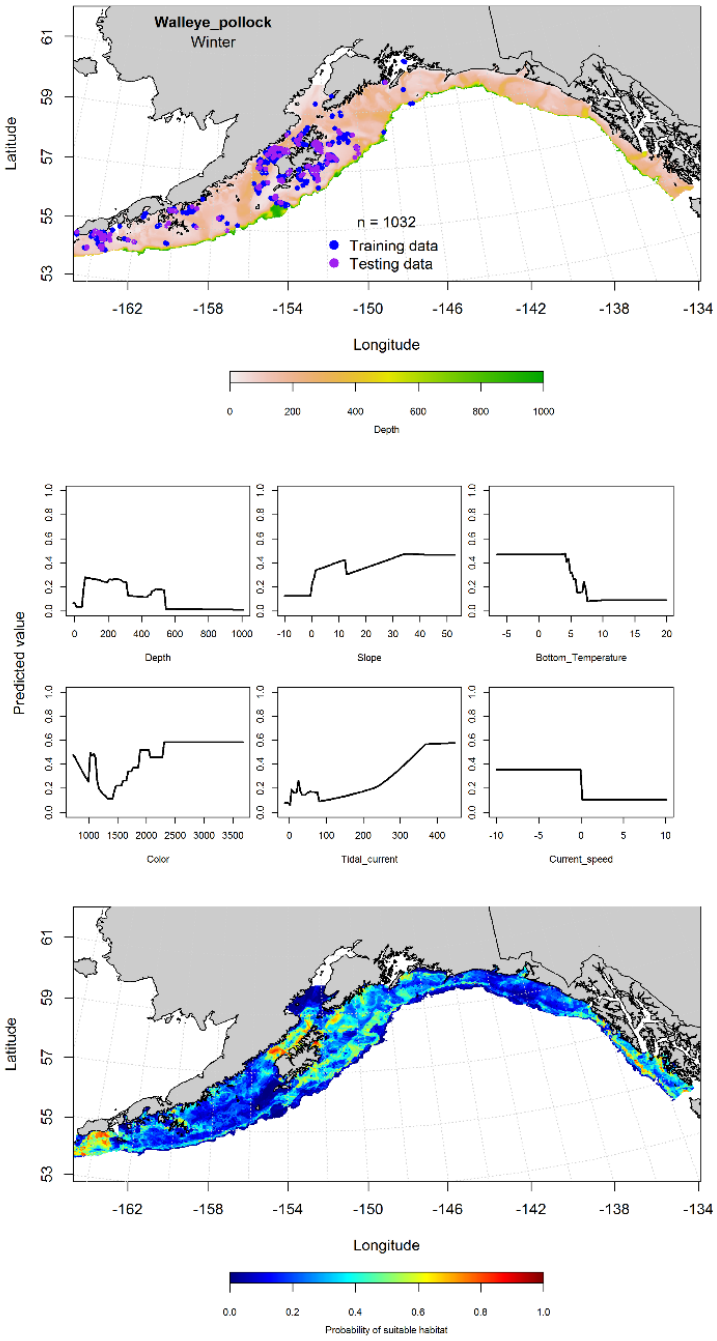

Figure 80. -- Locations of walleye pollock from winter (December-February 2001-2015) commercial fisheries catches in the Gulf of Alaska (top panel), with training (blue dots) and testing (purple dots) data indicated, maximum entropy (MaxEnt) model effects (center panel), and the predicted probability of suitable adult walleye pollock habitat (bottom panel).

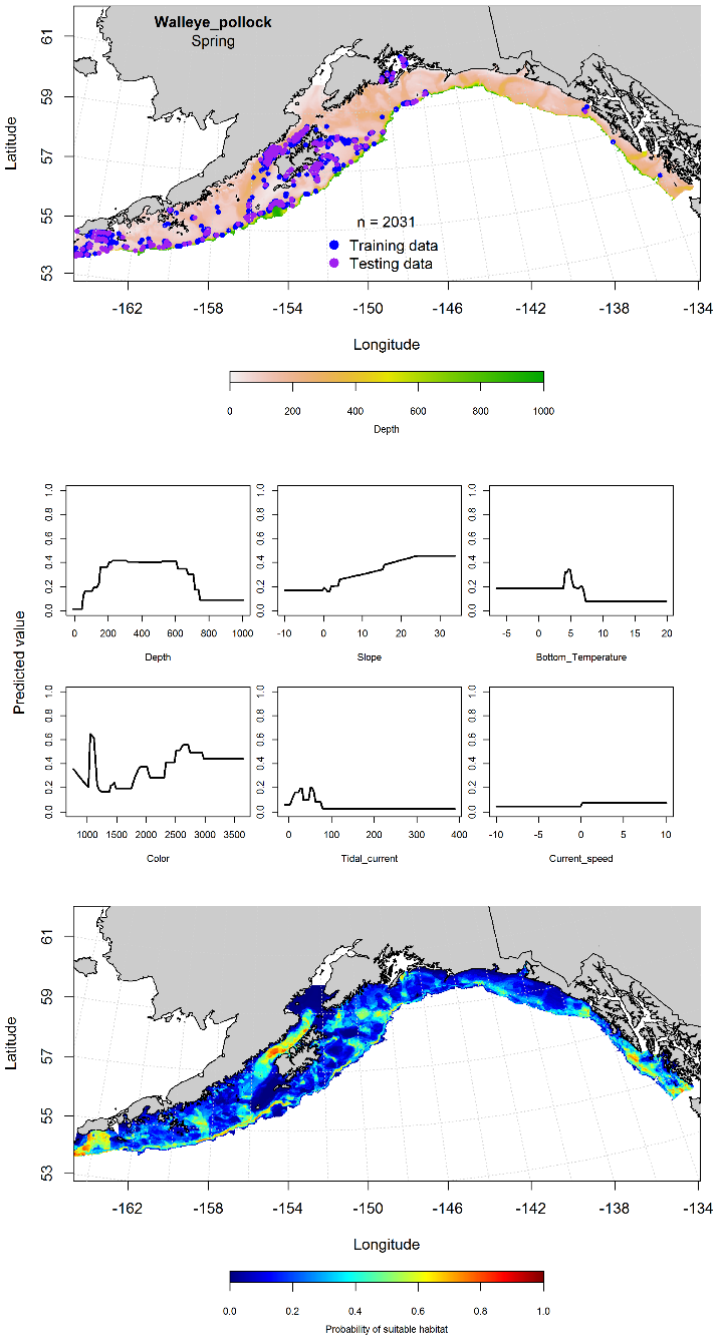

Figure 81. -- Locations of walleye pollock from spring (March-May 2001-2015) commercial fisheries catches in the Gulf of Alaska (top panel), with training (blue dots) and testing (purple dots) data indicated, maximum entropy (MaxEnt) model effects (center panel), and the predicted probability of suitable adult walleye pollock habitat (bottom panel).

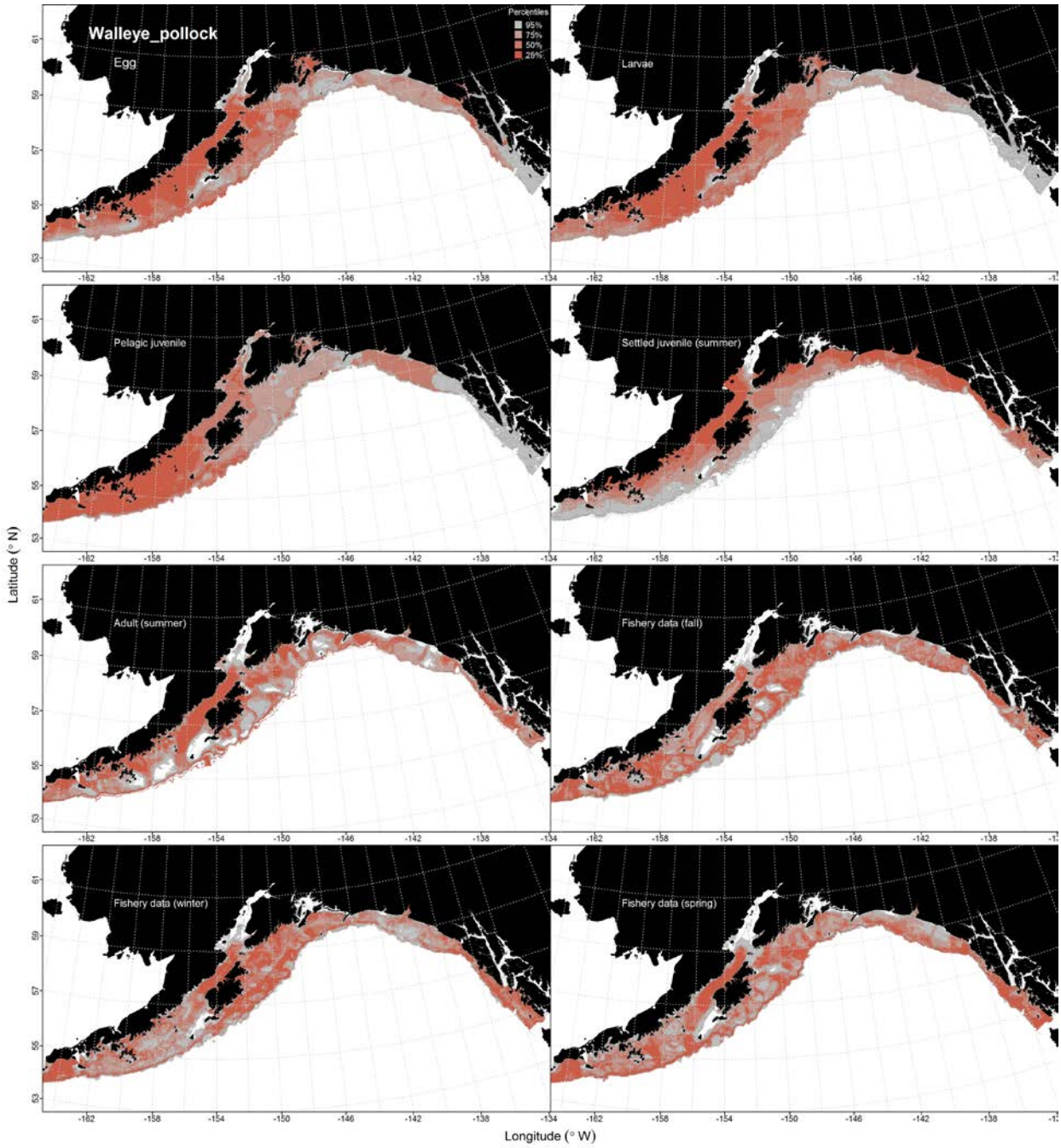

Figure 82. -- Habitat predicted for walleye pollock eggs, pelagic larvae, and pelagic juveniles from EcoFOCI ichthyoplankton surveys (1991-2012), settled juveniles and adults from RACE-GAP summertime bottom trawl surveys (1993-2013), and predicted from presence in commercial fishery catches (2001-2015) from fall, winter, and spring in the Gulf of Alaska.

Pacific Cod (*Gadus macrocephalus*)

Early life history stages of Pacific cod -- There were no instances of Pacific cod eggs observed in the EcoFOCI collections.

There were 2,348 catches of larval Pacific cod, the majority of which were from the central and western GOA (Fig. 83). The MaxEnt model indicated that sea surface temperature, bottom depth, and surface current speed were the most important factors explaining larval cod distribution (relative importance: 0.42, 0.27, and 0.12, respectively). The model AUCs were 0.88 (training data) and 0.81 (test data), with 79% of the training data and 81% of the test data correctly classified. The model predicted suitable habitat for larval Pacific cod in the central and western GOA, particularly around Shelikof Gully (Fig. 83).

There were 73 catches of pelagic juvenile Pacific cod in the EcoFOCI collections, these largely occurred in the central and western GOA (Fig. 84). The MaxEnt model indicated that sea surface temperature, ocean color, and bottom depth were the most important factors explaining pelagic juvenile cod habitat distribution (relative importance: 0.50, 0.26, and 0.15, respectively). The model AUCs were 0.88 (training data) and 0.82 (test data). The model predicted that pelagic juvenile Pacific cod habitat was prevalent throughout the central and western GOA, with areas of highest probability habitats concentrated near the Alaska Peninsula and Shumagin Islands (Fig. 84).

Juvenile and adult Pacific cod distribution in the bottom trawl survey -- The catches of settled juvenile Pacific cod in summer bottom trawl surveys indicate this species is broadly distributed across the GOA (Fig. 85). A GAM predicting the abundance of settled juvenile Pacific cod explained 27% of the variability in CPUE for training data, and 25% of the variability for the test data.

Geographic location, bottom depth, and ocean color were the most important variables explaining the abundance of settled juvenile Pacific cod. Predictions of settled juvenile Pacific cod abundance vary across the GOA, with the highest abundance occurring around Kodiak Island and the western Alaska Peninsula (Fig. 85).

A GAM predicting the abundance of adult Pacific cod explained 24% of the variability in CPUE for the training data, and 23% of the variability for the test data. Geographic location, bottom depth, and slope were the most important variables describing the abundance of adult Pacific cod in RACE-GAP summer bottom trawl catches. Adult Pacific cod abundance predictions varied across the GOA, but were highest along the western Alaska Peninsula (Fig. 86).

Pacific cod distribution in commercial fisheries -- Distribution of Pacific cod in commercial fisheries catches from the GOA was generally consistent across fall, winter, and spring. The AUC of the fall MaxEnt model was 0.88 for the training data (79% correctly classified) and 0.78 for the test data (78% correctly classified). Bottom depth and ocean color were the most important model variables determining probable suitable habitat of Pacific cod (relative importance: 0.41 and 0.19, respectively). The model predicted that suitable habitat of Pacific cod occurs throughout the GOA, but the greatest probabilities of suitable habitat was predicted in the central and western GOA (Fig. 87).

In the winter, bottom depth and ocean color were the most important variables predicting suitable Pacific cod habitat (relative importance: 0.58 and 0.16, respectively). The AUC of the winter MaxEnt model was 0.87 for the training data and 0.77 for the test data. The model correctly classified 78% of the predictions from the training data and 77% of the predictions from the test data.

The highest predicted probability of suitable habitat for Pacific cod was in the central and western GOA (Fig. 88).

In the spring, ocean color and bottom depth were the most important variables determining suitable habitat of Pacific cod (relative importance: 0.31 and 0.27, respectively). The AUC of the spring MaxEnt model was 0.86 for the training data and 0.77 for the test data. The model correctly classified 79% of the predictions from the training data and 77% of the predictions from the test data. As with the fall and winter predictions, the model predicted that the highest probability Pacific cod habitat was in the central and western GOA (Fig. 89).

Pacific cod essential fish habitat maps and conclusions-- Larval and pelagic juvenile Pacific cod habitat was predicted to occur throughout the central and western GOA (Fig. 90). Summertime habitat for settled juvenile and adult Pacific cod was also predicted throughout the central and western GOA, although adult habitats tended to be more broadly distributed and to include deeper areas than the juveniles (Fig. 90). The fall, winter, and spring distribution of Pacific cod habitat predicted from their presence in commercial catches was essentially the same throughout year, but slightly more concentrated at deeper depths during the spring (Fig. 90).

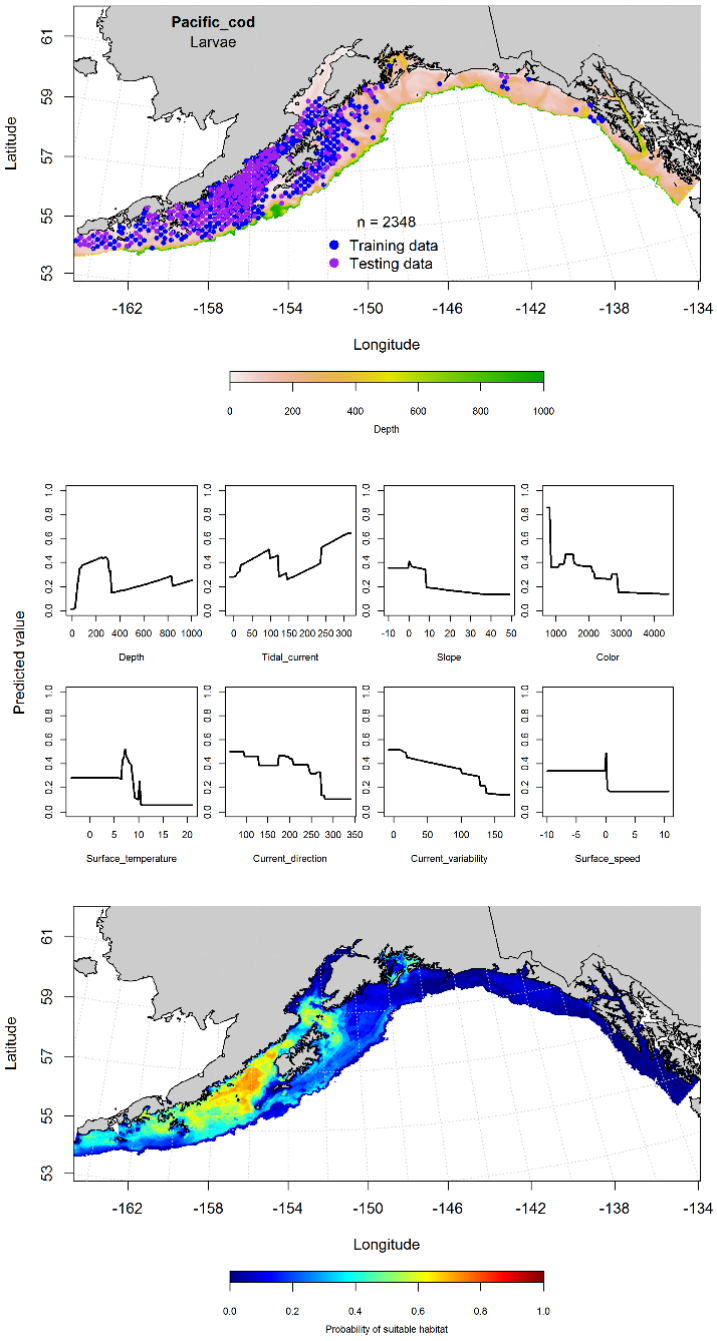

Figure 83. -- Distribution of pelagic Pacific cod larvae observations from EcoFOCI ichthyoplankton surveys (April-September 1991-2012) in the Gulf of Alaska (top panel) with training (blue dots) and testing (purple dots) data indicated, maximum entropy (MaxEnt) model effects (center panel), and the predicted probability of suitable pelagic Pacific cod larval habitat (bottom panel).

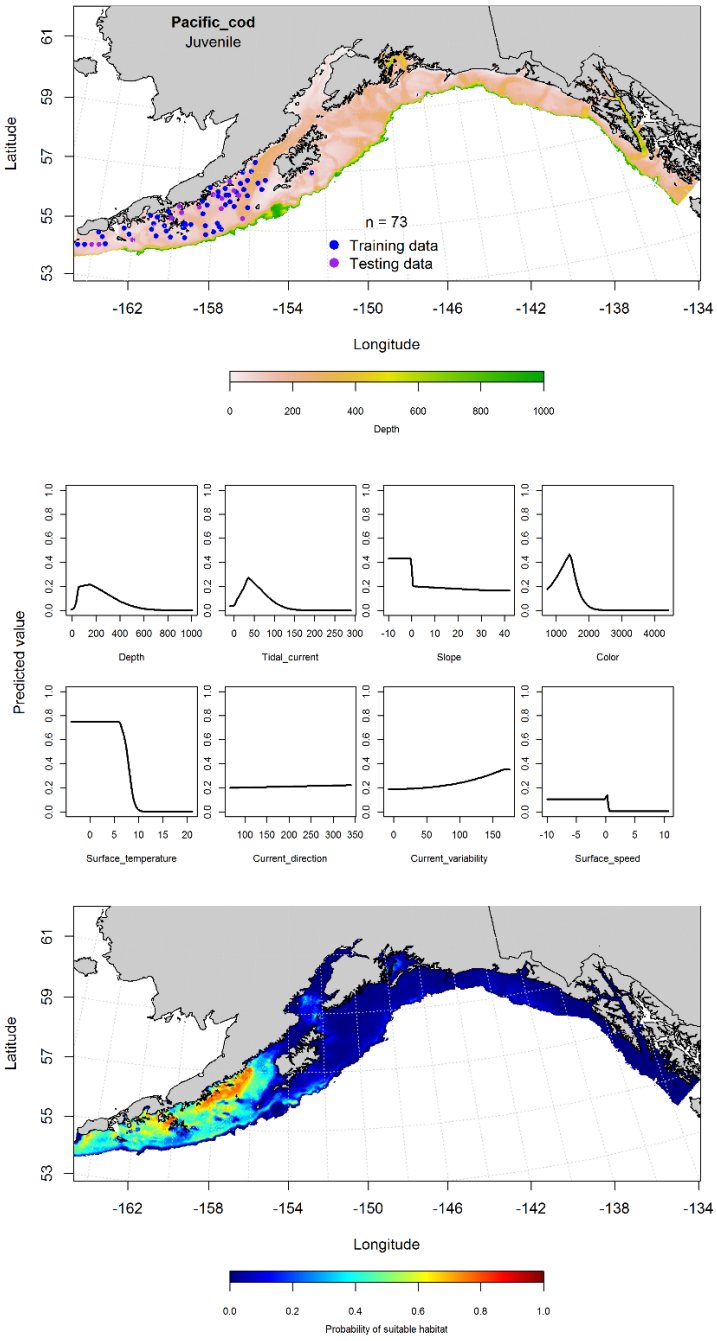

Figure 84. -- Distribution of pelagic juvenile Pacific cod observations from EcoFOCI ichthyoplankton surveys (April-September 1991-2012) in the Gulf of Alaska (top panel) with training (blue dots) and testing (purple dots) data indicated, maximum entropy (MaxEnt) model effects (center panel), and the predicted probability of suitable pelagic juvenile Pacific cod habitat (bottom panel).

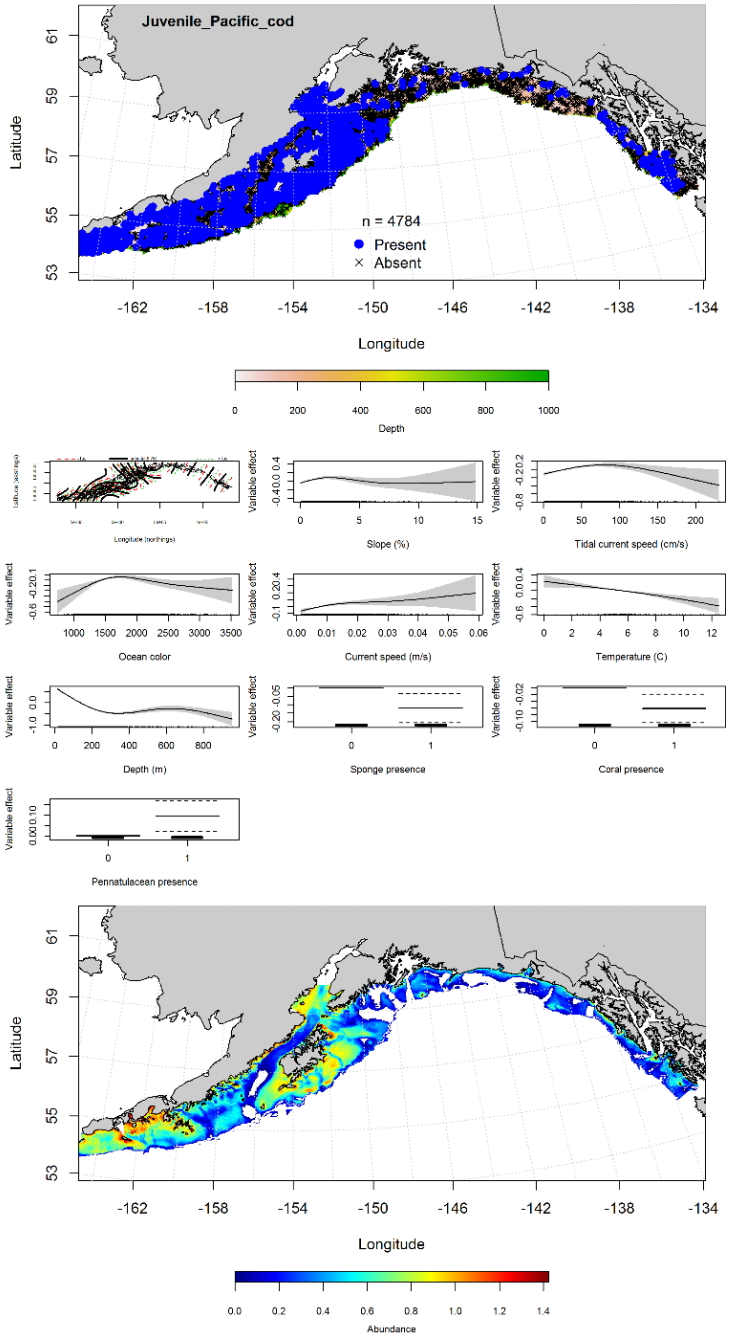

Figure 85. -- Presence of settled juvenile Pacific cod from RACE-GAP summer bottom trawl surveys (1993-2013) in the Gulf of Alaska (top panel) with training (blue dots) and testing (purple dots) data indicated, generalized additive model (GAM) effects (center panel), and the GAM-predicted abundance of settled juvenile Pacific cod (bottom panel).

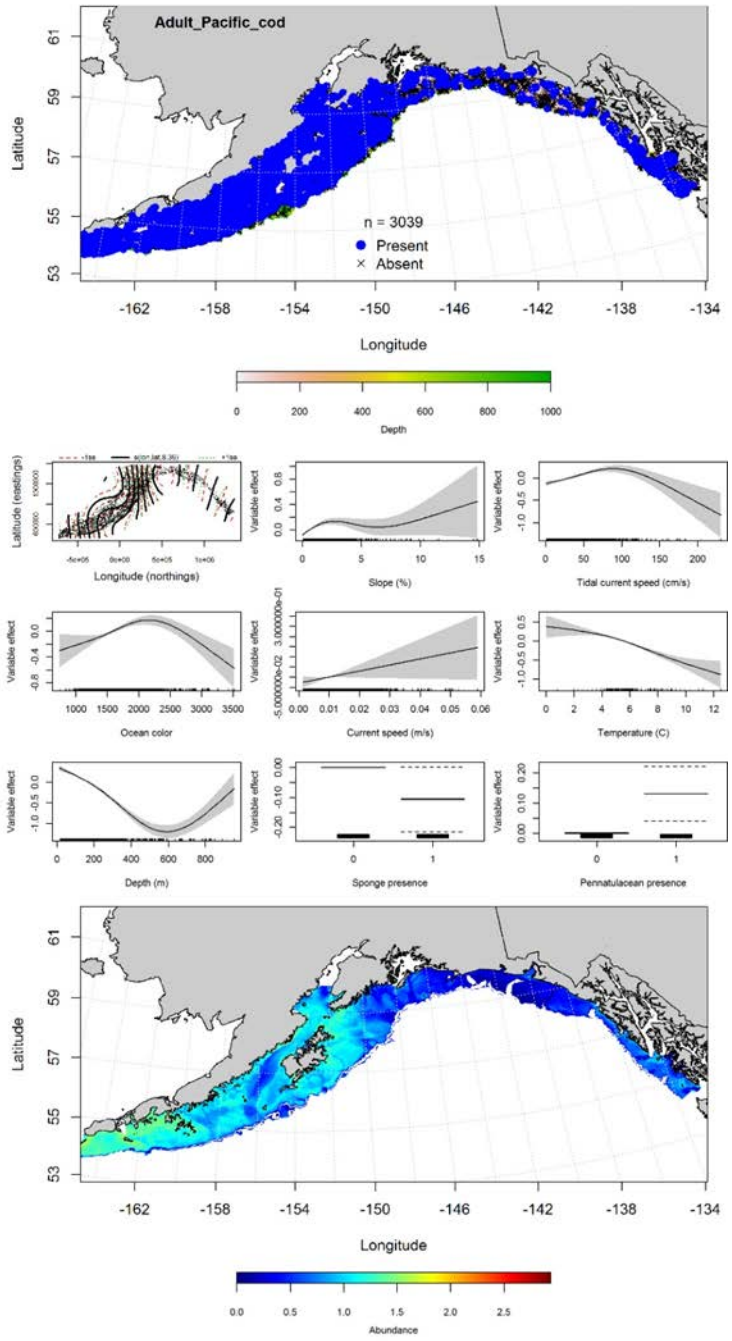

Figure 86. -- Presence of adult Pacific cod from RACE-GAP summer bottom trawl surveys (1993-2013) in the Gulf of Alaska (top panel) with training (blue dots) and testing (purple dots) data indicated, generalized additive model (GAM) effects (center panel), and the GAM-predicted abundance of adult Pacific cod (bottom panel).

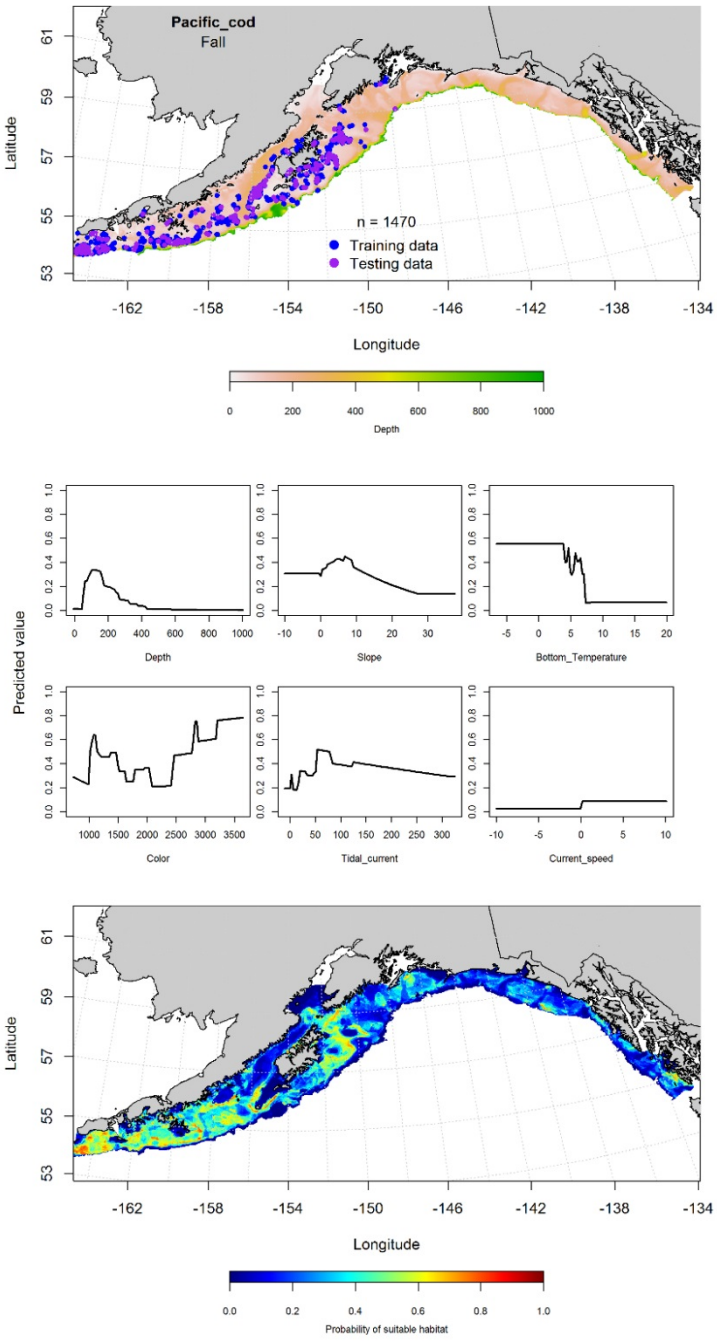

Figure 87. -- Locations of Pacific cod from fall (September-November 2001-2015) commercial fisheries catches in the Gulf of Alaska (top panel), MaxEnt model effects (middle panels), and predicted probability of suitable habitat for Pacific cod based on the model (bottom panel).

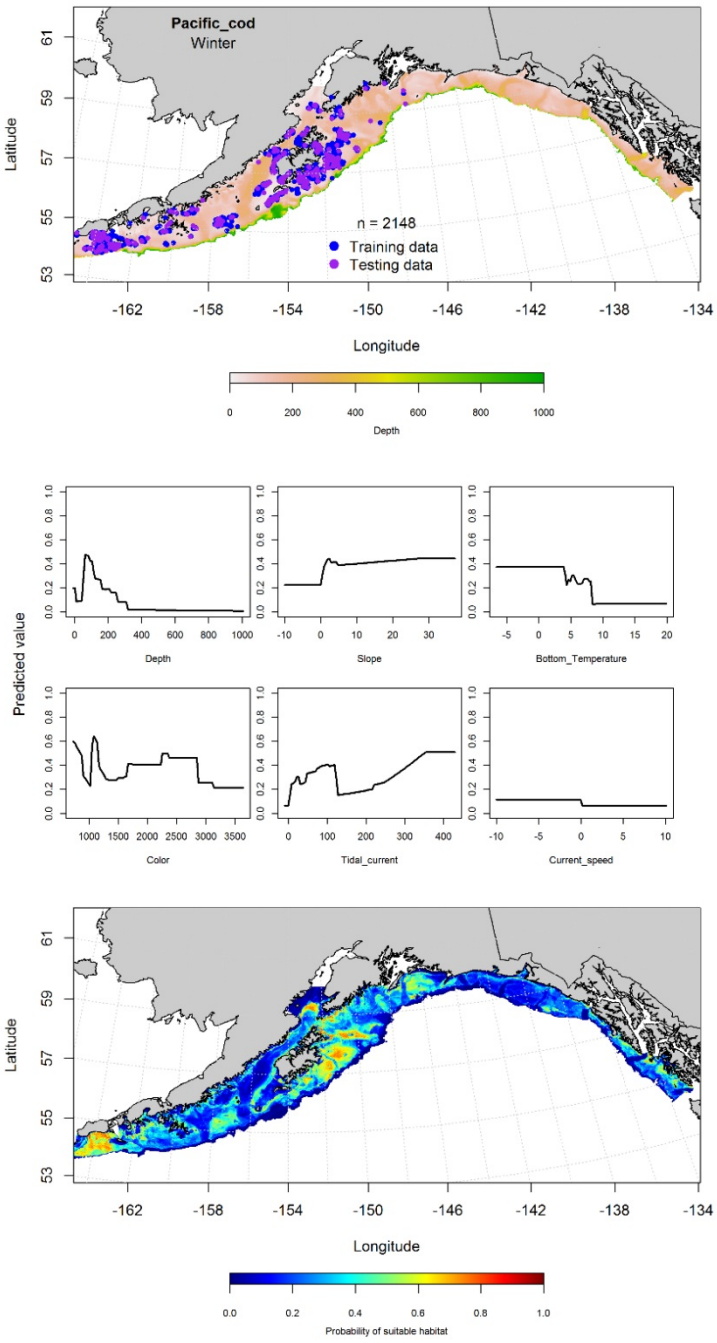

Figure 88. -- Locations of Pacific cod from winter (December-February 2001-2015) commercial fisheries catches in the Gulf of Alaska (top panel), with training (blue dots) and testing (purple dots) data indicated, maximum entropy (MaxEnt) model effects (center panel), and the predicted probability of suitable Pacific cod habitat (bottom panel).

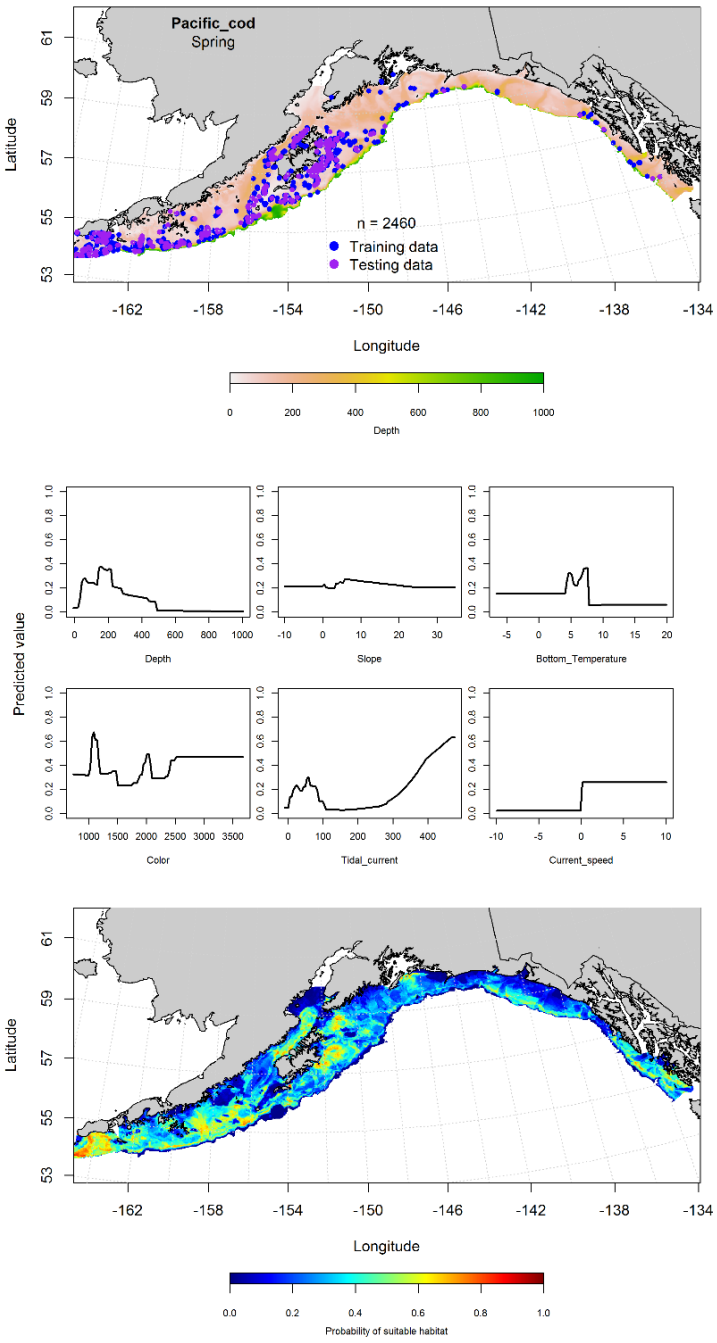

Figure 89. -- Locations of Pacific cod from spring (March-May 2001-2015) commercial fisheries catches in the Gulf of Alaska (top panel), with training (blue dots) and testing (purple dots) data indicated, maximum entropy (MaxEnt) model effects (center panel), and the predicted probability of suitable Pacific cod habitat (bottom panel).

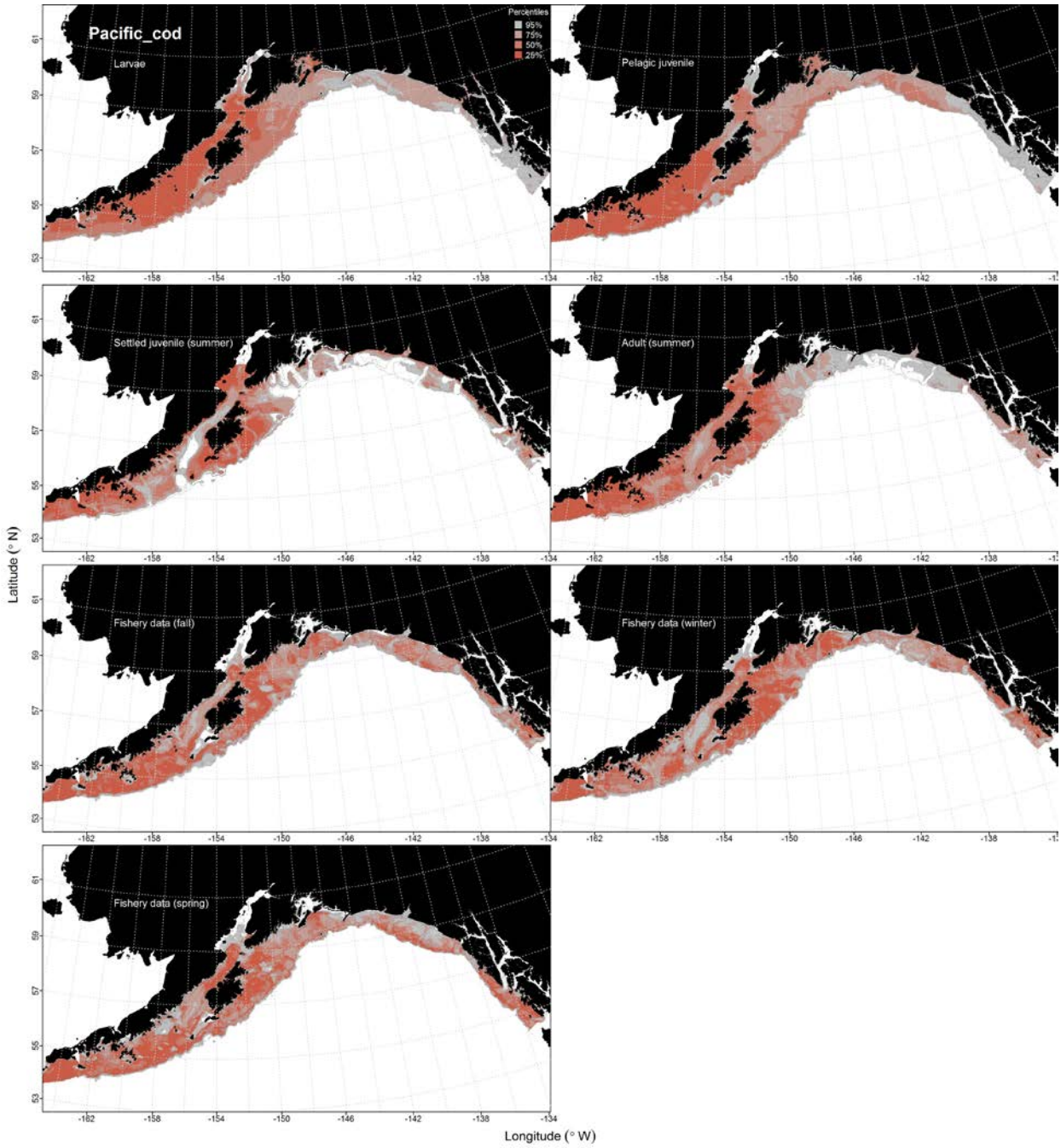

Figure 90. -- Habitat predicted for pelagic Pacific cod larvae and juveniles from EcoFOCI ichthyoplankton surveys (1991-2012), settled juveniles and adults from RACE-GAP summertime bottom trawl surveys (1993-2013), and predicted from presence in commercial fishery catches (2001-2015) from fall, winter, and spring in the Gulf of Alaska.

Yellow Irish Lord (*Hemilepidotus jordani*)

Early life history stages of yellow Irish lord -- There were no observation of yellow Irish lord eggs in the in the EcoFOCI collections.

There were 45 identified records (30 larvae and 15 pelagic juveniles) of yellow Irish lord in the EcoFOCI collections. A majority of these larvae (Fig. 91) and pelagic juveniles (Fig. 92) were observed in the central and western GOA. These occurrences did not provide sufficient data to parameterize a MaxEnt model for these life stages of yellow Irish lord.

Juvenile and adult yellow Irish lord distribution in the bottom trawl survey -- The catch of yellow Irish lord in summer bottom trawl surveys indicates this species is broadly distributed in the central and western GOA. A MaxEnt model was used to predict the suitable habitat of settled juvenile yellow Irish lord from RACE-GAP bottom trawl survey catches. The AUC of the model was 0.92 for the training data and 0.82 for the testing data. Bottom depth and ocean color were the most important predictors in the model (relative importance: 0.80 and 0.07, respectively). The model predicted that suitable yellow Irish lord habitat was distributed throughout GOA, but the most probable habitats were in the central GOA, around Kodiak Island and in the western GOA along the Alaska Peninsula (Fig. 93).

An hGAM was used to predict the distribution of adult yellow Irish lord abundance. The PA GAM resulted in an AUC of 0.88 for the training data and 0.87 for the test data. Geographic position, ocean color, and bottom current speed were the most important predictors of the probability of yellow Irish lord presence in the model (Fig. 94). Adult yellow Irish lord were predicted to occur throughout the GOA, though their highest probability of presence was in the western GOA (Fig. 94).

The CPUE GAM explained 29% of the variability of the training data set but only 5% of the test data set. Geographic position, maximum tidal current, and bottom current speed were the most important variables explaining the CPUE of adult yellow Irish lord. The highest predicted abundances occurred along the inner and middleshelf in central and western GOA, but even in these areas abundances were relatively modest (Fig. 94).

Yellow Irish lord distribution in commercial fisheries -- The distribution of adult yellow Irish lord in commercial fisheries catches from the GOA was seasonally consistent. In the fall, maximum tidal current, slope, and bottom depth were the most important model variables (relative importance: 0.51, 0.21, and 0.17, respectively). The AUC of the fall MaxEnt model was 0.98 for the training data and 0.89 for the test data. The model correctly classified 92% of the predictions from the training data and 89% of the predictions from the test data. The model predicted limited suitable habitat for yellow Irish lord which was primarily concentrated around Chirikof Island and Semidi Banks (Fig. 95).

In the winter, ocean color, bottom current speed, and bottom depth were the most important variables predicting suitable habitat of yellow Irish lord (relative importance: 0.42, 0.34, and 0.16, respectively). The AUC of the winter MaxEnt model was 0.87 for the training data and 0.78 for the test data. The model correctly classified 85% of the predictions from the training data and 90% of the predictions from the test data. The model predicted a patchy distribution of suitable habitat for yellow Irish lord, with the highest probability areas of occurrence concentrated near Unimak Island (Fig. 96).

In the spring, bottom depth, ocean color, and maximum tidal current were the most important variables determining suitable habitat of yellow Irish lord (relative importance: 0.45, 0.33, and 0.08, respectively). The AUC of the spring MaxEnt model was 0.89 for the training data and 0.81 for the

test data. The model correctly classified 91% of the predictions from the training data and 86% of the predictions from the test data. Similar to winter predictions, the spring model predicted the highest probability of suitable habitat for yellow Irish lord near Unimak Island with an additional hotspot near Kodiak Island in the central GOA (Fig. 97).

Yellow Irish lord essential fish habitat maps and conclusions-- Settled juvenile yellow Irish lord summertime habitat was predicted by the MaxEnt model to be distributed throughout the GOA with pockets of probable habitat present from Unimak Pass in the west well into southeast Alaska. In contrast, predictions of adult yellow Irish lord summertime presence and abundance were largely concentrated around Kodiak Island and the western Alaska Peninsula (Fig. 98). Potential adult yellow Irish lord habitat predicted from commercial catches in the fall, winter, and summer were all more broadly distributed than that predicted from summer bottom trawl survey data (Fig. 98). These differences may, in part, be related to fishing effort and species targeted by the commercial fisheries, compared to the effort of the trawl surveys that does not target any single species or complex of species.

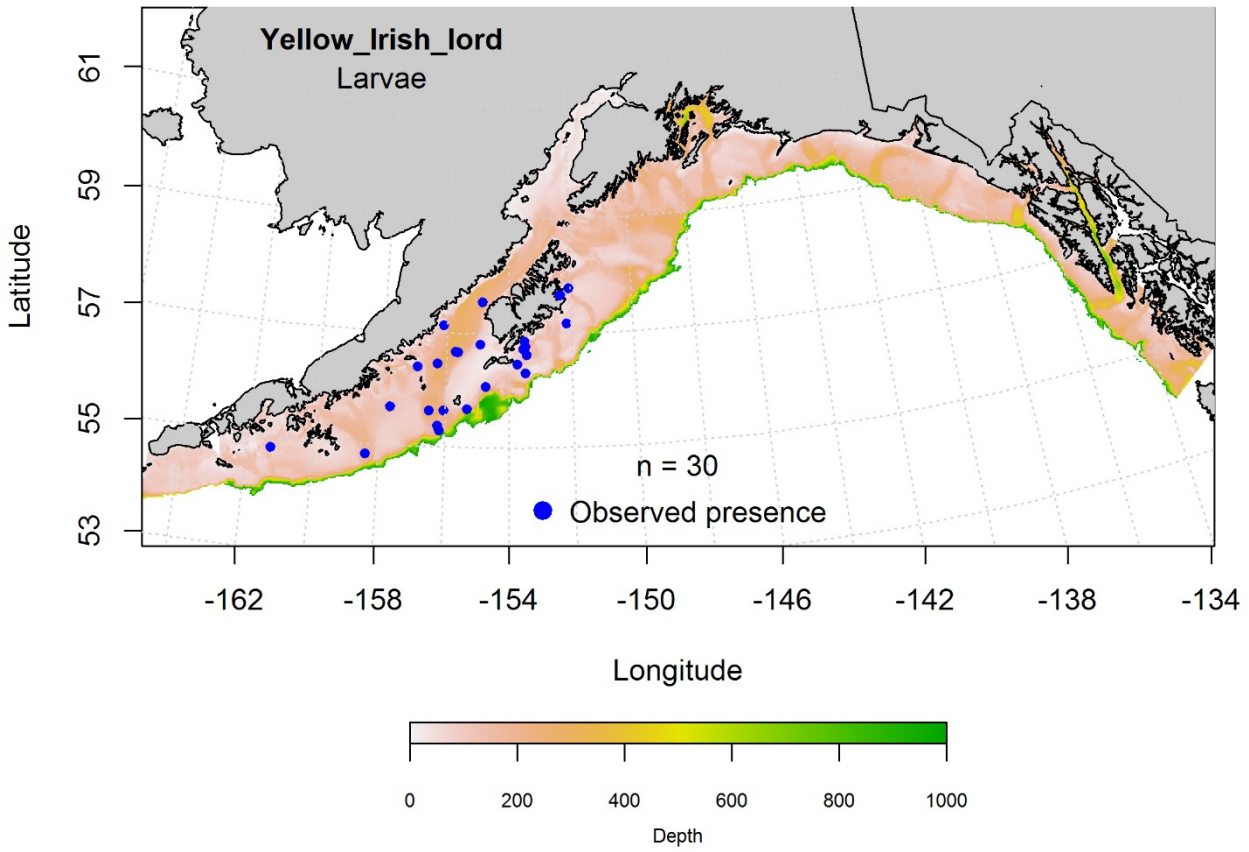

Figure 91. -- Distribution of pelagic yellow Irish lord larvae observations from EcoFOCI ichthyoplankton surveys (April-September 1991-2012) in the Gulf of Alaska.

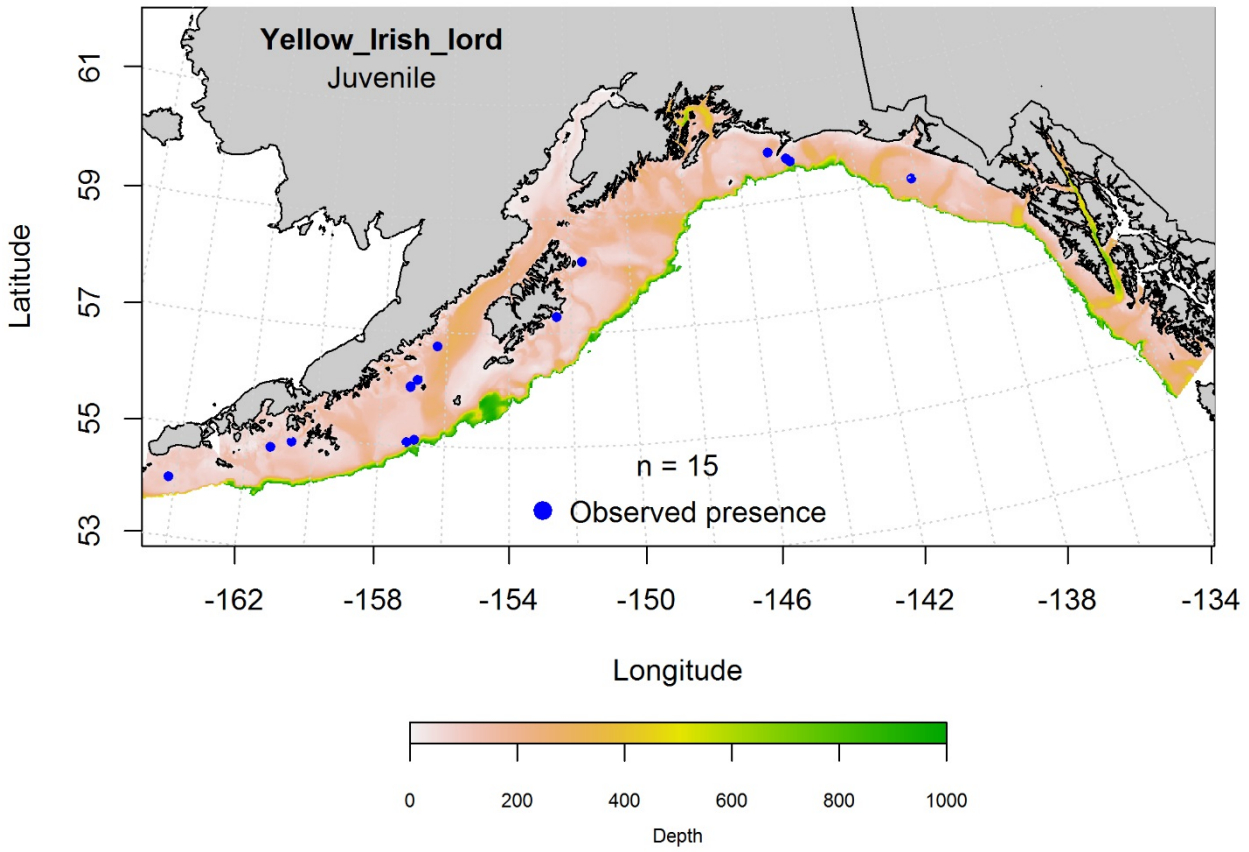

Figure 92. -- Distribution of pelagic juvenile yellow Irish lord observations from EcoFOCI ichthyoplankton surveys (April-September 1991-2012) in the Gulf of Alaska.

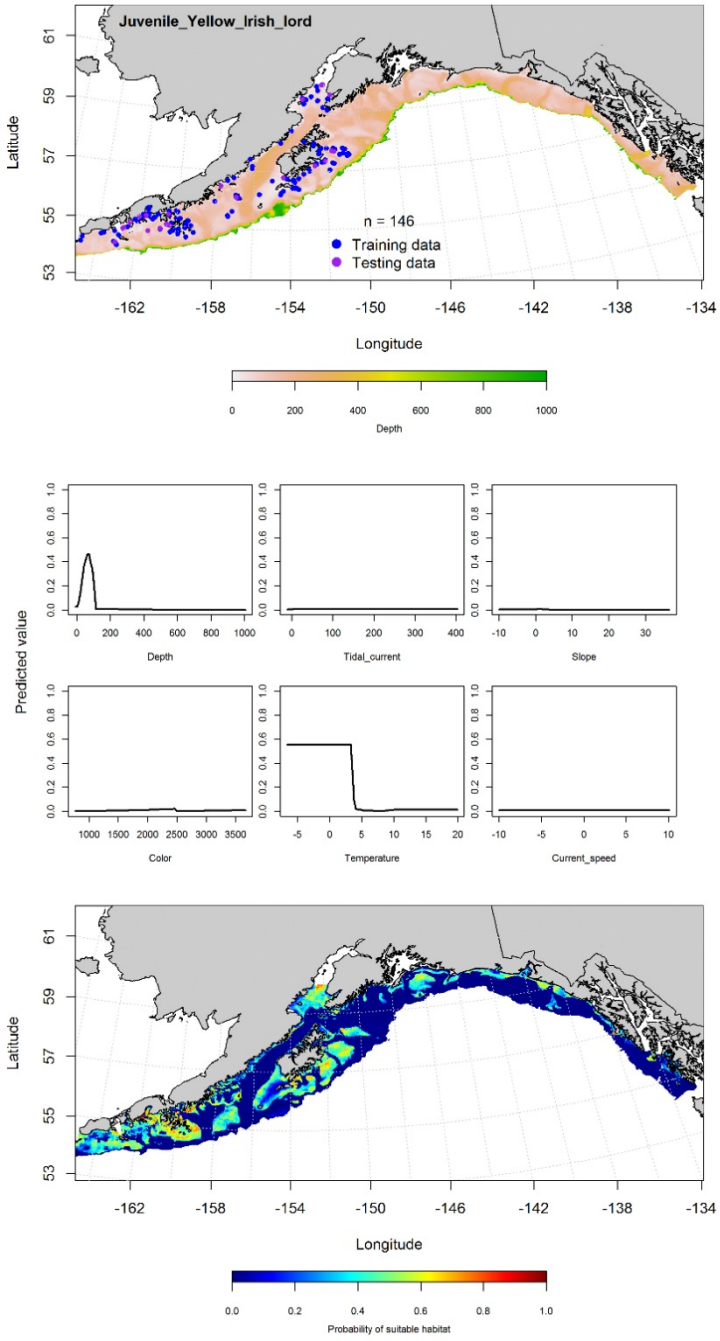

Figure 93. -- Presence of settled juvenile yellow Irish lord from RACE-GAP summer bottom trawl surveys (1993-2013) in the Gulf of Alaska (top panel) with training (blue dots) and testing (purple dots) data indicated, maximum entropy (MaxEnt) model effects (center panel), and the MaxEnt-predicted probability of suitable juvenile yellow Irish lord habitat (bottom panel).

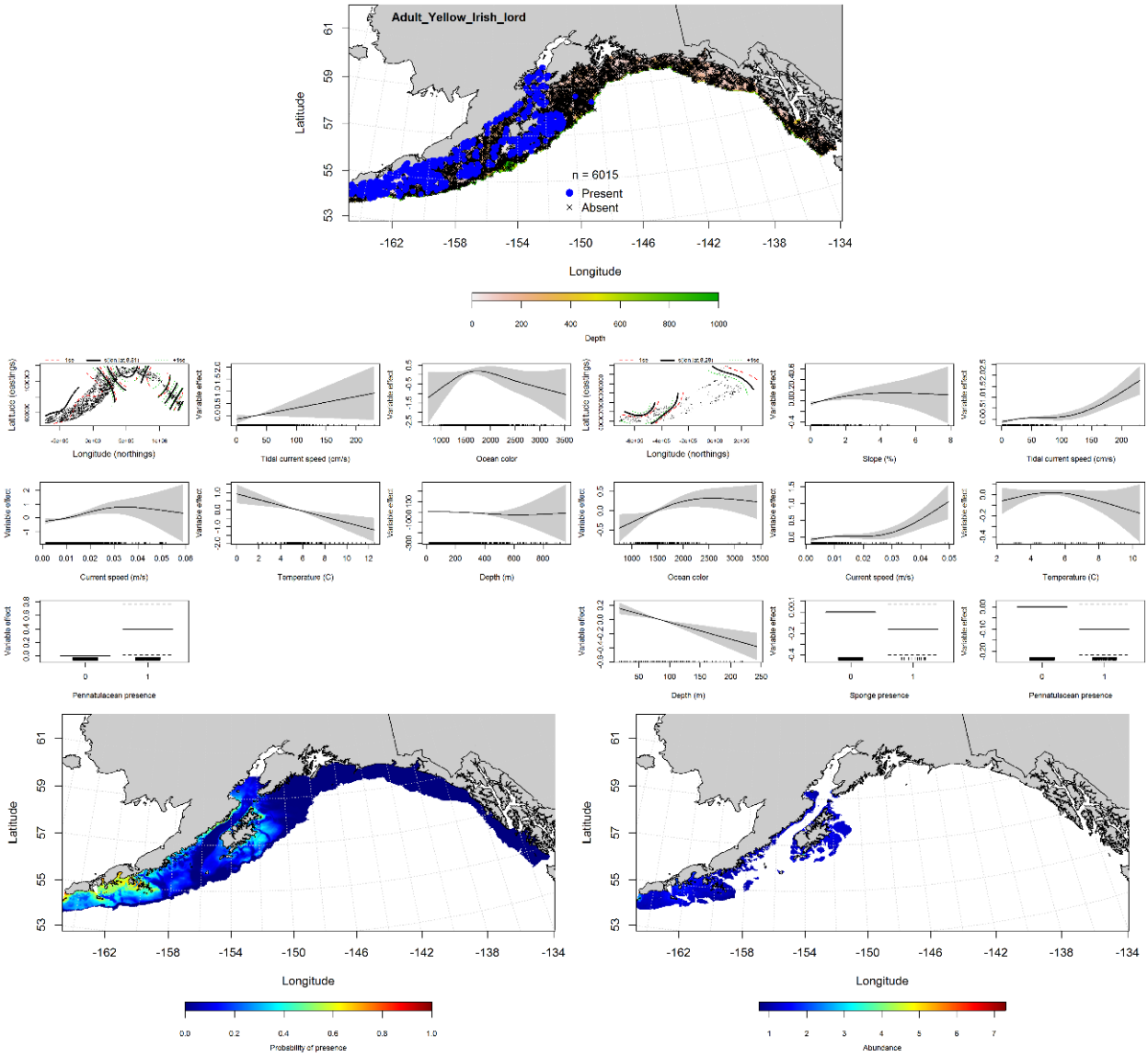

Figure 94. --Distribution of adult yellow Irish lord in 1993-2013 RACE-GAP summer bottom trawl surveys conducted in the Gulf of Alaska (upper panel). Effects of retained habitat covariates in the best fitting generalized additive presence-absence models (PA GAM; left center panel) and abundance (CPUE GAM; right center panel). Predicted spatial distribution of the probability of presence (bottom left panel) and abundance of adult yellow Irish lord based on the models (bottom right panel).

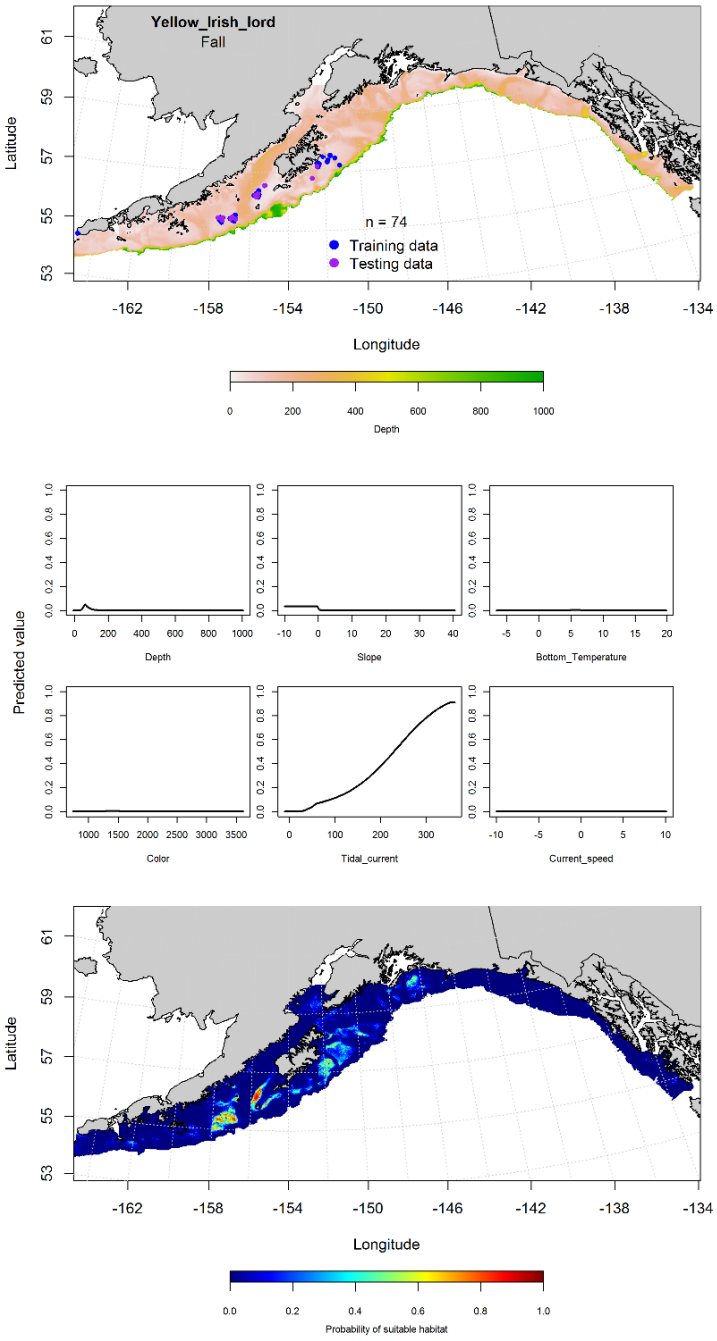

Figure 95. -- Locations of yellow Irish lord from fall (September-November 2001-2015) commercial fisheries catches in the Gulf of Alaska (top panel), MaxEnt model effects (middle panels), and predicted probability of suitable habitat for yellow Irish lord based on the model (bottom panel).

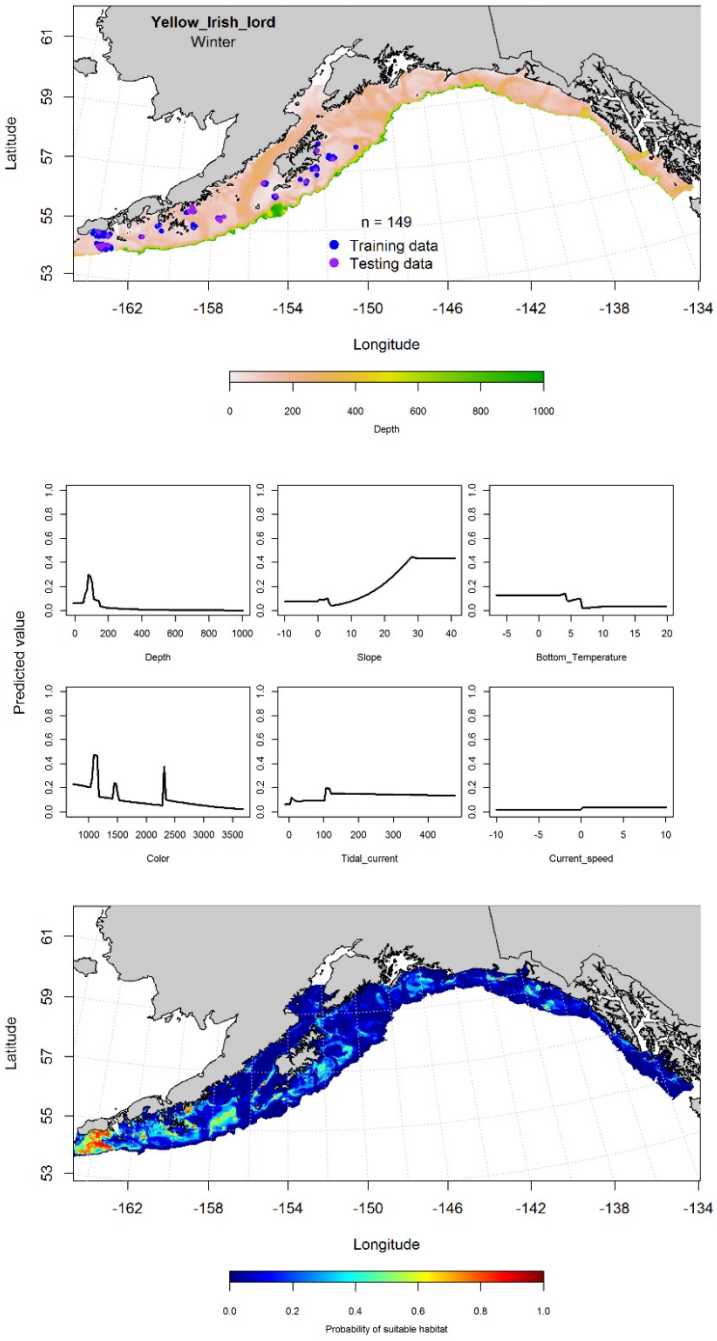

Figure 96. -- Locations of yellow Irish lord from winter (December-February 2001-2015) commercial fisheries catches in the Gulf of Alaska (top panel), with training (blue dots) and testing (purple dots) data indicated, maximum entropy (MaxEnt) model effects (center panel), and the predicted probability of suitable yellow Irish lord habitat (bottom panel).

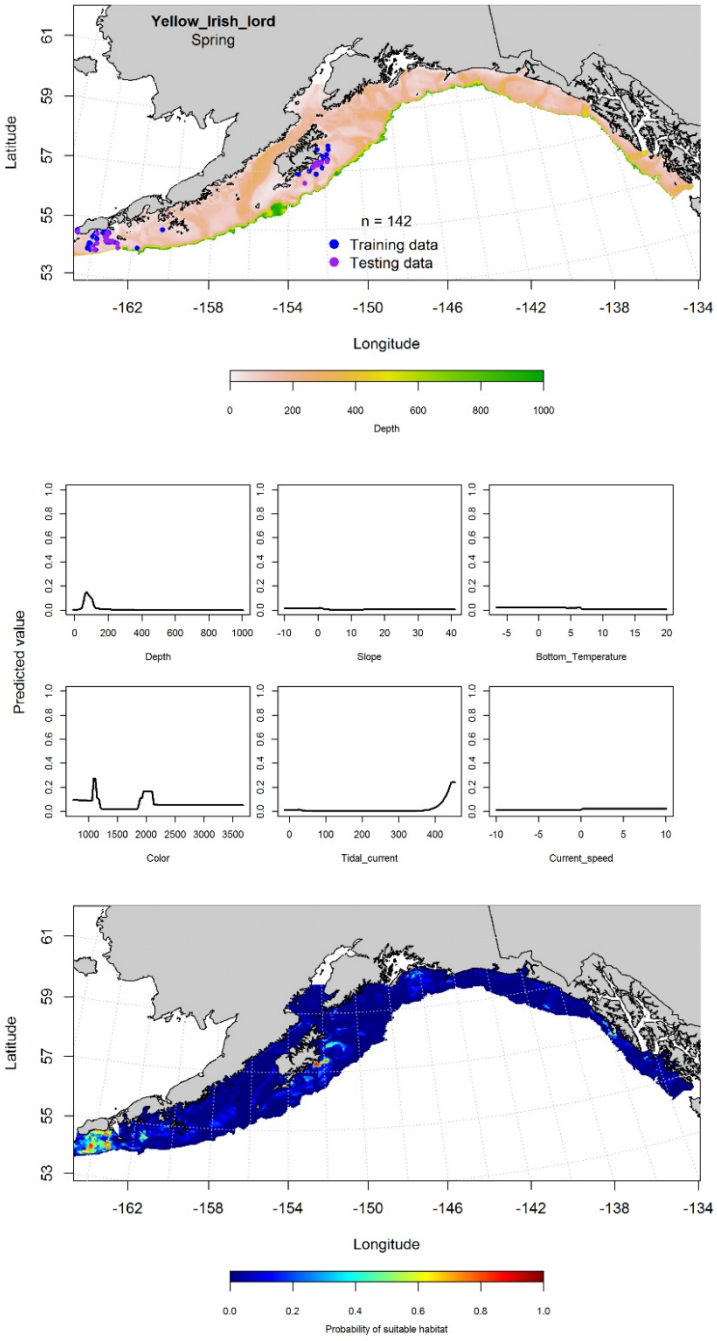

Figure 97. -- Locations of yellow Irish lord from spring (March-May 2001-2015) commercial fisheries catches in the Gulf of Alaska (top panel), with training (blue dots) and testing (purple dots) data indicated, maximum entropy (MaxEnt) model effects (center panel), and the predicted probability of suitable yellow Irish lord habitat (bottom panel).

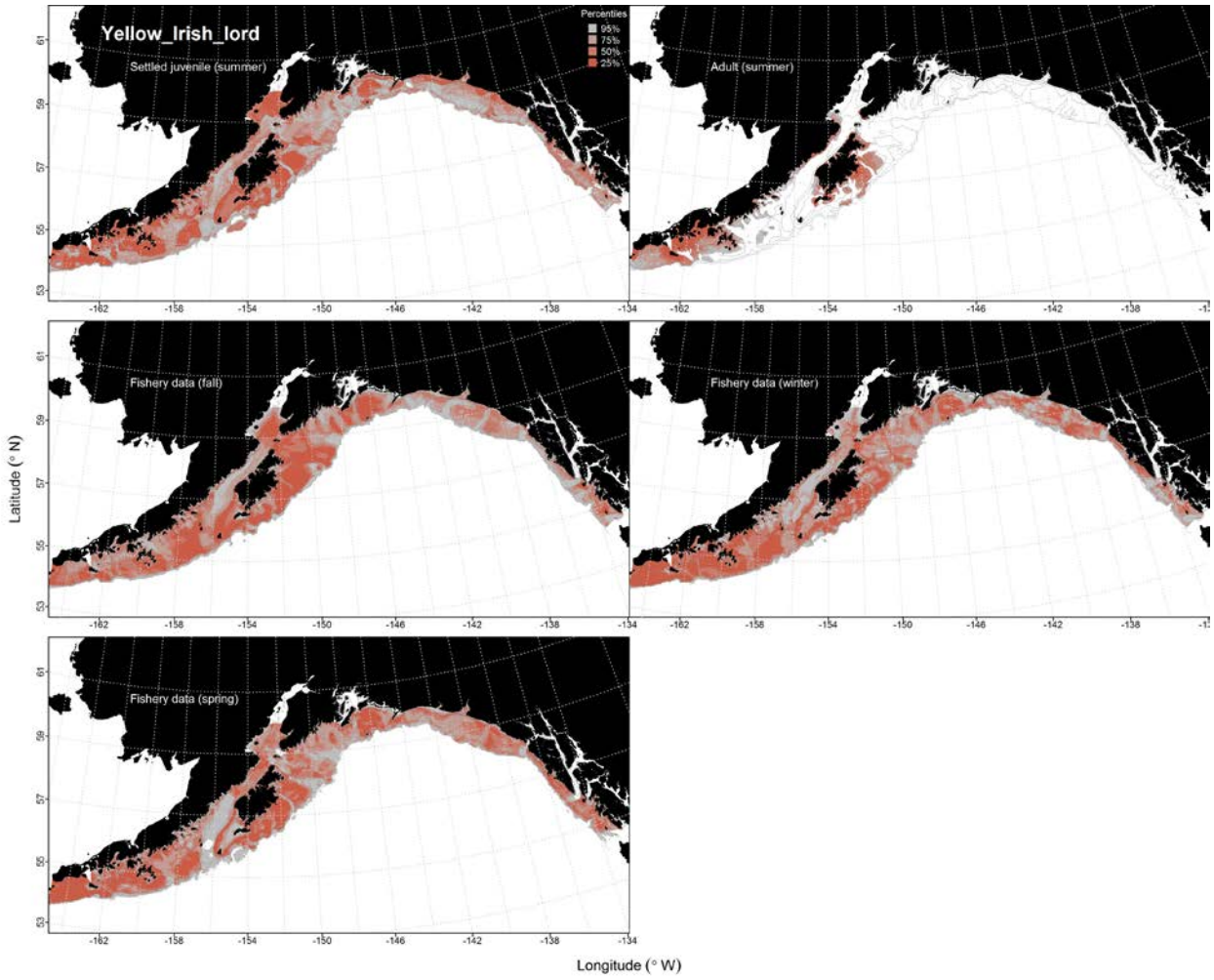

Figure 98. -- Habitat predicted for settled juvenile and adult yellow Irish lords from RACE-GAP summertime bottom trawl surveys (1993-2013) and predicted from presence in commercial fishery catches (2001-2015) from fall, winter, and spring in the Gulf of Alaska.

Bigmouth Sculpin (*Hemitripterus bolini*)

Early life history stages of bigmouth sculpin -- There were no observations of bigmouth sculpin eggs in the EcoFOCI collections.

There were eight observations of larval bigmouth sculpin (Fig. 99), and one instance of a pelagic juvenile bigmouth sculpin in the EcoFOCI collections (Fig. 100); however, these were not sufficient to model either of these life stages.

Juvenile and adult bigmouth sculpin distribution in the bottom trawl survey -- The catch of bigmouth sculpin in summer bottom trawl surveys indicates this species is broadly distributed across the central and western GOA, but occurs relatively rarely. A MaxEnt model predicting suitable habitat of settled juvenile bigmouth sculpin had an AUC of 0.84 for the training data and 0.62 for the test data. Bottom depth, maximum tidal current, and bottom temperature were the most important variables predicting the probability of suitable habitat of settled juvenile bigmouth sculpin (relative importance: 0.41, 0.20, and 0.18, respectively). The model predicted a patchy distribution of suitable habitat for settled juvenile bigmouth sculpin, which was highest in the western GOA, along the Alaska Peninsula, and in the eastern GOA off Cape St. Elias (Fig. 101).

A MaxEnt model predicting suitable habitat of adult bigmouth sculpin had an AUC of 0.87 for the training data and 0.74 for the test data. Bottom depth, maximum tidal current, and slope were the most important model variables (relative importance: 0.63, 0.17, and 0.08, respectively). The model correctly classified 80% of the predictions from the training data and 74% of the predictions from the test data. The model predicted that suitable habitat of adult bigmouth sculpin occurs throughout the GOA, though it was highest in central GOA, on Portlock Bank and in the western GOA, near Shumagin and Shelikof Gullies (Fig. 102).

Bigmouth sculpin distribution in commercial fisheries -- The distribution of adult bigmouth sculpin in commercial fisheries catches was generally consistent in fall, winter, and spring. In the fall, there were 35 observations of adult bigmouth sculpin from the central and western GOA (Fig.103) which were not sufficient data to build a MaxEnt model.

In the winter, bottom depth, slope, and maximum tidal current were the most important predictors of suitable habitat of adult bigmouth sculpin in the MaxEnt model (relative importance: 0.34, 0.31, and 0.19, respectively). The AUC of the winter MaxEnt model was 0.88 for the training data and 0.82 for the test data, with 82% of the cases in the training data set, and 84% of the test data predicted correctly. Suitable habitat for bigmouth sculpin was predicted to occur throughout the GOA, with the highest probability of suitable habitat occurring near Kodiak Island and off Prince William Sound (Fig. 104).

In the spring, bottom current speed, bottom depth, and bottom temperature were the most important variables for predicting suitable habitat of bigmouth sculpin in the MaxEnt model (relative importance: 0.36, 0.33, and 0.17, respectively). The AUC of the spring MaxEnt model was 0.79 for the training data and 0.69 for the test data. The model correctly classified 71% of the predictions from the training data set and 69% of the test data. The model predicted that suitable habitat for bigmouth sculpin occurred throughout the GOA; areas with the highest probability of suitable habitat occurred in the western GOA (Fig. 105).

Bigmouth sculpin essential fish habitat maps and conclusions-- Potential summertime habitat for settled juvenile and adult bigmouth sculpin were both extensively distributed throughout the GOA (Fig. 106). The winter and spring distribution of bigmouth sculpin habitat based on their presence in commercial catches was similar to that predicted from summer trawl survey data, except during

spring when higher suitability habitat tended to be slightly more concentrated in the western GOA (Fig. 106).

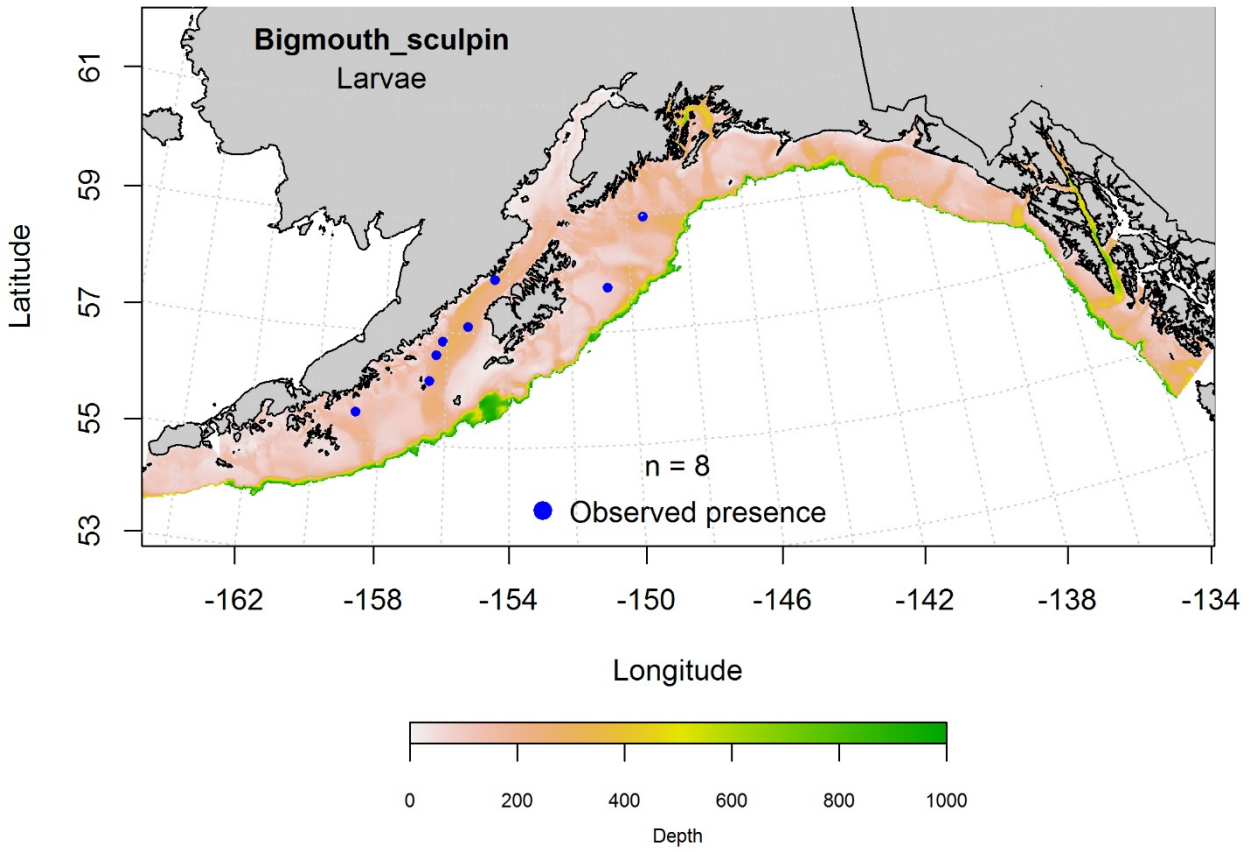

Figure 99. -- Distribution of pelagic bigmouth sculpin larvae observations from EcoFOCI ichthyoplankton surveys (April-September 1991-2012) in the Gulf of Alaska.

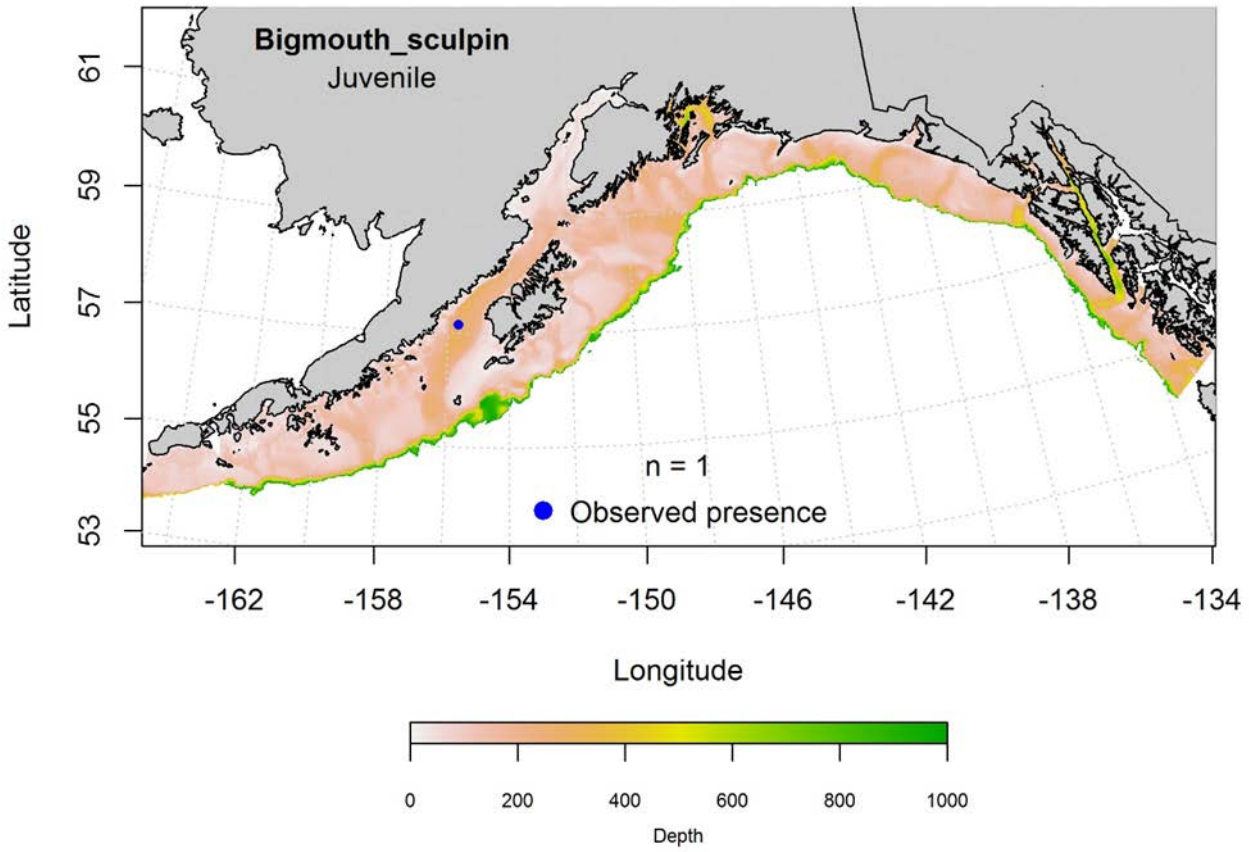

Figure 100. -- Distribution of pelagic juvenile bigmouth sculpin observations from EcoFOCI ichthyoplankton surveys (April-September 1991-2012) in the Gulf of Alaska.

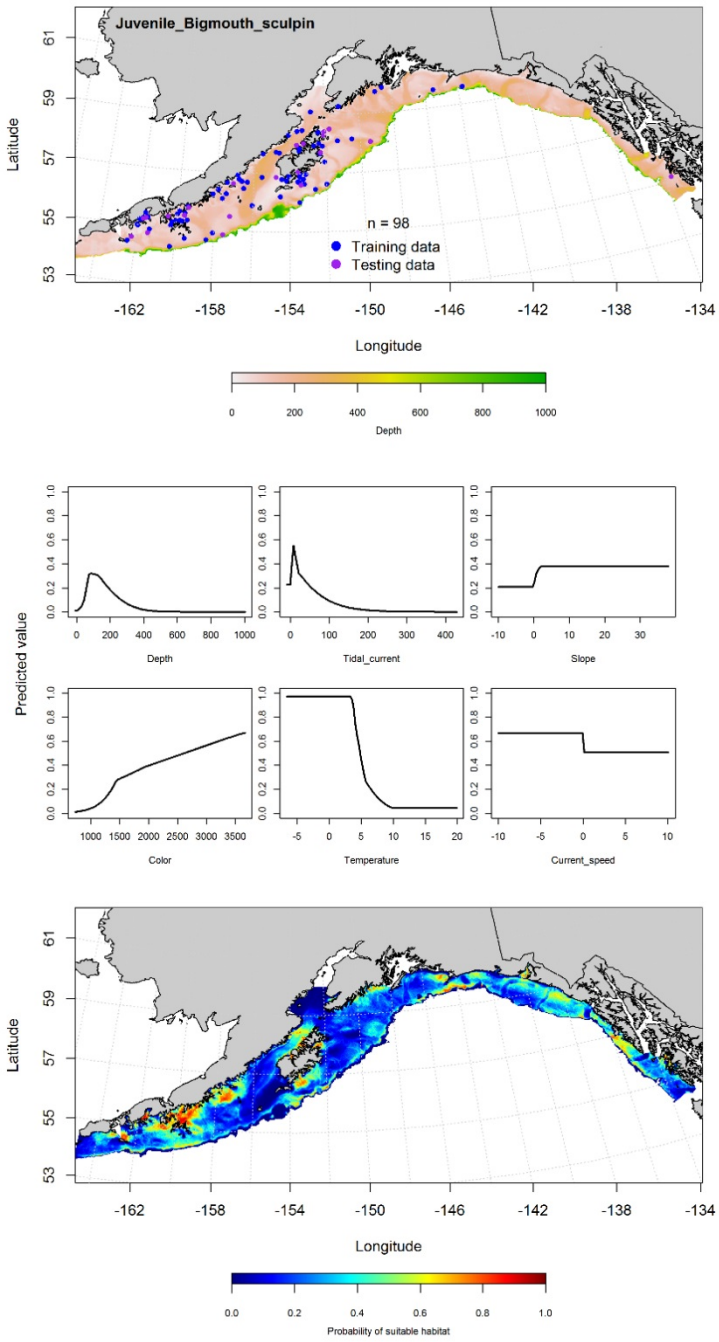

Figure 101. -- Presence of settled juvenile bigmouth sculpin from RACE-GAP summer bottom trawl surveys (1993-2013) in the Gulf of Alaska (top panel) with training (blue dots) and testing (purple dots) data indicated, maximum entropy (MaxEnt) model effects (center panel), and the MaxEnt-predicted probability of suitable juvenile bigmouth sculpin habitat (bottom panel).

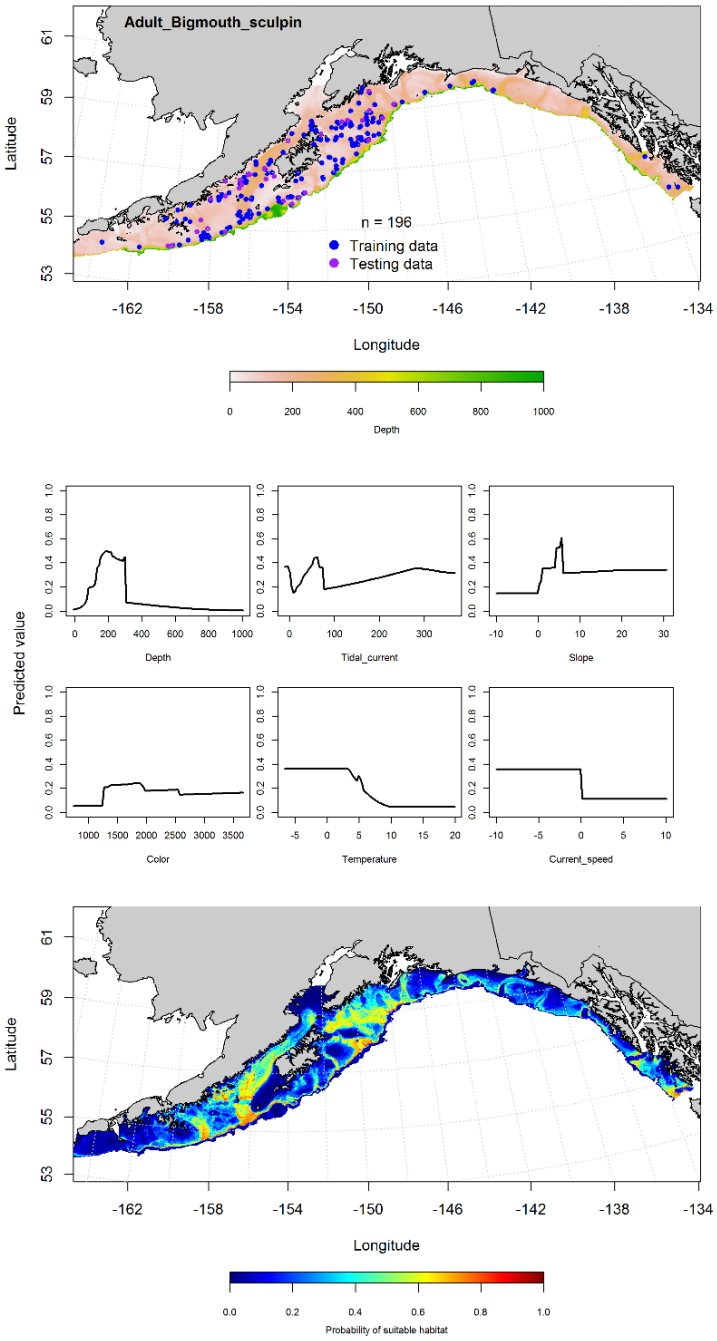

Figure 102. -- Presence of adult bigmouth sculpin from RACE-GAP summer bottom trawl surveys (1993-2013) in the Gulf of Alaska (top panel) with training (blue dots) and testing (purple dots) data indicated, maximum entropy (MaxEnt) model effects (center panel), and the MaxEnt-predicted probability of suitable adult bigmouth sculpin habitat (bottom panel).

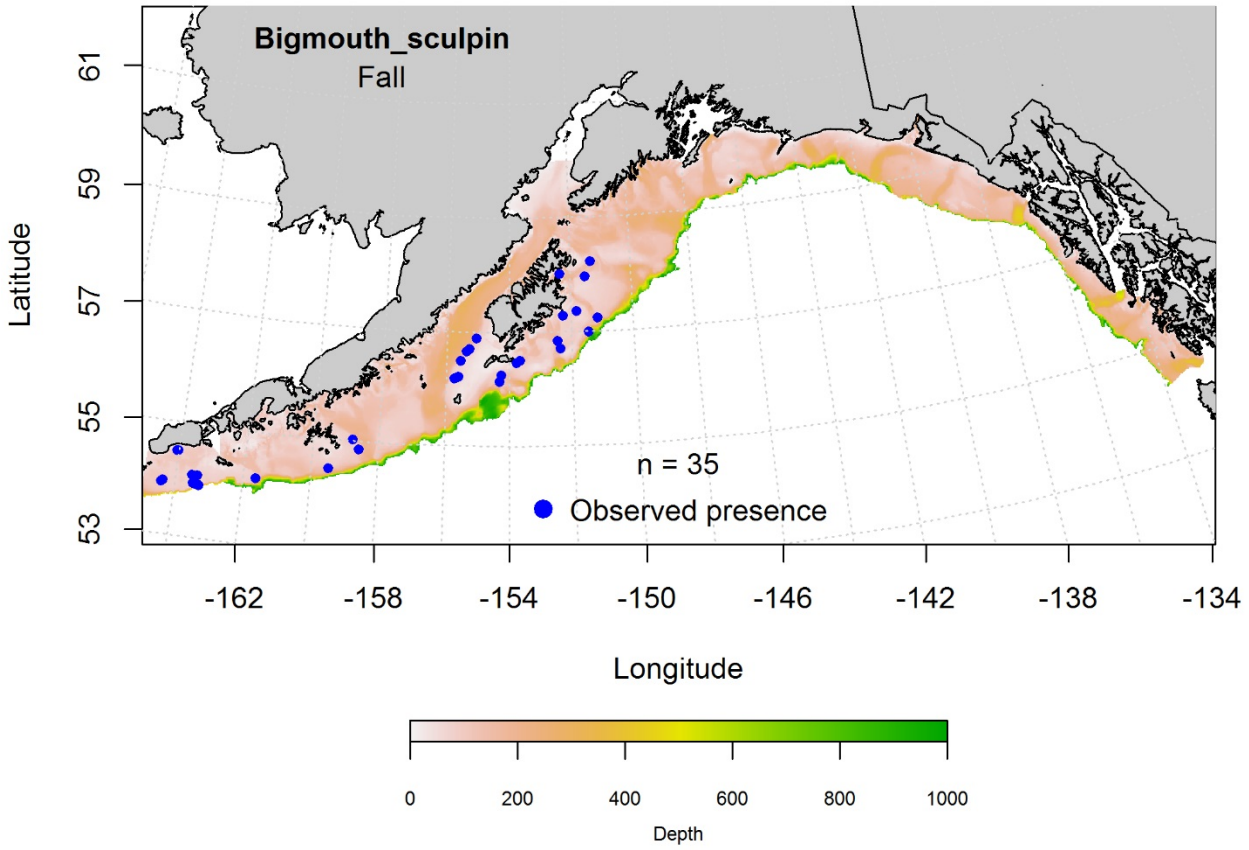

Figure 103. -- Locations of bigmouth sculpin from fall (September-November 2001-2015) commercial fisheries catches in the Gulf of Alaska.

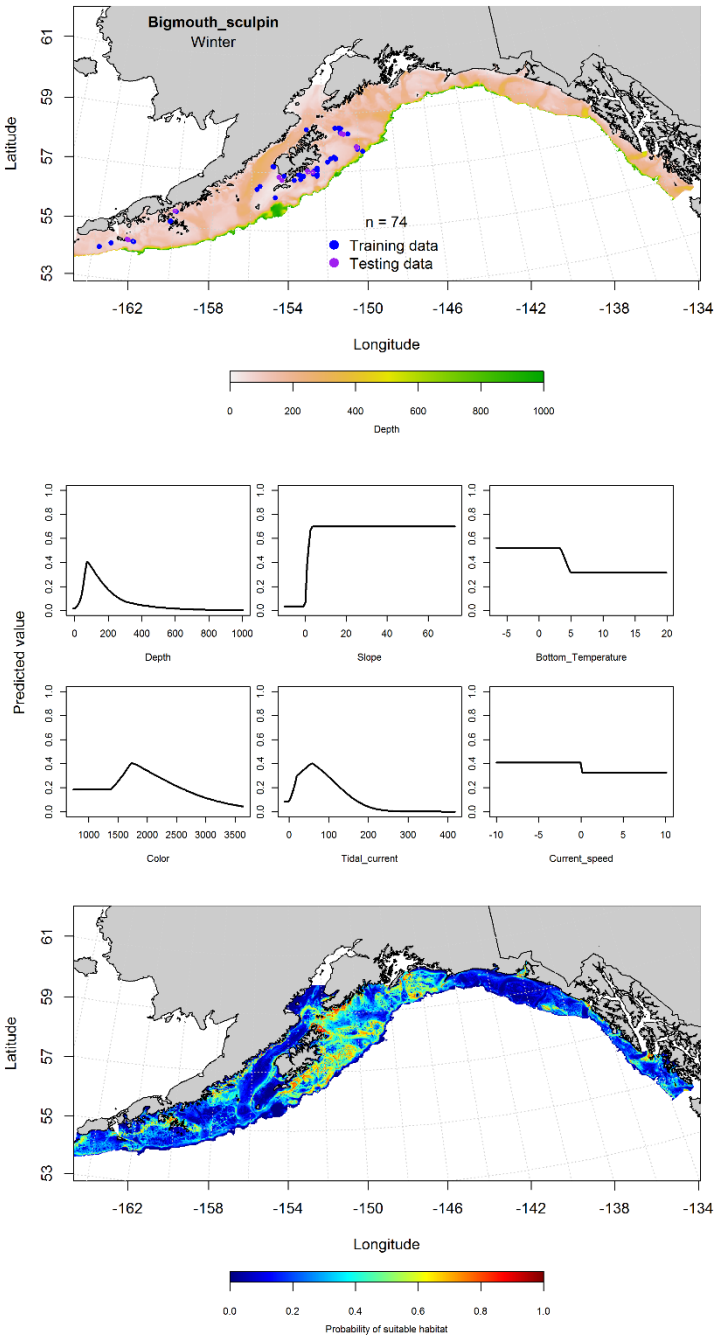

Figure 104. -- Locations of bigmouth sculpin from winter (December-February 2001-2015) commercial fisheries catches in the Gulf of Alaska (top panel), with training (blue dots) and testing (purple dots) data indicated, maximum entropy (MaxEnt) model effects (center panel), and the predicted probability of suitable adult bigmouth sculpin habitat (bottom panel).

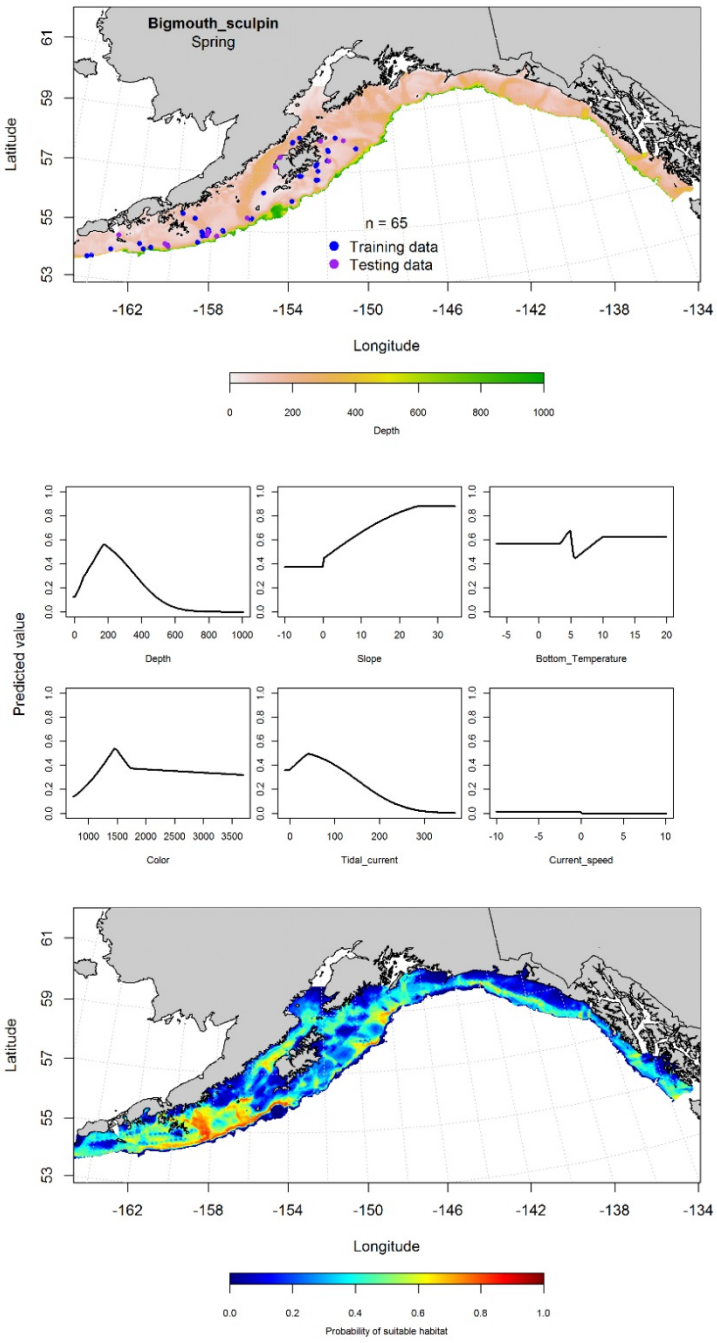

Figure 105. -- Locations of bigmouth sculpin from spring (March-May 2001-2015) commercial fisheries catches in the Gulf of Alaska (top panel), with training (blue dots) and testing (purple dots) data indicated, maximum entropy (MaxEnt) model effects (center panel), and the predicted probability of suitable adult bigmouth sculpin habitat (bottom panel).

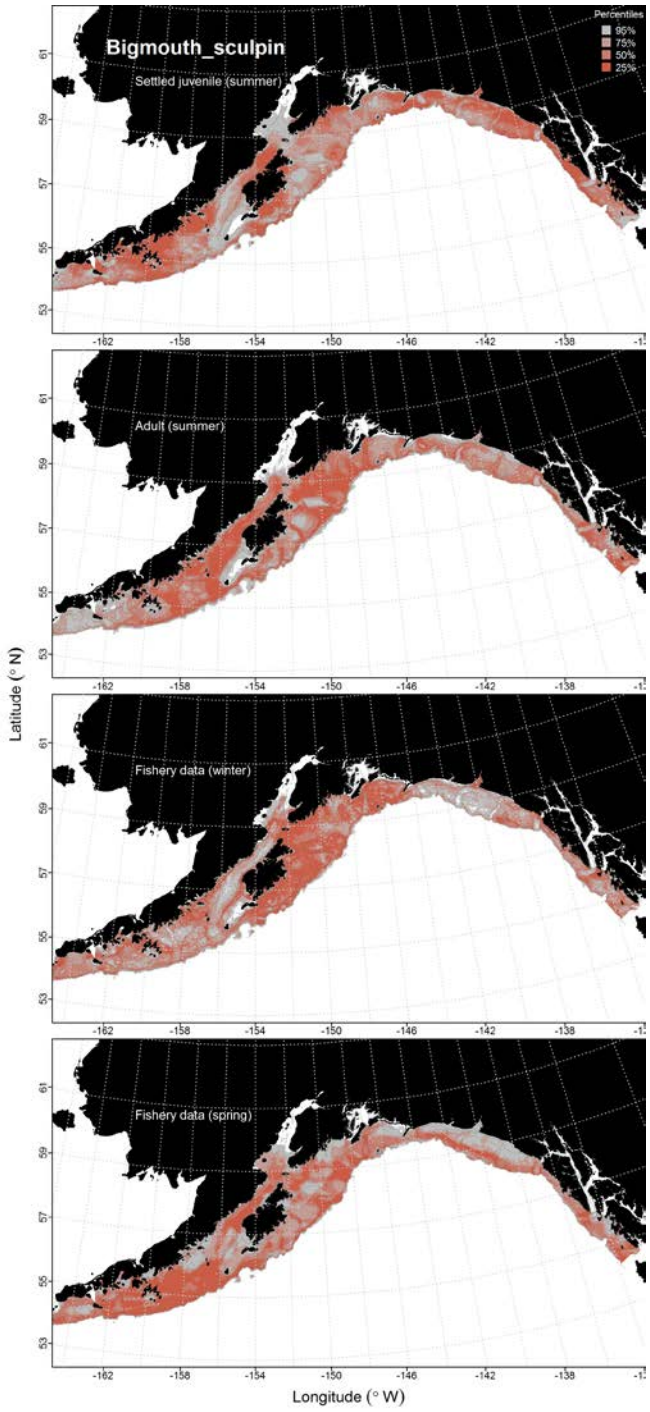

Figure 106. -- Habitat predicted for settled juvenile and adult bigmouth sculpin from RACE-GAP summertime bottom trawl surveys (1993-2013) and predicted from presence in commercial fishery catches (2001-2015) from winter and spring in the Gulf of Alaska.

Great Sculpin (*Myoxocephalus polyacanthocephalus*)

Early life history stages of great sculpin -- There were no records of any great sculpin eggs, larvae, or pelagic juvenile stages in the EcoFOCI collections.

Juvenile and adult great sculpin distribution in the bottom trawl survey -- The catch of great sculpin during the summer bottom trawl surveys indicates this species is distributed throughout the central and western GOA. A MaxEnt model predicting suitable habitat of settled juvenile great sculpin had an AUC of 0.94 for the training data and 0.86 for the test data. The model correctly classified 80% of the predictions from the training data and 86% of the predictions from the test data. Bottom depth and maximum tidal current were the most important model variables (relative importance: 0.64 and 0.16, respectively). The model predicted that suitable habitat of settled juvenile great sculpin was concentrated in relatively small areas; particularly in the western GOA around the Shumagin Islands, in the central GOA off Kodiak, and in the eastern GOA off Baranof Island (Fig. 107).

A MaxEnt model was used to predict suitable habitat of adult great sculpins. The AUC was 0.90 for the training data and 0.75 for the testing data. The model correctly classified 82% of predictions from the training data and 75% of the predictions from the test data. Bottom depth, maximum tidal current, and ocean color were the most important model variables (relative importance: 0.62, 0.21, and 0.07, respectively). The model predicted that suitable habitat of adult great sculpin was concentrated in relatively small areas around the Shumagin Islands, Kodiak, and Baranof Island similar to predictions of suitable habitat for settled juveniles (Fig. 108).

Great sculpin distribution in commercial fisheries -- Observations of great sculpin from commercial fisheries catches were limited. There were four observations in fall (Fig. 109), 34 in winter (Fig. 110), and 23 in the spring (Fig. 111). These observations all occurred in the central and western GOA and were insufficient to build a MaxEnt model for any of the three seasons considered.

Great sculpin essential fish habitat maps and conclusions-- Juvenile and adult great sculpin habitat was distributed throughout the region, although settled juvenile habitat was slightly more concentrated in shallower depths than the adults (Fig. 112).

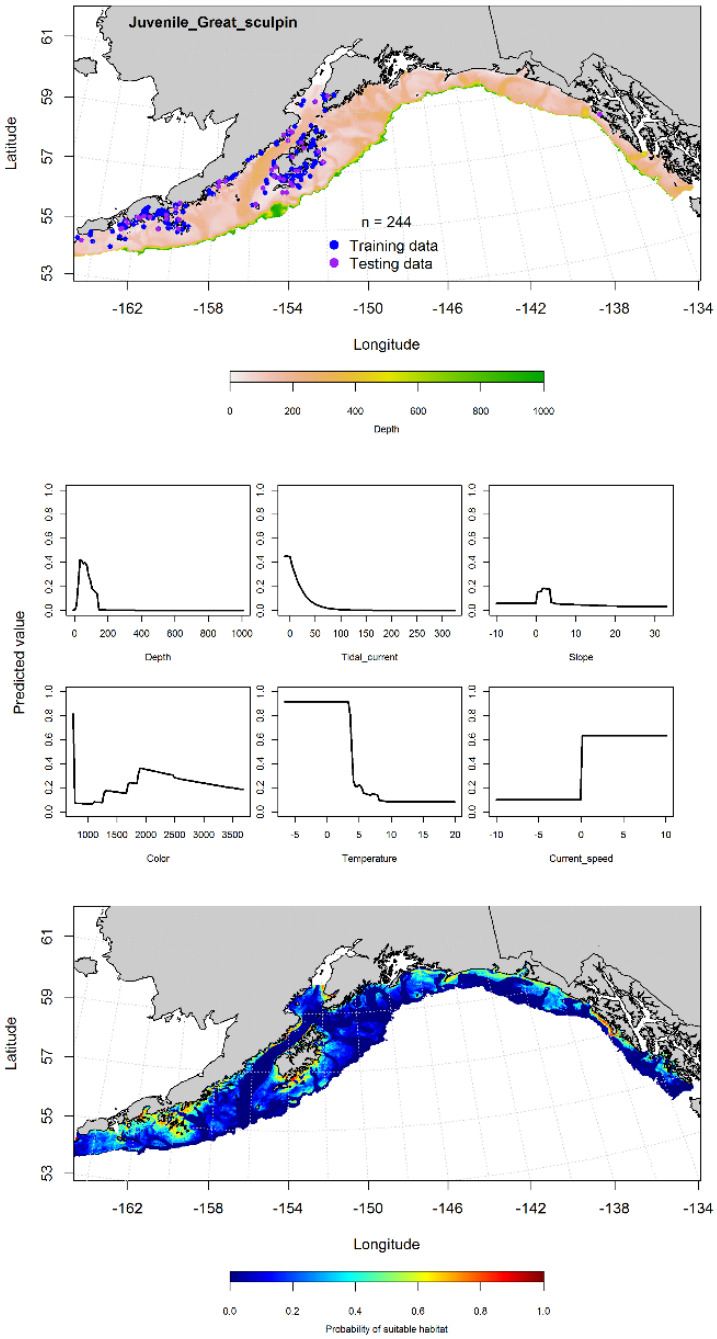

Figure 107. -- Presence of settled juvenile great sculpin from RACE-GAP summer bottom trawl surveys (1993-2013) in the Gulf of Alaska (top panel) with training (blue dots) and testing (purple dots) data indicated, maximum entropy (MaxEnt) model effects (center panel), and the MaxEnt-predicted probability of suitable juvenile great sculpin habitat (bottom panel).

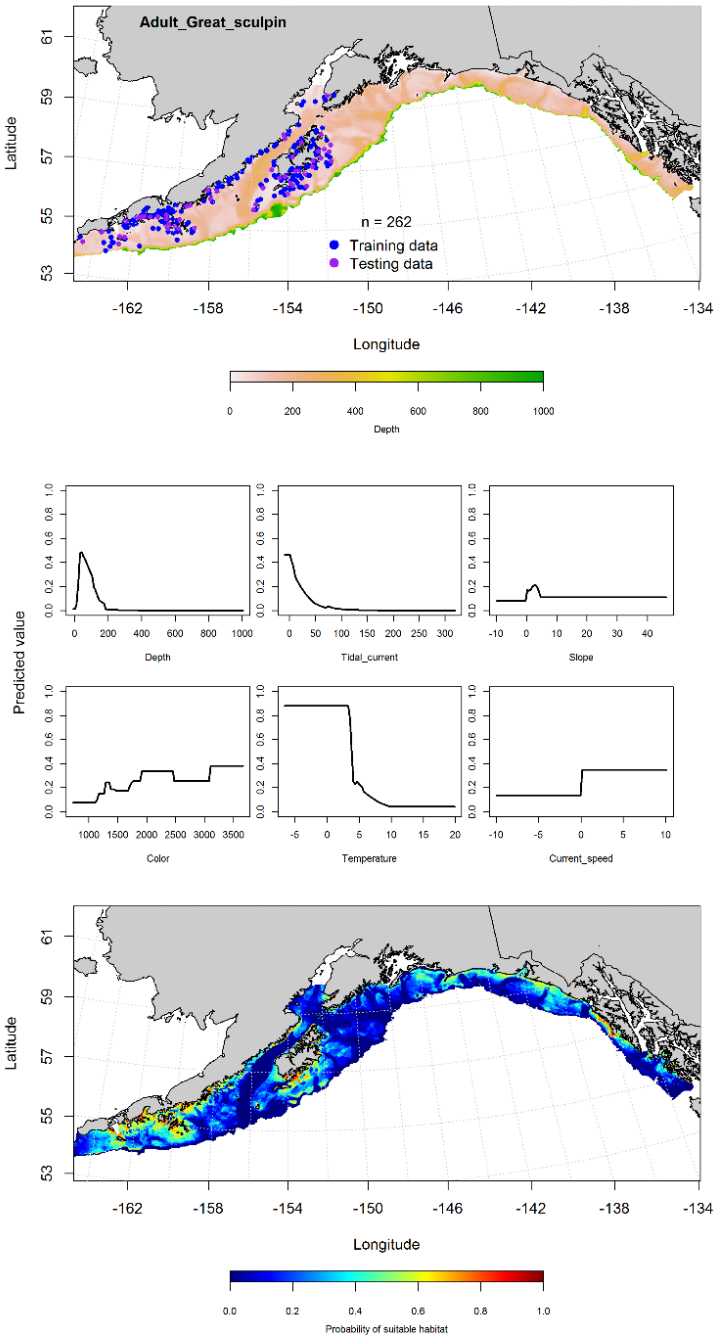

Figure 108. -- Presence of adult great sculpin from RACE-GAP summer bottom trawl surveys (1993-2013) in the Gulf of Alaska (top panel) with training (blue dots) and testing (purple dots) data indicated, maximum entropy (MaxEnt) model effects (center panel), and the MaxEnt-predicted probability of suitable adult great sculpin habitat (bottom panel).

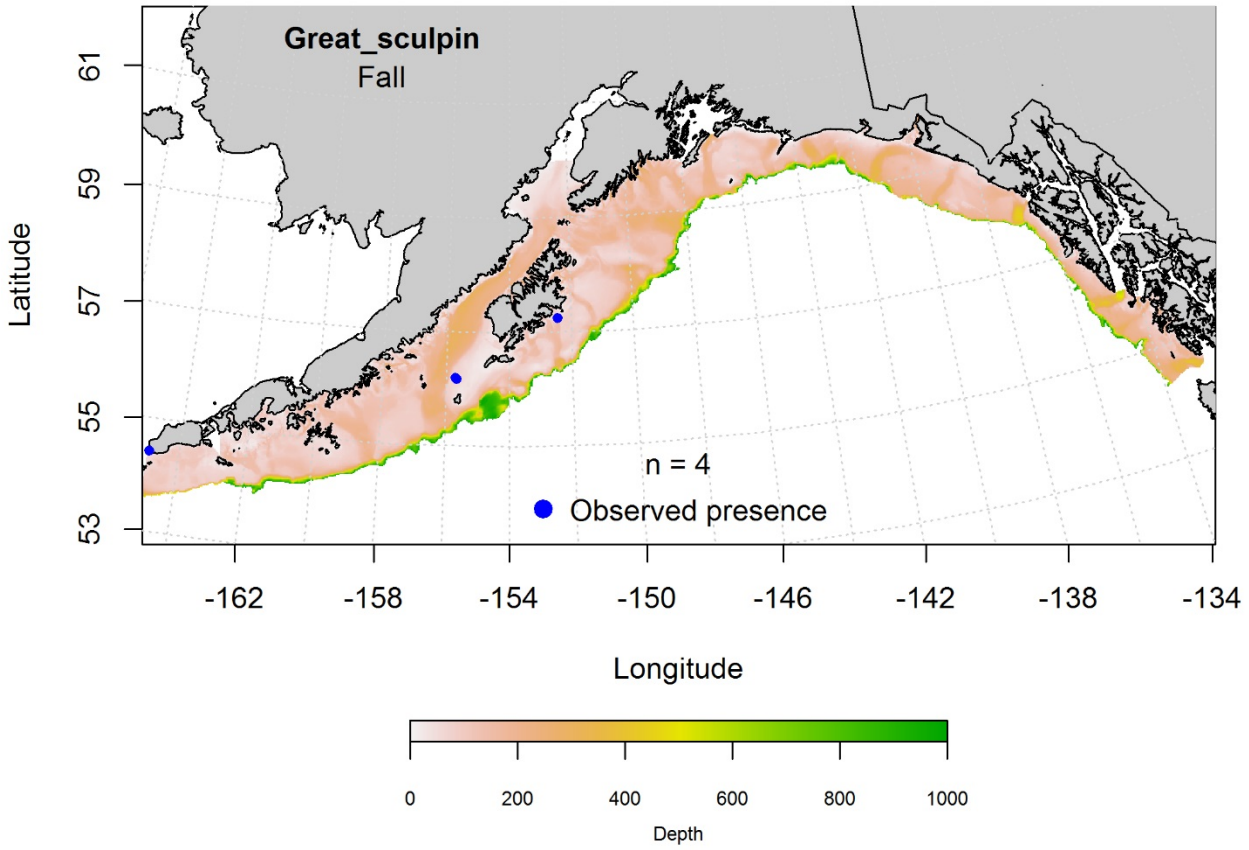

Figure 109. -- Locations of great sculpin from fall (September-November 2001-2015) commercial fisheries catches in the Gulf of Alaska.

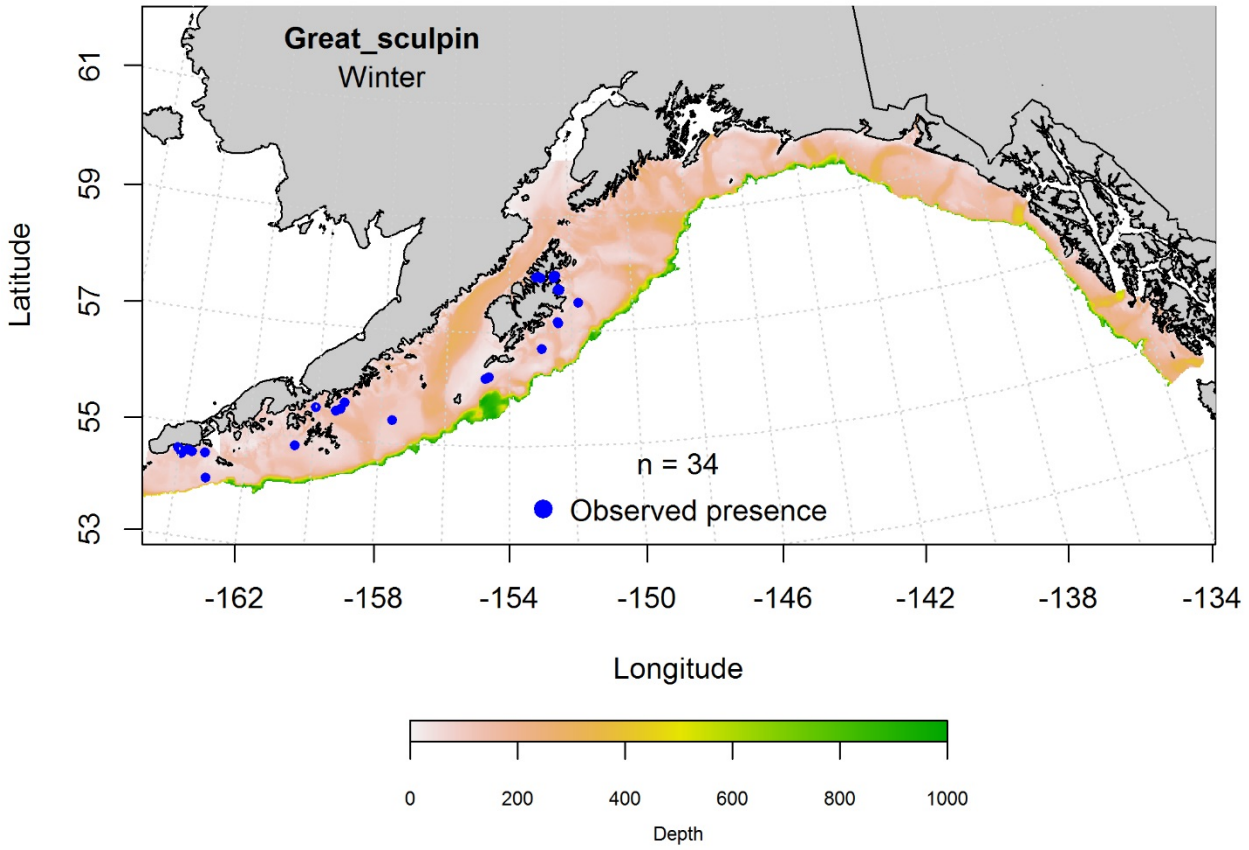

Figure 110. -- Locations of great sculpin from winter (December-February 2001-2015) commercial fisheries catches in the Gulf of Alaska.

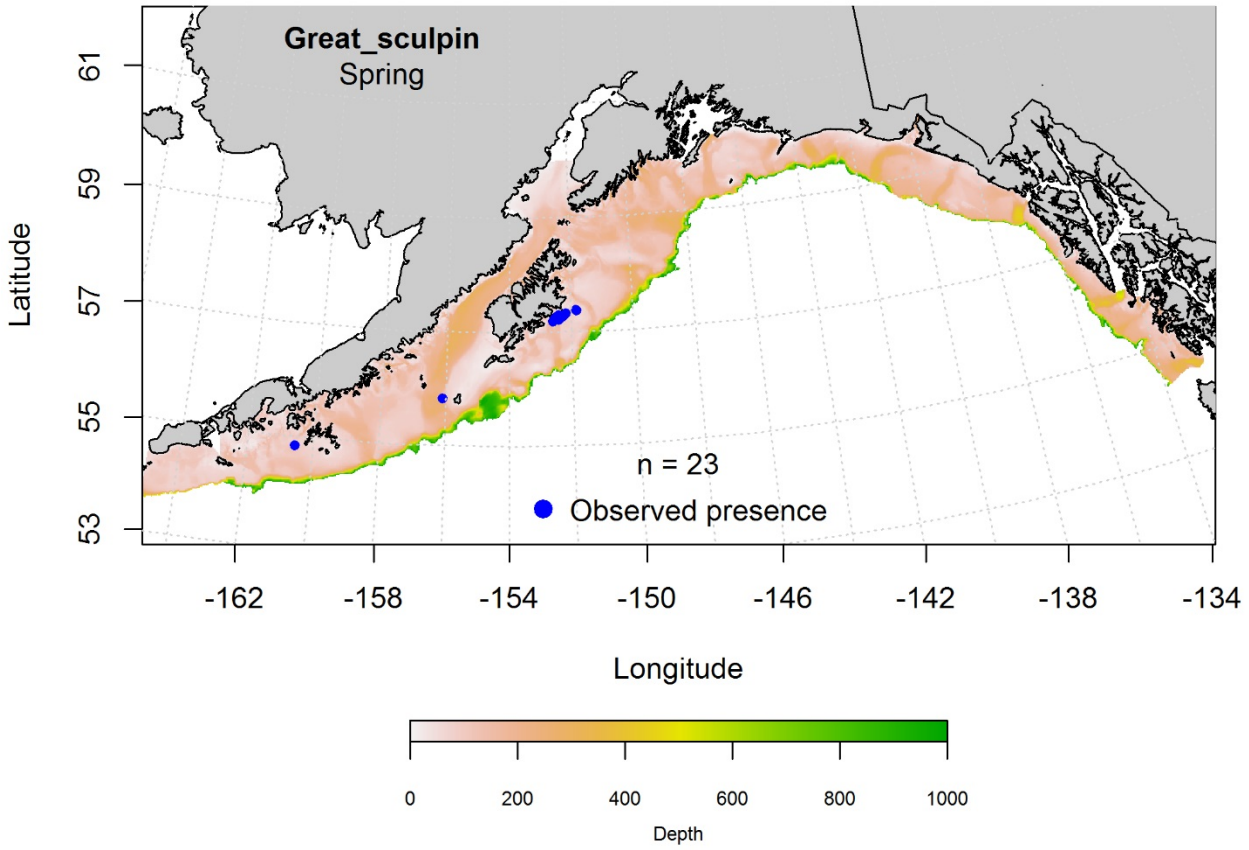

Figure 111. -- Locations of great sculpin from spring (March-May 2001-2015) commercial fisheries catches in the Gulf of Alaska.

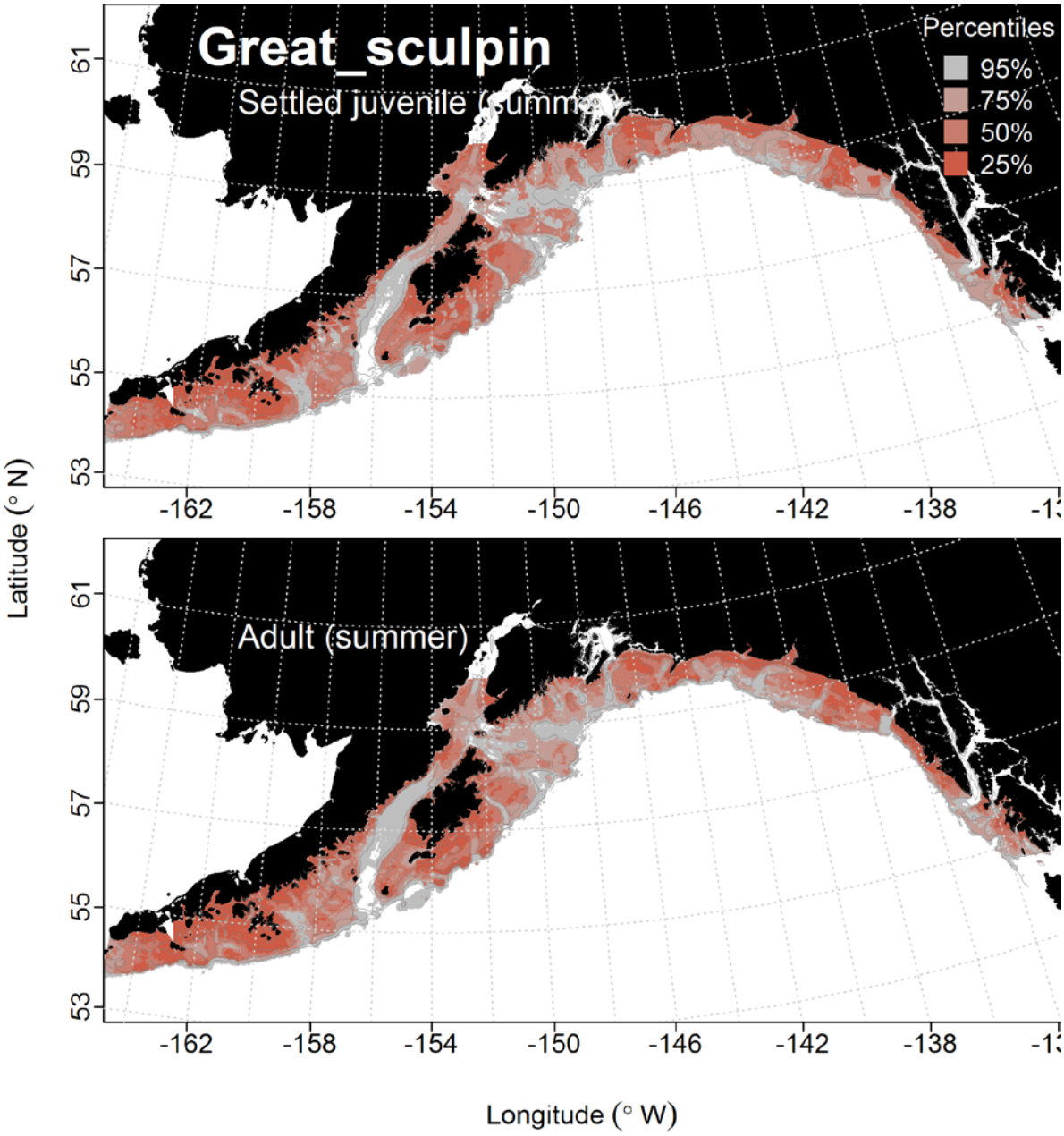

Figure 112. -- Habitat predicted for great sculpin juveniles and adults from RACE-GAP summertime bottom trawl surveys (1993-2013) in the Gulf of Alaska.

Atka Mackerel (*Pleurogrammus monopterygius*)

Early life history stages of Atka mackerel -- There were no observations of eggs or pelagic juvenile Atka mackerel observed in the EcoFOCI collections. There was not expectation to find eggs in ichthyoplankton collections because Atka mackerel spawn adherent, demersal eggs. There were 13 observations of larval Atka mackerel, most of which occurred in the central GOA (Fig. 113). These occurrences did not provide sufficient data to build a MaxEnt model for larval Atka mackerel distribution.

Juvenile and adult Atka mackerel distribution in the bottom trawl survey -- There were no observations of settled juvenile Atka mackerel during the summer trawl surveys.

An hGAM predicting the probability of adult Atka mackerel presence had an AUC of 0.85 for both the training data and testing data. Geographic position, bottom temperature, and maximum tidal current speed were the most important model variables for predicting the probability of adult Atka mackerel presence (Fig. 114). The model predicted the highest probabilities of presence were off Unimak Island (Fig. 114). Geographic location and bottom depth were the most important variables describing adult Atka mackerel abundance in the CPUE GAM. This model explained 11% of the variance in the training data, but only 9% of the variance in the test data. The model predicted a high CPUE of adult Atka mackerel in the western GOA, particularly on Sanak Bank (Fig. 114).

Atka mackerel distribution in commercial fisheries -- The distribution of Atka mackerel based on commercial fisheries catches remained similar in fall, winter, and spring. In the fall, ocean color, bottom temperature, and bottom depth were the most important model variables for predicting

probability of suitable Atka mackerel habitat (relative importance: 0.35 0.35, and 0.14, respectively). The AUC of the fall MaxEnt model was 0.97 for the training data and 0.85 for the test data. The model correctly predicted 97% of the training data and 85% of the test data. Suitable Atka mackerel habitat was predicted to occur throughout the western GOA with the higher abundances occurring off Unimak Island (Fig. 115).

In the winter, bottom depth and ocean color were the most important variables determining the probability of suitable habitat of Atka mackerel (relative importance: 0.46, 0.40, and 0.04, respectively (Fig. 116). The AUC of the winter MaxEnt model was 93% for the training data and 78% for the test data. The model correctly classified 88% of the predictions from the training data and 78% in the predictions from the test data. Suitable habitat for this species was predicted to occur across the inner and middle shelf in central and western GOA, with the highest abundances occurring off Unimak Island (Fig. 116).

In the spring, ocean color and bottom depth were the most important variables determining the probability of suitable habitat for Atka mackerel (relative importance: 0.36 and 0.28, respectively). The AUC of the spring MaxEnt model was 96% for the training data and 84% for the test data. The model correctly classified 89% of the predictions from the training data and 84% of the predictions from the test data. As with the fall and winter, the model predicted probable suitable habitat of Atka mackerel in western GOA, particularly off Unimak Island (Fig. 117).

Atka mackerel essential fish habitat maps and conclusions-- Predictions of potential adult Atka mackerel habitat were highest in the central and western GOA (Fig. 118). Potential Atka mackerel habitat predicted from commercial catches was more broadly distributed than that predicted from summer bottom trawl survey data (Fig. 118). These differences may, in part, be related to fishing

effort and species targeted by the commercial fisheries, compared to the effort of the trawl surveys that does not target any single species or complex of species. There were no marked seasonal differences in the predictions of Atka mackerel habitat from the commercial fisheries data.

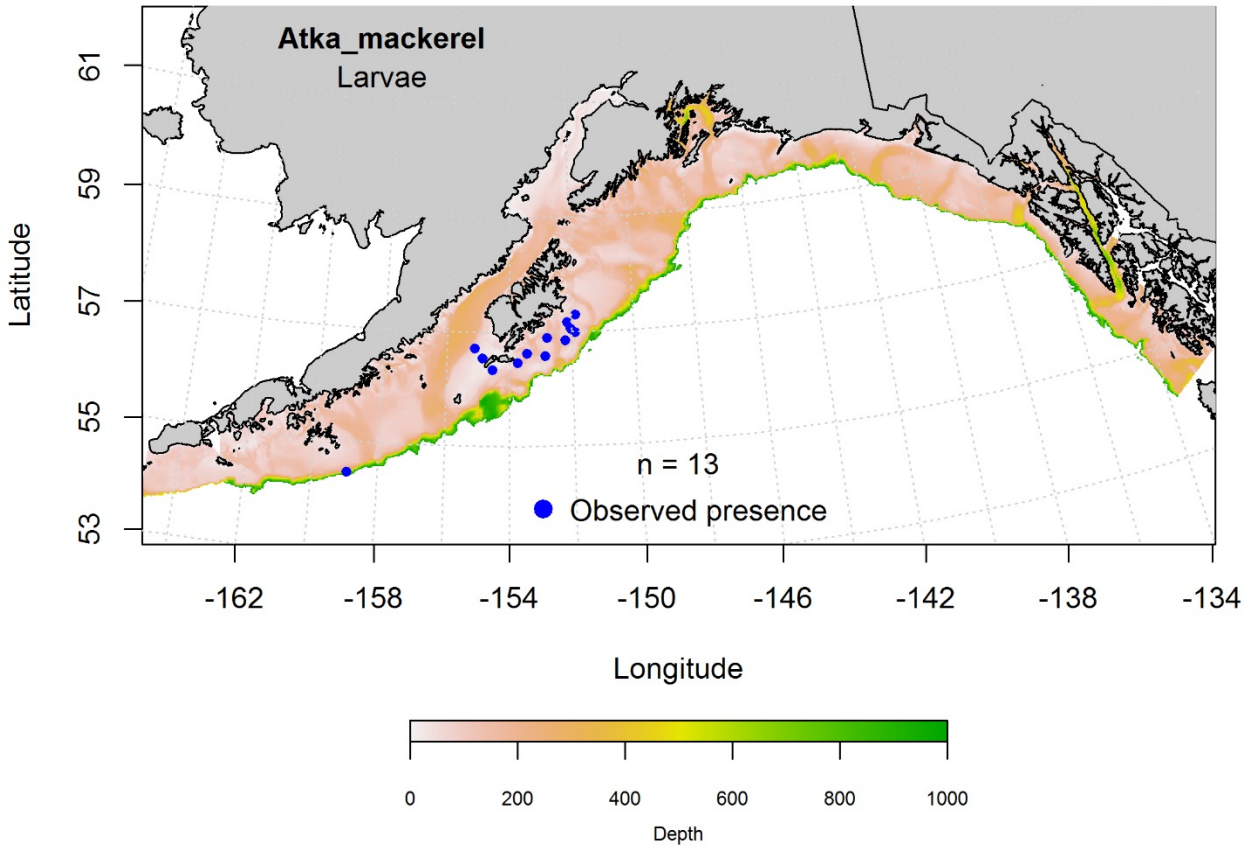

Figure 113. -- Distribution of pelagic Atka mackerel larvae observations from EcoFOCI ichthyoplankton surveys (April-September 1991-2012) in the Gulf of Alaska.

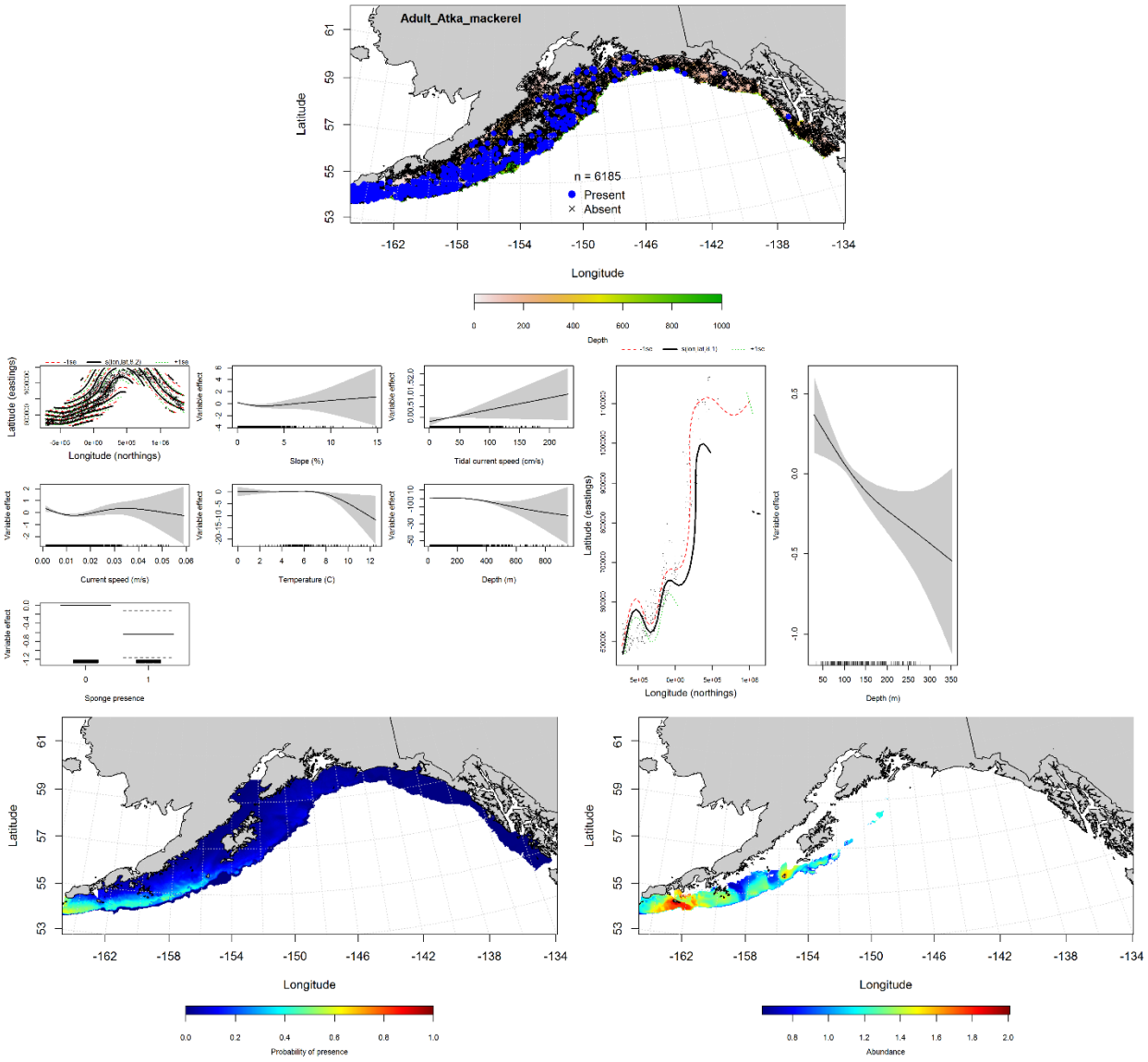

Figure 114. -- Distribution of adult Atka mackerel in 1993-2013 RACE-GAP summer bottom trawl surveys conducted in the Gulf of Alaska (upper panel). Effects of retained habitat covariates in the best fitting generalized additive presence-absence models (PA GAM; left center panel) and abundance (CPUE GAM; right center panel). Predicted spatial distribution of the probability of presence (bottom left panel) and abundance of adult Atka mackerel based on the models (bottom right panel).

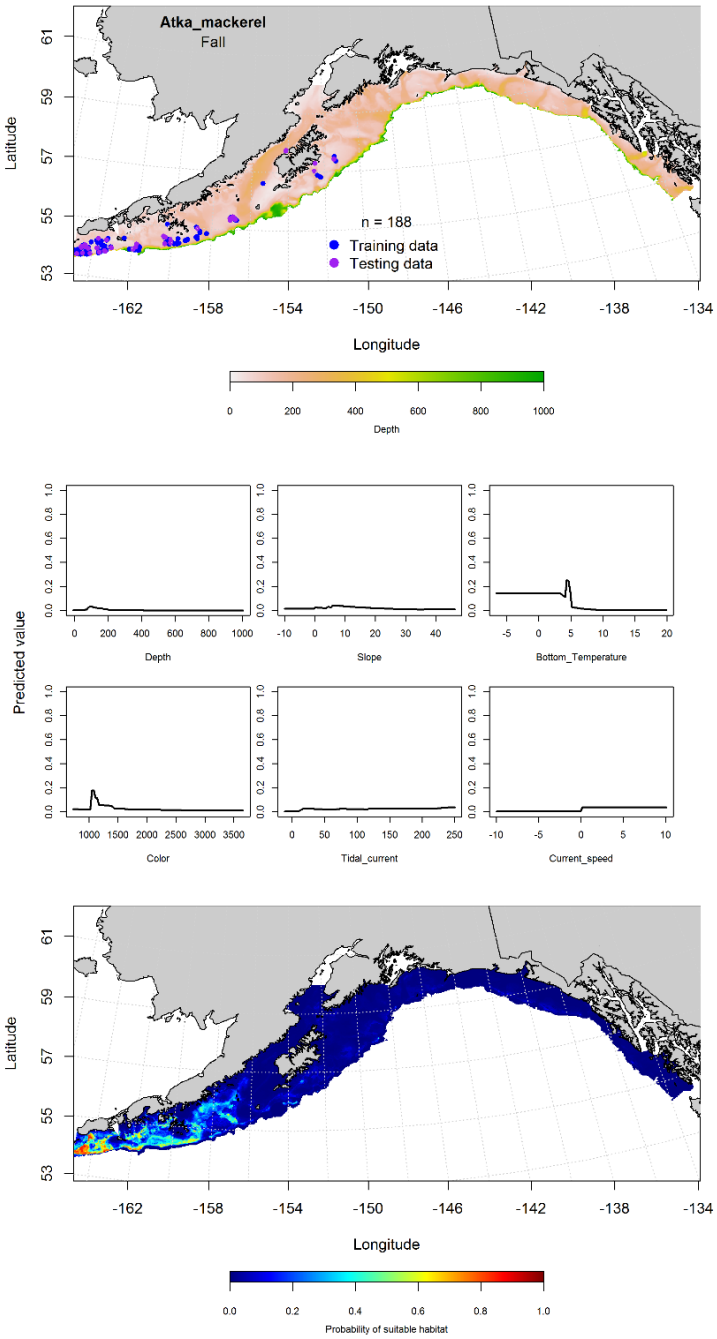

Figure 115. -- Locations of Atka mackerel from fall (September-November 2001-2015) commercial fisheries catches in the Gulf of Alaska, MaxEnt model effects (middle panels), and predicted probability of suitable habitat for Atka mackerel based on the model (bottom panel).

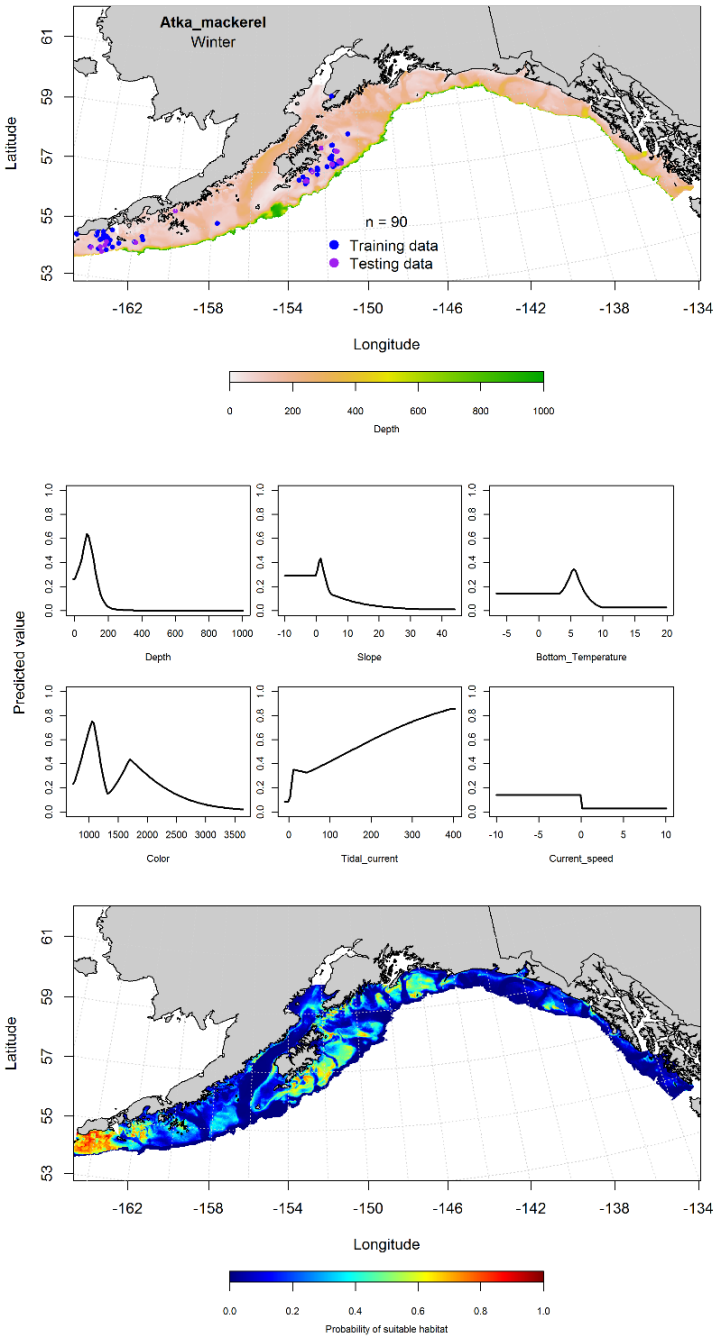

Figure 116. -- Locations of Atka mackerel from winter (December-February 2001-2015) commercial fisheries catches in the Gulf of Alaska (top panel), with training (blue dots) and testing (purple dots) data indicated, maximum entropy (MaxEnt) model effects (center panel), and the predicted probability of suitable adult Atka mackerel habitat (bottom panel).

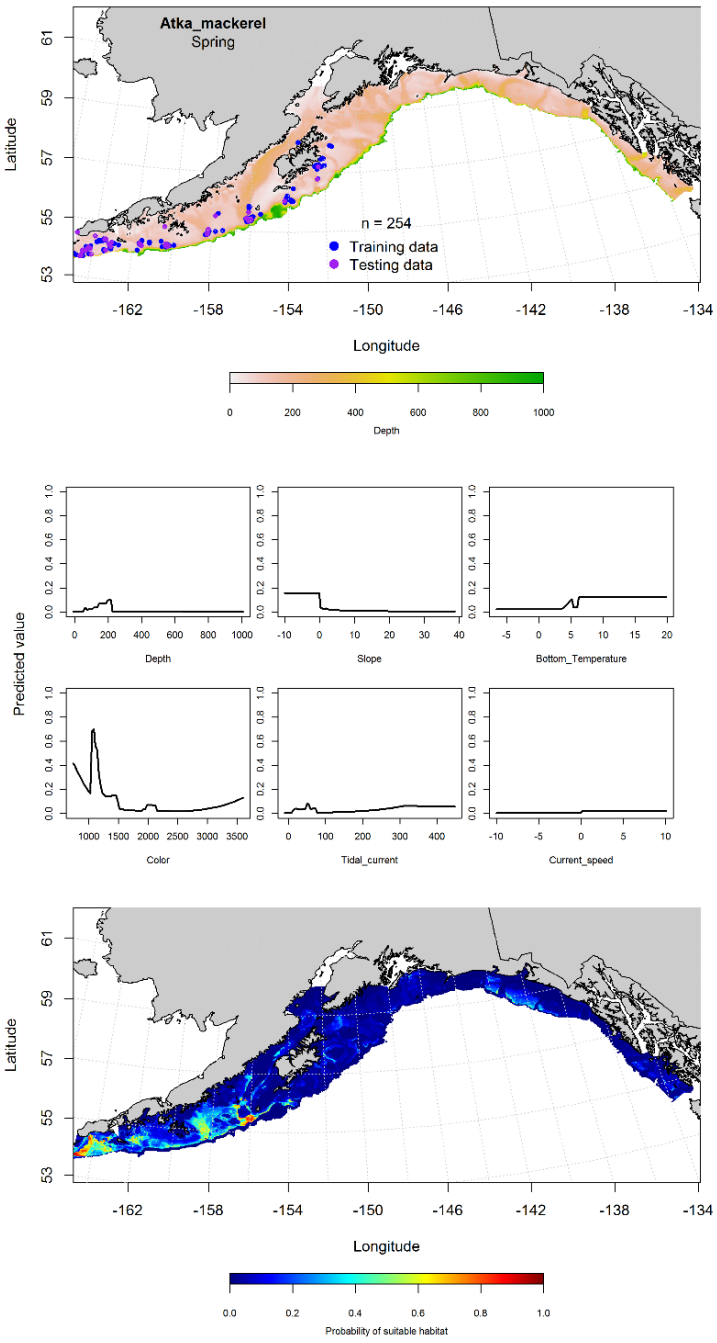

Figure 117. -- Locations of Atka mackerel from spring (March-May 2001-2015) commercial fisheries catches in the Gulf of Alaska (top panel), with training (blue dots) and testing (purple dots) data indicated, maximum entropy (MaxEnt) model effects (center panel), and the predicted probability of suitable adult Atka mackerel habitat (bottom panel).

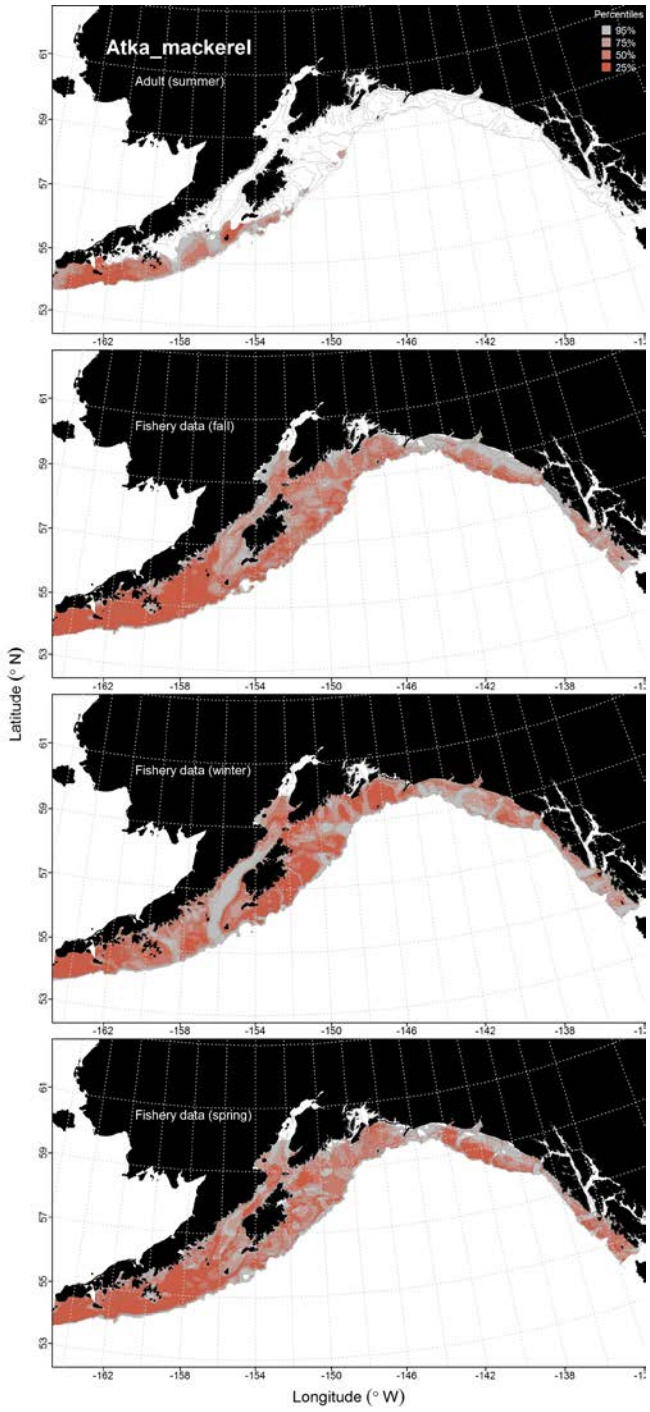

Figure 118. -- Habitat predicted for adult Atka mackerel from RACE-GAP summertime bottom trawl surveys (1993-2013) and predicted from presence in commercial fishery catches (2001-2015) from fall, winter, and spring in the Gulf of Alaska.

Rockfishes (*Sebastes* spp.)

Early life history stages of *Sebastes* spp. -- Larvae and pelagic juvenile rockfishes (*Sebastes* spp.) are difficult to distinguish from their close congeners using visible characters alone. Early life stages of *Sebastes* spp. were visually identified from EcoFOCI ichthyoplankton samples and thus were limited to generic classification. Rockfishes are ovoviviparous with internal fertilization so there was no expectation of encountering *Sebastes* spp. eggs in oceanographic survey samples. Thus, species distribution modeling was conducted on pelagic larval and juvenile rockfishes under the combined generic classification of *Sebastes* spp.

Distribution of early life history stages of *Sebastes* spp. in the GOA -- Larval rockfishes were encountered on EcoFOCI ichthyoplankton surveys (1991-2012) in GOA between April and October and were distributed from Unimak Pass into southeast Alaska (Fig. 119). A MaxEnt model spatially predicted the probability of suitable larval *Sebastes* spp. across the Gulf. Bottom depth and surface temperature accounted for a combined 60.4% of the relative importance of the habitat covariate predictors used for formulate the MaxEnt. Model effects were maximal between 200 and 800 m depths and at surface temperatures around 10°C. The MaxEnt fits to the training and test data were acceptable (AUC = 0.79 and 0.70, respectively) and correctly classified 70% of predicted cases from either data set. The concentrations of high probability suitable habitat were predicted to occur in the Chirikof and Kodiak regions of the GOA.

There were 19 occurrences of pelagic juvenile *Sebastes* spp. in EcoFOCI ichthyoplankton collections between April and September (Fig. 120). These observations occurred in the Chirikof and Kodiak regions of the central and western GOA. This level of prevalence did not provide sufficient data to build a MaxEnt model for pelagic juvenile *Sebastes* spp.

Pacific Ocean Perch (*Sebastes alutus*)

Settled juvenile and adult Pacific ocean perch distribution in the bottom trawl survey -- An hGAM was used to predict the distribution of settled juvenile Pacific ocean perch (POP) abundance. The PA GAM indicated that geographic position, bottom depth, and bottom temperature were the most important variables explaining the presence or absence of settled juvenile POP. The AUC of the model was 0.86 for the training data and 0.85 for the test data. The model correctly classified 78% of the predictions from both the training and test data. The areas of predicted highest probability of suitable habitat were concentrated near the outer shelf in the central and eastern GOA (Fig. 121). The abundance GAM found geographic position, ocean color, and bottom depth were the most important predictors of CPUE. This model explained 17% of the variability in the training data and 14% in the test data and predicted that the highest CPUE of settled juvenile POP occurred in the eastern GOA, along the outer shelf off Icy Bay and Prince of Wales Island (Fig. 121).

A GAM predicting the abundance of adult POP explained 33% of the variability in CPUE in the training data and 35% of the variability in the test data. Bottom depth, slope, and maximum tidal current were the most important variables explaining the catch of adult POP. Adult POP were distributed throughout the GOA, but concentrations of higher abundance were predicted in deeper areas along the outer shelf (Fig. 122).

Pacific ocean perch distribution in commercial fisheries -- The distribution of Pacific ocean perch occurrence in commercial fisheries catches varied through fall, winter, and spring. The AUC of the fall MaxEnt model was 0.93 for the training data and 0.78 for the test data. The model correctly classified 84% of the predictions from the training and 78% of the predictions from the test data.

Bottom depth, ocean color, and bottom temperature were the most important model variables (relative importance: 0.38, 0.20, and 0.13, respectively). Suitable fall POP habitat was predicted to be concentrated in deeper areas of the central GOA, particularly in Chiniak and Shelikof Gullies, and in the western GOA off Unimak Island (Fig. 123).

In winter, POP were less prevalent in commercial catches and their occurrence was more spatially constrained relative to fall and spring. Ocean color, maximum tidal current, and bottom temperature were the most important variables predicting the distribution of suitable habitat for POP (relative importance: 0.31, 0.19, and 0.17, respectively). The AUC of the winter MaxEnt model was 0.97 for the training and 0.75 for the test dat. The model correctly classified 93% of the predictions from the training data and 75% of the predictions from the test data. Suitable winter POP habitat was predicted to be patchy in distribution throughout the central GOA, with the highest suitability habitats occurring on Albatross Bank (Fig. 124).

In the spring, bottom depth and ocean color were the most important model variables predicting POP distributions (relative importance: 0.41, 0.17, and 0.16, respectively). The AUC of the spring model was 0.95 for the training data and 0.84 for the test data. The model correctly classified 89% of the predictions from the training and 84% of the predictions from the test data. As with the fall and winter, the spring model predicted suitable POP habitat was concentrated in deeper portions of the central GOA, particularly around Shelikof Gully, as well as in the western GOA, off Unimak Island (Fig. 125).

Early life stage *Sebastes* spp. and Pacific ocean perch essential fish habitat maps and conclusions-- Habitat of rockfish ELHS in general, and POP specifically, was predicted to extend across the GOA from west to east (Fig. 126). High probabilities of suitable larval *Sebastes* spp.

habitat were predicted in the western and central GOA regions of Chirikof and Kodiak. Predictions of habitat distribution for settled juvenile POP rockfish collected in summertime bottom trawl surveys indicate they could be found in higher abundance on the middle and outer shelf in the eastern and central GOA. Adult POP habitat was more broadly distributed than that of settled juveniles with higher abundances of adults predicted on the middle and outer shelf throughout the GOA. Probable POP habitat predicted from their presence in commercial catches was similar to that predicted from bottom trawl survey catches, and was widely distributed throughout the GOA (Fig. 126). The extent of POP habitat does not appear to vary much seasonally across the GOA.

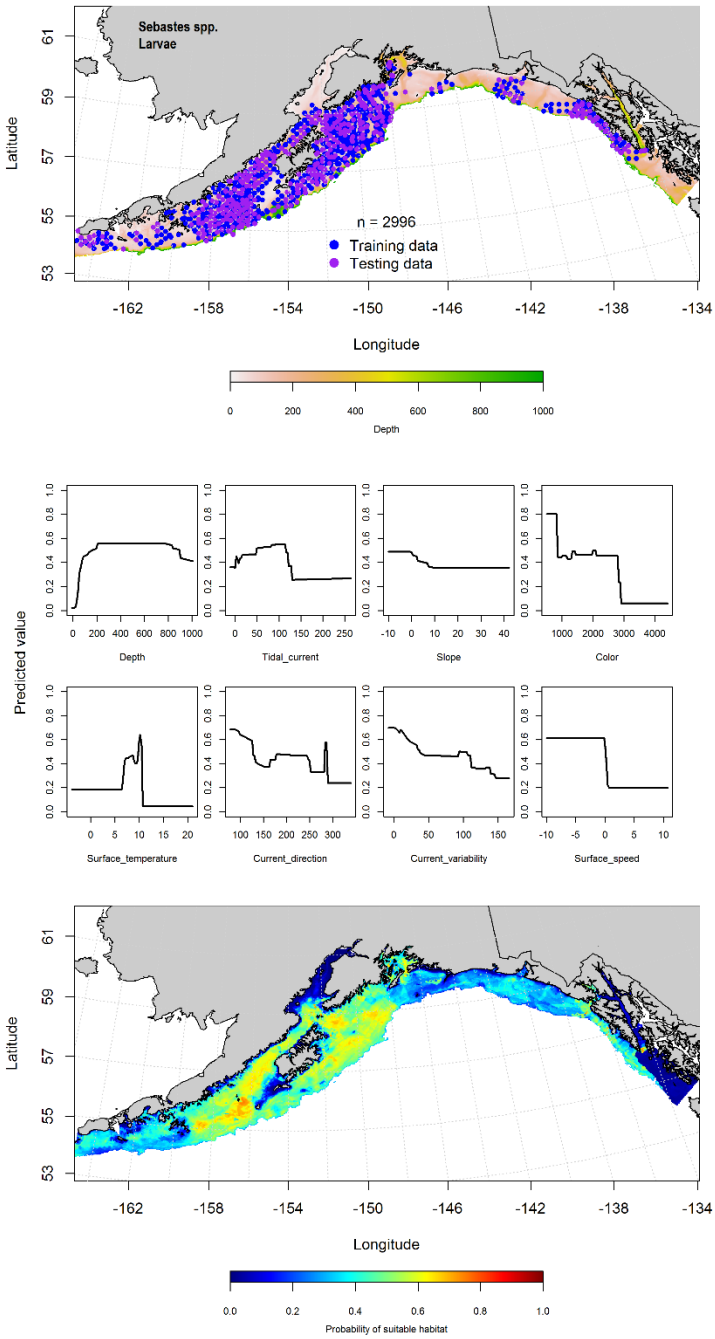

Figure 119. --Distribution of pelagic *Sebastes* spp. larvae observations from EcoFOCI ichthyoplankton surveys (April-October 1991-2012) in the Gulf of Alaska (top panel) with training (blue dots) and testing (purple dots) data indicated, maximum entropy (MaxEnt) model effects (center panel), and the predicted probability of suitable pelagic *Sebastes* spp. larval habitat (bottom panel).

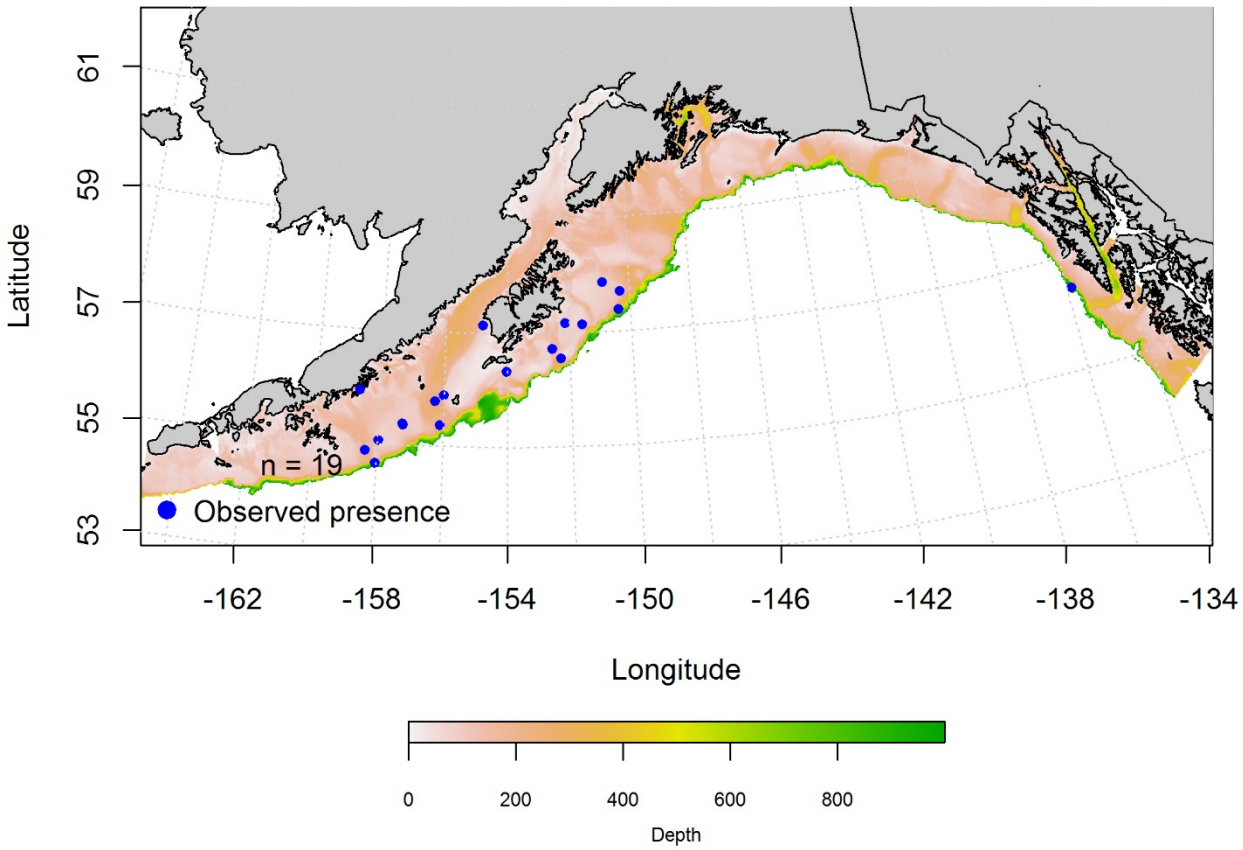

Figure 119. -- Distribution of pelagic Sebastes spp. juvenile observations from EcoFOCI ichthyoplankton surveys in the Gulf of Alaska (April-September 1991-2012).

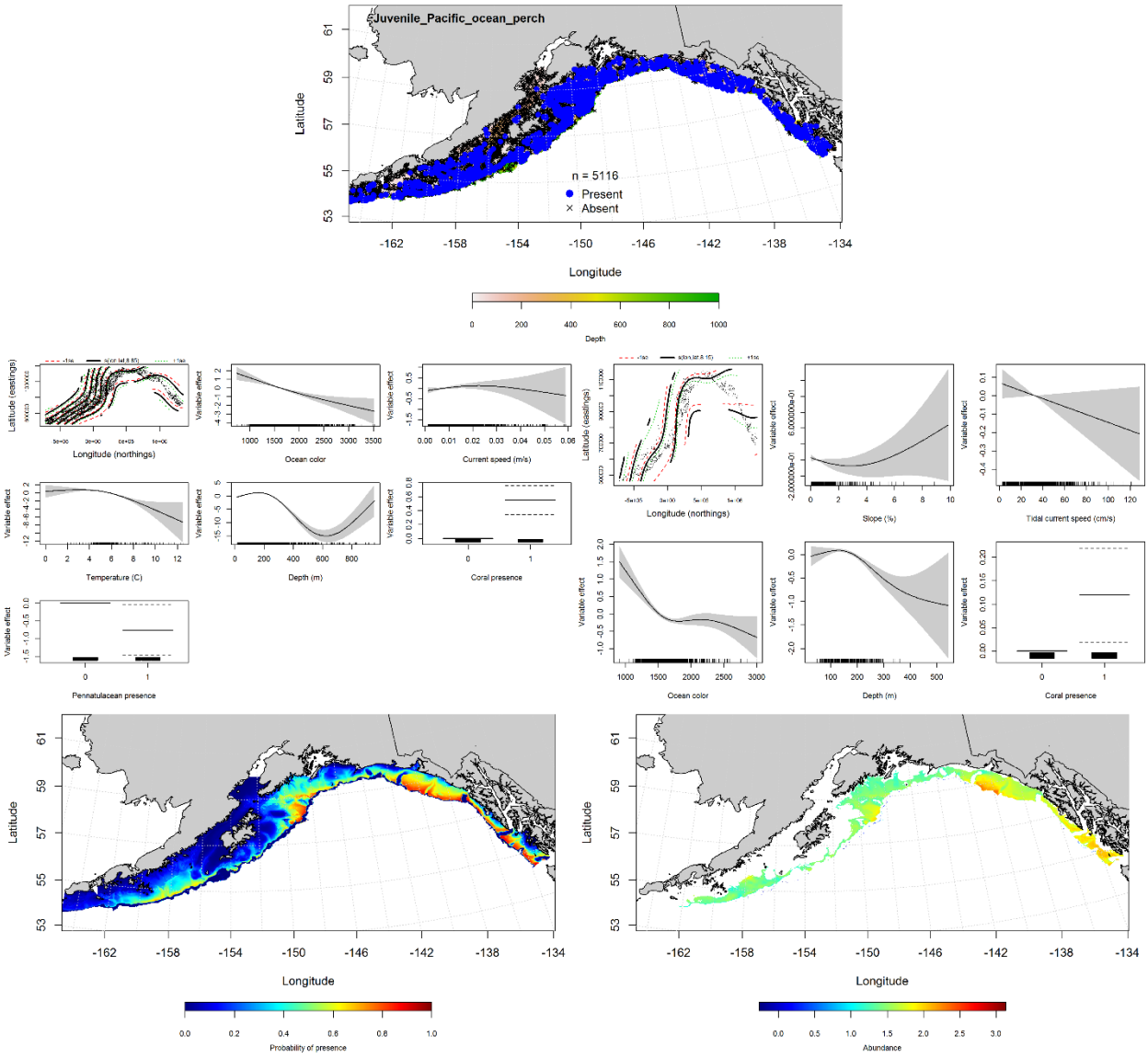

Figure 120. -- Distribution of settled juvenile Pacific ocean perch in1993-2013 RACE-GAP summer bottom trawl surveys conducted in the Gulf of Alaska (upper panel). Effects of retained habitat covariates in the best fitting generalized additive presence-absence models (PA GAM; left center panel) and abundance (CPUE GAM; right center panel). Predicted spatial distribution of the probability of presence (bottom left panel) and abundance of settled juvenile Pacific ocean perch based on the models (bottom right panel).

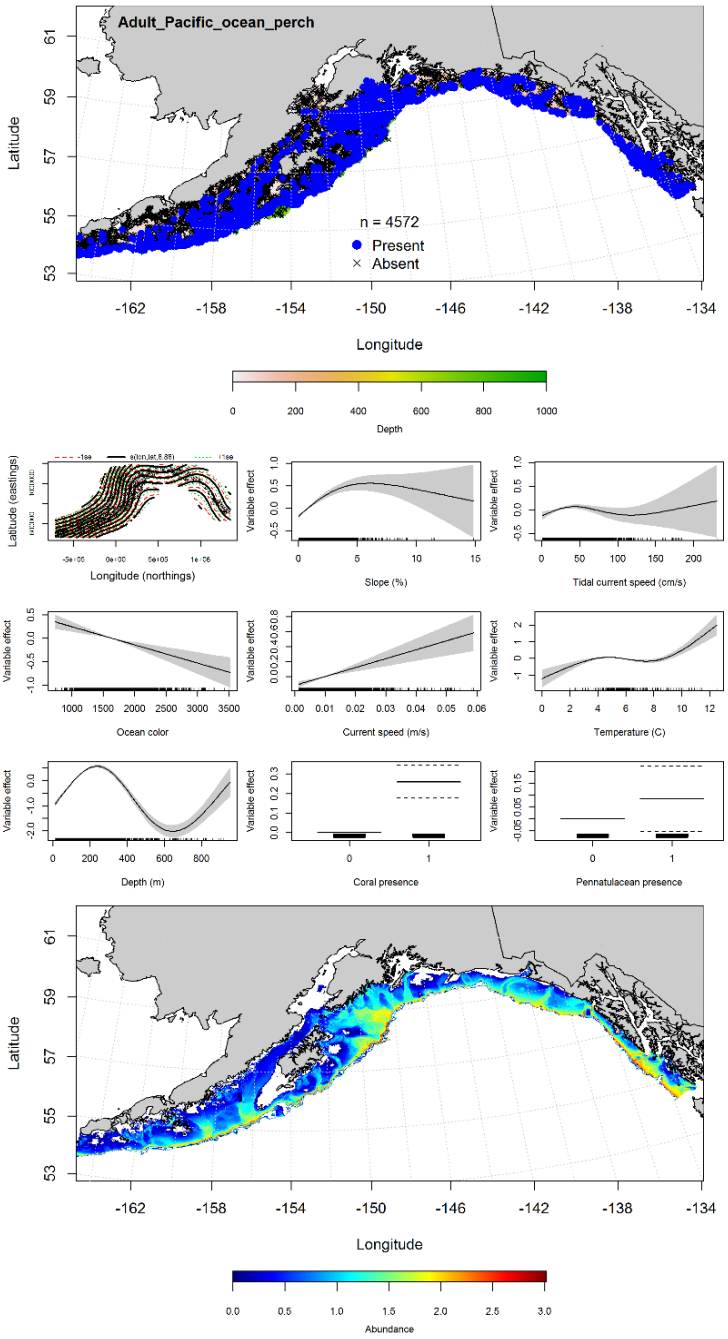

Figure 121. -- Catches of adult Pacific ocean perch from RACE-GAP summer bottom trawl surveys (1993-2013) in the Gulf of Alaska (top panel), significant relationships between CPUE and environmental variables in the best fitting generalized additive model (GAM; middle panels), and the GAM-predicted abundance of adult Pacific ocean perch (bottom panel).

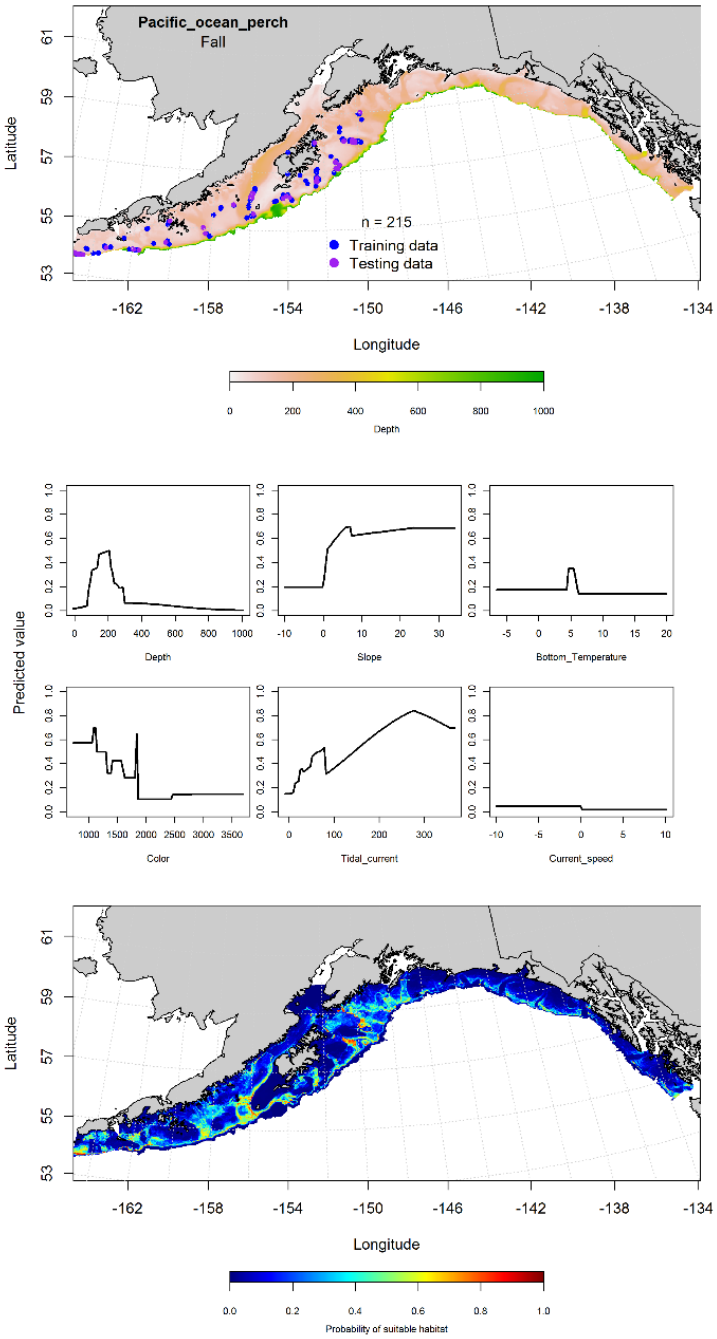

Figure 122. -- Locations of Pacific ocean perch from fall (September-November 2001-2015) commercial fisheries catches in the Gulf of Alaska, MaxEnt model effects (middle panels), and predicted probability of suitable habitat for Pacific ocean perch based on the model (bottom panel).

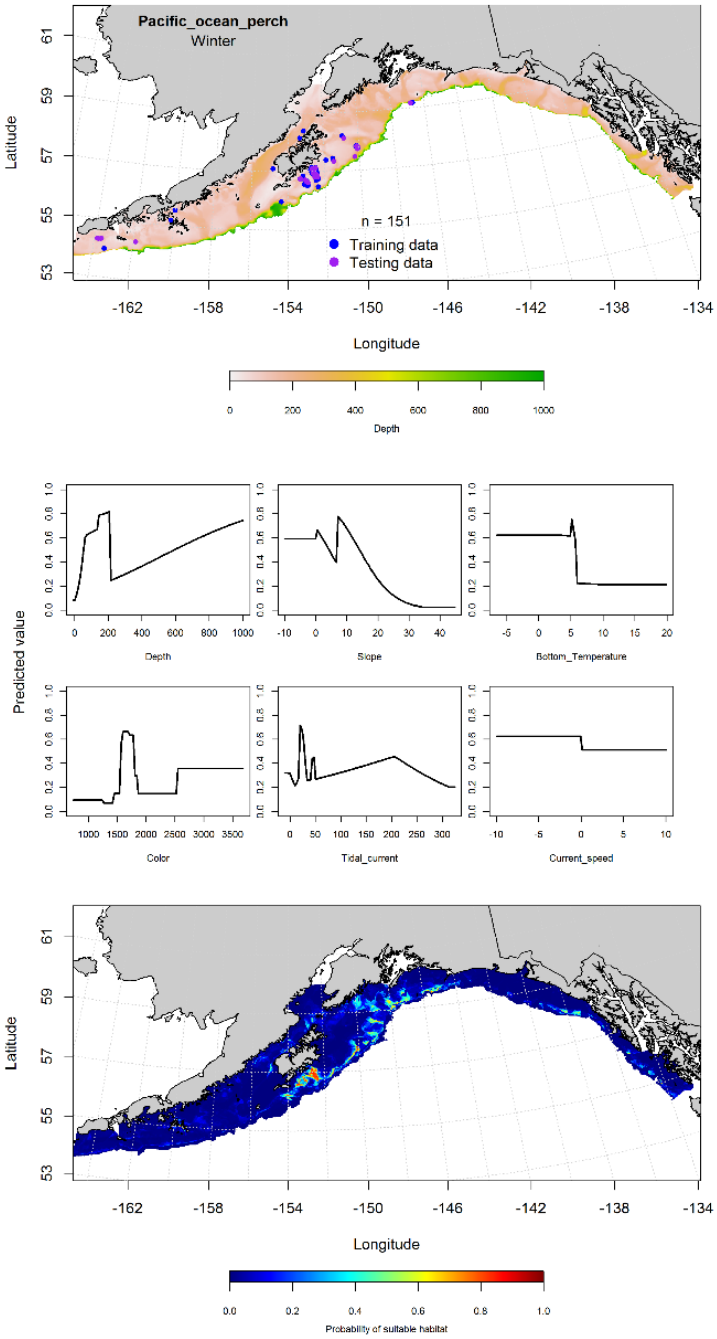

Figure 123. -- Locations of Pacific ocean perch from winter (December-February 2001-2015) commercial fisheries catches in the Gulf of Alaska (top panel), with training (blue dots) and testing (purple dots) data indicated, maximum entropy (MaxEnt) model effects (center panel), and the predicted probability of suitable Pacific ocean perch habitat (bottom panel).

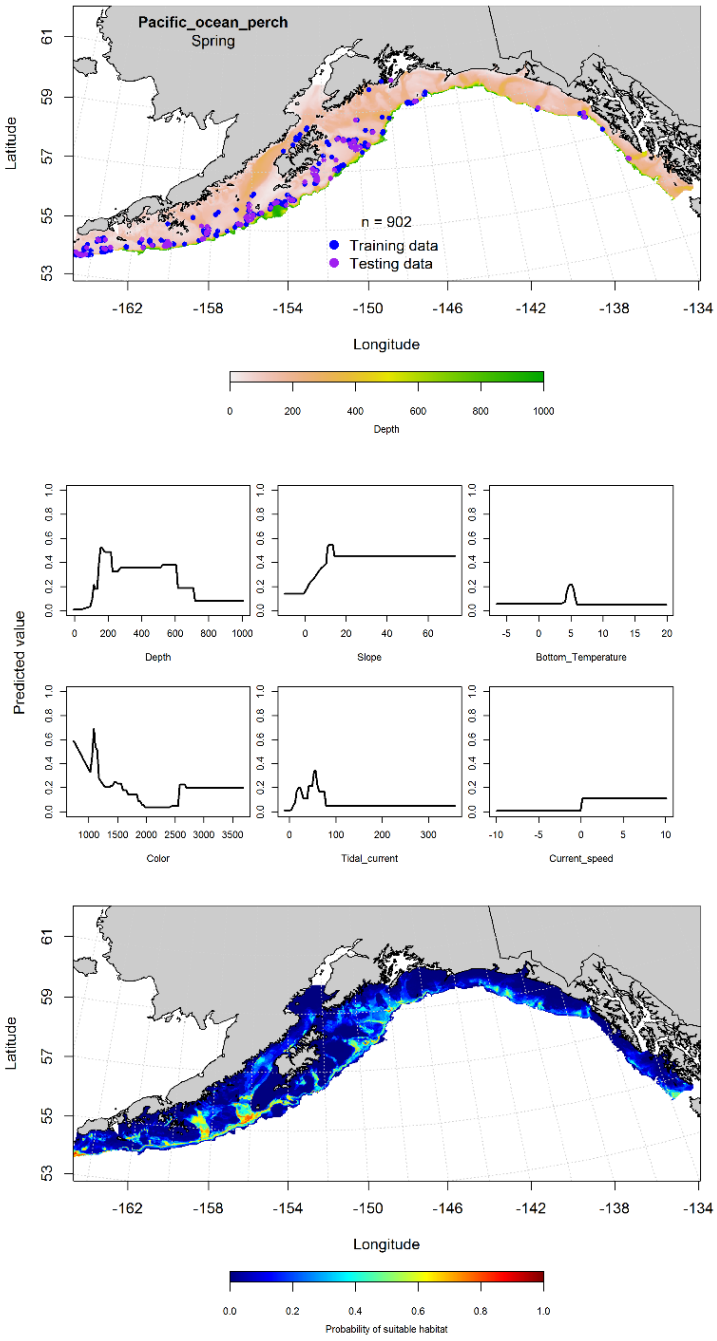

Figure 124. -- Locations of Pacific ocean perch from spring (March-May 2001-2015) commercial fisheries catches in the Gulf of Alaska (top panel), with training (blue dots) and testing (purple dots) data indicated, maximum entropy (MaxEnt) model effects (center panel), and the predicted probability of suitable Pacific ocean perch habitat (bottom panel).

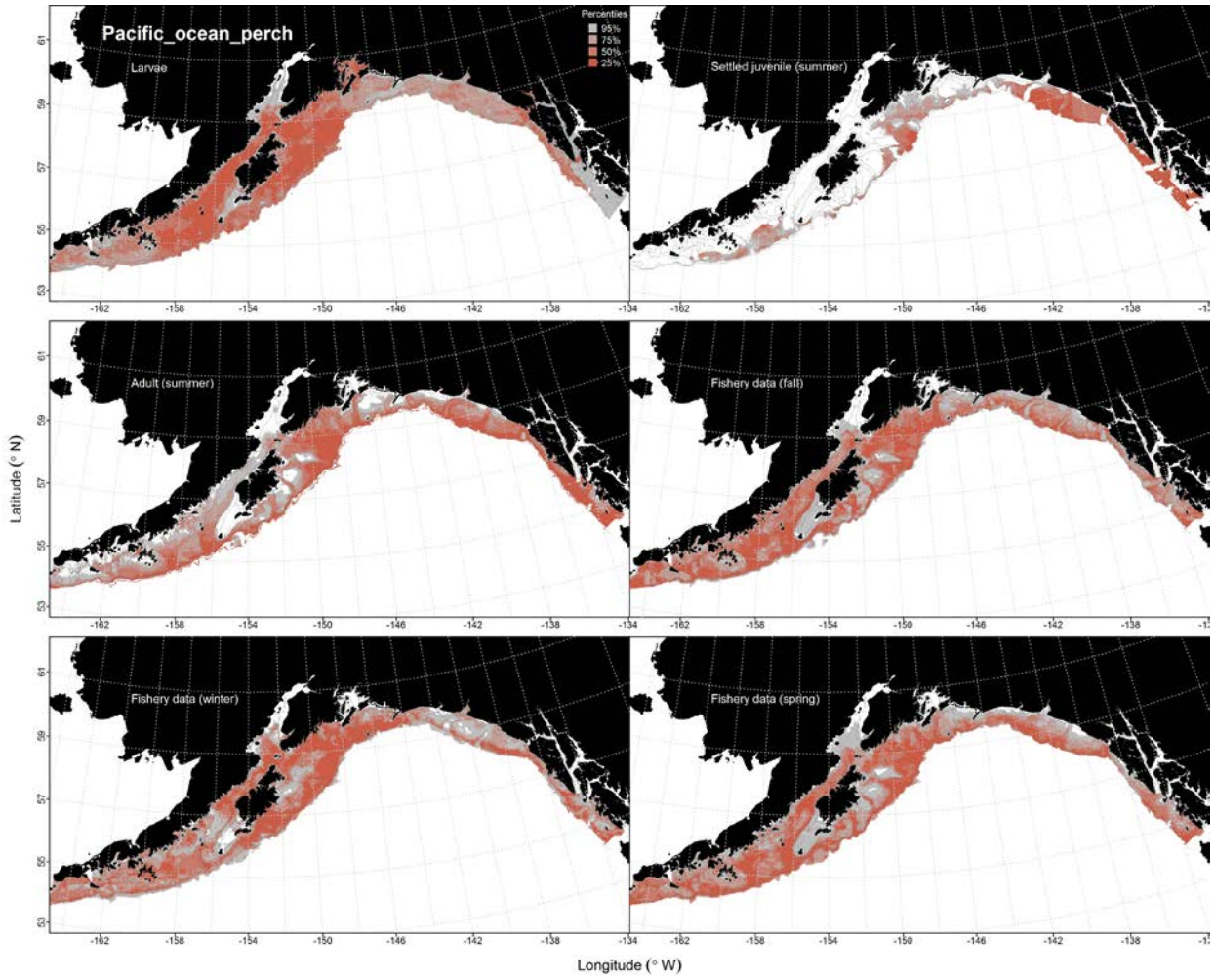

Figure 125. -- Habitat predicted for Pacific ocean perch pelagic larvae from EcoFOCI ichthyoplankton surveys (1991-2012), settled juveniles and adults from RACE-GAP summertime bottom trawl surveys (1993-2013), and predicted from presence in commercial fishery catches (2001-2015) from fall, winter, and spring in the Gulf of Alaska.

Rougheye Rockfish (*Sebastes aleutianus*)

Rougheye (*Sebastes aleutianus*) and blackspotted rockfish (*S. melanostictus*) were considered a single species until recently when blackspotted rockfish were resurrected as a distinct species and rougheye rockfish were re-described (Orr and Hawkins 2008). In the bottom trawl survey operations the species have been separated since 2006. In the VOE-CIA data from commercial fisheries observers, rougheye and blackspotted rockfishes are reported as they are landed; as a complex (i.e., "rougheye/blackspotted rockfish").

Juvenile and adult rougheye rockfish distribution in the bottom trawl survey -- An hGAM was used to predict the distribution of settled juvenile rougheye rockfish abundance from RACE GAP summer bottom trawl survey catches. The PA GAM indicated that geographic position, bottom depth, and slope were the most important model predictors of settled juvenile rougheye rockfish presence. The AUC of the model was 0.92 for the training and 0.91 for the test data. The PA GAM correctly classified 84% of the training data and 84% of test data. The highest predicted presence of settled juvenile rougheye rockfish was in the central and eastern GOA (Fig. 127). The CPUE GAM found geographic position and bottom depth were the most important predictors of CPUE. This model explained 23% of the variability in the training data and 15% in the test data. The model predicted the highest CPUE of settled juvenile rougheye rockfish in the central GOA off Prince William Sound (Fig. 127).

A MaxEnt model was used to predict the probability of suitable habitat for adult rougheye rockfish. Bottom depth and bottom temperature were found to be the most important model predictors of the probability of suitable adult rougheye habitat (relative importance: 0.87 and 0.08,

respectively). The AUC of the MaxEnt model was 0.92 for the training data and 0.84 for the testing data. The model correctly classified 84% of the predictions from both the training and test data. Suitable habitat of adult rougheye rockfish was highest near the shelf break in the central and western GOA, as well as in the eastern GOA, around Cape Ommaney and in Spencer Gully (Fig. 128).

Rougheye/blackspotted rockfish complex distribution in commercial fisheries -- The distribution of the rougheye/blackspotted rockfish complex from commercial fisheries catches in the GOA was similar in fall and winter, but much more extensive in spring. In the fall, bottom depth, slope, and bottom temperature were the most important predictors of the probability of suitable rougheye/blackspotted rockfish habitat (relative importance: 0.34, 0.26, and 0.21, respectively). The AUC of the MaxEnt model was 0.94 for the training data and 0.78 for the test data. The model correctly predicted 87% of the training data and 78% of the test data. Suitable habitat for rougheye/blackspotted rockfish was predicted near the shelf break, particularly in the western GOA (Fig. 129).

In the winter, maximum tidal current, bottom depth, and bottom current speed were the most important variables determining the probability of suitable rougheye/blackspotted rockfish habitat in the GOA (relative importance: 0.34, 0.31, and 0.21, respectively). The AUC of the winter MaxEnt model was 0.95 for the training data and 0.94 for the test data. The model correctly predicted 91% of the training data and 94% of the test data. Suitable habitat of rougheye/blackspotted rockfish was predicted to be concentrated near the shelf break in the central and eastern GOA, as well as in Chiniak Gully off Kodiak Island (Fig. 130).

In the spring, bottom depth, slope, and bottom temperature were the most important variables determining the probability of suitable rougheye/blackspotted rockfish habitat (relative importance:

0.71, 0.10, and 0.10, respectively). The AUC of the spring MaxEnt model was 0.95 for the training data and 0.87 for the test data. The model correctly classified 89% of the predictions from the training data and 87% of the predictions from the test data. As in the fall and winter, the model predicted suitable habitat concentrated along the shelf break across the GOA study area (Fig. 131).

Rougheye rockfish essential fish habitat maps and conclusions -- Predicted settled juvenile rougheye rockfish summer habitat predominantly occurred in eastern GOA (Fig. 132). In contrast, predicted adult rougheye rockfish habitat was much more widely distributed throughout the GOA, with higher suitability habitats concentrated at deeper depths and along the outer shelf (Fig. 132). The distribution of probably habitat predicted from commercial catches of adult rougheye/blackspotted rockfish was similar to that predicted from the bottom trawl surveys (Fig. 132). Predicted fall, winter, and spring habitat distributions from commercial catches were similar across seasons, but slightly more concentrated at deeper depths during the spring

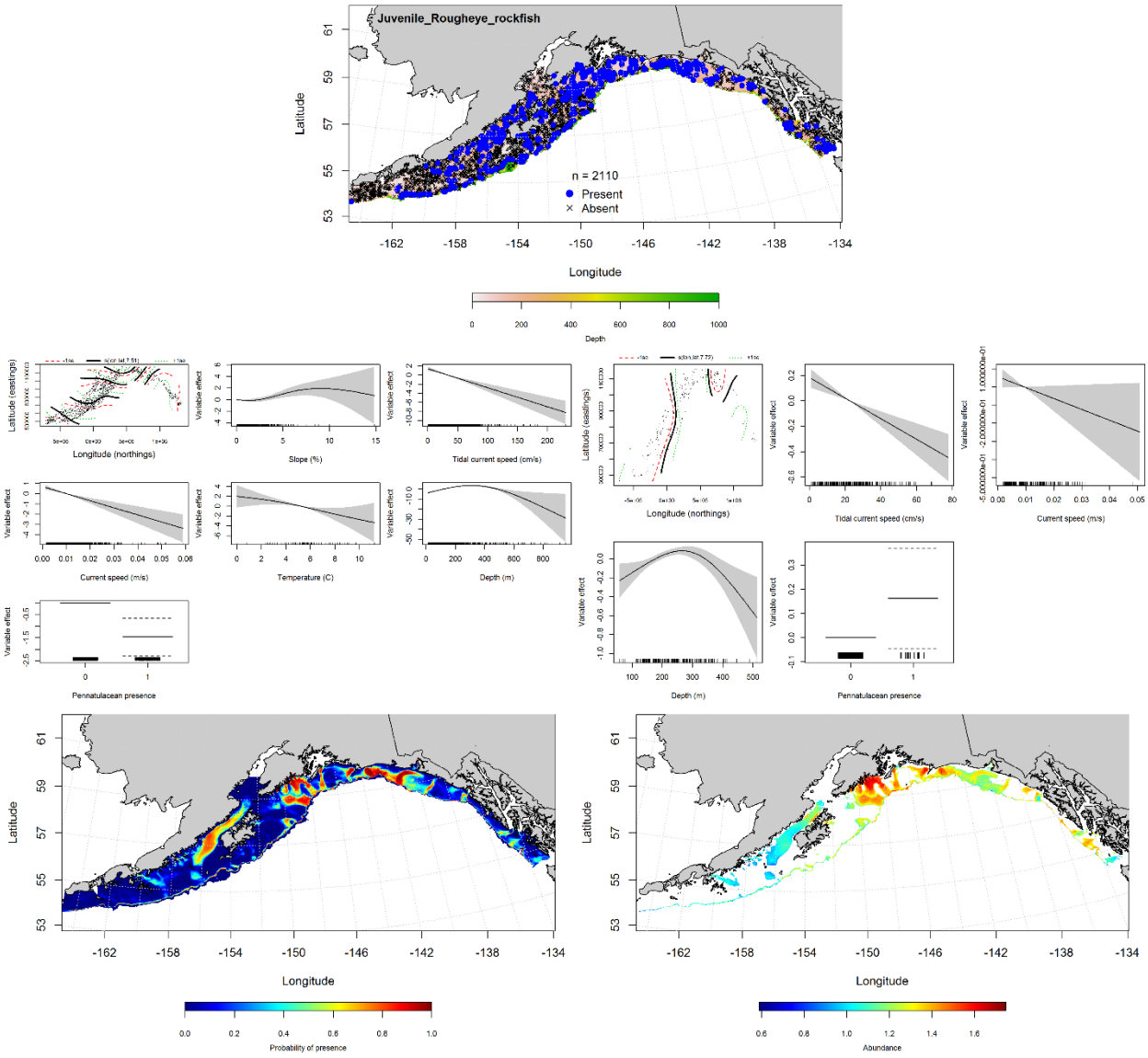

Figure 126. -- Distribution of settled juvenile rougheye rockfish in 1993-2013 RACE-GAP summer bottom trawl surveys conducted in the Gulf of Alaska (upper panel). Effects of retained habitat covariates in the best fitting generalized additive presence-absence models (PA GAM; left center panel) and abundance (CPUE GAM; right center panel). Predicted spatial distribution of the probability of presence (bottom left panel) and abundance of settled juvenile rougheye rockfish based on the models (bottom right panel).

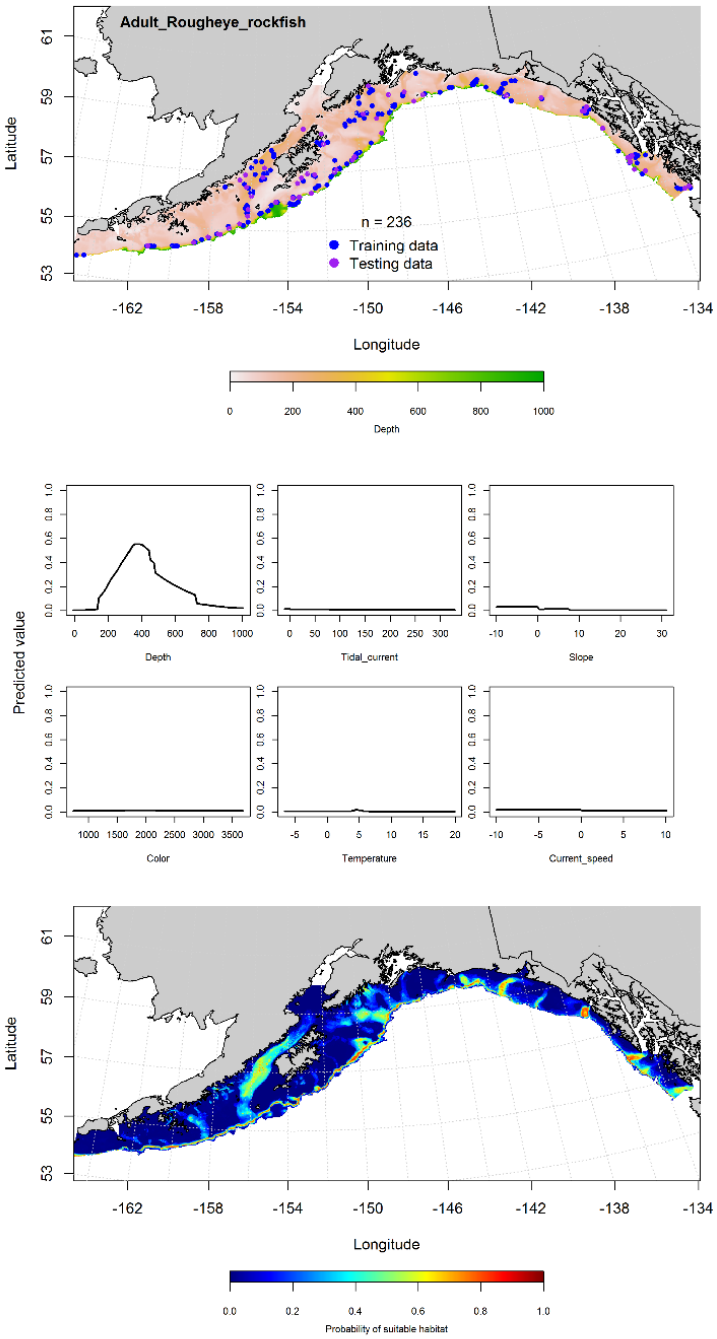

Figure 127. -- Presence of adult rougheye rockfish from RACE-GAP summer bottom trawl surveys (1993-2013) in the Gulf of Alaska (top panel) with training (blue dots) and testing (purple dots) data indicated, maximum entropy (MaxEnt) model effects (center panel), and the MaxEnt-predicted probability of suitable adult rougheye rockfish habitat (bottom panel).

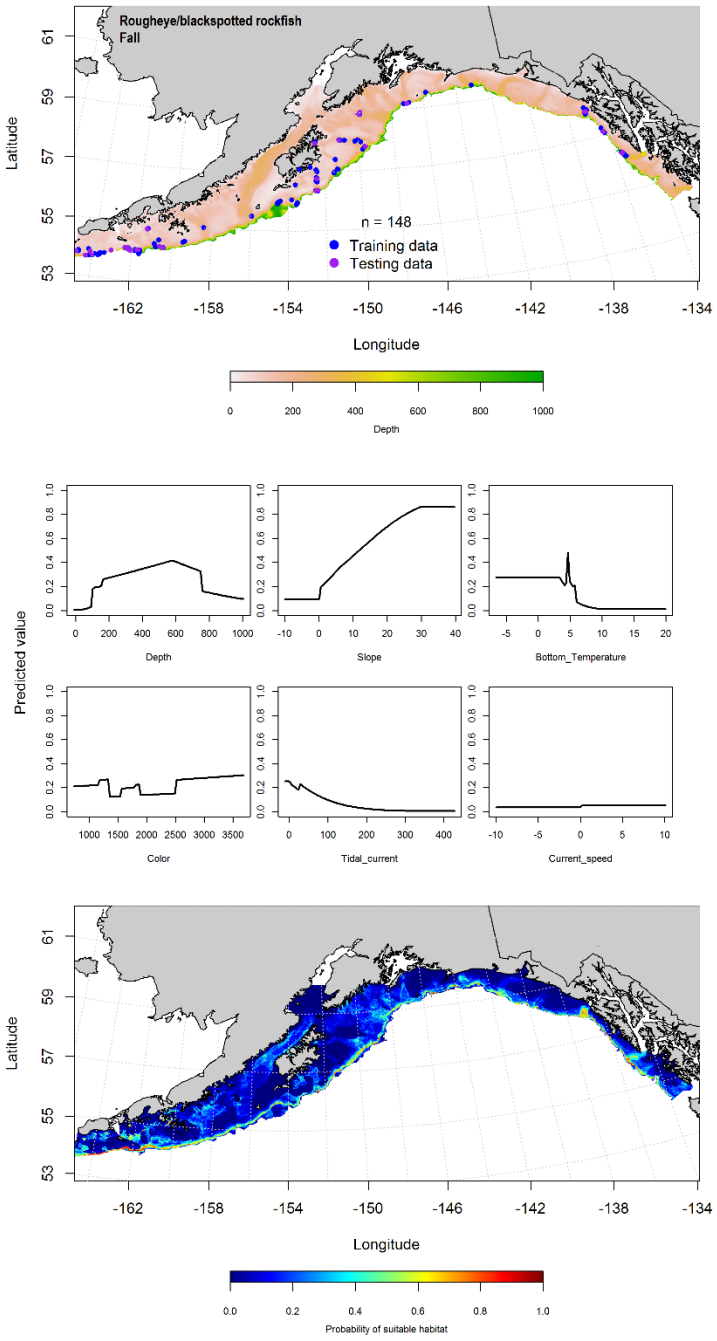

Figure 128. -- Locations of rougheye rockfish from fall (September-November 2001-2015) commercial fisheries catches in the Gulf of Alaska (top panel), MaxEnt model (middle panels), and predicted probability of suitable habitat for rougheye rockfish based on the model (bottom panel).

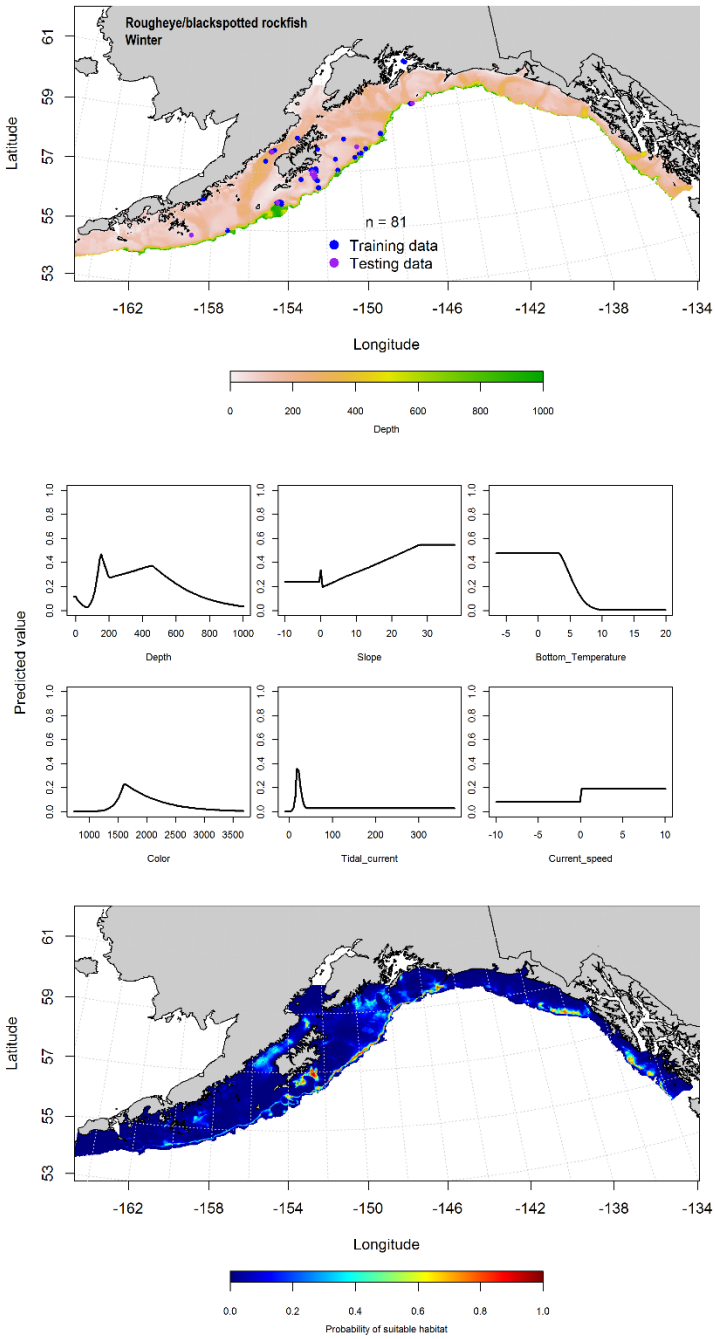

Figure 129. -- Locations of rougheye rockfish from winter (December-February 2001-2015) commercial fisheries catches in the Gulf of Alaska (top panel), with training (blue dots) and testing (purple dots) data indicated, maximum entropy (MaxEnt) model effects (center panel), and the predicted probability of suitable adult rougheye rockfish habitat (bottom panel).

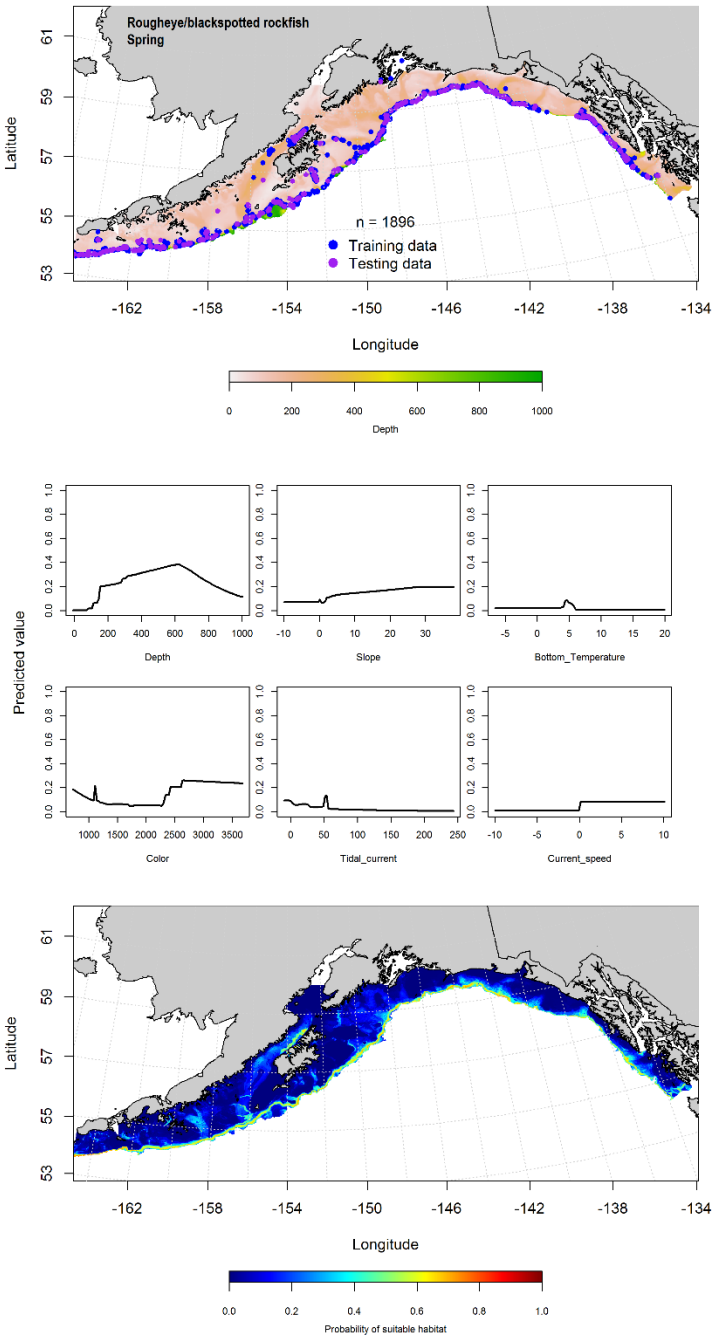

Figure 130. -- Locations of rougheye rockfish from spring (March-May 2001-2015) commercial fisheries catches in the Gulf of Alaska (top panel), with training (blue dots) and testing (purple dots) data indicated, maximum entropy (MaxEnt) model effects (center panel), and the predicted probability of suitable adult rougheye rockfish habitat (bottom panel).

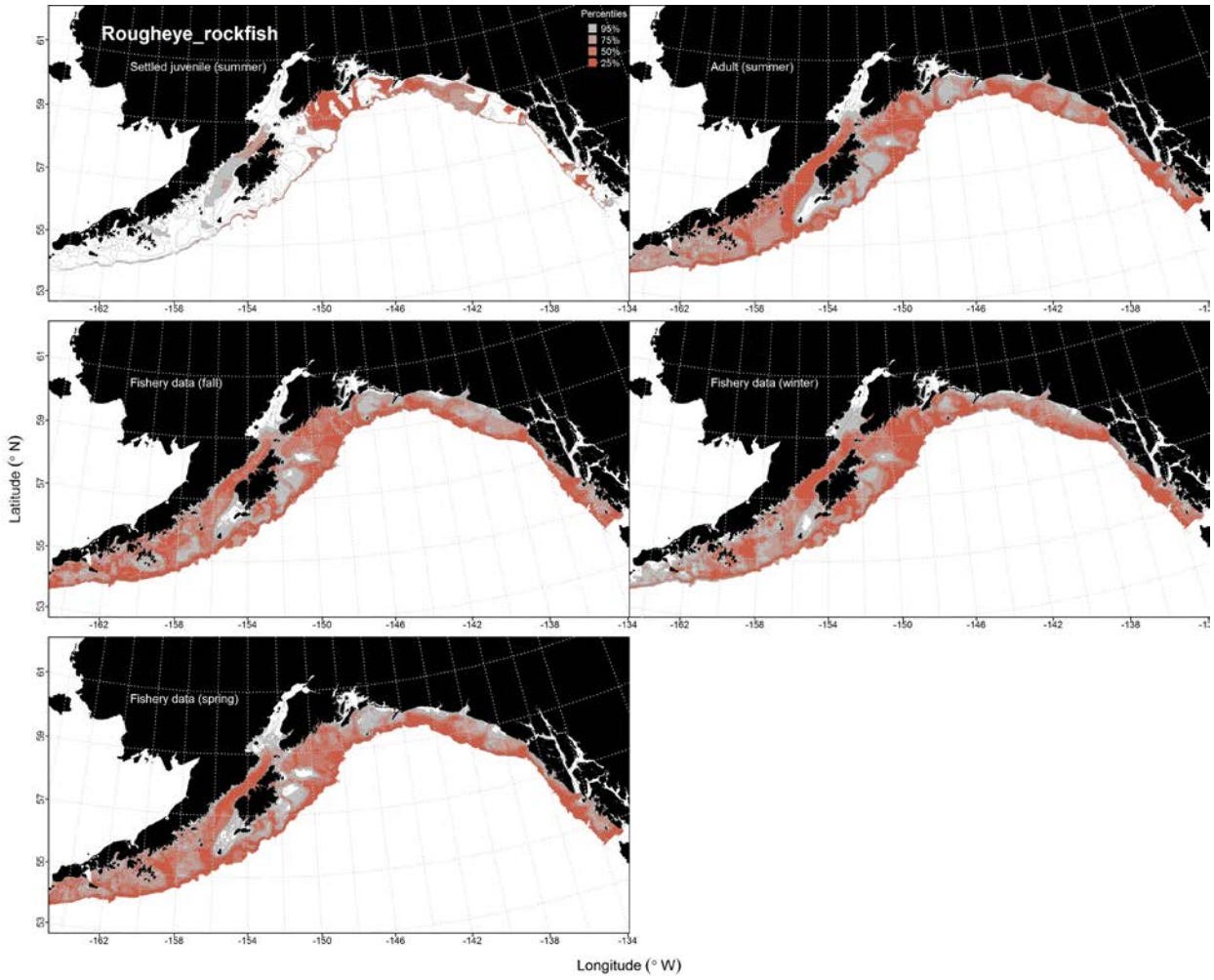

Figure 131. -- Predicted habitat distribution for settled juvenile and adult rougheye rockfish from RACE-GAP summertime bottom trawl surveys (1993-2013) and predicted from presence in commercial fishery catches of rougheye/blackspotted rockfish complex (2001-2015) from the fall, winter, and spring in the Gulf of Alaska.

Redbanded Rockfish (*Sebastes babcocki*)

Juvenile and adult redbanded rockfish distribution in the bottom trawl survey -- The catches of settled juvenile redbanded rockfish in summer bottom trawl surveys were broadly distributed throughout the GOA (Fig. 133). An hGAM was used to predict the distribution of settled juvenile redbanded rockfish abundance. The PA GAM had an AUC 0.94 for the training data and 0.93 for the testing data. The model correctly classified 87% of the predictions from both the training and test data. The most important variables explaining the presence of settled juvenile redbanded rockfish were geographic position, maximum tidal current, and slope. Settled juveniles were predicted to be distributed along the outer shelf throughout the eastern GOA (Fig. 133). The CPUE GAM found that maximum tidal current, bottom depth, and geographic location were the most influential habitat covariates explaining the abundance of settled juvenile redbanded rockfish. The model explained 25% of the variability in the training data and 26% of the variability in the test data. The areas of highest predicted abundance were predicted throughout the eastern GOA in submarine canyons and along the shelf edge (Fig. 133).

A MaxEnt model based on adult redbanded rockfish catches in the bottom trawl survey indicated that bottom depth and bottom current speed were the most important variables predicting suitable redbanded rockfish habitat. The AUC of the model was 0.94 for the training data and 0.77 for the test data. The model correctly classified 88% of the predictions from the training data and 77% of the predictions from the test data. The model predicted that the probability of suitable habitat for adult redbanded rockfish was highest in the eastern GOA, along the outer shelf, and in the central GOA in Shelikof Gully (Fig. 134).

Redbanded rockfish distribution in commercial fisheries -- The distribution of redbanded rockfish occurrence in commercial fisheries catches was sparse and varied across the fall, winter, and spring seasons. There were 39 observations of redbanded rockfish during the fall (Fig. 135) and 20 during the winter (Fig. 136). These data were insufficient to build a MaxEnt model in either season.

In the spring, redbanded rockfish were more prevalent than during other seasons, and bottom depth, bottom current speed, and bottom temperature were the most important variables determining suitable habitat of redbanded rockfish (relative importance: 0.36 and 0.30, respectively). The AUC of the spring MaxEnt model was 0.94 for the training data and 0.90 for the test data. The model correctly classified 88% of the predictions from the training and 90% of the predictions from the test data and predicted suitable habitat of redbanded rockfish across the GOA. Areas with higher probability of suitable habitat were concentrated near the shelf break (Fig. 137).

Redbanded rockfish essential fish habitat maps and conclusions -- Summer- time habitat of settled juvenile redbanded rockfish was largely concentrated along the outer shelf in the eastern GOA (Fig. 138). In contrast, summer habitat of adult redbanded rockfish was more broadly distributed on the middle and outer shelf throughout the GOA (Fig. 138). The spring distribution of redbanded rockfish habitat was similar to that predicted from the summer bottom trawl surveys, although slightly more concentrated at deeper depths (Fig. 138).

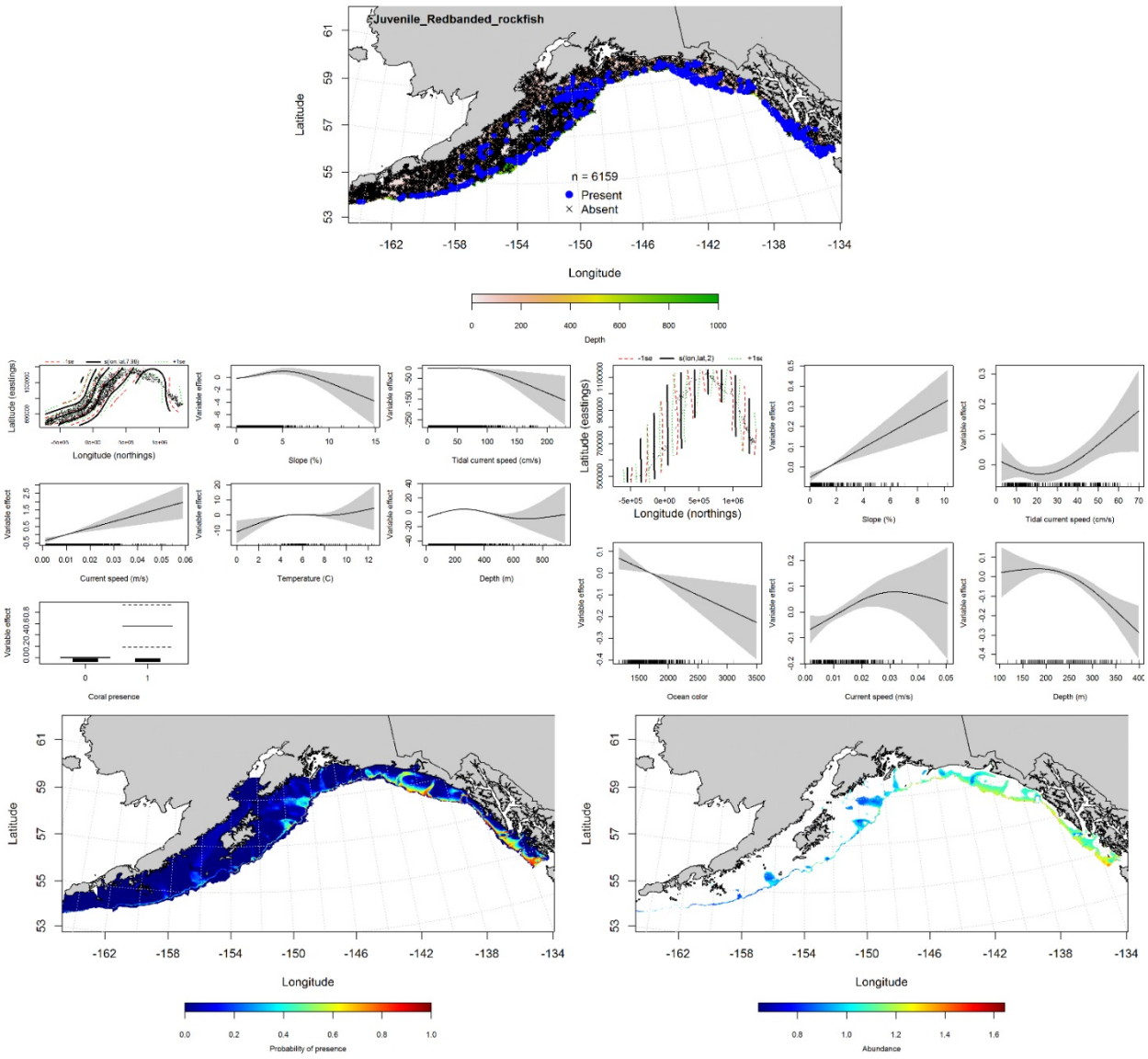

Figure 132. -- Distribution of settled juvenile redbanded rockfish in 1993-2013 RACE-GAP summer bottom trawl surveys conducted in the Gulf of Alaska (upper panel). Effects of retained habitat covariates in the best fitting generalized additive presence-absence models (PA GAM; left center panel) and abundance (CPUE GAM; right center panel). Predicted spatial distribution of the probability of presence (bottom left panel) and abundance of settled juvenile redbanded rockfish based on the models (bottom right panel).

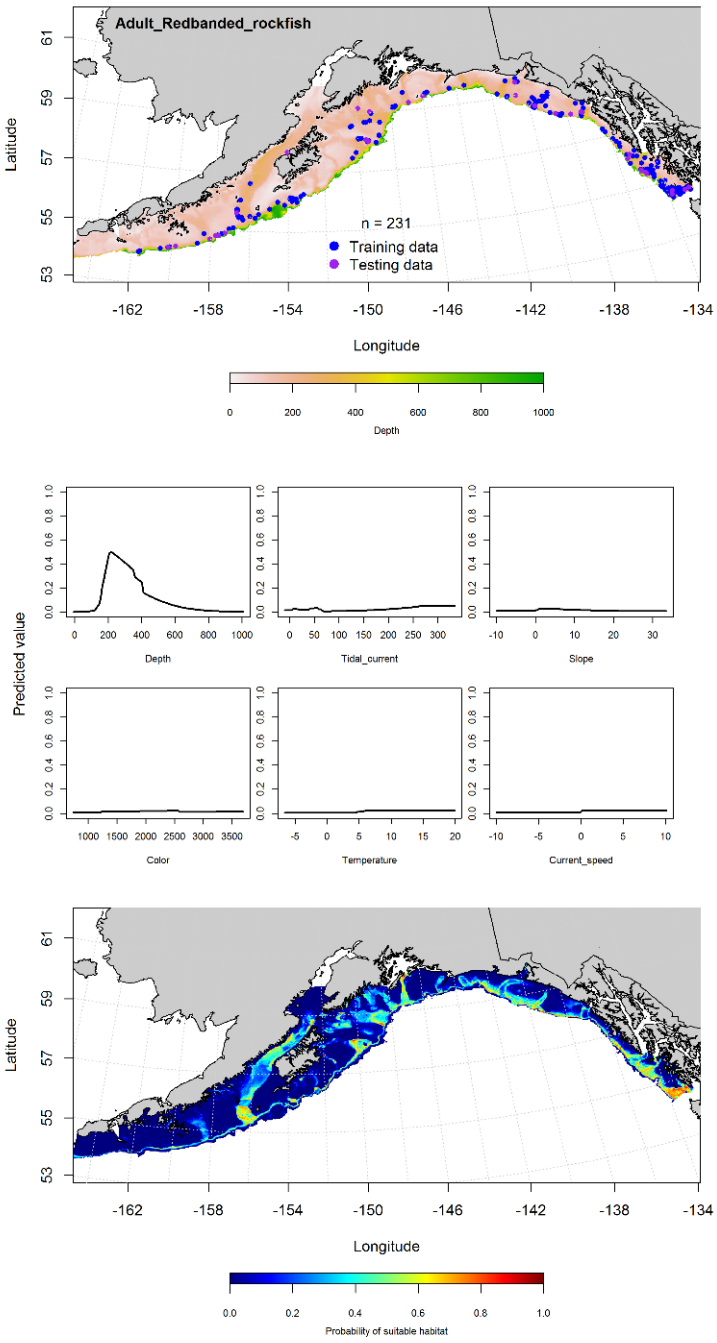

Figure 133. -- Catches of adult redbanded rockfish from RACE-GAP summer bottom trawl surveys (1993-2013) in the Gulf of Alaska (top panel), maximum entropy model (MaxEnt) effects (middle panels), and the MaxEnt-predicted probability of suitable adult redbanded rockfish habitat (bottom panel).

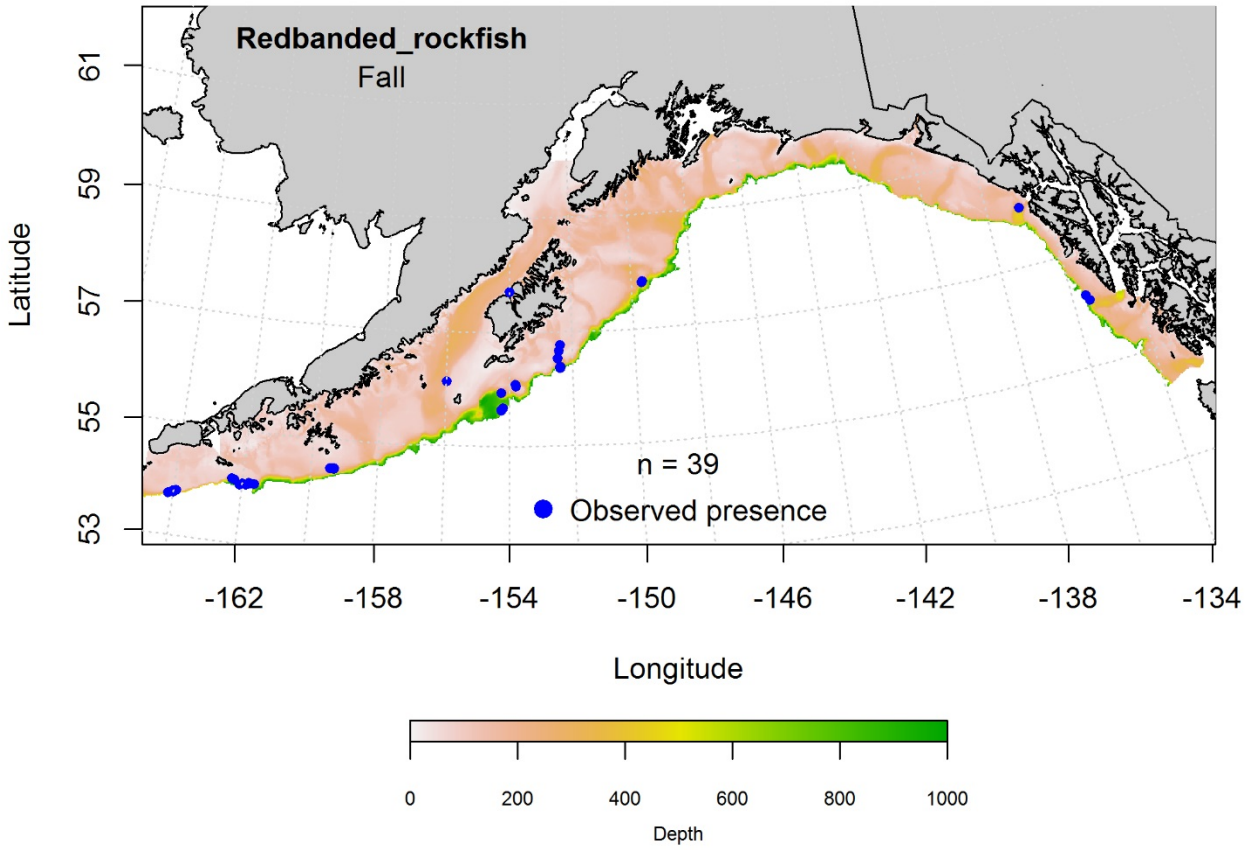

Figure 134. -- Locations of redbanded rockfish from fall (September-November 2001-2015) commercial fisheries catches in the Gulf of Alaska.

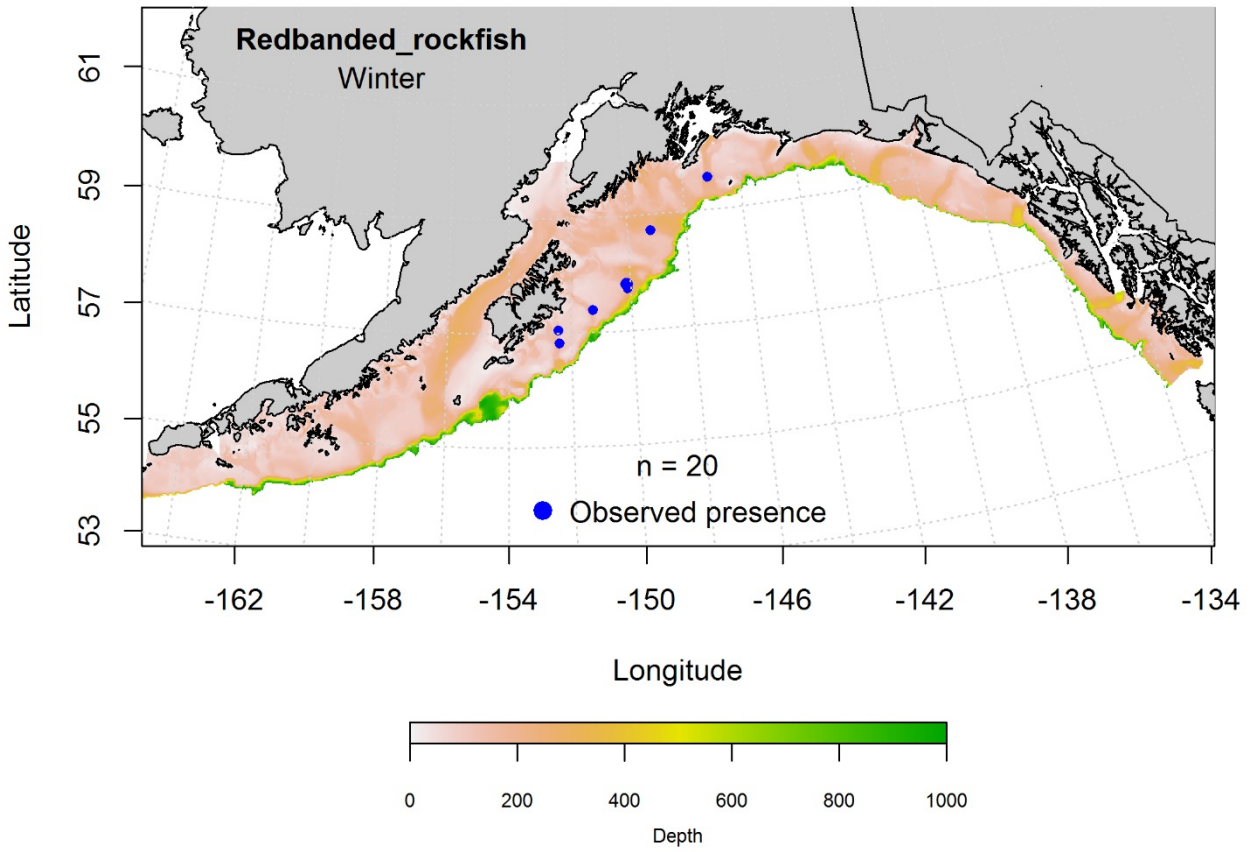

Figure 135. -- Locations of redbandeded rockfish from winter (December-February 2001-2015) commercial fisheries catches in the Gulf of Alaska.

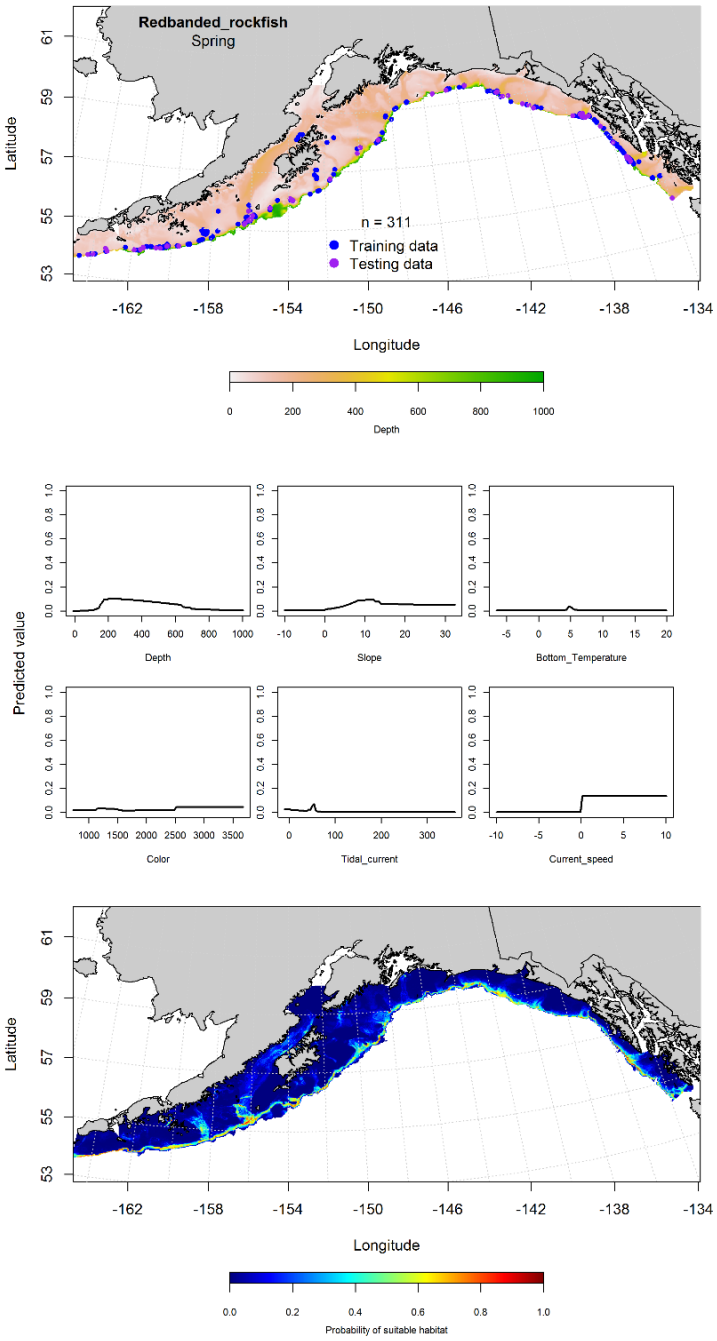

Figure 136. -- Locations of redbanded rockfish from spring (March-May 2001-2015) commercial fisheries catches in the Gulf of Alaska (top panel), with training (blue dots) and testing (purple dots) data indicated, maximum entropy (MaxEnt) model effects (center panel), and the predicted probability of suitable redbanded rockfish habitat (bottom panel).

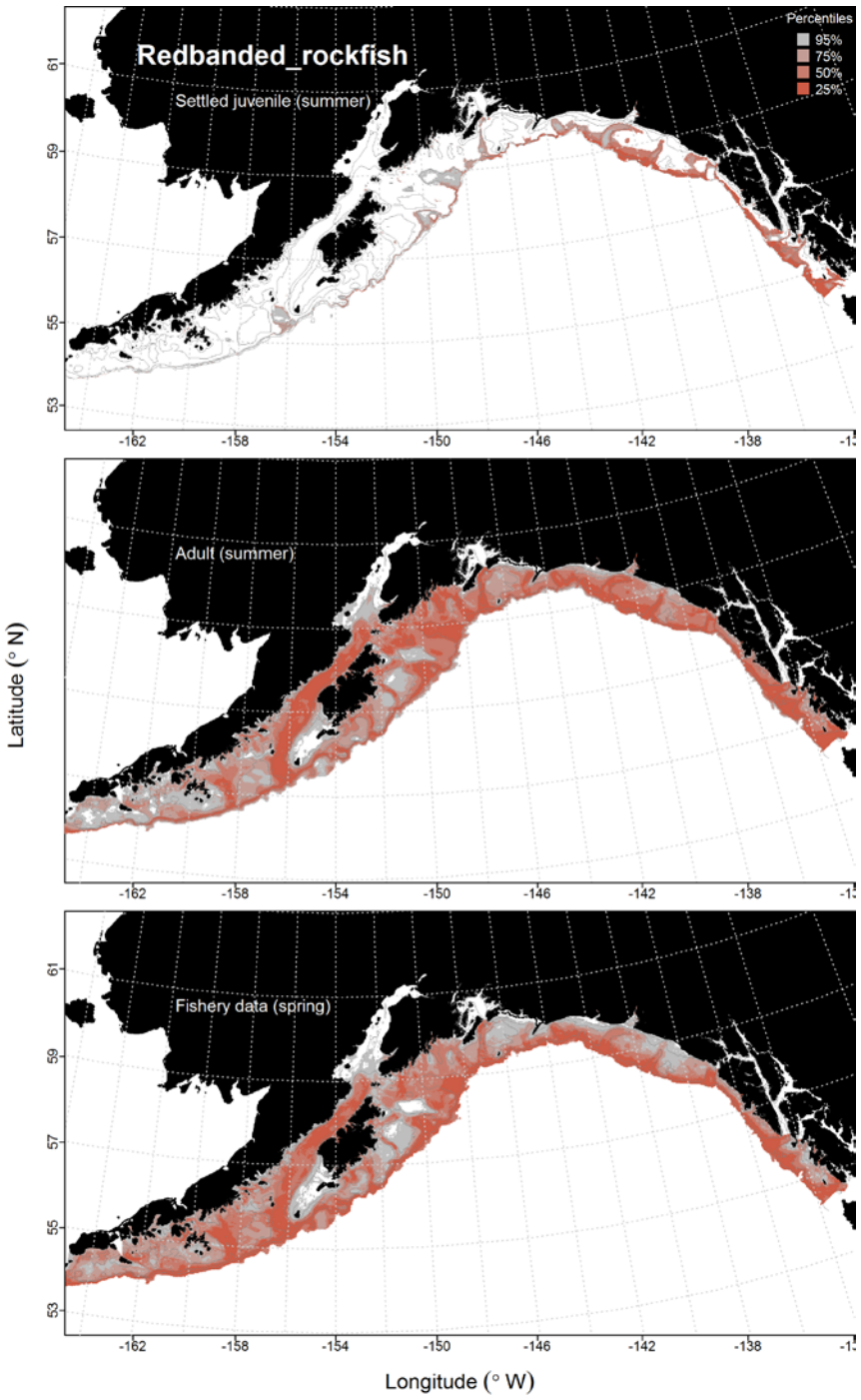

Figure 137. -- Predicted habitat for settled juvenile and adult redbanded rockfish from RACE-GAP summertime bottom trawl surveys (1993-2013) and predicted from presence in commercial fishery catches (2001-2015) from spring in the Gulf of Alaska.

Northern Rockfish (*Sebastes polyspinis*)

Juvenile and adult northern rockfish distribution in the bottom trawl survey -- The distribution of settled juvenile northern rockfish catches in summer bottom trawl surveys indicate this life stage is found in the central and western GOA (Fig. 139). A MaxEnt model was used to predict the suitable habitat of settled juvenile northern rockfish. The AUC of the model was 0.89 for the training data and 0.71 for the testing data. The model correctly classified 78% of the predictions from the training data and 75% of the predictions from the test data. The most important variables determining suitable habitat for settled juvenile northern rockfish were bottom depth, bottom current speed, and maximum tidal current (relative importance: 0.58, 0.13, and 0.10, respectively). The highest probability of suitable habitat of settled juvenile northern rockfish was concentrated in the central GOA, around Portlock and Albatross Banks, and in the western GOA, near Semidi Bank and the Shumagin Islands (Fig. 139).

An hGAM was used to predict the distribution of adult northern rockfish abundance from RACE-GAP summer bottom trawl survey catches. The PA GAM indicated that geographic location, maximum tidal current, and bottom depth were the most important model variables predicting adult northern rockfish presence. The AUC was 0.89 for the training data and 0.87 for the test data. The model correctly classified 89% of the predictions from the training and 81% of the predictions from the test data. The model predicted the highest probability of presence along the outer shelf in the central and western GOA (Fig. 140). The CPUE GAM found geographic location was the most influential variable for predicting abundance. The model explained 17% of the variance in the training data, but only 6% in the test data. The model predicted the highest CPUE on the outer shelf in the central and western GOA (Fig. 140).

Northern rockfish distribution in commercial fisheries -- In the fall commercial catches, bottom depth, bottom current speed, and ocean color were the most important variables determining the distribution of northern rockfish (relative importance: 0.28, 0.24, and 0.18, respectively). The AUC of the MaxEnt fall model was 0.93 for the training data and 0.81 for the test data. The model correctly classified 85% of the predictions from the training observations and 81% of the predictions from the testing observations. The model predicted suitable habitat of northern rockfish was distributed in the central and western GOA with the highest probabilities of suitable habitat in the western GOA, along the middle and outer shelf (Fig. 141).

In the winter commercial catches, bottom depth, bottom current speed, ocean color, and bottom temperature were the most important variables determining suitable habitat of northern rockfish (relative importance: 0.34, 0.18, and 0.17, respectively). The AUC of the MaxEnt model was 0.93 for the training data and 0.82 for the test data. The model correctly classified 85% of the predictions from the training data and 82% of predictions from the test data. The model predicted suitable habitat of northern rockfish throughout the GOA, with the highest probabilities occurring on Albatross Bank (Fig. 142).

In the spring commercial catches, maximum tidal current, bottom depth, ocean color, and bottom current speed were the most important model variables determining the distribution of northern rockfish (relative importance: 0.27, 0.26, and 0.20, respectively). The AUC of the MaxEnt model was 0.93 for the training data and 0.82 for the test data. The model correctly predicted 84% of the training data and 82% of the test data. Suitable habitat for northern rockfish was predicted throughout the GOA, with the highest suitability concentrated between Shelikof Gully and Unimak Island (Fig. 143).

Northern rockfish essential fish habitat maps and conclusions -- In general, predicted habitat for settled juvenile northern rockfish was extensively distributed throughout the GOA (Fig. 144). In contrast, adult northern rockfish habitat based on predicted abundance was concentrated along the outer shelf in the central and western GOA (Fig. 144). The fall, winter, and spring distribution of probable northern rockfish habitat based on their presence in commercial catches was essentially the same across the three seasons, and it was widely distributed throughout the GOA (Fig. 144).

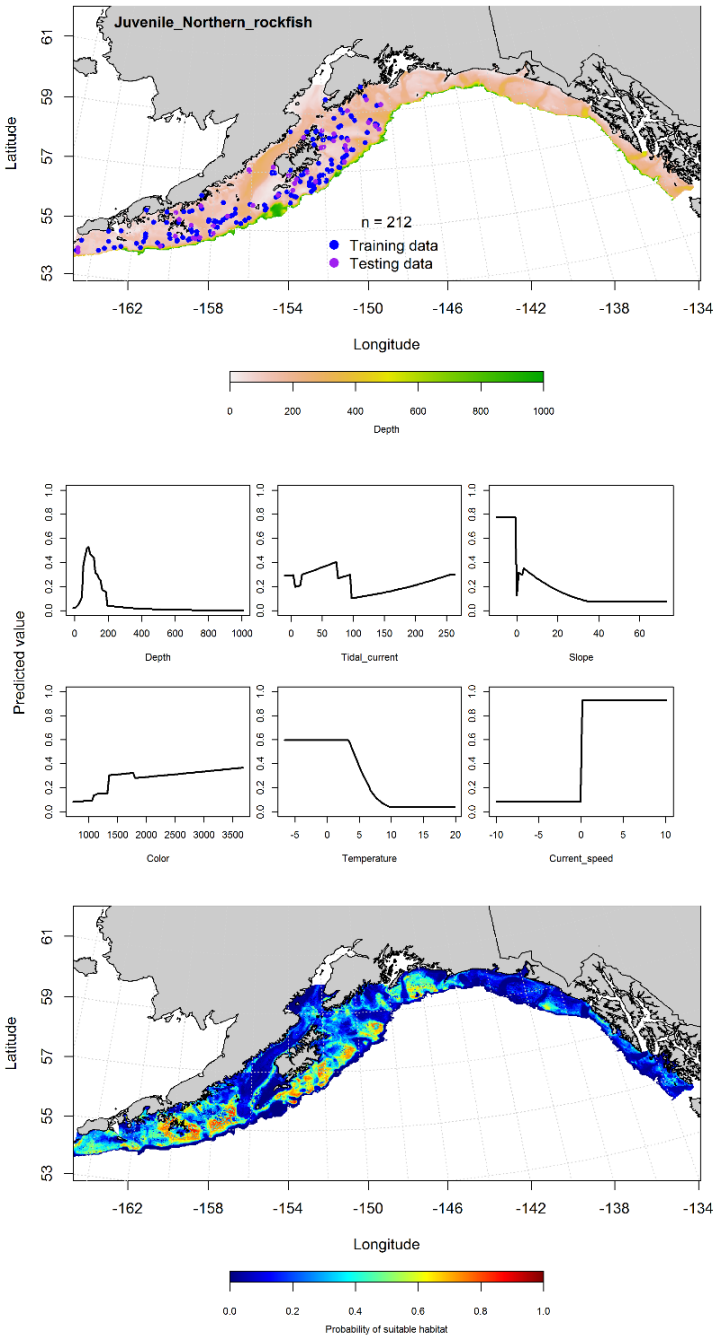

Figure 138. -- Presence of settled juvenile northern rockfish from RACE-GAP summer bottom trawl surveys (1993-2013) in the Gulf of Alaska (top panel) with training (blue dots) and testing (purple dots) data indicated, maximum entropy (MaxEnt) model effects (center panel), and the MaxEnt-predicted probability of suitable juvenile northern rockfish habitat (bottom panel)

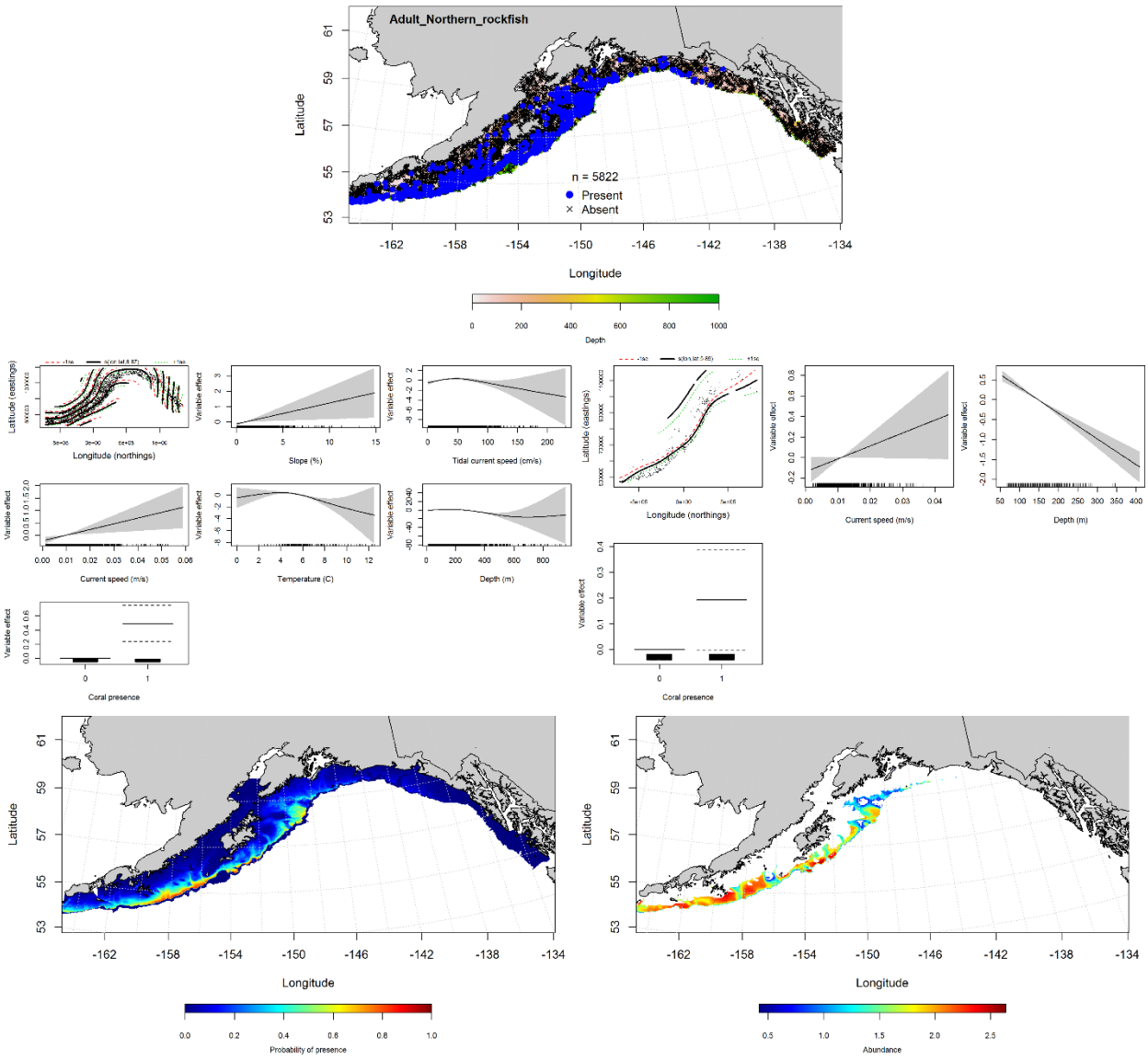

Figure 139. -- Distribution of adult northern rockfish in 1993-2013 RACE-GAP summer bottom trawl surveys conducted in the Gulf of Alaska (upper panel). Effects of retained habitat covariates in the best fitting generalized additive presence-absence models (PA GAM; left center panel) and abundance (CPUE GAM; right center panel). Predicted spatial distribution of the probability of presence (bottom left panel) and abundance of adult northern rockfish based on the models (bottom right panel).

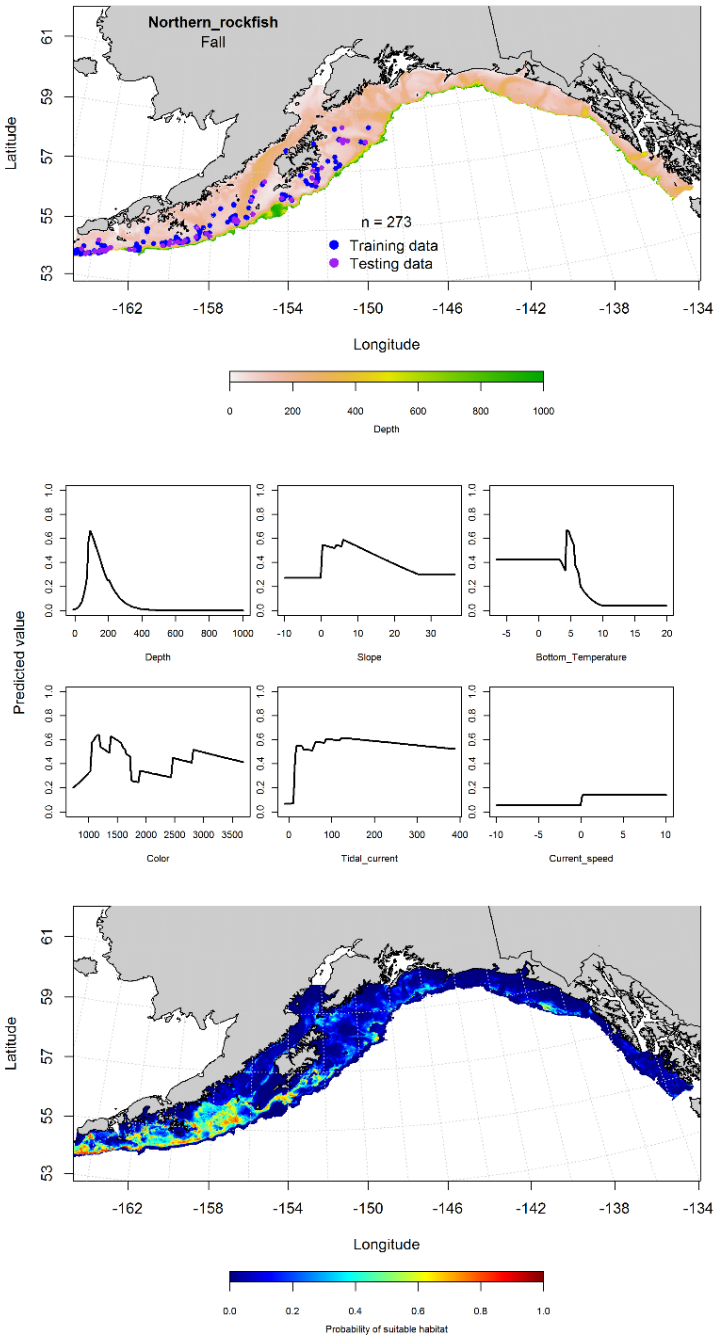

Figure 140. -- Locations of northern rockfish from fall (September-November 2001-2015) commercial fisheries catches in the Gulf of Alaska (top panel), MaxEnt model effects (middle panels), and predicted probability of suitable habitat for northern rockfish based on the model (bottom panel).

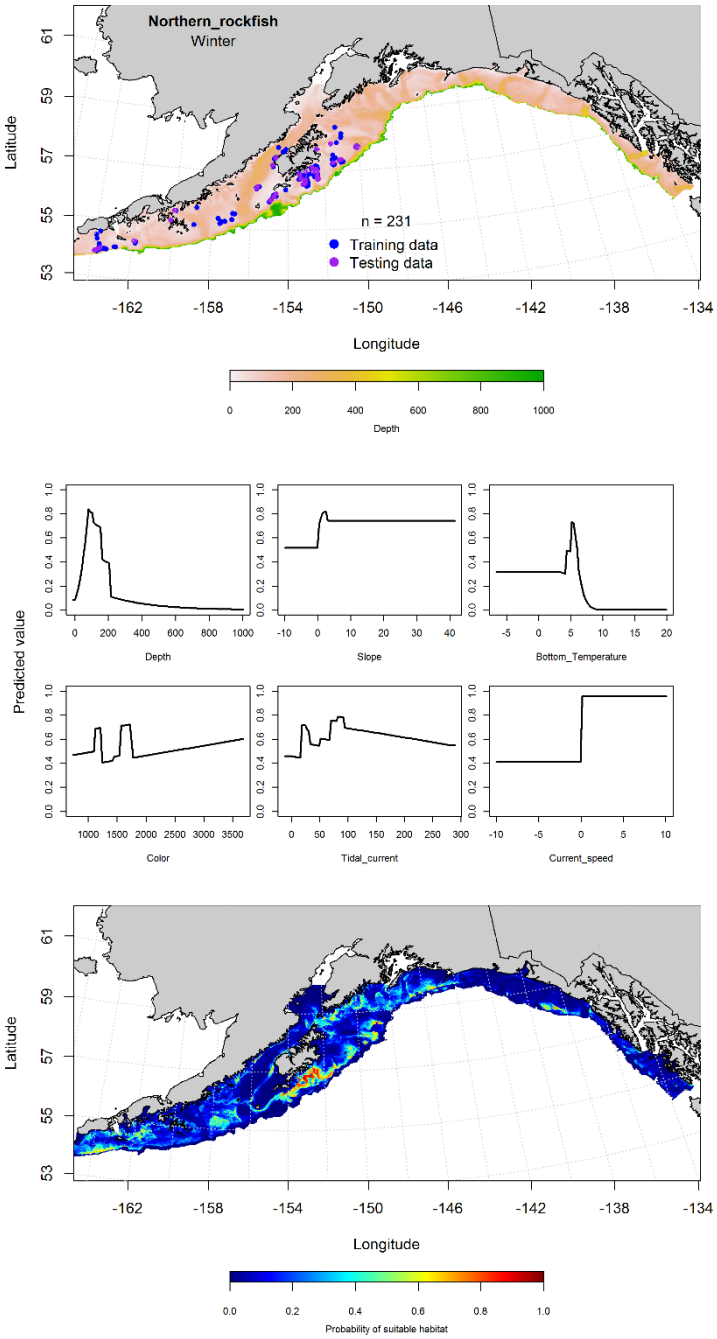

Figure 141. -- Locations of northern rockfish from winter (December-February 2001-2015) commercial fisheries catches in the Gulf of Alaska (top panel), with training (blue dots) and testing (purple dots) data indicated, maximum entropy (MaxEnt) model effects (center panel), and the predicted probability of suitable adult northern rockfish habitat (bottom panel).

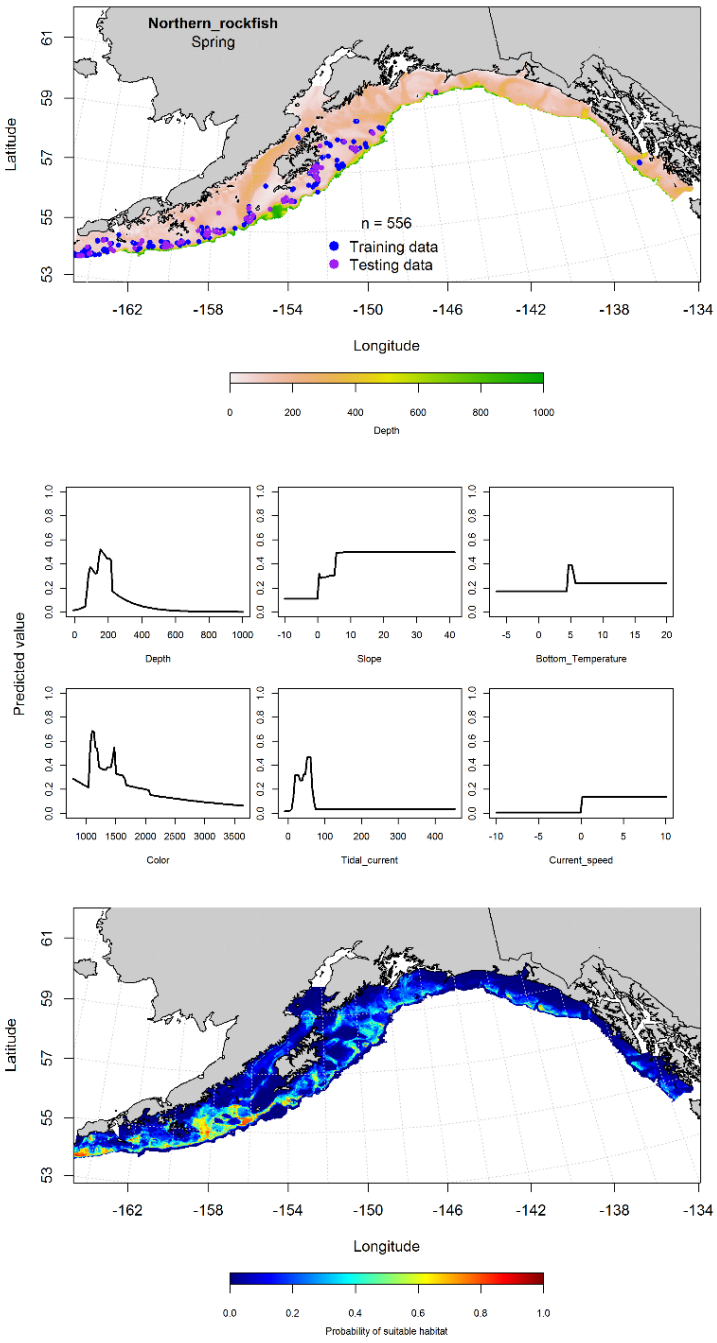

Figure 142. -- Locations of northern rockfish from spring (March-May 2001-2015) commercial fisheries catches in the Gulf of Alaska (top panel), with training (blue dots) and testing (purple dots) data indicated, maximum entropy (MaxEnt) model effects (center panel), and the predicted probability of suitable adult northern rockfish habitat (bottom panel).

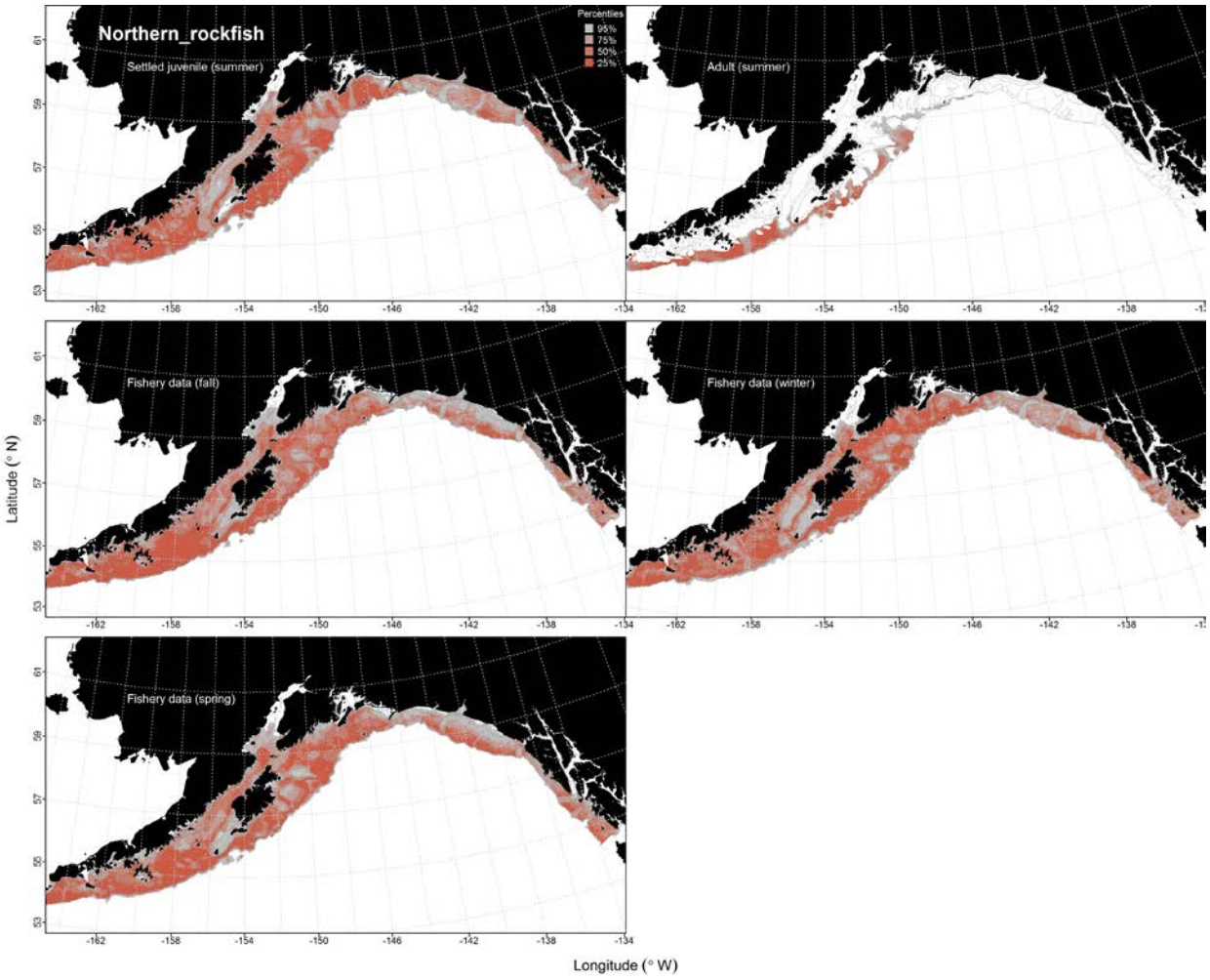

Figure 143. -- Predicted habitat for settled juvenile and adult northern rockfish from RACE-GAP summertime bottom trawl surveys (1993-2013) and predicted inform their presence in commercial fishery catches (2001-2015) from the fall, winter, and spring in the Gulf of Alaska.

Shortraker Rockfish (*Sebastes borealis*)

Juvenile and adult shortraker rockfish distribution in the bottom trawl survey -- A MaxEnt model was used to predict the probability of suitable settled juvenile shortraker habitat. The model AUC was 0.97 for the training data and 0.94 for the test data. The model correctly classified 78% of the predictions from the training data and 75% of the predictions from the test data. Bottom depth and bottom temperature were the important habitat covariates predicting the probability of suitable settled juvenile shortraker habitat (relative importance: 0.76 and 0.10, respectively). Suitable settled juvenile shortraker habitat was primarily predicted near the shelf break across the GOA (Fig. 145).

An hGAM was used to predict the distribution of adult shortraker rockfish abundance. The AUC for the PA GAM was 0.97 for both the training and the test data. Geographic location, bottom depth, and slope were the most important variables explaining the probability of presence of adult shortraker rockfish. The model correctly classified 92% of the predictions from both the training and test data. The model predicted the highest probability of presence in deeper water all across the GOA (Fig. 146). Bottom temperature, bottom depth, and ocean color were the most important variables retained in the CPUE GAM. The model explained 35% of the variance in the training data and 23% in the test data. The model predicted higher adult shortraker rockfish abundance near the shelf break across the GOA, with the highest CPUE occurring off Cape St. Elias (Fig. 146).

Shortraker rockfish distribution in commercial fisheries -- The distribution of shortraker rockfish in commercial fisheries catches varied across the fall, winter, and spring seasons modeled. In the fall, bottom depth, bottom temperature, and slope were the most important variables determining the distribution of shortraker rockfish (relative importance: 0.32, 0.24, and 0.21, respectively). The AUC of the fall MaxEnt model was 0.94 for the training data and 0.85 for the test data. The model

predicted that the probability of suitable shortraker rockfish habitat was highest near the shelf break across the GOA (Fig. 147).

In the winter, there were 46 observations of shortraker rockfish. Most of these were from the central GOA (Fig. 148). However, these data were too few to build a MaxEnt model.

In the spring, bottom depth and slope were the most important variables determining the distribution of shortraker rockfish (relative importance: 0.74 and 0.14, respectively). The AUC of the MaxEnt model was 0.96 for the training data and 0.90 for the test data. The model correctly classified 91% of the predictions from the training and 90% of the predictions from the test data. The model predicted probability of suitable shortraker rockfish habitat was concentrated along the shelf break across the GOA (Fig. 149).

Shortraker rockfish essential fish habitat maps and conclusions -- Probable settled juvenile shortraker rockfish habitat was distributed along the shelf break of the GOA (Fig. 150). In contrast, adult shortraker rockfish habitat was concentrated at continental slope depths (> 200 m) across the GOA and extended inshore from the shelf break along the axes of submarine canyons in the central and eastern GOA. Probable suitable habitat predicted from fall commercial catches was more broadly distributed across deeper areas of the middle and outer shelf of the western GOA while springtime habitat looked similar to summertime habitat predictions and was constrained to the GOA shelf break (Fig. 150). Distribution of shortraker rockfish habitat did not vary much seasonally with the possible exception of potential habitat on the middle and outer shelf in fall.

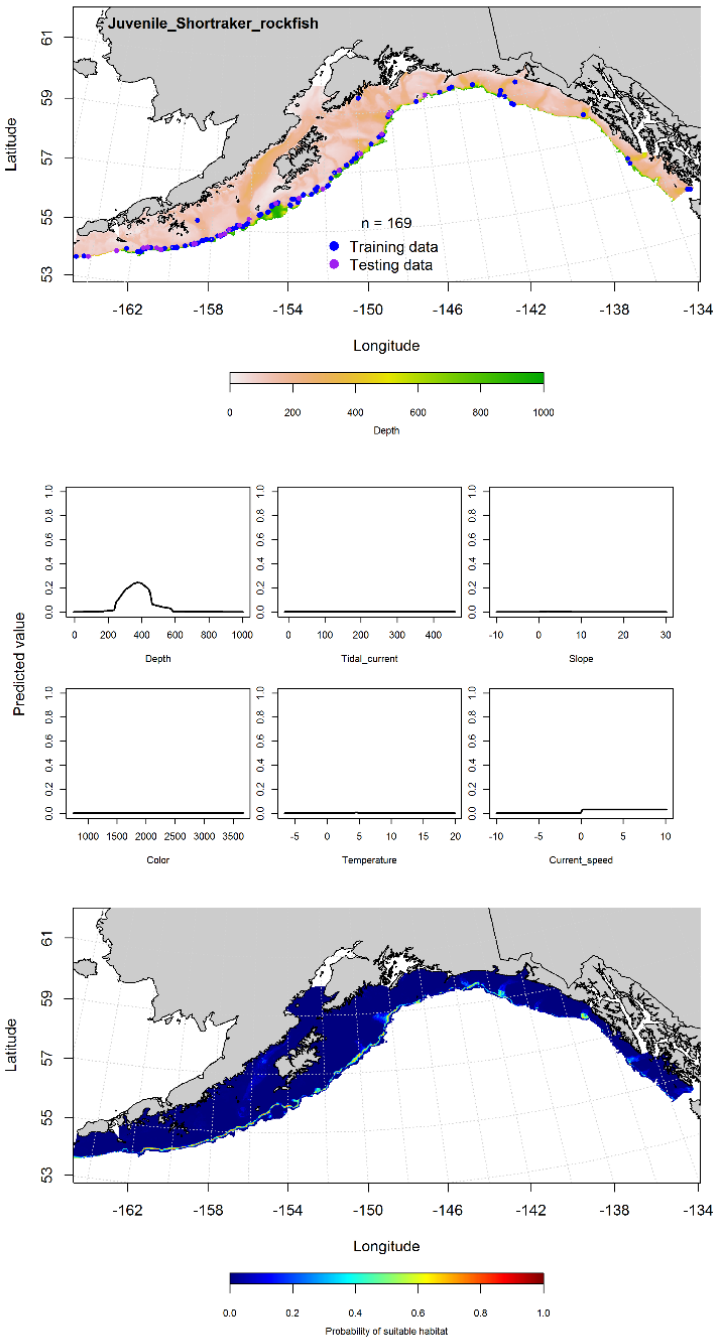

Figure 144. -- Presence of settled juvenile shortraker rockfish from RACE-GAP summer bottom trawl surveys (1993-2013) in the Gulf of Alaska (top panel) with training (blue dots) and testing (purple dots) data indicated, maximum entropy (MaxEnt) model effects (center panel), and the MaxEnt-predicted probability of suitable juvenile shortraker rockfish habitat (bottom panel).

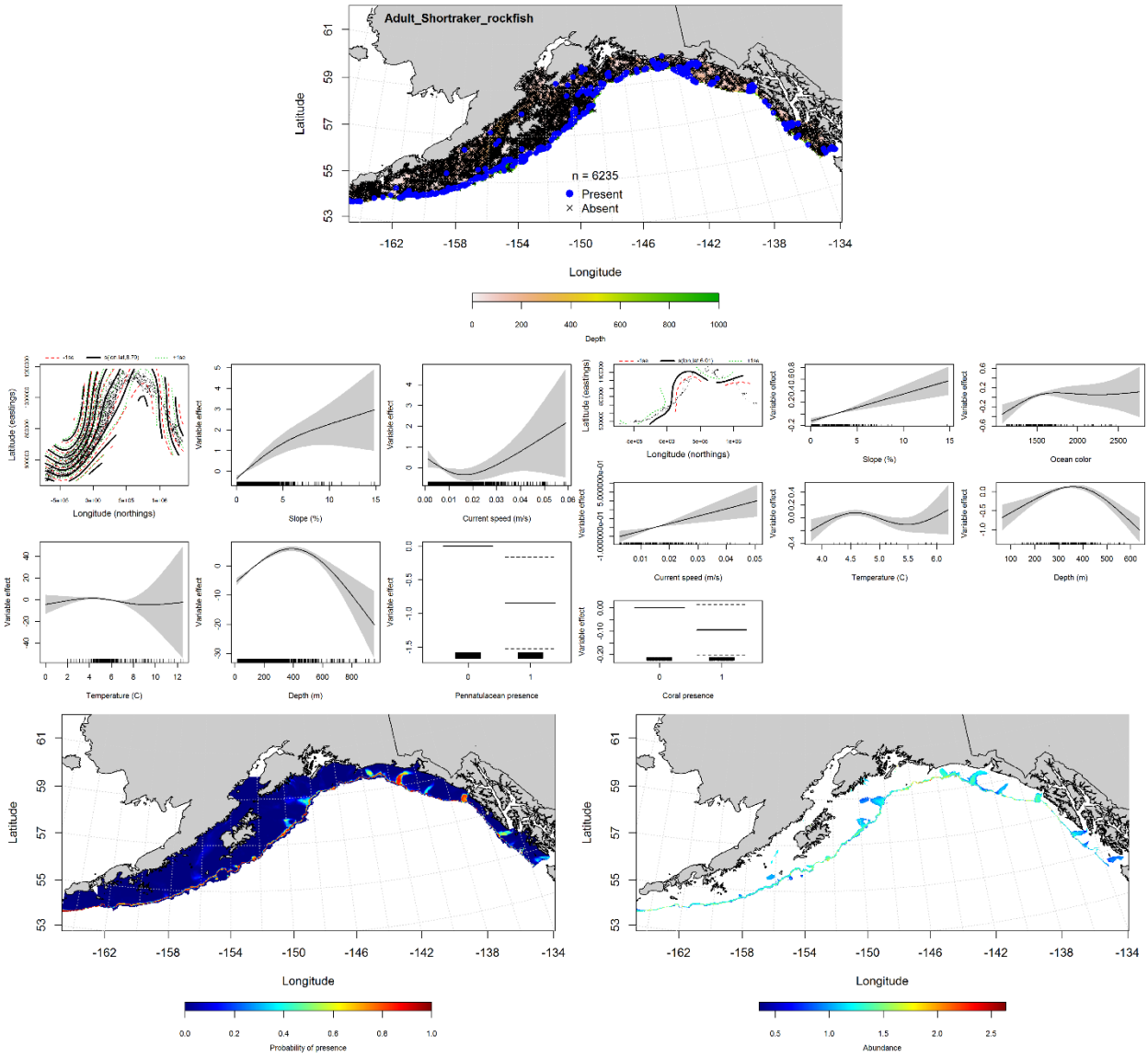

Figure 145. -- Distribution of adult shortraker rockfish in 1993-2013 RACE-GAP summer bottom trawl surveys conducted in the Gulf of Alaska (upper panel). Effects of retained habitat covariates in the best fitting generalized additive presence-absence models (PA GAM; left center panel) and abundance (CPUE GAM; right center panel). Predicted spatial distribution of the probability of presence (bottom left panel) and abundance of adult shortraker rockfish based on the models (bottom right panel).

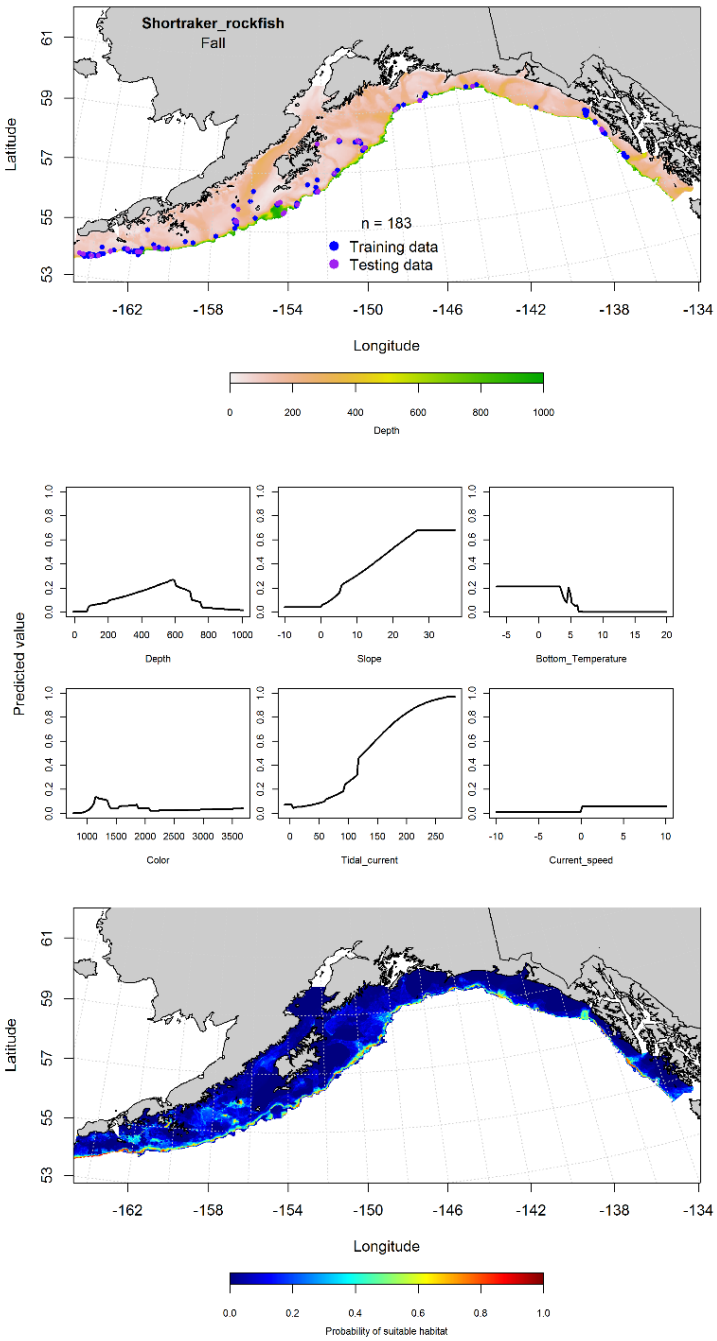

Figure 146. -- Locations of shortraker rockfish from fall (September-November 2001-2015) commercial fisheries catches in the Gulf of Alaska (top panel), MaxEnt model effects (middle panels), and predicted probability of suitable habitat for shortraker rockfish based on the model (bottom panel).

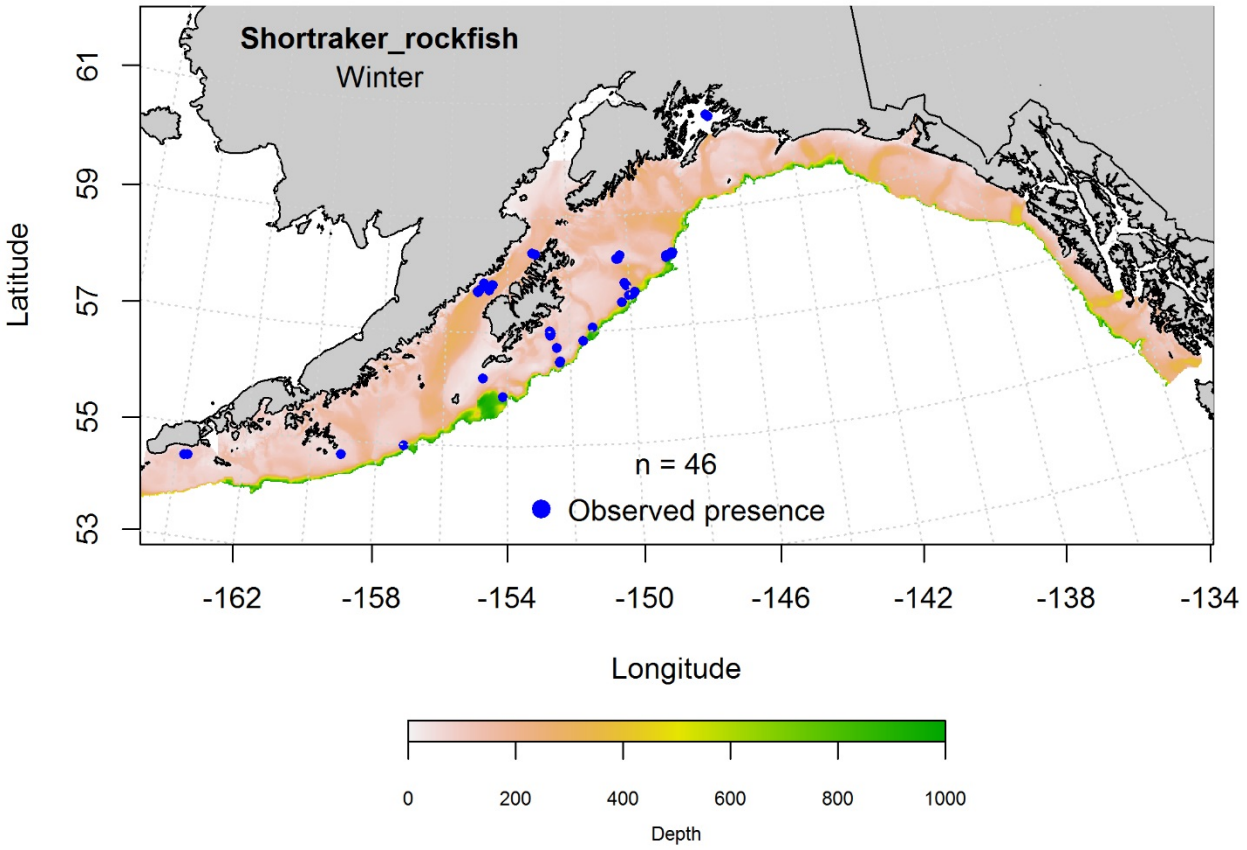

Figure 147. -- Locations of shortraker rockfish from winter (December-February 2001-2015) commercial fisheries catches in the Gulf of Alaska.

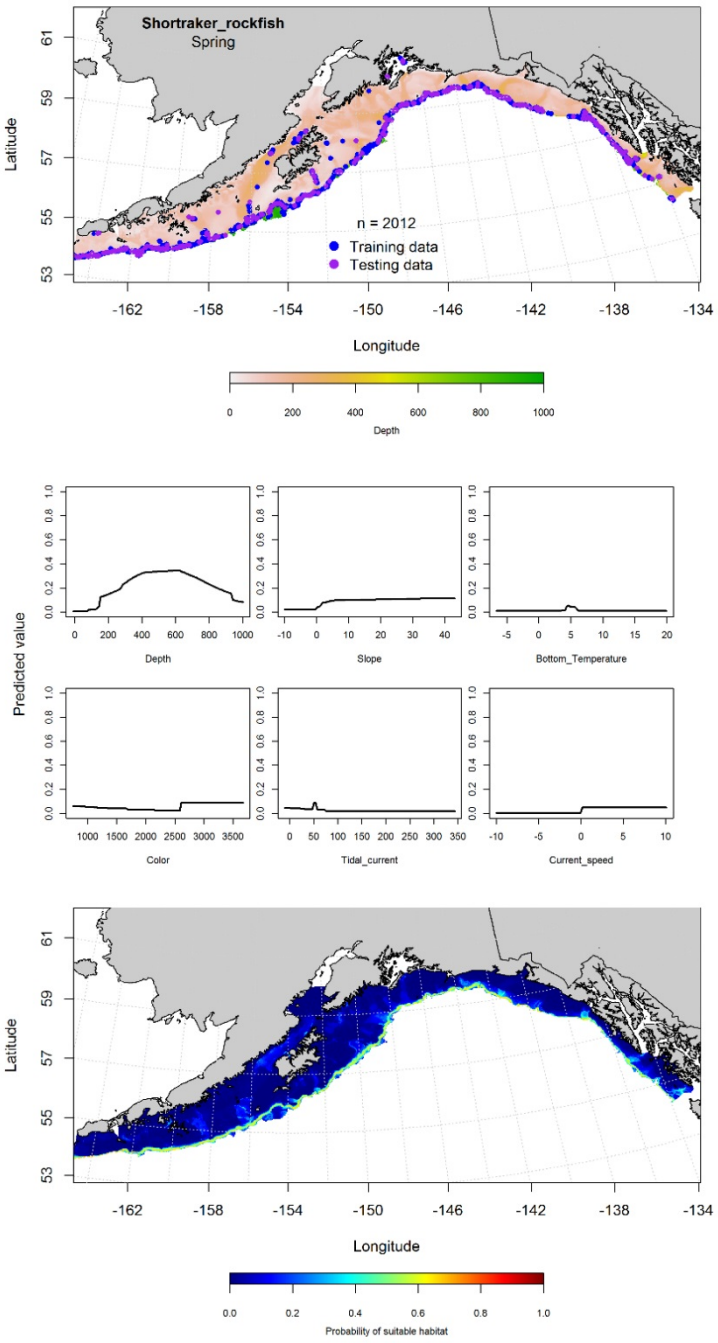

Figure 148. -- Locations of shortraker rockfish from spring (March-May 2001-2015) commercial fisheries catches in the Gulf of Alaska (top panel), with training (blue dots) and testing (purple dots) data indicated, maximum entropy (MaxEnt) model effects (center panel), and the predicted probability of suitable adult shortraker rockfish habitat (bottom panel).

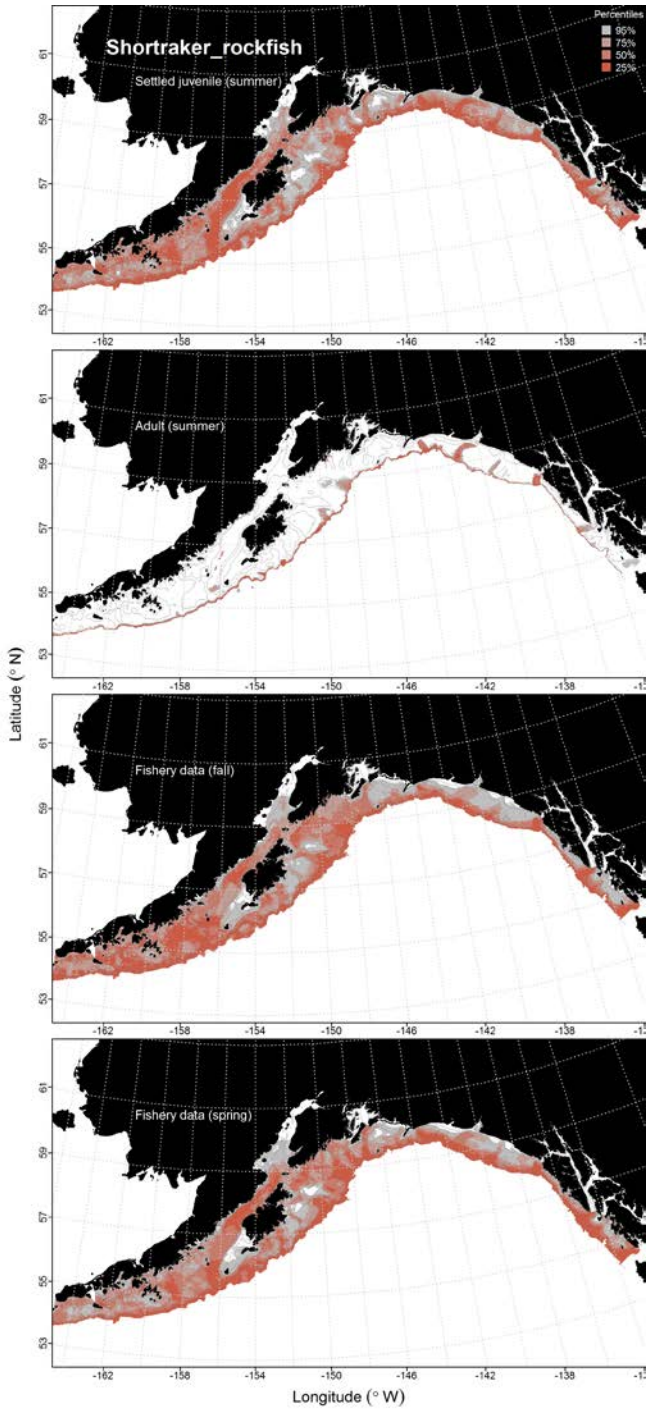

Figure 149. -- Predicted habitat for settled juvenile and adult shortraker rockfish from RACE-GAP summertime bottom trawl surveys (1993-2013) and predicted from their presence in commercial fishery catches (2001-2015) from the fall and spring in the Gulf of Alaska.

Silvergray Rockfish (*Sebastes brevispinis*)

Juvenile and adult silvergray rockfish distribution in the bottom trawl survey -- A MaxEnt model indicated that bottom temperature, bottom depth, and maximum tidal current were the important variables predicting settled juvenile silvergray rockfish habitat suitability (relative importance: 0.37, 0.37, and 0.09, respectively). The model AUC was 0.88 for the training data and 0.63 for the test data. The model correctly classified 80% of the predictions from the training data and 71% of the predictions from the test data. Suitable settled juvenile silvergray rockfish habitat was predicted extensively throughout the central and eastern GOA, with the highest suitability areas concentrated off southeast Alaska and Cape St. Elias (Fig. 151).

An hGAM was used to predict the distribution of adult silvergray rockfish abundance. The PA GAM resulted in an AUC of 0.95 for the training data and 0.92 for the test data. The model correctly classified 85% of the predictions from both the training and test data. The PA GAM indicated that geographic location, bottom temperature, and ocean color were the most important model variables. The model predicted the highest probability of presence for adult silvergray rockfish was along the outer shelf in the eastern GOA (Fig. 152). The CPUE GAM found geographic location, bottom temperature, and bottom depth were the most influential variables on CPUE. The CPUE GAM explained 26% of the variability in the training data and 10% of the variability in the test data. The model predicted the highest CPUE in the eastern GOA, particularly around Prince of Wales Island (Fig. 152).

Silvergray rockfish distribution in commercial fisheries -- Observations of silvergray rockfish from commercial fisheries catches in the GOA were relatively rare. There were 7 observations during the fall (Fig. 153); 14 during the winter (Fig. 154); and 15 during the spring (Fig. 155). These

observations were from across the GOA, but were insufficient to build a MaxEnt model from their presence in commercial catches.

Silvergray rockfish essential fish habitat maps and conclusions -- Probable settled juvenile silvergray rockfish habitat was predicted to be extensively distributed throughout the GOA (Fig. 156). In contrast, adult silvergray rockfish habitat was predicted to be largely concentrated on the continental shelf in the eastern GOA, particularly between Dixon Entrance and Yakutat (Fig. 156).

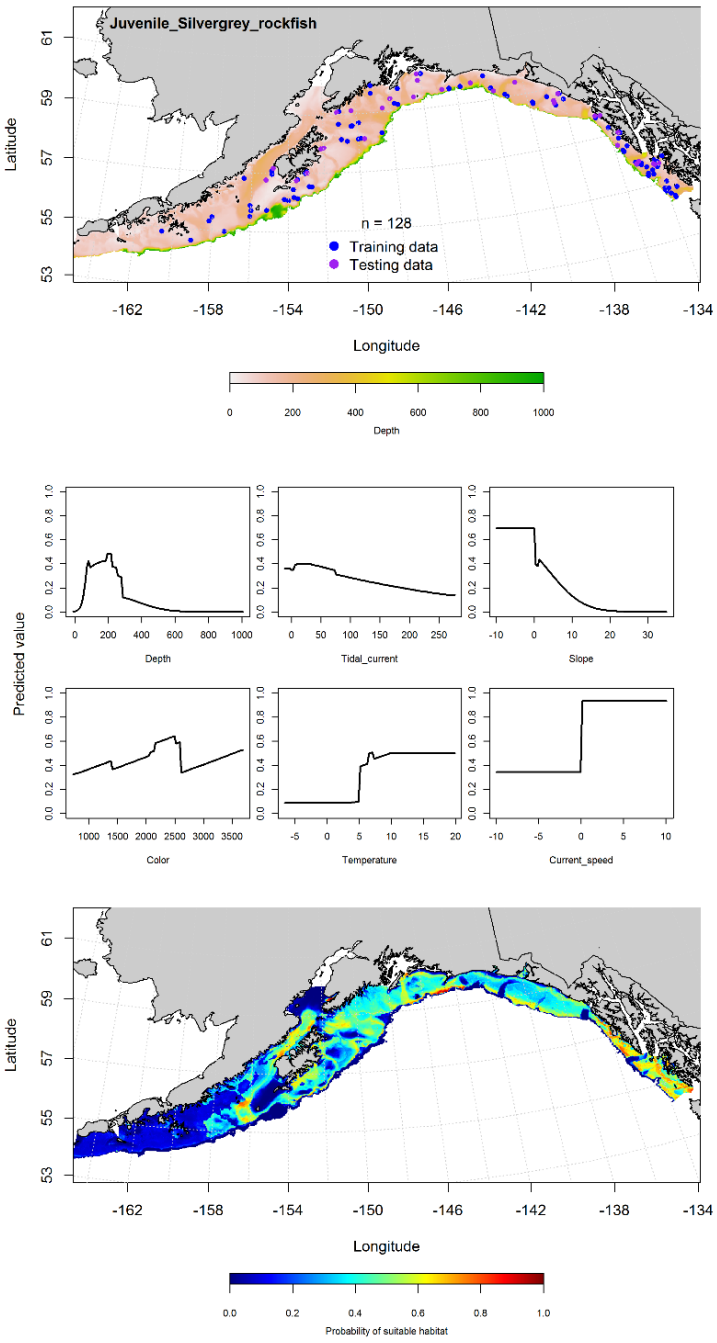

Figure 150. -- Presence of settled juvenile silvergray rockfish from RACE-GAP summer bottom trawl surveys (1993-2013) in the Gulf of Alaska (top panel) with training (blue dots) and testing (purple dots) data indicated, maximum entropy (MaxEnt) model effects (center panel), and the MaxEnt-predicted probability of suitable juvenile silvergray rockfish habitat (bottom panel).

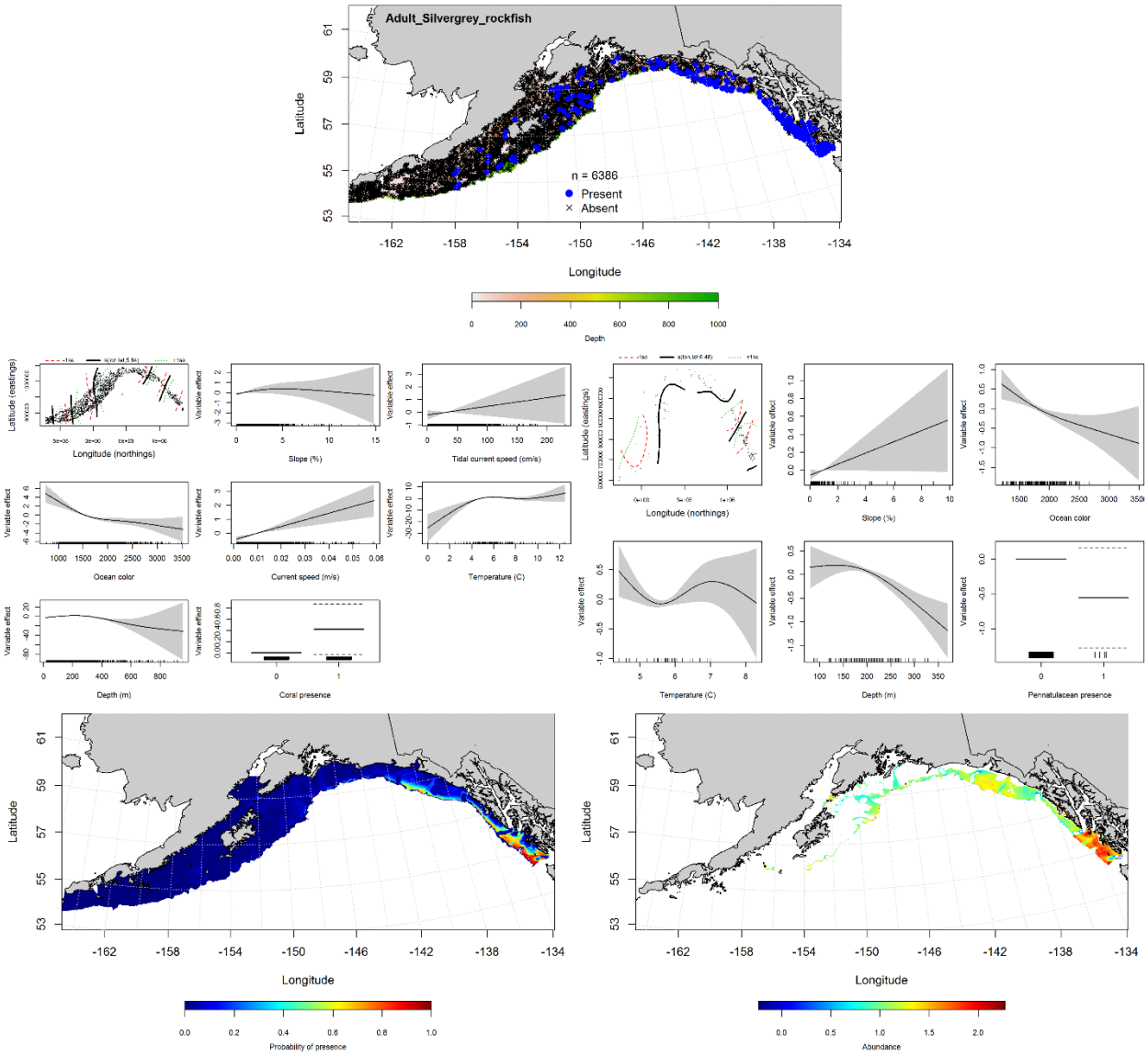

Figure 151. -- Distribution of adult silvergray rockfish in 1993-2013 RACE-GAP summer bottom trawl surveys conducted in the Gulf of Alaska (upper panel). Effects of retained habitat covariates in the best fitting generalized additive presence-absence models (PA GAM; left center panel) and abundance (CPUE GAM; right center panel). Predicted spatial distribution of the probability of presence (bottom left panel) and abundance of adult silvergray rockfish based on the models (bottom right panel).

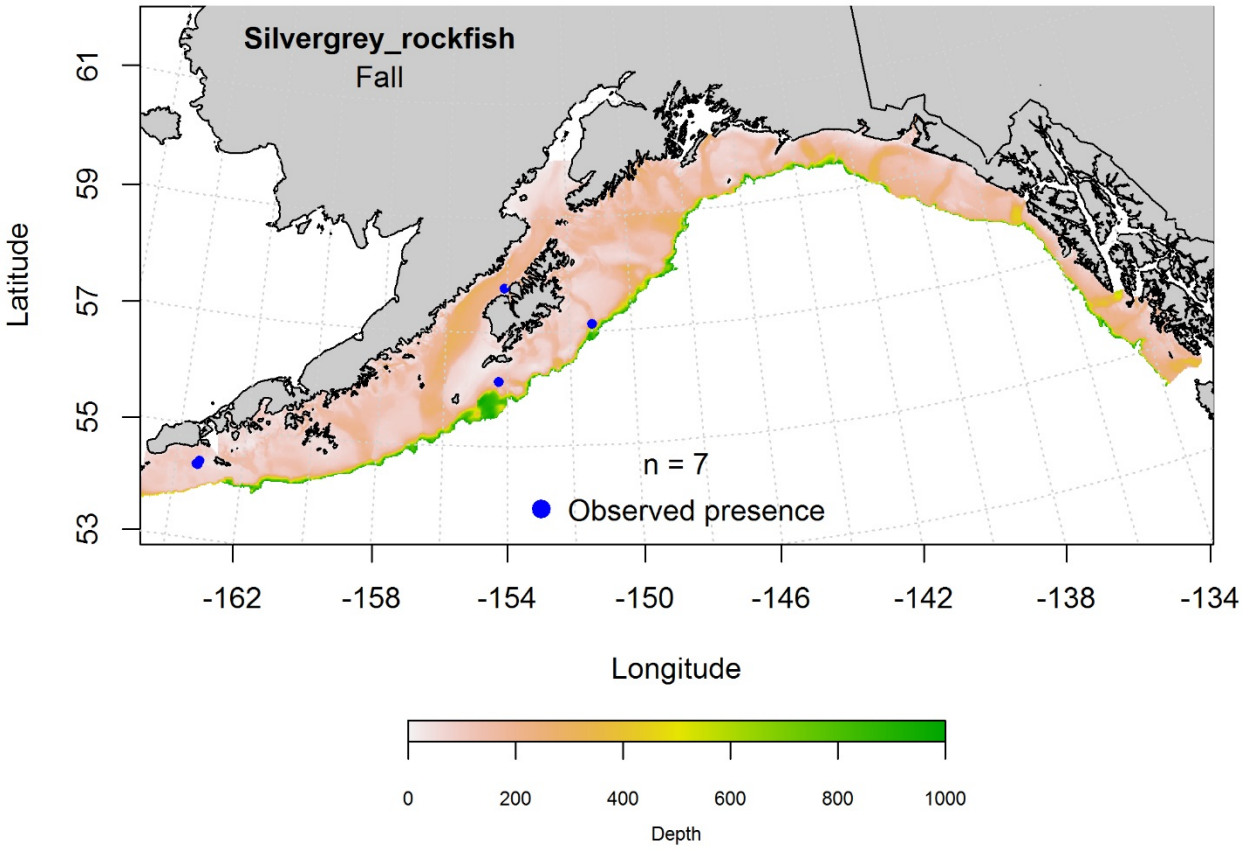

Figure 152. -- Locations of silvergray from fall (September-November 2001-2015) commercial fisheries catches in the Gulf of Alaska.

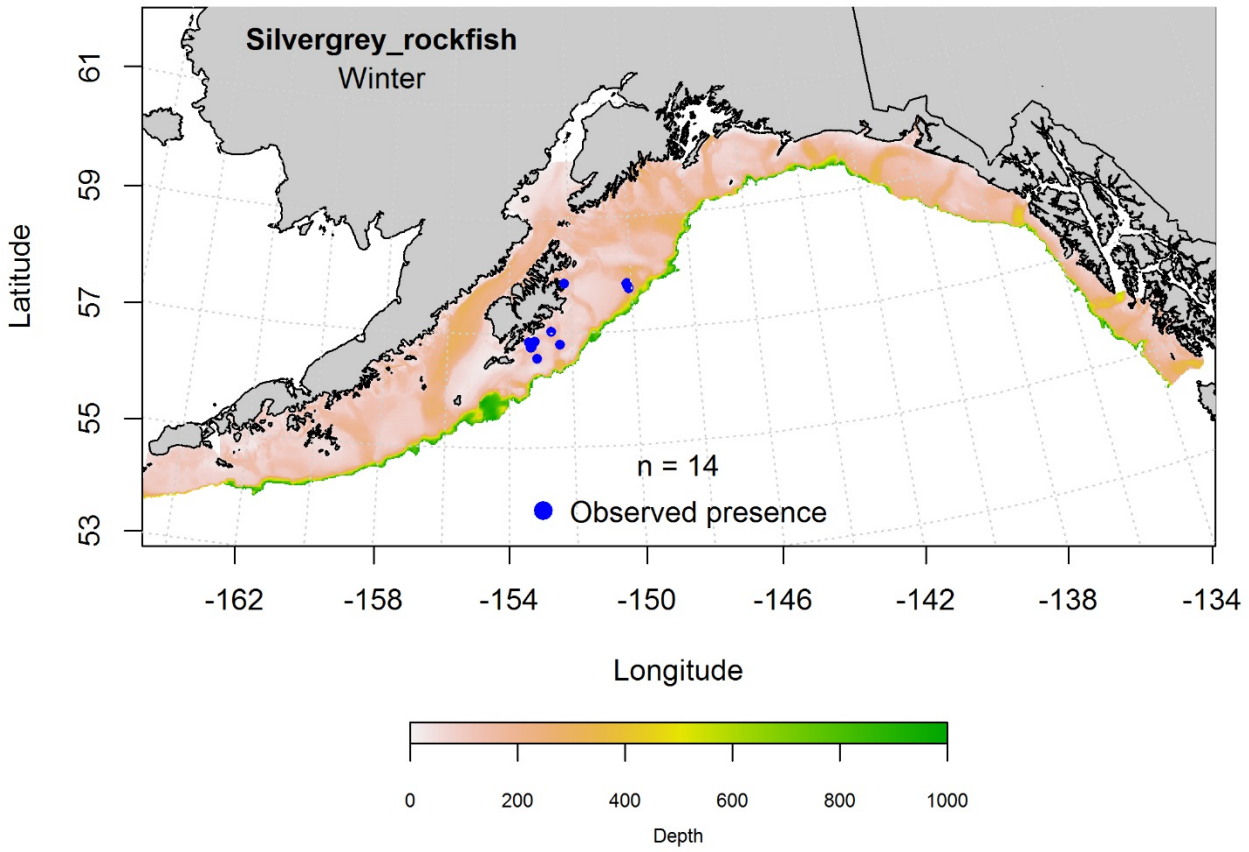

Figure 153. -- Locations of silvergray rockfish from winter (December-February 2001-2015) commercial fisheries catches in the Gulf of Alaska.

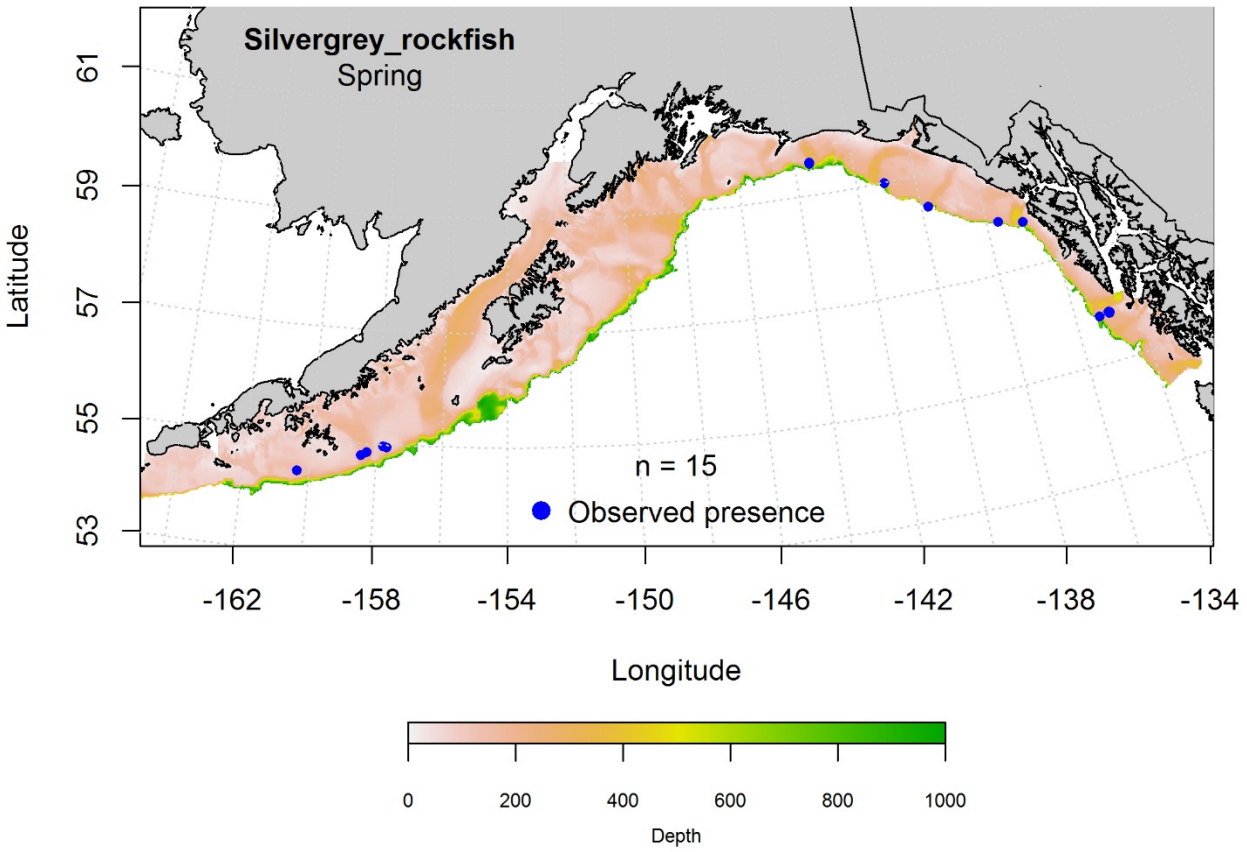

Figure 154. -- Locations of silvergray rockfish from spring (March-May 2001-2015) commercial fisheries catches in the Gulf of Alaska.

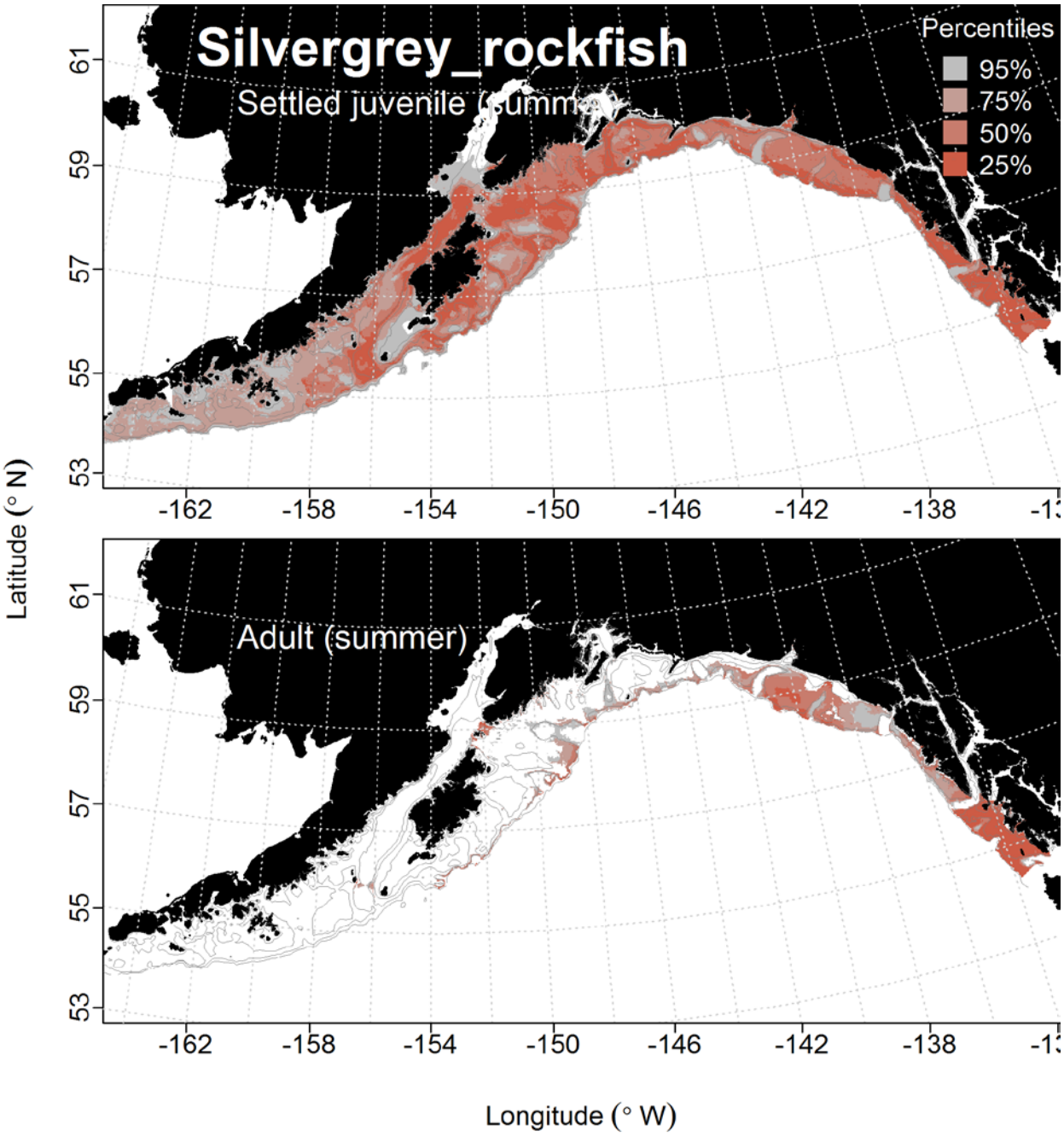

Figure 155. -- Distribution of settled juvenile and adult silvergray rockfish predicted from RACE-GAP summertime bottom trawl surveys (1993-2013) in the Gulf of Alaska.

Dark Rockfish (*Sebastes ciliatus*)

Juvenile and adult dark rockfish distribution in the bottom trawl survey -- There were no catches of settled juvenile dark rockfish in the bottom trawl survey.

There were 74 catches of adult dark rockfish in the bottom trawl survey. The AUC of the MaxEnt model for adult dark rockfish was 0.90 for the training data and 0.78 for the test data. The model correctly classified 83% of the predictions from the training data and 78% of the predictions from the test data. Bottom depth and bottom temperature were the most important variables explaining the distribution of adult dark rockfish (relative importance: 0.50 and 0.27, respectively). Adult dark rockfish suitable habitat was predicted across the western GOA, though higher near the Shumagin Islands (Fig. 157).

Dark rockfish distribution in commercial fisheries -- Observations of dark rockfish in commercial fisheries catches were limited. There were 27 observations during the fall (Fig. 158); 13 during the winter (Fig. 159); and 32 during the spring (Fig. 160). The distribution of these observations was generally concentrated in the central and western GOA, but were insufficient to build a MaxEnt model for dark rockfish.

Dark rockfish essential fish habitat maps and conclusions -- Summertime habitat of adult dark rockfish was predicted from RACE-GAP bottom trawl survey catches. It was distributed across the GOA, though areas with higher probabilities of suitable habitat tended to be more concentrated in the central and western GOA (Fig. 161).

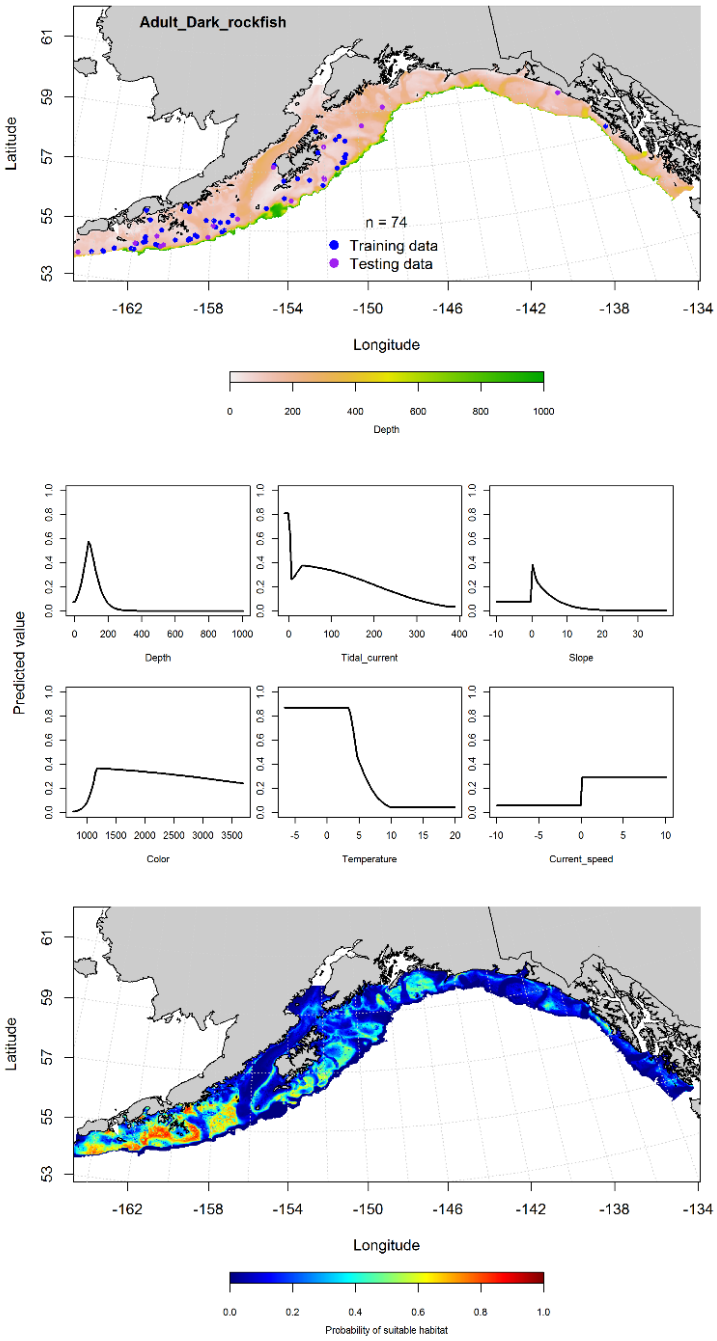

Figure 156. -- Presence of adult dark rockfish from RACE-GAP summer bottom trawl surveys (1993-2013) in the Gulf of Alaska (top panel) with training (blue dots) and testing (purple dots) data indicated, maximum entropy (MaxEnt) model effects (center panel), and the MaxEnt-predicted probability of suitable adult dark rockfish habitat (bottom panel).

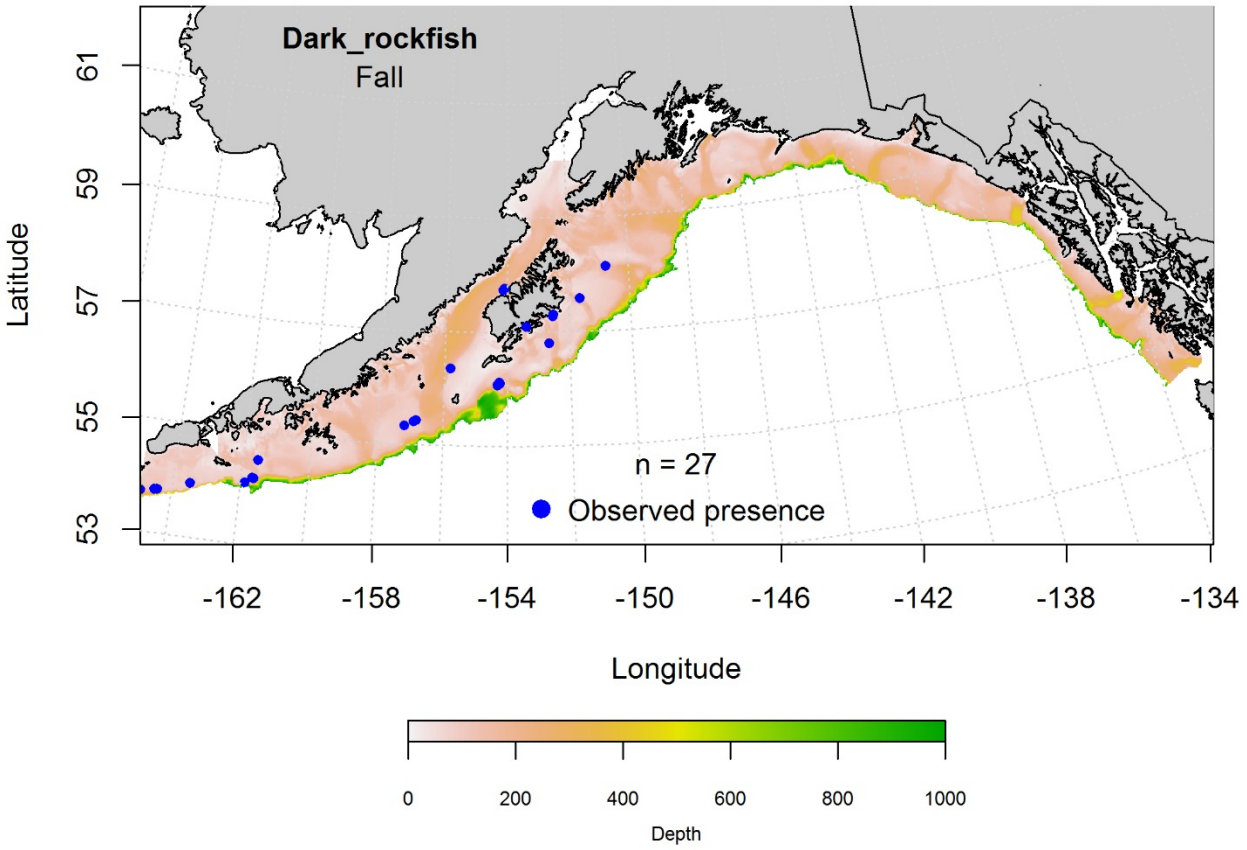

Figure 157. -- Locations of dark rockfish from fall (September-November 2001-2015) commercial fisheries catches in the Gulf of Alaska.

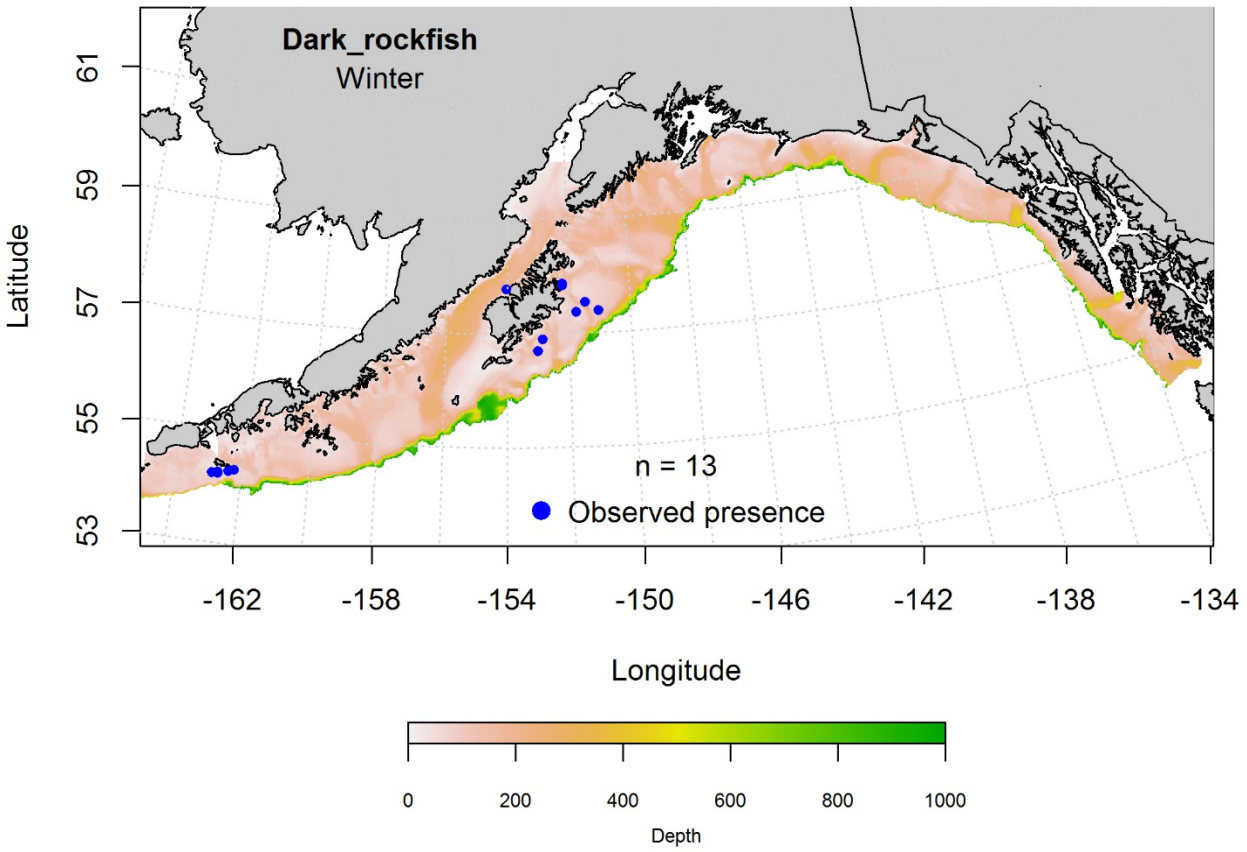

Figure 158. -- Locations of dark rockfish from winter (December-February 2001-2015) commercial fisheries catches in the Gulf of Alaska.

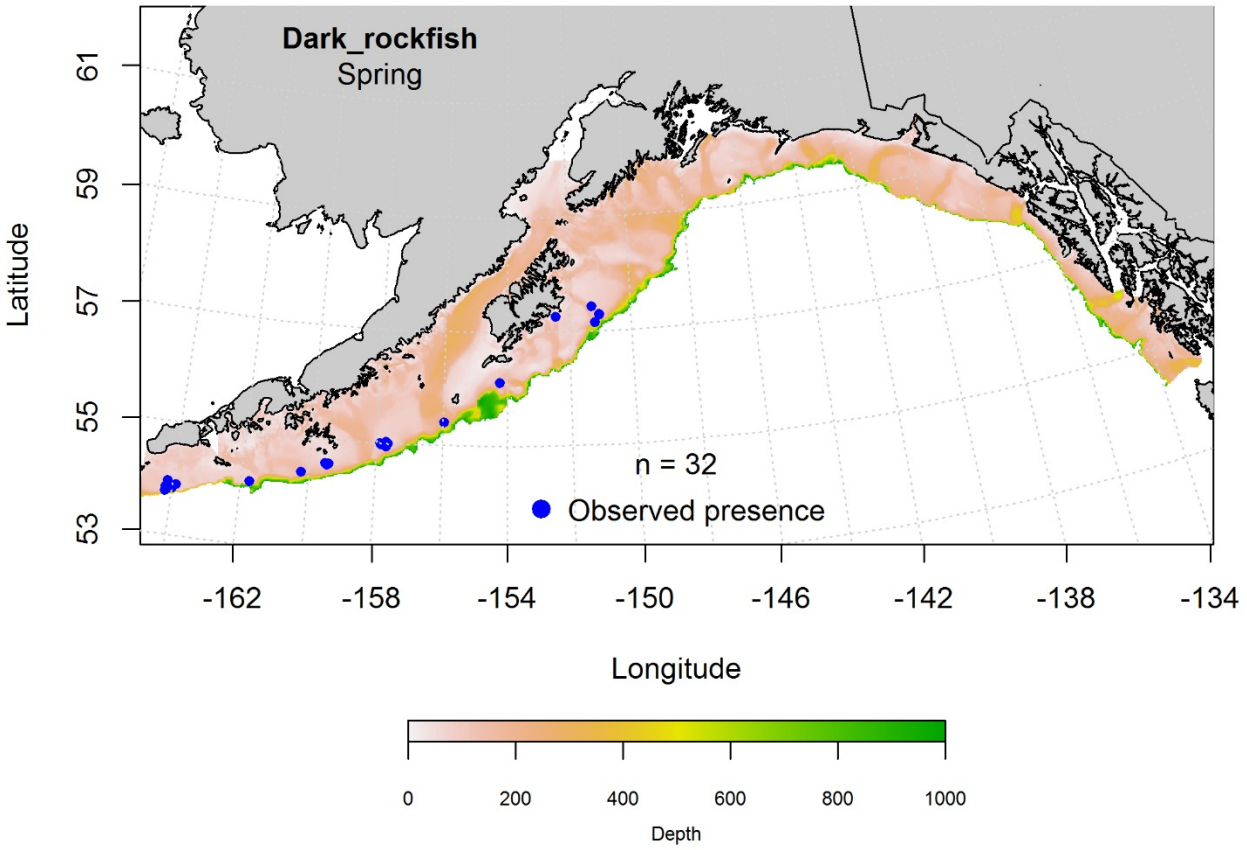

Figure 159. -- Locations of dark rockfish from spring (March-May 2001-2015) commercial fisheries catches in the Gulf of Alaska.

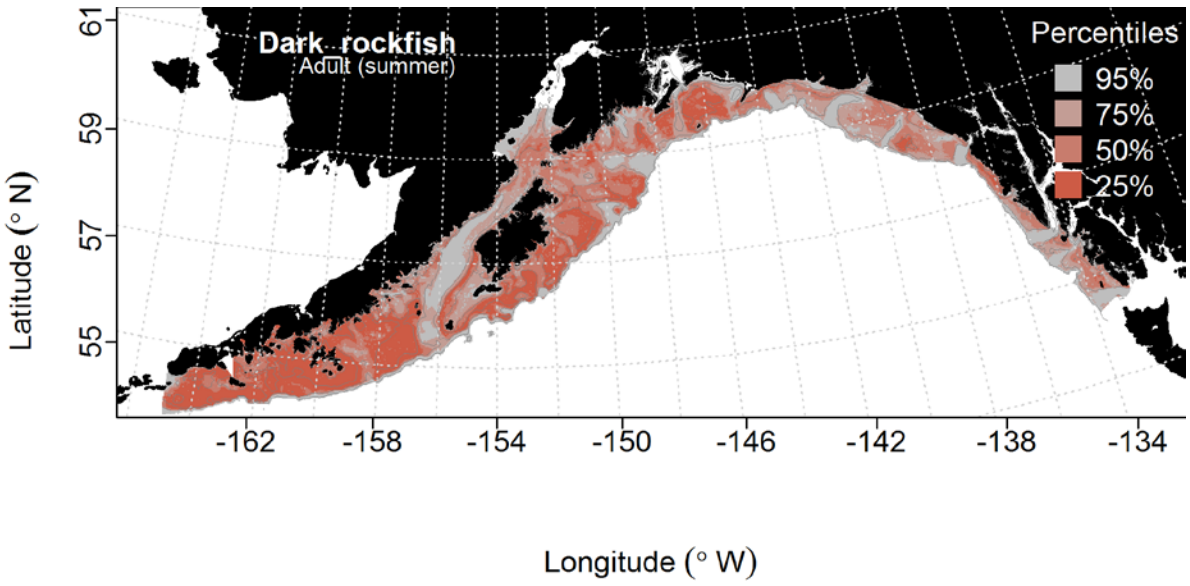

Figure 160. -- Distribution of predicted habitat of adult dark rockfish from RACE-GAP summertime bottom trawl surveys (1993-2013) in the Gulf of Alaska.

Quillback Rockfish (*Sebastes maliger*)

Juvenile and adult quillback rockfish distribution in the bottom trawl survey -- There were no observations of settled juvenile quillback rockfish during the summer trawl survey.

There were 58 observations of adult quillback rockfish from the bottom trawl survey, most of which occurred in the central and eastern GOA (Fig. 162). The MaxEnt model predicting suitable habitat of adult quillback rockfish had an AUC of 0.90 for the training data and 0.93 for the test data. The model correctly classified 82% of the predictions from the training data and 93% of the predictions from the test data. Bottom depth, ocean color, and maximum tidal current were the important variables explaining the distribution of adult quillback rockfish (relative importance: 0.41, 0.37, and 0.34, respectively). Suitable habitat of adult quillback rockfish was predicted along the inner shelf in the eastern GOA, with the highest suitability areas occurring off Southeast Alaska and at Wessels Reef off Prince William Sound (Fig. 162).

Quillback rockfish distribution in commercial fisheries

Observations of quillback rockfish from commercial fisheries catches were limited, with six observations during the fall (Fig. 163), two from the winter (Fig. 164), and five during the spring (Fig. 165). These observations were primarily from the central GOA, but were insufficient in to build a MaxEnt model for quillback rockfish.

Quillback rockfish essential fish habitat maps and conclusions -- Potential summertime adult quillback rockfish habitat was predicted to be distributed throughout the GOA, though higher

suitability areas tended to be more concentrated on the middle and inner shelf in central and eastern GOA (Fig. 166).

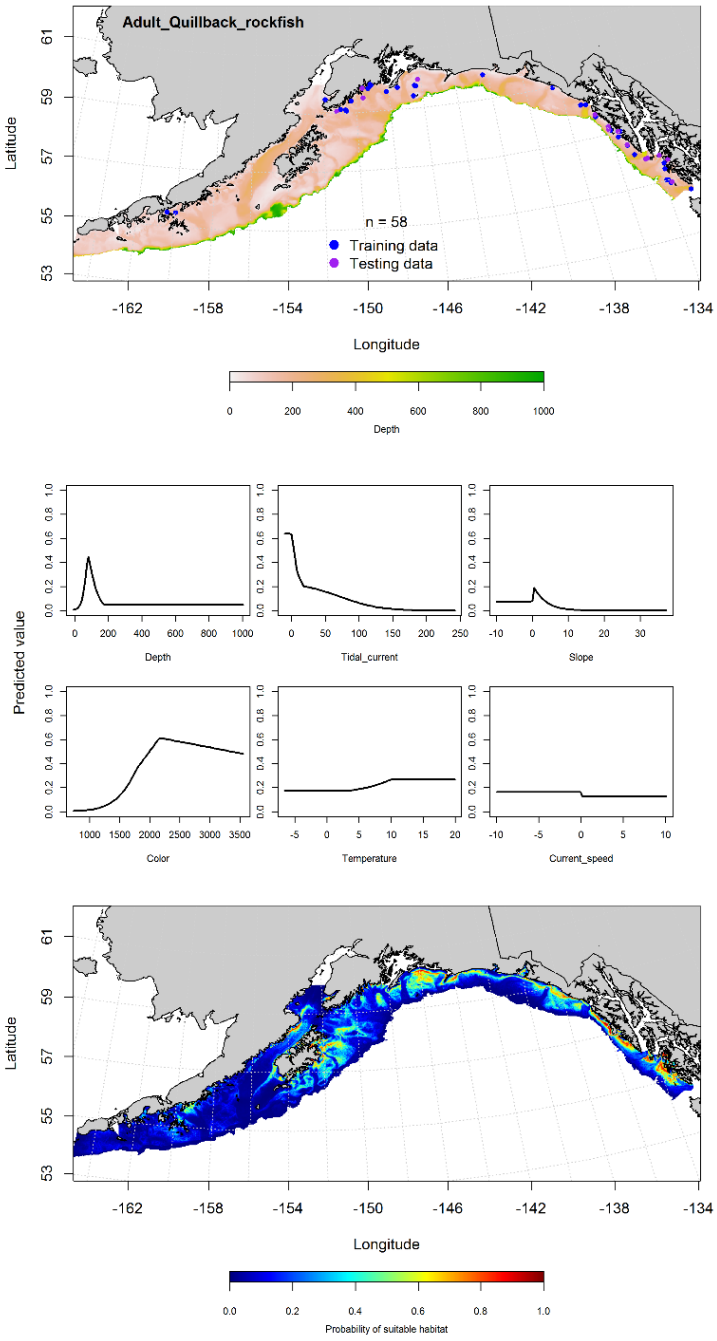

Figure 161. -- Presence of adult quillback rockfish from RACE-GAP summer bottom trawl surveys (1993-2013) in the Gulf of Alaska (top panel) with training (blue dots) and testing (purple dots) data indicated, maximum entropy (MaxEnt) model effects (center panel), and the MaxEnt-predicted probability of suitable adult quillback rockfish habitat (bottom panel).

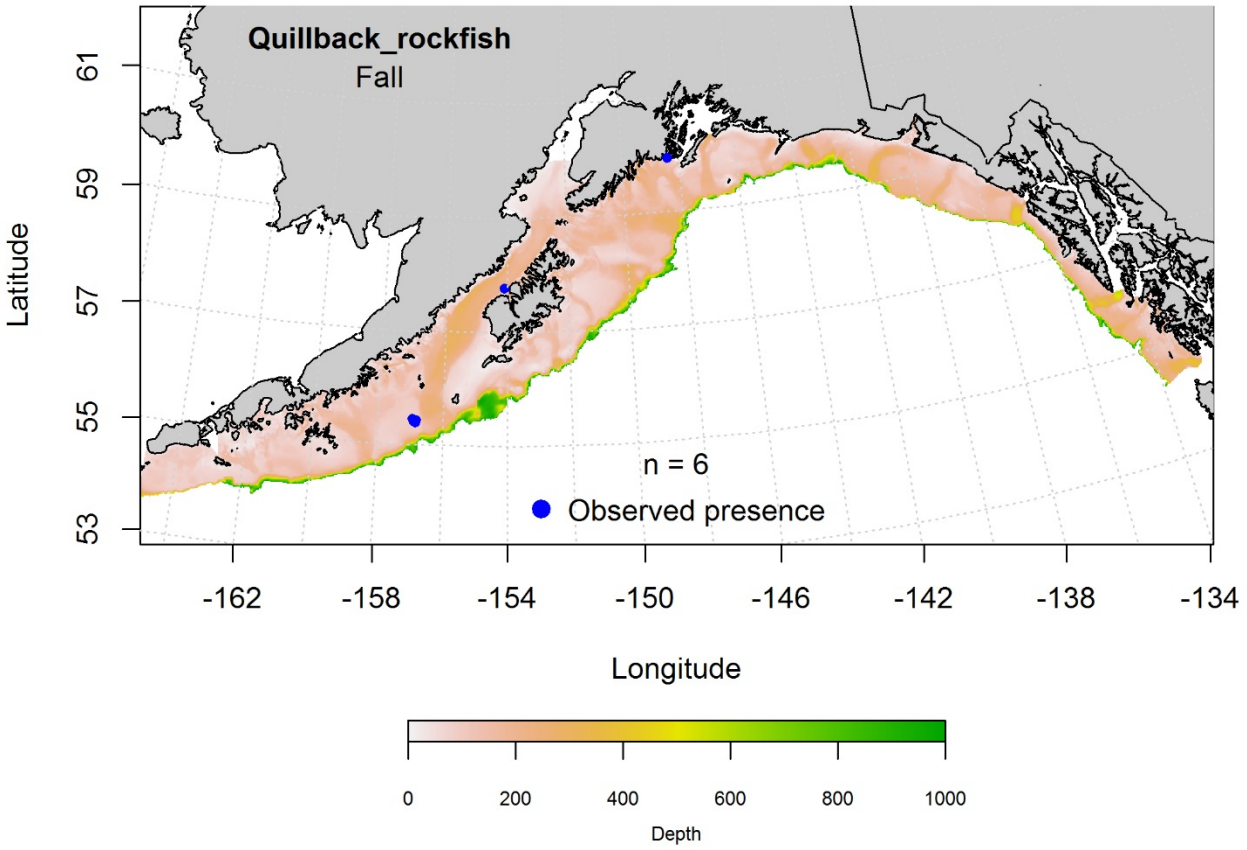

Figure 162. -- Locations of quillback rockfish from fall (September-November 2001-2015) commercial fisheries catches in the Gulf of Alaska.

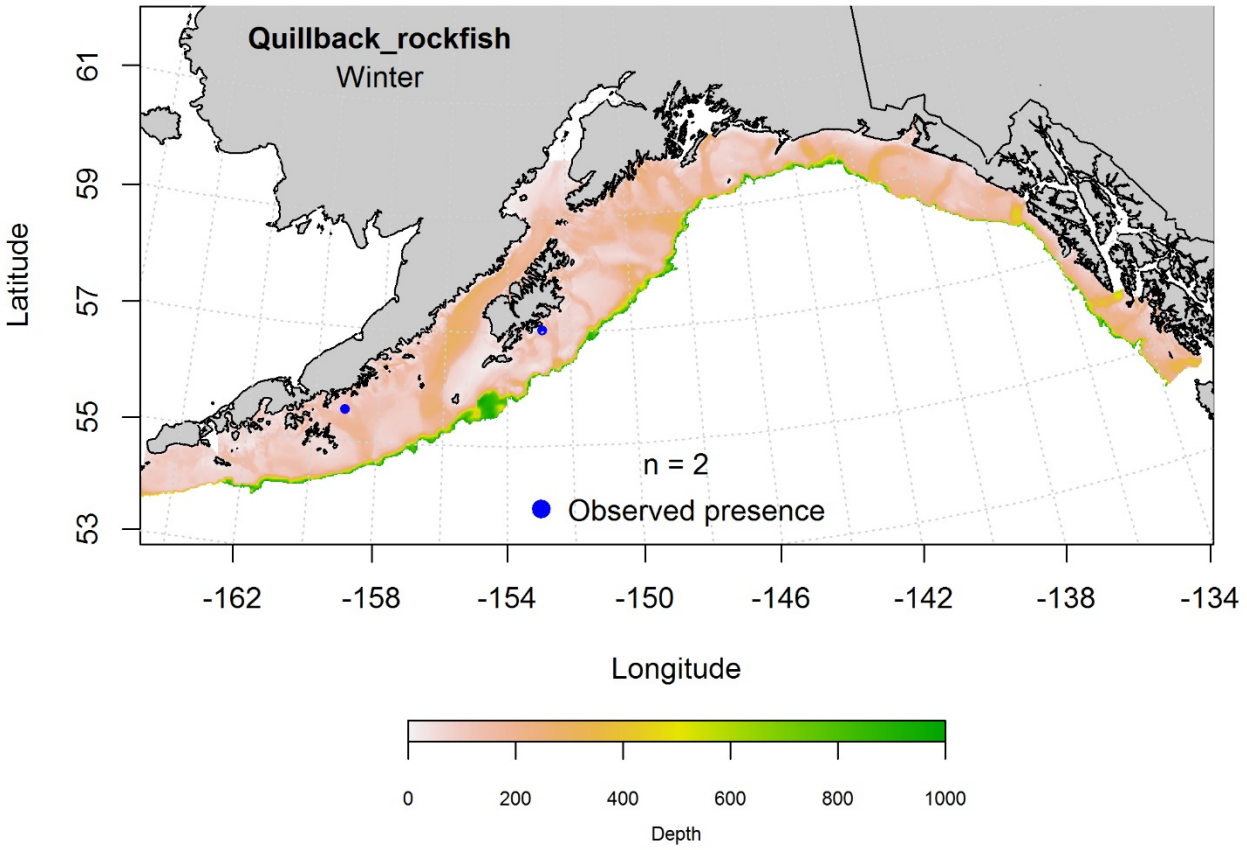

Figure 163. -- Locations of quillback rockfish from winter (December-February 2001-2015) commercial fisheries catches in the Gulf of Alaska.

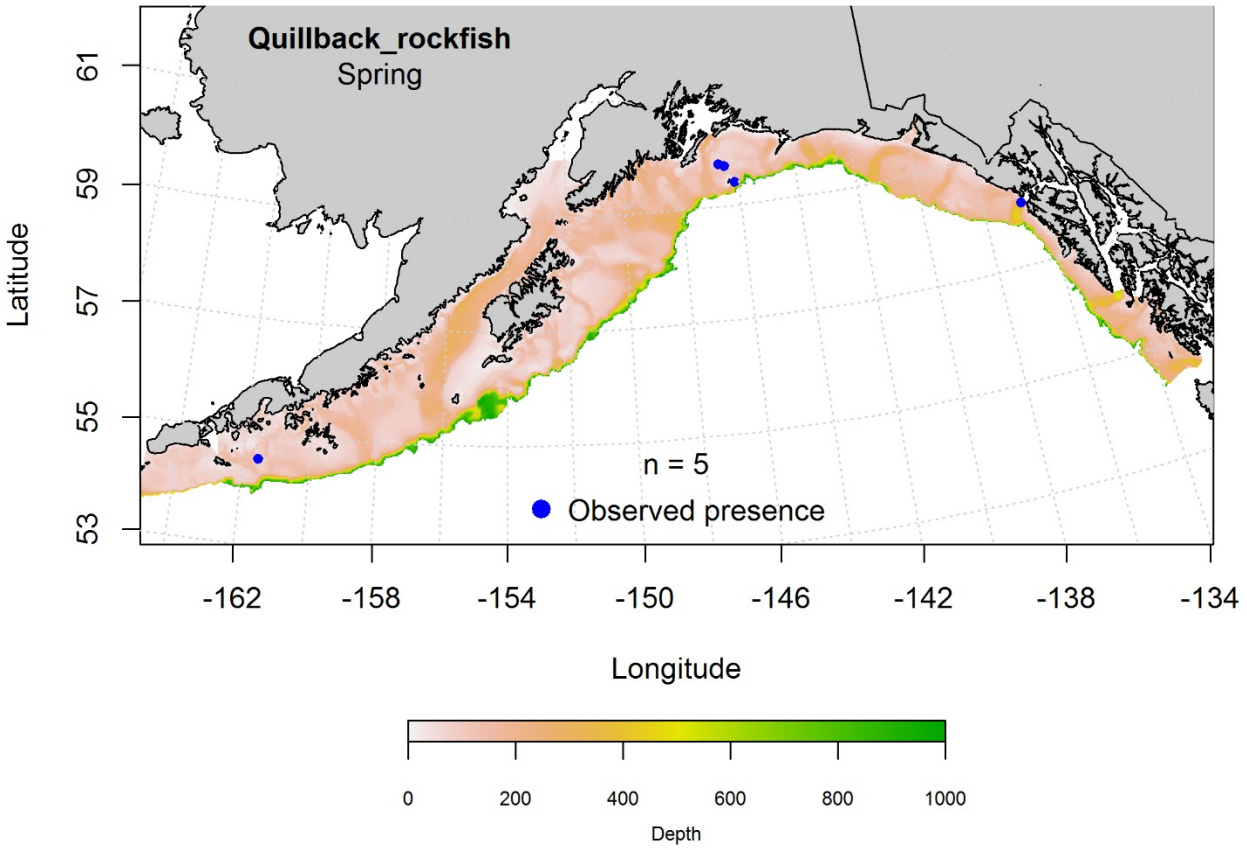

Figure 164. -- Locations of quillback rockfish from spring (March-May 2001-2015) commercial fisheries catches in the Gulf of Alaska.

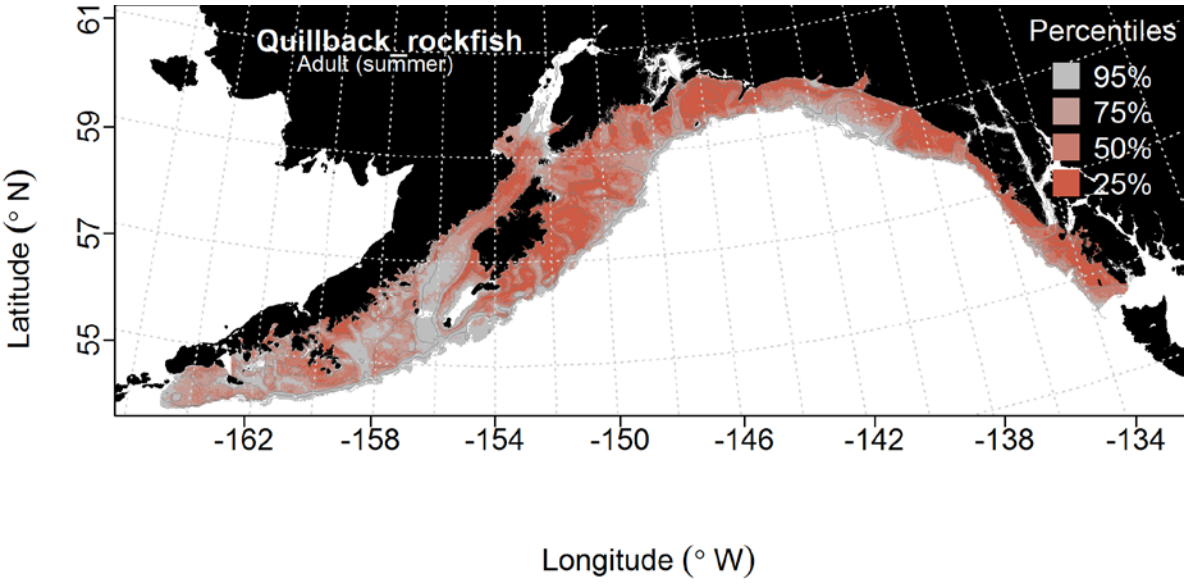

Figure 165. -- Distribution of predicted habitat of adult quillback rockfish from RACE-GAP summertime bottom trawl surveys (1993-2013) in the Gulf of Alaska.

Black Rockfish (*Sebastes melanops*)

Juvenile and adult black rockfish distribution in the bottom trawl survey -- There were no instances of settled juvenile black rockfish observed during the summer trawl surveys.

There were 50 observations of adult black rockfish from the bottom trawl surveys, these were widely distributed though the GOA (Fig. 167). The AUC of the MaxEnt model for adult black rockfish had an AUC of 0.87 for the training data and 0.90 for the test data. The model correctly classified 84% of the predictions from the training data and 90% of the predictions from the test data. Bottom depth, maximum tidal current, and slope were the important model variables (relative importance: 0.52, 0.17, and 0.17, respectively). The model predicted suitable habitat of adult black rockfish primarily in shallow near-shore waters, with the highest suitability habitats concentrated in eastern GOA, around Cordova; in the central GOA, around Kodiak; and throughout the western GOA (Fig. 167).

Black rockfish distribution in commercial fisheries -- Observations of black rockfish from commercial fisheries catches were limited. There were 13 observations from during the fall (Fig. 168), 20 during the winter (Fig. 169), and 34 during the spring (Fig. 170). These observations were from the central and western GOA, but were insufficient to build model a MaxEnt model for black rockfish.

Black rockfish essential fish habitat maps and conclusions -- Adult black rockfish habitat predicted from MaxEnt modeling was extensively distributed throughout the inner and middle shelf across the GOA (Fig. 171).

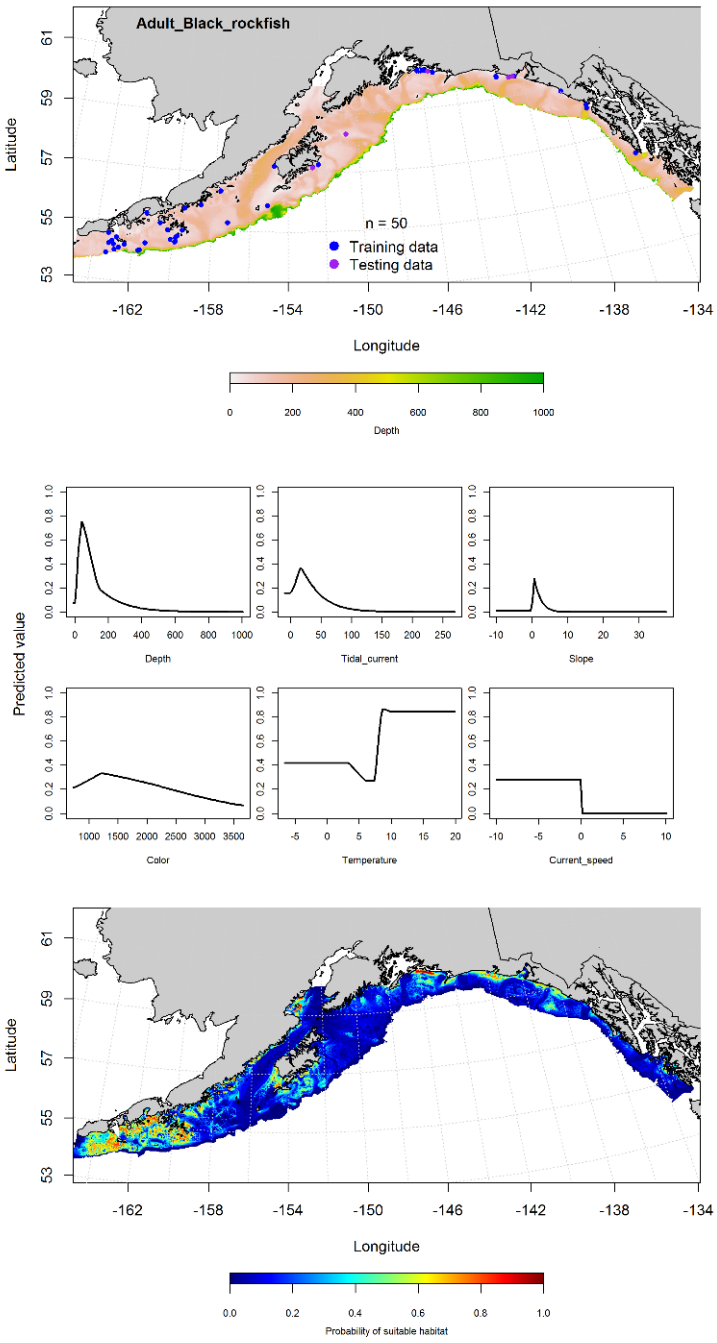

Figure 166. -- Presence of adult black rockfish from RACE-GAP summer bottom trawl surveys (1993-2013) in the Gulf of Alaska (top panel) with training (blue dots) and testing (purple dots) data indicated, maximum entropy (MaxEnt) model effects (center panel), and the MaxEnt-predicted probability of suitable adult black rockfish habitat (bottom panel).

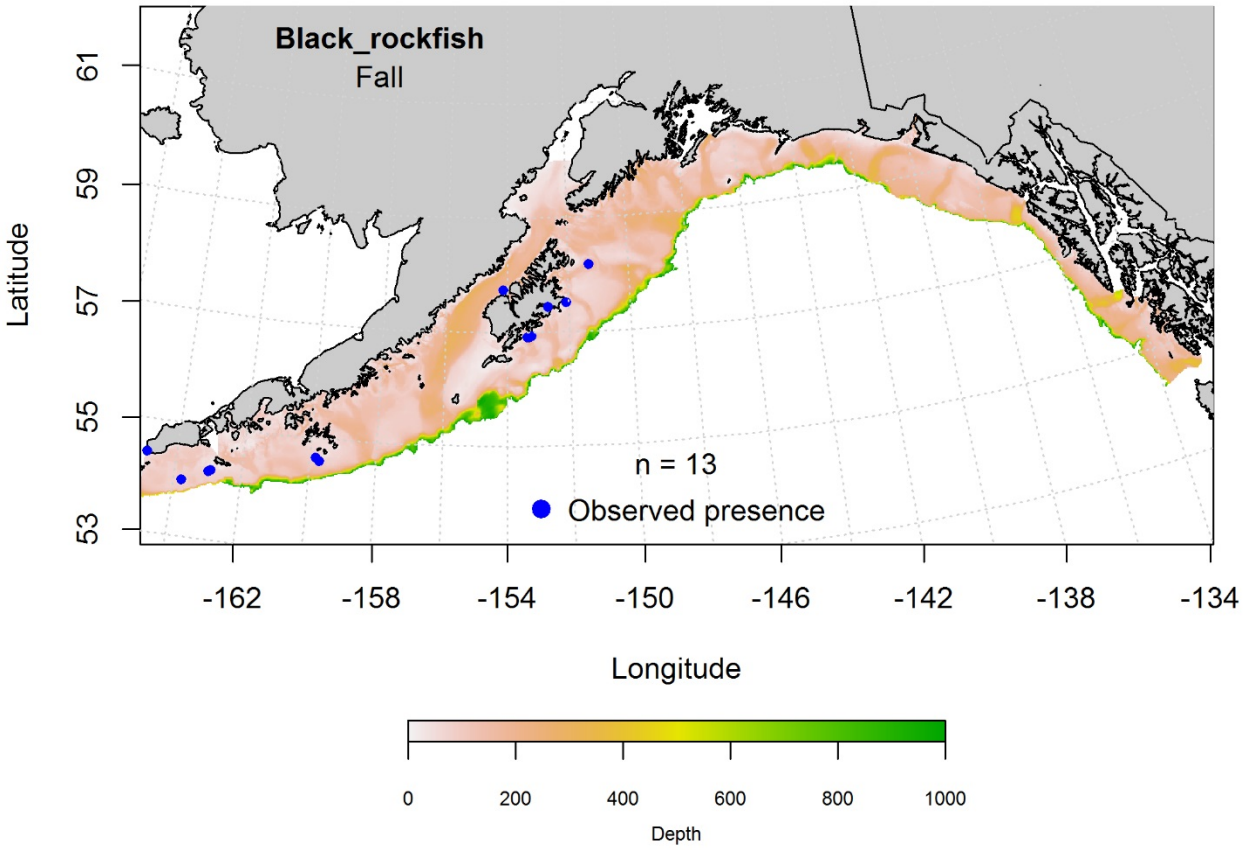

Figure 167. -- Locations of fall (September-November 2001-2015) commercial fisheries catches of black rockfish.

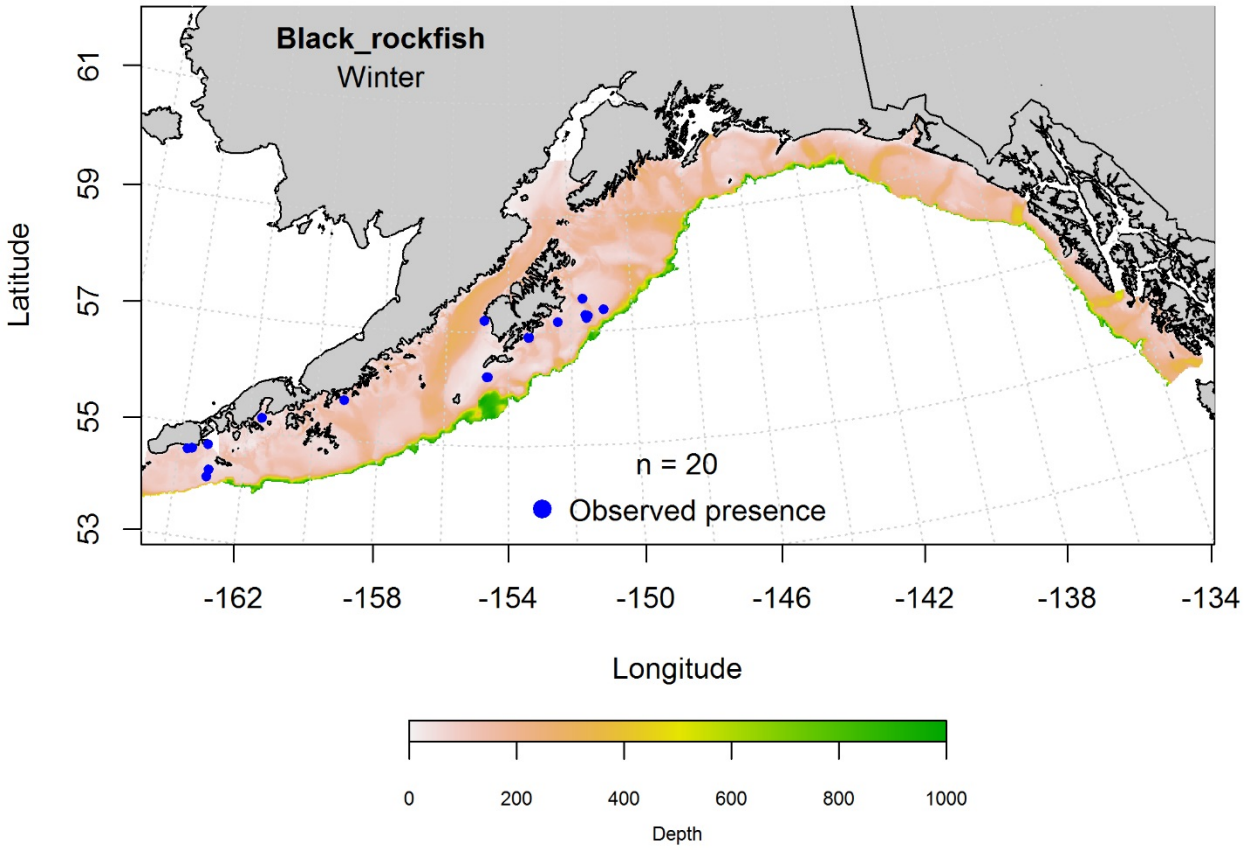

Figure 168. -- Locations of black rockfish from winter (December-February 2001-2015) commercial fisheries catches in the Gulf of Alaska.

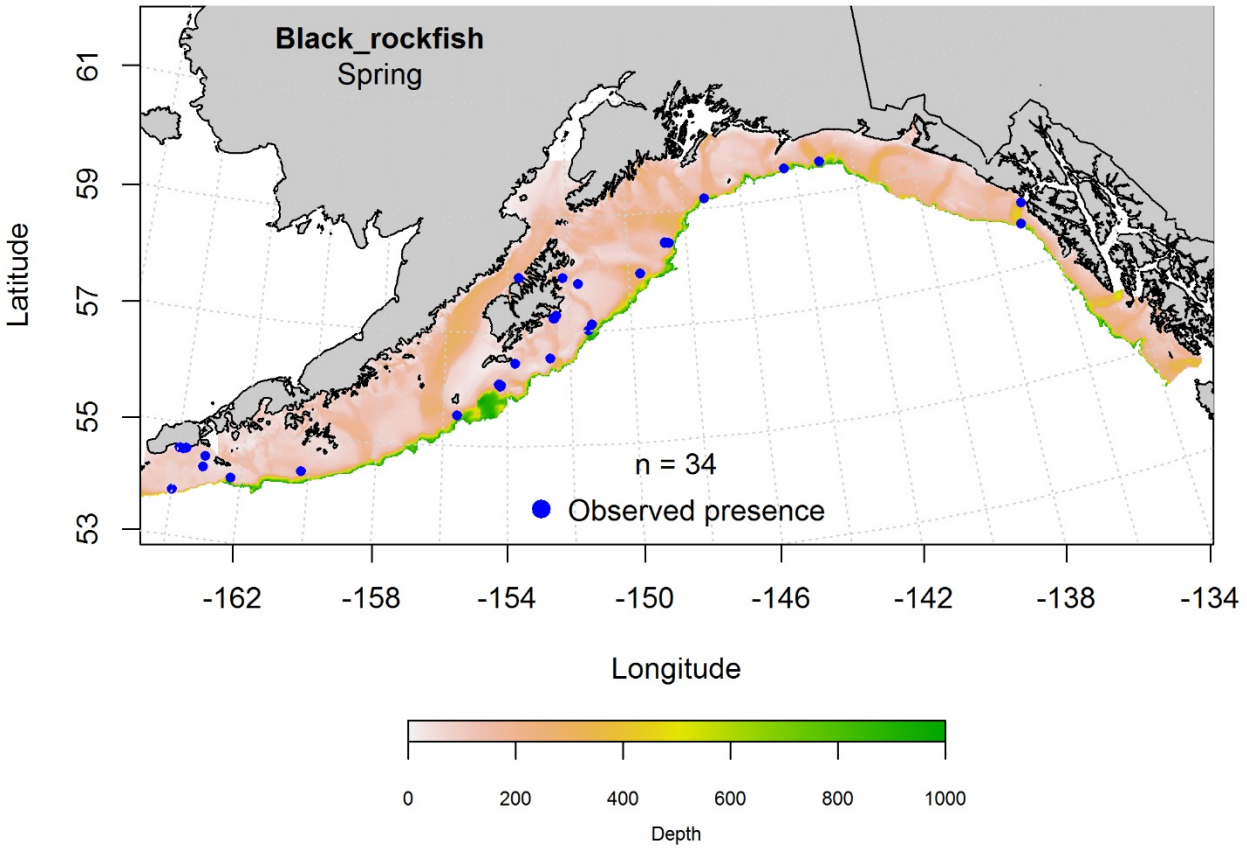

Figure 169. -- Locations of black rockfish from spring (March-May 2001-2015) commercial fisheries catches in the Gulf of Alaska.

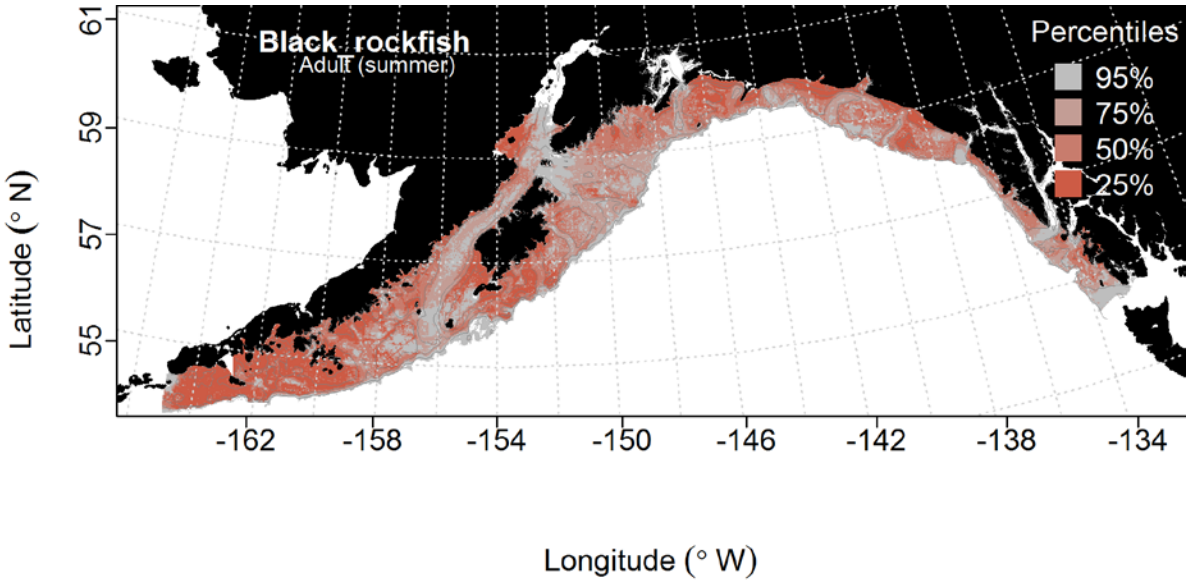

Figure 170. -- Distribution of predicted habitat of adult black rockfish from RACE-GAP summertime bottom trawl surveys (1993-2013) in the Gulf of Alaska.

Blackspotted Rockfish (*Sebastes melanostictus*)

Rougheye (*Sebastes aleutianus*) and blackspotted rockfish (*S. melanostictus*) were considered a single species until recently when blackspotted rockfish were resurrected as a distinct species and rougheye rockfish were re-described (Orr and Hawkins 2008). In the bottom trawl survey operations the species have been separated since 2006. In the VOE-CIA data from commercial fisheries observers, rougheye and blackspotted rockfishes are reported as they are landed; as a complex (i.e., "rougheye/blackspotted rockfish").

Juvenile and adult blackspotted rockfish distribution in the bottom trawl survey -- The MaxEnt model predicting probability of suitable habitat of settled juvenile blackspotted rockfish had an AUC of 0.90 for the training data and 0.75 for the test data. The model correctly classified 80% of the predictions from the training data and 75% of the predictions from the test data. Bottom depth and bottom temperature were the most important variables explaining the distribution of settled juvenile blackspotted rockfish (relative importance: 0.84, and 0.08, respectively). The model predicted probable suitable settled juvenile blackspotted rockfish habitat throughout the GOA, with higher suitability areas concentrated near the shelf break (Fig. 172).

A MaxEnt model was used to predict the distribution of suitable habitat for adult blackspotted rockfish. Bottom depth and bottom temperature were again the most important variables in the model (relative importance: 0.81, 0.10, and 0.07, respectively). The AUC was 0.97 for the training data and 0.91 for the test data. The model correctly classified 90% of the predictions from the training data and 91% of the predictions from the test data. Adult blackspotted rockfish habitat was predicted to be similarly distributed to that of the juveniles; near the shelf break across the GOA (Fig. 173).

Blackspotted rockfish distribution in commercial fisheries -- Blackspotted and rougheye rockfish are combined in the VOE-CIA commercial fisheries observer data. Distribution modeling for the rougheye/blackspotted rockfish complex when present in commercial catches is summarized in the rougheye rockfish section above.

Blackspotted rockfish essential fish habitat maps and conclusions -- The distribution of probable settled juvenile and adult blackspotted rockfish summertime habitat was similar for these life stages. Predicted habitat was distributed across the GOA, with the highest probabilities concentrated near the shelf break and in deeper areas of the middleshelf (Fig. 174).

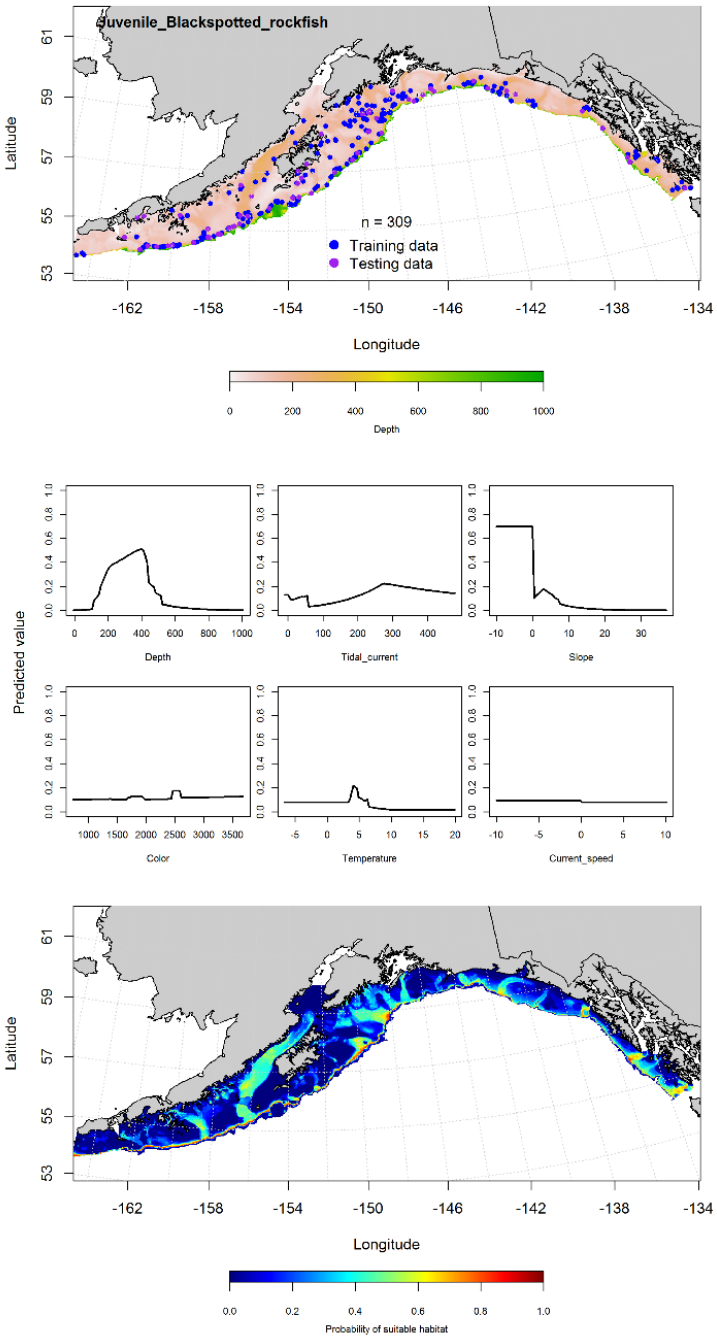

Figure 171. -- Presence of settled juvenile blackspotted rockfish from RACE-GAP summer bottom trawl surveys (1993-2013) in the Gulf of Alaska (top panel) with training (blue dots) and testing (purple dots) data indicated, maximum entropy (MaxEnt) model effects (center panel), and the MaxEnt-predicted probability of suitable juvenile blackspotted rockfish habitat (bottom panel).

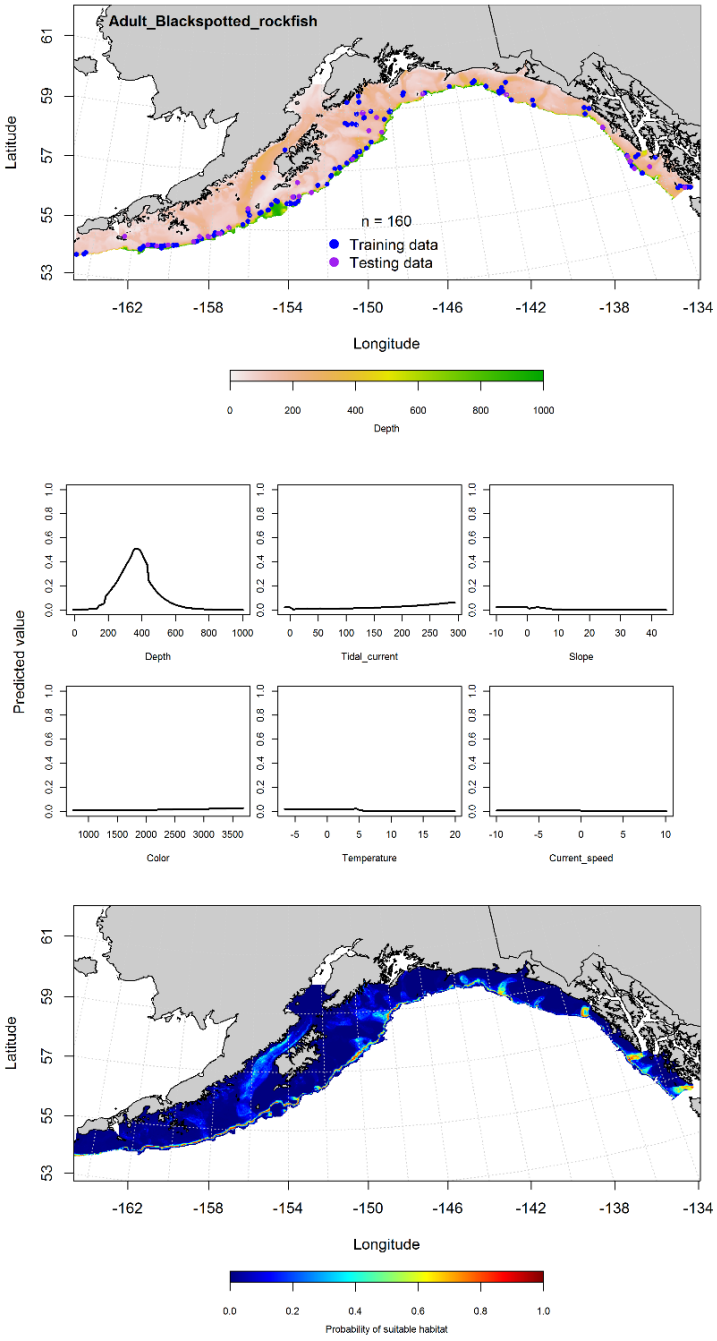

Figure 172. -- Presence of adult blackspotted rockfish from RACE-GAP summer bottom trawl surveys (1993-2013) in the Gulf of Alaska (top panel) with training (blue dots) and testing (purple dots) data indicated, maximum entropy (MaxEnt) model effects (center panel), and the MaxEnt-predicted probability of suitable adult blackspotted rockfish habitat (bottom panel).

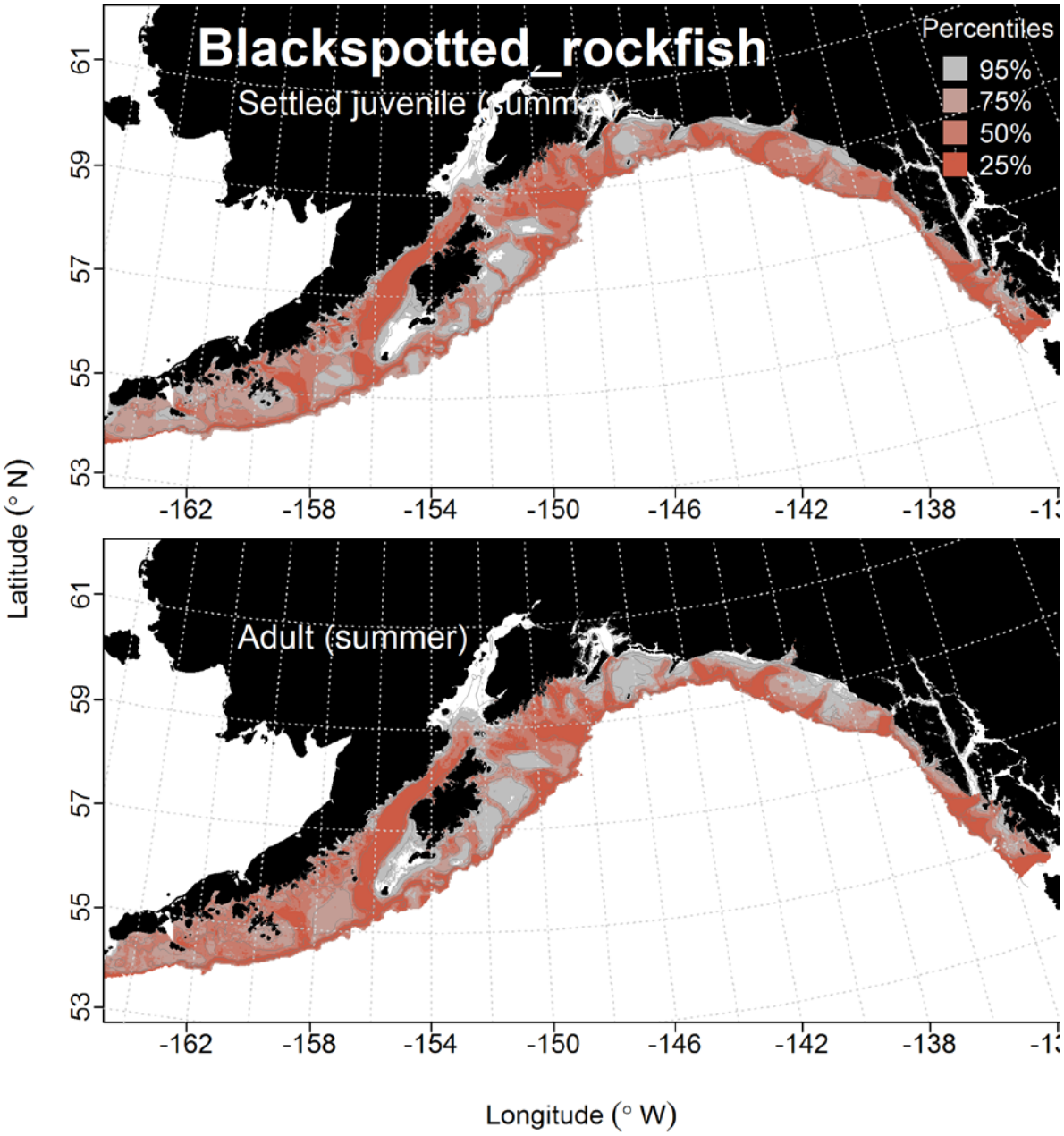

Figure 173. -- Distribution of predicted habitat of settled juvenile and adult blackspotted rockfish from RACE-GAP summertime bottom trawl surveys (1993-2013) in the Gulf of Alaska.

Redstriped Rockfish (*Sebastes proriger*)

Juvenile and adult redstriped rockfish distribution in the bottom trawl survey -- The locations of the summer bottom trawl survey catches of settled juvenile redstriped rockfish, indicate that this species is broadly distributed throughout the GOA (Fig. 175). The AUC of the MaxEnt model used to predict probability of suitable habitat was 0.89 for the training data and 0.73 for the test data. The model correctly predicted 87% of the training data and 78% of the test data. The most important model variables were bottom depth and bottom current speed (relative importance: 0.46, 0.24, and 0.22, respectively). The highest probability of suitable habitat for settled juvenile redstriped rockfish was mapped to deeper areas of the eastern GOA, including off Prince of Wales and Baranof Islands, and in the central GOA, along Shelikof Strait (Fig. 175).

A MaxEnt model was used to predict the suitable habitat of adult redstriped rockfish. The AUC of the model was 0.94 for the training data and 0.77 for the testing data. The most important variables in the model were bottom depth and bottom current speed (relative importance: 0.46, 0.24, and 0.22, respectively). The model predicted the highest probability of suitable habitat for adult redstriped rockfish in eastern GOA, off Prince of Wales, and in the central GOA, off the Baranof Islands (Fig. 176).

Redstriped rockfish distribution in commercial fisheries -- Observations of redstriped rockfish in commercial fisheries catches from the GOA were limited. There were 19 observations of redstriped rockfish during the fall (Fig. 177), three during the winter (Fig. 178), and 13 during the spring (Fig. 179). These observations were concentrated in the central and western GOA and were not enough to model commercial catches of redstriped rockfish.

Redstriped rockfish essential fish habitat maps and conclusions -- In general, predictions of probable settled juvenile and adult restriped rockfish habitat were similarly distributed for these two life stages. The highest probability for suitable redstriped rockfish habitat was distributed throughout most of the middle and outer shelf in the central and eastern GOA (Fig. 180).

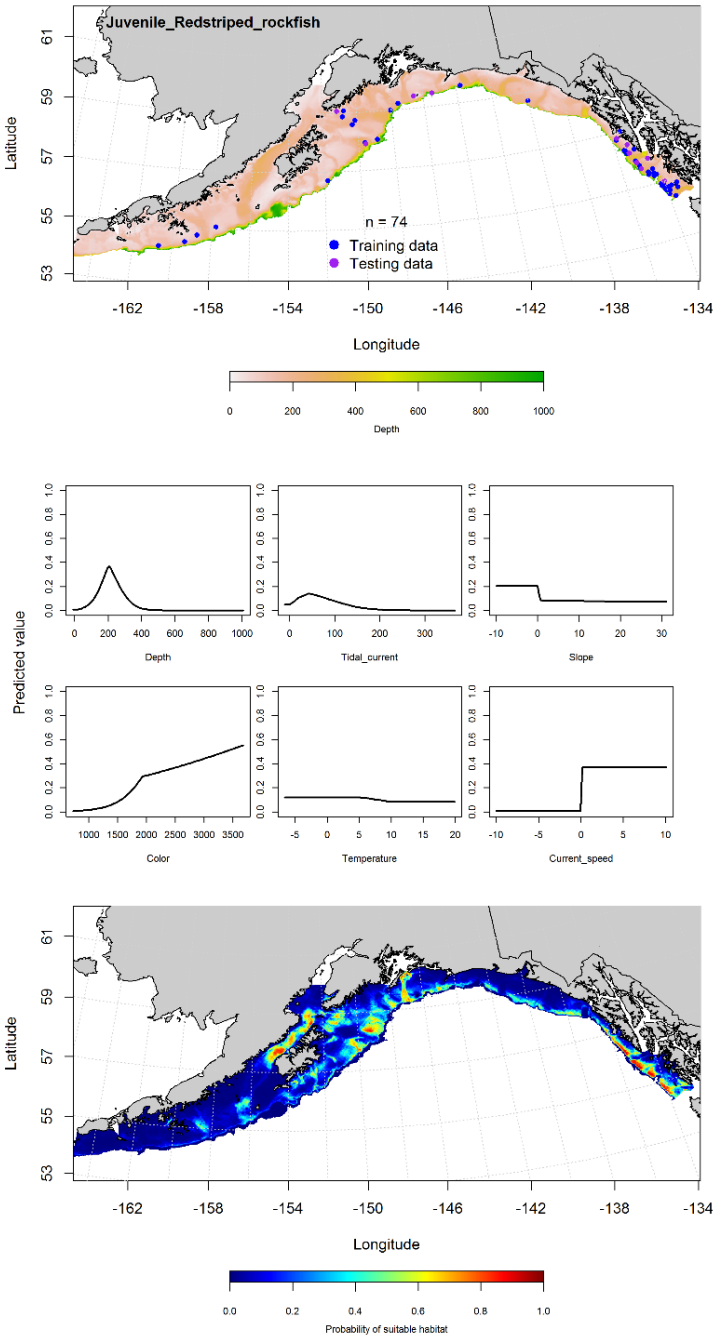

Figure 174. -- Presence of settled juvenile redstriped rockfish from RACE-GAP summer bottom trawl surveys (1993-2013) in the Gulf of Alaska (top panel) with training (blue dots) and testing (purple dots) data indicated, maximum entropy (MaxEnt) model effects (center panel), and the MaxEnt-predicted probability of suitable juvenile redstriped rockfish habitat (bottom panel).

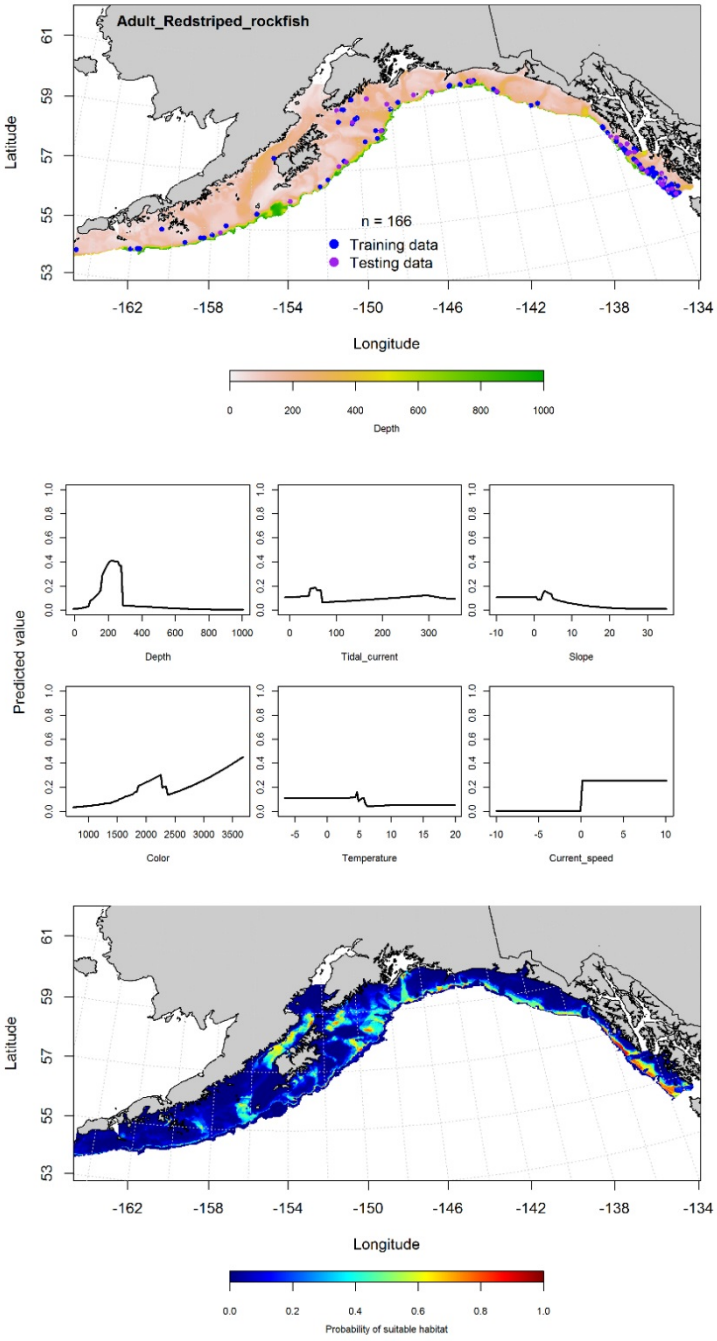

Figure 175. -- Presence of adult redstriped rockfish from RACE-GAP summer bottom trawl surveys (1993-2013) in the Gulf of Alaska (top panel) with training (blue dots) and testing (purple dots) data indicated, maximum entropy (MaxEnt) model effects (center panel), and the MaxEnt-predicted probability of suitable adult redstriped rockfish habitat (bottom panel).

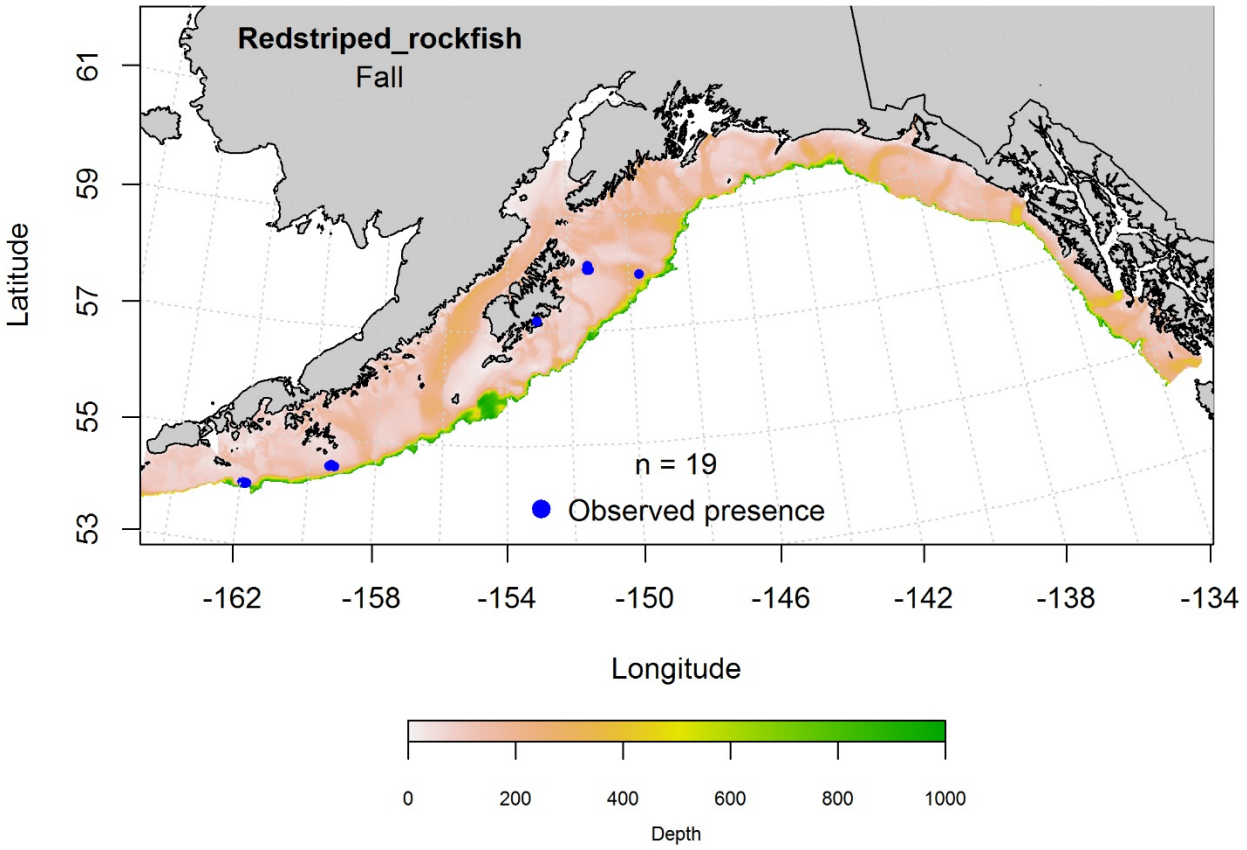

Figure 176. -- Locations of redstriped rockfish from fall (September-November 2001-2015) commercial fisheries catches in the Gulf of Alaska.

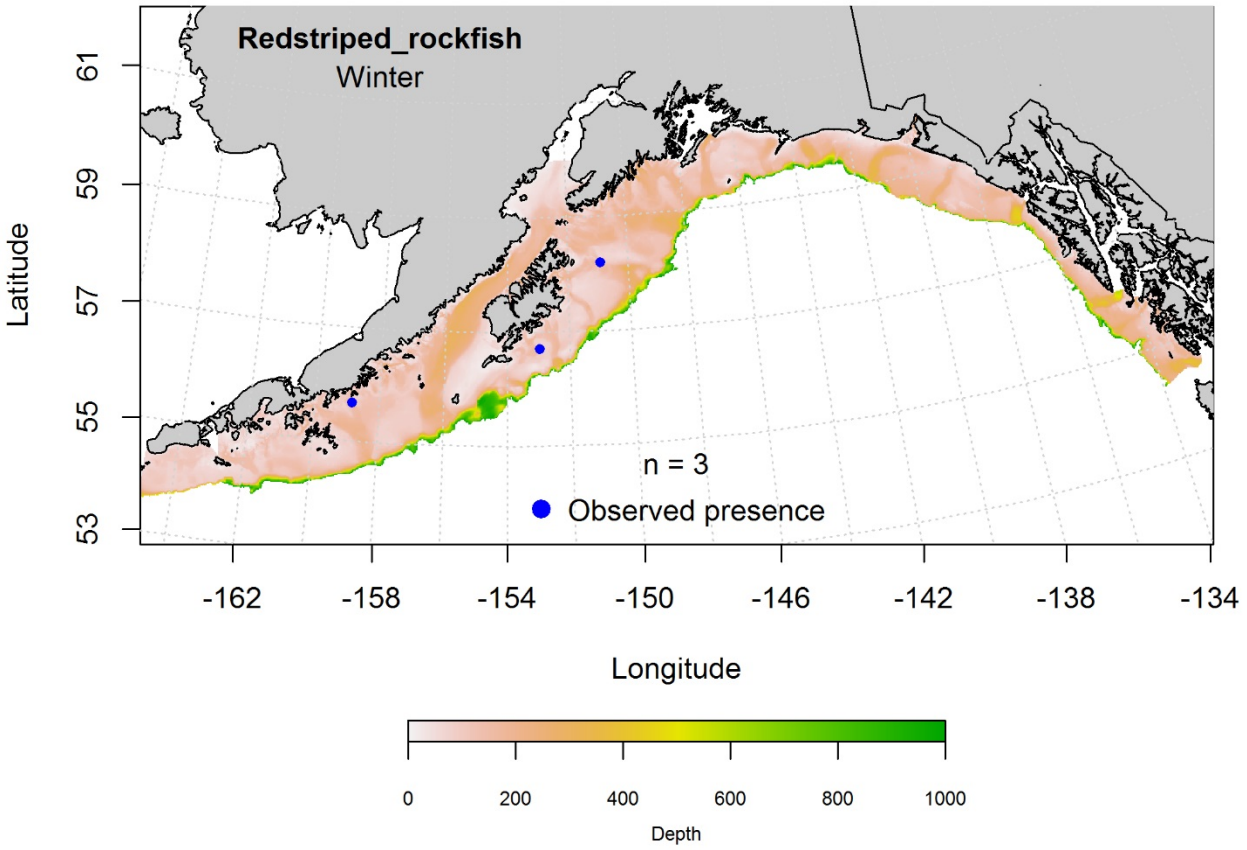

Figure 177. -- Locations of redstriped rockfish from winter (December-February 2001-2015) commercial fisheries catches in the Gulf of Alaska.

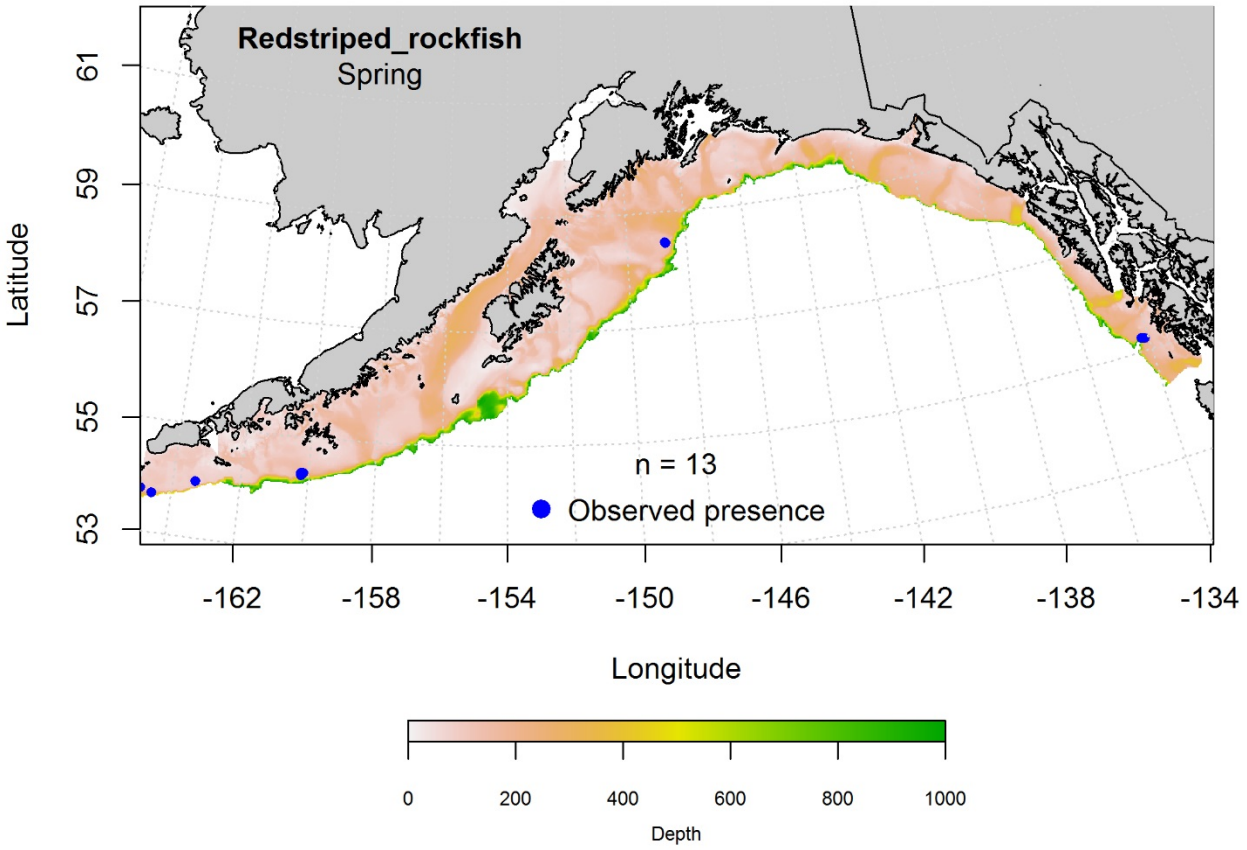

Figure 178. -- Locations of redstriped rockfish from spring (March-May 2001-2015) commercial fisheries catches in the Gulf of Alaska.

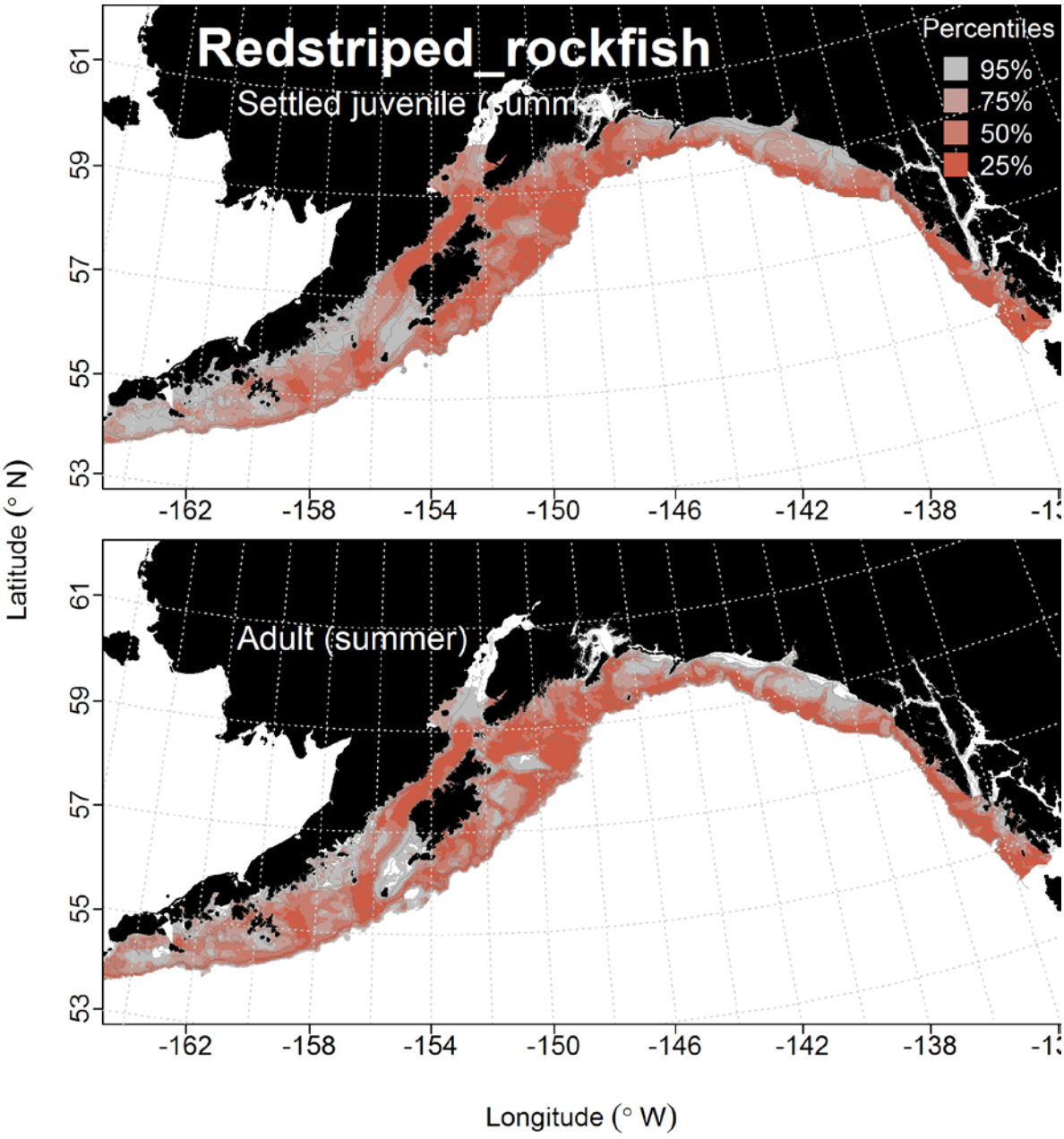

Figure 179. -- Distribution of predicted habitat of settled juvenile and adult redstriped rockfish from RACE-GAP summertime bottom trawl surveys (1993-2013) in the Gulf of Alaska.

Yelloweye Rockfish (*Sebastes ruberrimus*)

Juvenile and adult yelloweye rockfish distribution in the bottom trawl survey -- The catch of settled juvenile yelloweye rockfish from summer bottom trawl survey indicates this species is broadly distributed across the GOA (Fig. 181). A MaxEnt model was used to predict the suitable habitat of settled juvenile yelloweye rockfish. The AUC of the model was 0.96 for the training data and 0.75 for the testing data. The model correctly classified 90% of the predictions from the training data and 75% of the predictions from the test data. The most important variables in the model were bottom depth and bottom current speed (relative importance: 0.58 and 0.19, respectively). The model predicted suitable habitat for settled juvenile yelloweye rockfish occurred throughout the central and western GOA, though it was highest east of Portlock Bank (Fig. 181).

The catch of adult yelloweye rockfish in summer bottom trawl surveys was similar to that of the settled juveniles (Fig. 182). A MaxEnt model predicting suitable habitat of adult yelloweye rockfish explained 82% of the variability in the training data and 70% of the test data. The AUC was 0.94 for the training data and 0.77 for the testing data. The most important variables in the model were bottom depth, bottom temperature, and bottom current speed (relative importance: 0.55, 0.15, and 0.13, respectively). Suitable adult yelloweye rockfish habitat was predicted on the middle and outer shelf across the GOA, with higher probability areas concentrated in the central GOA, east of Portlock Bank; as well as in the eastern GOA, off Baranof Island (Fig. 182).

Yelloweye rockfish distribution in commercial fisheries -- In the fall, bottom temperature and bottom depth were the most important variables determining the distribution of yelloweye rockfish (relative importance: 0.37 and 0.24, respectively). The AUC of the MaxEnt fall model was 0.97 for the training data and 0.92 for the test data. Suitable habitat of yelloweye rockfish was predicted near

the shelf break in the western GOA, though higher probability around the Shumagin and Unimak islands (Fig. 183).

In the winter, there were 46 observations of adult yelloweye rockfish from commercial fisheries catches. Most of these observations were from the central and western GOA; however, there were not enough to model (Fig. 184).

In the spring, bottom temperature and bottom depth were again the most important variables predicting yelloweye rockfish distributions (relative importance: 0.38 and 0.22, respectively). The AUC of the spring MaxEnt model was 0.92 for the training data and 0.72 for the test data. The model predicted suitable habitat of yelloweye rockfish throughout the GOA, though highest along the Alaska Peninsula and off Unimak Island (Fig. 185).

Yelloweye rockfish essential fish habitat maps and conclusions -- Yelloweye rockfish habitat predicted by the modeling is widely distributed throughout the GOA for both settled juvenile and adult life stages from summer bottom trawl surveys (Fig. 186). In contrast, predicted yelloweye rockfish habitat based on commercial catches is widely distributed in the central and western GOA, but in the eastern-GOA it is more concentrated along the outer shelf (Fig.186). There does not appear to be much seasonal variability to the habitat distribution.

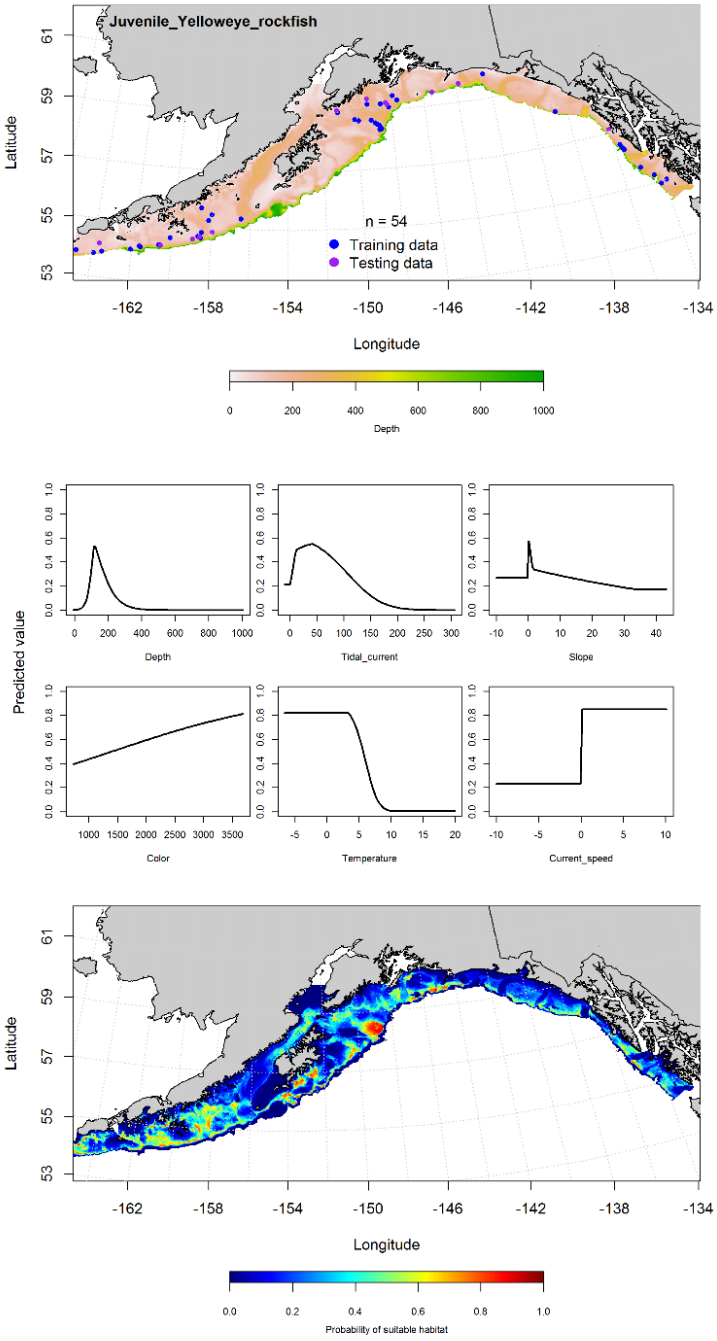

Figure 180. -- Presence of settled juvenile yelloweye rockfish from RACE-GAP summer bottom trawl surveys (1993-2013) in the Gulf of Alaska (top panel) with training (blue dots) and testing (purple dots) data indicated, maximum entropy (MaxEnt) model relationships between probability of juvenile presence and habitat covariates (center panel), and the MaxEnt-predicted probability of suitable juvenile yelloweye rockfish habitat (bottom panel).

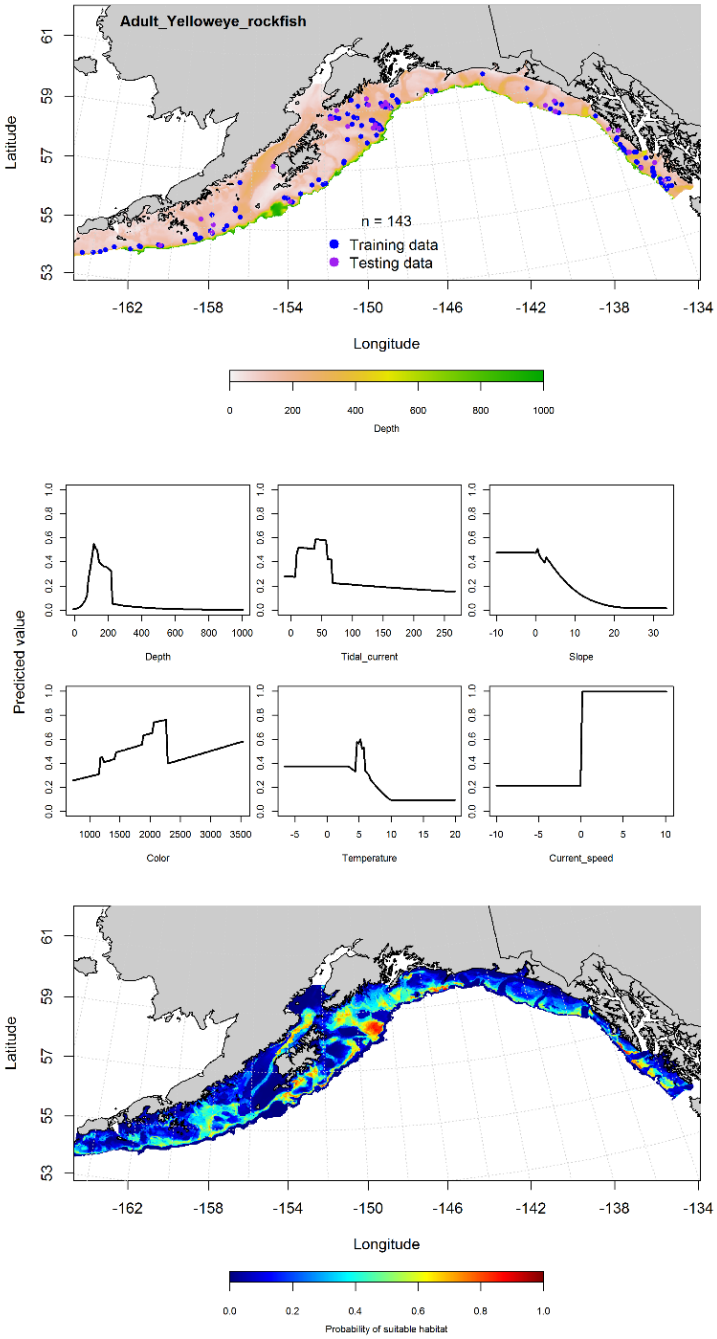

Figure 181. -- Presence of adult yelloweye rockfish from RACE-GAP summer bottom trawl surveys (1993-2013) in the Gulf of Alaska (top panel) with training (blue dots) and testing (purple dots) data indicated, maximum entropy (MaxEnt) model effects (center panel), and the MaxEnt-predicted probability of suitable adult yelloweye rockfish habitat (bottom panel).

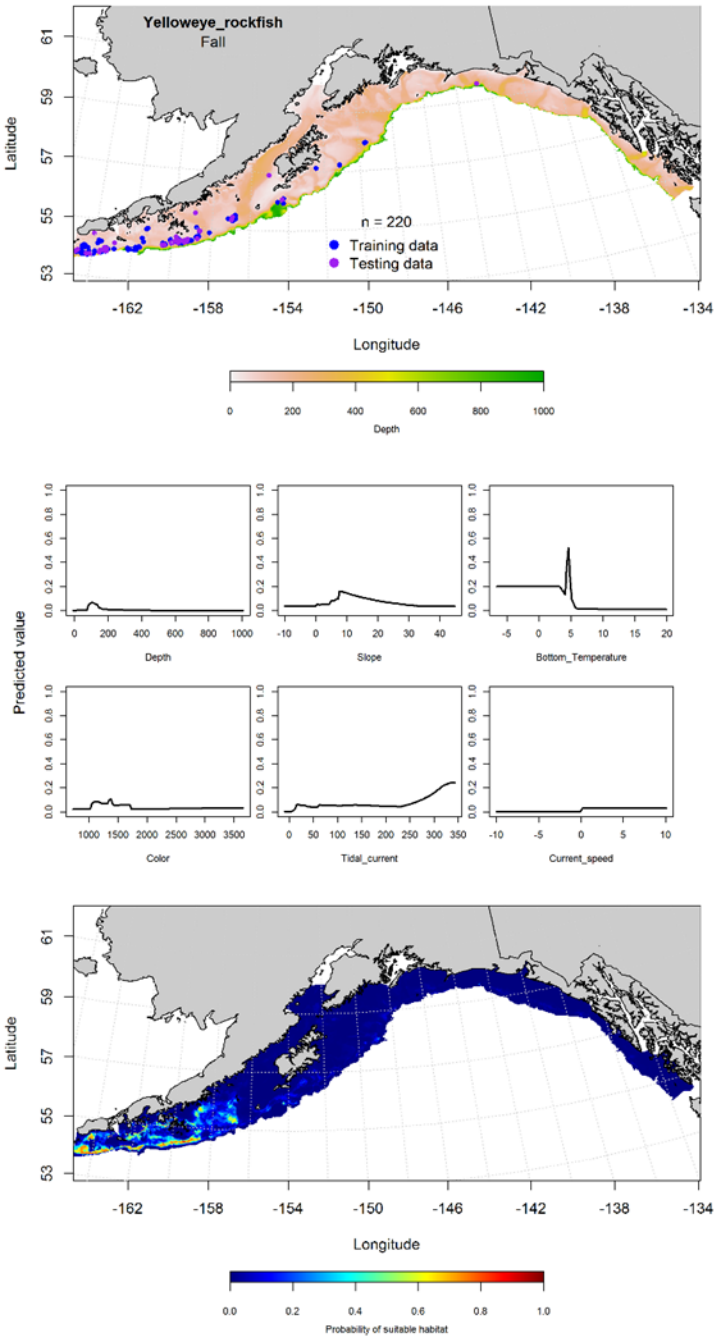

Figure 182. -- Locations of yelloweye rockfish from fall (September-November 2001-2015) commercial fisheries catches in the Gulf of Alaska (top panel), MaxEnt model effects (middle panels), and predicted probability of suitable habitat for yelloweye rockfish based on the model (bottom panel).

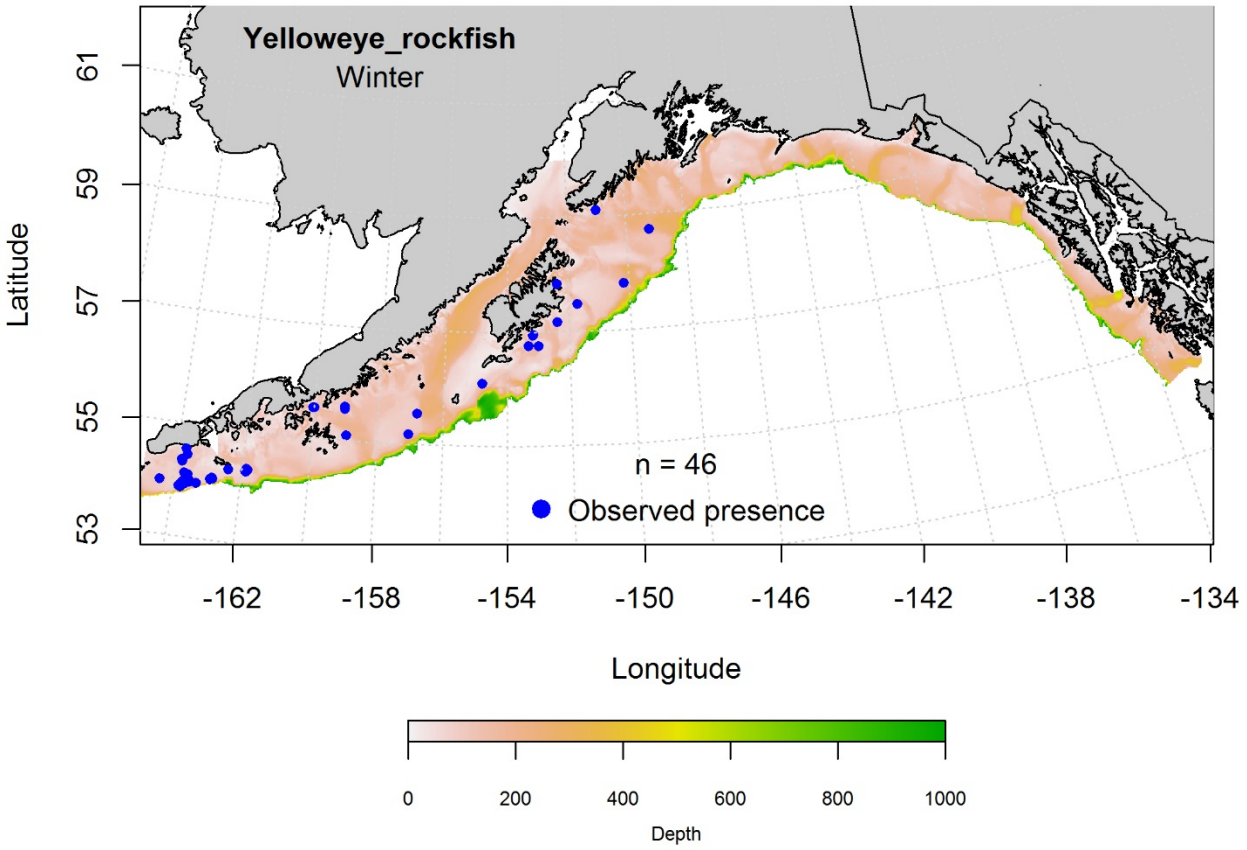

Figure 183. -- Locations of yelloweye rockfish from winter (December-February 2001-2015) commercial fisheries catches in the Gulf of Alaska.

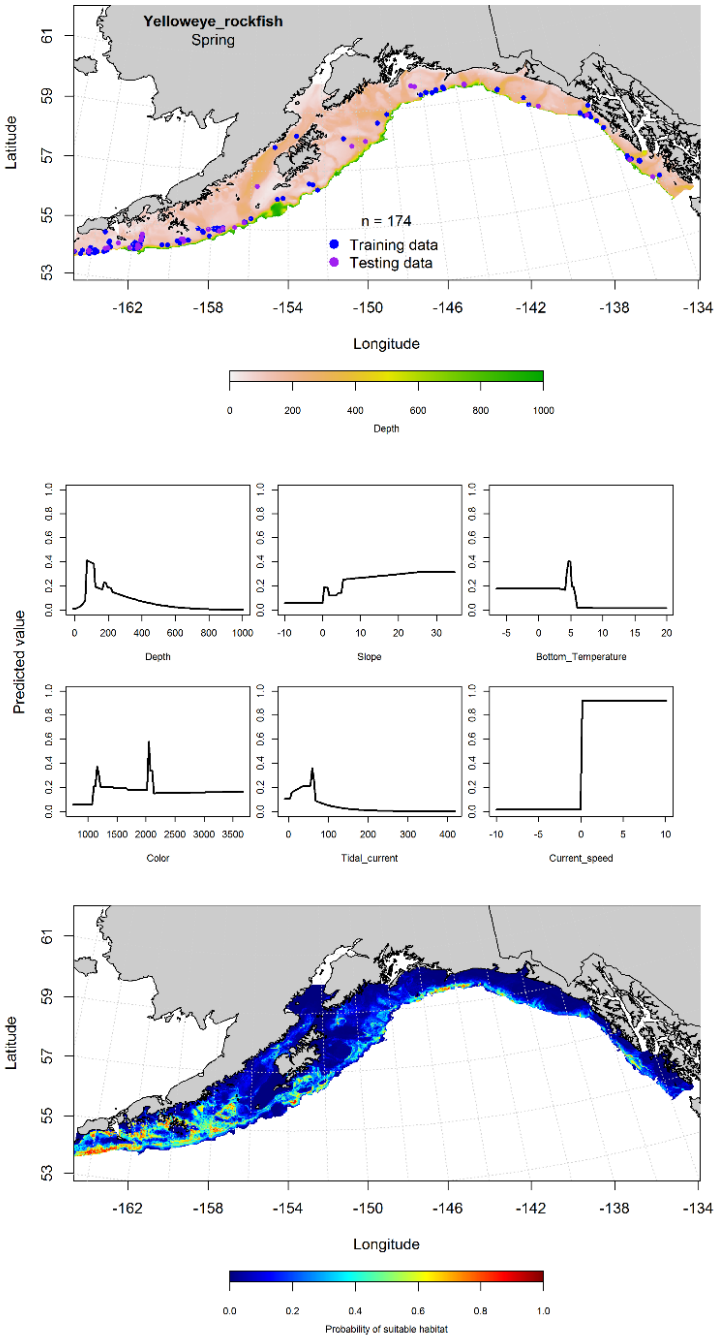

Figure 184. -- Locations of yelloweye rockfish from spring (March-May 2001-2015) commercial fisheries catches in the Gulf of Alaska (top panel), with training (blue dots) and testing (purple dots) data indicated, maximum entropy (MaxEnt) model effects (center panel), and the predicted probability of suitable adult yelloweye rockfish (bottom panel).

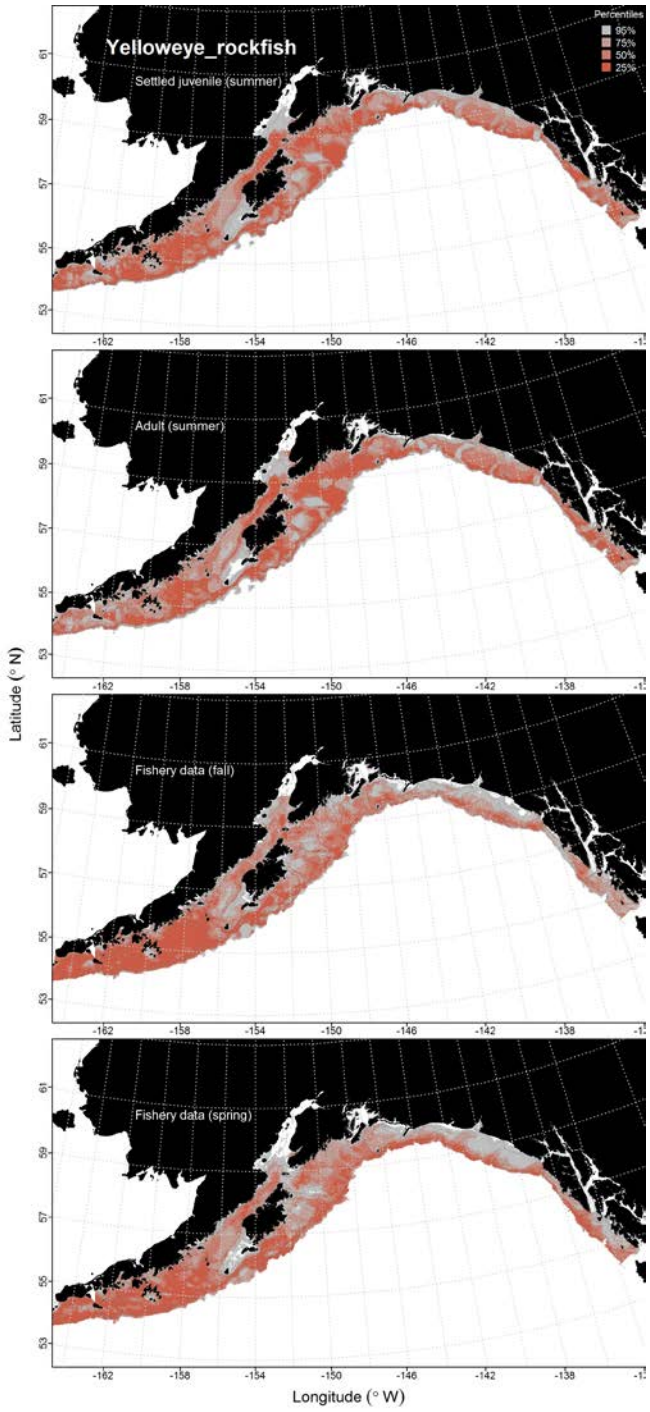

Figure 185. -- Predicted habitat for yelloweye rockfish life history stages based on species distribution modeling. Larval stages are shown above in the Pacific ocean perch section (Sebastes spp.). Predicted habitat for settled juveniles and adults are based on RACE-GAP summertime bottom trawl surveys (1993-2013), and predicted presence in commercial fishery catches (2001-2015) from the fall and spring in the Gulf of Alaska.

Dusky Rockfish (*Sebastes variabilis)*

Juvenile and adult dusky rockfish distribution in the bottom trawl survey -- The catch of settled juvenile dusky rockfish in summer bottom trawl surveys indicates this species is broadly distributed across the central and western GOA (Fig. 187). A MaxEnt model was used to predict the distribution of suitable settled juvenile dusky rockfish habitat. The AUC for the model was 0.82 for the training data and 0.75 for the test data. The model correctly classified 81% of the predictions from the training data and 75% of the predictions from the test data. The most important variables predicting the probability of suitable habitat were bottom depth and bottom current speed (relative importance: 0.82 and 0.09, respectively). The model predicted suitable habitat of settled juvenile dusky rockfish along the inner and middleshelf, particularly in the western GOA, around the Shumagin Islands; as well as in the central GOA, around Albatross Bank and Wessels Reefs (Fig. 187).

An hGAM was used to predict the distribution of adult dusky rockfish abundance. The AUC of the PA GAM was 0.82 for the training data and 0.79 for the test data. Geographic location, maximum tidal current, and bottom temperature were the most important variables explaining the probability of presence of adult dusky rockfish. The model correctly classified 75% of the predictions from both the training and the test data. The highest probability of presence was predicted to occur along the outer shelf in the central and western GOA (Fig. 188). Geographic location and ocean color were the most important variables in the CPUE GAM; however, the model only explained 10% of the variability of the training data set and 5% of the test data set. The areas of highest abundance in the central GOA were off Portlock Bank, while in the western GOA they were off Unimak Island (Fig. 188).

Dusky rockfish distribution in commercial fisheries -- In the fall, bottom depth, maximum tidal current and ocean color were the most important variables in the model determining suitable habitat of dusky rockfish (relative importance: 0.28, 0.22, and 0.22, respectively). The AUC of the fall MaxEnt model was 0.93 for the training data and 0.81 for the test data. The areas of predicted highest probability of suitable habitat in the western GOA were off Unimak Island and the Sandman Reefs, while in the central GOA, they were off Albatross and Portlock banks (Fig. 189).

In the winter, ocean color, bottom current speed, and bottom depth were the most important variables determining suitable habitat of dusky rockfish (relative importance: 0.32, 0.17, and 0.17, respectively). The AUC of the MaxEnt model was 0.93 for the training data and 0.78 for the test data. The model predicted suitable habitat of dusky rockfish in the central and western GOA, particularly along Albatross Bank and the Kenai Peninsula (Fig. 190).

In the spring, maximum tidal current, bottom depth, and bottom current speed were the most important variables determining suitable habitat of dusky rockfish (relative importance: 0.24, 0.22, and 0.20, respectively). The AUC of the spring MaxEnt model was 0.90 for the training data and 0.79 for the test data. The model predicted suitable habitat of dusky rockfish along the outer shelf in the western GOA, particularly around Semidi Bank and Unimak Island (Fig. 191).

Dusky rockfish essential fish habitat maps and conclusions -- Summertime habitat for settled juvenile dusky rockfish adults was predicted along the inner and middleshelf throughout the GOA (Fig. 191). In contrast, predicted habitats for adult dusky rockfish was concentrated along the outer shelf (Fig. 192). The fall, winter, and spring distribution of dusky rockfish based on commercial catches were essentially the same throughout the seasons (Fig. 192).

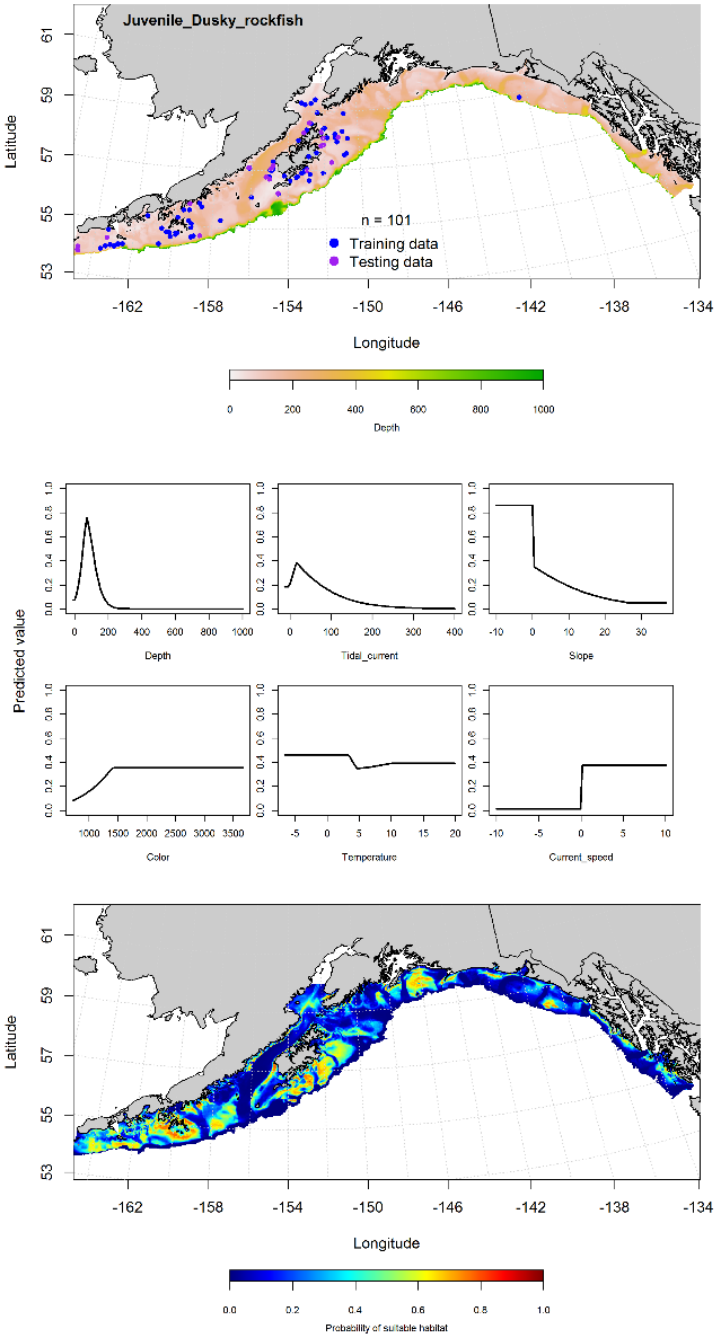

Figure 186. -- Presence of settled juvenile dusky rockfish from RACE-GAP summer bottom trawl surveys (1993-2013) in the Gulf of Alaska (top panel) with training (blue dots) and testing (purple dots) data indicated, maximum entropy (MaxEnt) model relationships between probability of juvenile presence and habitat covariates (center panel), and the MaxEnt-predicted probability of suitable juvenile dusky rockfish habitat (bottom panel).

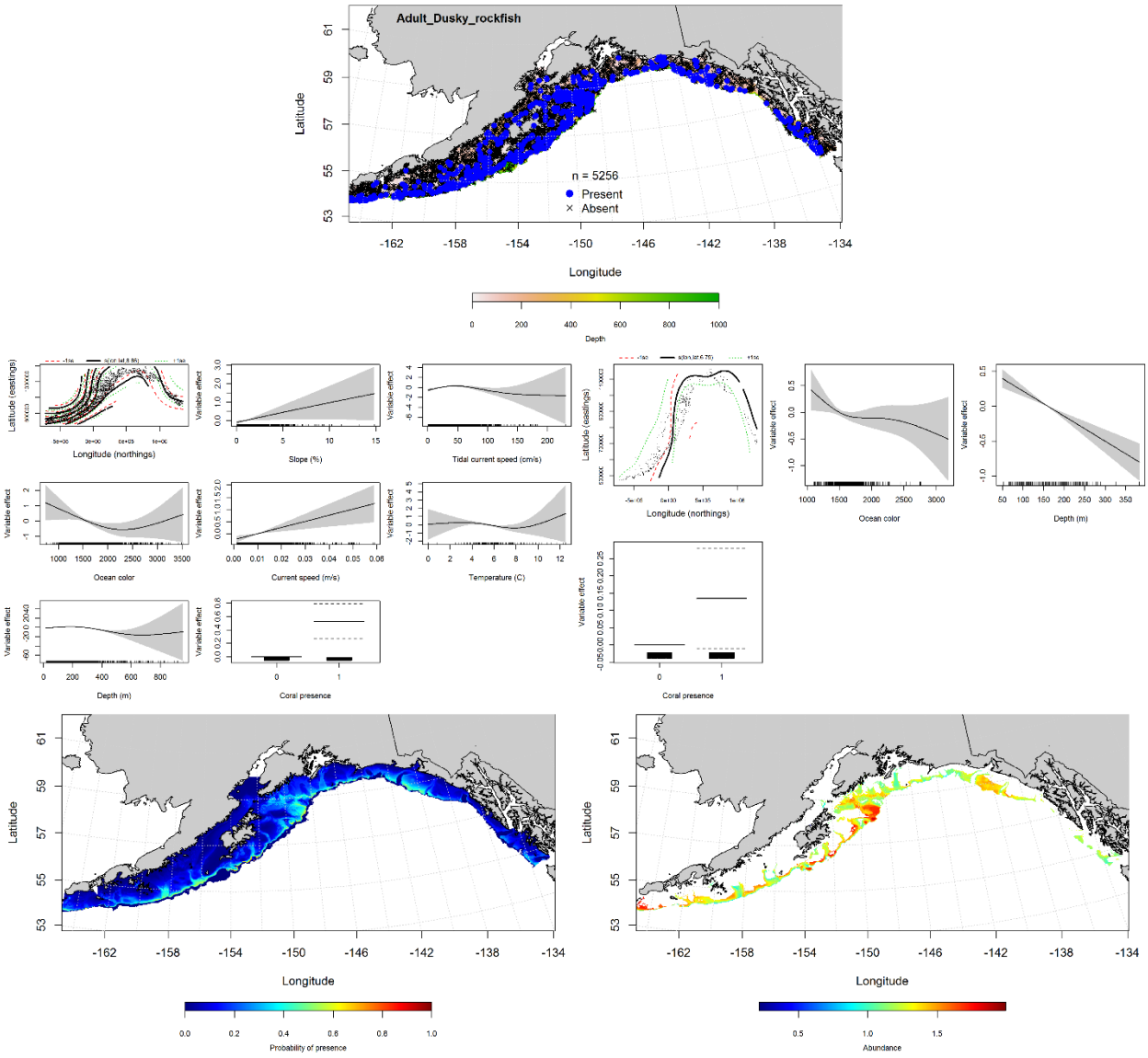

Figure 187. -- Distribution of adult dusky rockfish in 1993-2013 RACE-GAP summer bottom trawl surveys conducted in the Gulf of Alaska (upper panel). Effects of retained habitat covariates in the best fitting generalized additive presence-absence models (PA GAM; left center panel) and abundance (CPUE GAM; right center panel). Predicted spatial distribution of the probability of presence (bottom left panel) and abundance of adult dusky rockfish based on the models (bottom right panel).

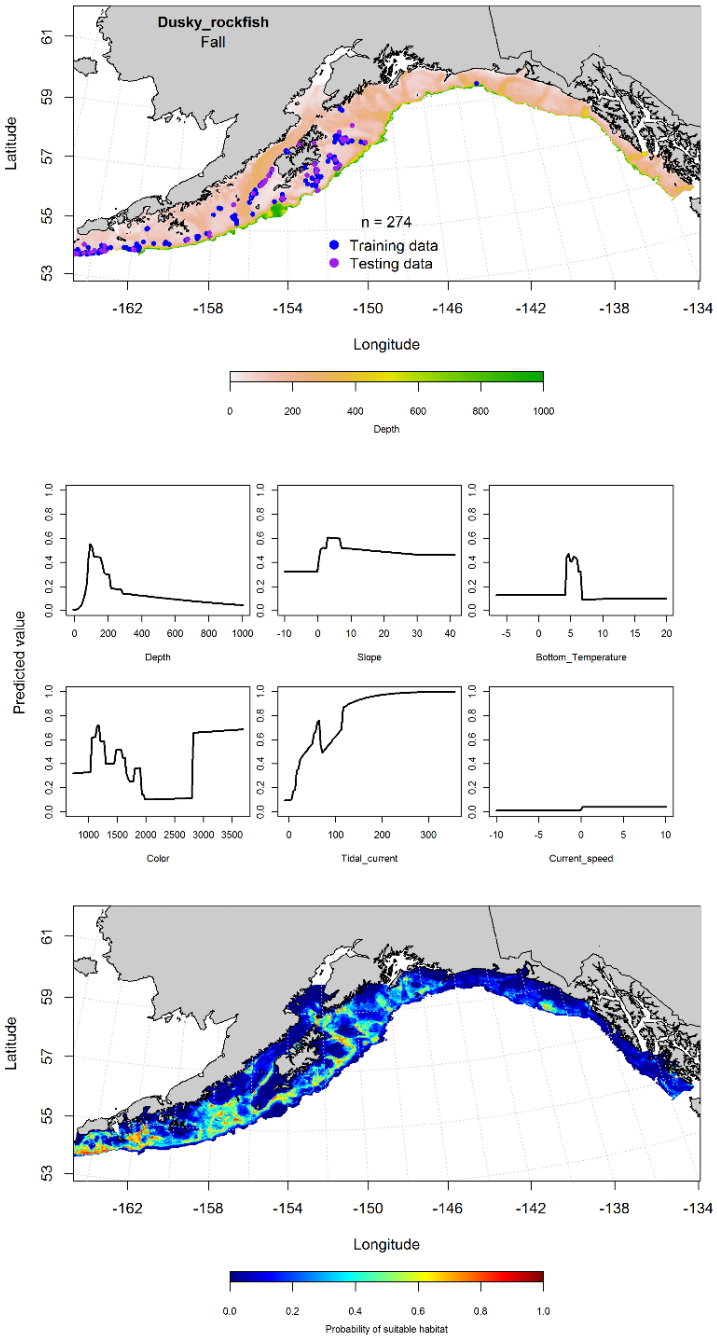

Figure 188. -- Locations of dusky rockfish from fall (September-November 2001-2015) commercial fisheries catches in the Gulf of Alaska (top panel), MaxEnt model effects (middle panels), and predicted probability of suitable habitat for dusky rockfish based on the model (bottom panel).

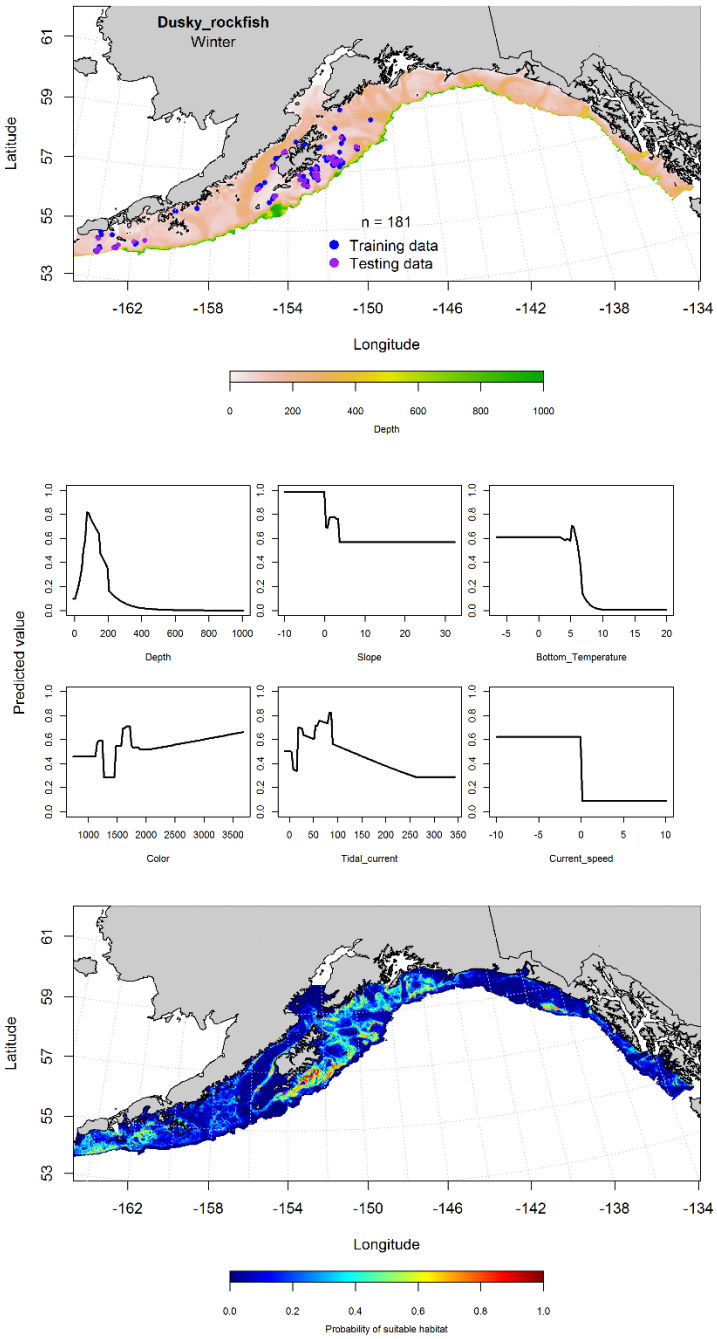

Figure 189. -- Locations of dusky rockfish from winter (December-February 2001-2015) commercial fisheries catches in the Gulf of Alaska (top panel), with training (blue dots) and testing (purple dots) data indicated, maximum entropy (MaxEnt) model effects (center panel), and the predicted probability of suitable adult dusky rockfish habitat (bottom panel).

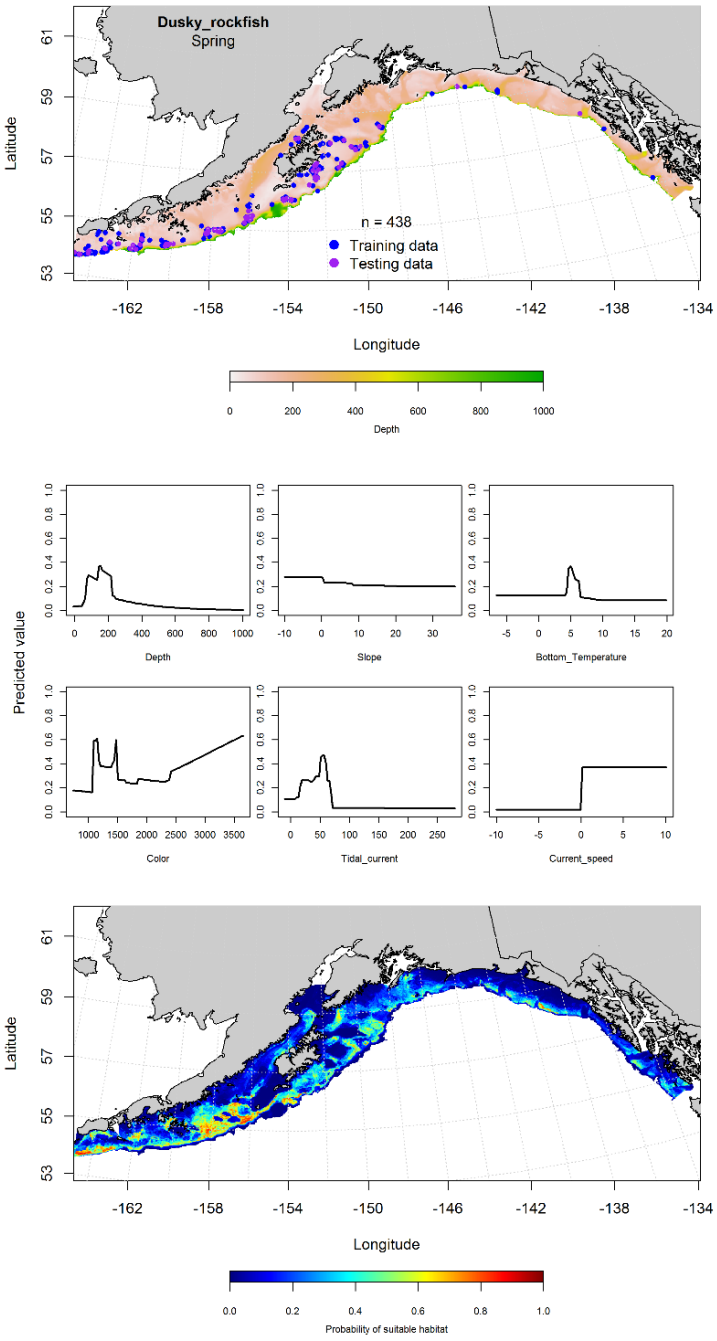

Figure 190. -- Locations of dusky rockfish from spring (March-May 2001-2015) commercial fisheries catches in the Gulf of Alaska (top panel), with training (blue dots) and testing (purple dots) data indicated, maximum entropy (MaxEnt) model effects (center panel), and the predicted probability of suitable adult dusky rockfish (bottom panel).

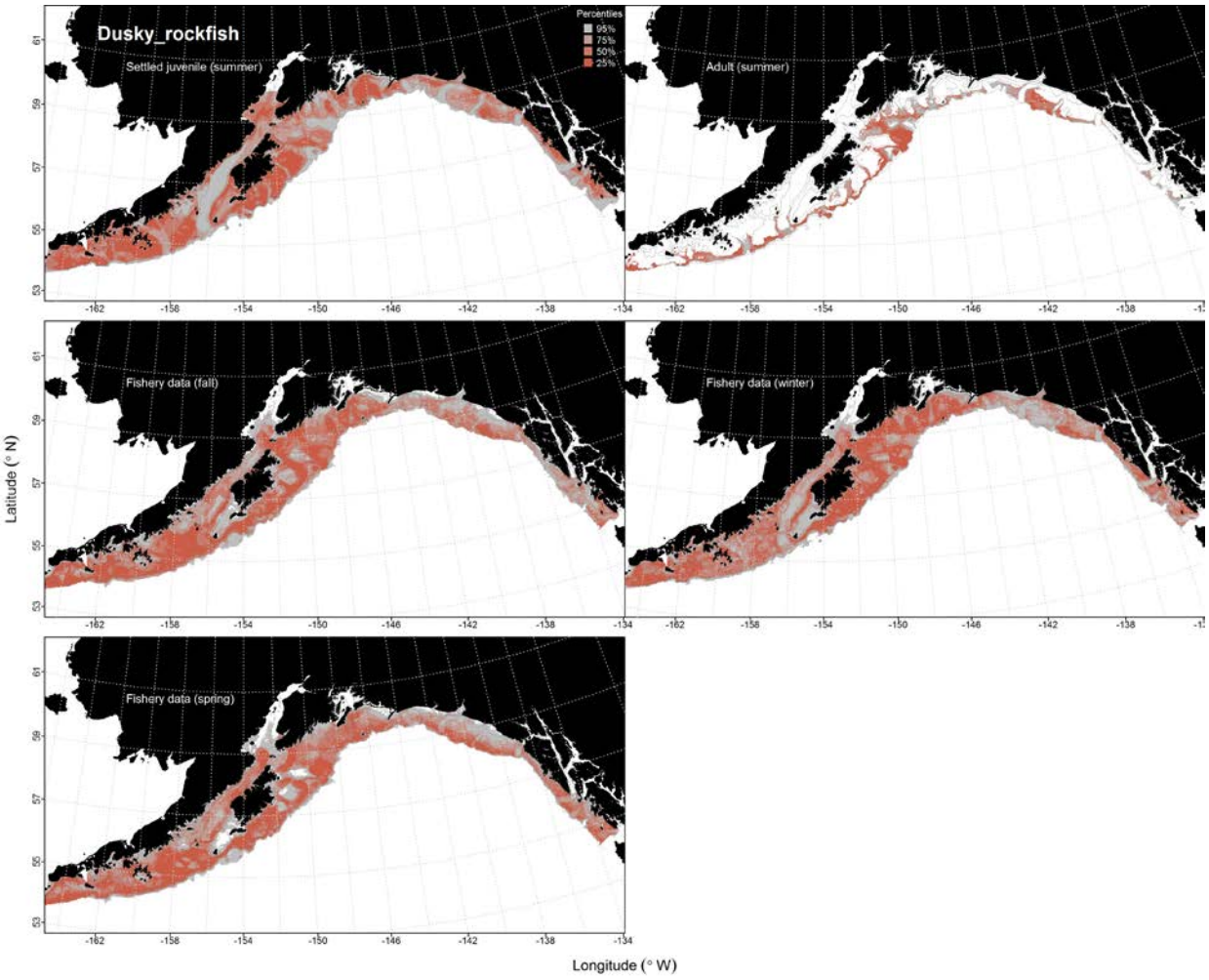

Figure 191. -- Predicted habitat for dusky rockfish life history stages based on species distribution modeling. Larval stages are shown above in the Pacific ocean perch section (Sebastes spp.). Predicted habitat for settled juveniles and adults are based on RACE-GAP summertime bottom trawl surveys (1993-2013), and predicted presence in commercial fishery catches (2001-2015) from the fall, winter, and spring in the Gulf of Alaska.

Harlequin Rockfish (*Sebastes variegatus*)

Juvenile and adult harlequin rockfish distribution in the bottom trawl survey -- The catch of settled juvenile harlequin rockfish from summer bottom trawl surveys indicates this species is broadly distributed throughout the GOA. A MaxEnt model predicting the probability of suitable habitat of settled juvenile harlequin rockfish resulted in AUCs of 0.89 for the training data and 0.72 in the test data. The model correctly classified 83% of the predictions from the training data and 72% of the predictions from the test data. Bottom depth, bottom temperature, and bottom current speed were the most important variables explaining suitable habitat of settled juvenile harlequin rockfish (relative importance: 0.34, 0.30, and 0.16, respectively). The model predicted suitable habitat across the middle and outer shelf, particularly off Southeast Alaska, and in the central GOA, off Portlock Bank (Fig. 193).

An hGAM was used to predict the distribution of adult harlequin rockfish abundance. The AUC of the PA GAM was 0.82 for the training data and 0.79 for the test data. The model correctly classified 87% of the predictions from the training data and the 84% of the predictions from the test data. Geographic location, maximum tidal current, and ocean color were the most important variables. A relatively low probability of presence was predicted for adult harlequin rockfish, with the highest probability concentrated near the shelf break across the GOA (Fig. 194).

Harlequin rockfish distribution in commercial fisheries -- Observations of harlequin rockfish from commercial fisheries data were limited, with 28 records of adult harlequin rockfish from during the fall (Fig. 195), and three during the winter (Fig. 196). These observations all occurred either in the central or western GOA; however, there were not enough to model.

In the spring, bottom depth, maximum tidal current, and bottom current speed were the most important variables determining suitable habitat of harlequin rockfish (relative importance: 0.36, 0.30, and 0.16, respectively). The AUC of the spring MaxEnt model was 0.96 for the training data and 0.88 for the test data. The model correctly classified 85% of the predictions from the training data and 88% of the predictions from the test data. The model predicted suitable habitat of harlequin rockfish near the shelf break in the central and western GOA, particularly around the Shelikof and Shumagin Gullies (Fig. 197).

Harlequin rockfish essential fish habitat maps and conclusions -- Summertime habitat for settled juvenile harlequin rockfish was predicted to be broadly distributed across the central and eastern GOA (Fig. 198). Predicted summertime habitat for adult harlequin rockfish was concentrated along the outer shelf throughout the GOA (Fig. 198). In contrast, springtime harlequin rockfish habitat based on commercial catches was predicted to be broadly distributed throughout the middle and outer shelf (Fig. 198). This difference in the predicted distribution of adult harlequin rockfish habitat, is likely due to the limited number of observations (n = 64) used create the commercial catch model. As a result, the predicted habitat results from the commercial catch model should be interpreted with caution.

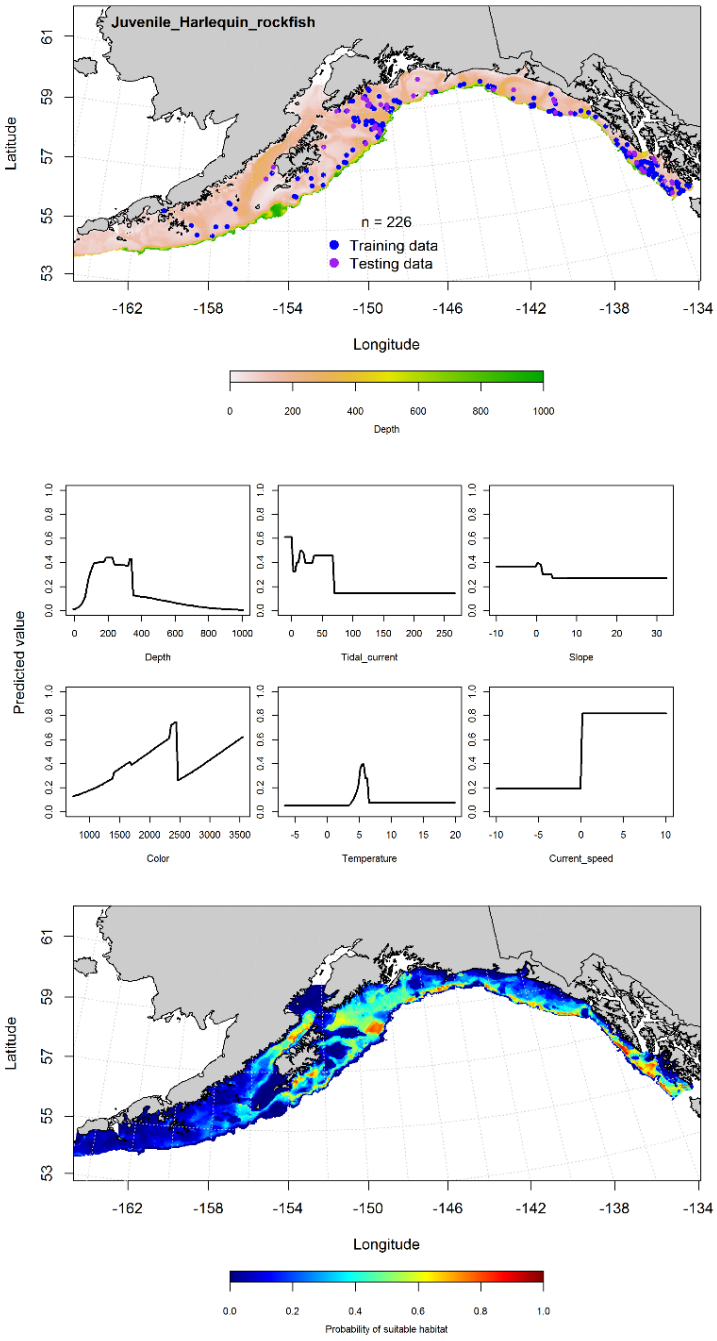

Figure 192. -- Presence of settled juvenile harlequin rockfish from RACE-GAP summer bottom trawl surveys (1993-2013) in the Gulf of Alaska (top panel) with training (blue dots) and testing (purple dots) data indicated, maximum entropy (MaxEnt) model relationships between probability of juvenile presence and habitat covariates (center panel), and the MaxEnt-predicted probability of suitable juvenile harlequin rockfish habitat (bottom panel).

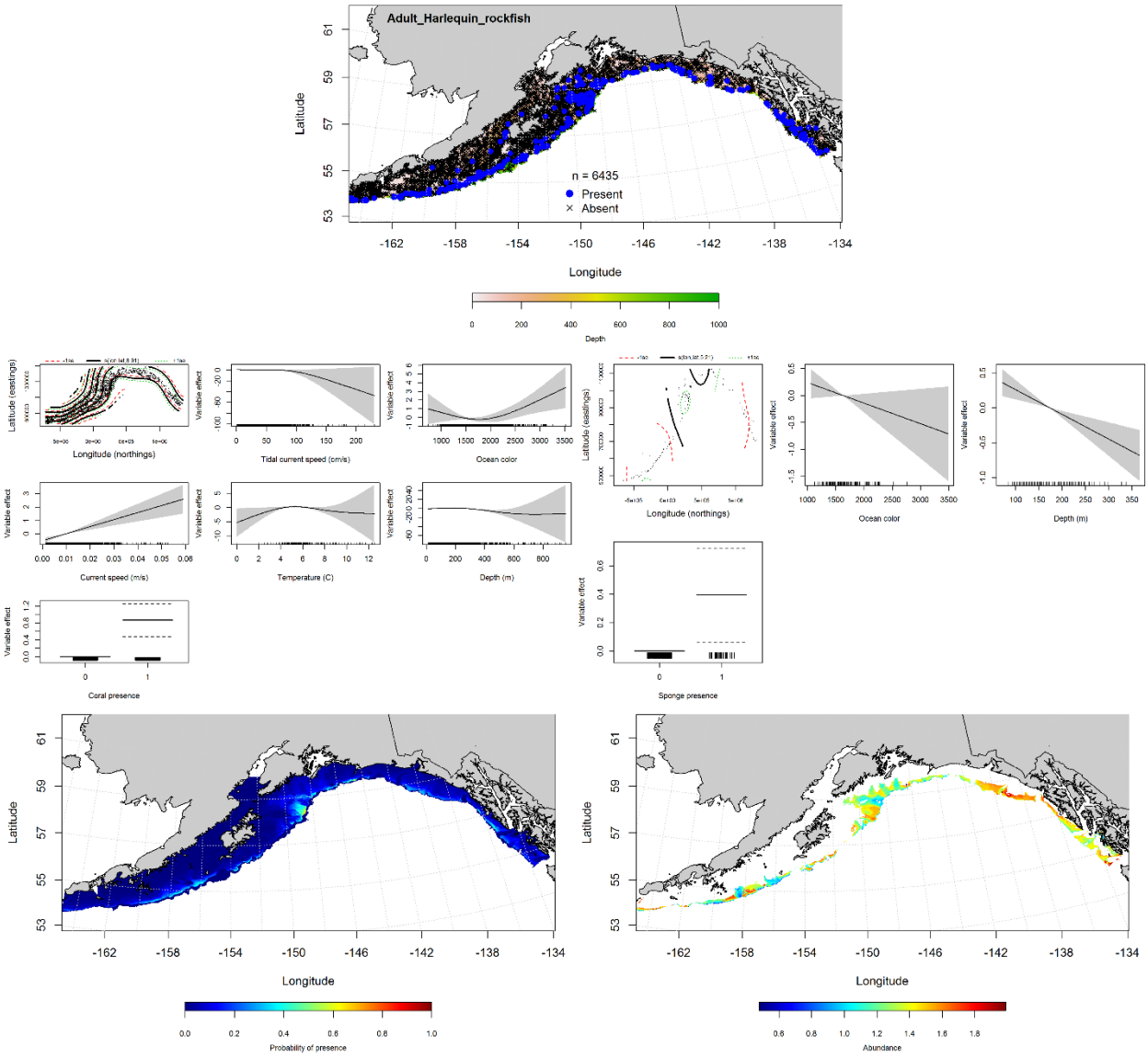

Figure 193. -- Distribution of adult harlequin rockfish in 1993-2013 RACE-GAP summer bottom trawl surveys conducted in the Gulf of Alaska (upper panel). Effects of retained habitat covariates in the best fitting generalized additive presence-absence models (PA GAM; left center panel) and abundance (CPUE GAM; right center panel). Predicted spatial distribution of the probability of presence (bottom left panel) and abundance of adult harlequin rockfish based on the models (bottom right panel).

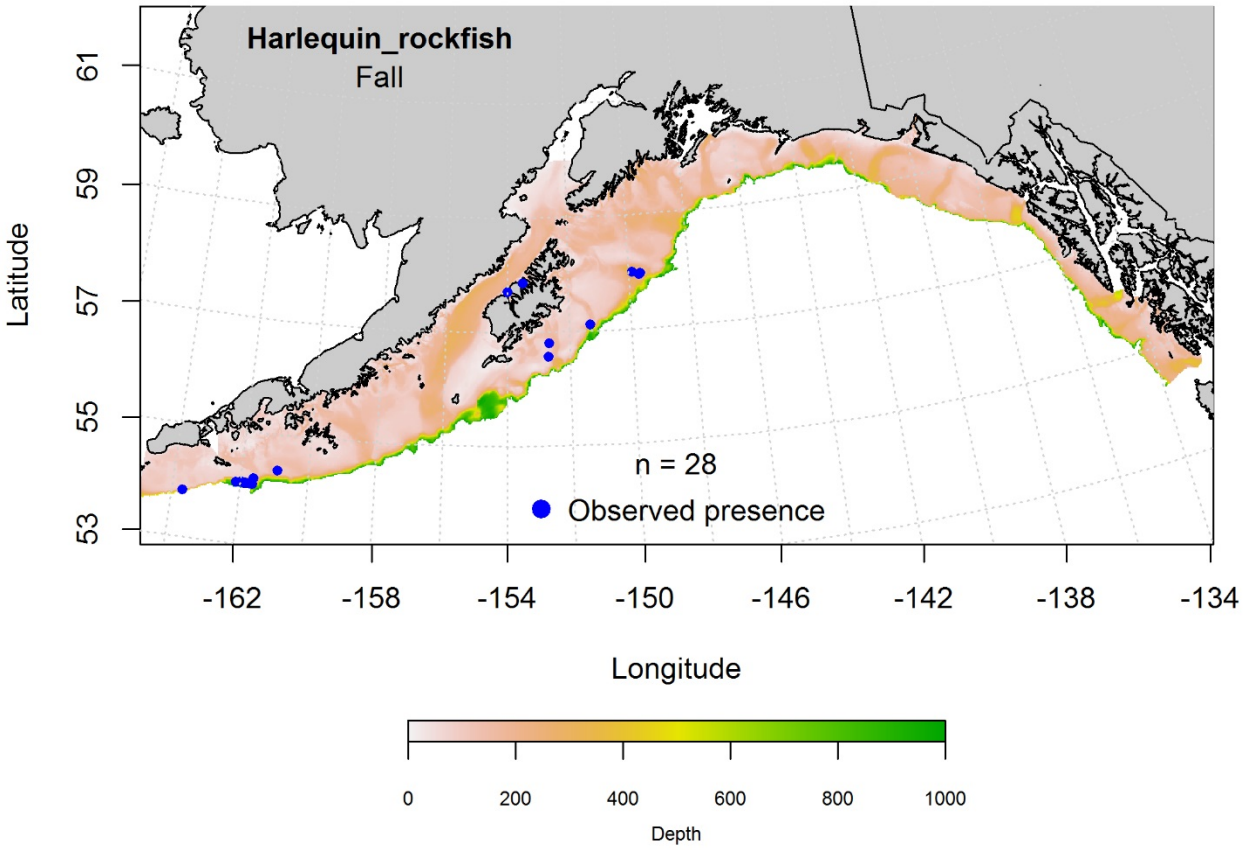

Figure 194. -- Locations of harlequin rockfish from fall (September-November 2001-2015) commercial fisheries catches in the Gulf of Alaska.

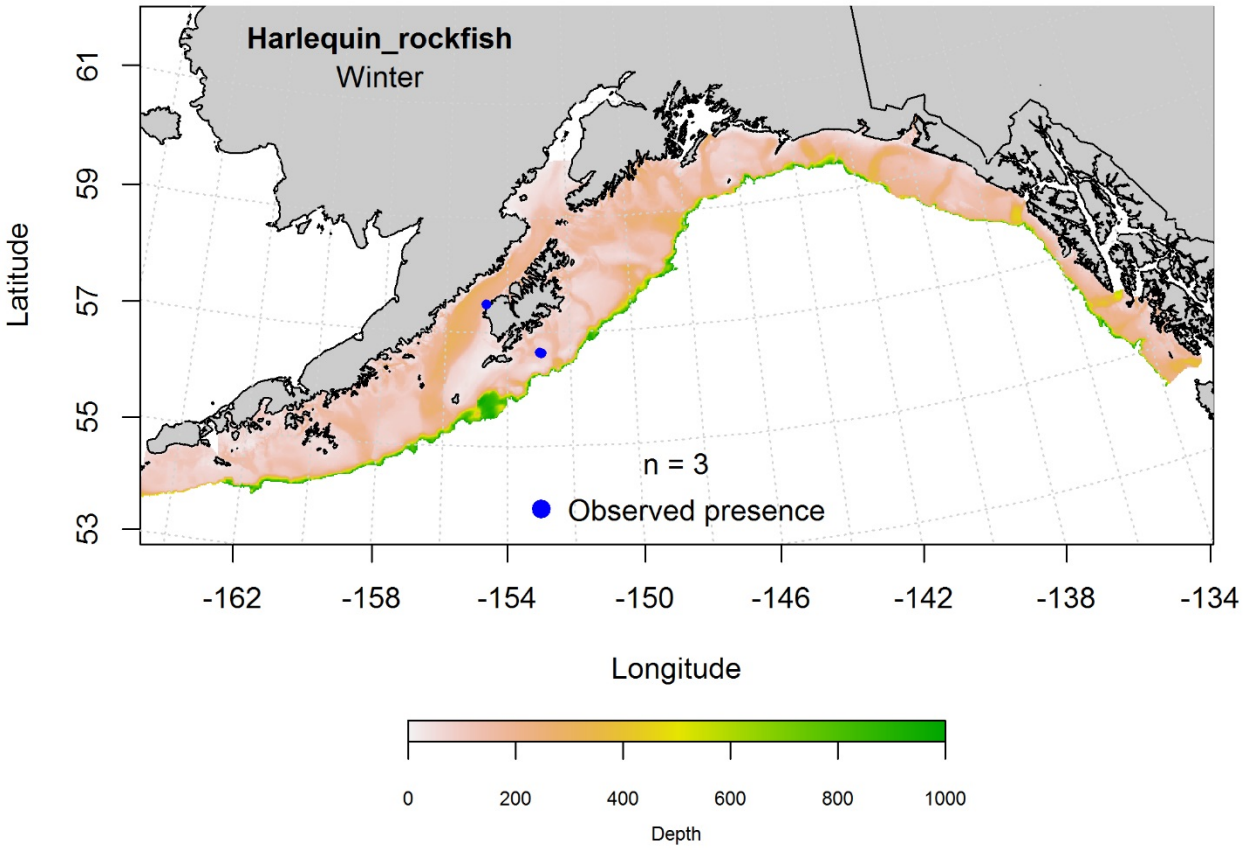

Figure 195. -- Locations of harlequin rockfish from winter (December-February 2001-2015) commercial fisheries catches in the Gulf of Alaska.

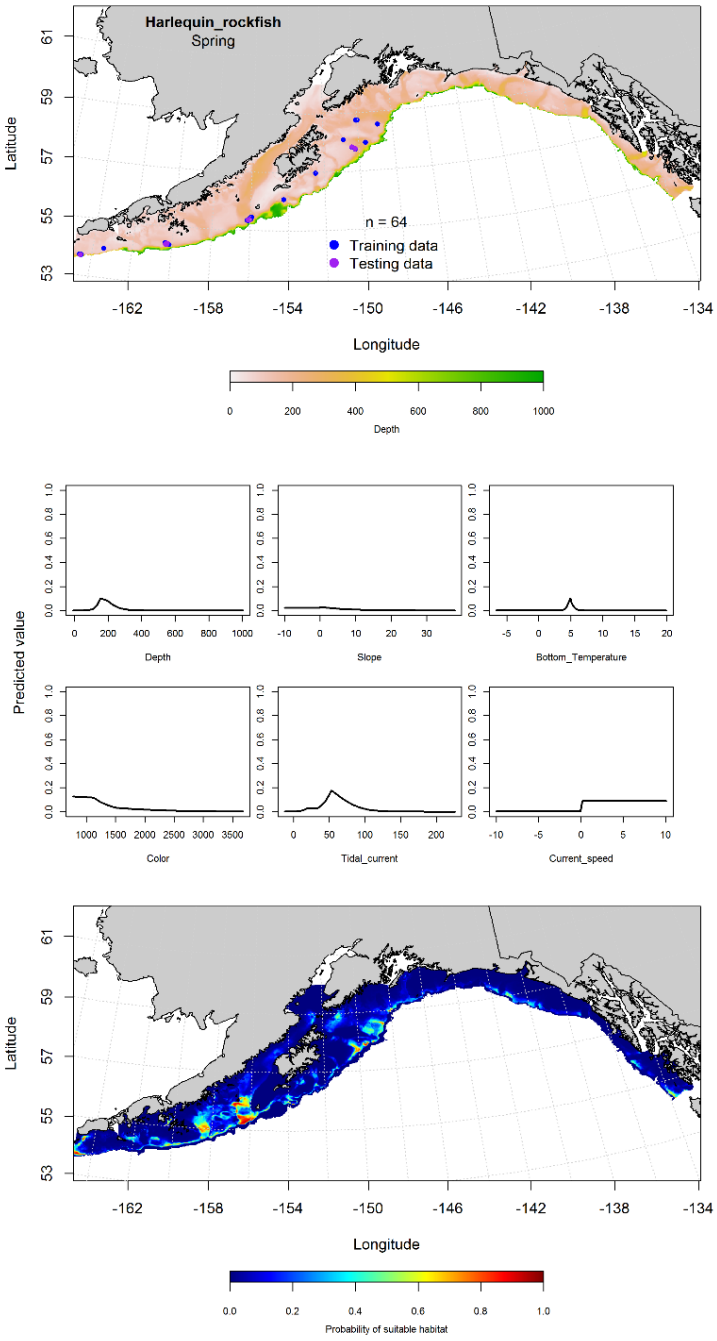

Figure 196. -- Locations of harlequin rockfish from spring (March-May 2001-2015) commercial fisheries catches in the Gulf of Alaska (top panel), with training (blue dots) and testing (purple dots) data indicated, maximum entropy (MaxEnt) model effects (center panel), and the predicted probability of suitable adult harlequin rockfish (bottom panel).

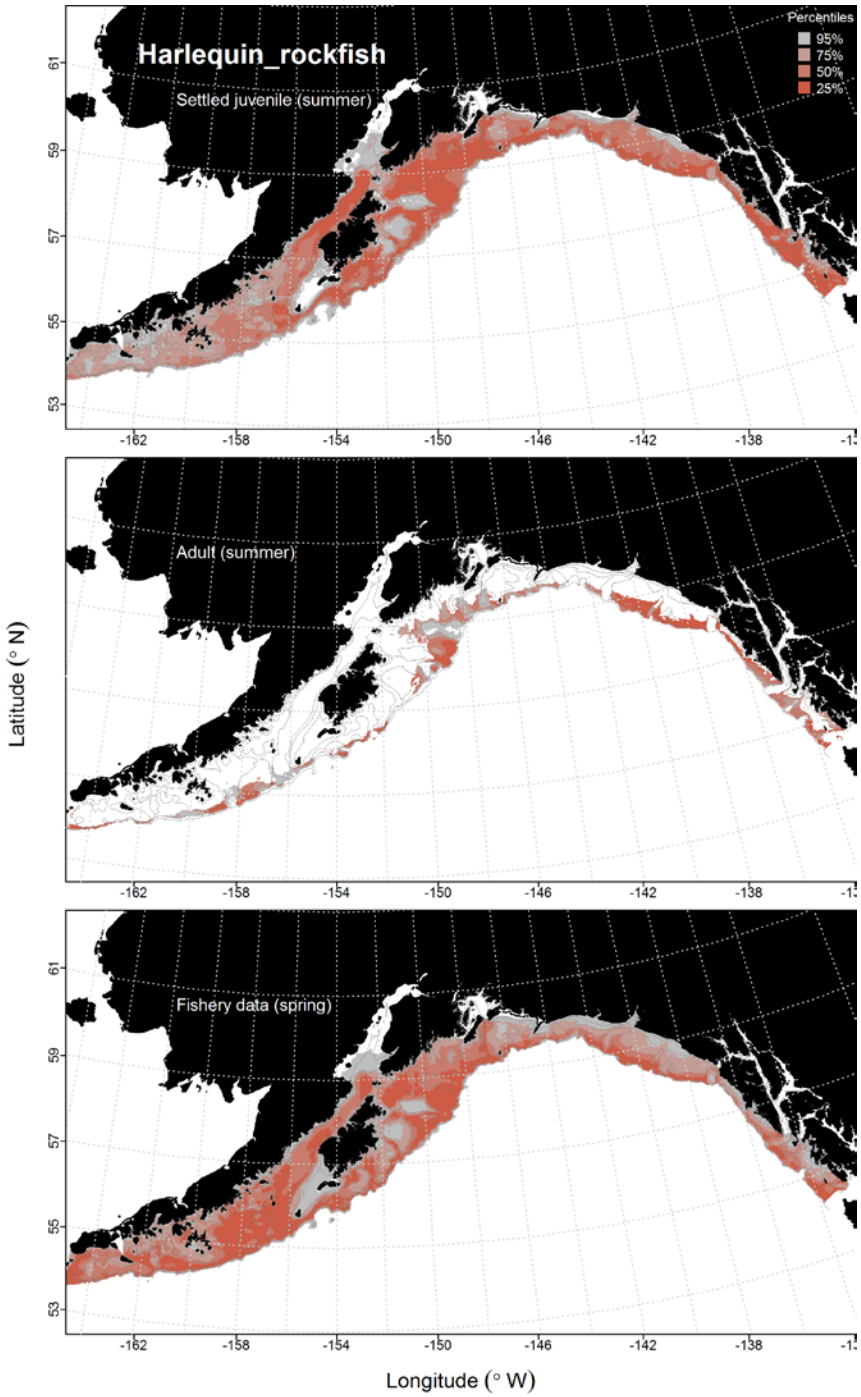

Figure 197. -- Predicted habitat for harlequin rockfish life history stages based on species distribution modeling. Larval stages are shown above in the Pacific ocean perch section (*Sebastes* spp.). Predicted habitat for settled juveniles and adults are based on RACE-GAP summertime bottom trawl surveys (1993-2013), and predicted presence in commercial fishery catches (2001-2015) from the fall, winter, and spring in the Gulf of Alaska.

Pygmy Rockfish (*Sebastes wilsoni*)

Juvenile and adult pygmy rockfish distribution in the bottom trawl survey -- There were no observations of settled juvenile pygmy rockfish during the summer time trawl surveys.

There were 57 observations of adult pygmy rockfish. The MaxEnt model predicting probability of suitable habitat of adult pygmy rockfish had an AUC of 0.91 for the training data and 0.67 for the test data. The model correctly classified 80% of the predictions from the training data and 67% of the predictions from the test data. Bottom depth and bottom temperature were the most important model variables (relative importance: 0.52, 0.17, and 0.17, respectively). Suitable habitat for adult pygmy rockfish was concentrated along the middle and outer shelf, particularly in the eastern GOA, between Prince of Wales Island and Yakutat (Fig. 199).

Pygmy rockfish distribution in commercial fisheries -- There were two observations of adult pygmy rockfish from commercial fisheries catches during the spring (Fig. 200), therefore these data were not modeled.

Pygmy rockfish essential fish habitat maps and conclusions -- Pygmy rockfish habitat predicted by the modeling is extensively distributed across the eastern and central GOA (Fig. 201).

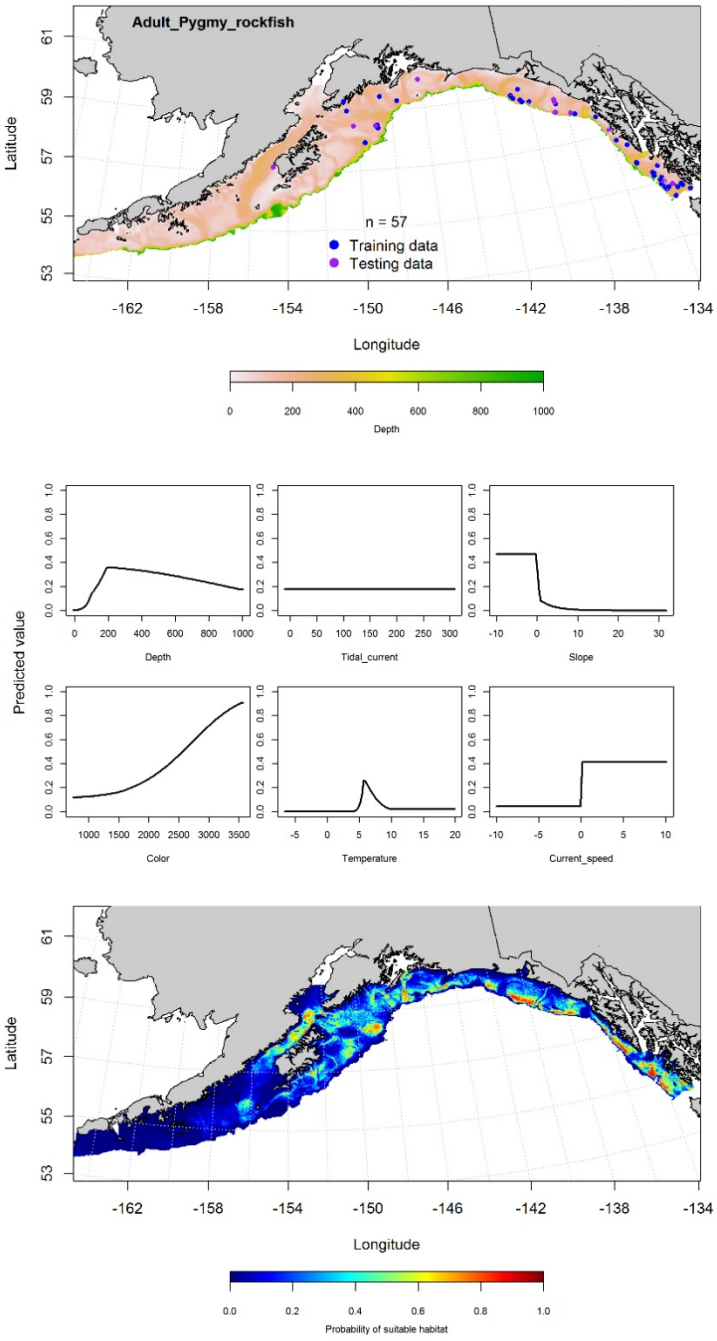

Figure 198. -- Presence of adult pygmy rockfish from RACE-GAP summer bottom trawl surveys (1993-2013) in the Gulf of Alaska (top panel) with training (blue dots) and testing (purple dots) data indicated, maximum entropy (MaxEnt) model effects (center panel), and the MaxEnt-predicted probability of suitable adult pygmy rockfish habitat (bottom panel).

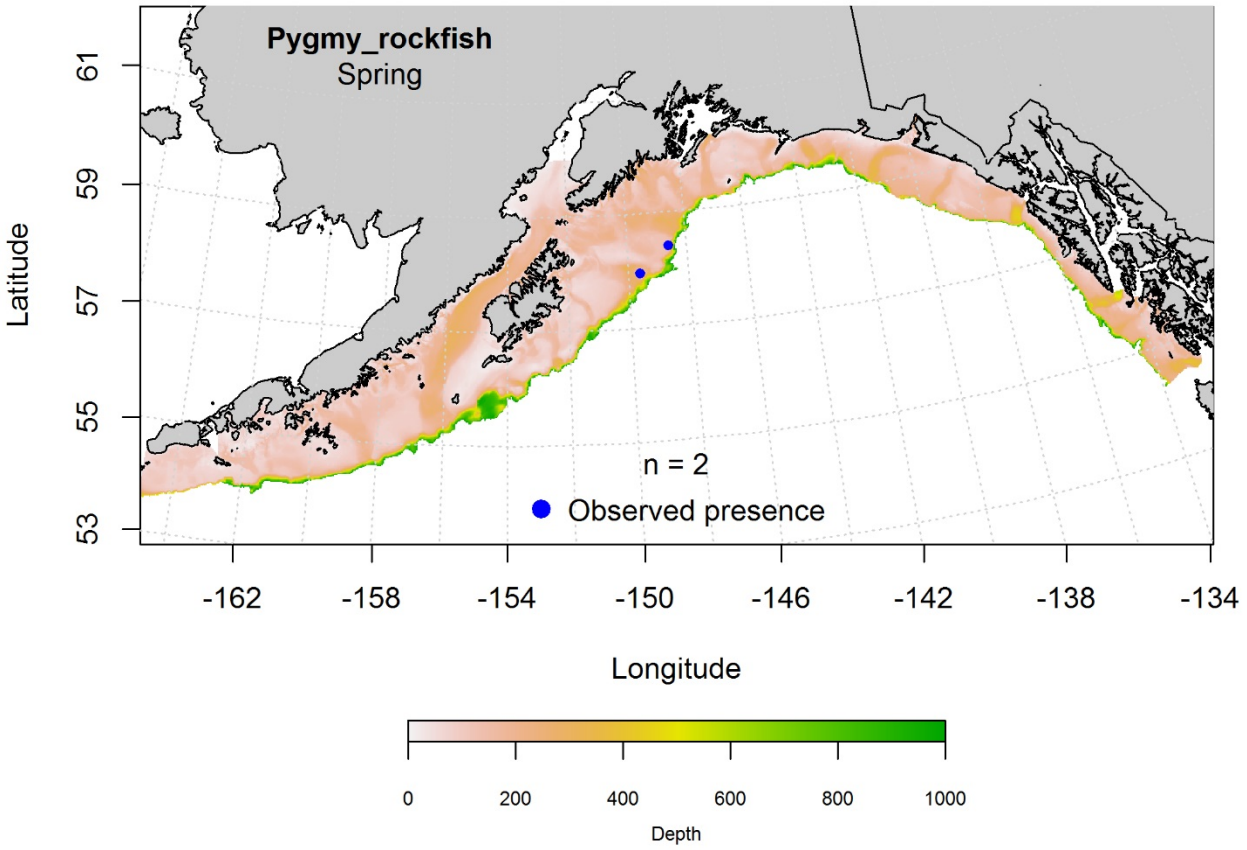

Figure 199. - Locations of pygmy rockfish from spring (March-May 2001-2015) commercial fisheries catches in the Gulf of Alaska.

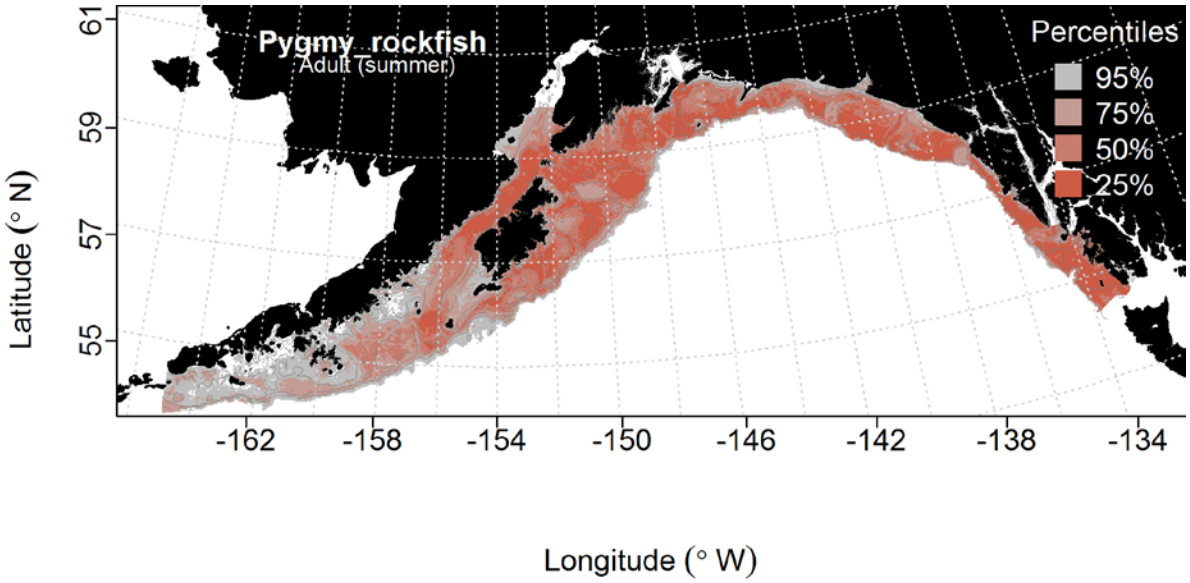

Figure 200. -- Predicted habitat for pygmy rockfish life history stages based on species distribution modeling. Larval stages are shown above in the Pacific ocean perch section (*Sebastes* spp.). Predicted habitat for settled adults are based on RACE-GAP summertime bottom trawl surveys (1993-2013) in the Gulf of Alaska.

Sharpchin Rockfish (*Sebastes zacentrus*)

Juvenile and adult sharpchin rockfish distribution in the bottom trawl survey -- An hGAM was used to predict the distribution of settled juvenile sharpchin rockfish abundance. The PA GAM indicated that geographic location, ocean color, and bottom temperature were the most important variables in the model. The AUC of the model was 0.95 for the training and 0.93 for the test data. The model correctly classified 87% of the predictions from the training data and 86% of the predictions from the test data. The highest predicted probability of presence for settled juvenile sharpchin rockfish was concentrated along the outer shelf in the eastern GOA, particularly off Prince of Wales Island and between Alsek and Yakutat Valley (Fig. 202). The CPUE GAM found geographic location, bottom temperature, and bottom depth were the most important predictors of CPUE. Overall, the hurdle model explained 29% of the variability in the training data and 18% in the test data. The highest CPUE of settled juvenile sharpchin rockfish was predicted to occur near the shelf break in the eastern GOA (Fig. 202).

Bottom depth, bottom current speed, and bottom temperature were the most important variables explaining the distribution of adult sharpchin rockfish (relative importance: 0.58, 0.23, and 0.15, respectively). The MaxEnt model had an AUC of 0.92 for the training data and 0.83 for the test data. The model correctly classified 83% of the predictions from the training data and 81% of the predictions from the test data. Habitat of adult sharpchin rockfish was predicted to occur along the outer shelf across the GOA, with the highest suitable areas concentrated in the eastern GOA (Fig. 203).

Sharpchin rockfish distribution in commercial fisheries -- There were ten records of sharpchin rockfish from commercial fisheries data during the fall (Fig. 204) and one observation from the winter (Fig. 205), therefore these data were not modeled.

In the spring, bottom depth and bottom current speed were the most important model variables (relative importance: 0.41, 0.19, and 0.17, respectively). The AUC of the spring model was 0.98 for the training data and 0.95 for the test data. The model correctly classified 91% of the predictions from the training data and 95% of the predictions from the test data. Sharpchin rockfish suitable habitat was predicted in relatively small areas concentrated in the western GOA, including around Shelikof and Shumagin Gullies (Fig. 206).

Sharpchin rockfish essential fish habitat maps and conclusions -- In general, habitat for settled juvenile sharpchin rockfish was concentrated in deeper areas of the eastern and central GOA (Fig. 207). The predicted distribution of adult sharpchin rockfish habitat was more extensive than that of the juveniles, and include much of the middle and outer shelf across the GOA. The spring distribution of adult sharpchin rockfish habitat was similar to that predicted based on the summer trawl surveys; however, higher suitability habitat tended to be slightly more concentrated near shelf break and in Shelikof Strait (Fig. 207).

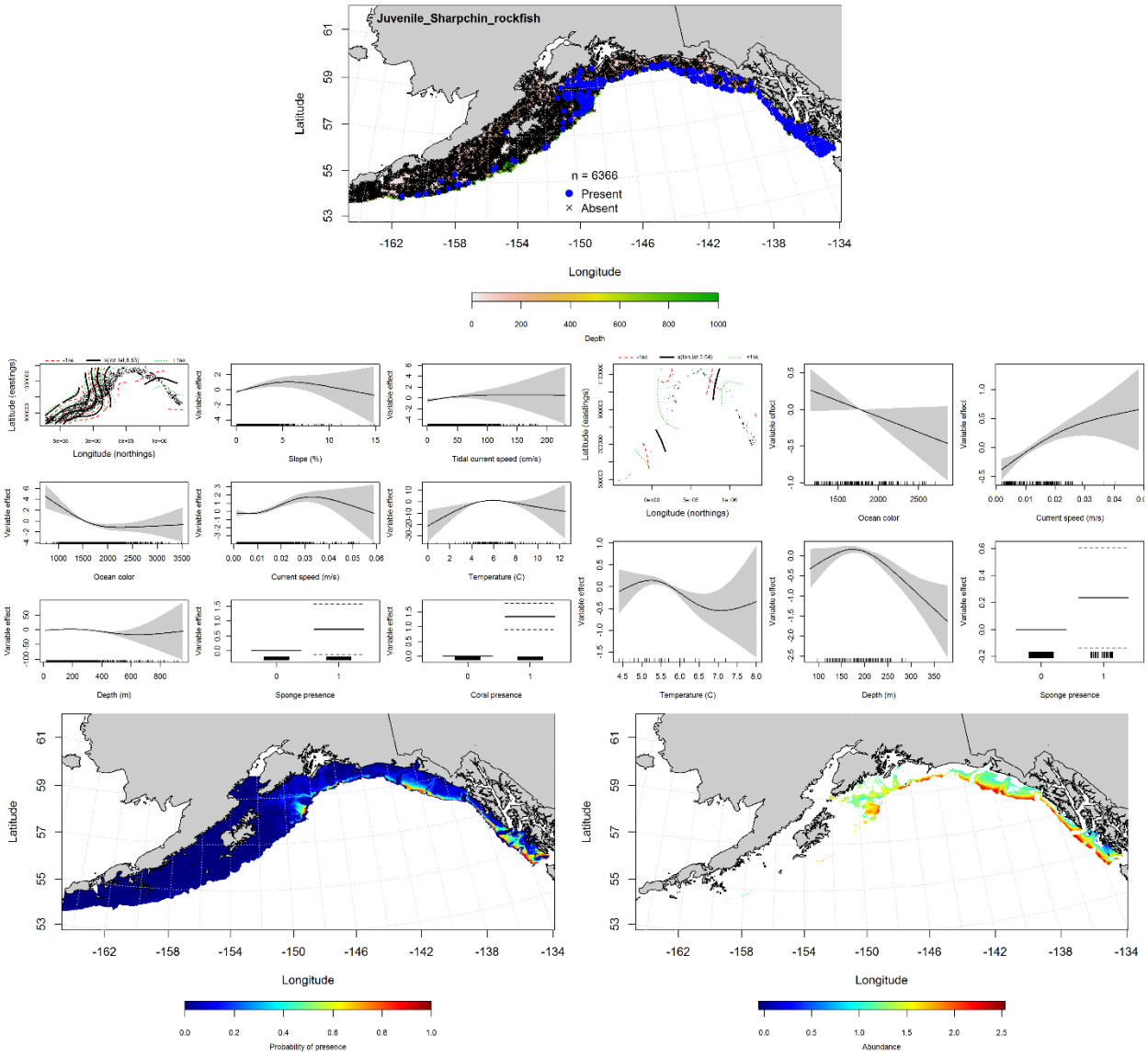

Figure 201. -- Distribution of settled juvenile sharpchin rockfish in 1993-2013 RACE-GAP summer bottom trawl surveys in the Gulf of Alaska (upper panel). Effects of retained habitat covariates in the best fitting generalized additive presence-absence models (PA GAM); left center panel) and abundance (CPUE GAM; right center panel). Predicted spatial distribution of the probability of presence (bottom left panel) and abundance of settled juvenile sharpchin rockfish based on the models (bottom right panel).

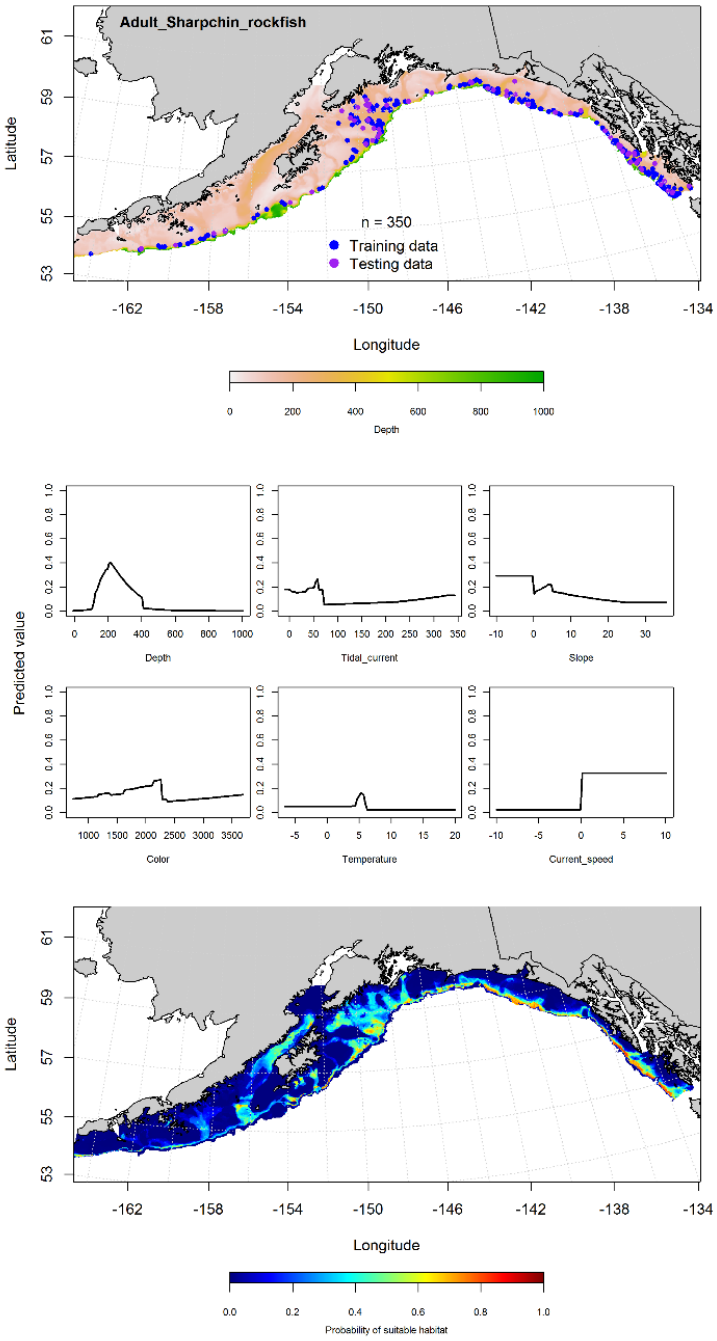

Figure 202. -- Presence of adult sharpchin rockfish from RACE-GAP summer bottom trawl surveys (1993-2013) in the Gulf of Alaska (top panel) with training (blue dots) and testing (purple dots) data indicated, maximum entropy (MaxEnt) model effects (center panel), and the MaxEnt-predicted probability of suitable adult sharpchin rockfish habitat (bottom panel).

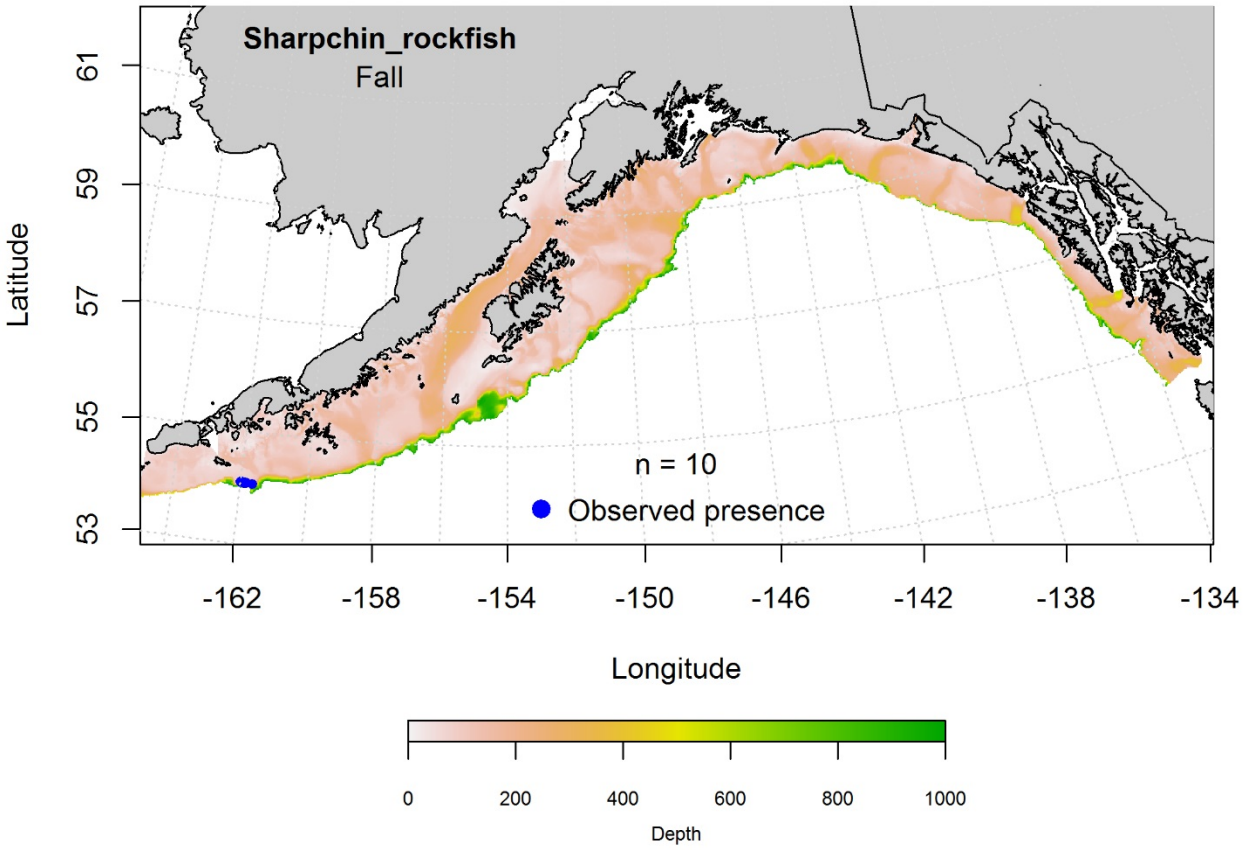

Figure 203. - Locations of sharpchin rockfish from fall (September-November 2001-2015) commercial fisheries catches in the Gulf of Alaska.

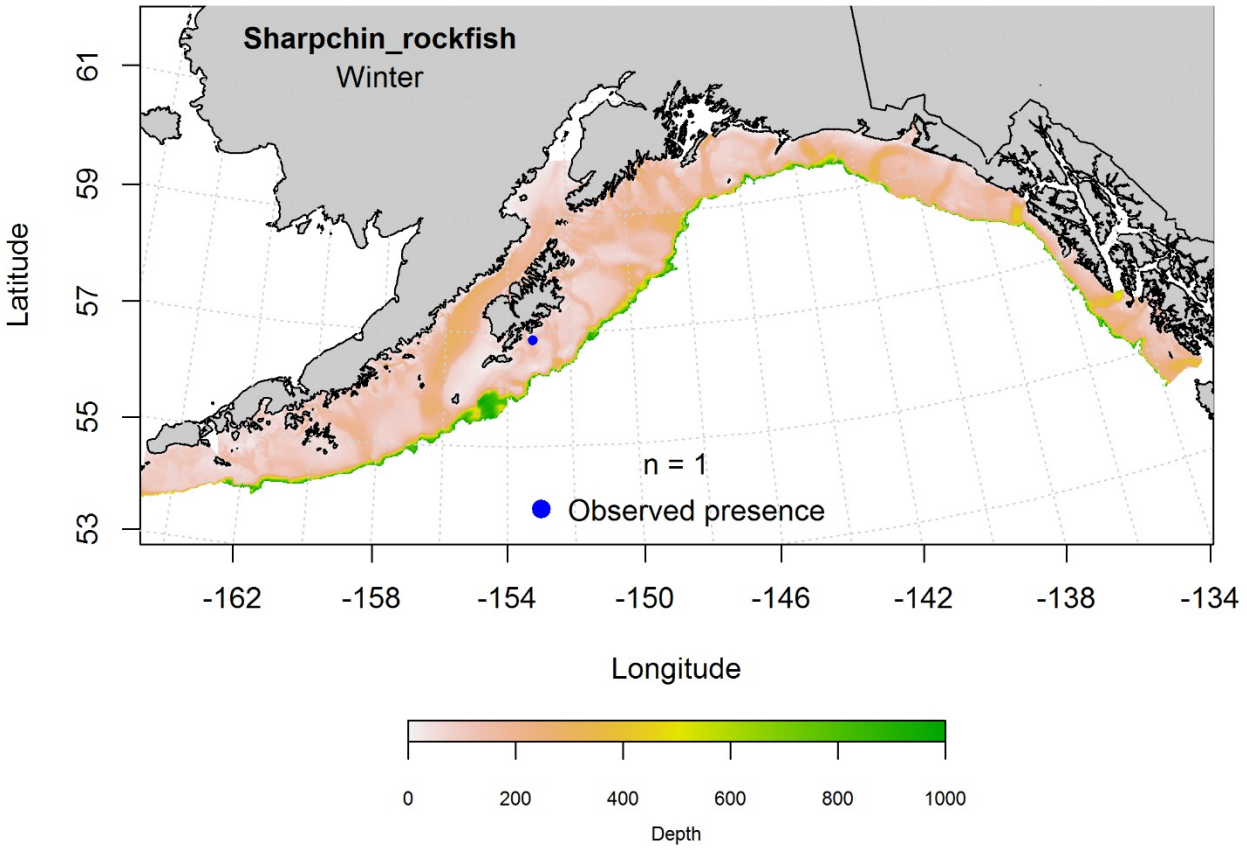

Figure 204. -- Locations of sharpchin rockfish from winter (December-February 2001-2015) commercial fisheries catches in the Gulf of Alaska.

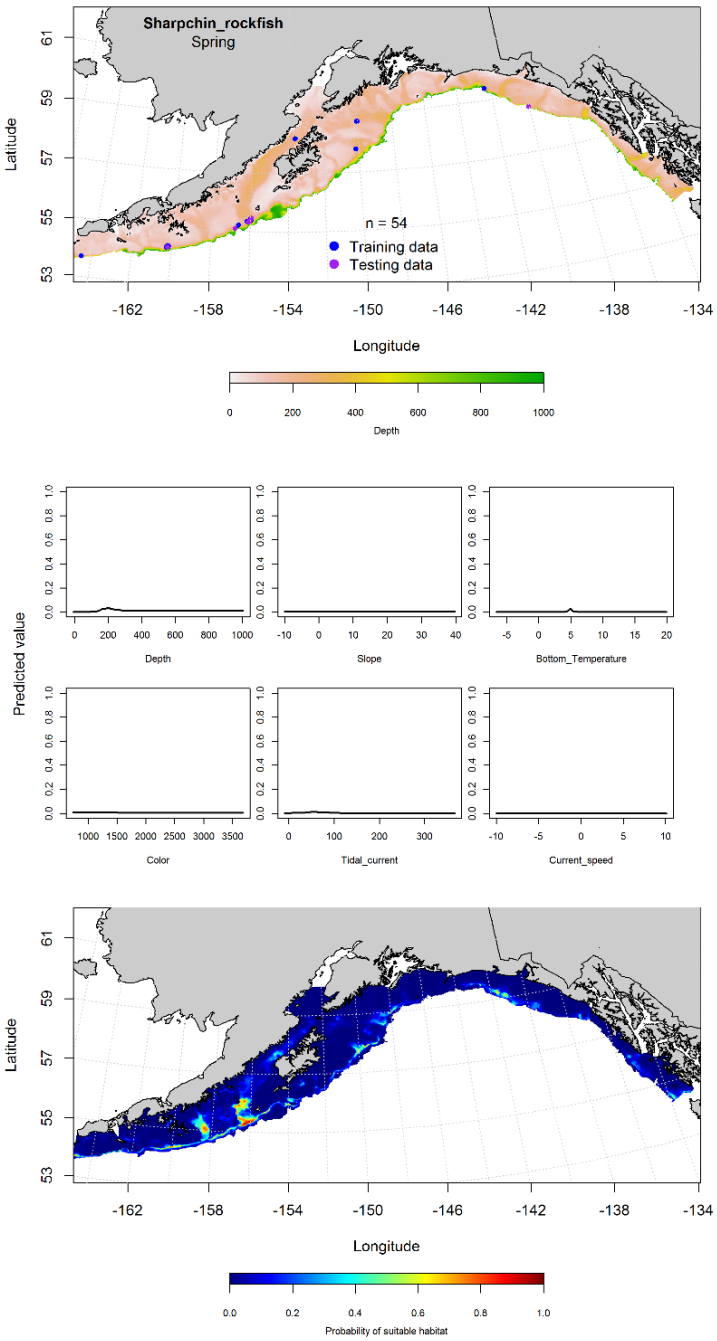

Figure 205. -- Locations of sharpchin rockfish from spring (March-May 2001-2015) commercial fisheries catches in the Gulf of Alaska (top panel), with training (blue dots) and testing (purple dots) data indicated, maximum entropy (MaxEnt) model effects (center panel), and the predicted probability of suitable adult sharpchin rockfish (bottom panel).

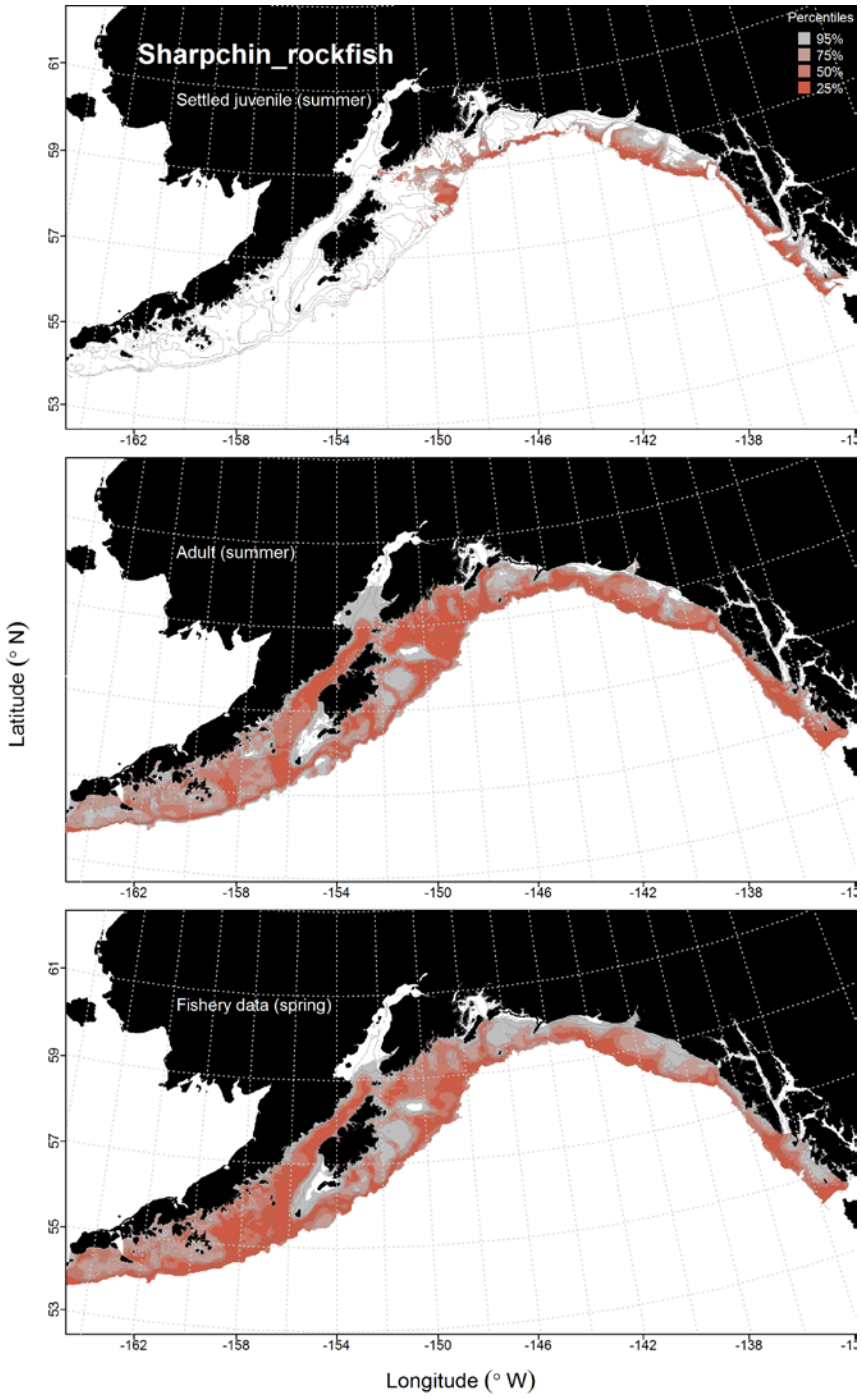

Figure 206. -- Predicted habitat for sharpchin rockfish life history stages based on species distribution modeling. Larval stages are shown above in the Pacific ocean perch section (*Sebastes* spp.). Predicted habitat for settled juveniles and adults are based on RACE-GAP summertime bottom trawl surveys (1993-2013), and predicted presence in commercial fishery catches (2001-2015) from the spring in the Gulf of Alaska.

Shortspine Thornyhead (*Sebastolobus alascanus*)

Early life history stages of shortspine thornyhead -- Shortspine thornyhead eggs and larvae cannot be distinguished from other species in the genus, including longspine thornyhead (*Sebastolobus altivelis*), as a result all observations were combined at the genus level (*Sebastolobus*) for analysis. There were 48 instances of *Sebastolobus* spp. eggs observed in the EcoFOCI collections. These observations were distributed across the GOA; however, there were not enough cases to model (Fig. 208).

There were 30 catches of *Sebastolobus* spp. larvae during the spring and summer. Most were from the central GOA (Fig. 209); however, there were not enough observations to model.

There were no observations of pelagic juvenile *Sebastolobus* spp. in the EcoFOCI collections.

Juvenile and adult shortspine thornyhead distribution in the bottom trawl survey - An hGAM was used to predict the distribution of settled juvenile shortspine thornyhead abundance. The PA GAM indicated that geographic location, bottom depth, and ocean color were the most important model variables. The AUC of the model was 0.98 for both the training data and the test data. The model correctly classified 93% of the predictions from the training data and 94% of the predictions from the test data. The areas of predicted highest presence were concentrated along outer shelf across the GOA (Fig. 210). Geographic location, bottom depth, and maximum tidal current were the most important variables in the CPUE GAM. The model explained 40% of the variance in the training data and 41% in the test data. The highest CPUE for settled juvenile shortspine thornyhead were predicted to occur in deeper areas along the outer shelf (Fig. 210).

An hGAM was used to predict the distribution of adult shortspine thornyhead abundance. The AUC of the PA GAM was 0.98 for both the training data and the test data. Geographic location, ocean color, and slope were the most important variables determining the presence or absence of adult shortspine thornyhead. The model correctly classified 92% of the predictions from the training data and 93% the predictions from the test data. The highest probability of presence was similar in distribution to that predicted for the settled juveniles (primarily along the outer shelf, Fig. 211). Geographic location, bottom depth, bottom current speed, and ocean color were the most important variables in the CPUE GAM. The model explained 55% of the variance in the training data and 59% in the test data. The model predicted the highest CPUE of adult shortspine thornyhead to occur in deeper waters across the GOA (Fig. 211).

Shortspine thornyhead distribution in commercial fisheries -- In the fall, bottom depth, slope, and bottom temperature were the most important variables determining suitable habitat of shortspine thornyhead (relative importance: 0.43, 0.22, and 0.19, respectively). The AUC of the MaxEnt model was 0.95 for the training data and 0.85 for the test data. The model correctly classified 90% of the predictions from the training data and 85% of the predictions from the test data. In the fall, suitable habitat of shortspine thornyhead highest near the shelf break, particularly in the western GOA (Fig. 212).

In the winter, bottom depth, bottom current speed, and maximum tidal current were the most important variables determining suitable habitat of shortspine thornyhead (relative importance: 0.40, 0.36, and 0.12, respectively). The AUC of the MaxEnt model was 0.99 for the training data and 0.96 for the test data. The model correctly classified 94% of the predictions from the training data and 96% of the predictions from the test data. The highest suitability habitats were predicted in the

central GOA, off Albatross and Portlock banks; and in the eastern GOA, off Cape Ommaney and Prince of Wales Island (Fig. 213).

In the spring, bottom depth and slope were the most important variables determining suitable habitat of shortspine thornyhead (relative importance: 0.82 and 0.11, respectively). The AUC of the spring MaxEnt model was 0.97 for the training data and 0.93 for the test data. The model correctly classified 93% of the predictions from both the training and test data. The probability of occurrence for shortspine thornyhead were highest near the shelf break, across the GOA (Fig. 214).

Shortspine thornyhead essential fish habitat maps and conclusions -- Predicted summertime habitat of shortspine thornyhead settled juveniles and adults was similar throughout the GOA (Fig. 215). These habitats were concentrated along the outer shelf at depths greater than 200 m. Shortspine thornyhead habitat, based on commercial fishery data, was more broadly distributed, although still largely concentrated in deeper areas of the middle and outer shelf (Fig. 215).

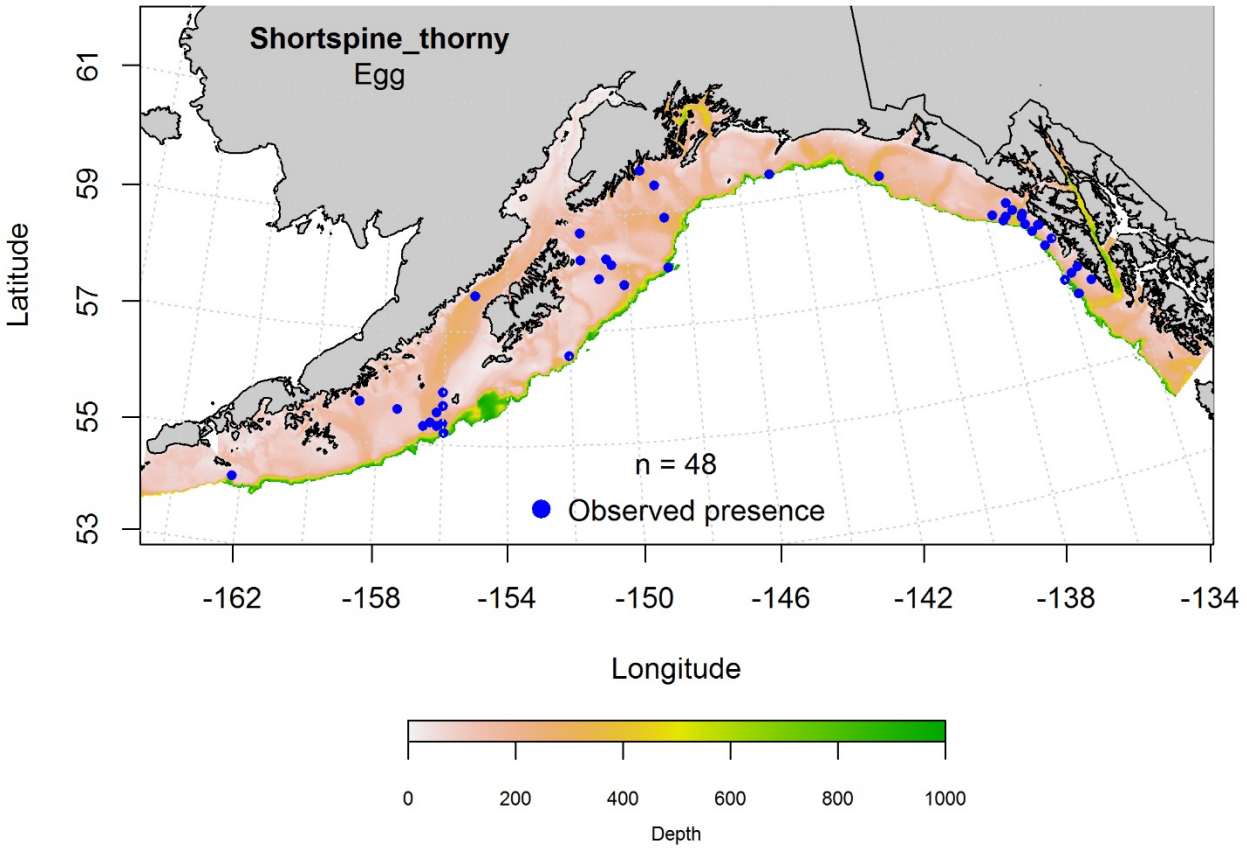

Figure 207. -- Distribution of *Sebastolobus* spp eggs from EcoFOCI ichthyoplankton surveys (January-March 1991-2013).

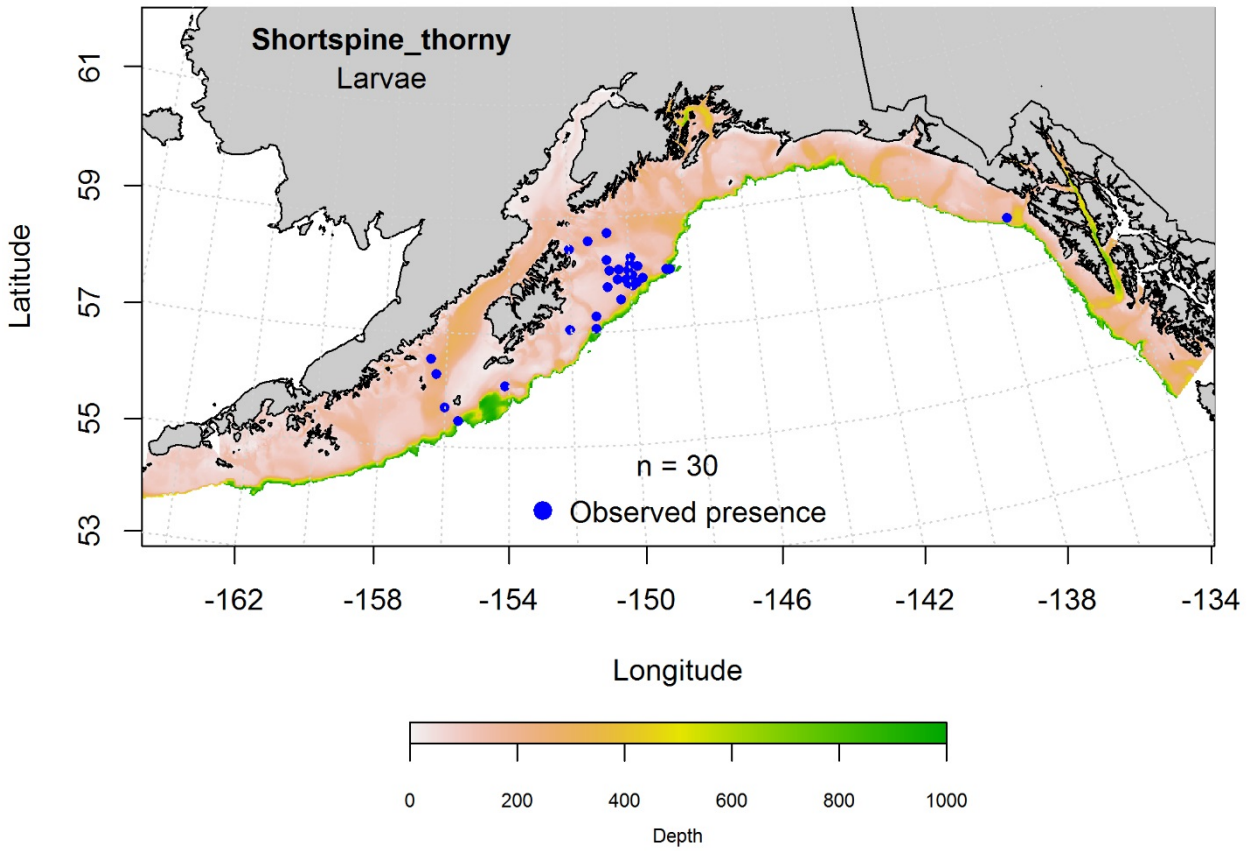

Figure 208. -- Distribution of pelagic *Sebastolobus* spp. larvae observations from EcoFOCI ichthyoplankton surveys (April-September 1991-2012) in the Gulf of Alaska.

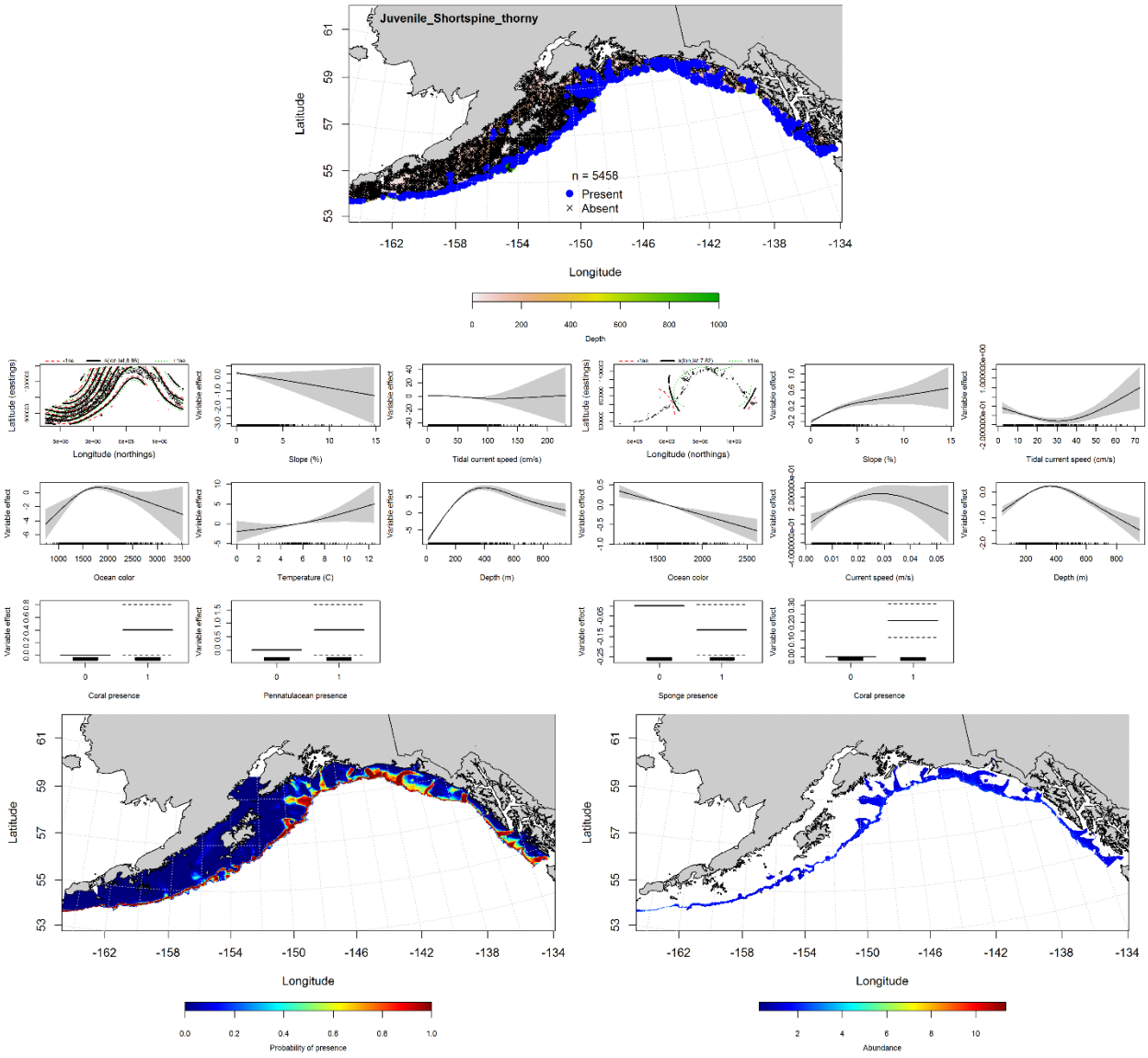

Figure 209. -- Distribution of settled juvenile shortspine thornyhead in 1993-2013 RACE-GAP summer bottom trawl surveys conducted in the Gulf of Alaska (upper panel). Effects of retained habitat covariates in the best fitting generalized additive presence-absence models (PA GAM; left center panel) and abundance (CPUE GAM; right center panel). Predicted spatial distribution of the probability of presence (bottom left panel) and abundance of settled juvenile shortspine thornyhead based on the models (bottom right panel).

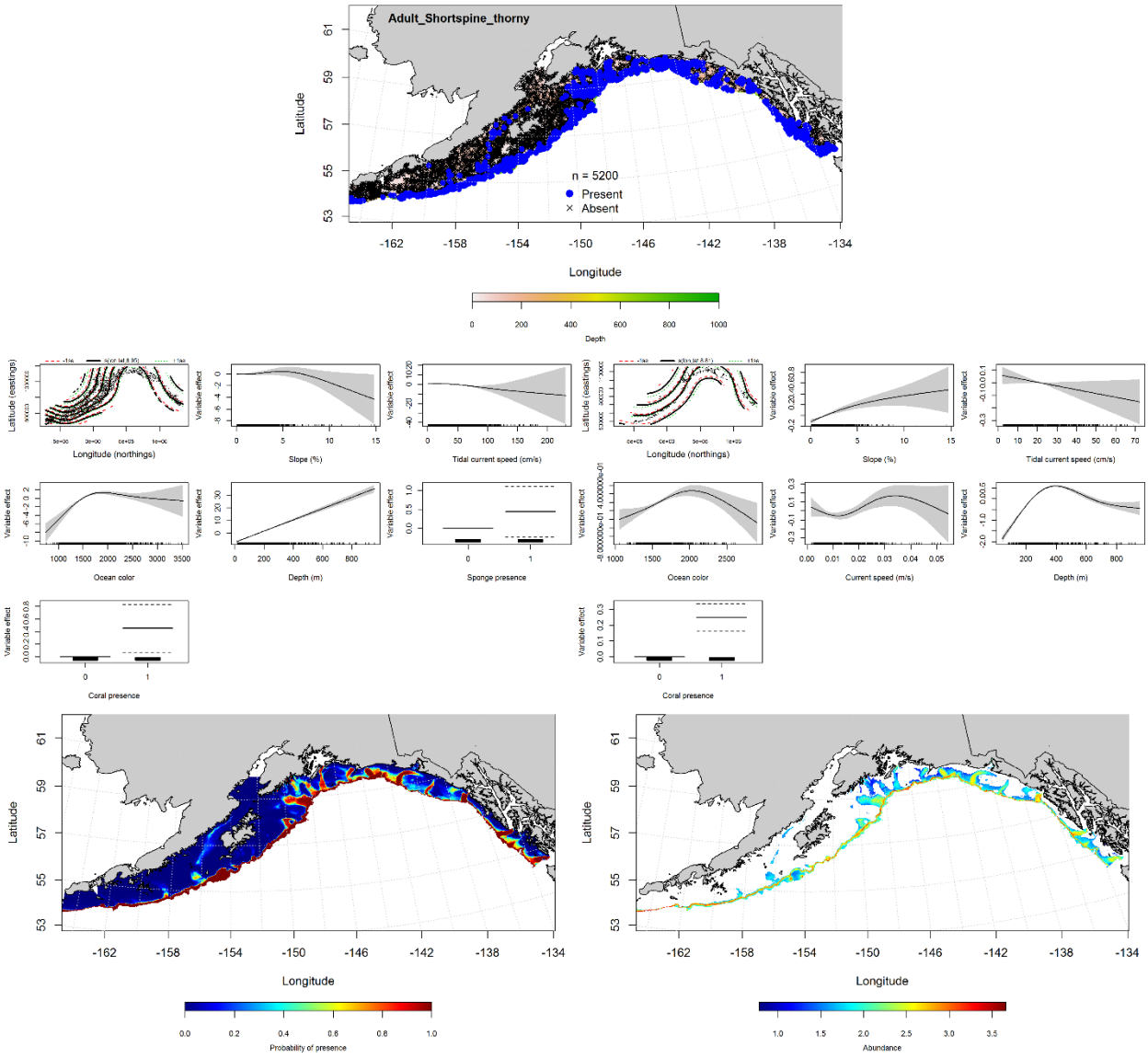

Figure 210. -- Distribution of adult shortspine thornyhead in 1993-2013 RACE-GAP summer bottom trawl surveys conducted in the Gulf of Alaska (upper panel). Effects of retained habitat covariates in the best fitting generalized additive presence-absence models (PA GAM; left center panel) and abundance (CPUE GAM; right center panel). Predicted spatial distribution of the probability of presence (bottom left panel) and abundance of adult shortspine thornyhead based on the models (bottom right panel).

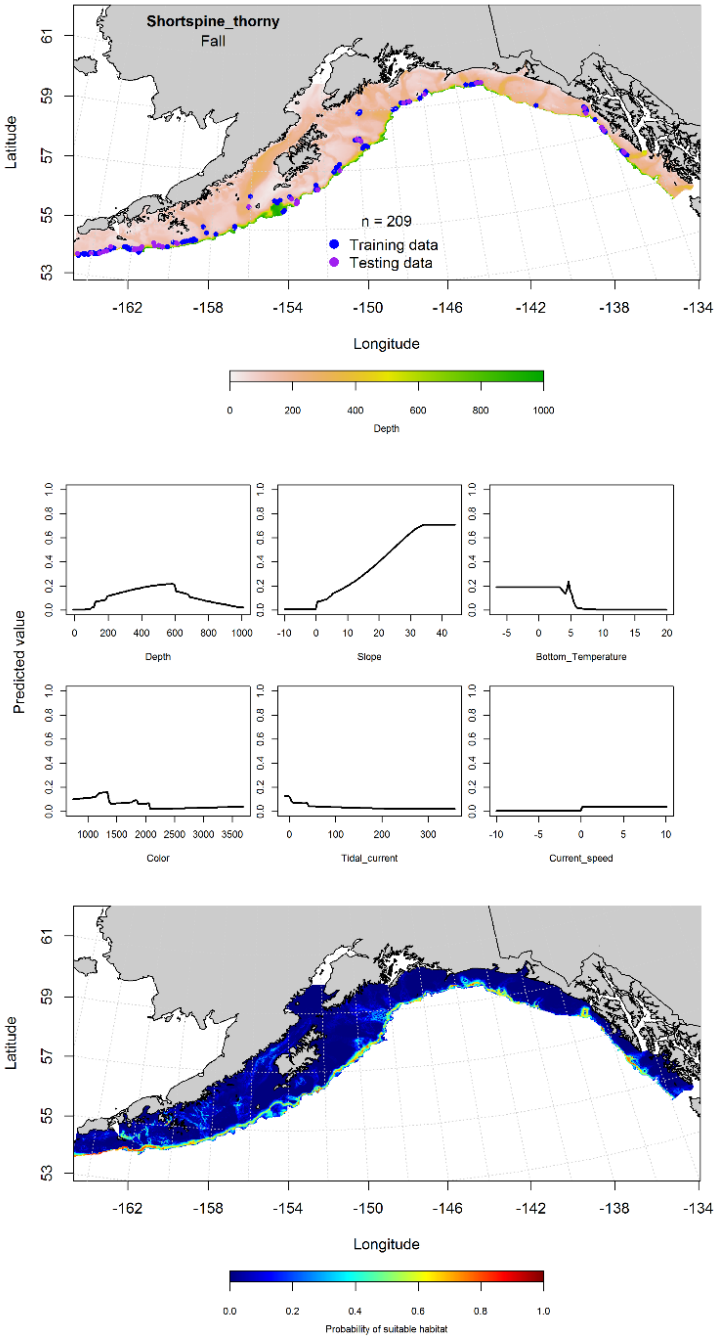

Figure 211. -- Locations of shortspine thornyhead from fall (September-November 2001-2015) commercial fisheries catches in the Gulf of Alaska (top panel), MaxEnt model effects (middle panels), and predicted probability of suitable habitat for shortspine thornyhead based on the model (bottom panel).

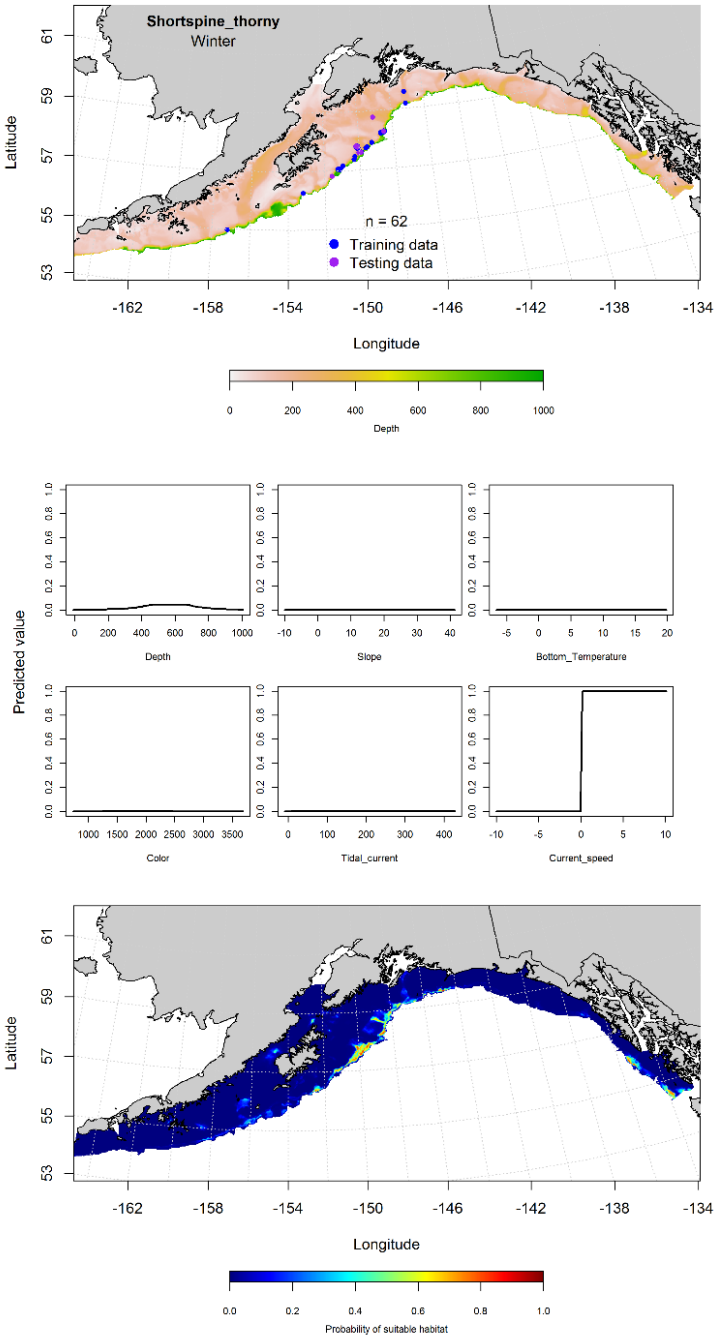

Figure 212. -- Locations of shortspine thornyhead from winter (December-February 2001-2015) commercial fisheries catches in the Gulf of Alaska (top panel), with training (blue dots) and testing (purple dots) data indicated, maximum entropy (MaxEnt) model effects (center panel), and the predicted probability of suitable adult shortspine thornyhead habitat (bottom panel).

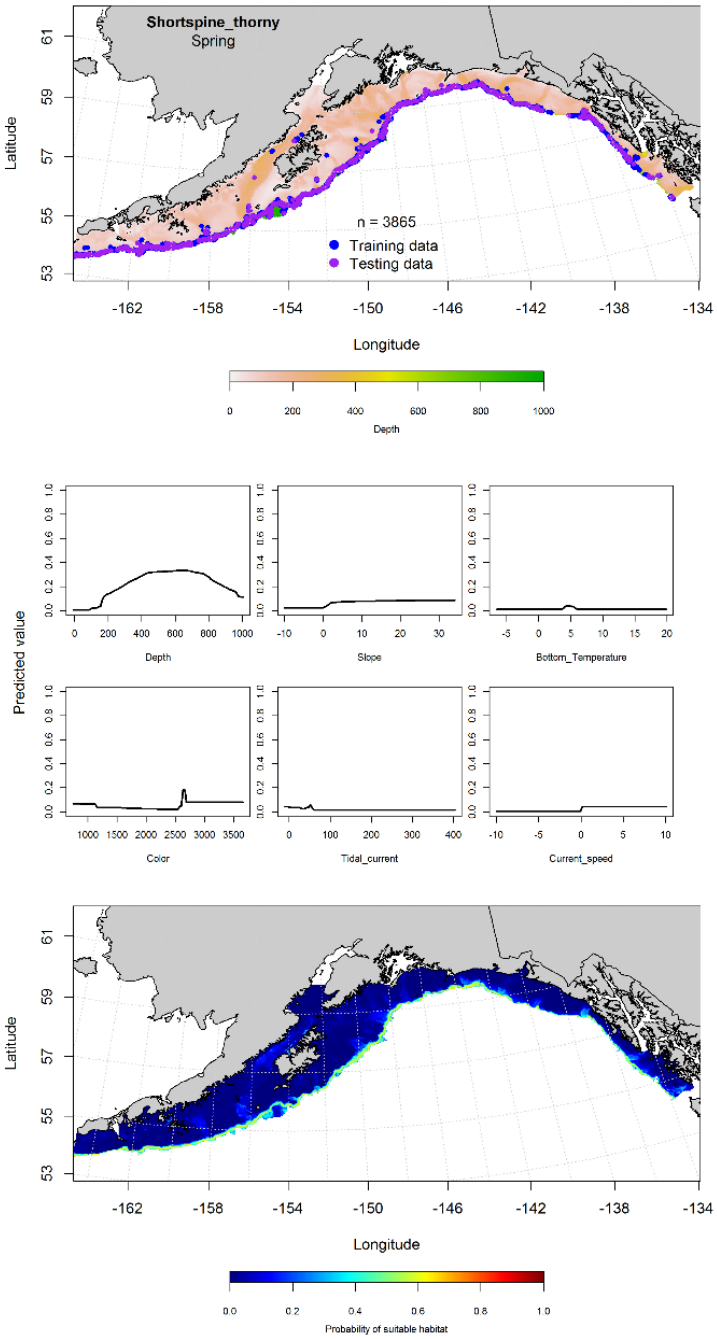

Figure 213. -- Locations of shortspine thornyhead from spring (March-May 2001-2015) commercial fisheries catches in the Gulf of Alaska (top panel), with training (blue dots) and testing (purple dots) data indicated, maximum entropy (MaxEnt) model effects (center panel), and the predicted probability of suitable adult shortspine thornyhead (bottom panel).

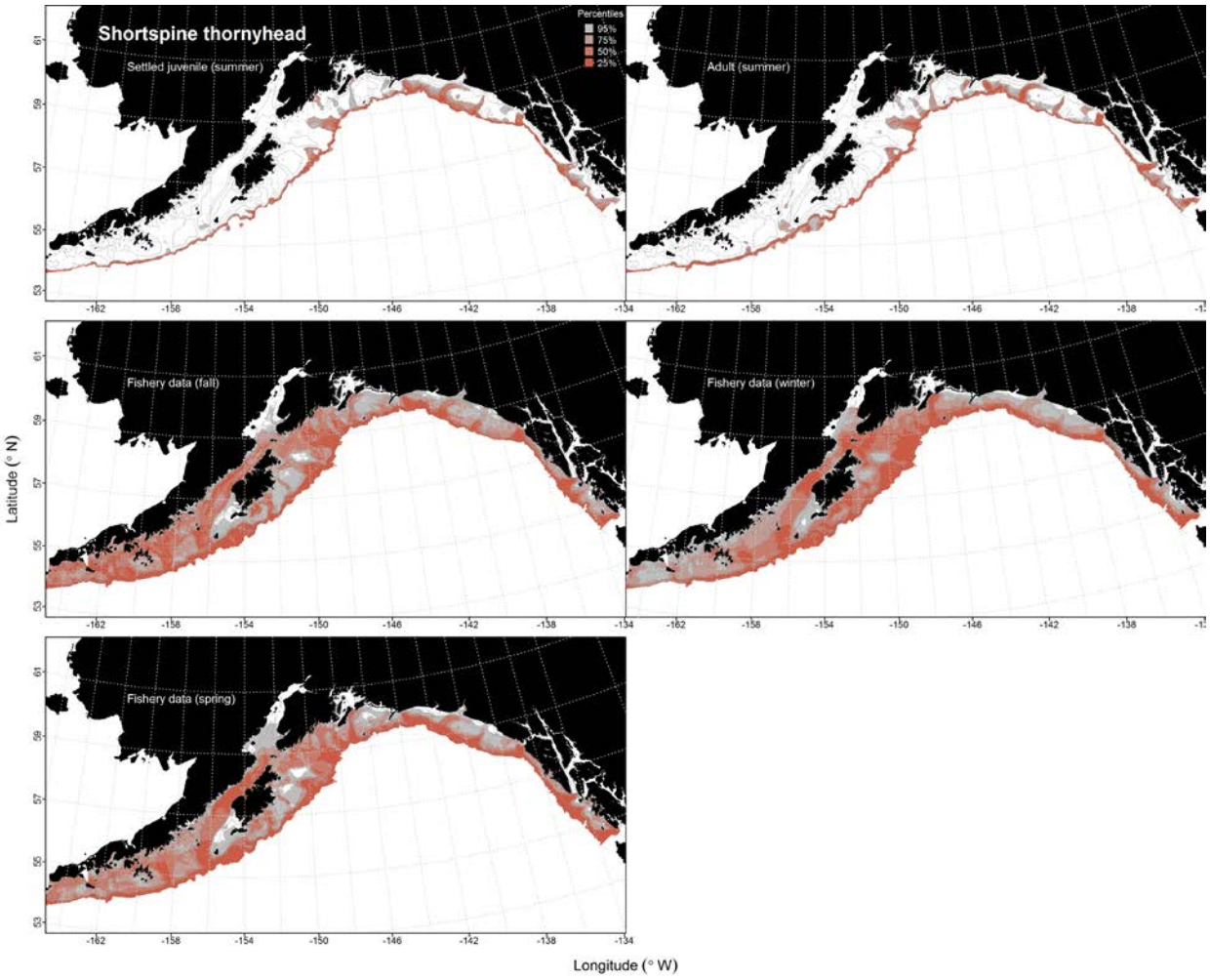

Figure 214. -- Predicted habitat for shortspine thornyhead life history stages based on species distribution modeling. Predicted habitat for settled juveniles and adults are based on RACE-GAP summertime bottom trawl surveys (1993-2013), and predicted presence in commercial fishery catches (2001-2015) from the fall, winter, and spring in the Gulf of Alaska.

Longspine Thornyhead (*Sebastolobus altivelis*)

Early life history stages of longspine thornyhead - See section above (shortspine thornyhead) for distribution models based on the combined *Sebastolobus* spp. ELHS.

Juvenile and adult longspine thornyhead distribution in the bottom trawl survey -- There were no observations of settled juvenile longspine thornyhead rockfish during the summer trawl survey.

A MaxEnt model predicting suitable habitat of adult longspine thornyhead rockfish had an AUC of 1.00 for the training data and 0.95 for the test data. It correctly classified 98% of the training data and 95% of the test data. Bottom depth and bottom temperature were the most important variables explaining the probability of suitable habitat for longspine thornyheads (relative importance: 0.85, and 0.09, respectively). The highest probability of suitable habitat was predicted on the continental slope (> 200 m) across the GOA (Fig. 216). However, this distribution likely underestimates the actual distribution of longspine thornyhead since trawl survey data were collected from 1,000 m depth and this species is typically found between 201 and 1,756 m (Love et al. 2005).

Longspine thornyhead distribution in commercial fisheries -- There were no observations of longspine thornyhead rockfish from commercial fisheries catches during either the fall or the winter.

A MaxEnt model was used to predict the suitable habitat of longspine thornyhead during the spring. The AUC of the model was 0.93 for the training data and 0.92 for the testing data. The model correctly classified 89% of the predictions from the training data and 92% of the predictions from the test data. The most important habitat covariates were bottom depth and slope (relative importance 0.71 and 0.17, respectively). The model predicted that the probability of suitable habitat of longspine

thornyhead rockfish was highest near the shelf break, particularly between Albatross Bank and Cape St. Elias in the central GOA, and off Baranof Island in the eastern GOA (Fig. 217).

Longspine thornyhead rockfish essential fish habitat maps and conclusions -- Summertime habitat of adult longspine thornyhead was distributed across the GOA but core habitat was predicted to be in deeper water along the shelf break and in submarine canyons (Fig. 218). Essential longspine thornyhead habitat predicted from springtime commercial catches was similarly distributed at deeper depths and near the shelf break (Fig. 218).

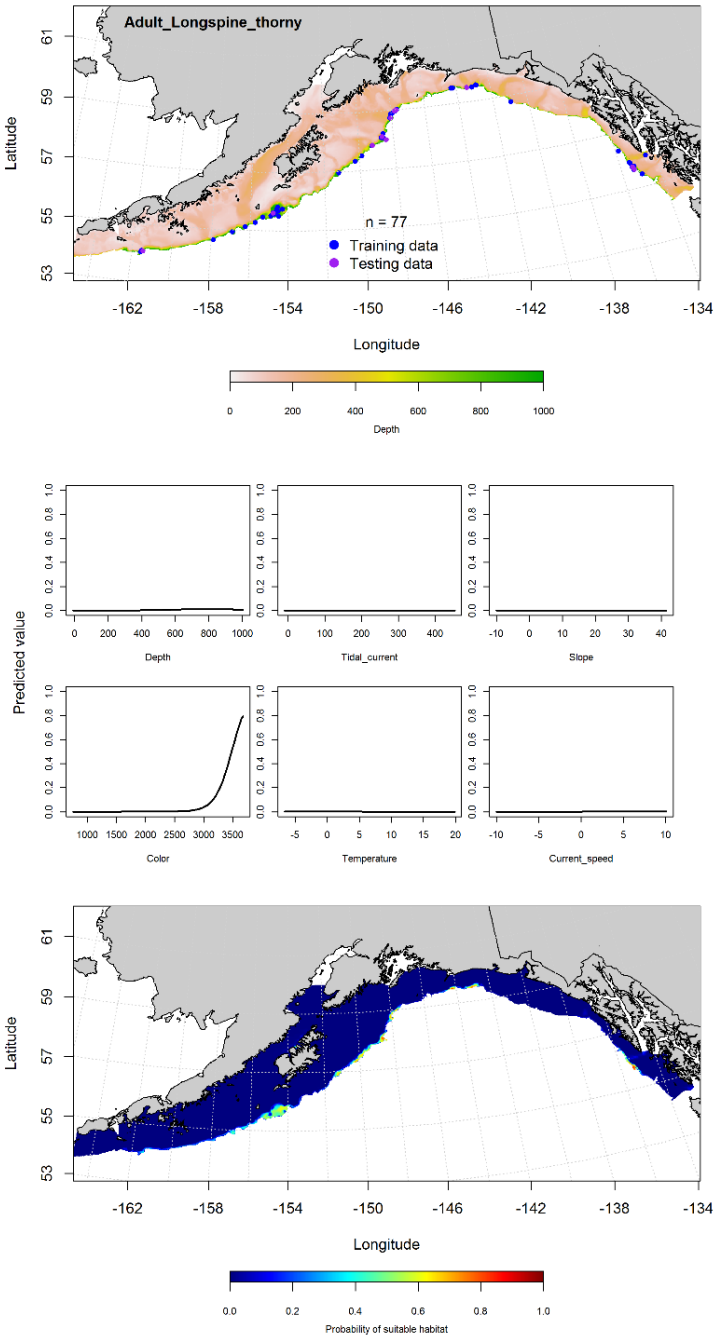

Figure 215. -- Catches of adult longspine thornyhead from RACE-GAP summer bottom trawl surveys (1993-2013) in the Gulf of Alaska (top panel), significant relationships between CPUE and environmental variables in the best fitting generalized additive model (GAM; middle panels), and the GAM-predicted abundance of adult longspine thornyhead (bottom panel).

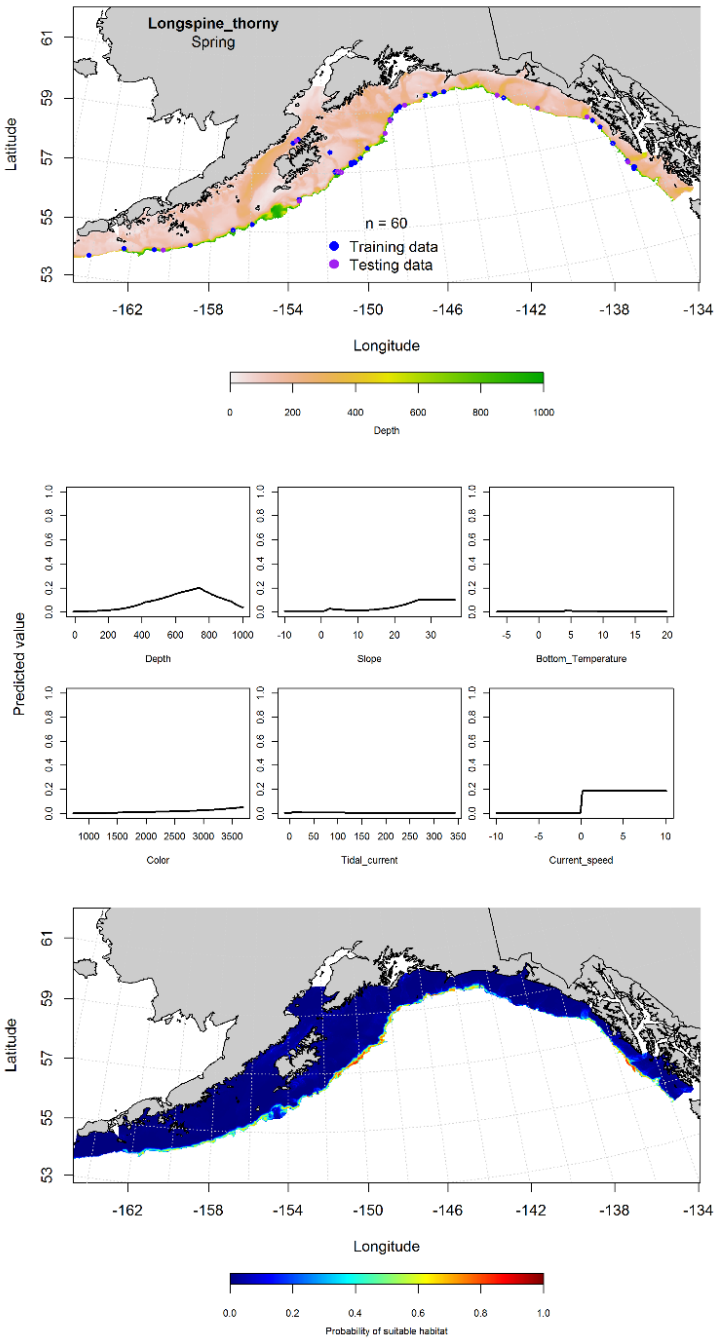

Figure 216. -- Locations of longspine thornyhead from spring (March-May 2001-2015) commercial fisheries catches in the Gulf of Alaska (top panel), with training (blue dots) and testing (purple dots) data indicated, maximum entropy (MaxEnt) model effects (center panel), and the predicted probability of suitable adult longspine thornyhead (bottom panel).

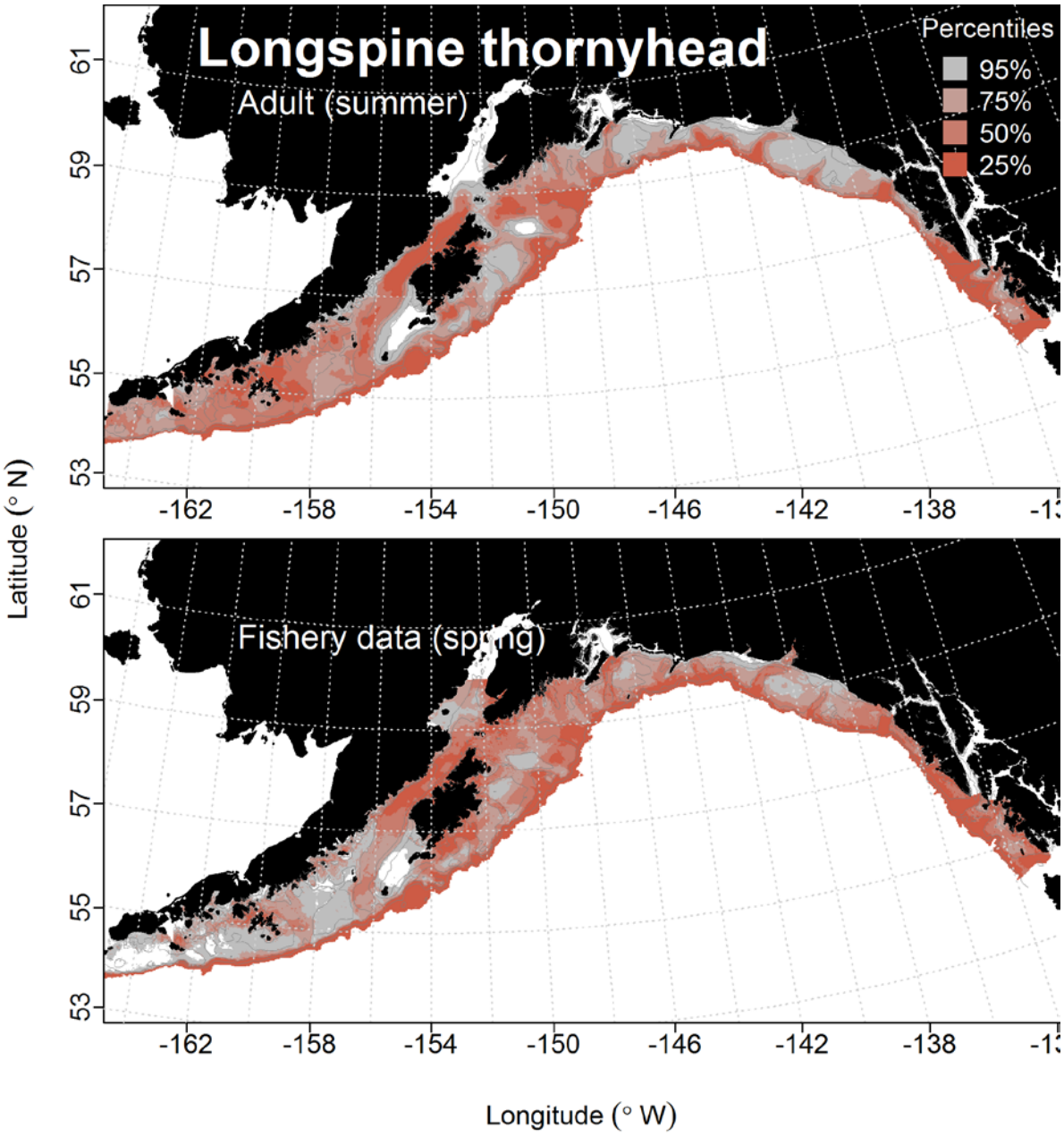

Figure 217. -- Habitat predicted for adult longspine thornyhead from RACE-GAP summertime bottom trawl surveys (1993-2013), and predicted from presence in commercial fishery catches (2001-2015) from spring in the Gulf of Alaska.

Skates

Early life history information for skates is limited and early life stages of skates are not available to EcoFOCI ichthyoplankton surveys nor are they reliably available to our GOA bottom trawl. Skates lay benthic eggs in nurseries in Alaska (Hoff 2010) that are typically small areas with high concentrations of eggs on the outer continental shelf and upper slope in the GOA (J. Hoff, AFSC, pers. comm.). These eggs hatch competent live pups. This early life strategy employed by skates eliminated the possibility of building SDMs for skate ELHS based on the data available to us at this time.

Alaska Skate (*Bathyraja parmifera*)

Juvenile and adult Alaska skate distribution in the bottom trawl survey -- A MaxEnt model predicting suitable habitat of settled juvenile Alaska skate had an AUC of 0.79 for the training data and 0.63 for the test data. The model correctly classified 67% of the predictions from the training data and 63% of the predictions from the test data. Bottom depth and bottom temperature were the most important variables predicting settled juvenile Alaska skate habitat suitability (relative importance: 0.57 and 0.27, respectively). The settled juvenile Alaska skate model predicted the highest probability of suitable habitat in deeper depths along the Alaska Peninsula (Fig. 219).

A MaxEnt model predicting suitable habitat of adult Alaska skate had AUCs of 0.73 for the training and 0.50 for the test data. The model correctly classified 69% of the predictions from the training data and 50% of the predictions from the test data. Depth and ocean color were the most important variables explaining the distribution of adult Alaska skate suitable habitat. Maximum tidal current, bottom depth, and ocean color were the most important variables explaining the distribution of adult Alaska skate (relative importance: 0.46, 0.30, and 0.14, respectively). The model predicted

the highest probability of suitable habitat in the western GOA, particularly off Unimak Island (Fig. 220).

Alaska skate distribution in commercial fisheries -- In the fall, ocean color and bottom depth were the most important variables determining the distribution of Alaska skate (relative importance: 0.69, 0.18, and 0.06, respectively). The AUC of the fall MaxEnt model was 0.95 for the training data and 0.86 for the test data. The model correctly classified 88% of the predictions from the training data and 86% of the predictions from the test data. Suitable habitat of Alaska skate was predicted in a few locations, mostly notably off Unimak Island and on Chirikof Bank (Fig. 221).

In the winter, bottom depth, bottom current speed, and ocean color were the most important variables predicting the distribution of Alaska skate (relative importance: 0.38, 0.24, and 0.23, respectively). The AUC of the winter MaxEnt model was 0.95 for the training data, 0.81 for the test data. The model correctly classified 87% of the predictions from the training data and 81% of the predictions from the test data. The model predicted a patchy distribution of suitable habitat for Alaska skate, with the highest probabilities of occurrence predicted off Unimak Island (Fig. 222).

In the spring, ocean color, current speed, and bottom depth were again the most important variables determining the distribution of Alaska skate (relative importance: 0.34, 0.22, and 0.20, respectively). The AUC of the spring MaxEnt model was 0.93 for the training data and 0.69 for the test data. The model correctly classified 85% of the predictions from the training data and 69% of the predictions from the test data. The model predicted suitable of Alaska skate habitat was concentrated near the shelf break in the eastern and central GOA, and more broadly distributed throughout the western GOA, particularly off Unimak Island (Fig. 223).

Alaska skate essential fish habitat maps and conclusions -- Predicted summertime habitat of Alaska skate settled juveniles was broadly distributed on the middle and outer shelf throughout the GOA (Fig. 224). Predicted habitat of Alaska skate adults was similar to the juveniles (Fig. 224). The fall, winter, and spring distribution of Alaska skate habitat was essentially the same throughout the seasons (Fig. 224). Areas of higher predicted habitat were concentrated in the western GOA, near Unimak Island and the Alaska Peninsula, as well as in the central GOA, on Albatross and Portlock banks.

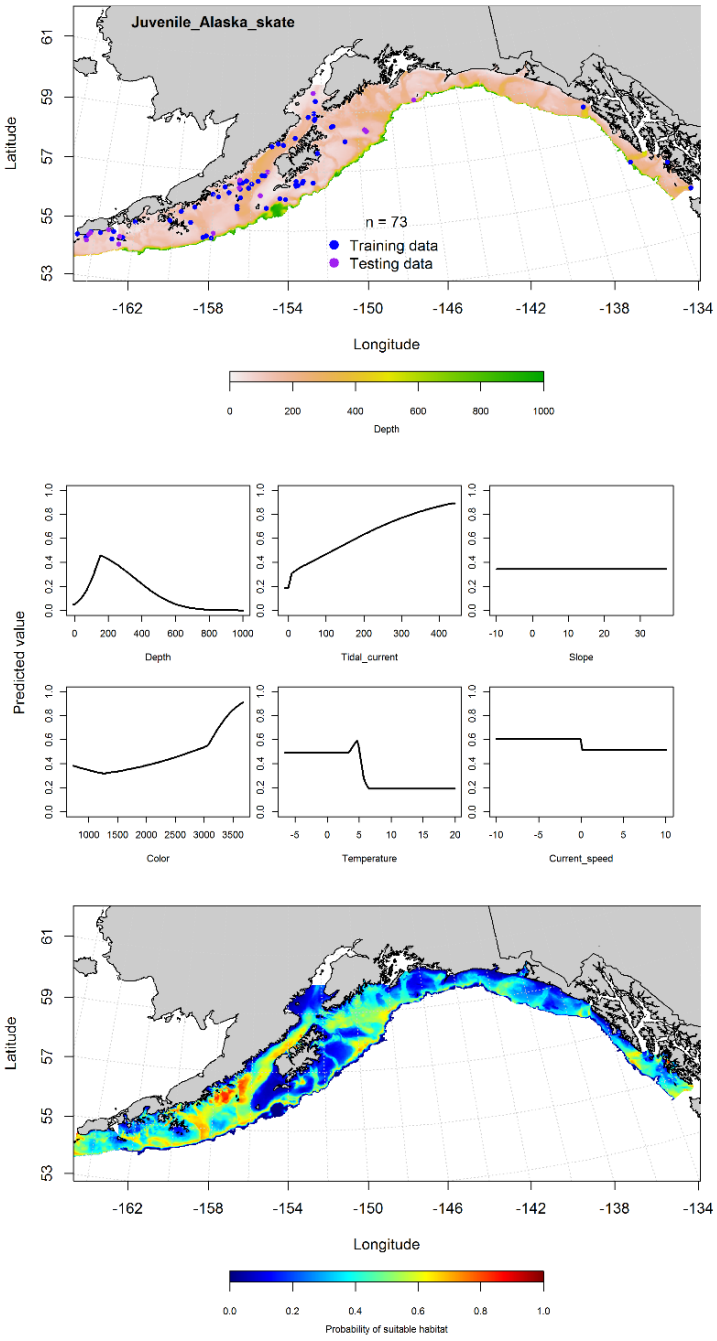

Figure 218. -- Presence of settled juvenile Alaska skate from RACE-GAP summer bottom trawl surveys (1993-2013) in the Gulf of Alaska (top panel) with training (blue dots) and testing (purple dots) data indicated, maximum entropy (MaxEnt) model relationships between probability of juvenile presence and habitat covariates (center panel), and the MaxEnt-predicted probability of suitable juvenile Alaska skate habitat (bottom panel).

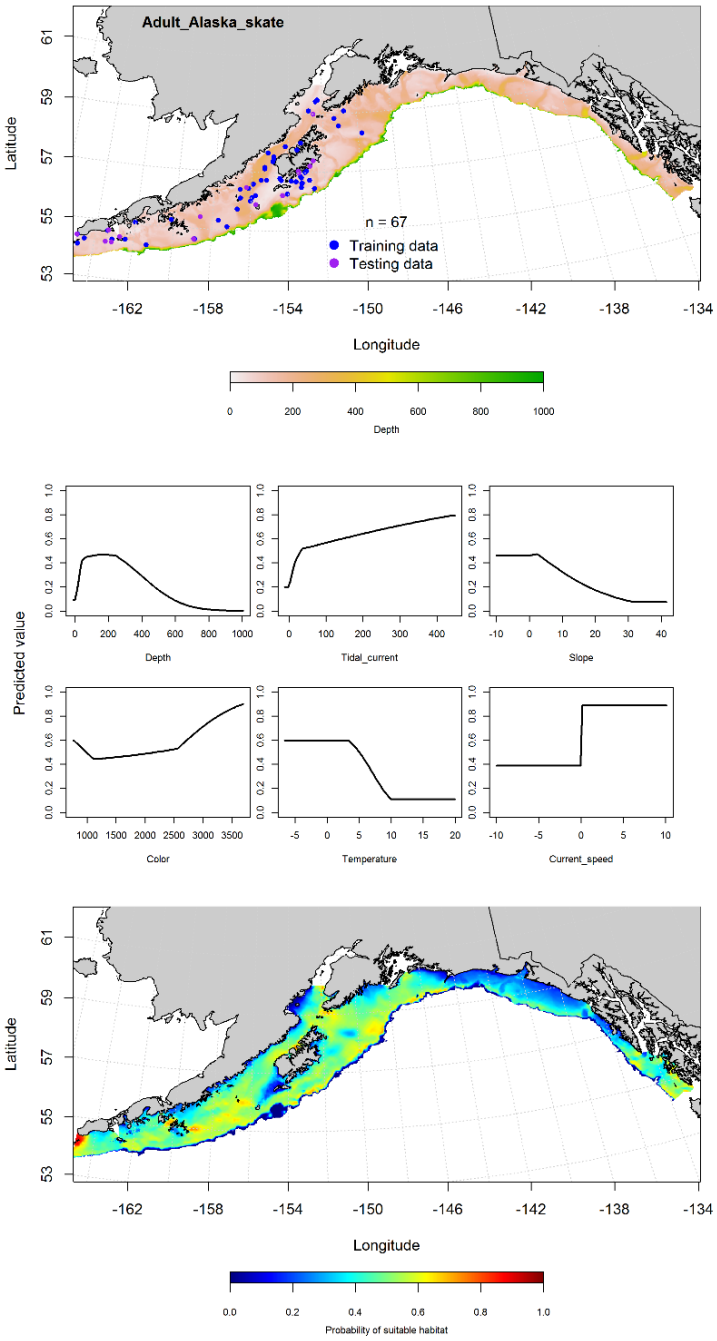

Figure 219. -- Presence of adult Alaska skate from RACE-GAP summer bottom trawl surveys (1993-2013) in the Gulf of Alaska (top panel) with training (blue dots) and testing (purple dots) data indicated, maximum entropy (MaxEnt) model effects (center panel), and the MaxEnt-predicted probability of suitable adult Alaska skate habitat (bottom panel).

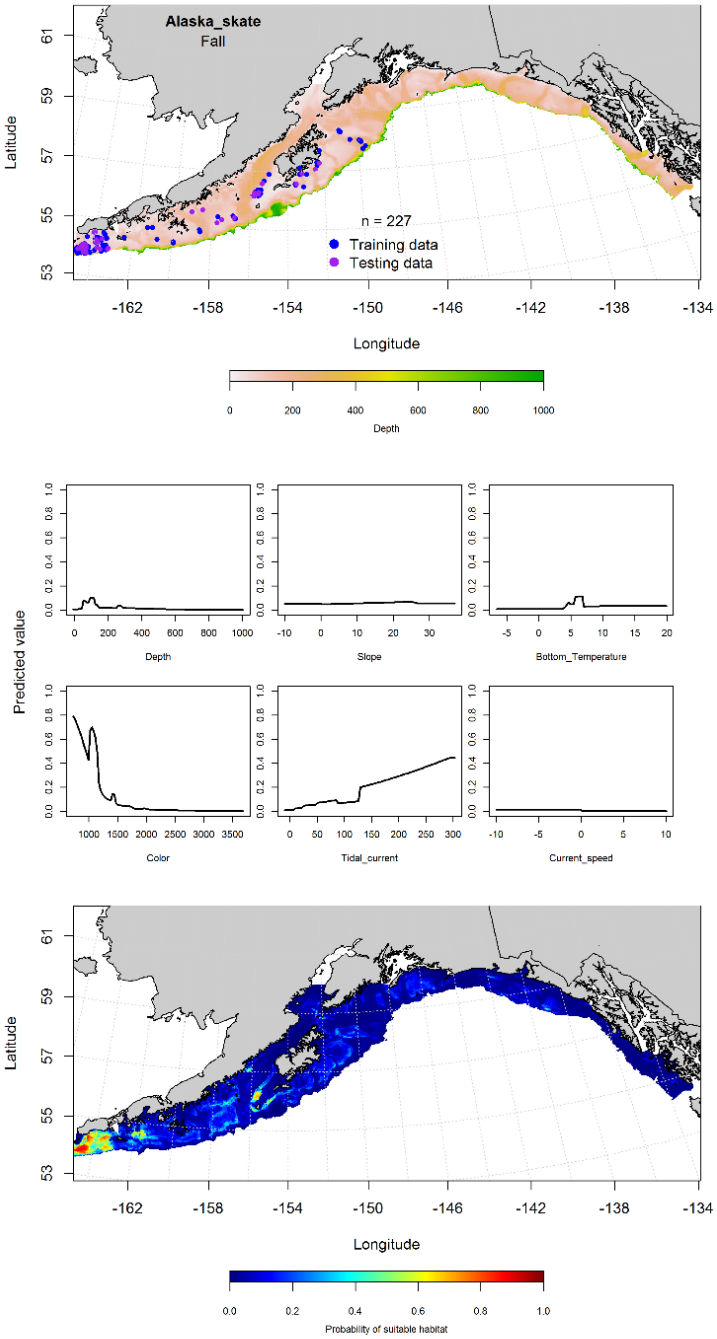

Figure 220. -- Locations of Alaska skate from fall (September-November 2001-2015) commercial fisheries catches in the Gulf of Alaska (top panel), MaxEnt model effects (middle panels), and predicted probability of suitable habitat for Alaska skate based on the model (bottom panel).

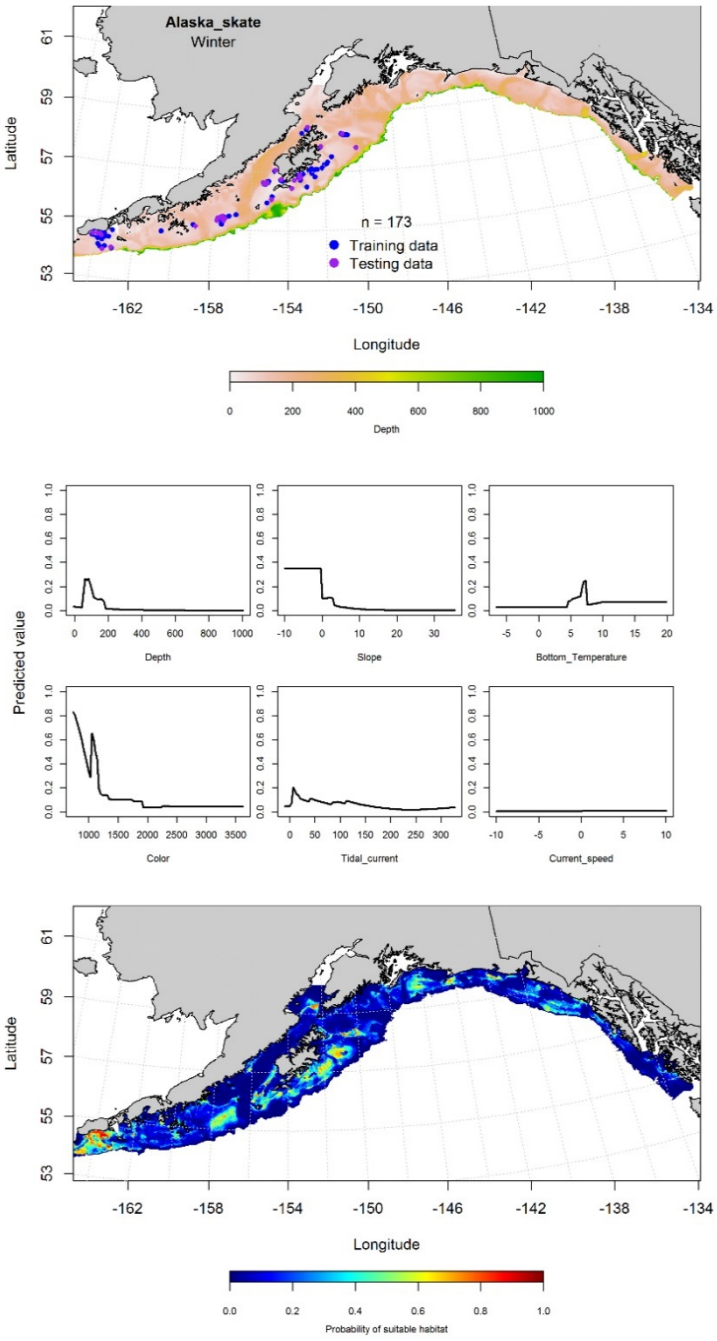

Figure 221. -- Locations of Alaska skate from winter (December-February 2001-2015) commercial fisheries catches in the Gulf of Alaska (top panel), with training (blue dots) and testing (purple dots) data indicated, maximum entropy (MaxEnt) model effects (center panel), and the predicted probability of suitable adult Alaska skate habitat (bottom panel).

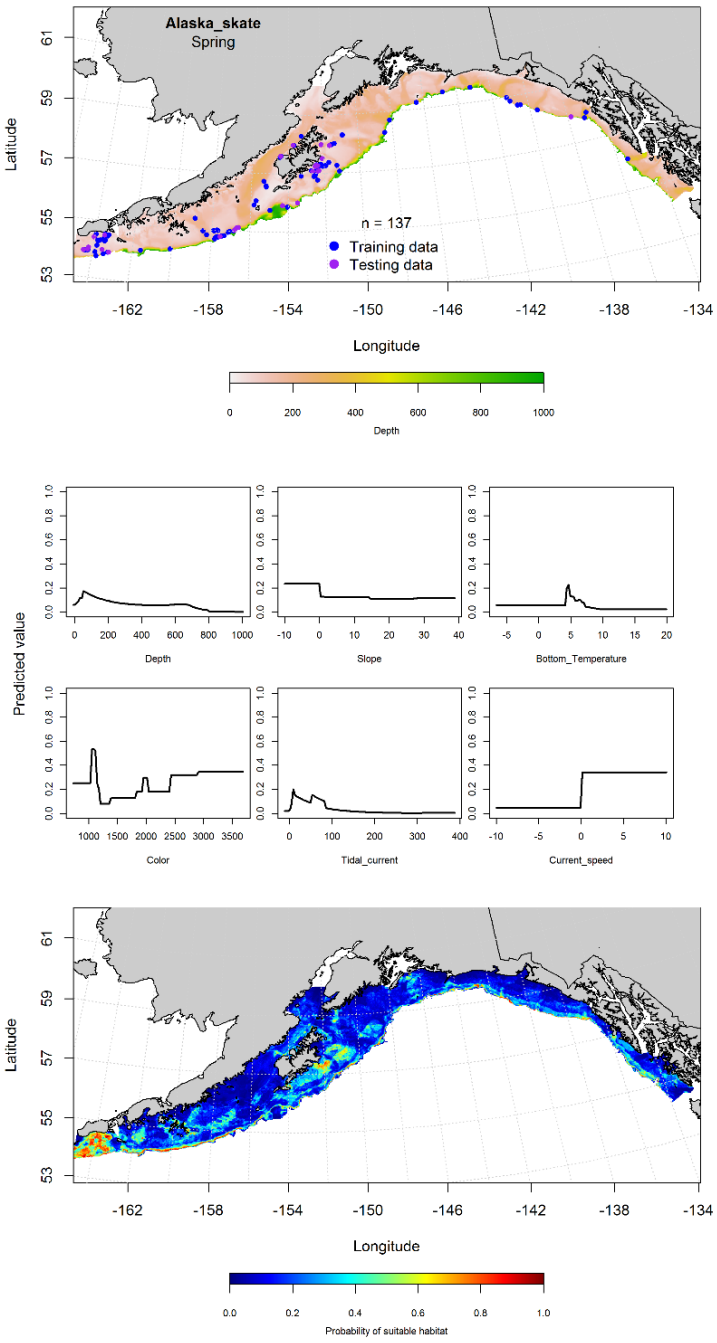

Figure 222. -- Locations of Alaska skate from spring (March-May 2001-2015) commercial fisheries catches in the Gulf of Alaska (top panel), with training (blue dots) and testing (purple dots) data indicated, maximum entropy (MaxEnt) model effects (center panel), and the predicted probability of suitable adult Alaska skate (bottom panel).

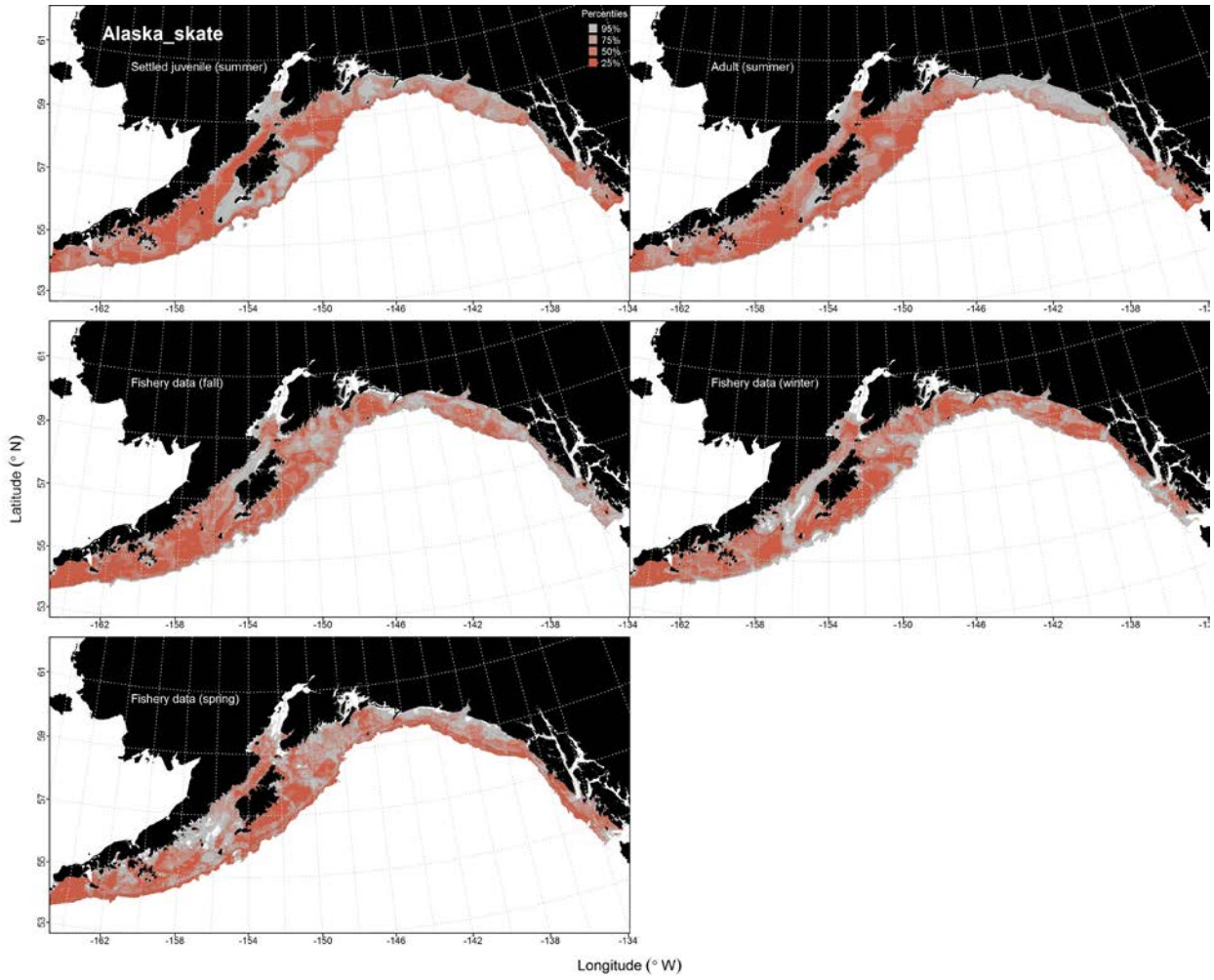

Figure 223. -- Habitat predicted for settled juvenile and adult Alaska skate from RACE-GAP summertime bottom trawl surveys (1993-2013), and predicted from presence in commercial fishery catches (2001-2015) from fall, winter, and spring in the Gulf of Alaska.

Aleutian Skate (*Bathyraja aleutica*)

Juvenile and adult Aleutian skate distribution in the bottom trawl survey -- An hGAM was used to predict the distribution of settled juvenile Aleutian skate abundance. The AUC for the PA GAM was 0.79 for both the training and the test data. Geographic location, slope, and bottom depth were the most important model variables. The model predicted the highest probability of presence for settled juvenile Aleutian Skate was in the central GOA, around Shelikof Strait and Shelikof Gully (Fig. 225). Overall, the CPUE GAM explained 15% of the variability in the training data and 9% in the test data. Geographic location, bottom depth, bottom current speed, and ocean color were the most important determinants of CPUE. The model predicted the highest CPUE occurred in Shelikof Strait and Shelikof Gully (Fig. 225).

A MaxEnt model predicting the probability of suitable habitat of adult Aleutian skate resulted in an AUC of 0.86 for the training data and 0.72 for the test data. The model correctly classified 79% of the predictions from the training data and 72% of the predictions from the test data. Bottom depth, bottom temperature, and ocean color were the most important model variables (relative importance: 0.59, 0.22, and 0.12, respectively). The model predicted suitable habitat of Aleutian skate throughout the GOA, though highest in the western GOA, around Semidi Bank; as well as in the central GOA, along Shelikof Strait (Fig. 226).

Aleutian skate distribution in commercial fisheries -- In the fall, ocean color and bottom depth were the most important variables determining suitable habitat of Aleutian skate (relative importance: 0.52 and 0.20, respectively). The AUC of the fall MaxEnt model was 0.95 for the training data and 0.84 for the test data. The model correctly classified 88% of the predictions from the training data and 84% of the predictions from the test data. The model predicted suitable habitat

of Aleutian skate was highest along the outer shelf in the western GOA, particularly off Unimak Island (Fig. 227).

In the winter, bottom depth, bottom current speed, and ocean color were the most important variables determining suitable habitat of Aleutian skate habitat (relative importance: 0.54, 0.15, and 0.14, respectively). The AUC of the winter MaxEnt model was 0.93 for the training data and 0.82 for the test data. The model correctly classified 87% of the predictions from the training data and 81% of the predictions from the test data. The model predicted suitable of Aleutian skate habitat was patchy in distribution, with the highest suitability habitats concentrated in the western GOA off Unimak Island, and in the central GOA around Albatross and Portlock banks (Fig. 228).

In the spring, bottom depth, and bottom temperature were the most important variables determining suitable habitat of Aleutian skate habitat (relative importance: 0.61, 0.19, and 0.07, respectively). The AUC of the MaxEnt spring model was 0.92 for the training data and 0.81 for the test data. The model correctly classified 85% of the predictions from the training data and 69% of the predictions from the test data. The model predicted suitable habitat of Aleutian skate was highest near the shelf break throughout the GOA (Fig. 229).

Aleutian skate essential fish habitat maps and conclusions -- Summertime habitat of Aleutian skate settled juveniles was predicted to be concentrated in deeper areas of the central GOA, including Shelikof Strait and Shelikof Gully (Fig. 230). In contrast, habitat for adult Aleutian skate was predicted to be more extensively distributed throughout GOA (Fig. 230). Similar to adult summertime bottom trawl survey data observations, the habitat predicted from commercial catches of Aleutian skate was distributed throughout the GOA (Fig. 230). The fall, winter, and spring

distribution of Aleutian skate habitat was generally the same in each season, though more probable near the outer shelf during the spring.

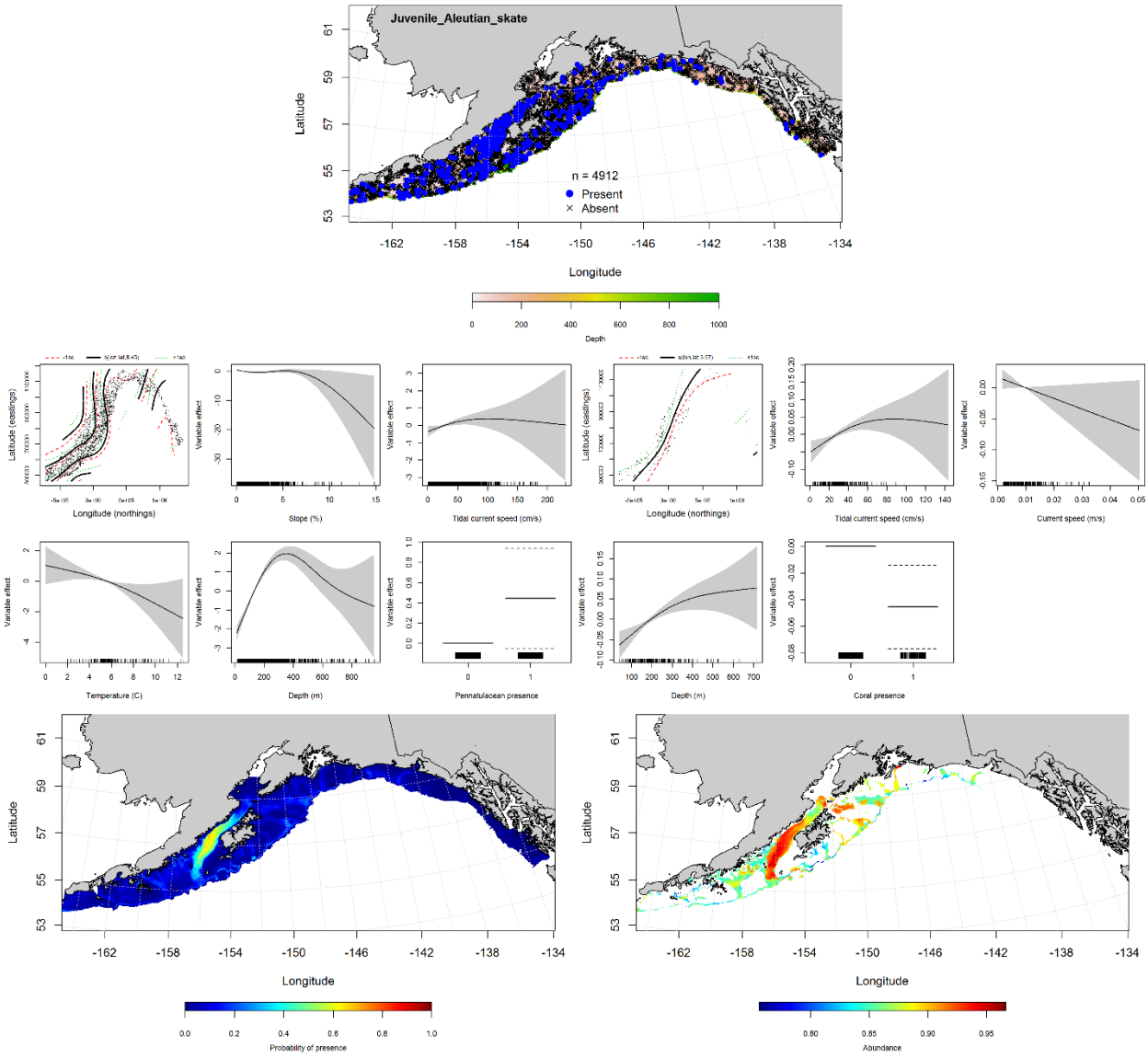

Figure 224. -- Distribution of settled juvenile Aleutian skate in 1993-2013 RACE-GAP summer bottom trawl surveys conducted in the Gulf of Alaska (upper panel). Effects of retained habitat covariates in the best fitting generalized additive presence-absence models (PA GAM; left center panel) and abundance (CPUE GAM; right center panel). Predicted spatial distribution of the probability of presence (bottom left panel) and abundance of settled juvenile Aleutian skate based on the models (bottom right panel).

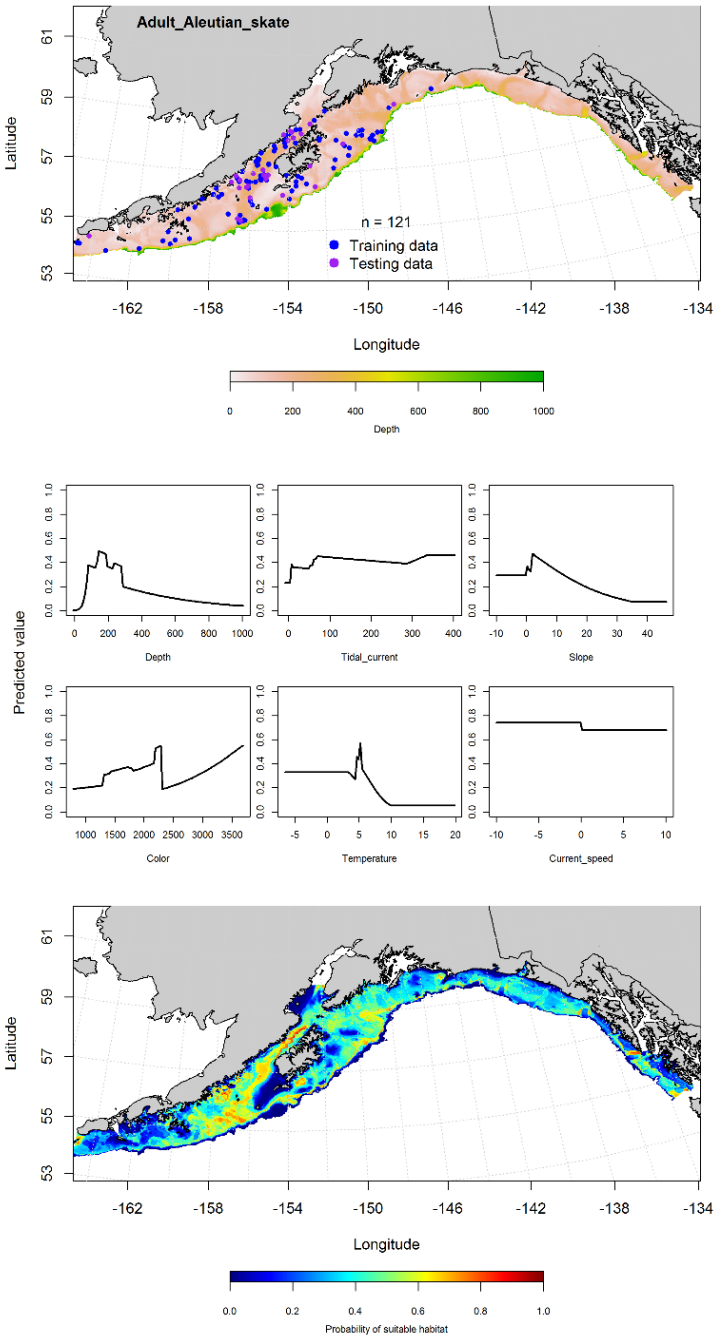

Figure 225. -- Presence of adult Aleutian skate from RACE-GAP summer bottom trawl surveys (1993-2013) in the Gulf of Alaska (top panel) with training (blue dots) and testing (purple dots) data indicated, maximum entropy (MaxEnt) model effects (center panel), and the MaxEnt-predicted probability of suitable adult Aleutian skate habitat (bottom panel).

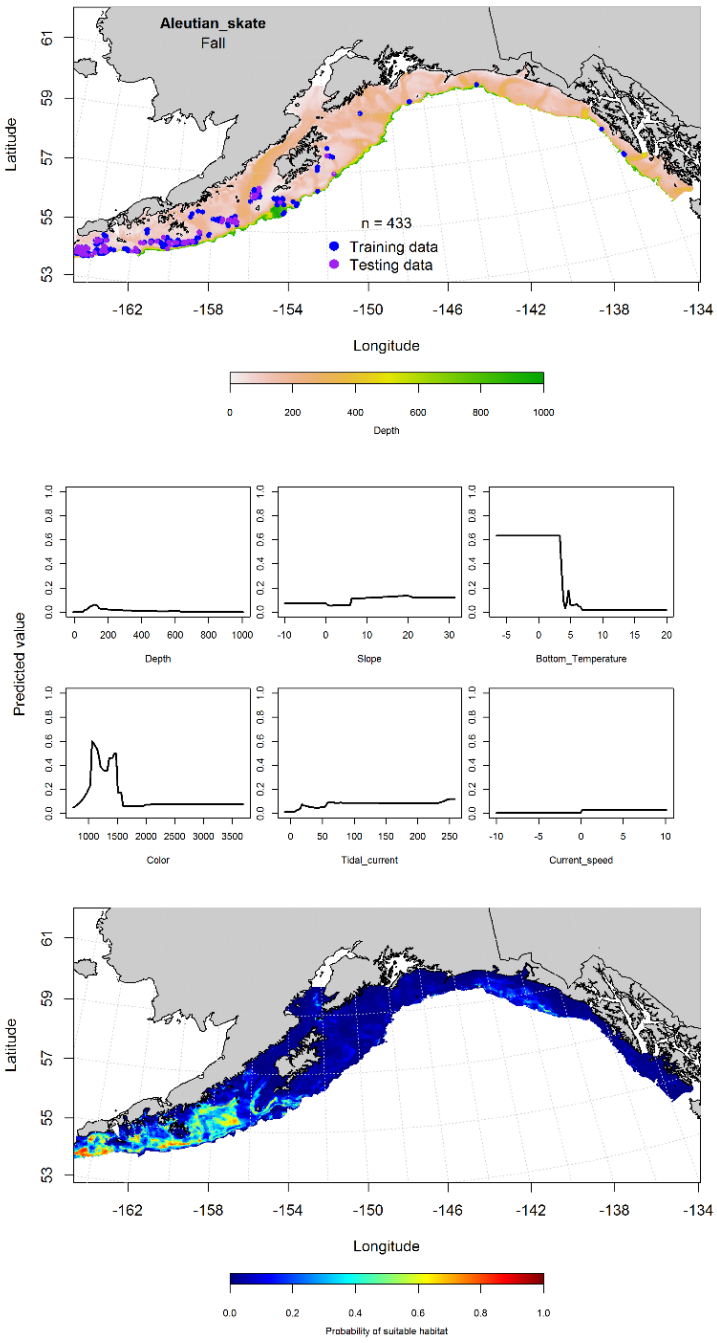

Figure 226. -- Locations of Aleutian skate from fall (September-November 2001-2015) commercial fisheries catches in the Gulf of Alaska (top panel), MaxEnt model effects (middle panels), and predicted probability of suitable habitat for Aleutian skate based on the model (bottom panel).

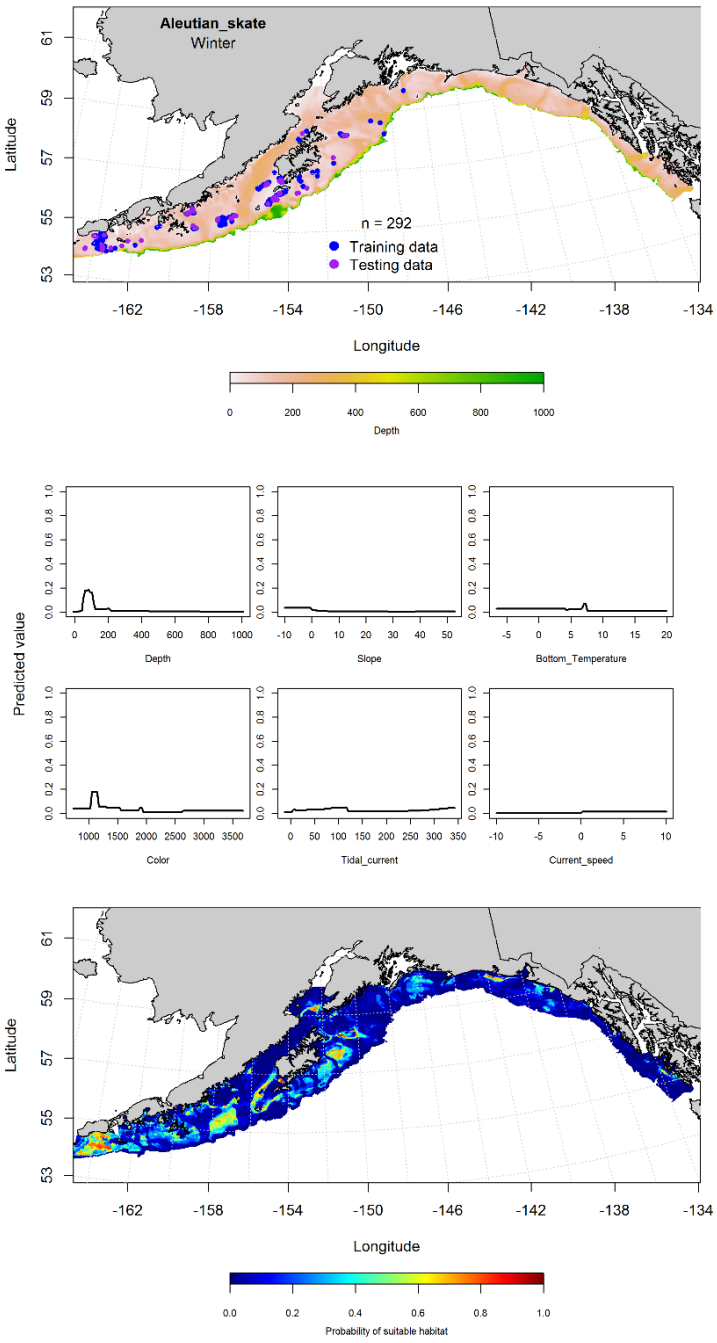

Figure 227. -- Locations of Aleutian skate from winter (December-February 2001-2015) commercial fisheries catches in the Gulf of Alaska (top panel), with training (blue dots) and testing (purple dots) data indicated, maximum entropy (MaxEnt) model effects (center panel), and the predicted probability of suitable adult Aleutian skate habitat (bottom panel).

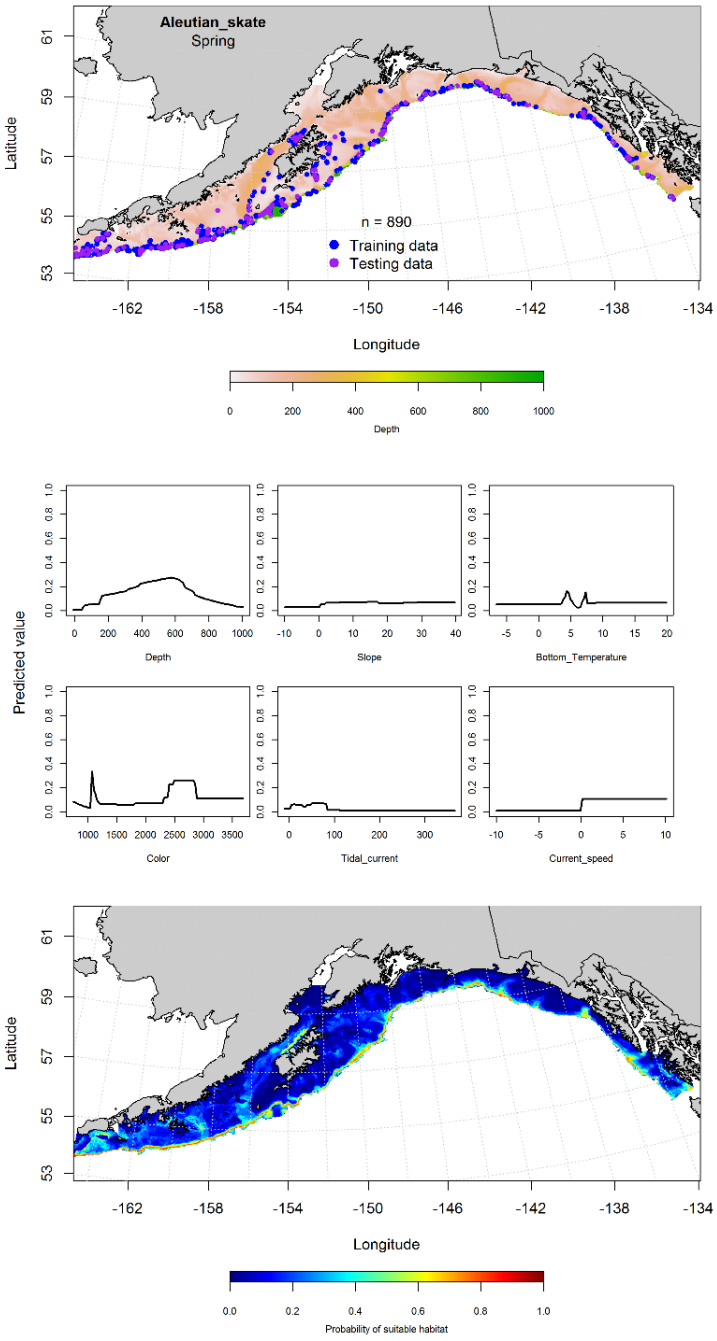

Figure 228. -- Locations of Aleutian skate from spring (March-May 2001-2015) commercial fisheries catches in the Gulf of Alaska (top panel), with training (blue dots) and testing (purple dots) data indicated, maximum entropy (MaxEnt) model effects (center panel), and the predicted probability of suitable adult Aleutian skate (bottom panel).

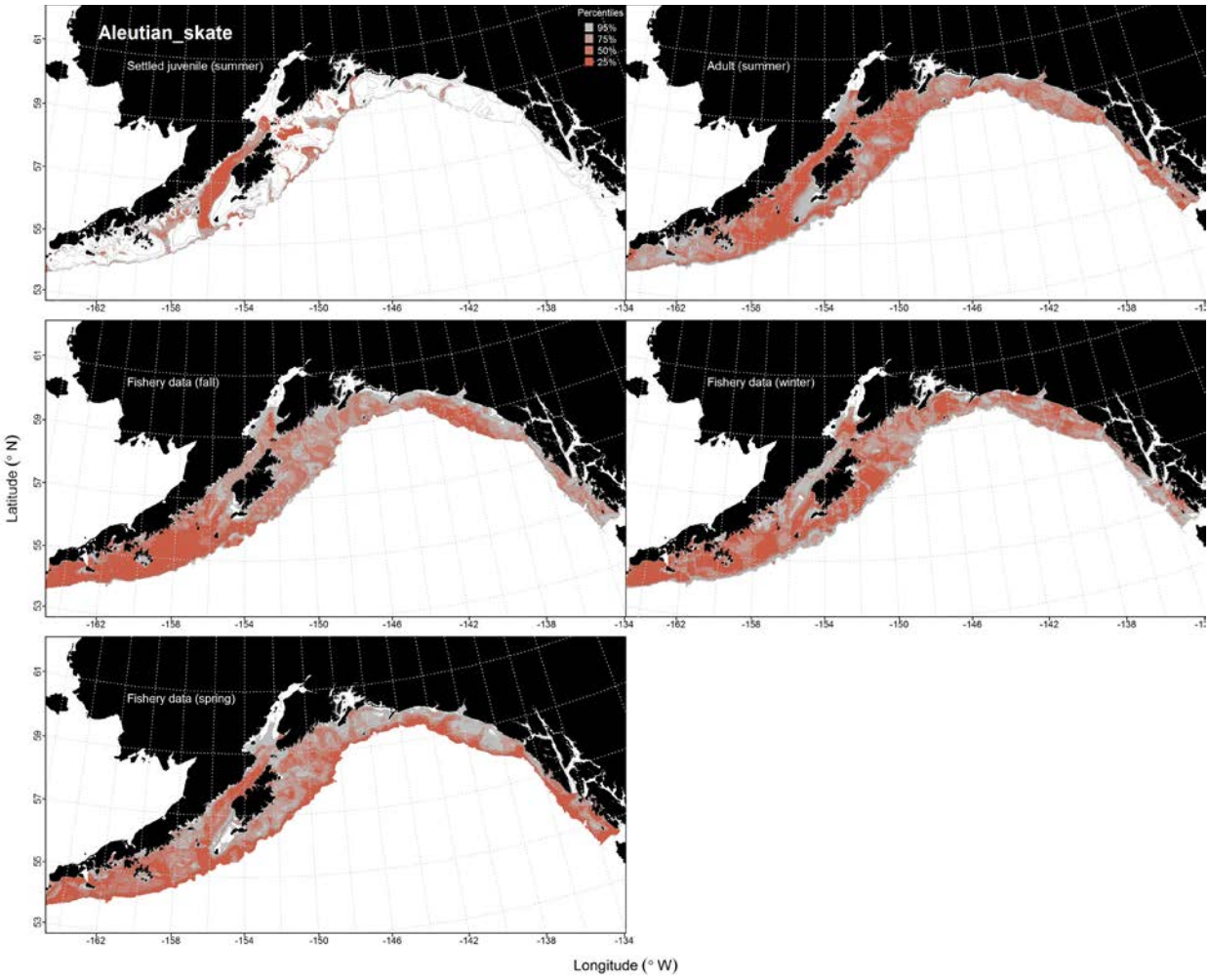

Figure 229. -- Habitat predicted for settled juvenile and adult Aleutian skate from RACE-GAP summertime bottom trawl surveys (1993-2013), and predicted from presence in commercial fishery catches (2001-2015) from fall, winter, and spring in the Gulf of Alaska.

Bering Skate (*Bathyraja interrupta*)

Juvenile and adult Bering skate distribution in the bottom trawl survey -- Although there were enough data points to use hGAMs to predict the distribution of settled juvenile Bering skate, the resulting models were very poor fits to the data, so a MaxEnt approach was used instead. The MaxEnt model predicting the probability of suitable habitat for settled juvenile Bering skate had an AUC of 0.85 for the training data and 0.74 for the test data. The model correctly classified 78% of the predictions from the training data and 74% of the predictions from the test data. Bottom depth, maximum tidal current, and bottom temperature were the most important variables determining the distribution of settled juvenile Bering skate (relative importance: 0.62, 0.12, and 0.11, respectively). Predicted suitable habitat of settled juvenile Bering skate was distributed throughout the central and eastern GOA, but highest in Marmot Gully and between Albatross and Portlock banks (Fig. 231).

A MaxEnt model predicting the probability of suitable habitat of adult Bering skate resulted in an AUC of 0.80 for the training data and 0.72 for the test data. The model correctly classified 73% of the predictions from the training data and 72% of the predictions from the test data. Bottom depth, bottom temperature, and maximum tidal current were the most important variables explaining the probability of suitable habitat of adult Bering skate (relative importance: 0.43, 0.18, and 0.14, respectively). The model predicted that suitable habitat of adult Bering skate was found throughout the GOA, but was highest in the central GOA around Shelikof Strait and Portlock Bank; as well as in the eastern GOA, off Baranof Island (Fig. 232).

Bering skate distribution in commercial fisheries -- There were no records of Bering skates reported in the VOE-CIA database.

Bering skate essential fish habitat maps and conclusions -- Summertime habitat of Bering skate settled juveniles and adults were similarly distributed throughout the GOA. Predictions of juvenile and adult Bering skate habitat were highest in the central GOA, around Shelikof Strait and Marmot Gully; as well as in the eastern GOA, along the middle and outer shelf (Fig. 233).

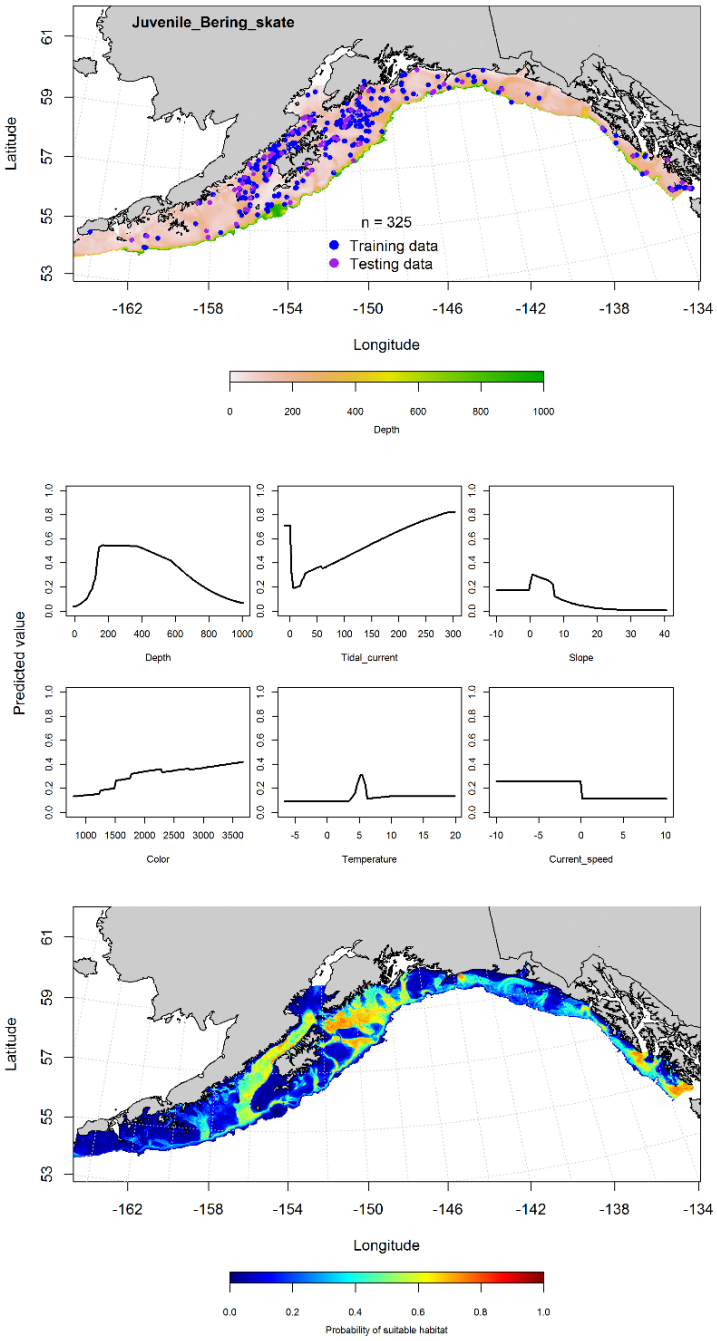

Figure 230. -- Presence of settled juvenile Bering skate from RACE-GAP summer bottom trawl surveys (1993-2013) in the Gulf of Alaska (top panel) with training (blue dots) and testing (purple dots) data indicated, maximum entropy (MaxEnt) model relationships between probability of juvenile presence and habitat covariates (center panel), and the MaxEnt-predicted probability of suitable juvenile Bering skate habitat (bottom panel).

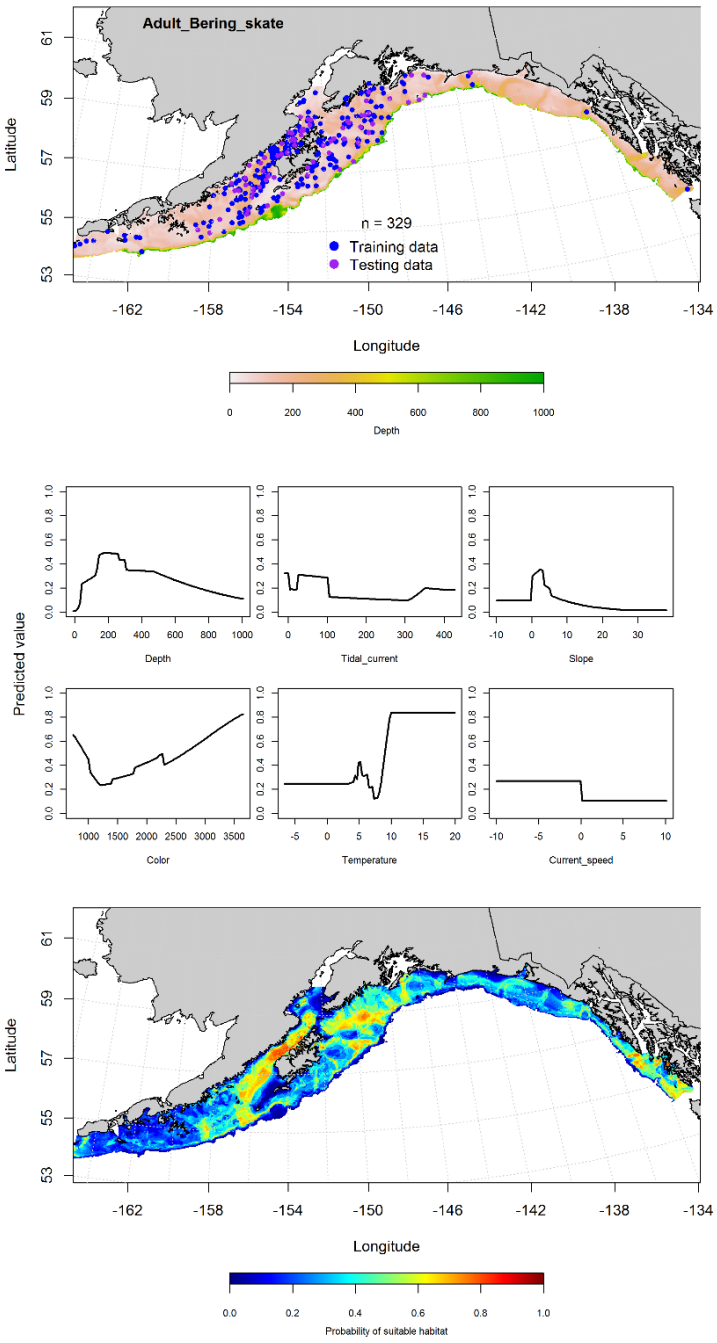

Figure 231. -- Presence of adult Bering skate from RACE-GAP summer bottom trawl surveys (1993-2013) in the Gulf of Alaska (top panel) with training (blue dots) and testing (purple dots) data indicated, maximum entropy (MaxEnt) model effects (center panel), and the MaxEnt-predicted probability of suitable adult Bering skate habitat (bottom panel).

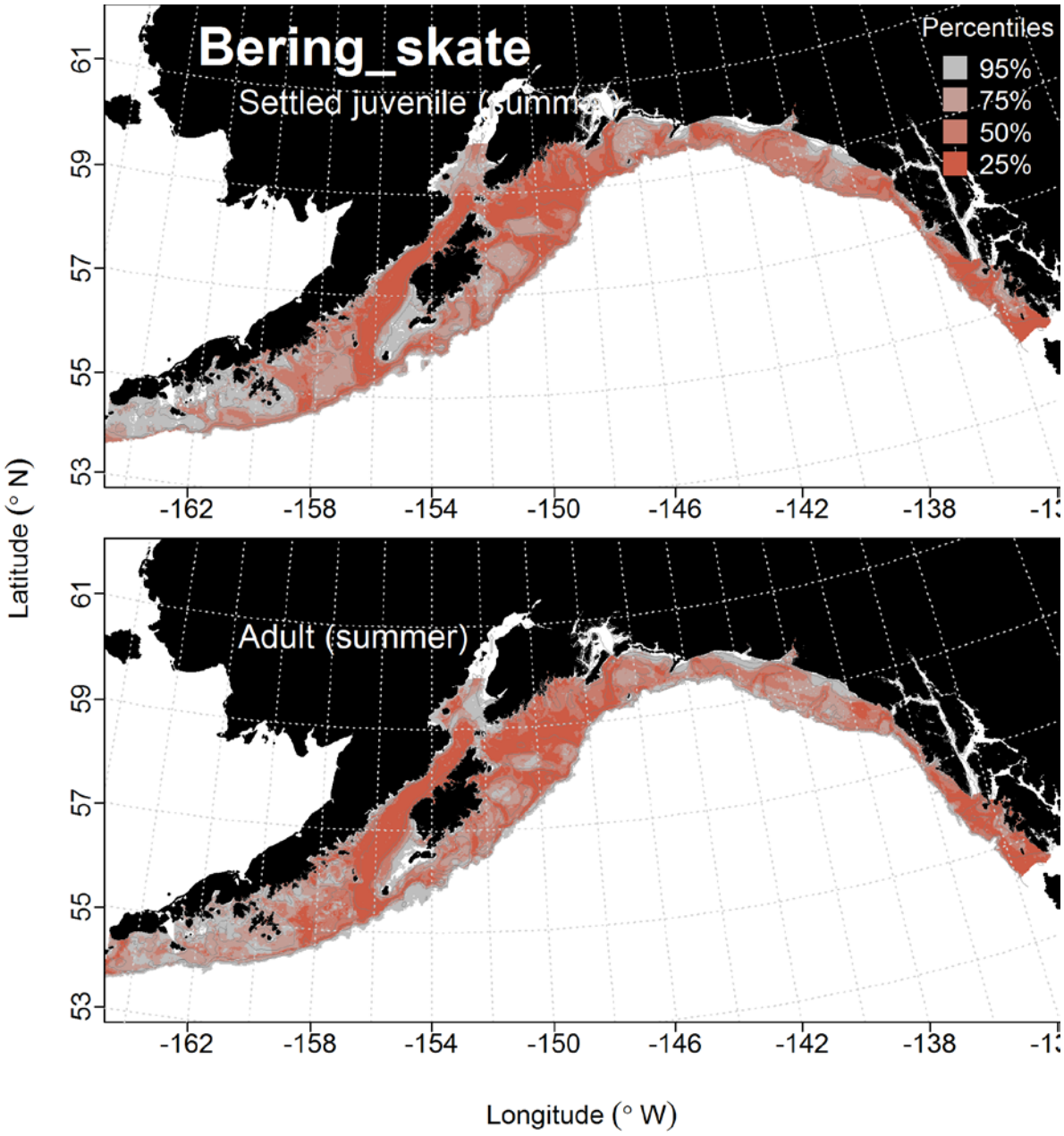

Figure 232. -- Predicted habitat for settled juvenile and adult Bering skate based on RACE-GAP summertime bottom trawl surveys (1993-2013) in the Gulf of Alaska.

Invertebrates

Octopus Unidentified

Early life history stages of octopus unidentified -- Early life history stages of octopus were not reliably sampled by EcoFOCI data, therefore the ELHS of these organisms were not modeled.

Octopus unidentified distribution in the bottom trawl survey -- A MaxEnt model predicting the probability of suitable habitat of octopus resulted in an AUC of 0.80 for the training data and 0.72 for the test data. The model correctly classified 73% of the predictions from both the training and the test data. Bottom temperature, bottom depth, and bottom current speed were the most important variables explaining the probability of suitable habitat of octopus (relative importance: 0.35, 0.27, and 0.16, respectively). Predicted suitable habitat occurred across the GOA, but was highest along the outer shelf near the Shumagin Islands (Fig. 234).

Octopus unidentified distribution in commercial fisheries -- Commercial fisheries catches of unidentified octopus were generally consistent throughout all seasons. In the fall, ocean color, bottom depth, and bottom current speed were the most important variables determining the probability of suitable habitat of unidentified octopus (relative importance: 0.48, 0.26, and 0.12, respectively). The AUC of the fall MaxEnt model was 0.83 for the training data and 0.79 for the test data. The model correctly classified 77% of the predictions from the training data and 79% of the predictions from the test data. The model predicted suitable habitat of unidentified octopus occurred in the central and

western GOA, though the highest predicted probability of suitable habitat was predicted off Unimak Island (Fig. 235).

In the winter, bottom depth, bottom current speed, and maximum tidal current were the most important variables determining the distribution of suitable unidentified octopus habitat (relative importance: 0.53, 0.17, and 0.12, respectively). The AUC of the winter MaxEnt model was 0.91 for the training data and 0.76 for the test data. The model correctly classified 81% of the predictions from the training data and 76% of the predictions from the test data. As with the fall, the winter model predicted suitable habitat of unidentified octopus in the central and western GOA, although there was clear clustering of higher suitability habitats in the western GOA off Unimak Island, and in the central GOA around Albatross and Portlock banks (Fig. 236).

In the spring, bottom temperature, maximum tidal current, and bottom depth were the most important variables determining probable suitable habitat of unidentified octopus (relative importance: 0.40, 0.20, and 0.17, respectively). The AUC of the spring MaxEnt model was 0.88 for the training data and 0.74 for the test data. The model correctly classified 82% of the predictions from the training data and 74% of the predictions from the test data. The model predicted suitable habitat of unidentified octopus near the outer shelf throughout the GOA, with the highest suitability areas concentrated in the western GOA along the Alaska Peninsula and off Unimak Island (Fig. 237).

Octopus unidentified essential fish habitat maps and conclusions -- Predicted habitat for octopus was distributed throughout the GOA, although higher suitability areas tended to be concentrated along outer shelf in the eastern and central GOA, while being more broadly distributed in the western GOA (Fig. 238). The fall, winter, and spring distribution of octopus habitat was generally consistent

throughout all seasons, though higher probability habitat was predicted along the outer shelf during the spring (Fig. 238).

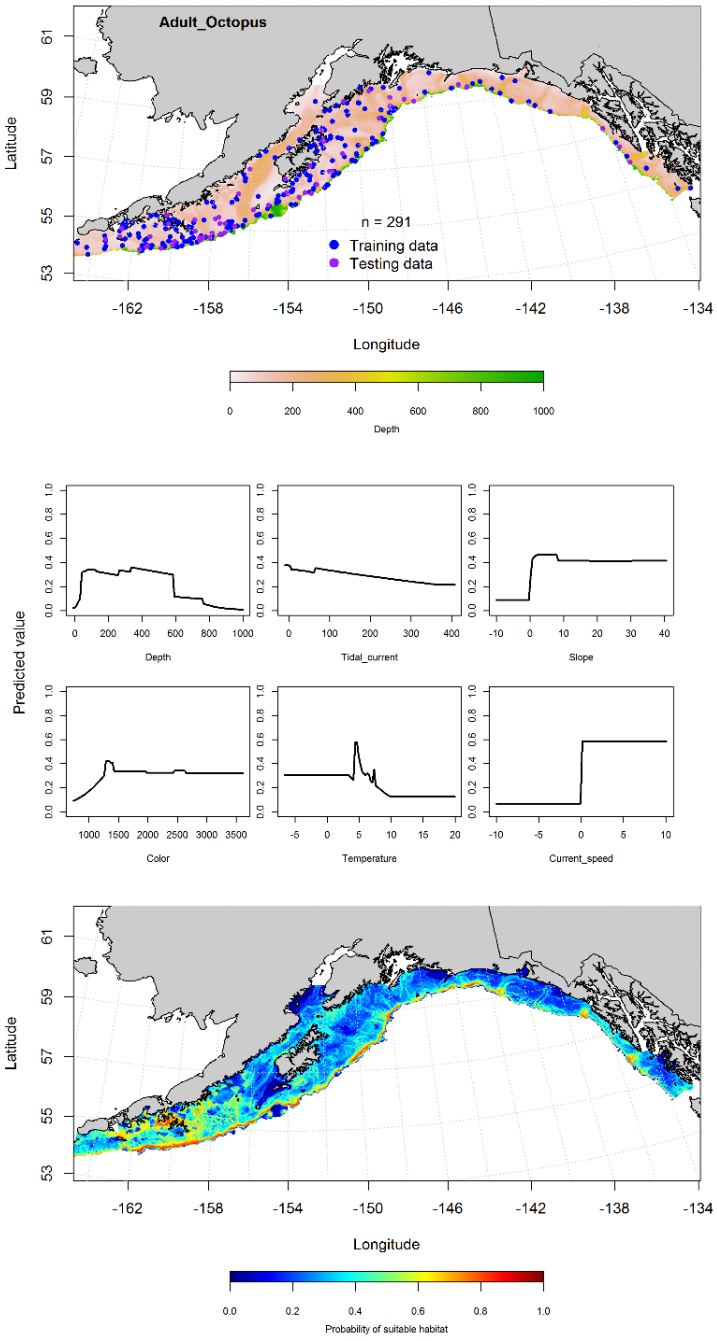

Figure 233. -- Presence of adult octopus unidentified from RACE-GAP summer bottom trawl surveys (1993-2013) in the Gulf of Alaska (top panel) with training (blue dots) and testing (purple dots) data indicated, maximum entropy (MaxEnt) model relationships between probability of adult presence and habitat covariates (center panel), and the MaxEnt-predicted probability of suitable adult octopus unidentified habitat (bottom panel).

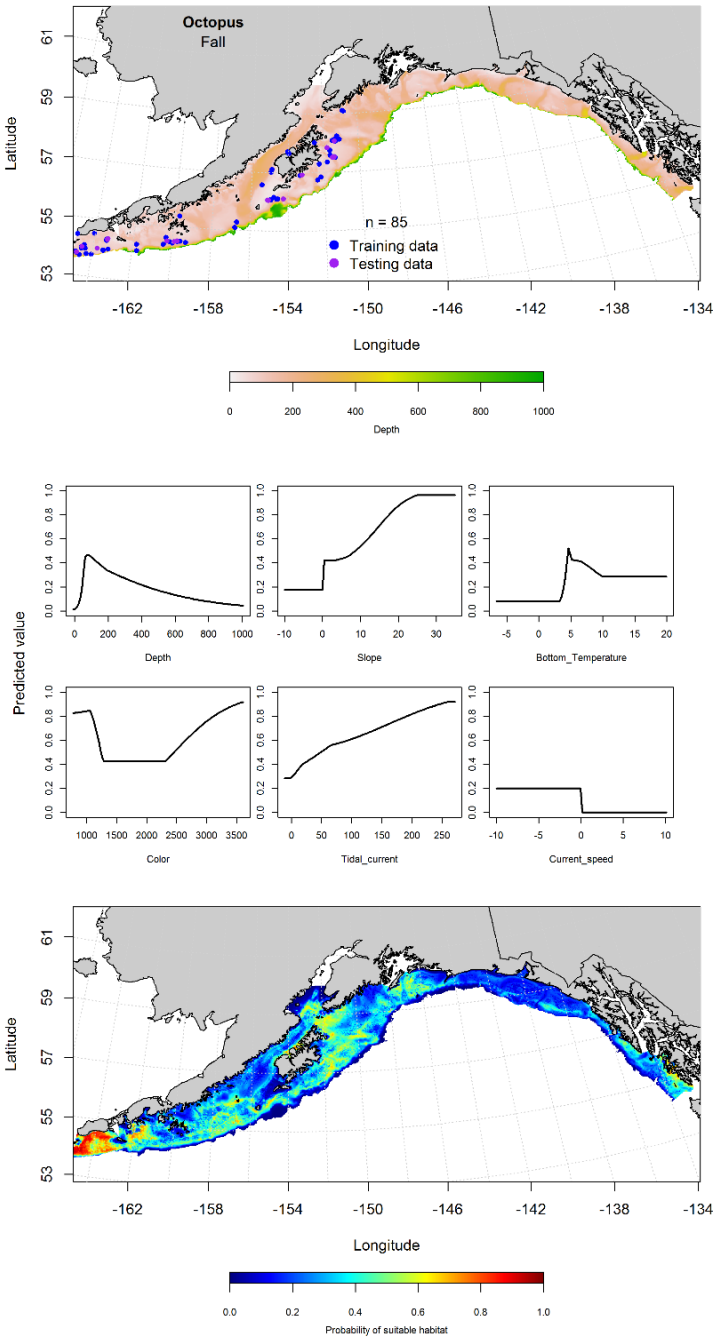

Figure 234. -- Locations of octopus unidentified from fall (September-November 2001-2015) commercial fisheries catches in the Gulf of Alaska (top panel), relationships between probability of presence and environmental variables for the MaxEnt model (middle panels), and predicted probability of suitable habitat for octopus unidentified based on the model (bottom panel).

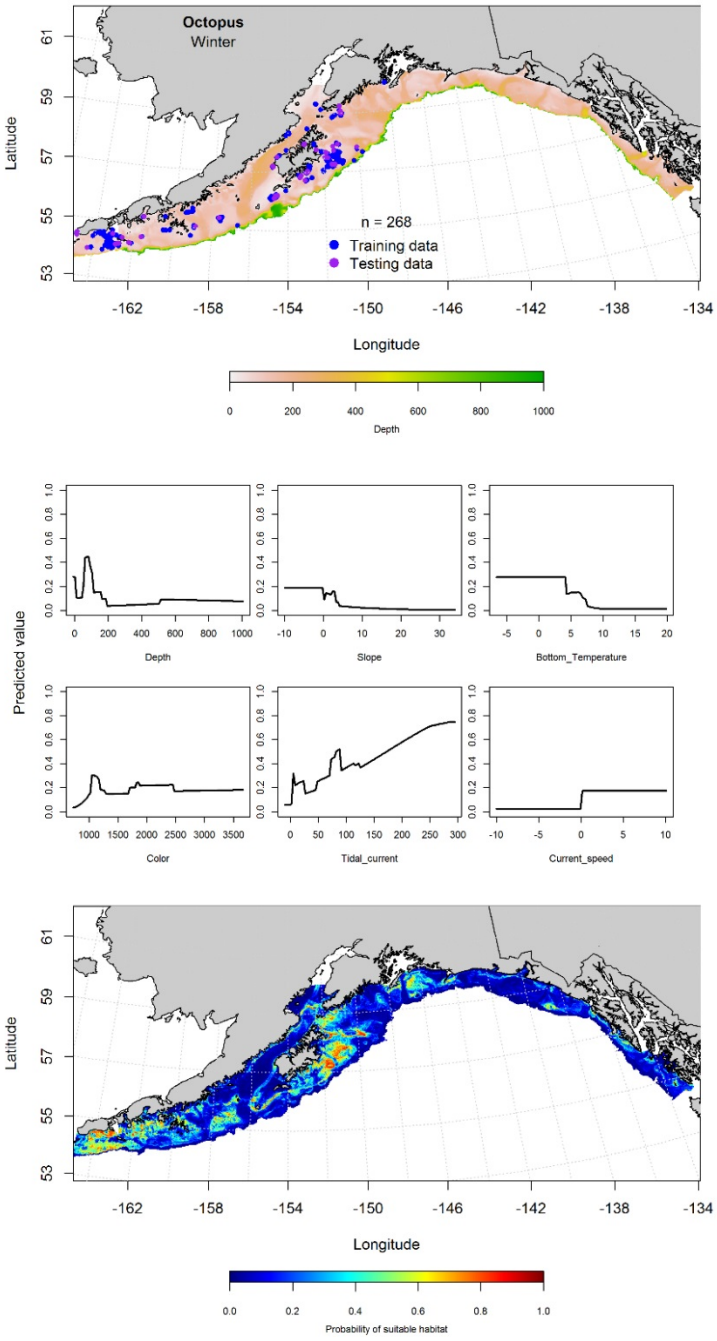

Figure 235. -- Locations of octopus unidentified from winter (December-February 2001-2015) commercial fisheries catches in the Gulf of Alaska (top panel), with training (blue dots) and testing (purple dots) data indicated, maximum entropy (MaxEnt) model effects (center panel), and the predicted probability of suitable adult octopus unidentified habitat (bottom panel).

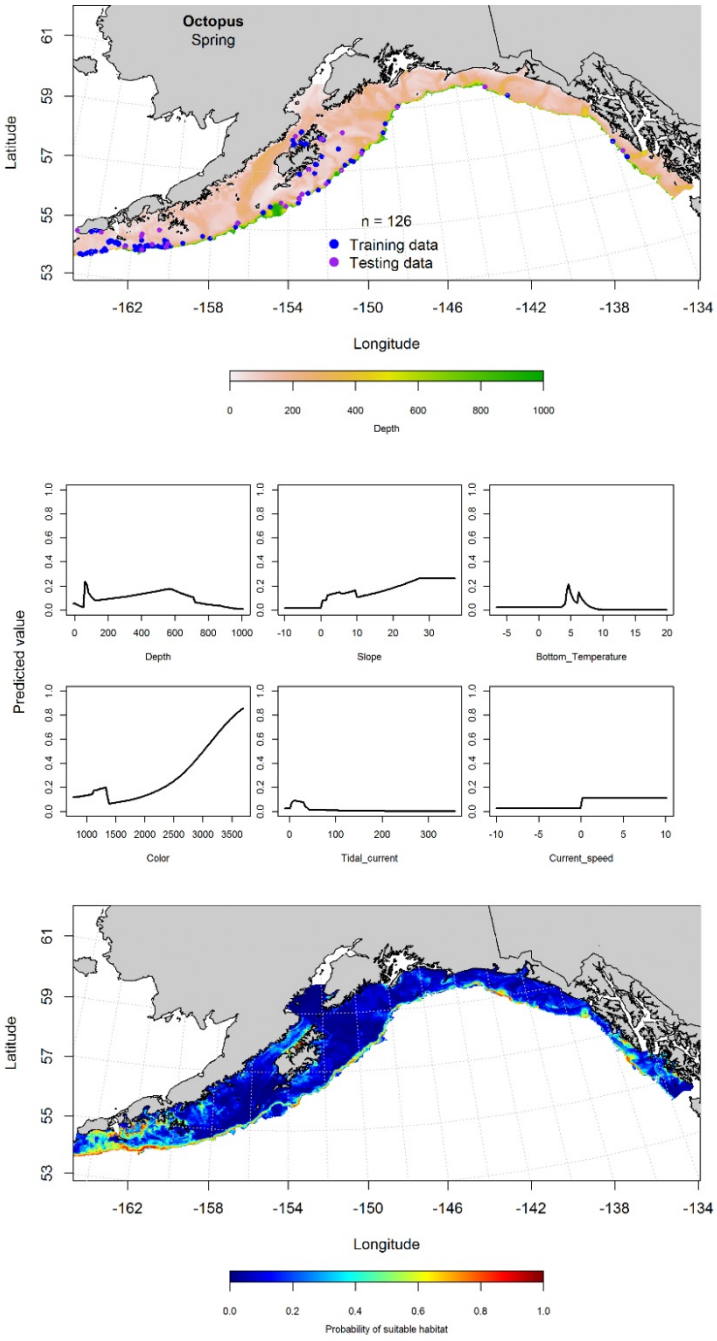

Figure 236. -- Locations of octopus unidentified from spring (March-May 2001-2015) commercial fisheries catches in the Gulf of Alaska (top panel), with training (blue dots) and testing (purple dots) data indicated, maximum entropy (MaxEnt) model effects (center panel), and the predicted probability of suitable adult octopus unidentified (bottom panel).

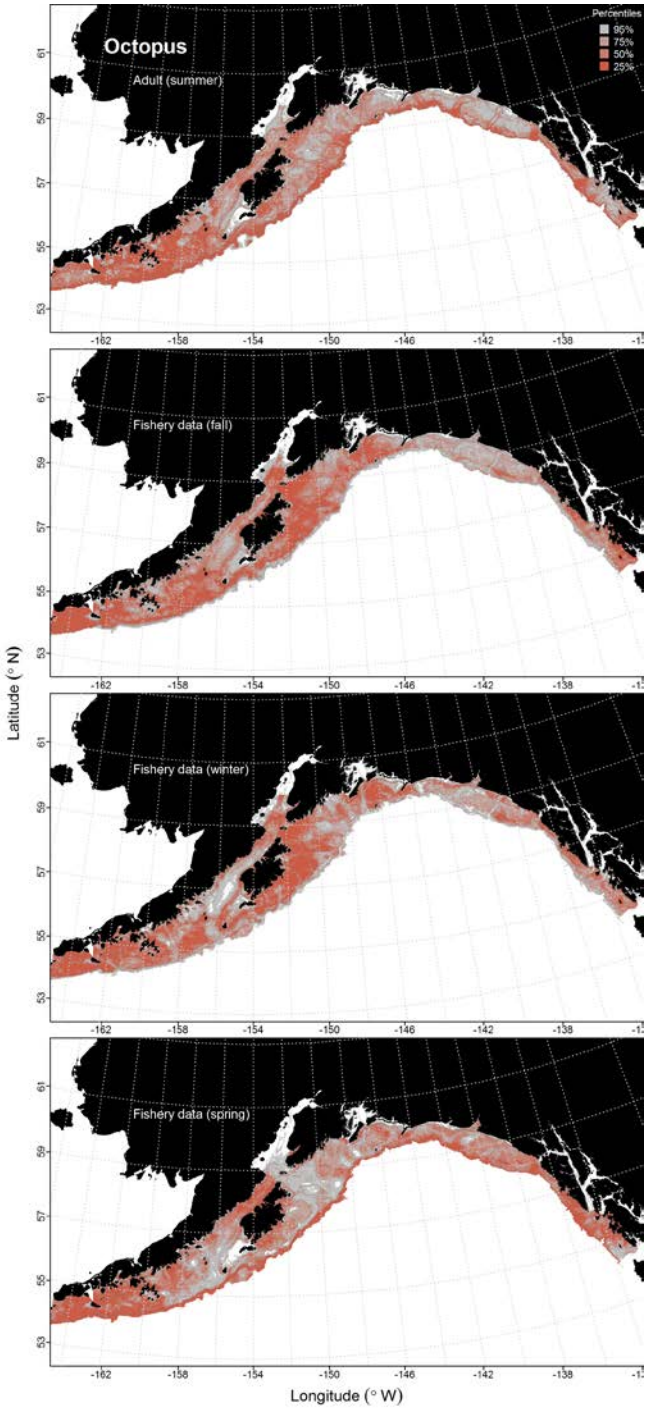

Figure 237. -- Habitat predicted for unidentified octopus from RACE-GAP summertime bottom trawl surveys (1993-2013), and predicted from presence in commercial fishery catches (2001-2015) from fall, winter, and spring in the Gulf of Alaska.

ACKNOWLEDGMENTS

We are grateful to Robert McConnaughey, John Olson, and Wayne Palsson for their reviews of this report. We also thank the numerous stock assessment scientists from the AFSC for their helpful reviews and criticisms. This project was funded by the AKRO/AFSC Essential Fish Habitat Research Funds.

CITATIONS

Abookire, A. A. 2006. Reproductive biology, spawning season, and growth of female rex sole (*Glyptocephalus zachirus*) in the Gulf of Alaska. Fish. Bull., U.S. 104(3):350-359.

Abookire, A. A., and B. J. Macewicz. 2003. Latitudinal variation in reproductive biology and growth of female Dover sole (*Microstomus pacificus*) in the North Pacific, with emphasis on the Gulf of Alaska stock. J. Sea Res. 50(2):187-197.

Alverson, D. L., and W. T. Pereyra. 1969. Demersal fish explorations in the northeastern Pacific Ocean – An evaluation of exploratory fishing methods and analytical approaches to stock size and yield forecasts. J. Fish. Res. Bd. Can. 26:1985-2001.

Behrenfeld, M. J., and P. G. Falkowski. 1997. Photosynthetic rates derived from satellite-based chlorophyll concentration. Limnnol. Oceanogr. 42: 1−20.

Chilton, E. A. 2010. Maturity and growth of female dusky rockfish (*Sebastes variabilis*) in the central Gulf of Alaska. Fish. Bull., U.S. 108(1):70-79.

Cochran W. G. 1977. Sampling Techniques, Third Edition. 428 p. John Wiley and Sons, New York, New York.

Cooper, D. W., S. F. McDermott, and J. N. Ianelli. 2010. Spatial and temporal variability in Atka mackerel female maturity at length and age. Mar. Coast. Fish.: Dynam. Manage. Ecosys. Sci. 2(1): 329-338.

Cragg, J. G. 1971. Some statistical models for limited dependent variables with application to the demand for durable goods. Econometrica. 39: 829−844.

Danielson, S., E. Curchitser, K. Hedstrom, T. Weingartner, and P. Stabeno. 2011. On ocean and sea ice modes of variability in the Bering Sea. J. Geophys. Res. 116: C12034, doi: 10.1029/2011JC007389.

DeLong, A. K., and J. S. Collie. 2004. Defining Essential Fish Habitat: A Model-Based Approach. Rhode Island Sea Grant, Narragansett, R.I. 4 p.

DeLong, E. R., D. M. DeLong, and D. L. Clarke-Pearson. 1988. Comparing the areas under two or more correlated receiver operating characteristic curves: a nonparametric approach. Biometrics 44: 837−845.

Dorn, M., K. Aydin, B. Fissel, D. Jones, W. Palsson, K. Spalinger, and S. Stienessen. 2016. Assessment of the Walleye Pollock Stock in the Gulf of Alaska. In: Stock assessment and fishery evaluation report for the groundfish resources of the Gulf of Alaska. North Pac. Fish. Mgmt. Council, Anchorage, AK, section 1:45-174.

Ebert, D. A., W. D. Smith, D. L. Haas, S. M. Ainsley, and G. M. Cailliet. 2007. Life history and population dynamics of Alaskan skates: providing essential biological information for effective management of bycatch and target species. Final Report to the North Pacific Research Board, Project 510. North Pacific Research Board, 1007 W. 3rd Ave., STE 100, Anchorage, AK 99501.

Egbert, G. D. and S. Y. Erofeeva. 2002. Efficient inverse modeling of barotropic ocean tides. J. Atmos. Ocean. Technol. 19: 183−204.

Elith, J., S. J. Phillips, T. Hastie, M. Dudík, Y. E. Chee, and C. J. Yates. 2011. A statistical explanation of MaxEnt for ecologists. Divers. Distrib. 17(1), 43-57.

Hastie, T. J. and R. J. Tibshirani. 1990. Generalized additive models. Chapman & Hall, London.

Hoff, G. R. 2010. Identification of skate nursery habitat in the eastern Bering Sea. Mar. Ecol. Progr. Ser. 403:243-254.

Hosmer, D. W. and S. Lemeshow. 2005. Assessing the fit of the model in applied logistic regression, 2nd edn. John Wiley & Sons, Hoboken, NJ.

Laman, E., C. N. Rooper, K. Turner, S. Rooney, D. Cooper, and M. Zimmermann. 2017. Model-based Essential Fish Habitat Definitions for Eastern Bering Sea Groundfish. U.S. Dep. Commer., NOAA Tech. Memo. NMFS-AFSC-357, 265 p. doi:10.7289/V5/TM-AFSC-357.

Laman, E., C. N. Rooper, K. Turner, S. Rooney, D. Cooper, and M. Zimmermann. in press. Using species distribution models to describe essential fish habitat in Alaska. Can. J. Fish. Aquat. Sci. dx.doi.org/10.1139/cjfas-2017-0181.

Love, M. S., C. W. Mecklenberg, T. A. Mecklenberg, and L. K. Thorsteinson. 2005. Resource inventory of marine and estuarine fishes of the West Coast and Alaska: a checklist of north Pacific and Arctic Ocean species from Baja California to the Alaska-Yukon Border. U.S. Dep. Int., U.S. Geological Survey, Biological Resources Division, Seattle, Washington, 98104, OCS Study MMS 2005-030 and USGS/NBII 2005-001.

Lozier, J. D., P. Aniello, and M. J. Hickerson. 2009. Predicting the distribution of Sasquatch in western North America: anything goes with ecological niche modeling. J. Biogeogr. 36:1623-1627.

Matarese, A. C., D. M. Blood, S. J. Picquelle, and J. L. Benson. 2003. Atlas of abundance and distribution patterns of ichthyoplankton from the Northeast Pacific Ocean and Bering Sea ecosystems based on research conducted by the Alaska Fisheries Science Center (1972-1996). U.S. Dep. Commer., NOAA Professional Paper, NMFS-1, 281 p.

Matta, M. E. 2006. Aspects of the life history of the Alaska skate, *Bathyraja parmifera*, in the eastern Bering Sea. M.S. thesis, Univ. Washington, Seattle, WA.

McConnaughey, R. A. and S. E. Syrjala. 2009. Statistical relationships between the distributions of groundfish and crabs in the eastern Bering Sea and processed returns from a single-beam echosounder. ICES J. Mar. Sci. 66:1425-1432.

Nichol, D. G. 1997. Effects of geography and bathymetry on growth and maturity of yellowfin sole, *Pleuronectes asper*, in the eastern Bering Sea. Oceanograph. Lit. Rev., *12*(44), 1548.

Orr, J. W., and S. Hawkins. 2008. Species of the rougheye rockfish complex: Resurrection of *Sebastes melanostictus* (Matsubara, 1934) and a redescription of *Sebastes aleutianus* (Jordan and Evermann, 1898) (Teleostei: Scorpaeniformes). Fish. Bull., U.S. 106:111-134.

Phillips, S. J., R. P. Anderson, and R. E. Schapire. 2006. MaxEnt modeling of species geographic distributions. Ecol. Model. 190:231-59.

Potts, J., and J. Elith. 2006. Comparing species abundance models. Ecol Modell 199:153−163.

R Core Development Team. 2013. R: A language and environment for statistical computing. R Foundation for Statistical Computing, Vienna, Austria. URL http://www.R-project.org/.

Rooper, C. N. 2008. An ecological analysis of rockfish (*Sebastes* spp.) assemblages in the North Pacific Ocean along broad-scale environmental gradients. Fish. Bull., U.S. 106(1):1-11.

Rooper, C. N., M. Zimmermann, M. M. Prescott, and A. J. Hermann. 2014. Predictive models of coral and sponge distribution, abundance and diversity in bottom trawl surveys of the Aleutian Islands, Alaska. Mar. Ecol. Prog. Ser. 503:157-176.

Rooper, C. N., M. F. Sigler, P. Goddard, P. Malecha, R. Towler, K. Williams, R. Wilborn and M. Zimmermann. 2016. Validation and improvement of species distribution models for structure-forming invertebrates in the eastern Bering Sea with an independent survey. Mar. Ecol. Prog. Ser. 551:117-130.

Sagarese, S. R., M. G. Frisk, R. M. Cerrato, K. A. Sosebee, J. A. Musick, and P. J. Rago. 2014. Application of generalized additive models to examine ontogenetic and seasonal distributions of spiny dogfish (*Squalus acanthias*) in the northeast (US) shelf large marine ecosystem. Can. J. Fish. Aquat. Sci. 71: 847−877.

Sigler, M. F., C. N. Rooper, G. R. Hoff, R. P. Stone, R. A. McConnaughey, and T. K. Wilderbuer. 2015. Faunal features of submarine canyons on the eastern Bering Sea slope. Mar. Ecol. Prog. Ser. 526: 21−40.

Stark, J. W. 2004. A comparison of the maturation and growth of female flathead sole in the central Gulf of Alaska and south-eastern Bering Sea. J. Fish Biol. 64(4):876-889.

Stark, J. W. 2007. Geographic and seasonal variations in maturation and growth of female Pacific cod (*Gadus macrocephalus*) in the Gulf of Alaska and Bering Sea. Fish. Bull., U.S. 105(3):396-407.

Stark, J. W. 2012(a). Female maturity, reproductive potential, relative distribution, and growth compared between arrowtooth flounder (*Atheresthes stomias*) and Kamchatka flounder (*A. evermanni*) indicating concerns for management. J. Appl. Ichthyol. 28(2):226-230.

Stark, J. W. 2012(b). Contrasting maturation and growth of northern rock sole in the eastern Bering Sea and Gulf of Alaska for the purpose of stock management. N. Amer. J. Fish. Manage. 32(1):93-99.

Stauffer G. 2004. NOAA protocols for groundfish bottom trawl surveys of the Nation's fishery resources. U.S. Dep. Commer., NOAA Tech. Memo. NMFS-F/SPO-65, 205 p.

Tenbrink, T. T., and T. K. Wilderbuer. 2015. Updated maturity estimates for flatfishes (Pleuronectidae) in the eastern Bering Sea, with implications for fisheries management. Mar. Coast. Fish. Dy. Manage. Ecosys. Sci. 7:474–482.

Tenbrink, T. T. and C. E. Hutchinson. 2009. Age, growth, and mortality of the plain sculpin, *Myoxocephalus jaok,* in the eastern Bering Sea. North Pacific Research Board Project Final Report. North Pacific Research Board, 1007 W 3rd Ave STE100, Anchorage, AK 99501.

Tenbrink, T. T., and T. W. Buckley. 2013. Life-history aspects of the yellow Irish lord (*Hemilepidotus jordani*) in the Eastern Bering Sea and Aleutian Islands. Northwest. Natural. 94(2):126-136.

Turner, K., C. N. Rooper, E. Laman, S. C. Rooney, D. W. Cooper, and M. Zimmermann. 2017. Model-based essential fish habitat definitions for Aleutian Island groundfish species. U.S. Dep. Commer., NOAA Tech. Memo. NMFS-AFSC-360, 239 p.

Venables, W. N., and B. D. Ripley. 2002. Modern applied statistics with S, 4th edn. Springer Science+Business Media, New York, NY.

von Szalay, P. G., and N. W. Raring. 2016. Data report: 2015 Gulf of Alaska bottom trawl survey. U.S. Dep. Commer., NOAA Tech. Memo. NMFS-AFSC-325.

Wakabayashi, K., R. G. Bakkala, and M. S. Alton. 1985. Methods of the Japan demersal trawl surveys, p. 7-29. *In* R. G. Bakkala and K. Wakabayashi (Editors), Results of cooperative Japan groundfish investigations in the Bering Sea during May-August 1979. Int. N. Pac. Fish. Comm. Bull. 44.

Watson, D. F., and G. M. Philip. 1985. A refinement of inverse distance weighted interpolation. Geo-processing 2(4):315-327.

Wood, S. N. 2006. Generalized additive models: an introduction with R. Chapman & Hall/CRC Press, Boca Raton, FL.

Zaur, A. F., E. N. Ieno, N. J. Walker, A. A. Saveliev, and G. M. Smith. 2009. Mixed effects models and extensions in ecology with R. Springer, New York.

Zimmermann, M., and M. M. Prescott. 2015. Smooth sheet bathymetry of the bathymetry of the central Gulf of Alaska. U.S. Dep. Commer., NOAA Tech. Memo. NMFS-AFSC-287, 54 p.

Zimmermann, M. 1997. Maturity and fecundity of arrowtooth flounder, *Atheresthes stomias*, from the Gulf of Alaska. Fish. Bull., U.S. 95(3):598-611.

Zimmermann, M. and J. L. Benson. 2013. Smooth sheets: How to work with them in a GIS to derive bathymetry, features and substrates. U.S. Dep. Commer., NOAA Tech. Memo. NMFS-AFSC-249, 52 p.

Zimmermann, M. and M. M. Prescott. 2014. Smooth sheet bathymetry of Cook Inlet, Alaska. U.S. Dep. Commer., NOAA Tech. Memo. NMFS-AFSC-275, 32 p.

RECENT TECHNICAL MEMORANDUMS

Copies of this and other NOAA Technical Memorandums are available from the National Technical Information Service, 5285 Port Royal Road, Springfield, VA 22167 (web site: *www.ntis.gov)*. Paper and electronic (.pdf) copies vary in price.

AFSC-

372 LANG, C. A., J. I. RICHAR, and R. J. FOY. 2018. The 2017 eastern Bering Sea continental shelf and northern Bering Sea bottom trawl surveys: Results for commercial crab species, 233 p. NTIS number pending.

371 RODGVELLER, C. J., K. B. ECHAVE, P-J. F. HULSON, and K. M. COUTRÉ. 2018. Age-at-maturity and fecundity of female sablefish sampled in December of 2011 and 2015 in the Gulf of Alaska, 31 p. NTIS number pending.

370 GUTHRIE, C. M. III, HV. T. NGUYEN, A. E. THOMSON, K. HAUCH, and J. R. GUYON. 2018. Genetic stock composition analysis of the Chinook salmon bycatch samples from the 2016 Gulf of Alaska trawl fisheries, 226 p. NTIS number pending.

369 SHELDEN, K. E. W., K. T. GOETZ, R. C. HOBBS, L. K. HOBERECHT, K. L. LAIDRE, B. A. MAHONEY, T. L. MCGUIRE, S. A. NORMAN, G. O'CORRY-CROWE, D. J. VOS, G. M. YLITALO, S. A. MIZROCH, S. ATKINSON, K. A. BUREK-HUNTINGTON, and C. GARNER. 2018. Beluga whale, *Delphinapterus leuca*s, satellite-tagging and health assessments in Cook Inlet, Alaska, 1999 to 2002, 226 p. NTIS No. PB2018-100721.

368 FRITZ, L., K. CHUMBLEY, R. TOWELL, K. LUXA, and J. CUTLER. 2018. Short-term survival rates of branded Steller sea lion pups, 33 p. NTIS No. PB2018-100686.

367 STRASBURGER, W. W., J. H. MOSS, K. A. SIWICKE, E. M. YASUMIISHI, A. I. PINCHUK, and K H. FENSKE. 2018. Eastern Gulf of Alaska ecosystem assessment, July through August 2017, 105 p. NTIS No. PB2018-100602.

366 WHITTLE, J. A., C. M. KONDZELA, HV. T. NGUYEN, K. HAUCH, D. CUADRA, and J. R. GUYON. 2018. Genetic stock composition analysis of chum salmon from the prohibited species catch of the 2016 Bering Sea walleye pollock trawl fishery and Gulf of Alaska groundfish fisheries, 56 p. NTIS No. PB2018-100474.

365 GUTHRIE, C. M. III, HV. T. NGUYEN, A. E. THOMSON, K. HAUCH, and J. R. GUYON. 2018. Genetic stock composition analysis of the Chinook salmon (*Oncorhynchus tshawytscha*) bycatch from the 2016 Bering Sea walleye pollock (*Gadus chalcogrammus*) trawl fishery, 32 p. NTIS No. PB2018-100476.

364 SULLIVAN, J., and C. FAUNCE. 2018. Alternative sampling designs for the 2018 Annual Deployment Plan of the North Pacific Observer Program, 30 p. NTIS No. PB2018-100475.

363 STRASBURGER, W. W., J. H. MOSS, K. A. SIWICKE, and E. M. YASUMIISHI. 2018. Results from the eastern Gulf of Alaska ecosystem assessment, July through August 2016, 90 p. NTIS No. PB2018-100430.

362 ORR, A. J., J. D. HARRIS, K. A. HIRSCHBERGER, R. L. DELONG, G. S. SANDERS, and J. L. LAAKE 2017. Qualitative and quantitative assessment of use of offshore oil and gas platforms by the California sea lion (*Zalophus californianus*), 72 p. NTIS No. PB2018-100078.